IVK

CNRS

Centre National de la Recherche Scientifique

INFN

Istituto Nazionale di Fisica Nucleare

VIRGO

FINAL DESIGN REPORT

Code: VIR-TRE-1000-13

Issue:1

Date:01/05/97

VIRGO * A joint CNRS-INFN Project
Project Office: INFN-Sezione di Pisa*Via Livornese, 1291-56010 San Piero a Grado, Pisa.Italy.
Secretariat: Telephone.(39) 50 880 352 * FAX.(39) 50 880 350 * e-mail claudia@galileo.pi.infn.it

CHANGE RECORD

Issue/Rev	*Date*	*Section affected*	*Reason/ remarks*
1	19/06/97	All	Update of June 95-Version 0

10. INTRODUCTION

This document is an updated version of the technical part of the «Final Design, version 0», issued in October 1995. Since then, the goals of the project, the expected performance, and the cost have only very slightly evolved, but the planning has drifted and many technical details have been fixed or have evolved, so that an update of the technical design report was considered as necessary.

The project organization is described separately in the Management plan, issued in November 1996.

Programmatic aspects have been initially given in the second part of the «Final Design, version 0» and are regularly updated ib several documents: Council reports, Staff Distribution, Work Breakdown Structure, Work Package Description.

10.1 Foreword

Virgo is a project of construction of a large laser interferometer aiming at the direct detection of gravitational waves emitted by various astrophysical sources. The initial discovery phase will open the road to the new field of gravitational wave astrophysics: Virgo must be considered both as an experiment and as a step towards a future observatory.

Virgo is being designed and built by physicists and technicians from INFN in Italy and CNRS in France.

10.2 Historical background

The scientific goals and the principles of the project were described in the Virgo proposal, submitted to both institutions in May 1989. This led to the signature of a declaration of common interest between CNRS and INFN, in September 1991.

Costs and planning estimates provided in the Final Conceptual Design document in March 1992, were the basis for the final approval of the project and for the cooperation agreement signed by CNRS and INFN in June 1994.

10.3 Collaboration CNRS, INFN

The collaboration agreement between INFN and CNRS concerning the realization of Virgo was signed in June 1994. It defines the general rules of the collaboration and the role of the Virgo Council. This document concerns exclusively the construction of Virgo.

10.4 Scientific objectives

Virgo has three levels of scientific objectives :

- to realize or to participate in the first direct detections of gravitational radiation
- to test the dynamical aspects of the theory of General Relativity through the measurement of the properties of gravitational waves
- to initiate the new field of gravitational waves astrophysics

10.5 Project Description

The Virgo facilities will be erected in Cascina (Tuscany). They consist mainly in a large vacuum vessel containing the interferometer, and a few buildings. The vacuum vessel is L shaped, with two, 3 km long, orthogonal arms (the tubes). The tubes have an internal diameter of 1.2m. They house a number of baffles designed to trap the scattered light, which leave a free aperture of 1m in diameter.

They are connected to vertical tanks (the towers), which house the low frequency seismic isolation systems (the superattenuators) suspending each optical element of the interferometer.

The initial interferometer is a recycled Michelson interferometer, containing a 3 km Fabry-Perot cavity in each arm. The vertex area contains the suspended input bench and detection bench, the beamsplitter, the input mirrors of the cavities, and a recycling mirror, each element being associated with a superattenuator and a tower.

The tubes are protected by light concrete/metal structures (the tunnels) at ground level. At all the extremities small buildings house the towers and associated equipment and maintain proper environmental conditions (temperature, cleanliness, vibrations,...). The largest one (about 1000 m^2) is the central building which contains seven towers. In the central area, three additional smaller buildings house the computing system (control-command building), some technical facilities (technical building), and the extremity of the mode-cleaner (a 144 m long optical filtering cavity). The facilities are designed for a minimal lifetime of 20 years. They allow for some modifications of the interferometer geometry, and for the future addition of at least a second interferometer.

These constructions are described below. The document is split in five chapters corresponding to five « systems » (infrastructure, vacuum, interferometer optics, interferometer suspensions, and electronics). Each system is split in subsystems, and finally items. Most subsystems, and all items, are under the responsibility of one single group.

10.6 Performance goals and main requirements

Figure 1 shows the spectral sensitivity curves of VIRGO, from 1 Hz to 10 kHz.

The full (upper) curve represents the expected equivalent noise level for the initial interferometer. From low to high frequencies, the sensitivity will be limited by seismic noise, by the thermal noise of the last isolation stage, by the thermal noise of the mirrors, and finally by the quantum noise of the optical detection system. The numerical data injected in this model have been measured on existing materials and components which will be used in VIRGO: they correspond to the present state of the art.

A negligible fraction of the spectrum may be spoiled by very narrow « noise peaks » corresponding to mechanical resonance frequencies in the last isolation stage, which are not represented here. The very low frequency part of the spectrum (below 10 Hz) could be partly spoiled by the interferometer locking system.

The expected sensitivity is such that, according to astrophysicists estimates, the initial Virgo should be able to detect a few events per year.

The dotted (lower) curve shows the ultimate sensitivity level which could be achieved in Cascina. This curve does not constitute a realistic sensitivity goal, but rather shows that the facilities being built will not become rapidly obsolete : approaching this level of sensitivity would allow the observation of a large fraction of the Universe, with the detection of many events per hour.

The ultimate limitations are: seismic noise below 3 Hz, fluctuating gravity gradients (atmospheric and ground motions) up to 10 Hz, the « standard quantum limit » up to 2 kHz, and residual pressure fluctuations in the vacuum system, at higher frequencies.

In practice, there are already indications that it will be possible to enhance the initial sensitivity by about an order of magnitude at all frequencies above 5 Hz, while reaching the ultimate sensitivity would require very large, and yet unconceivable, improvements in the interferometer's thermal noise and shot-noise.

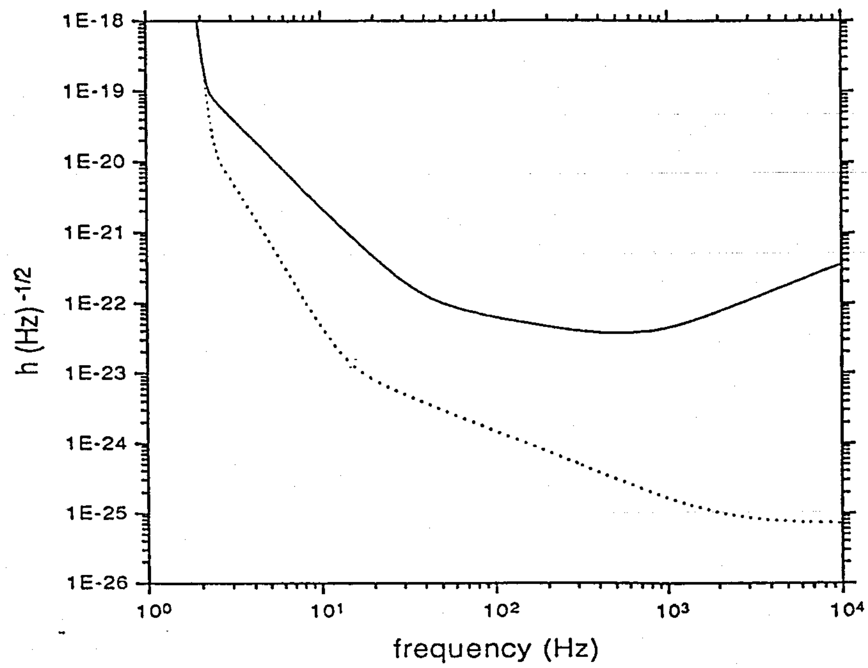

Figure 1: Spectral sensitivity curve of VIRGO

10.7 Strategy for development

The construction of Virgo will be achieved according to the following scheme :

- Construction and equipment of the central buildings.
- Installation of the "test interferometer" in the central building. This test interferometer will be used as a real size test bench for most essential subsystems of Virgo in order to perform their qualification before the end of the construction.
- Construction of the North and West arms (tunnels, vacuum tube, assembly and end buildings)
- Installation of the final optics and control systems
- Tests and commissioning
- Operation

The achievement of Virgo ultimate objectives requires the continuation of R&D. Typical R&D activities are:

- understanding and improving thermal noise
- improving the shot-noise level
- understanding low frequency noise sources
- understanding and suppressing non stationary noises
- improving the working rate

These R&D activities remain to be organized and funded

13. System Studies

Table of Contents

13.1 Modelling

Modelling refers to the physical studies and the corresponding numerical estimates necessary for making technological decisions, or compromises, on a quantitative basis. This kind of activity is going on in all the laboratories of the collaboration, and a minimal coordination is necessary to avoid useless duplication of efforts, as well as to trigger some studies which otherwise could be missing. The results of these studies may or may not be used as inputs for the general simulation program (SIESTA).

Following studies have been so far performed (non exhaustive list).

- Thermal effects in Laser optics (Orsay)
  Study of the temperature induced stresses in the YAG crystal, optimization of the optical path

- Interferometer configurations (Orsay)
  Analytical formulas for recycling interferometers

- Non-linear effects in cavities (Orsay)
  Stability of Virgo under dynamical temperature gradients in the mirrors, and radiation pressure effects

- Optics studies for specifying optical elements (Cooperation Orsay-Paris)
  Static simulation of resonant Fabry-Perot cavities in a recycling configuration, involving imperfect mirrors

- Scattered light noise evaluation (Cooperation Pisa-Orsay-Lyon)
  Emission, propagation, modulation and recombination of light scattered by the mirrors, analytical study, Monte Carlo estimates, physical measurements, design of baffles

- Electrostatic actuators for moving mirrors (Cooperation Orsay-Napoli)
  Calculation of the force generated by electrodes on a silica blank

- Magnetic effects in Bechers (Cooperation Orsay-Annecy)
  Noise due to interaction of the marionetta coils with a thin metallic wall : seismic excitation of the wall, Foucault currents, dissipation.

- Modulation studies (Orsay)
  Modulation/Demodulation schemes
  Noise due to a jitter in the modulation frequency

- Alignment (Frascati, Orsay, Annecy)
  Representation of weakly misaligned mirrors by modal expansion

- Interferometer simulation (Annecy, Orsay)
  Dynamical models of interferometers for global control

- Thermal noise (Orsay, Perugia)
  Models of cylindrical acoustic resonators for mirror thermal noise estimates

- Dynamics of superattenuator (Pisa, Orsay)
  Model of the chain of coupled oscillators involved in a SA with all relevant degrees of freedom

13.2 Locking

13.2.1 Locking function and concept

Virgo is a complex system which final performance depends of the interaction between all sub-systems. As an example, the effect of the various sources of noise of the laser light source (frequency, power, pointing fluctuations) is proportional to the asymmetry of the interferometer optics, which is the result of optical components imperfections and of their misalignments. It is the task of the control system to manage these interactions. The task of the locking activity is to define the most adequate control strategy for ensuring that the position of the interferometer components and the laser parameters remain inside a range of values which provides the optimal sensitivity for Virgo.

Locking is then a typical System activity, which involves a coordination between subsystems.

The control strategy must be based on realistic performance achievable by each subsystem. Each sub-system has to provide information and shall contribute to the definition of the strategy.

Most of the effects to be expected as well as most of the transfer functions can be computed or derived from experimental tests, so the locking studies are principally based on simulations. It is believed that there is less to learn from the experimental study of small mock-up interferometers than from piecewise study of elementary, but real items.

The main simulation tools are MATLAB for the design of solutions and SIESTA for the test of solutions.

The locking is also the place where the need for new or more accurate models arises.

After a satisfying strategy has been developed and (partially) tested on the test interferometer, the locking activity will naturally evolve towards the definition of the « h reconstruction » strategy, which is in some way the inversion of the locking strategy.

13.2.2 Locking requirements

The main requirement of the locking is to bring and maintain the interferometer in a regime that permits to reach the nominal sensitivity.

This main requirement can be split in three points:

1. The locking has to limit the residual motion of the mirrors below a certain value
2. The locking has to be robust against:

- Various resonances (violin modes, vertical thermal modes of the suspensions)
- Coupling due to the alignment
- Inaccuracy of the mechanical and optical models

3. Moreover this has to be done under the following constraint: the forces needed on the marionette and the reference mass, in order to maintain the residual motion within acceptable range, shall not introduce noise due to the electronic of the actuators.

The first point of the requirements is the consequence of the power needed in the cavities and is also the consequence of :

- The dynamic range of the photodiodes electronic and the ADC
- The power fluctuation of the laser

These last requirements can be expressed in term of length variations (see Figure 2).The locking group has shown that we have to maintain the four following lengths :

13.2.2.1 Fabry-Perot cavities lengths (L_1 and L_2)

In order to keep the two Fabry-Perot at resonance we have:

$$\Delta L_1 \text{ and } \Delta L_2 < \frac{1}{10}.\frac{\lambda}{4F} = 5\ 10^{-4}\lambda$$

where :
$F = 5C$ is the finesse of the Fabry-Perot
$\lambda = 1.064\ 10^{-6}$ m is the laser wavelength

13.2.2.2 Recycling cavity equivalent length

This length is :

$$\Delta L_r = \Delta(\frac{l_1 + l_2}{2} + \frac{2}{\pi} F \frac{L_1 + L_2}{2})$$

We have to keep the recycling cavity at resonance

$$\Delta L_r < \frac{1}{10} . \frac{\lambda}{4F_r} = 1.6\ 10^{-4} \lambda$$

where :
$F_r = 150$ is the finesse of the recycling

13.2.2.3 Dark fringe offset

This length is :

$$\Delta L_d = \Delta(l_1 - l_2 + \frac{2}{\pi} F(L_1 - L_2))$$

In that case we have two conditions :
First we have to not overload the photodiodes electronics, then the phase fluctuation has to be :

$$\Delta\phi_d < \sqrt{\frac{2h\nu}{\eta P}} \sqrt{n_{pd}}\, r$$

because the phase variation divided by the dynamic range has to be less than the shot noise.

Or equivalently in term of length:

$$\Delta L_d < \frac{\lambda}{4\pi} \sqrt{\frac{2h\nu}{\eta P_b}} \sqrt{n_{pd}}\, r = 3.3\ 10^{-4} \lambda$$

where :
$P_b = 1$kW is the power on the beam splitter
$\eta = 0.85$ is the efficiency
$2h\nu = 3.7\ 10^{-19}$ J
n_{pd}=16 is the number of photodiodes
$r = 5\ 10^7 \mathrm{Hz}^{-1/2}$ is the dynamic range of one photodiode
$\sqrt{\frac{2h\nu}{\eta P_b}}$ is the shot noise spectral density in phase units

The second condition is due to the laser power fluctuation, in that case we have :

$$\Delta\phi_d < \sqrt{\frac{2h\nu}{\eta P}} / \frac{\delta P}{P}$$

Because the length varaition has to be less than the shot noise devided by the laser fluctuation.

Or equivalently in term of length:

$$\Delta L_d < \frac{\lambda}{4\pi} \sqrt{\frac{2h\nu}{\eta P}} / \frac{\delta P}{P} = 1.6\ 10^{-4} \lambda$$

where :

$\frac{\delta P}{P} = 10^{-8}\ Hz^{-1/2}$ is the laser power fluctuation

Finally, for this length, we have to maintain :

$$\Delta L_d < \min\left(\frac{\lambda}{4\pi}\sqrt{\frac{2h\nu}{\eta P_b}}\sqrt{n_{pd}}\,r, \frac{\lambda}{4\pi}\sqrt{\frac{2h\nu}{\eta P}} / \frac{\delta P}{P}\right) = 1.6\ 10^{-4}\lambda$$

Table 1 summarise all these requirements.

Length :	ΔL_1 and ΔL_2	ΔL_r	ΔL_d
Maximal variation :	$5\ 10^{-4}\lambda$	$1.6\ 10^{-4}\lambda$	$1.6\ 10^{-4}\lambda$

Table 1: Locking requirements in term of equivalent lengths

13.2.3 Locking interfaces

The systems/subsystems which are concerned by the locking activity are :

- **All interferometer subsystems** in particular,
- **Global control** where the strategy's software is implemented
- **Infrastructure.** The exact position of each tower, is related to the modulation frequency
- **Links.** Their length is related to the towers position
- **SW Tools, simulation.** They are the main basis for locking studies

13.2.4 Selection of solutions

The problem of the locking has been split in two parts. The first one deals with the lengths recovery and the second one deals with the control of the mirrors.

13.2.4.1 Lengths recovery

The frontal (Schnupp) modulation technique (Flaminio and Heitmann PJT 93-021) has been selected due to its simplicity and robustness (see the frontal modulation scheme in part 4100).

In order to stabilize the interferometer, we need at least four independent signals coming from photodiodes. The χ^2 method is a way to use all the available information in order to reconstruct four independent signals, this permits to deal with malfunctioning diodes and to extend the linear range of measurement (Barsuglia and Cavalier VIR-NOT-LAL-1390-051).

For instance two strategies have been tested (see Figure 2):

- Use of photodiodes D1 D2 D7 and D8 (Barsuglia NTS 096-23)
- Use of photodiodes D1 D2 D5 in phase and quadrature (Flaminio and Heitman PJT 093-021)

All the robustness tests have not been yet done, there is a need to work on this aspect (TBD).

It has been shown that the dynamic behavior of the optical model (the model between the position of the mirrors and the photodiode signals) has to be taken into accounts in order to achieve control stability (Mehmel NTS 096-40 and NTS 096-23).

The frequency modulation of the laser has to be chosen in order to satisfy a low laser frequency fluctuation (min 8 MHz) and in order to be within the bandwidth of the photodiodes electronics (max. 10 Mhz). This range of possible frequencies seems to agree with the alignement constraints (TBC).

In this range there is a large choice of frequencies (Heitmann PJT 094-007). It is sufficient that the side bands are resonant in the recycling cavity and anti resonant in the Fabry-Perot. This choice has an influence on the optical model and then on the locking. We have to test the different possible solutions, in order to have the most robust control strategy (TBD).

Remark :

For the test interferometer a modulation frequency around 12.56 Mhz has been chosen.

13.2.4.2 Control of mirrors

An important problem is the bandwidth of the control. For instance due to requirements and due to the expected open loop displacement of the mirrors we need at least an open loop gain of 10^6 (TBC) around 5 Hz.

If we assume a full decoupled technique (inversion of the optical model and the same compensator on each mirror, Mehmel NTS 096-23) and if we call $L(j\omega)$ the open loop transfer function from one length to the same length, then the closed loop transfer function is given by :

$$\frac{1}{1+L(j\omega)}$$

The needed accuracy for $L(j\omega)$ depends on the bandwidth of the control. If the unity gain frequency is low (around 10 Hz) then the controller is difficult to realize because the gain has to decrease rapidly. But in that case, it is not necessary to have a good knowledge of $L(j\omega)$ above this frequency. On the contrary, if the unity gain is high (around 1kHz) the controller is much more easy to realize, but we have to know the high frequency behavior of $L(j\omega)$, which includes the optical and the mechanical models.

13.2.4.3 Remarks

1. Even if we do not use a decoupled technique, we have to know precisely $L(j\omega)$ quite above the unity gain frequency.
2. We have decided to use a sampling frequency of 10 kHz for the control, so the maximal value for the unity gain frequency is around 1kHz.
3. The bandwidth has an influence on the transfer function between gravitational waves and detection. In any case, this transfer function (which may include the control strategy if the bandwidth is large) has to be known for the detection of gravitational waves.All tests have been done with a unity gain frequency of 30 Hz.

The second problem is the maximal forces available on both the marionette and the reference mass. Most of the simulation tests have been done with the only control on the reference mass. However, some studies have shown that it is not possible to act only on the reference mass. A solution has been proposed that permits to lower the force needed on the reference mass (Flaminio NTS096-06) but we need informations on the maximal forces delivered by the actuators (TBD).

The third problem is the acquisition of the locking (TBD). SIESTA seems to be the tool that permits to test the acquisition of the locking by using fast simulation. For the acquisition strategy, the χ^2 method could be useful.

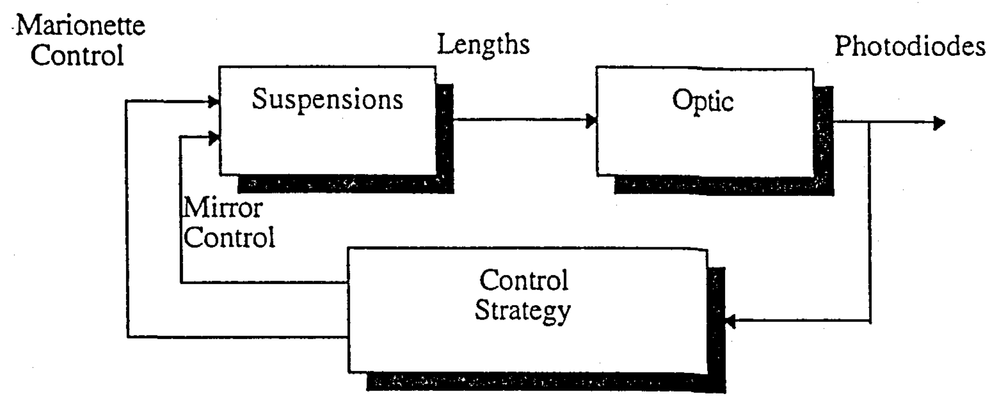

Figure 1 : Locking Scheme

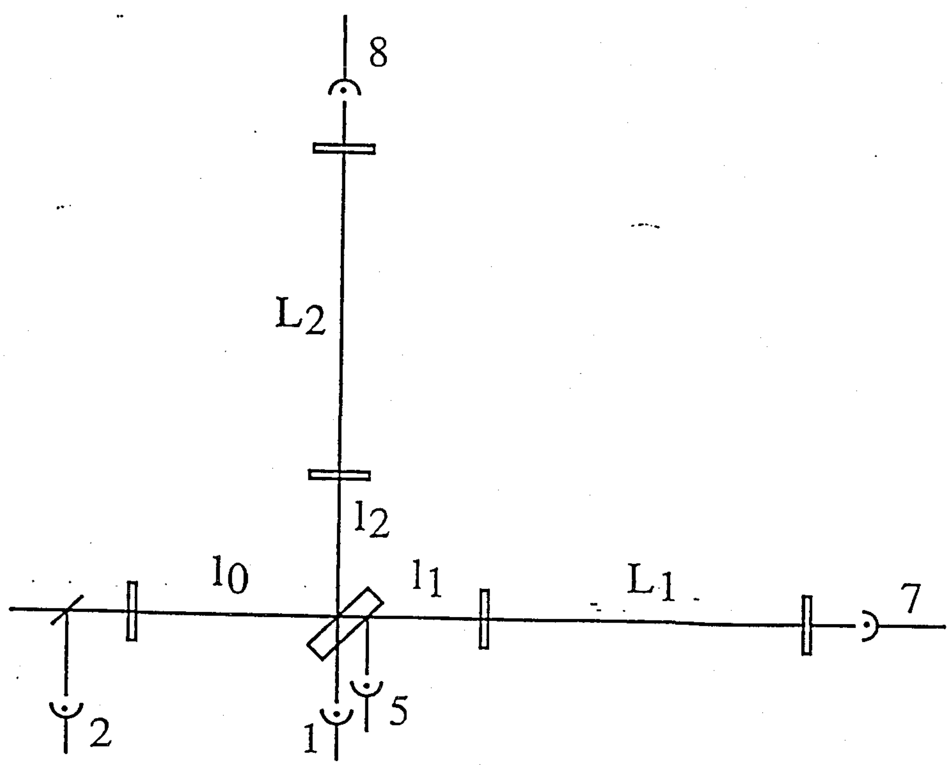

Figure 2 : Scheme of the interferometer

13.3 Facility Geometry

13.3.1 Scope

The alignment of the optical and mechanical elements on the 3 km arms requires the development of specific methodologies. By facility geometry we understand all the means necessary to provide physical references necessary during the assembly to achieve the required positioning tolerances.

13.3.2 Summary of Requirements

13.3.2.1 Angle between the two arms

The angle must be about 90°. There is no precise requirement on this angle which will anyway be known within the accuarcy of the GPS absolute measurements (< 10cm over 3 Km).

13.3.2.2 Angle between arms plane and Mode Cleaner beam

The mode cleaner needs to be in the same plane as the two arms within 1 mrd.(It is to be reminded that the North arm is horizontal but the west arm has a slope of 2 meters over 3 Km).

13.3.2.3 Distance input to terminal towers

The absolute distance must be set within ± 0.25 meter.
This precision is defined by the modulation wavelength (c/12MHz) divided by 100.

13.3.2.4 Tubes positioning

Tube axis

The tube axis must stay inside a cylinder of 50 mm radius centered on the line defined by the beam splitter and the end mirror.

Longitudinal distance precision:

The supports of the tube lay on the concrete slab on top of pillars.
Each tube section must be positionned within ± 5 mm with respect to the neighbouring one.

Straightness of the tube .

The tube does not follow the earth curvature which would give a sag of about 20 cm over 3 km but is straight. Local measurements must therefore be corrected.

13.3.2.5 Towers positioning

13.3.2.5.1 Separating roof, global tuning allowed

The mirror position is defined by the center of the separating roof. All errors added the separating roof must be positioned with an absolute accuracy of ± 25 mm which is the range of movement of the separating roof.

13.3.2.5.2 Towers Center

The reference surface is the square upper flange.
The position of the real center of the tower (crossing of the axis) is not materially defined (It can be deduced indirectly within about one cm precision from the manufacturing tolerances).
So and by definition the Center of the tower is at 1630 mm below the crossing of the marks on the upper flange
Once the tower is in place, its deformations may be, during the baking or with time, up to 1mm.

During the baking the tower expands and may not come back exactly to the initial position. The displacement of the tower "center " would be about 7 mm during the baking. It is estimated that the center may come back within ± 2 mm from its initial position.

The movements of the towers can be measured with the targets on the upper flange.

13.3.2.5.3 Towers positioning error

It is estimated that the towers may be position within ± 5mm (better if possible). TBC

It can be distinghished between:

the absolute position of all the towers,

and the relative precision of the towers respective one to another.

13.3.2.6 Mode Cleaner requirements

The Mode Cleaner tower longitudinal position has to be set within ± 1cm from the theoretical position .

Mode cleaner Tube axis precision : The tube axis must stay inside a cylinder of 50 mm diameter centered on the line defined by the Injection tower and the Mode cleaner tower axis.

13.3.3 Interfaces:

The definition of geometrical references is needed for the installation of the following parts:

Infrastructures	WBS 2000
Towers lower parts	WBS 3310
Tests interferometer Assembly	WBS 6100
Modules realization	WBS 3110
Mode Cleaner tube	WBS 3130
Tube assembly	WBS 6300

13.3.4 Principles.

The basic idea is to make use of the high absolute accuracy of Global Positioning Systems. GPS provides positions on the geoid referred to several satellites emitting radio signals. Measurements can be done only in open air.

A first network of reference points to be measured by this GPS method will be installed: at least five points outside the buildings, permanently accessible and measurable, and several points inside the buildings measurable before the roofs are put in place.

This network will be linked to the local geodesic network. It will give the reference from which all the other distances will be measured.

A second reference points network will be installed inside the central building and the tunnels. The positions of the secondary reference points will be measured relative to the first reference network by classical topographic method. (with a special theodolite equipped with a telemeter). It is from this secondary network that the positions of the towers lower parts or the tube will be measured.

Each tower or tube modules will be equipped with targets. The mechanical references and dimensions of each elements will be measured relative to the targets, before assembly on site.

So from the measurement of the tragets one knows the position of the element. Possible long term evolution can also be monitored with the same system.

The central buildings are rather full of equipment and hence obstruction of lines of sight must be avoided.

Five points inside the central building will be installed and their position measured before the roof installation . Some points will be visible from the outside. By this way it will be possible to link the points inside to the external references.

13.3.5 Instrument accuracy

13.3.5.1 GPS Measurement.

The expected precision of the GPS measurements for each point are :
in planimetry : standard deviation $\sigma = 5$ mm
In altimetry : standard deviation $\sigma = 10$ mm

13.3.5.2 Theodolite measurements

The leveling of the buildings and the tunnel can be done by leveling theodolites which can currently give an accuracy of about 1 arcsecond.
Lengths can be measured with specially equipped theodolites. The accuracy is:
0.8 mm +1 ppm *Distance(mm)

13.4 Electro-Magnetic Compatibility (EMC)

13.4.1 E.M.C. General

The useful detection frequency range of Virgo is from 0 to about 20 Mhz. The main frequencies used are shown on the figure below.

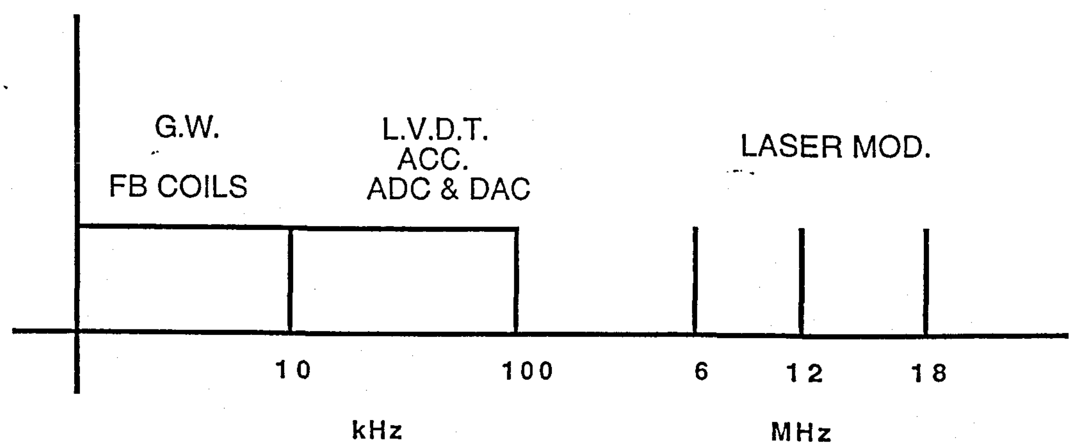

It is important that undesired signals coming from outside or from other instruments inside the buildings are kept at a sufficiently low level not to interfere with the useful signals.
For this reason, electromagnetic interference suppression methods that at least reduce, if not completely eliminate, unwanted effects must be used.
E.M.C. means to study, to foresee, and (possibly) to solve problems that can arise by the coexistence of such a lot of instruments into a noisy area.
Potential interference sources are:
A) "Outside" sources:

A1) Interference from external sources (e.g. radio transmitter, lightning, etc.)
A2) Interference existing on the 220Vac mains supply (ENEL)

B) "Internal" sources

B1) Interference produced from instruments in the building

B1.1) Propagated by the 220Vac mains supply
B1.2) Propagated magnetically and/or electrically
B2) Voltage differences due to an imperfect grounding of instruments

Let us see, for each item, details and possible solutions.

13.4.2 External disturbances.

Some measurements have been performed in the area of the central building, in the frequency range from 40 kHz to 100 MHz (Fig. 1340.1). It seems that the most relevant source of E. M. noise is the 100 kW 1 MHz "COLTANO" AM transmitter, about 6 km from the building (Fig.1340.2).

To reduce the impact of this and any other signal that could be present in the future (airport radar, Monte Serra TV and Radio transmitters, etc.), it's convenient to shield the buildings. The shielding effectiveness is inversely proportional to the longest dimension (not the total area) of an opening in the shielding net (because the openings behave as slot antennas), and to the frequency (Fig 1340.3).

Equation 1340.1 can be used to calculate the shielding effectiveness, or the susceptibility to EMI leakage or penetration of an opening in an enclosure:

$$\text{SHIELDING EFFECTIVENESS (dB)} = 20\log_{10}\left(\frac{\lambda}{2\,L}\right) \qquad \text{(Eq. 1340.1)}$$

In our case, with λ=300m and L=4m, at least 30 dB of attenuation @ 1 MHz can be expected using only the metal supporting structure. In case it's necessary to increase this attenuation, it will be useful to interconnect the structure with a narrower web, using clamping tools (Fig. 1340.4) and copper strips. No shielding is necessary on the floor, because attenuation is very high through the ground (Fig. 1340.5).

For the same problem it could be useful to ground the vacuum tubes every 15 meters (TBC), avoiding resonance problems.

13.4.3 Internal disturbances

We will probably have no problems arising from the mains supply, because all the electronics will be powered from an insulated Uninterrupted Power Supply; we must only be careful not to leave mains cables "after" and "before" the UPS running together for long distances. If this will not be possible, it could be necessary to use shielded cables with the "clean" power supply (TBC).

This precaution will not be sufficient if our own electronics disturbs the mains, spreading noise on the cables. Simple rules to avoid this are: use (whenever possible) linear power supplies, not switching; ask the manufacturers which EMC directive instruments comply to, and use only those instruments (crates, power supply, P.C., etc.) declaring compliance to FCC, VDE, IEC or similar directives; in case the instruments are home made the project must follow EMC criteria. Other rules can be found in the bibliography at the end of the chapter.

The same guidelines are to be followed for the noise radiated magnetically and/or electrically; the following approach shall be followed :

a) the "photodiode and mixer" system could detect the laser modulating signal also; it will be necessary to shield the source (signal generator + power amplifier + Pockels cell) and the receiver (photodiode + mixer) correctly.

b) position sensors (LVDT) and accelerometers, working at close frequencies (10 kHz to 50 kHz), could interact with each other, generating unwanted beat effects and/or cross/talk; moreover, some of these high frequency signals can go through (for grounding problems) the anti-aliasing filters at the input of every ADC system, with unpredictable results.

c) all signals at the output of the sensors are of very low level (near the noise limit), and the connections between these sensors and the instruments must be reliable.

For all these reasons, it is absolutely necessary to use, as much as possible, differential inputs and outputs, with the aid of twisted and shielded cables. This system will also avoid ground-loop problems.

Likewise on the airplanes, no RF transmission will be allowed into the buildings; a 1W hand-held radio at a distance of 1 meter can generate an electric field of 5.5V/m, as in equation. 1340.2:

$$\text{ELECTRIC FIELD INTENSITY, in V/m,} = 5.5\left(\frac{\sqrt{W_{erp}}}{m}\right) \qquad \text{(Eq. 1340.2)}$$

That means no cellular phones, no cordless, etc. in critical areas during normal operation.

13.4.4 Grounding concepts

The safety ground is not able to assure an equipotential ground system, especially at high frequencies: a wire length of $\lambda/4$ and its odd multiple is like an "open" connection; it's necessary to use connections as short as possible in Virgo.

For this reason, during the construction of the main building, a net (8 mm iron rods) has been embedded into the concrete floor, with a square mesh of about 2.7 meters (Fig. 1340.6). In this manner it's easy to have very short ground connections if desired, because every 2.7 meters, a short iron rod welded at every cross point of the mesh comes out vertically.

On the walls, the rods are joined to the metal supporting structure of the building (Fig. 1340.7); somewhere (in more than one point) there will be connections with the safety ground.

13.4.5 Cabling

As stated before, very low level signals are expected in VIRGO; it's important to have high noise rejection on the cables connecting the sensors inside the towers to their electronics.

With a simple test set-up, some measurements have been made that show how an external field is induced at the inputs of a differential amplifier (Fig. 1340.8); it's clear that the best choice is the use of a shielded twisted pair cable, or the use of a special kind of coaxial cable (e.g. shielded coaxial), with the inner conductor connected to one input (+), the inner shield to the other input (-), and the outer shield grounded at the receiver end only.

However, these configurations leads to a high number of cables, and to a high number of connection from the vacuum tower to the out.

This is an "open point" to be discussed with other groups, particularly with Cabling, Vacuum and Electronics.

Finally, it's almost impossible to foresee the EMC problems that will arise in Virgo; every decision must be a trade-off between the costs of the current choice (and its efficiency), and those of a more effective but more costly (and perhaps unnecessary) solution.

Bibliography:

Henry W. Ott: "**Noise reduction techniques in electronic systems**", second edition, John Wiley & Sons, Inc., New York.

Hugh W. Denny: "**Grounding for the control of EMI**", Interference Control Technologies, Inc., Gainesville, Virginia.

Ralph Morrison: "**Grounding and shielding techniques in instrumentation**", third edition, John Wiley & Sons, Inc., New York.

Paul Brokaw: "**An I.C. amplifier user's guide to decoupling, grounding, and making things go right for a change**", Analog Devices Application Note.

Walt Jung and John McDonald: "**Noise reduction and filtering for switching power supply**", Analog Devices Application Note.

Adolfo A. Garcia: "EMI/RFI considerations", Analog Devices Application Note.

John McDonald: "Sensors and Cable shielding", Analog Devices Application Note.

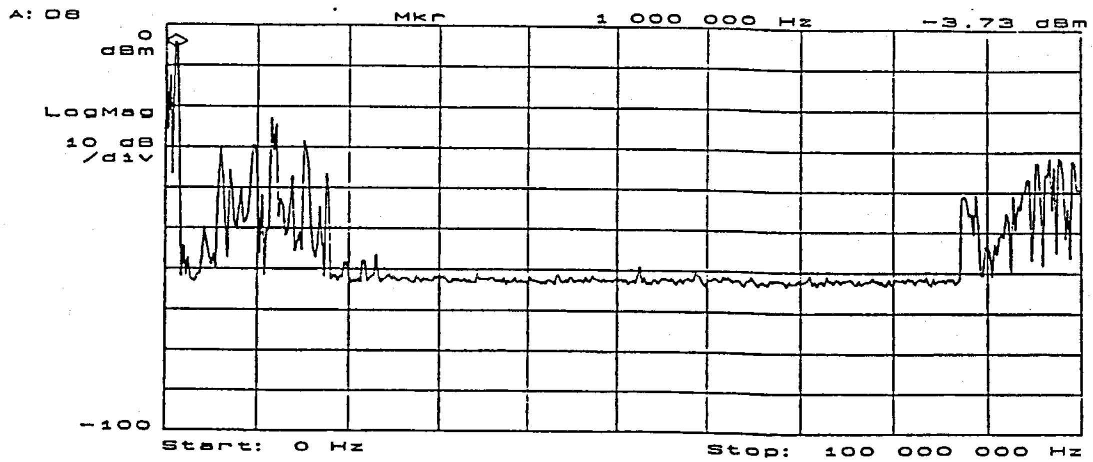

Fig. 1340.1 0 to 100 MHz spectrum measured in the area of the central building

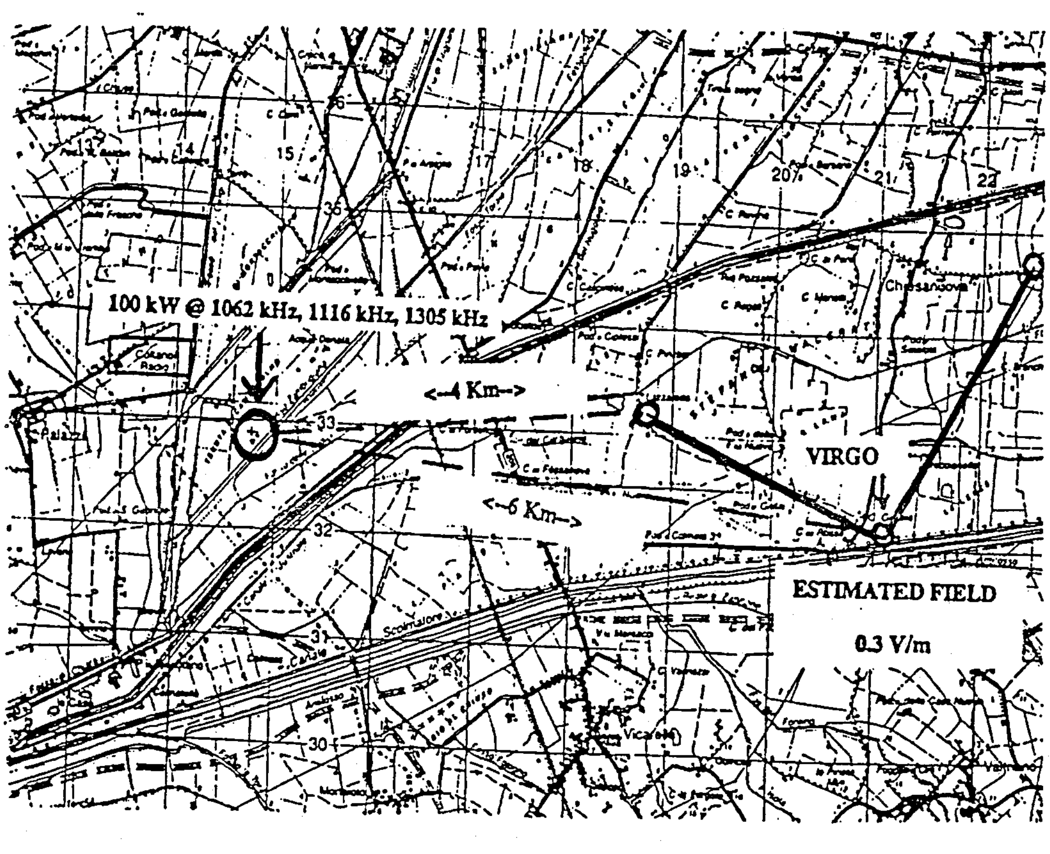

Fig. 1340.2 VIRGO area plant

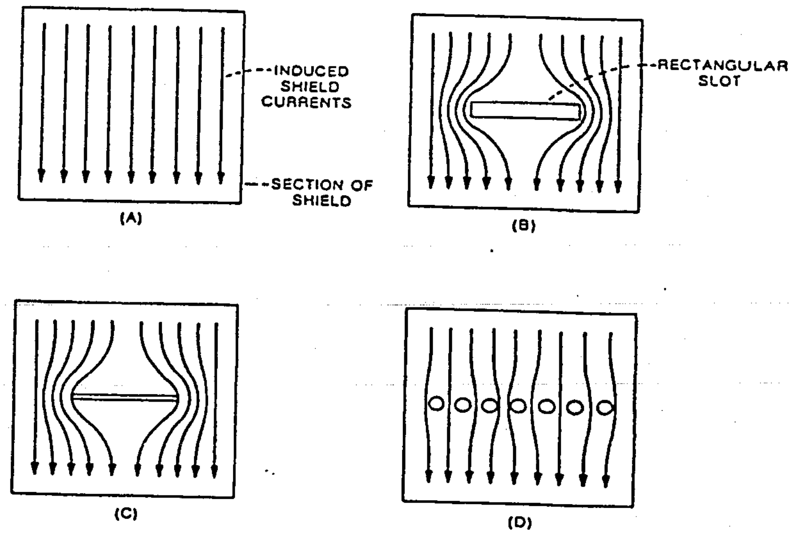

Effect of shield discontinuity on magnetically induced shield current.

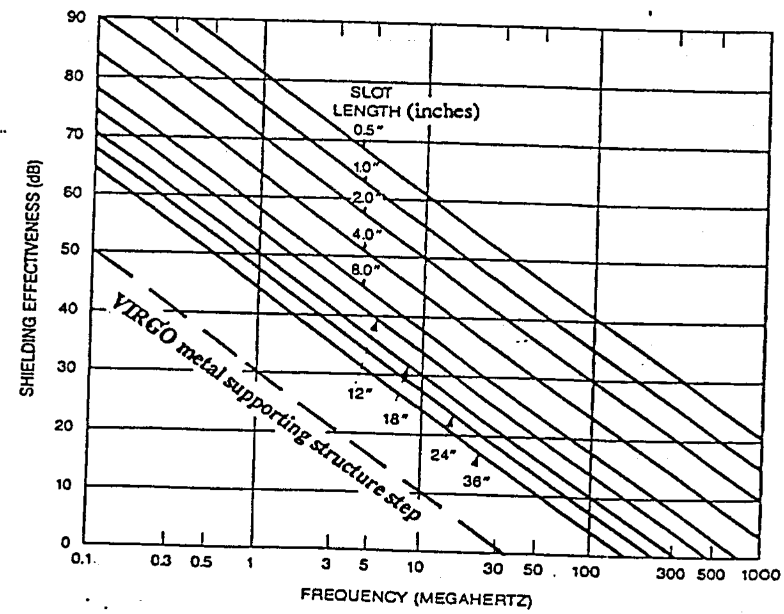

Fig. 1340.3 Shielding effectiveness vs. Frequency and maximum slot length for a single aperture

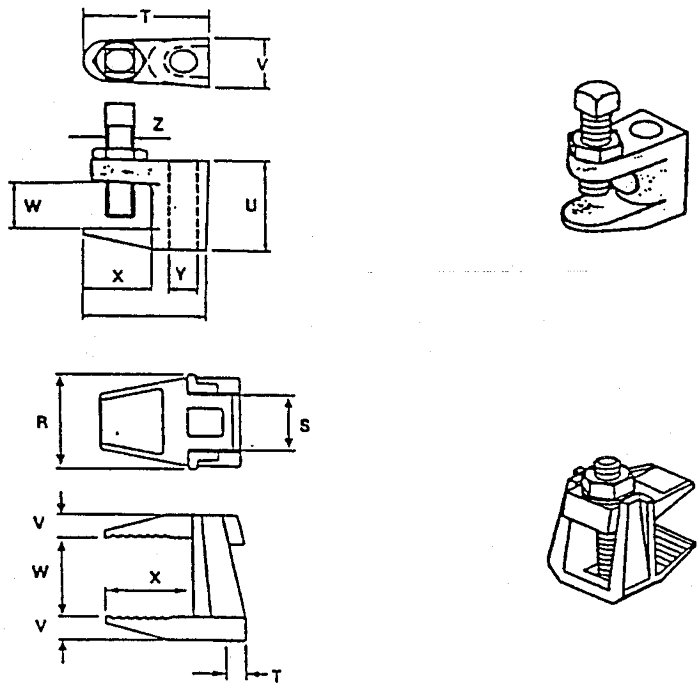

Fig. 1340.4 Two kinds of clamping tools useful for interconnection between the metal supporting structure

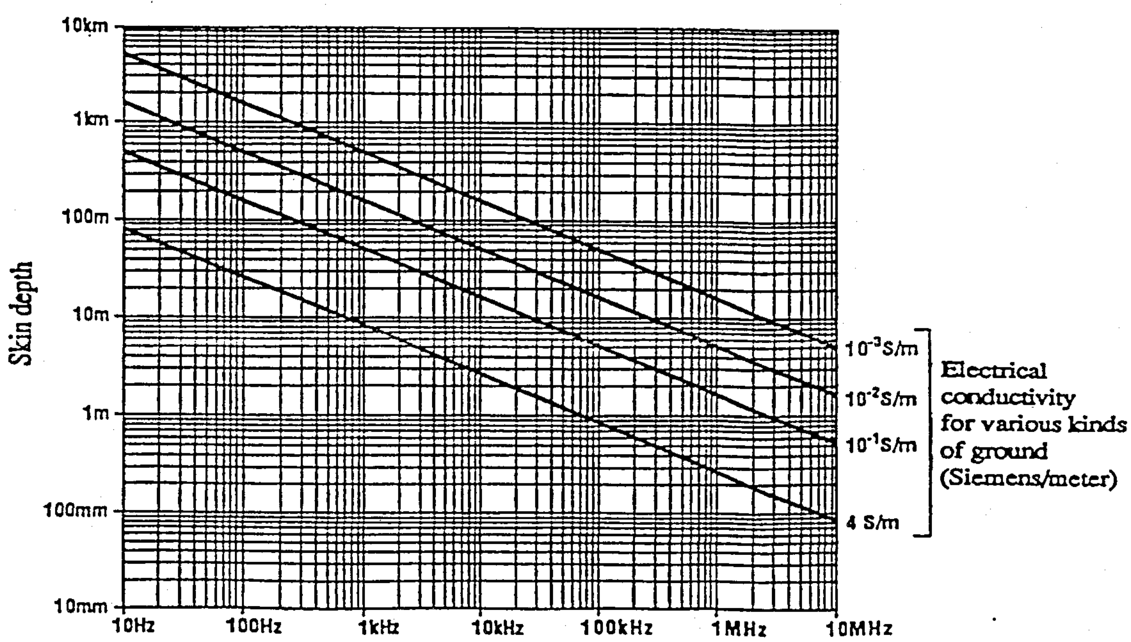

Fig. 1340.5 RF ground penetration vs. Frequency

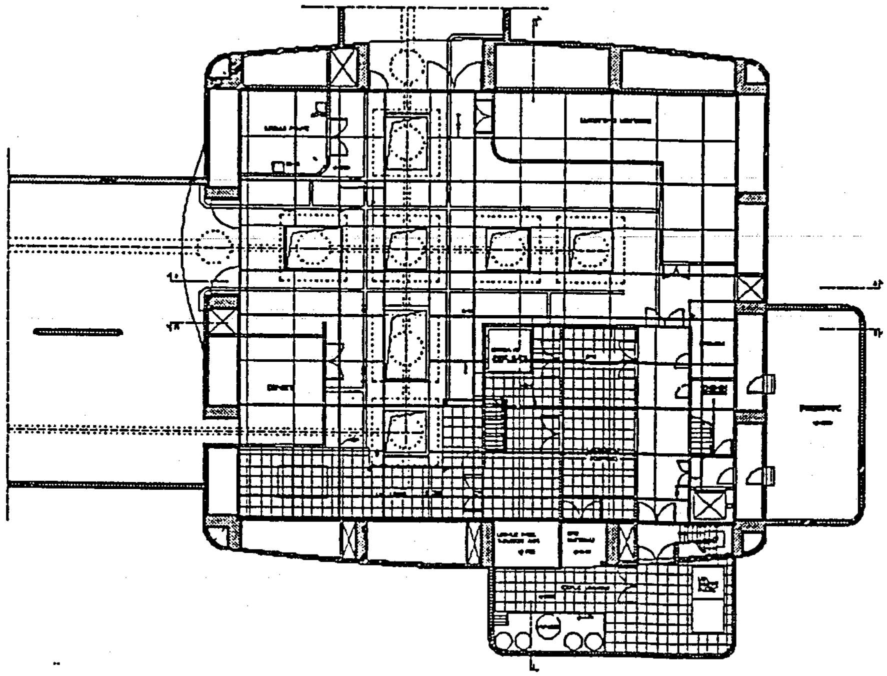

Fig. 1340.6 VIRGO central building plant, with the 2.7 meters square mesh overlapped

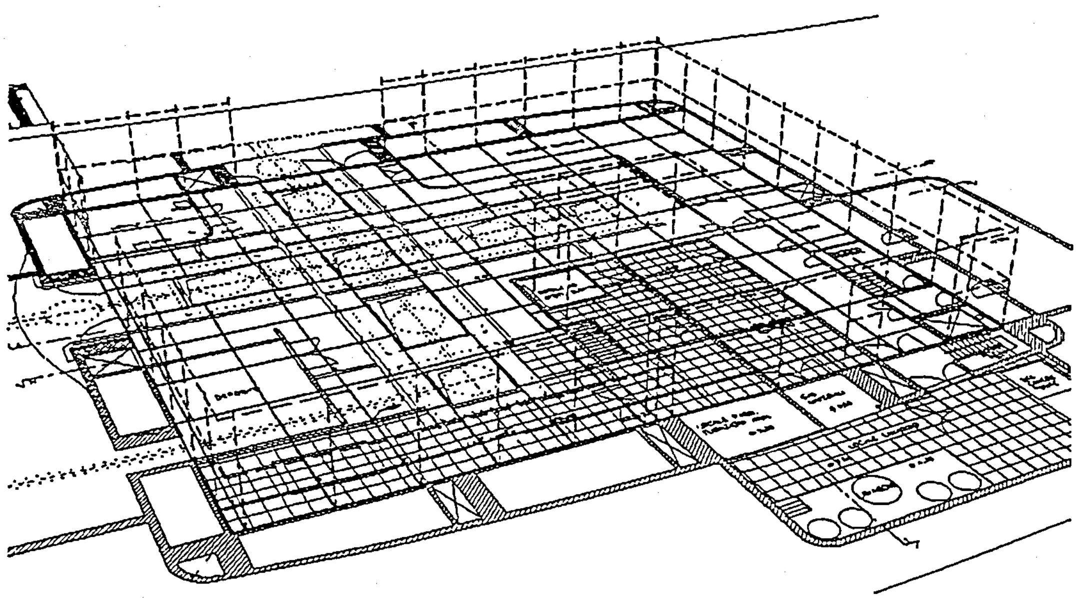

Fig. 1340.7 Perspective plant of Fig. 1340.6

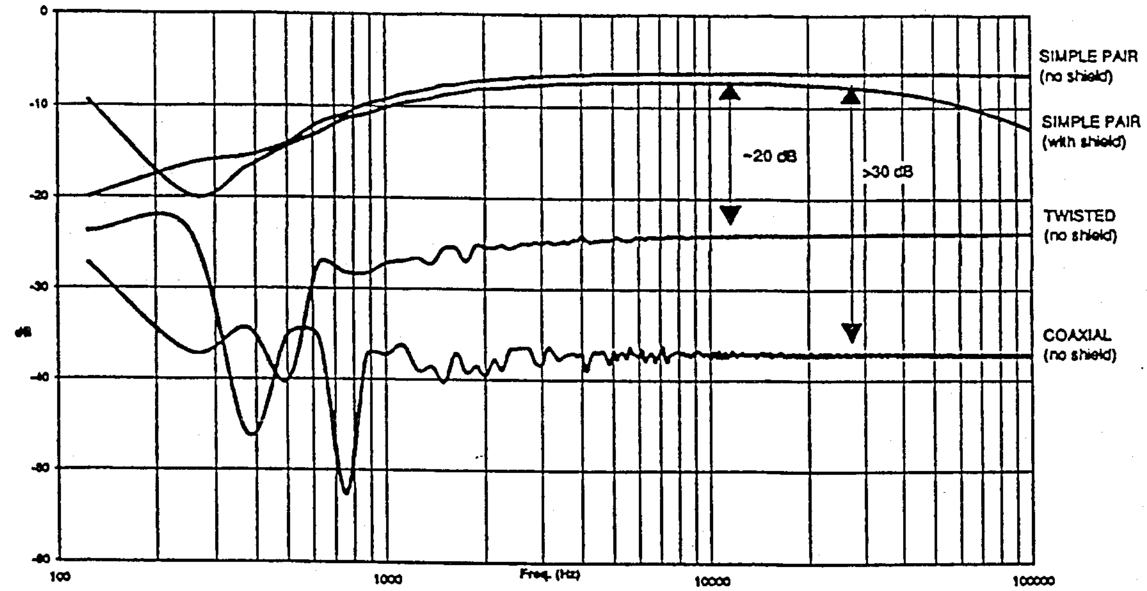

Fig. 1340.8 Noise rejection for various kinds of cables

20. INFRASTRUCTURE

Table of Contents

20.1 Infrastructure function and concept

The infrastructure for the VIRGO Project consists of the buildings and the tunnels, with their equipment, necessary to the interferometer installation on the Cascina site.

In the next paragraphs the infrastructures designed to accept the VIRGO interferometer (the tunnels hiding the long vacuum pipes and the relative assembly halls, the experimental halls and the laboratories) will be described together with the chosen site, its characteristics and arrangement (roads, bridges, fence, drain channels).

The executive design of the "central area buildings" has been completed; for this set of buildings the shown drawings correspond to what is really being built. On the contrary the drawings of the “arms and terminal buildings”, when shown, correspond to the preliminary design.

20.2 Infrastructure requirements

20.2.1 General requirements

The installation of the VIRGO interferometer has to satisfy the following requirements :

- build a detector and an infrastructure frame capable of a 20 years operation time;
- keep the performances of the detector at the limits of present technologies;
- build the apparatus on a flat, controlled area, as far as possible away from mechanical vibration sources, as roads, trains, etc., within a reasonably short distance from one of the collaborating laboratories;
- give a minimum perturbation to the geological, biological and economical equilibrium of the surrounding region.

The stability requirements for a safe VIRGO operation are summarized in what follows.

- The foundations of the experimental halls have to guarantee the stability of the Super Attenuators suspension points, located at the top of the vacuum tanks. (The suspension points shall not move more than 1 mm per day and, in a 20 year period, the overall displacement must stay well within the adjustment range of a few cm in all directions. Tidal effects and thermal dilatation are expected to produce movements up to 0.2 mm with 6, 12, 24 hour periods.)
- The foundations of the tunnels have to guarantee the stability of the tube. (it is required to have the center of any pipe cross-section always inside an ideal 5 cm radius cylinder. The realignment of the supports shall not occur more than once in a year.

20.2.2 Site requirements

To satisfy the requirements listed before, the site has been selected according to the following rules :

- keep the distance of the tube from farm houses above a minimum of 50 m
- keep the distance of the mirrors above a minimum of 500 m from main roads and of 200m from electrical power lines.
- reduce to a minimum the number of crossed lanes and irrigation channels
- keep the expenses for the acquisition of the land much lower than the cost of the apparatus itself;
- allow to build the halls and the tunnels with standard foundation.

20.3 Infrastructure description

20.3.1 General description

The area needed for VIRGO in Cascina (fig. 2000.2) consists of five laboratory areas, about 40000 m^2 each, connected by two orthogonal land strips 30 m wide and 3 km long. An additional area, consisting of a small land strips along each side of the main two, is needed to realize country roads and the drain channels outside the fence, to satisfy the requirement of "Comune di Cascina".

The tunnels, placed on the main land strips, make two orthogonal arms in the North and West direction. Each tunnel hides the 3 km vacuum pipe.

There are four experimental halls : at the crossing point of the arms there is the "central building" containing, under vacuum inside the towers (vacuum tanks), the pendulum chains, called Super Attenuators (SA), that supports the various optical parts; at the other ends of the tunnels there are the "terminal buildings" where are installed the chains supporting the other two mirrors of the interferometer; a fourth hall, containing the mode-cleaner mirror, is located at 140 m from the central one, along the West arm, .

At 100 m from the central hall there are the "control building" and a "technical building" for electricity and thermal plants.

At half way of the arms there are the "assembly buildings" for the vacuum pipe assembly.

A service road, running along the arms, connects all the buildings.

Apart the service road and a round zone around the central building, the remaining area will be arranged with trees and grass.

20.3.2 Access roads

The access to the site is good, through already existing paved roads, linked to the Pisa-Firenze motor-way. The most relevant distances are : 15 km from Pisa, 8 km from Cascina, 21 km from INFN laboratory in San Piero a Grado (fig. 2000.1). The Pisa-Firenze railway has a stop in Cascina and an almost dismissed railway runs at about 5 km West of the central zone; it could be useful for tube elements delivery, during the installation phase.

The VIRGO area will be closed by a fence. Controlled access to the VIRGO area will be only through the central zone, even if it could be possible also through the terminal zones. In fact all three zones are within a distance of 0 - 100 m from already existing roads.

20.3.3 The site

20.3.3.1 Site choice

A very accurate search has been performed in a 100 km radius region around Pisa. Much more distant sites have also been investigated : the INFN National Laboratories at GranSasso and Legnaro and a site in the South of Italy, that was being considered to install large air shower detectors. All morphological, technical and administrative aspects have been investigated, including detailed seismic noise measurements. A site has been selected as very suitable for the installation in the Comune di Cascina (fig. 2000.1); the Mayor assures full collaboration to solve administrative problems in the land acquisition procedure. Outstanding characteristics of this site are the perfect flatness (+/-0.5 m) and the low population density.

The relevance of the noises generated by sources as roads and electrical lines has been investigated theoretically and experimentally and possible screening methods have been suggested, while not necessary in the chosen situation.

20.3.3.2 Site morphology

The vertical profiles of the two arms have been carefully measured and they turn out to be flat within +/- 0.5 m. Only in a 100 m radius zone, around the arm crossing, the ground level is 2 m higher; a clever architectural design uses this characteristics to allow to circulate freely around the central area, despite the presence of the tunnels, and to use more efficiently the central building volume, entering at the first floor.

The plane of the interferometer will be horizontal in the North - South direction, but inclined by 2 m over 3 km, in the East - West direction. Being this slope perfectly tolerable for the apparatus operation, it will not be corrected.

Only a few crossings have to be foreseen : a few irrigation channels and one paved road on each arm. The channels are only a few meters wide and do not represent a problem. The small roads will get bridges to allow the crossing of the VIRGO tunnels. Three smaller bridges will be built for unpaved country roads.

20.3.3.3 Site geology and stability

The site geological survey, performed along the two whole arms, included penetrometric tests, core borings and water table height measurements. The study reached a depth of 50-60 m and, at few locations, 180 m. Undisturbed core samples have been collected at different depths and laboratory analyzed. The complete study is contained in detailed reports, where all the data are collected and possible foundation types are envisaged, to meet the stability requirements.

Main feature of the ground is a surface clay layer, 4 m thick, with a low load capability, followed by a sequence of softer and stronger clay and sand layers, extending down to a gravel layer situated at a depth variable between 30 m and 60 m. Beyond the gravel layer (5 m thick minimum), there is consolidated clay extending few hundred meter deep.

Given the tight requirements, a study of the ground motion expected in the next 20 years has been performed. The study included :

- precision measurements of the ground level up to 20 km away from the site
- collection of historical data on the ground level
- measurements of the water height in existing and on purpose drilled wells
- collection of historical data on the water height
- use of the ground knowledge acquired through the quoted geological measurements
- development of a computer program for the dynamical simulation of the interaction between solid and liquid phases in the ground
- tuning of the simulation program on the available historical data
- computing of the ground level evolution in the next 20 years.

The comfortable result is that, despite an overall subsidence (ground lowering) reaching 15 cm at some point, the differential subsidence will be less than 5 cm. This means that the planarity of the site is expected to be preserved to better than +/-2.5 cm. This could even allow to do not readjust the vacuum tube alignment in the 20 year lifetime of the apparatus. It has to be remarked that also the gravel layer suffers of most of the subsidence, due to the underlying deep clay layer.

20.3.3.4 Seismic measurements

Seismic measurements have been performed on the chosen site, showing that it is normal/good from his point of view, the seism intensity being below $10^{-6}/n^2$ $mHz^{-1/2}$ in the whole relevant frequency range (0.5 Hz < n < 3000 Hz).

Ground vibration measurements have also been performed at different distances from ploughing tractors; the result is that, in the VIRGO site ground type, the effect reduces at the natural seism level at about 80 m distance from an operating machine. This does not give any problem for the mirrors, since their suspensions are located at the center of 100 m radius laboratory areas. Also the vibrations induced on the vacuum tube are not expected to be dangerous, even if ploughing tractors could go as close as 15 m to the tube axis; the baffle system designed to stop the diffused light is, in fact, performing well enough to get rid also of this problem. Moreover ploughing and other heavy agricultural works last few days per year and can be brought to coincide with apparatus maintenance periods, when data taking is, anyway, stopped.

FIGURE CAPTIONS

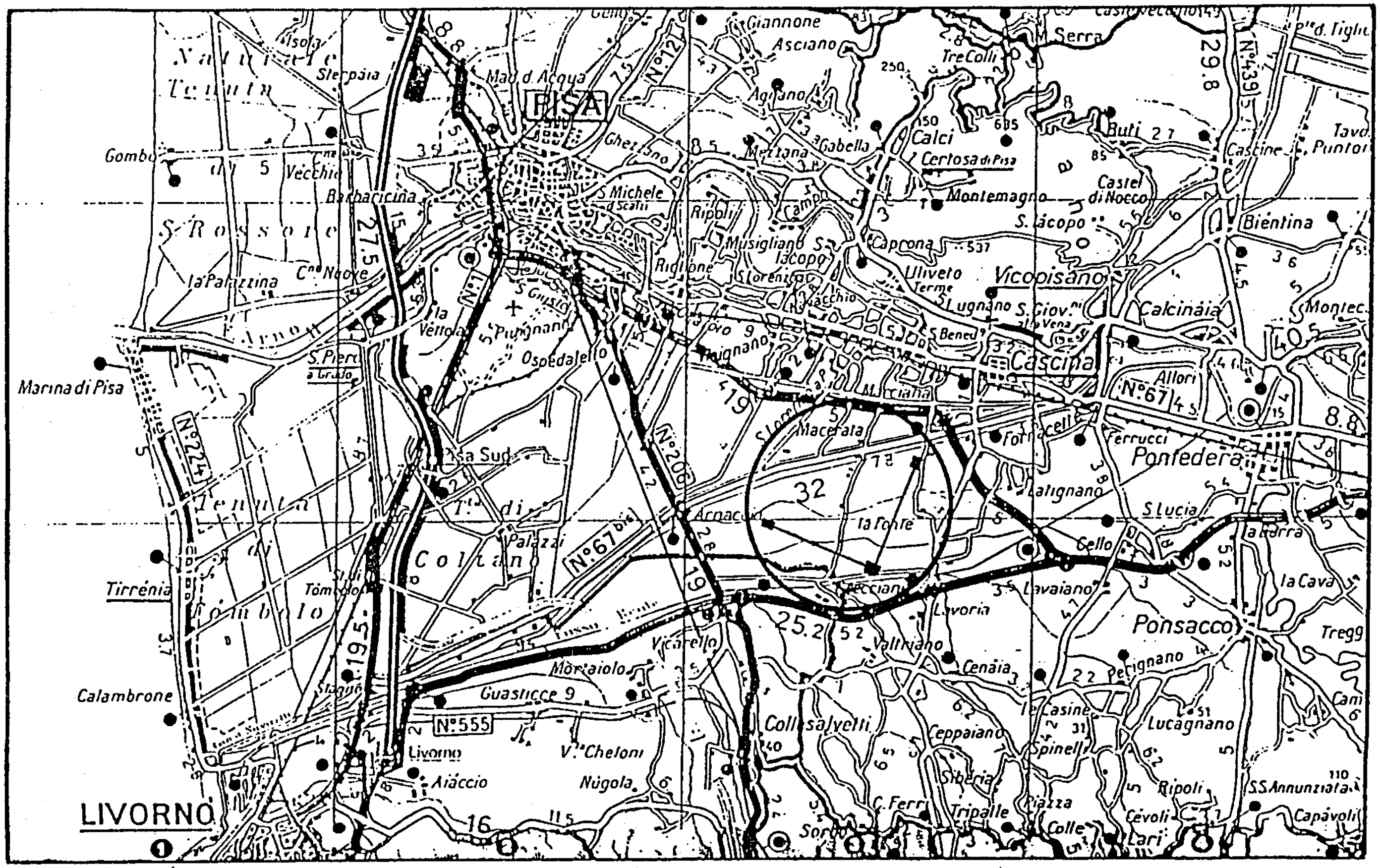

Sept. 1993 - De Carolis

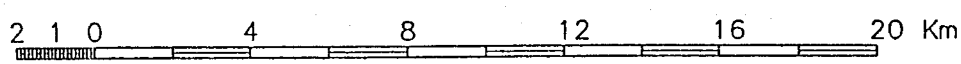

Fig. 2000.1

A = CENTRAL BUIDING
B = CONTROL BUILDING
C = SERVICE BUILDING
D = MODE CLEANER
E = ASSEMBLY BUILDING
F = TERMINAL BUILDING

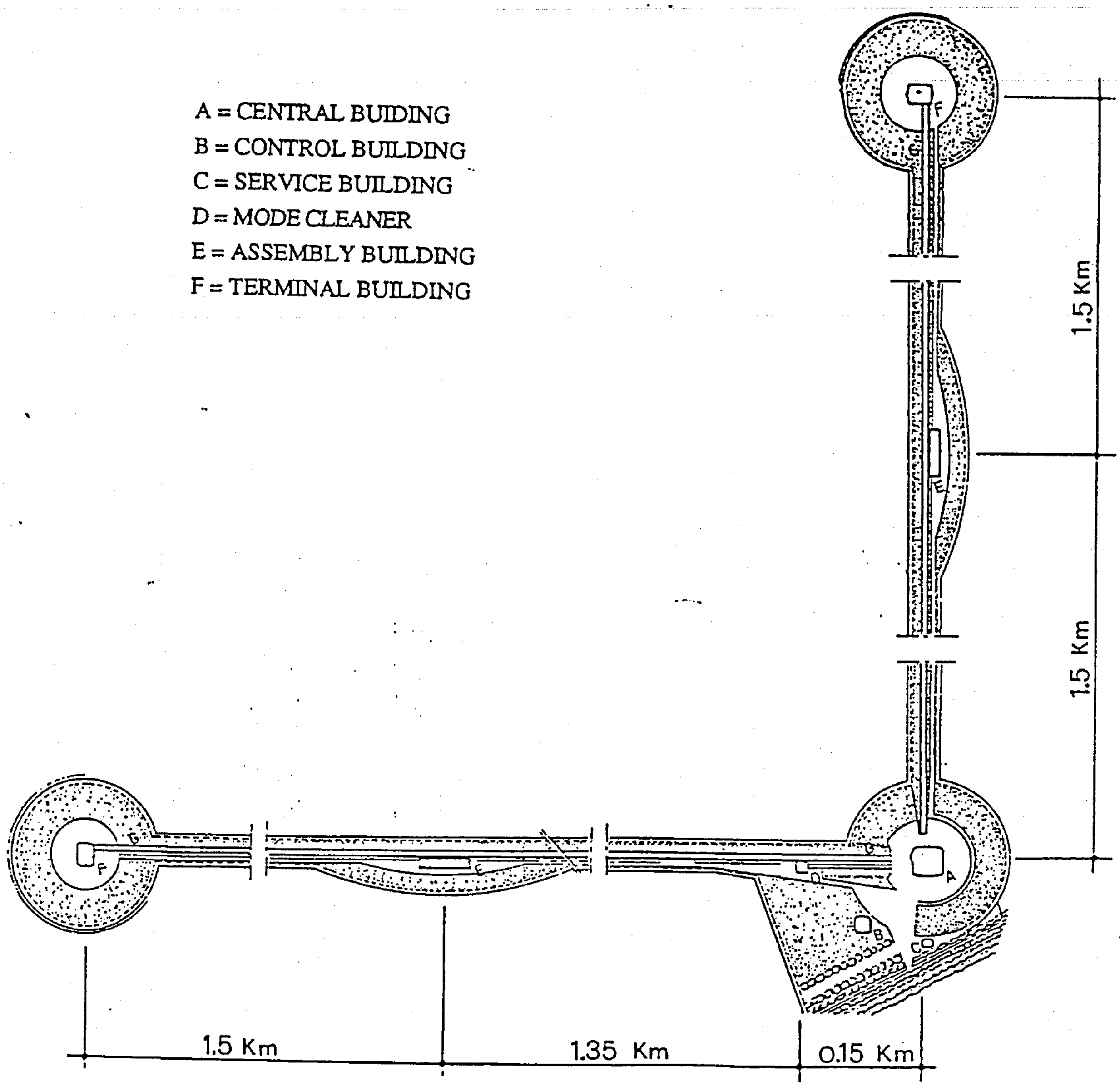

Fig. 2000.2

21. Central Area Buildings

21.1 "Central area buildings" function and concept

The "central area buildings" shall accommodate the towers, the pumping systems, the data acquisition system and the related equipment at the cross of the arms, providing two experimental halls, optic laboratories, assembly laboratories, data acquisition room, offices from which Virgowill be driven and data will be analyzed.

The "central building", at the crossing point of the two arms contains the main optical components, suspended to six independent AS chains, inside six large vertical vacuum tanks. Only the bottom part of a seventh tank will be installed, to have the possibility, in the future, to use the dual recycling technique; the installation of such an heavy object would be impossible later. A smaller building (mode cleaner building) contains the far mirror of the mode cleaner, also suspended in vacuum to a shorter suspension chain. In the "central building", inside appropriate rooms, are installed the lasers and part of the acquisition and control electronics.

The experimental halls are equipped with cranes to assemble or disassemble the vacuum tanks and the pendulum chains. They are controlled in temperature and humidity; the inner volume is kept in overpressure with respect to the outside and supplied only with filtered air, in order to be free of dust.

To avoid mechanical vibrations all equipment containing motors or moving parts (pumps, air conditioning, laser power supplies and cooling, etc.) will be mechanically isolated or confined well outside the experimental halls.

To avoid noises produced by human activity, the control room of the whole interferometer is located in a separate building (control building), 100 m apart from the central one, connected by a bunch of cables to the apparatus.

The foundations of the experimental halls (fig. 2100.2/a) consist of large drilled piles (ϕ 1200 and 30 m long) resting on the gravel layer. Such deep piles are necessary to guarantee the requested stability to inclination and not to avoid subsidence lowering. The piles support a strong concrete platform; on this platform rest the vacuum tanks. Under the main level there is a basement level, the "gallery", allowing to access the tanks bottom, where an aperture is located for optical equipment introduction; the gallery structure further contributes to the platform rigidity. The platform supports also the upper part of the experimental halls, composed by a very stiff and light steel structure enclosed between two walls, made of a metal sheet/thermal insulation sandwich. The hall structure has been designed in order to be free of high Q-factor mechanical resonance, below 7.5 Hz, since in this frequency range the SA performances become poor.

Most of the volume of the experimental halls is fully open, only a fraction of it, close to the outer walls, is subdivided in laboratories of standard height.

21.2 Central area buildings requirements

21.2.1 Central and M.C. building requirements

The experimental halls of the "central area buildings" (central building and mode cleaner building) have to satisfy the requirements figured out from the indications of the involved sub-system. They shall be characterized by :

- absence of high Q-factor mechanical resonance
- seismic noise less than $10^{-6}/\nu^2$ m $Hz^{-1/2}$

- controlled temperature inside the experimental halls : 22 ±2°C (TBC)
- controlled humidity inside the experimental halls : 55 ± 5%
- low dust level (overpressure 0.3 mbar)

In addition they shall provide :

- "Clean rooms" for Laser and Optic Laboratories
- a gallery for mirror installation
- a crane 5t (13000 mm minimum free distance from the floor)
- distance from the floor to the tube axis : 1100 mm
- relative displacement of super attenuator suspension points : less than 1 cm in 20 years (TBC)
- emergency generator unit
- UPS

21.2.2 Control building requirements

The control building has to satisfy the following requirements :

- contain a data acquisition room with cooling air and double floor
- contain a computer room
- contain a meeting room for minimum 50 people
- contain some offices
- have an emergency generator unit
- have UPS

21.3 Buildings and Equipment Description

21.3.1 The central building

This building covers an area of 26x30 m^2 and has a useful height of 15 m, to allow to lift up the upper parts of the vacuum tanks and to make accessible the pendulum chains. (figs. 2100.2).

The platform on which rest the vacuum tanks is stiffened by the double concrete wall constituting the perimeter of the main level (the level containing the axes of the interferometer).

Inside there are the gallery, in the basement (fig. 2100.2/a), and laboratories organized in three levels. Following the description of the site vertical profile, the gallery and the first level are underground; the first level is also called "main level" since it contains the plane defined by the interferometer beams, running at 1.1 m above the floor.

At the main level of the central building (fig. 2100.2/c) there are seven towers arranged as a cross, with the beam splitter tower at the center. In the South part of this floor, there are the clean rooms, one for the laser installation and the other for the optical parts assembly. A staircase and an aperture in the floor allow to bring to the gallery (fig. 2100.2/b) clean optical parts, which will be installed, from below, in the towers. For this purpose, also the gallery is a clean room, supplied with clean air through the towers.

At the main level there will be also : the large valves connecting the towers to the arm tubes, the large primary pumps for the arm tubes and the laboratory to assemble the SA chains. Inside two volumes protruding out of the rectangular shape of the building, there are the clean air generators, an optical and mechanical parts washing chain and the air conditioning machinery.

In the floor, along both sides of the tower cross, there are cable passages for power and service cables. Signal cables, coming out from the towers at 2.5 m height, reach the read out electronics, at the upper floor, on aerial cable trays.

At the large valves location, suitable apertures are available for tower bases and valves installation. The connection between the central building and the tunnels is made through transition rooms containing auxiliary equipment for the large valves; the transition room toward the West arm makes the connection also to the mode cleaner tunnel; it is therefore quite large and will be used for storage.

The personnel and truck entrances are located at the upper level (fig. 2100.2/d), coincident with the outer ground level. The truck entrance is closed and its removable roof will be opened to access the load with the crane, only after stopping the truck engine and waiting for dust deposition. People coming in through the personnel entrance will either stay in the reception and visiting gallery zone or enter the laboratory zone after changing shoes and dress.

The data acquisition room is located at this level; in this way the signal cables come out of the towers at about the same height of the double floor of this room. Through the double floor comes also the cooling air flow for the electronics racks. On this level there are also the electronic workshop and the toilets.

The upper and last level of the central building has a surface of about 150 m^2, divided in seven offices.

Five ton cranes will be available to assemble or disassemble the vacuum tanks and the pendulum chains; movable rented cranes will be used for the installation of the base of the tank since these pieces have a weight much larger (up to 20 ton) than all other pieces. All the inner surfaces accessible by the crane will be used as storage space for parts of the towers and other equipment.

21.3.2 The mode cleaner building

This building covers an area of 8x10 m^2 (fig. 2100.3). It is only 10 m high since it contains a small tower with a simpler SA. The tower position can be adjusted by +/-2.0 m along the mode cleaner beam.

Very little assembly space is required, since this hall is located only 140 m apart from the central hall, where the necessary technical facilities are available.

Five ton cranes will be available to assemble or disassemble the vacuum tanks and the pendulum chains; movable rented cranes will be used for the installation of the base of the tank.

21.3.3 The mode cleaner tunnel

This tunnel (fig. 2100.4) is parallel to the West arm and has a smaller cross-section with respect to that of the interferometer tunnel, since it contains a much smaller vacuum pipe (0.3 m diameter) and , being only 140 m long, does not contain pumps.

It is founded on piles, 32 cm in diameter and 26 m long, driven in the ground. Every 15 m there are two piles joined by a rectangular cap. The tunnel floor and walls are realized with a single concrete beam resting on the caps. The tunnel cover is a light one, made of sandwich plates (metal/insulation/metal).

21.3.4 The control building

This building (fig. 2100.5), located in the central zone, has a surface of 280 m^2 and is two floor high.

At ground floor there are : a 50 people meeting room, the guardian room, some offices and a small cafeteria. At first floor there are : the control room of the whole experiment, the computer room and some office space for people in shift.

Control and computer room are equipped with a double floor for cable passage and cooling air flowing to the electronics racks.

21.3.5 The technical building

The technical building (fig. 2100.6) contains the electrical power station and the climatisation plant for the central buildings. It is situated at the border of the central zone, in order to be easily reached for inspection and fuel supply. The building is divided in two halves, with two floors each. It contains : at the ground floor, the connection to the 15 kV power line, the diesel generator and the hot water generator; at the first floor, the transformers, the Uninterrupted Power Supply (UPS) and the water pumping units; on the roof, the chilled water generators. The water at the proper temperature, according to the season, is brought via insulated piping to the heat exchangers of the different buildings of the central zone.

21.3.6 Electric power supply

All the Virgo electrical network will be connected to the italian electricity company (ENEL) medium voltage network (15 kV) by a station located in the technical building. The total installed power will be 1100 kW and includes : illumination (inner and outer), air conditioning, white rooms, cranes, workshops, vacuum pumps, electronics and computers. A distribution line will deliver through five local transformers low voltage power (380/220 VAC) to the final panels.

In the central area will be installed a 600 kW transformer. Auxiliary power supply are foreseen for short and long break-downs. The Uninterrupted Power Supply (UPS) for fast interventions to keep working computers and electronics (150 kW, lasting 15 minutes) and diesel generators (IPS) for long term emergency power supply (250 kW).

Only the towers (TBC) will be connected to the general power supply to be baked-out (30 kW each).

21.3.7 Service fluids

There is one water circuit, for bathrooms, cleaning and general purposes. Bathrooms with showers will be sufficient for a 20 working persons occupancy in the central and the control building; for 10 persons in all other buildings. During construction phase, auxiliary services will be available in trailers.

Cooling water, for laser and vacuum pumps, will be produced locally in the experimental halls with closed circuit cooling systems.

Compressed air will be available only for vacuum valves actuation and for tool powering. In principle compressed air for cleaning purposes will not be allowed, to avoid dust propagation. Suitably large air reservoirs will be provided, in order to provide buffers for emergencies and to let the compressors work at long intervals and at controlled times.

An integrate vacuum cleaner system could be installed in each experimental halls (TBC).

21.3.8 Control cables

Signals coming from every part of the set-up will converge, along the tunnels, in the central building for local use and/or to be sent to the control building. It is foreseen to have a few hundred cables or fiber optics from each arm, demanding for a cross-section of the order of 100-200 cm^2 on the cable trays.

The infrastructure will provide the dedicated cable trays located at the right distance from the power cable ones. In addition, the twisted pair cables, but not their installation, will be provided.

21.4 Interface

The "central area buildings" sub-system interfaces with many other sub-systems, due to its function to accommodate many experimental facilities of Virgo.

In particular it interfaces with :

- tower sub-system mainly for the tower installation, the hall temperature, tower operation (power supply, cooling water, compressed air);
- super-attenuator sub-system for the filters washing machine, the S.A. installation, the stability of the suspension point, the S.A. operation;
- pumping sub-system for the installation and operation of tower pumping units, tube rough pumping and venting (power supply, cooling water, compressed air);
- tube sub-system for tube terminal parts and related large vacuum valves;
- electronics sub-system, for the accommodation of computers and cabling necessary to drive Virgo and to record the experimental data (two different areas); in particular the twisted pair cables will be furnished by infrastructure but the installation is in charge of the electronic sub-system;
- clean areas sub-system for the clean areas which will be lodged in the central building;
- tunnels and terminal buldings sub-system, regarding the tunnel linking to the central building.

FIGURE CAPTIONS

2100.1	Arrangement of central area on Cascina site
2100.2	Central experimental hall; a - vertical cross-section; b - gallery (second underground); c - main level (first underground); d - ground level
2100.3	Mode-cleaner building
2100.4	Mode cleaner tunnel cross-section
2100.5	Control building; a - ground floor; b - first floor
2100.6	Technical building; a - ground floor; b - first floor

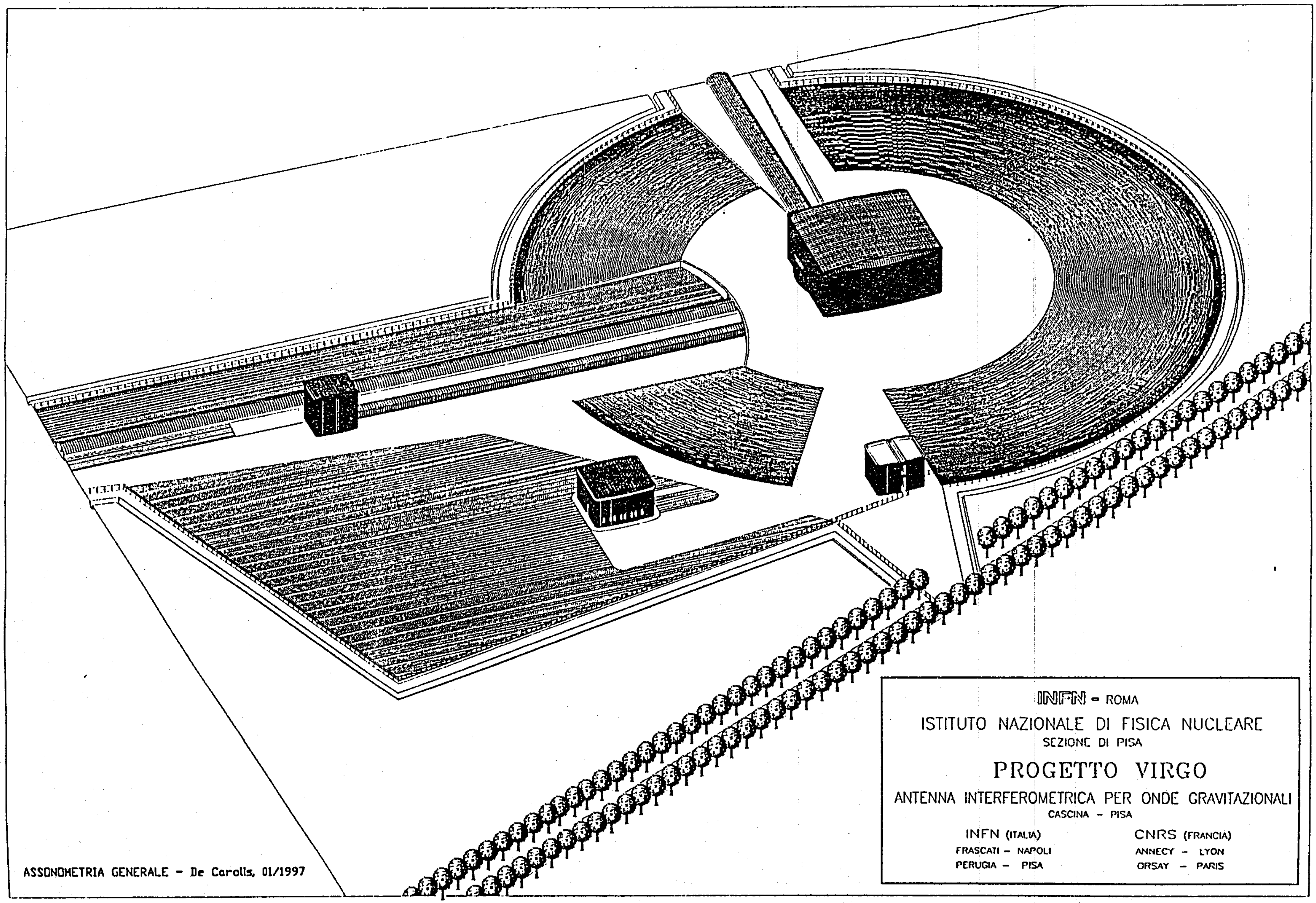
INFN - ROMA
ISTITUTO NAZIONALE DI FISICA NUCLEARE
SEZIONE DI PISA
PROGETTO VIRGO
ANTENNA INTERFEROMETRICA PER ONDE GRAVITAZIONALI
CASCINA - PISA
INFN (ITALIA)
FRASCATI - NAPOLI
PERUGIA - PISA
CNRS (FRANCIA)
ANNECY - LYON
ORSAY - PARIS
ASSONOMETRIA GENERALE - De Carolis, 01/1997

Fig. 2100.1

CENTRAL BUILDING

INFN Pisa, De Carolis 01/97

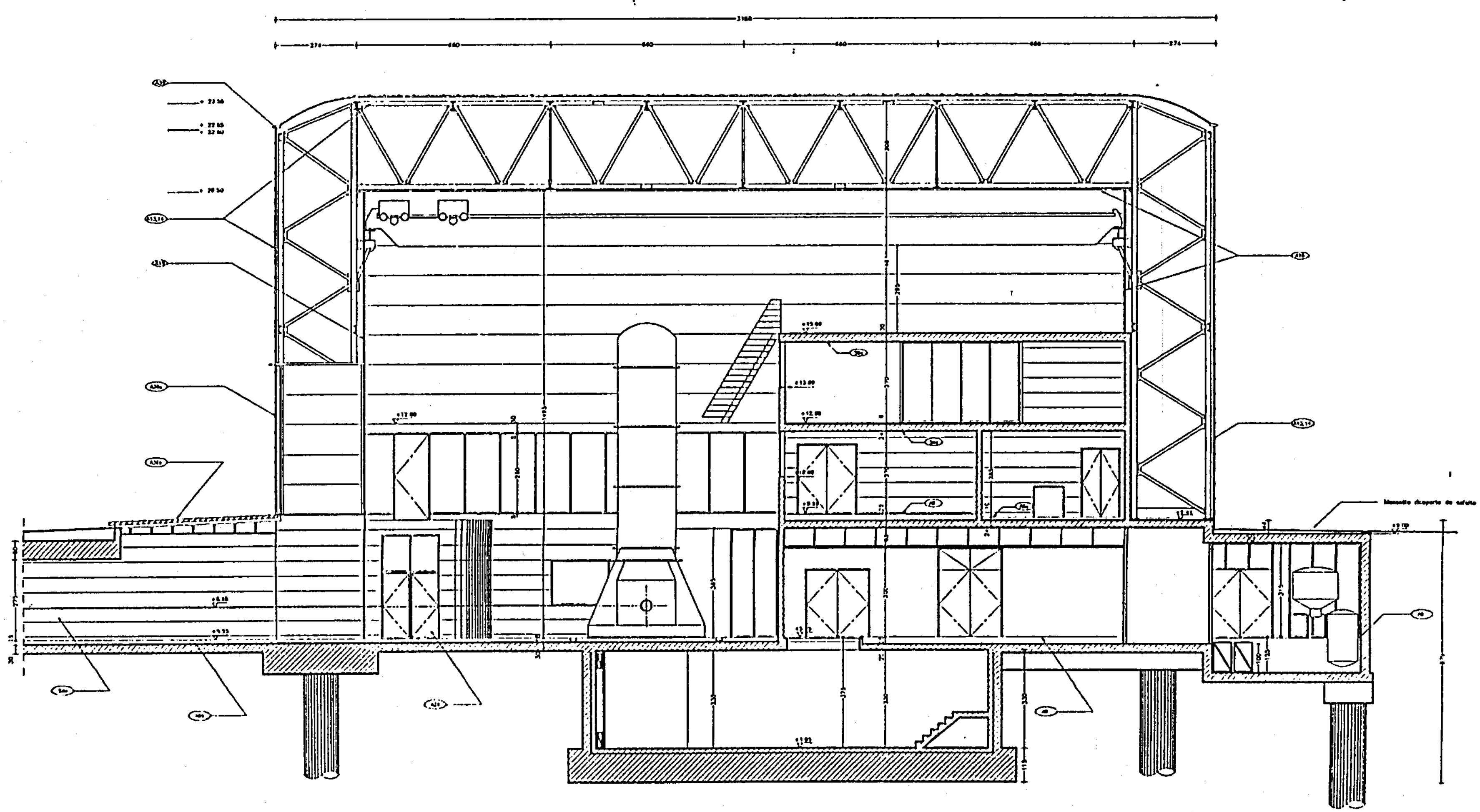

Fig. 2100.2/a

INFN Pisa, De Carolis 01/97

CENTRAL BUILDING

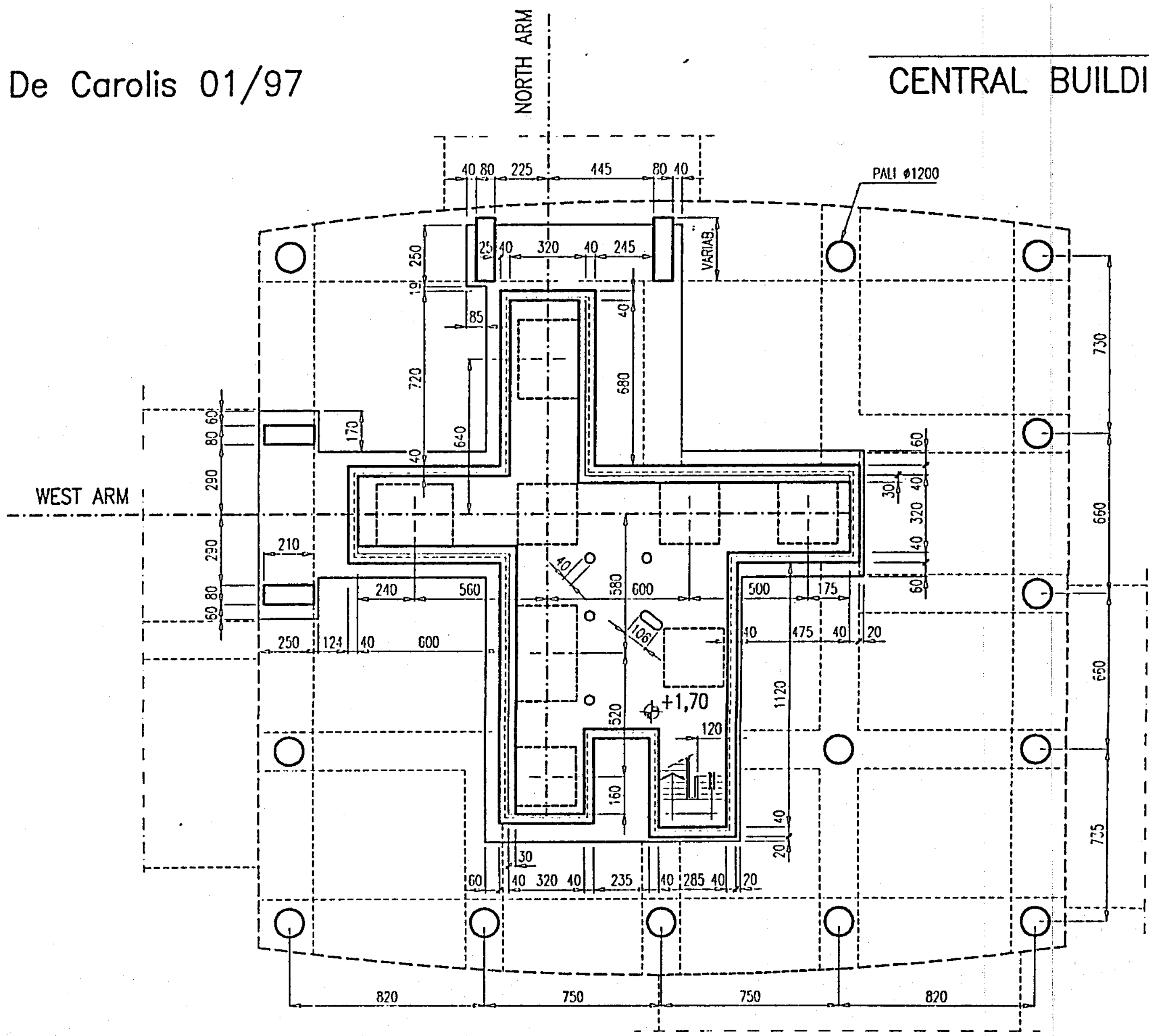

GALLERY (SECOND UNDERGROUND)

Fig. 2100.2/b

INFN Pisa, De Carolis 01/97

CENTRAL BUILDING

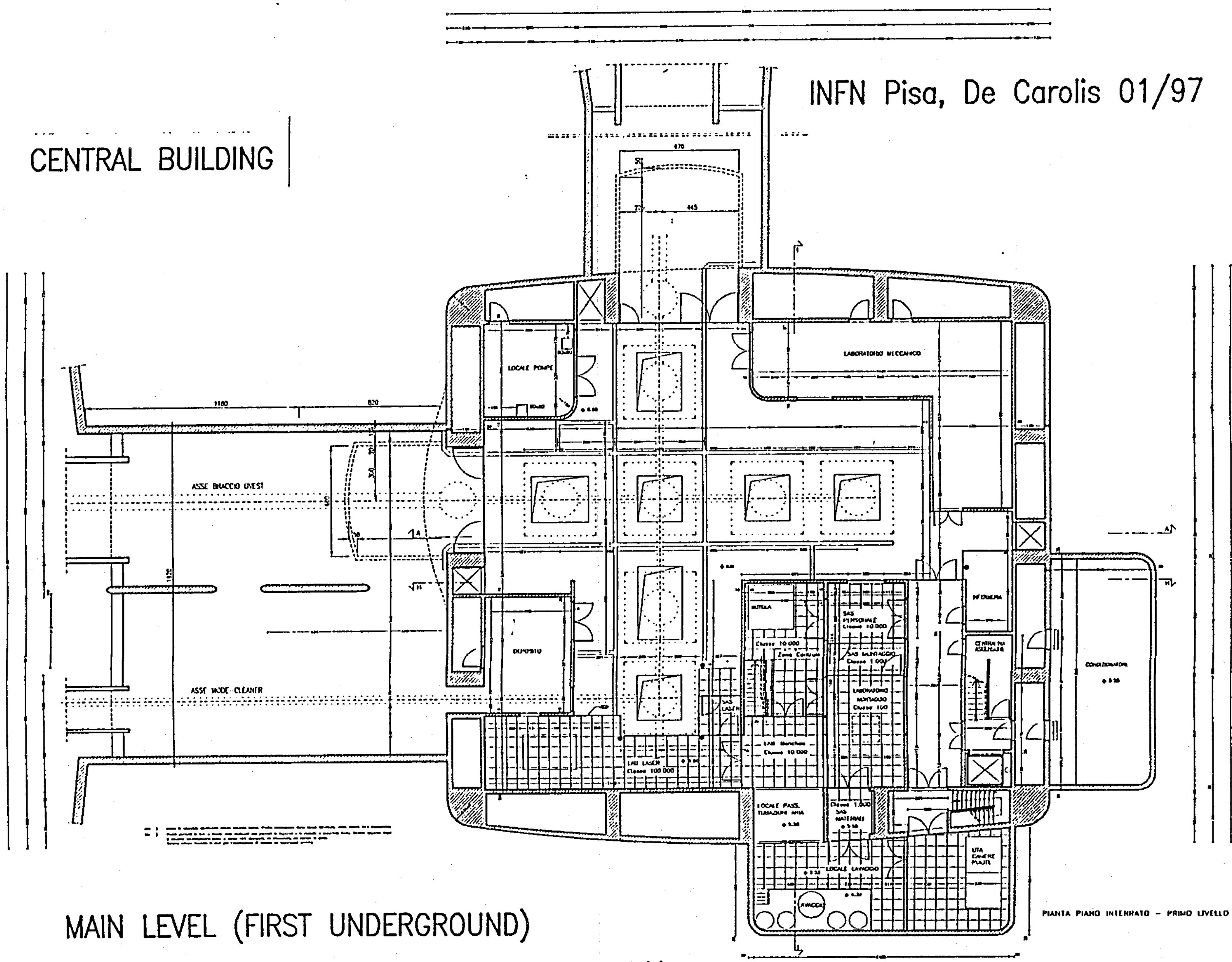

MAIN LEVEL (FIRST UNDERGROUND)

Fig. 2100.2/c

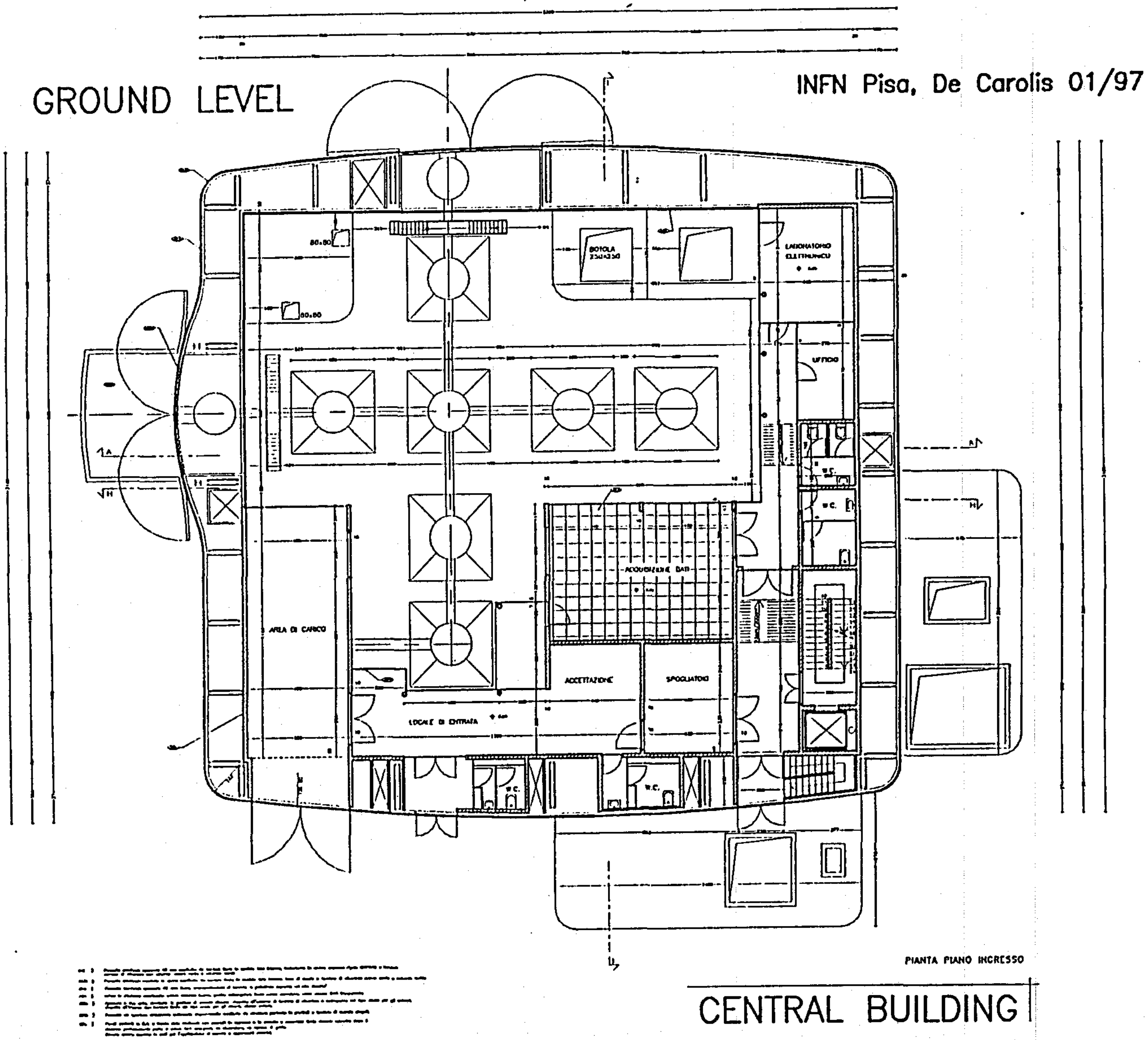
GROUND LEVEL
INFN Pisa, De Carolis 01/97
PIANTA PIANO INGRESSO
CENTRAL BUILDING

Fig. 2100.2/d

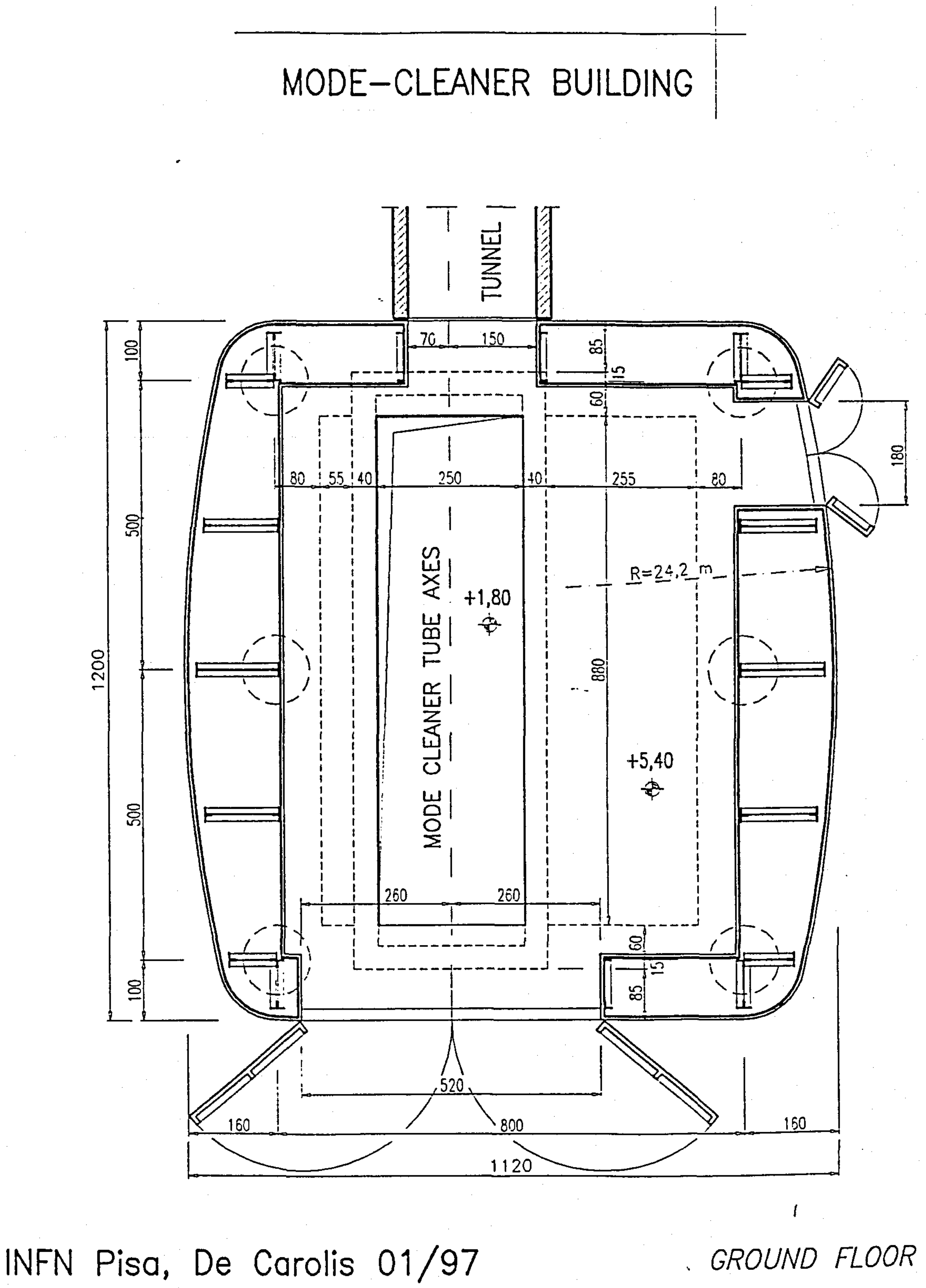
MODE-CLEANER BUILDING
TUNNEL
70
150
85
15
60
80
55
40
250
40
255
80
180
R=24,2 m
MODE CLEANER TUBE AXES
+1,80
880
+5,40
260
260
60
15
85
100
500
1200
500
100
520
160
800
160
1120
INFN Pisa, De Carolis 01/97
GROUND FLOOR

Fig. 2100.3

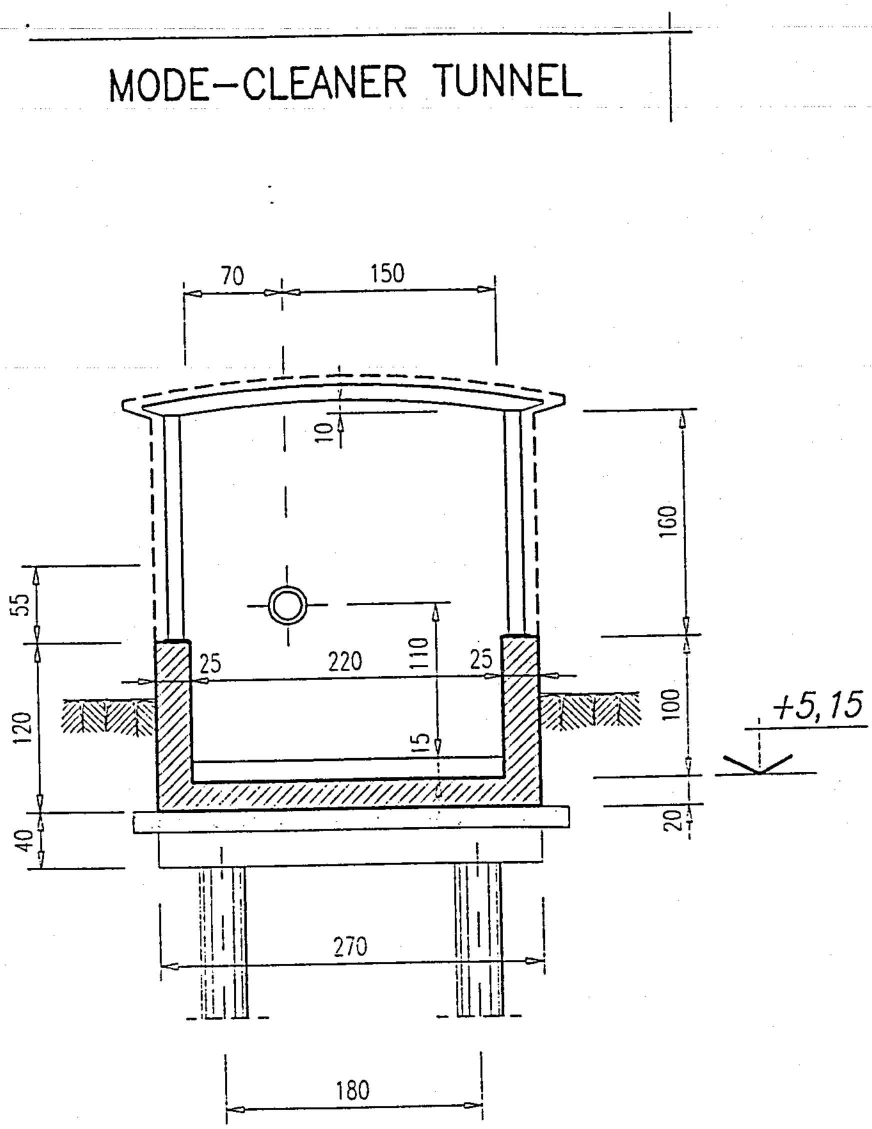

MODE–CLEANER TUNNEL
70
150
10
160
55
25
220
110
25
120
100
+5,15
15
20
40
270
180

Fig. 2100.4

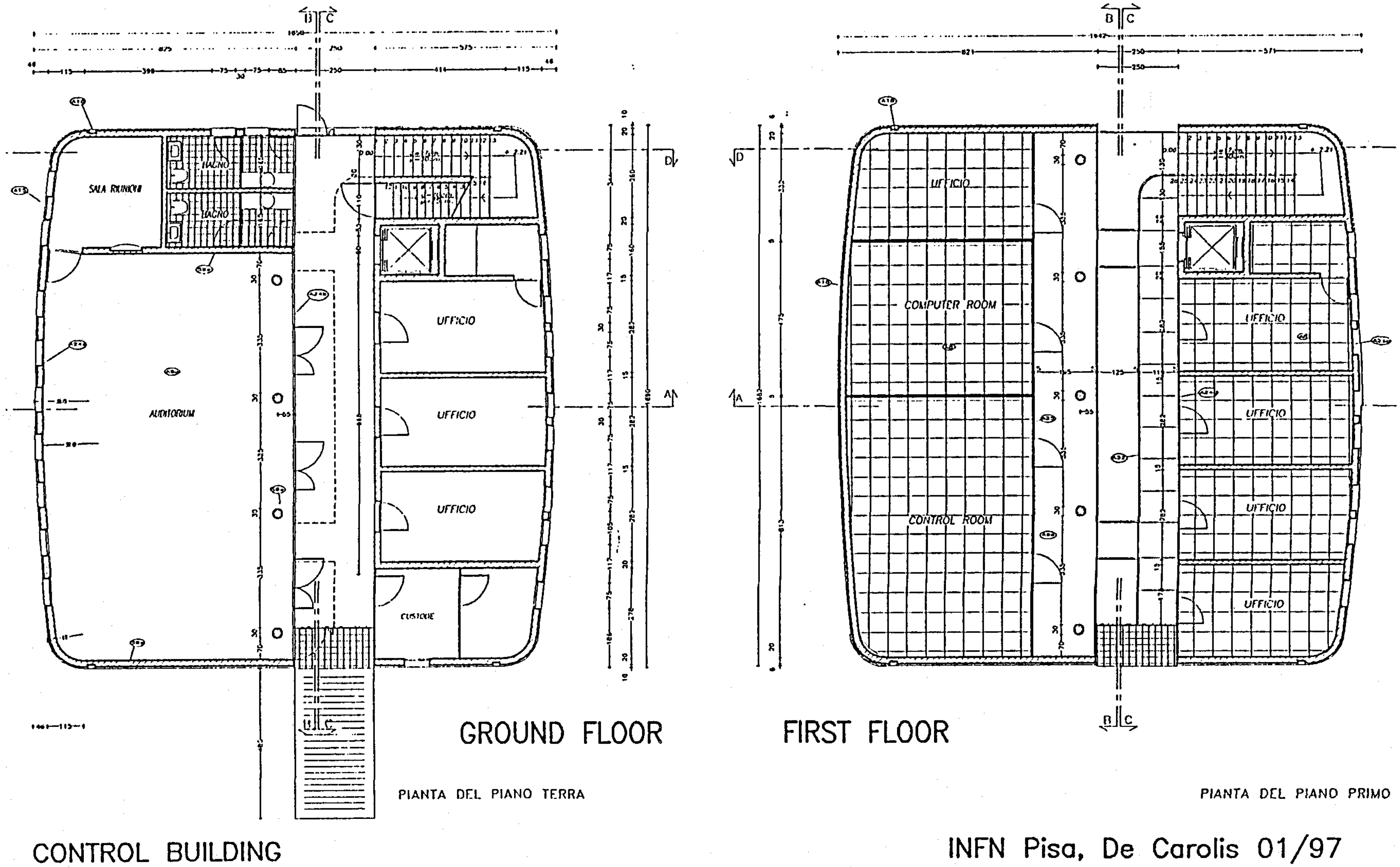
SALA RIUNIONI
BAGNO
BAGNO
AUDITORIUM
UFFICIO
UFFICIO
UFFICIO
CUSTODE
GROUND FLOOR
PIANTA DEL PIANO TERRA
UFFICIO
COMPUTER ROOM
CONTROL ROOM
UFFICIO
UFFICIO
UFFICIO
UFFICIO
FIRST FLOOR
PIANTA DEL PIANO PRIMO
CONTROL BUILDING
INFN Pisa, De Carolis 01/97

Fig. 2100.5

GROUND PLOOR

FIRST FLOOR

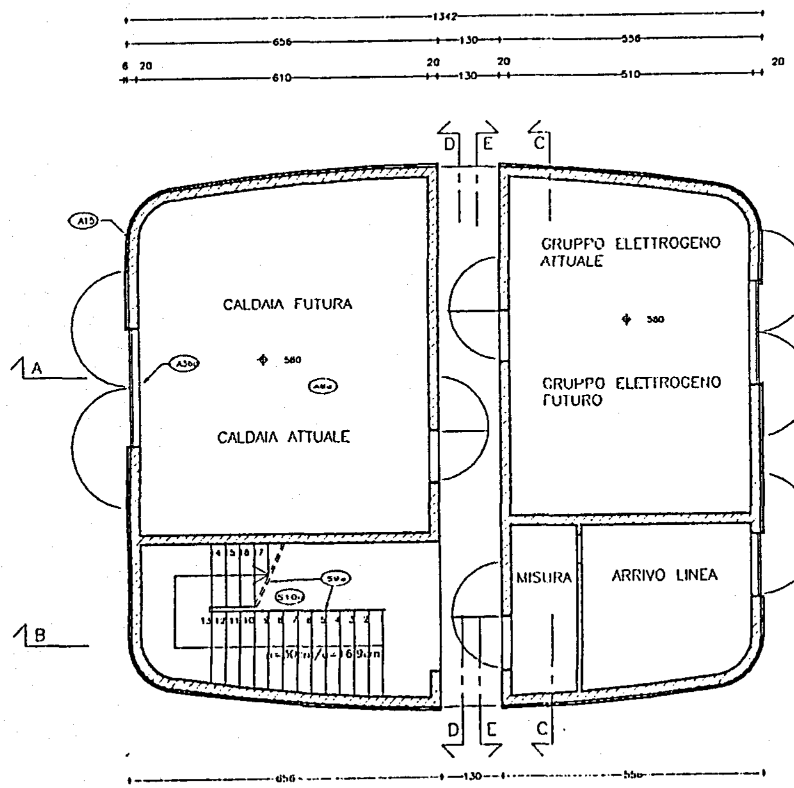

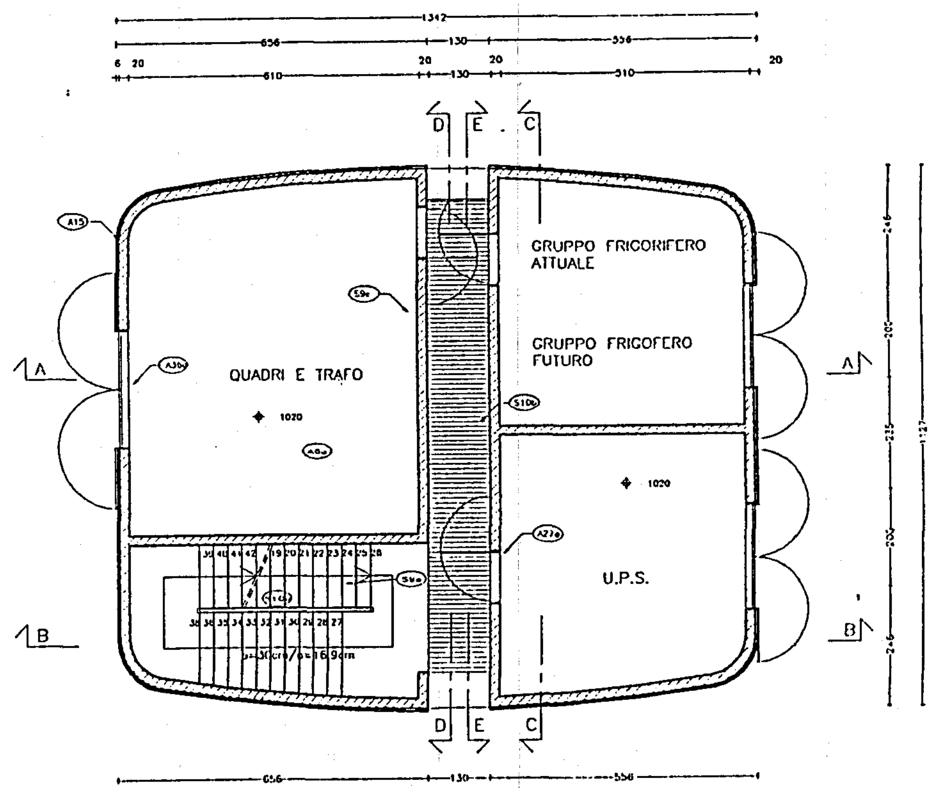

CONTROL BUILDING

INFN Pisa, De Carolis 01/97

Fig. 2100.6

22. Clean Areas

22.1 Clean areas function and concept

The clean areas of Virgo are the rooms, plants and all the necessary equipment which shall allow to assembly and to install the clean optics in the correct environment. The clean installations can be roughly divided in two types : the clean laboratories and the systems to provide filtered air to the towers during the installation of the clean optics. Both are located inside the buildings containing the towers and will be realized following the results obtained in the prototype installed in LAPP. During integration and operation the cleanliness, temperature, humidity and pressure of each room will be strictly controlled. The laboratories access will be limited to the personnel in charge of specific operations. During scientific operation the clean rooms may be shut down if no intervention on the payloads is foreseen.

22.2 Clean areas requirements

The clean areas have to satisfy the requirements schematically listed below.

- General requirements :
  - -avoid mechanical vibration sources
  - -avoid acoustic noise sources

- Class of cleanliness :

- Galleries :	not classified
- Optic laboratory :	100 operational
- Laser laboratory	100.000 at rest
- Benches laboratory	10.000 at rest (below the filter)
- Towers	100

- Temperature

- Galleries :	not classified
- Optic laboratory :	20° C
- Laser laboratory	22° C
- Benches laboratory	22° C
- Towers	20° C

- Humidity

- Galleries :	not classified
- laboratories	52 ± 3%
- towers	52 ± 3%

22.3 Clean areas description

The "clean areas" consist of 5 plants, complete of filters, conditioning system, electrical power, etc. They are :

- the laboratories plant in the central building

- the towers and gallery plant in the central building
- the mode cleaner tower and gallery plant
- the North terminal tower and gallery plant
- the West terminal tower and gallery plant

Each of them has the cleanliness class listed in the requirements part. The adopted technology to realize them is a standard one consisting of lining the walls with proper materials, using double floor and roof, filtering and recycling air, controlling temperature, humidity and overpressure.

The accessories as dresses, special shoes, gloves, etc. are part of the sub-system.

22.3.1 The laboratories in the central building

This plant includes the clean optics assembly laboratories, the laser laboratory, the benches preparation laboratory, the washing facility room (fig. 2200.1). The laboratories will be accessed through two different intermediate rooms (SAS) respectively for people and materials. The laser laboratory will be accessed from the tower hall; an additional door is foreseen in correspondence of the benches laboratory. The optic laboratory has an additional SAS for personnel. The tower gallery is accessed through a staircase and a trapdoor, respectively for the personnel and the materials, located in the central zone of this group. A crane to lift up and down the materials is located near to the trapdoor. Next to material SAS there is a washing facility room. The water cooling and heating units are installed in the technical building, in order to avoid the mechanical vibrations and acoustic noise in the central building. Only the air treatment unit is located in the central building, next to the laboratories.

22.3.2 The towers and gallery plant in the central building

This plant provides the clean air to the towers and the below gallery. An air flow of 1200 m^3h^{-1} will be provided to each tower via a ϕ 200 mm port. In the gallery, an additional air flow of 1200 m^3h^{-1} will be fed horizontally to each tank access. The gallery will be equipped as a clean area but not classified. During the optics installation, the tank access will be confined with a tent. Not more than two towers will be fed contemporary.

The water cooling and heating units are the same used for the clean laboratories plant. The air treatment unit is locate inside the tower hall, upon the "pumping storage room". Both flows will be extracted at the end of gallery and than recycled.

22.3.3 The towers and gallery plant in the mode cleaner building

This plant will be used only for the mode cleaner tower and is completely independent. It will provide only an air flow of 1200 m^3h^{-1} to the tower via a ϕ 200 mm port. The air flow will be extracted via the gallery and then recycled. Since this equipment is small, it will completely installed in the mode cleaner building. The gallery will be equipped as a clean area but not classified and accessed via a movable SAS, located on the gallery, to allow the tower displacement.

22.3.4 The towers and gallery plant in the terminal buildings

This plant is essentially of the same type described in 2200.3.2, but will provide only one tower.

In addition only one small clean laboratory in each terminal building is foreseen (TBC). In such small installation the same water cooling and heating units will supply the air treatment units for the tower and the clean laboratory.

22.4 Clean areas interface

The interfaces essentially concerns the central area building, in which the clean areas will be located, the laser sub-system for the laser operation, tower sub-system for the clean optics installation and the network sub-system for the communication.

FIGURE CAPTIONS

2200.1 Clean laboratories in the Central Building

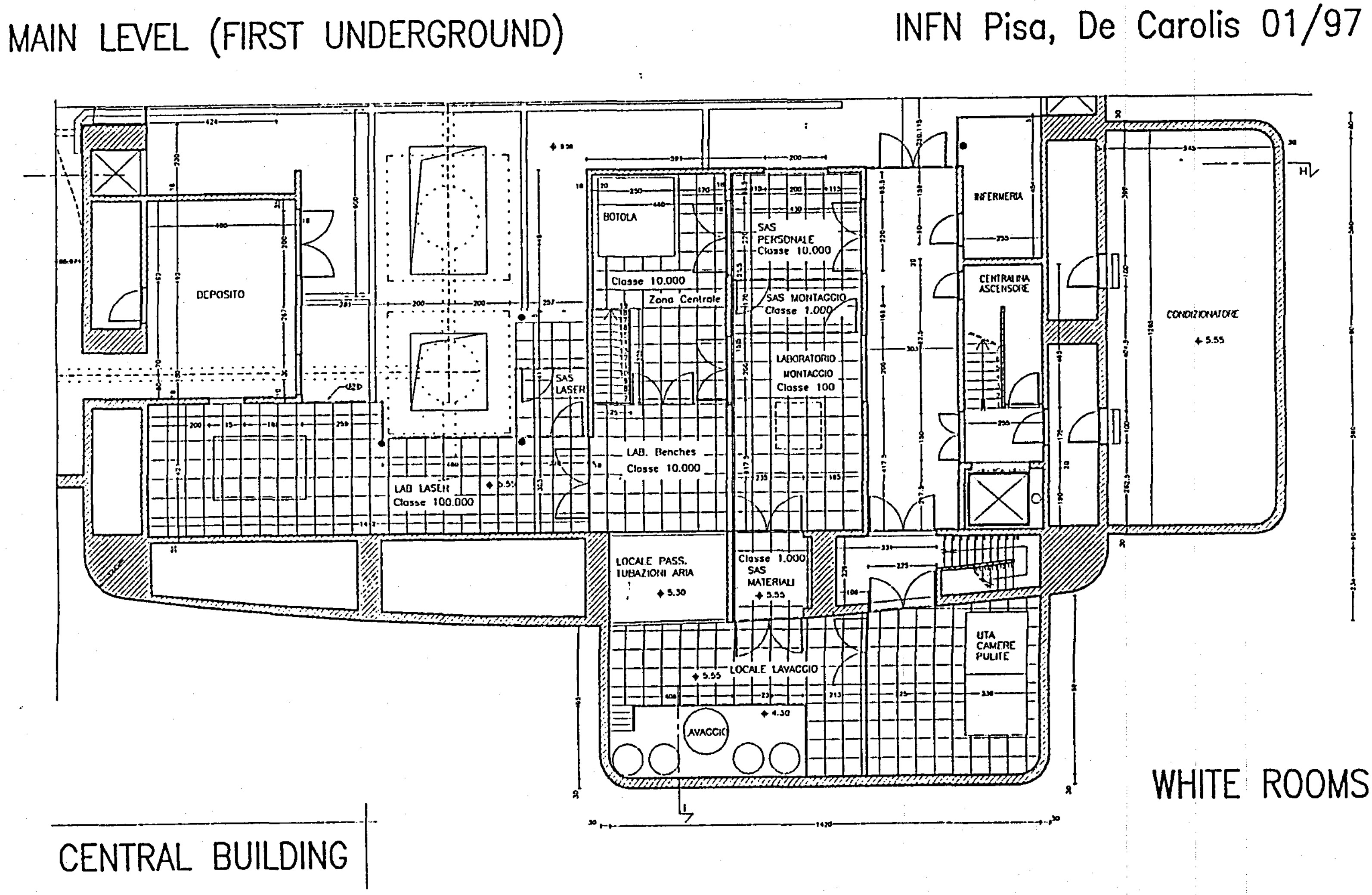
MAIN LEVEL (FIRST UNDERGROUND)
INFN Pisa, De Carolis 01/97
DEPOSITO
BOTOLA
Classe 10.000
Zona Centrale
SAS PERSONALE Classe 10.000
SAS MONTAGGIO Classe 1.000
LABORATORIO MONTAGGIO Classe 100
INFERMERIA
CENTRALINA ASCENSORE
CONDIZIONATORE
SAS LASER
LAB LASER Classe 100.000
LAB. Benches Classe 10.000
LOCALE PASS. TUBAZIONI ARIA
Classe 1.000 SAS MATERIALI
LOCALE LAVAGGIO
UTA CAMERE PULITE
WHITE ROOMS
CENTRAL BUILDING

Fig. 2200.1

23. Arms & terminal buildings

23.1 "Arms & terminal buidings" function and concept

The 1.2 m diameter vacuum pipes, containing the beams of the interferometer, will be installed inside a protection structure, the "tunnel", containing also all the cables connecting the central building with the terminal ones. The beam tube axis is at 1.45 m above tunnel floor.

Taking into account the nature of the ground, as described in the geology section, the tunnel could lay directly on the ground, since the expected subsidence is lower than the maximum tolerable displacement. In order to obtain perfectly straight arms and the correct slopes from the tunnel toward the sides of the land strip (this is necessary to collect water into the lateral drain channels and to improve the environmental aspect), the top ground layer, 1-2 m thick, will be rearranged. This could produce local ground disuniformity or compression, demanding deeper foundation resting on undisturbed ground layers. All the tube supports will be positioned directly on the tunnel foundation points. The movements of several points of the tunnels will be monitored in order to plan, if necessary, the re-alignment of the tube. Global rigid displacements preserving the complanarity of the apparatus will be neglected. The position of three points, necessary to define the directions and the lengths of the interferometer arms, can be easily determined with "standard" techniques, with a 1 cm error in three coordinates; this is largely sufficient for VIRGO. GPS systems, allowing relative precision below 1 cm, will be used for all alignment and positioning purposes.

The tunnels connect the central building with the terminal buildings, which are located at the end of each arm and contain the terminal towers. They are similar to the central building, but reduced in surface, since each of them contains only one tower. To avoid mechanical vibrations all equipment containing motors or moving parts (pumps, air conditioning, laser power supplies and cooling, etc.) will be mechanically isolated or confined well outside the buildings. The foundations have to guarantee the requested stability to inclination and not to avoid subsidence lowering.

At the middle of each arm a building dedicated to the tube assembly is located.

23.2 Arms and terminal buildings requirements

23.2.1 Tunnel requirements

The tunnel requirements, figured out from the indications of the involved sub-system, are schematically listed below :

- location as far as possible away from main roads, trains, etc.;
- distance from farm houses more than 50 m
- vertical displacement of any pipe cross section :
  - less than 0.5 cm per month
  - less than 1 cm per year
  - less than 15 cm (relative) in 20 years
- lateral displacement less than ± 5 cm total (in 20 years)
- correction of earth curvature
- alignment of tunnel floor better than 1 cm on 15 m
- minimum inner width 5m (TBC)
- minimum inner height 3.0 m (TBC)
- foundations every 15 m

- doors to enter every 300 m (TBC) in correspondence of the pumping stations (TBC)
- tube axis distance from the floor 1450 mm;
- aerators to evacuate 0.4 kW per meter of pipe (TBC)
- supply of 10 kW - 380 Vac each 300m
- supply of 10 kW - 220 Vac each 300m
- service road along the tunnels
- minimum height of bridges 3500 mm (TBC)

23.2.2 Terminal building requirements

The terminal building requirements, figured out from the indications of the involved sub-systems, are schematically listed below :

- Same general requirements as the Central Building
- Independent emergency electrical generator unit
- Independent UPS

23.2.3 Assembly building requirements

The assembly building requirements, figured out from the indications of the involved sub-system, are schematically listed below :

- allow the storage of some insulated tube modules ready for installation;
- accommodate a test bench for the tube modules;
- be connected to the tunnel;
- provide for the tube modules an easy access to the tunnel;
- allow the storage of tube supports, vacuum pumps and accessories;
- lodge an emergency electrical generator
- have an emergency generator unit

23.3 Arms & Terminal Buildings Description

23.3.1 The interferometer tunnels

The tunnel, designed above ground, has the cross-section shown in figure 2300.1, with an inner height of 3.0 m (TBC) and an inner width of 5.0 m (TBC). These dimensions are needed for installation and replacement of the vacuum pipe elements (as described in the relevant section), of the relative pumps and of the tools necessary for baffle installation. The passage for a man has to be easily allowed at any moment, for survey and maintenance purposes.

Hence, every 15 m, there are two piles, 32 cm in diameter and 24 m deep, joined by a single rectangular capital. The tunnel floor and walls are made by a single concrete beam, poured continuously on site, resting on the capitals.

The designed structure does not suffer resonance problems, due to the great dumping effect of the ground. This avoids vibrations that, transferred to the pipe, could modulate the cavity beams, through the diffused light phenomenon. Residual oscillations of the structure have, anyway, little relevance, since the tube supports rest on the capitals, directly connected to the piles, hence to the ground.

The tunnel floor will be aligned to better than 1 cm on 15 m, correcting for earth curvature. The floor will be smooth enough to allow the displacement of pipe elements from the assembly halls to the installation point, using suitable trolleys, guided by rails.

Doors to enter the tunnel are foreseen every 300 m (TBC), in correspondence of the pumping stations. On the wall opposite to doors there are cable trays for power and control cables and fluids.

The tunnel cover is a light one, made of curved sandwich plates (metal/insulation/metal) similar to those used for the outer walls of the buildings.

Aerators will be installed on tunnels roof, to evacuate the heat produced during vacuum pipe bake-out.

23.3.2 The terminal buildings

At the far ends of the two arms, two smaller experimental halls contain the end mirrors of the interferometer inside their vertical vacuum tanks.

The terminal buildings (fig. 2300.2) have a structure very similar to the central one, but reduced in surface (15x22 m^2) because they contain only one tower; the height is the same since the terminal towers contain a full size SA chain. Inside there is one inner floor, equipped with a clean laboratory, and a gallery. The temperature is controlled to +/- 2 °C and humidity is kept at 55 +/-5%. The inner volume is kept in overpressure with respect to the outside and supplied only with filtered air, in order to be free of dust.

Five ton cranes will be available to assemble or disassemble the vacuum tanks and the pendulum chains; movable rented cranes will be used for the installation of the base of the tank.

23.3.3 The pipe assembly halls

A vacuum pipe assembly hall will be built in the middle of each arm of the interferometer. The covered area will be 20x50 m^2 (TBC), with an useful height of 8 m. Trucks coming from the pipe factory will be unloaded in the delivery zone and the incoming vacuum pipe elements will be stored in the storage area (fig. 2300.3).

The preparation zone is a clean area where the pipe elements will be prepared for installation and mounted on suitable trolleys to be brought in position, along the tunnel.

One 5 ton crane will serve the delivery and preparation zones.

23.3.4 Electric power supply

The electrical power distribution along the arms will be achieved with two separate networks : one for installation and normal operation and one for bake-out of the vacuum system (TBD).

The medium voltage network (15 kV) will be connected to the technical building in the central area. A distribution line will deliver, through local transformers, 100 kW in each of the tube assembly zones and 150 kW in each of the terminal zones.

The total installed power includes : illumination (inner and outer), air conditioning, white rooms, cranes, workshops, vacuum pumps, electronics and computers.

An emergency generator unit (IPS) is foreseen for terminal and assembly buildings. The Uninterrupted Power Supply (UPS), for fast interventions to keep working computers and electronics, is foreseen only in the terminal buildings.

23.3.5 Service fluids

From the central area the water will be sent to the assembly building and to the terminal buildings. There will be one water circuit for bathrooms and cleaning purposes. Toilets and showers will be sufficient for 20 people for the assembly hall and 5 people in the terminal buildings. During construction phase, auxiliary services may be made available in trailers if necessary.

Cooling water, for vacuum pumps, will be produced locally in the terminal buildings and tunnels with closed circuit cooling systems.

In the terminal buildings compressed air will be available only for vacuum valves actuation and for tool powering. In the terminal buildings a suitable air reservoirs will be provided, in order to provide buffers for emergencies and to let the compressors work at long intervals and at controlled times.

In the assembly building compressed air will be available for many purposes.

23.3.6 Control cables

Signals coming from terminal buildings will converge, along the tunnels, in the central area. It is foreseen to have a few hundred cables or fiber optics from each arm, demanding for a cross-section of the order of 100-200 cm2 on the cable trays.

The infrastructure will provide the dedicated cable trays located at the right distance from the power cable ones.

23.3.7 Service road

A service road, 4 m wide, will allow displacement of cars and trucks along the interferometer. The road will become wider in correspondence of the tunnel accesses and around the buildings, to allow parking and truck crossing.

The whole VIRGO area will be closed by a fence and surrounded by a drain channel in order to collect water and to avoid any submersion of adjacent fields. To allow the maintenance of the drain channels there will be, between the fence and the drain channels (fig. 2300.4), a land strip 6 m large along each side of the arms.

23.3.8 Bridges

To allow the public paved roads to overcome the interferometer, two "large" bridges will be built.

In addition, to satisfy the prescription of "Comune di Cascina", three bridges on unpaved country lanes will be built too.

All the bridges have the similar structure. For economical and environmental reasons, the foreseen free distance from the service road is 3.5 m (fig. 2300.4).

23.4 Interface

The arms & terminal buildings interfaces are schematically below summarized :

- tube sub-system for the tube installation, operation, maintenance and survey;
- tube sub-system for the tube bake out;
- pumping sub-system for the pumps installation and electrical supply;
- central area buildings sub-system for the tunnel connection and alignment with the central area;
- tower sub-system mainly for the terminal tower installation and operation (power supply, cooling water, compressed air), the terminal building conditionings;
- super-attenuator sub-system for S.A. installation, stability of the suspension point, S.A. operation in the terminal buildings;
- pumping sub-system for the installation and operation of terminal towers pumping units;
- large vacuum valves sub-system for valves accomadation in the terminal buildings;
- electronic sub-system for computers and cabling accommodation in the terminal buildings and communication network installation.
- clean areas sub system for clean areas lodging in the terminal buildings.

FIGURE CAPTIONS

LONGITUDINAL SECTION

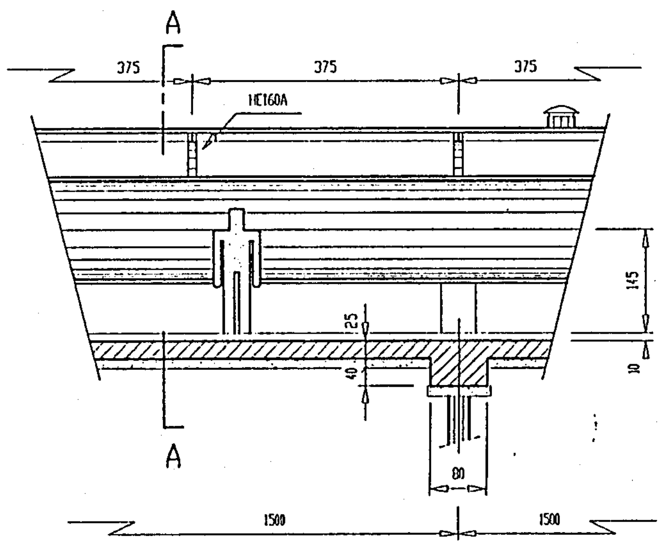

SECTION A–A

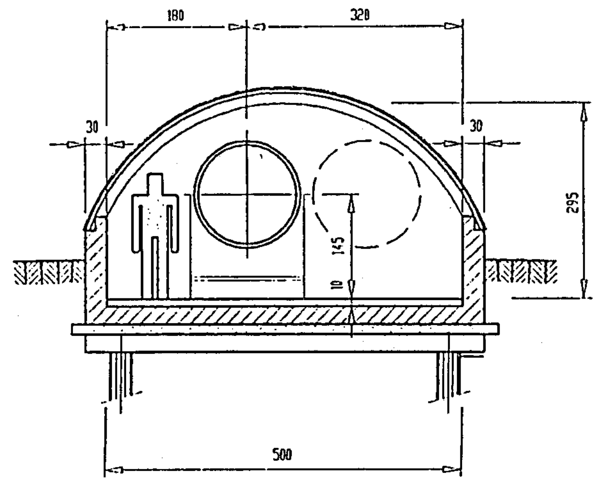

INFN Pisa, De Carolis 01/97

Fig. 2300.1

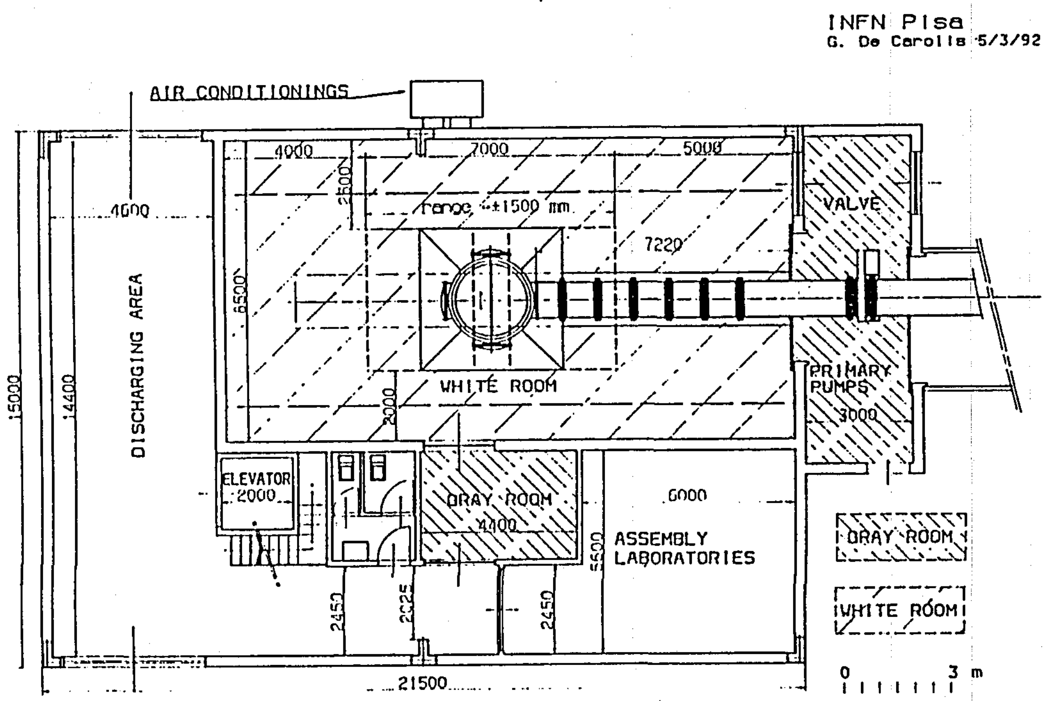
INFN Pisa
G. De Carolis 5/3/92
AIR CONDITIONINGS
4000
7000
5000
2500
range +±1500 mm.
7220
4000
6500
VALVE
WHITE ROOM
PRIMARY PUMPS
3000
15000
14400
DISCHARGING AREA
2000
ELEVATOR
2000
GRAY ROOM
4400
6000
5600
ASSEMBLY LABORATORIES
2450
2025
2450
21500
GRAY ROOM
WHITE ROOM
0
3 m

Fig. 2300.2

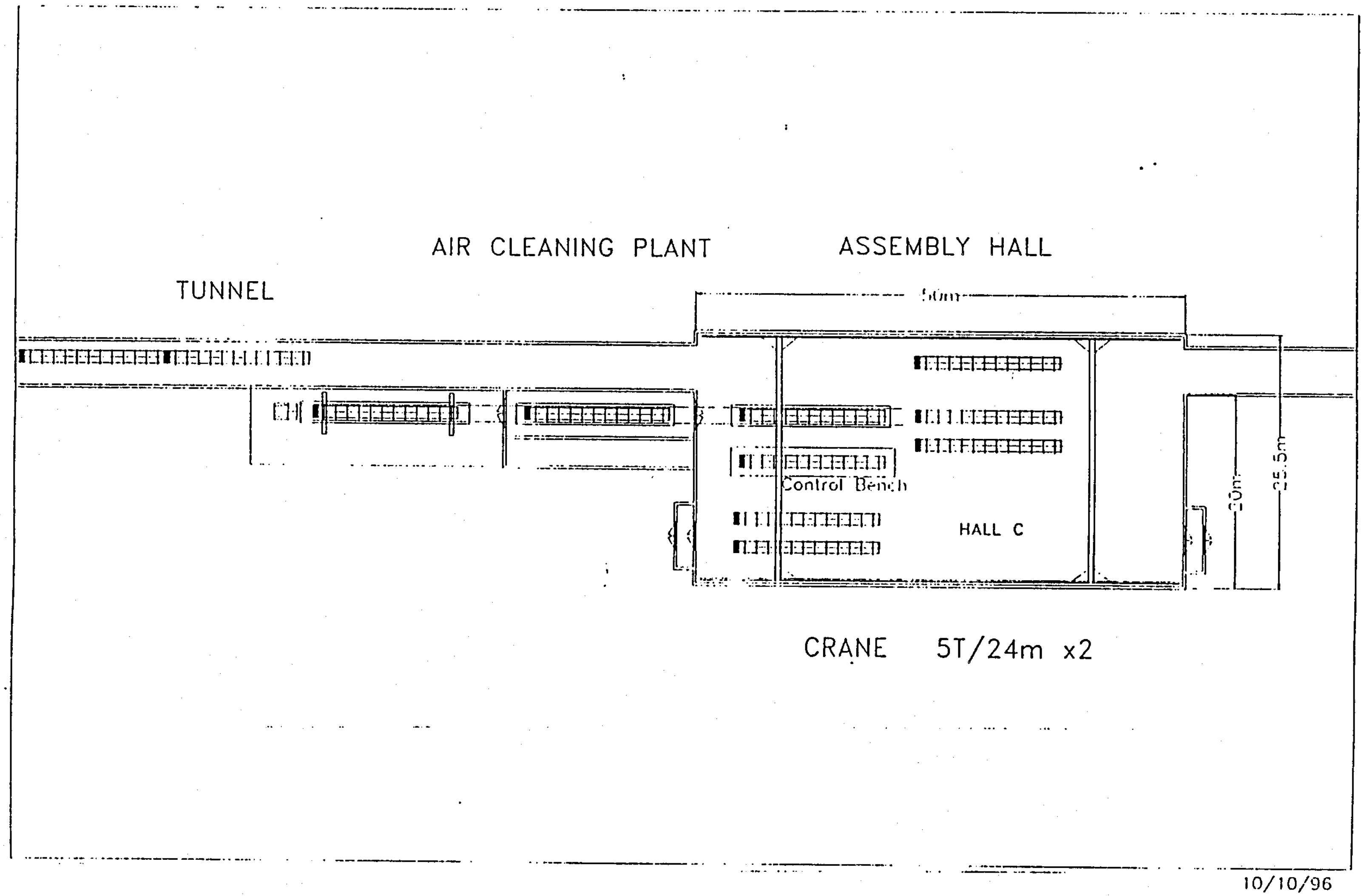
AIR CLEANING PLANT
ASSEMBLY HALL
TUNNEL
50m
Control Bench
HALL C
20m
25.5m
CRANE 5T/24m x2
10/10/96

Fig. 2300.3

TRANSVERSAL SECTION

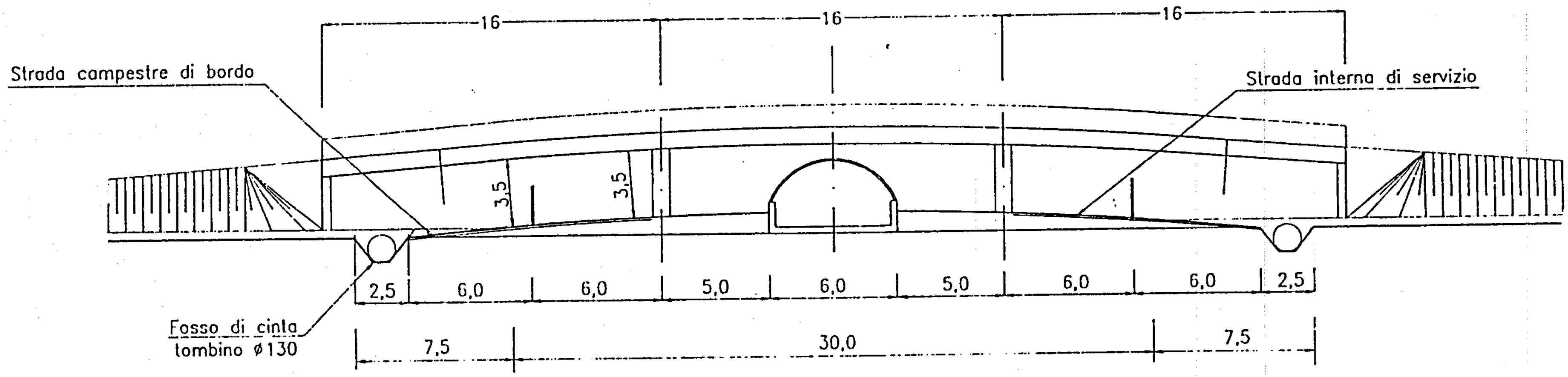

INFN Pisa, De Carolis 01/97

Fig. 2300.4

24. Miscellaneous equipment

To complete the infrastructure of Virgo, some additional equipments are needed. They are summarized below.

24.1.1 Set of electrical equipment

The terminal and assembly buildings will be powered with the medium voltage (15 kV) by an underground line connected to the technical building in the central area. This installation involves the following set of electrical equipments :

- two terminal power stations
- two middle power stations
- 15 kV power line along the arms .

24.1.2 Outer lighting plant

The central area and arms of Virgo will be provided by an outer lighting plant. The consistence of such plant has to be defined (TBD).

24.1.3 Security system

The buldings and the tunnels of Virgo will be provided with a security system. The organization of this system has still to be defined.

30. VACUUM

Table of Contents

30.1 Vacuum system description

The entire interferometer is put in vacuum in order to suppress several sources of noise, each one of them being strong enough at atmospheric pressure to prevent the observation of gravitational waves. They are :

- the transmission of acoustical noise to the mirrors,
- the damping of the mirror suspension and the corresponding increase of its thermal noise,
- the excitation of mirror motion by gas molecules brownian motion,
- the scattering of light by residual gas molecules,
- the random fluctuations of the refractive index.

This last one is by far the largest one related to vacuum. If one finds satisfactory conditions for it, then all the other ones will be fulfilled. The fluctuations of the number of molecules contained inside the volume of the light beam is the source of variations of the optical path length. These fluctuations may be produced either by the poissonian distribution of the molecules in steady vacuum or by the occurrence of sudden bursts of molecules. In both cases, the effect is proportional to the polarizability of the molecules. In practice one expects the dominant residual gas to be hydrogen which has a low polarizability.

In a steady vacuum, the poissonian fluctuations of the number of molecules within the beam are evaluated as if the ratio of the volume of the tube to the volume of the beam was infinity. The basic correlation time corresponds to the time for evacuating the molecules through the boundaries of the beam (or to the reverse). It is 60 μs for hydrogen and 180 μs for water vapour. This is to be compared to 10 μs for the light transit time between two mirrors and about 500 μs for the light storage time.

The vacuum system consists basically of two tubes, each 3 km long, joined in an L shape, containing the light beams and of ten towers disposed as shown in fig. 3000.1 and 3000.2, containing the antiseismic suspensions of the optical elements. All the vacuum vessels are made in stainless steel. Each tube and tower can be isolated from the connected elements by large gate valves (fig. 3000.2). The full volume can be divided in two parts: a ultra high vacuum (UHV) volume, where the light beams run, and a high vacuum (HV) volume, where the suspensions and other less demanding equipments are contained.

30.1.1 Tubes

The tubes, containing the Fabry-Perot cavities, hence most of the interferemeter optical path, will be in ultra high vacuum. This will be achieved by a relatively modest permanent pumping speed, thanks to air firing of the tube modules, adequate surface cleaning, subsequent 150 ℃ bake out.

Each 3 km tube has a diameter of 1.2 m. It is made of ten 300 m long sections. Every section will be built and tested separately for leaks and for ultimate vacuum after bake out, when ready the sections will be linked to build the full tubes.

30.1.2 Baffles

The baffles are necessary to stop the diffused light propagation inside the tubes and in the towers; they are distributed in the tube so as to cover completely its inner surface, as seen from the mirrors.

The baffles installed inside the tubes are made of stainless steel; the baffles installed in the towers and in the links (tower-tower and tower-large valve) are made of absorbing glass.

30.1.3 Towers

Seven of the ten towers (mirror towers) will be built in two parts, the so-called "upper tower" (tower upper part) and "lower tower" (tower lower part), connected by a small conductance. The lower towers which contain only clean optics, will be in UHV, as the 3 km tubes. This will be achieved with a relatively modest permanent pumping speed thanks to air firing of the vacuum vessels, adequate surface cleaning, subsequent 150°C bake out. During operation, lower towers and 3 km tubes will be in open communication, constituting one single vacuum vessel.

In contrast, the upper compartment of the mirror towers, which contain the superattenuators and the actuators (large outgassing rates) and the three other towers consisting of a single compartment, will require only HV, i.e. a pressure around 10^{-6} mbar.

30.1.4 Pumping system

The pumping system has been designed to allow for a high running efficiency of the antenna.

The tubes and the towers will be evacuated by dry pumps, starting from atmospheric pressure, in order to avoid oil back-streaming and air pollution in the environment; the two compartments of the mirror towers will be evacuated by the same dry pump.

Turbo pumps will be used for the permanent pumping of the high vacuum volumes and, during bake out, on the ultra-high vacuum volumes; in the end the permanent pumping of the ultra-high vacuum volumes will be achieved with large Ti sublimation pumps and small ion pumps.

The vacuum monitoring is done by separate instrumentation boxes.

All the pumps and the instrumentation boxes are connected to the large vacuum chambers through gate valves.

30.2 Vacuum system requirements

It is required the gas pressure noise not to be a limiting factor for the antenna sensitivity, that is, at least, one order of magnitude lower than the shot noise level. The relationship between the sensitivity of the antenna and the average pressure on the optical path has been derived in the 1990 Virgo proposal (Ref. 3000.1, see fig. 2-15-1 herein).

The target sensitivity of the antenna has been set to be $\tilde{h} = 10^{-23}\,\mathrm{Hz}^{-1/2}$. A pressure of hydrogen, in the absence of other gases of 2. 10^{-7} mbar (2. 10^{-5} Pa) would give a corresponding noise level of $\tilde{h} = 10^{-24}\,\mathrm{Hz}^{-1/2}$, in agreement with the above requirement. Due to their higher polarizability, a total pressure of 2. 10^{-8} mbar (2. 10^{-6} Pa) for most other gases, in the absence of hydrogen, would give the same noise level.

Having in mind future improvements of the antenna sensitivity by one order of magnitude, the ultimate pressure should be 100 times lower (the two quantities are related by a square law). This could be achieved either by a higher pumping speed or alternatively by a lower outgassing rate, far easier to perform. Virgo aims from the start to reach the ultimate hydrogen outgassing rate through an air firing treatment of the stainless steel at 400°C. This choice, while mandatory for future improvements, allows from the beginning considerable savings in the pumping system cost.

Furthermore, the residual gas must be free of hydrocarbons, in order to keep the optical surfaces clean. A partial pressure of less than 10^{-14} mbar (10^{-12} Pa) is required if one wants to avoid the cumulative deposition of a single layer of hydrocarbon molecules on the optics in 4 years. This value has been calculated using rather conservative (while not fully verified) hypotheses:

sticking probability of hydrocarbons on mirrors = 1; private communications suggest a more likely value of 0.1;

one monolayer of hydrocarbon molecules is harmful for Virgo operation; this is not proven, so as it is not known the hydrocarbons cross-section for infrared light (λ = 1.06 μm); depending on this cross-section the deposited hydrocarbons could either polymerise or eventually be photodesorbed, under the intense (10 kW) Fabry-Perot beam.

The retained target values for the average partial pressures on the optical path of the Virgo beams are:

Gas species	Partial pressure
H_2	1. 10^{-9} mbar (1. 10^{-7} Pa)
Σ other gases	1. 10^{-10} mbar (1. 10^{-8} Pa)
Hydrocarbons	1. 10^{-14} mbar (1. 10^{-12} Pa)

30.2.1 Bursts of molecules

The release of bursts of molecules inside the vacuum system can produce variations of the refractive index along the light beams, hence fake gravitational wave signals.

These phenomena are very difficult to assess; let us first describe the various possible sources and then try to develop their consequences on the behaviour of the antenna.

30.2.1.1 The possible sources

Mechanical motions of the inner part of the vacuum system is a well known source. It can be produced by vibrations. By far, the most dangerous, from practical experience, is the friction between metallic surfaces (actuation of vacuum valves).

Ion pumps have been found responsible for molecular bursts. This could originate from micro-fragments of titanium being extracted either from the cathode or sometimes from the anode. These objects, which have absorbed many molecules, bounce between the two electrodes and can release molecules bursts at some stage.

At the present time, the only possible policy is to try to observe these effects in laboratory conditions, and to minimize their consequences on the antenna.

30.2.1.2 The burst characteristics.

30.2.1.2.1 The time dependence

If the burst emission time is short, then the rise time of the pressure pulse is of the order of D/V_i (about 700 μs for hydrogen), where D is the tube diameter and V_i the molecule velocity. Otherwise, the rise time is longer.

The decay time is of the order of v/S where v is the volume pumped by each pumping station, having a pumping speed S; v/S is above 100 s for hydrogen, with 11 pumping stations on each 3 km tube.

This asymmetry between rise time and decay time gives a possible way of recognizing the signature of a pressure burst.

30.2.1.2.2 The dangerous level

Both statistical fluctuations of the number of molecules in the light beam and molecule bursts produce optical index variations. In consequence, the safe noise level ($\tilde{h} = 10^{-24}\,\mathrm{Hz}^{-1/2}$) is the same and it is equivalent to the statistical fluctuations for a hydrogen pressure of 2 10^{-7} mbar.

At this pressure, the number of molecules in the beam volume of diameter d, 10 cm, is 1.3 10^{17} and the variance 3.5 10^{8}. Assuming the burst of molecules to fill up the whole cross section of the tube, the number of released molecules having the same effect will be a factor

$(D/d)^2$ higher, that is $3.5\ 10^{10}$. Distributed over 1 m length of tube, it would produce a local pressure variation of $1.5\ 10^{-12}$ mbar.

Only the interferometer is capable of detecting such a small variation.

30.2.1.3 Strategies against bursts

During interferometer operation, no part in motion will be present inside the UHV compartment of the vacuum system. In the HV compartments, very limited motions of mechanical parts will be necessary to control the suspensions; great care has been put in avoiding frictions. Any molecule burst in HV will be transferred to the UHV compartment attenuated by a large factor, thanks to the double differential vacuum.

It is known that turbomolecular pumps and ion pumps can be themselves sources of molecule bursts. Studies on this subject has been performed in collaboration with G. Rupschuss (from P. T. B. - Berlin. Germany) and are reported in some Virgo internal reports (Ref. 3000.2); no definite conclusion has been reached so far, further studies are planned for the future.

The following precautions have been adopted so far in the permanent pumping system design:

turbomolecular pumps will be present only on the HV compartments; hence bursts generated by them, if any, will be attenuated by the differential vacuun system;

ion pumps will be located at one end of the titanium sublimation pots, hence the number of molecules reaching the tube would roughly be reduced by a factor of 10, for a fresh layer of titanium.

Furthermore, given the very low outgassing rates and the very low pressure foreseen for the vacuum system of Virgo, turbomolecular and ion pumps will work in very good conditions and one can expect burst events to be rare.

In data analysis, fake signals due to molecules bursts will be recognized through their peculiar time dependence.

30.2.2 Fluctuations of the tube volume

At the pressure of $2\ 10^{-7}$ mbar (see 3000.2.1.2.2.), a relative change of volume of $1/(3.5\ 10^8)$ in a time shorter than the time constant of the vacuum system, i.e. 100 s, would produce a change of refractive index at the level of the antenna sensitivity ($\tilde{h} = 10^{-24}\,\mathrm{Hz}^{-1/2}$). Such a volume change, 8.6 cm^3, could be generated by a longitudinal displacement of one face of a bellows convolution by 30 μm. Taking into account the large number of such objects, even when combining their actions statistically, these adiabatic changes could be a serious concern for the antenna. It is now foreseen that the pressure in the tube will be reduced by 2 and most probably 3 orders of magnitude, thus making such events unlikely.

30.3 References

3000.1 Virgo Proposal - 1990
3000.2 Rupschus et al. - 40th AVS Symposium, abstr. 256, program # VT-WEM1 - 1993

30.4 Figures

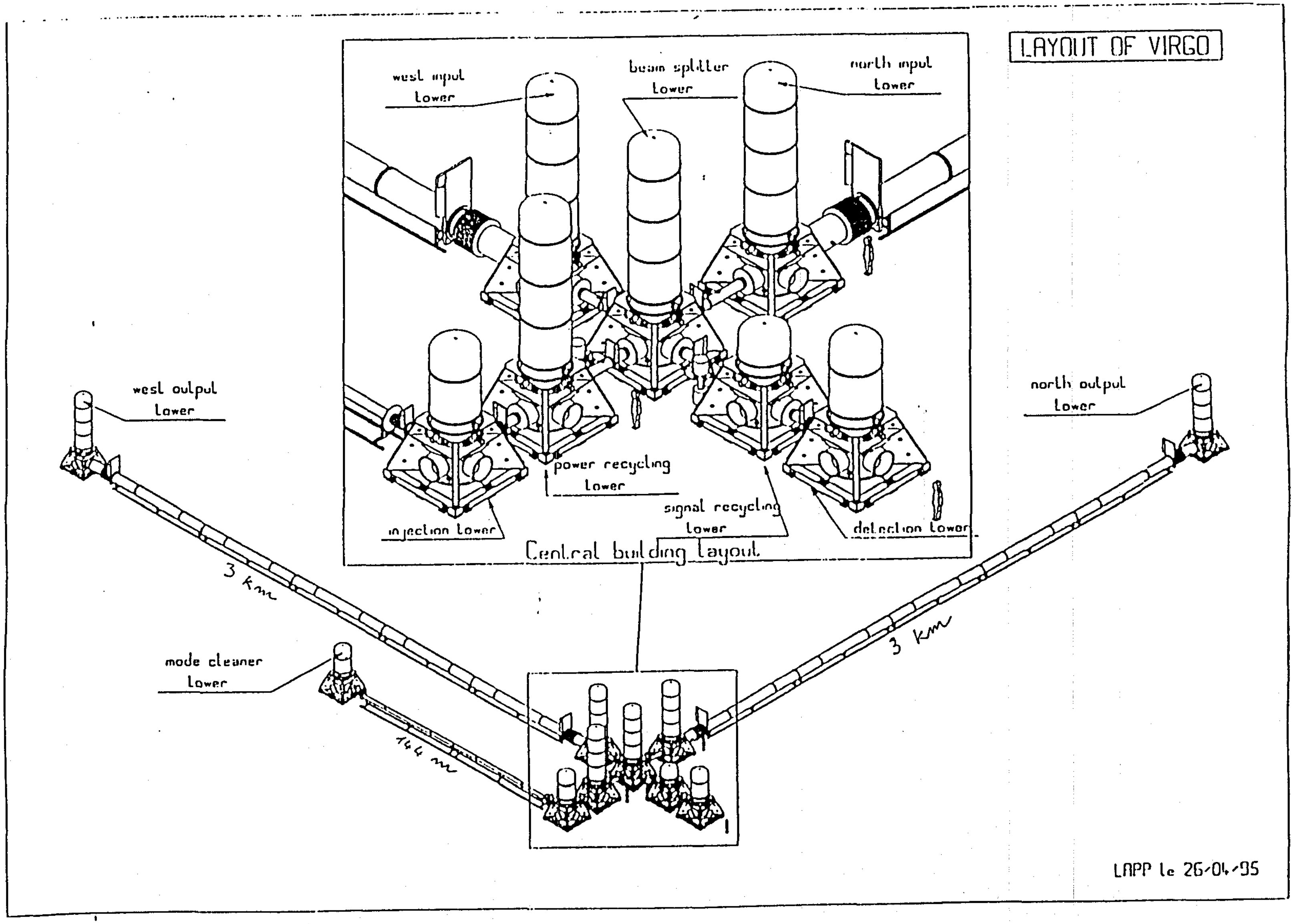

Fig. 3000.1 Vacuum system artists view

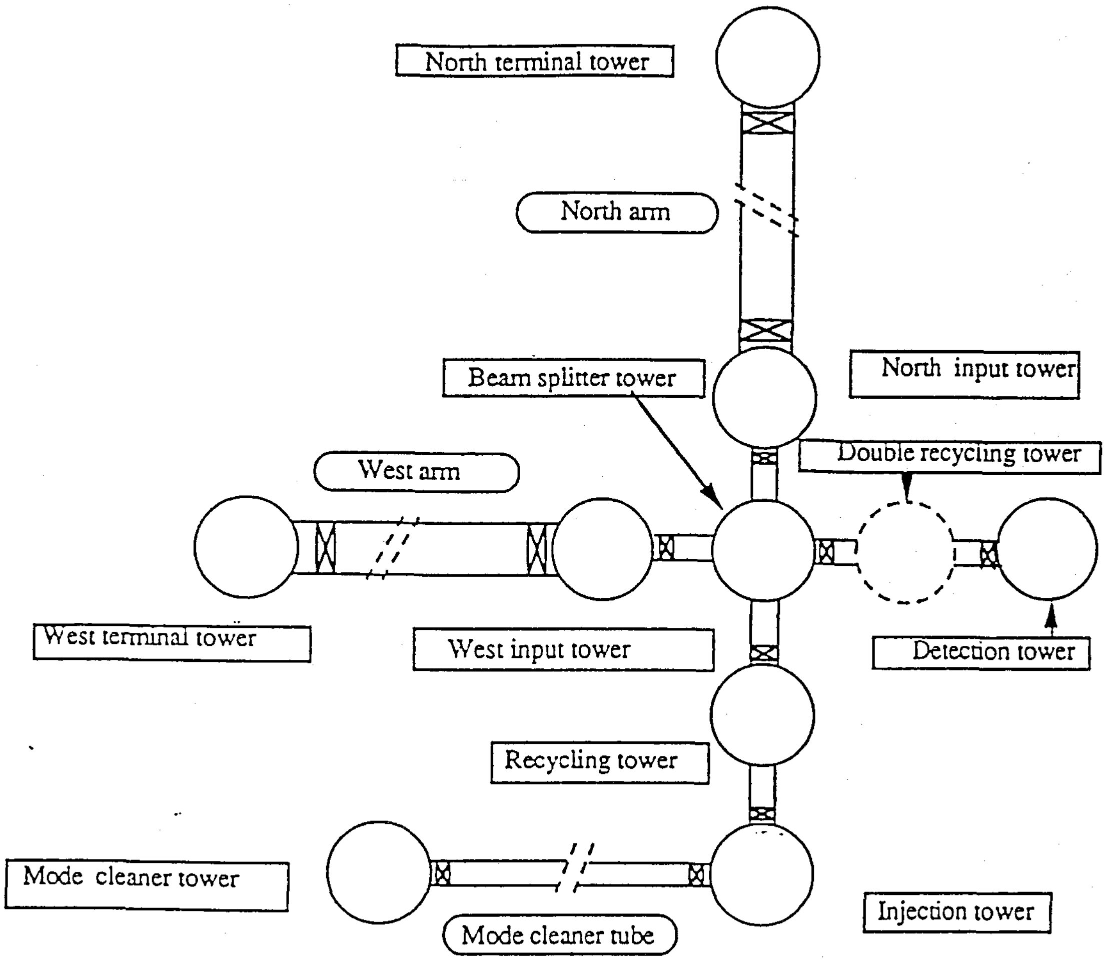

Fig. 3000.2 Vacuum system schematic lay-out

31. Tubes

Table of Contents

31.1 Tube function and concept

The vacuum tubes have been designed in order to provide a vacuum vessel for the two 3 km Fabry-Perot cavities; the tube diameter has been chosen, together with the baffle free aperture, in order to allow the installation of up to three interferometers in the same vacuum vessel. The ultimate pressure has been chosen (section 3000.2.) in order to keep the noise generated by pressure fluctuations well below other noise sources, even at an improved sensitivity of $\tilde{h} = 10^{-24}\,\mathrm{Hz}^{-1/2}$.

31.2 Requirements applicable to the tube

The requirements will be classified as physics requirements, necessary to preserve the interferometer performances, and design constraints, corresponding to practical choices, made in the development of the tube design.

31.2.1 Physics requirements

1. Length of each arm — 3000 m
2. Residual pressure — 10^{-9} mbar for H_2; 10^{-10} mbar for other gas species; 10^{-14} mbar for hydrocarbons
3. Inner diameter — 1200 mm
4. Presence of baffles in the tube
5. Minimum amplification of the seismic noise for any frequency, i.e. no mechanical resonance.

Requirement 1. corresponds to the arm length chosen to obtain the design sensitivity; requirement 2. is needed to preserve the sensitivity against optical index fluctuations; 3., 4. and 5. are required to control the noise due to scattered light, as described in the relevant section.

31.2.2 Design constraints

1. Outgassing rate — $5\ 10^{-14}$ mbar l s^{-1} cm^{-2} for H_2
2. Reference temperature — 20°C
3. Temperature range — +5°C, +160°C (TBC)
4. Working temperature range — +5°C, +40°C
5. Lifetime — 20 years
6. Viton valves at ends of arms — 1000 mm free diameter
7. Bake-out temperature — 150°C
8. Bake-out power — 250 W per meter of tube
9. Distance between pumping groups — 300 m
10. Straightness: the tube axis has to be contained within a 100 mm diameter cylinder
11. Distance between floor and tube axis — 1450 mm
12. Available tunnel cross-section — 5000 mm (horiz.), 2800 mm (vert.)

The previous values of the parameters have been chosen in the design process described in the following sections.

31.3 Tube interfaces

31.3.1 Tunnel

The tunnel function is to house the tube; the space available should be sufficient for all the installation operations, for replacing defective tube parts and to house the pumps installed at 300 m intervals (design constraints 11. and 12.).

The tube supports rest on the tunnel floor, which has to have the necessary stability (see Infrastructure section) with respect to earth movements, due mainly to subsidence. The supports adjustment range (+/-75 mm in the vertical direction) allows to keep the tube straightness, since the maximum floor expected movements are well within these limits.

In order to be free from resonance of the tunnel structure, which could enhance tube resonance, tube supports are directly clamped above the foundation piles.

The tube weight is a negligible load for the tunnel

No horizontal forces are transmitted to the tunnel structure, except in well determined points, every 300 m, at the ends of the sections. This will happen only during the vacuum test of each individual section; in this situation, the axial force put by atmospheric pressure on the section end covers will have to be supported by the tunnel.

In standard years, the temperature inside the tunnels is expected to range between 0°C and +40°C; hence, during operation, it will be easy to keep the tube temperature above +5°C, as required, using the bake-out system at a reduced current; the same holds for keeping the tunnel temperature below 40°C during bake-out, thanks to the ventilation system foreseen in the tunnel.

No provision has been made, yet, for exceptional situations, e.g. outside temperature -15°C for one week (can happen once in 50 years), accompanied by a long power failure; in this case there will be no mean to warm up the tube, with structural danger for bellows and lips, and to keep the pumps running, with the risk of freezing the cooling water. (TBC)

31.3.2 Pumping system

Suitable sets of three ports have to be provided at 300 m intervals: two CF200 and one CF63 ports for rough/intermediate pumping, permanent pumping, instrument bottles/venting, respectively.

31.3.3 Input and terminal towers

The arm length, hence the tube length, is given by the distance of each terminal tower from the corresponding input tower; this distance will be 3000 m, center to center, at the installation. At each end of each tube there are one large gate valve, one special module to link the tube to the valve and one special module to link the valve to the tower. After the first operation period, the correct arm lengths will be determined according to the mirror reflectivity, hence the tower distance will be adjusted, changing the valve/tower links length.

31.3.4 Light beams

During the final operation period, there will be possibly three interferometers installed in the vacuum system, with parallel beams, at about 500 mm one from the other. This situation requires a tube diameter of 1200 mm and a baffle free aperture of 1000 mm, in order to keep the tails of the gaussian beams far from tube walls and baffle edges. The number of baffles has been determined as a consequence, in order to intercept and absorb all the photons scattered off the mirrors.

This situation determines also the straightness requirement for the tube: the centre of every tube cross-section must stay inside a 50 mm diameter cylinder; the requirement refers in principle to baffle edges, and has been extended to the tube.

During initial operation this requirement could be much less tight, but has been kept unchanged, in order to preserve the tube integrity, from a mechanical point of view.

No quantitative requirement exists on dust contamination in the tubes (TBD); dust particles, falling through the light beam could simulate G.W. signals.

31.4 Selection of solutions

The tubes will be built assembling in the tunnels prefabricated elements ("modules" in the following). This choice has been immediately made, leaving the module length selection to a later stage as a compromise between a easy transport and a limited number of modules per arm. Each element will be made of a rigid part and a bellows to allow for thermal expansion up to 160 °C.

The assembly will proceed installing "sections" of 300 m to be closed with endcaps end separately tested for their ultimate performances.

When all tested, the sections will be joined together by means of connection pieces, in order to constitute a full 3 km tube.

The detailed tube structure will be described in the following.

31.4.1 Historical background

Many different solutions have been considered for the vacuum tube, since the Virgo proposal (Ref. 3000.1). A plain tube, with non stiffened wall, about 10 mm thick, has been discarded for cost of raw material and weight; a stiffened tube with thinner wall (about 5 mm) and a corrugated tube with thin walls (2 mm or less) have been retained for further study. The continuous spiral welding technique, proposed by LIGO for tube fabrication, has been discarded since not promptly available among European companies.

As far as the technique to join on site the modules, welding has been preferred as safer and cheaper with respect to bolted flanges.

In parallel, some relatively small scale prototyping work has been made, including two 12 m long, 1000 mm diameter, modules, made of 3 mm thick 304 stainless steel, reinforced with external stiffening rings; end covers were installed with bolted flanges and silver wire gaskets.

Very encouraging results have been obtained, including outgassing rates in the range 10^{-12} mbar l s^{-1} cm^{-2} and 10^{-14} mbar l s^{-1} cm^{-2} respectively, after 150 °C vacuum bake-out and after 400 °C air firing.

31.4.2 Final choice

Four years ago Virgo started two parallel programs at Pisa and at Orsay in order to study large scale prototypes of the vacuum tube and to perform the final choice. These were called respectively the Stiffened Tube (ST) and the Corrugated Tube (CT) prototypes. Both prototypes aimed at ultimate low hydrogen outgassing rates through either a prolonged air firing at 400 °C or a classical 950 °C vacuum firing. In the recent period, their results were analyzed in the light of the theory of hydrogen diffusion and solubility in the stainless steel matrix. The latter, besides the temperature dependence of the mechanism, was examined in connection with the existing hydrogen pressure arising either through water vapor dissociation during the elaboration of the alloy or from the natural hydrogen content in air. The analysis of the hydrogen content in stainless steel samples submitted to different treatments confirmed the capability of air firing to eliminate hydrogen from the bulk material (Ref. 3100.1).

One can summarize the results as follows.

Both kinds of prototypes experienced industrial fabrication and surface cleaning. After bake out for about a week at 150 °C, they presented similar outgassing rates for hydrogen, the dominant gas species, namely a few 10^{-12} mbar l cm^{-2} s^{-1}. The 48 m long Pisa prototype was then air fired at 380 °C for 100 hours maintaining a constant inner gas flow in order to eliminate the contamination by the hydrogen being released in the inner part of the tube. Subsequently an outgassing rate around 5 10^{-15} mbar l cm^{-2} s^{-1} was obtained after a standard bake out and pumping as described above.

At Orsay (Ref. 3100.2) a second corrugated prototype made of stainless steel sheets, 950 °C vacuum fired for 2 hours, gave an outgassing rate of 2.5 10^{-14} mbar l cm^{-2} s^{-1}. The difference with the rate obtained on the stiffened tube was attributed to the weld contamination by traces of water vapor dissociated by the argon arc discharge. In order to test this hypothesis, the first Orsay prototype was split into three elements. Each of these was air fired at 400 °C for about 38 hours, respecting the necessary precaution to evacuate the hydrogen released from the metal. After reconstituting the prototype and a standard bake out and pumping, an ultimate outgassing rate of hydrogen of 1.5 10^{-15} mbar l cm^{-2} s^{-1} was obtained. The improvement factor is sensibly in agreement with the reduction of the length of the welds, when comparing the second and the third test.

For an industrial construction of the tubes, Virgo took a conservative value of 5 10^{-14} mbar l cm^{-2} s^{-1} as the design hydrogen outgassing rate. This is more than an order of magnitude larger than the ultimate rate achieved. It is still compatible with a process involving a 400 °C air firing of the metal sheets which would exclude the treatment of the welds.

Other developments were made on bake out (heating tapes and current flowing in the tube wall, called IHS = impedance heating system), on thermal insulation, on pumping aspects (dry pumping for evacuation, permanent pumping with titanium sublimators and NEG, cryogenic pumping for the tower upper parts) and finally on instrumentation.

Hydrocarbon contamination after a normal cycle of bake out and pumping using a TMP and a mechanical forepump separated by a zeolite trap, was found to be close to the level required by Virgo.

All these efforts confirmed the feasibility of vacuum performances far better than the ones presently needed for Virgo, thus allowing for increased performances in other fields limiting the antenna sensitivity.

In order to make a choice between the CT and the ST solutions, a group of external experts (TTAG, i.e. Tube Technical Advisory Group) has been asked to advice the Virgo Direction. Although both solutions could meet the final requirements of Virgo, based on financial and practical considerations the ST solution was selected. It however incorporates some of the CT ideas, concerning essentially bellows, IHS and the technique to join modules.

Following the recommendations of the TTAG, the main choices for the stiffened tube construction are summarized below:

- module length 15 m, as a realistic approach to several problems such as transport, surface cleaning, etc.;
- wall thickness of 4 mm, together with the number of reinforcing rings was found to be adequate, thus lowering substantially the weight of steel needed without endangering the welding of the sub elements;
- the bellows were designed to work in the elastic regime in order to bring the safe number of cycles in accordance with the large number of modules and that of the bake-outs foreseen;
- modules will be joined welding together thin (2 mm) lips, thus allowing defecting modules removal by automatic and clean lip cutting;
- the different parts of the module were toleranced to achieve smooth and precise conditions for welding the lips;
- the heat treatment will be performed on the full module (including its bellows) thus allowing for extreme outgassing performances; the smaller thickness of the tube has also the advantage of reducing by one third the duration of the process;
- the bake out temperature was set to 150 °C, thus lowering the cost of this operation but calling for more stringent conditions so as to avoid accidental pollution;
- IHS was adopted.

31.5 Tube modules

31.5.1 Introduction

The modules consist in stainless steel stiffened tubes, 15 meter long, with a 1200 mm diameter, welded to each other through lips (Ref. 3100.3). Each 15 m long tube is equipped with a bellows to allow for dilatation. Most of the modules are "standard modules", one out of 20 is a pumping module, and in several places there is need for different "special modules". The modules and all their components have been modeled and optimized with the finite element program Systus. In particular, the size and spacing of stiffening rings have been designed to avoid any risk of buckling of the tube (Ref. 3100.4).

31.5.2 The modules

31.5.2.1 Standard Module

This module is shown in Fig. 3100.1. The wall is 4 mm thick, and the stiffener rings are 70 mm high and 8 mm thick, with a 1200 mm spacing. The tube is terminated by 2 lips (one at each end) described in 3100.5.3., which allow the welding to the adjacent modules. At one end of the module, a 10 convolution bellows allows for dilatation (see 3100.5.4.). These 2 items, made of 2 mm thick stainless steel, are assembled to the tube ends by welding. The module is supported through the two rings (16 mm thick) closer to the ends; on these "terminal rings" different accessories are fixed :

- feet for fixing the modules on support
- targets for alignment
- pieces for handling
- connectors to feed-in bake-out current.

31.5.2.2 Pumping modules

They are identical to standard modules, with three ports, two for respectively intermediate and permanent pumping, one for measuring instruments (Fig. 3100.2).

31.5.2.3 Special modules

1. Modules without bellows : at the extremity of every 300 m section, the first module has no bellows, it is only 14 m long and has feet distance as standard modules. This allows the mounting of all the sections separately, one after the other. Later on, the "missing bellows" are positioned and welded to two adjacent 300 meter sections, insuring the continuity of the 3 km long tube.
2. Links at the end of arms : special modules identical to standard modules but with different lengths are used to link the extremity towers to the large valves (these links are dismounting) and the large valves to the normal modules.

31.5.3 Lip joints

Modules will be joined together by means of 2 mm thick lips (Fig. 3100.1), following a technique developed for the Joint European Thorus. The ends (lips) of adjacent modules will be aligned and put in contact; when perfectly coincident (within 0.3 mm), the edges of the lips will be welded by an automatic machine, developed on purpose. Great care has to be put in avoiding pulling or transverse stresses on the lip welds.

In case of necessity, modules will be dismounted simply cutting out the lip welds; the automatic nibbling machine essentially removes an outer ring of the welded lips, reducing their radius by 3 mm and making them free from each other. Later on the module will be repositioned and re-welded at a smaller radius. The radial width of the lips is such as to allow three successive cut and weld sequences.

31.5.4 Bellows

Necessary for absorbing the dilatation of the tube - which rests on rigid supports fixed to the ground every 15 m - the bellows (Fig. 3100.3) are designed to operate in the elastic domain, in order to reduce the stresses on themselves and on the lip welds. They are made out of 2 mm thick stainless steel, with 10 convolutions. The bellows total extension range is 42 mm, allowing the tube to be operated from +5°C to +160°C. In case of very low outside temperature, the + 5°C minimum tube temperature will be obtained by the bake-out system.

31.5.5 Other components

In order to test individually each 300 m section, end caps have to be made, with 1 lip joint for their welding to the section terminal modules. When all the sections of one arm will be tested, the end caps will be removed by nibbling their lip welds, and replaced by "missing bellows" (3100.5.2.3.).

31.5.6 Raw material

All parts are made of stainless steel 1.4307/EN 10088 (X2CrNi 18-9). The thicknesses are 2 mm for lips and bellows, 4 mm for the tube walls, 8 and 16 mm for the stiffening rings. There is a special requirement for the elastic limit of the 2 mm sheets :

- $R_{p0.2} \geq$ 29 daN/mm^2 at 20°C
- $R_{p0.2} \geq$ 20 daN/mm^2 at 150°C

For 2 mm and 4 mm sheets a limit on inclusions content is also required.

More precise specifications about the material (~ 800 tons) can be found in the call for tender documents (Ref. 3100.3).

31.5.7 Cleaning

A careful cleaning of each module must be done at the end of its complete assembly, in order to get rid of all possible contamination.

For the washing a 2% concentration alkaline lye is used at 60°C.

Rinsing is done with tap water. The washing-rinsing cycle is done three times. A last rinsing with demineralized water is done at 60°C. Finally, the whole module is dried with radiant panels.

31.5.8 Thermal treatment

All the surfaces which are part of the UHV tank will be heated at 400°C in air, for desorbing hydrogen out of stainless steel, in order to get the outgassing rate as mentioned in the specifications ($Q < 5\ 10^{-14}$ mbar l s^{-1} cm^{-2} for H_2).

A clean oven with stainless steel walls and electrical heating is required.

The typical heating cycle will be :

- T increasing from 20°C to 400°C in at least 24 hours
- Constant T = (400 ± 10°C) for 72 hours
- Decrease to T = 20°C in at least 24 hours.

During the whole cycle an air flow will sweep the module for extracting the desorbed hydrogen.

31.5.9 Leak detection

The test must be performed in an air-controlled area. The vessels are closed by end caps and put on a test bench, flat Viton gaskets insure tightness.

The test must be done by qualified people in the presence of Virgo inspectors. The total leak must be smaller than 3 10^{-10} mbar l s^{-1} (He).

31.5.10 Connections to supports

The modules rest on supports through 2 feet welded to each terminal ring (Fig. 3100.4). In average the standard feet (on the right side in the figure) should not be submitted to any longitudinal stress (if two adjacent modules are identical), besides the force necessary to bend the elastic supports (see the relevant section). Only the eventual differences among modules can induce further stresses; but the total force is always smaller than 700 daN on each foot. The constraint induced on the tube wall is always smaller than the elastic limit.

For the 300 meter section tests, the longitudinal force due to atmospheric pressure on the end caps is 12 tons. Special feet have been designed and are welded on a doubled stiffened ring (on the left side in fig. 3100.4).

31.6 Tube assembly

The activities of receiving, storing, unpacking, preparing for installations of all the items before being entered into the tunnel are carried on in dedicated yard service areas properly equipped. Two different locations are assigned for these areas.

One location is close to the central building zone and is dedicated to modules reception, storage and thermal insulation equipping (fig. 3100.5). This area is unique for both tubes; it is a hall equipped with bridge crane for modules handling and fixed supports for modules laying.

The other location is aside each tunnel, at mid-length, where a workshop is built integrated with the tunnel (fig. 3100.6). In this workshop (called Tube Assembly Building in Infrastructure section) each thermally insulated module can be prepared before entering the tunnel. Prior to enter this clean area workshop the modules are to be cleaned. A dedicated plant installed externally to this workshop provides for the outside cleaning of modules. Inside this workshop a separate area is dedicated for minor item and accessory: bellows sections, valves, pumping and instrumentation groups, supports. Here the minor items can be stored, completed before assembly and receive brief inspection before being driven to their final position. In particular supports shall be cleaned with the same facilities of the modules. The halls of the service areas are equipped with bridge cranes, transport boogies, electrical mains and water.

The thermal insulation storage is located in the module storing area, close to one of the two main walls.

The covered service areas layout, their equipment distribution and characteristics have still to be revised (TBD).

31.6.1 Assembly strategy

The fabrication of the tube is conceived to be executed in steps. For being fabricated the tube is subdivided into modules, the majority of which is 15 m long; other components are also fabricated for completion, as described below. Each standard module includes a stiffened tube portion and a bellows. The modules are manufactured in workshop and arrive complete to site. Here they are equipped with thermal insulation prior to be erected in the tunnel onto the relevant supports, previously installed. Modules are connected together by welding. The connection is realized by a couple of facing lips, each belonging to one of the facing modules. The lip edges are fit–up and welded together. Major non destructive inspection on the welded joints is He leak test.

Due to the need of verifying on a step–by–step basis the vacuum quality reachable by the realized assembly, a number of adjacent assembled modules are made to constitute a "section". End caps are foreseen at one end of the extreme modules of each section for performing the site test. The tests are both He leak onto lip-welds executed on site (between adjacent modules and end caps) and the vacuum quality, measured by RGA (residual gas analyzer). First test requires 10^{-6} mbar pressure inside the section, second test requires 10^{-9} mbar, thus trough baking process. The space needed for the end caps volume is made available delaying the installation of the bellows from a special module (see 3100.5.2.3.) at one end of the testing section. The module at the other end of the testing section has pumping and vacuum measuring ports.

Once the sections are testes they are kept under vacuum (TBC) until there is the need of connecting them together to complete the tube. This operation is done by inserting the missing bellows in between each adjacent sections. The connection is realized via lip joints similarly welded and tested to those between modules. Other sections complete the tube at its ends. Thermal insulation continuity along the tube is restored after these items are erected.

Each completed tube is vacuum tested full length.

To be noted that the temporary removal of tube splice for baffles relocation is relatively easy by cutting out the lip weld at both ends of a module. The lips are dimensioned in order to allow a number of cutting and re-welding operations. It is also to be noted that lip welding is the last operation performed before closing the tube, i.e. confining its inside from the outside: to avoid contamination any activity inside the tube after the weld is completed is to be done under complete cleanness control.

31.6.2 Interfaces and attachments

To control the alignment of modules and link sections one target holder can be installed onto each foot. The holders are to be erected on site onto the proper positions predisposed on the items' feet. The correct positioning of target holders is made through mechanical coupling, compatible with the alignment tolerance value.

To facilitate the items handling one lifting lug is mounted in manufacturing workshop onto each terminal ring of each module and link section. The lugs may remain installed onto the terminal rings also during service (TBC).

31.6.2.1 Supports and Supporting Feet

The Modules lay onto supports by means of built-in feet. The feet are in number of four per module; the bellows have no feet. No other supporting points are foreseen, either allowed, for the Module.

Feet are connected to the supporting rings in the manufacturing workshop. Their lower surface is located within the tolerances indicated in construction documents.

31.6.2.2 Electrical connections for baking

To allow the baking operation for UHV by means of Joule effect, electrical connectors are bolted onto a number of tube terminal rings in selected locations along the tube itself, after the modules are installed in their final destination. Selected locations are the extreme rings of sections. The connectors are cabled to heating current power supplies installed along the tunnel.

31.6.3 Transport to Site

The Modules, the Links, the Bellows sections and the end caps are collected from manufacturing facilities completely assembled, mechanically complete and cleaned as ready to be installed.

31.6.3.1 Transport

Modules are transported to site onto adequate saddles. Modules are provided with temporary protective caps to keep the inside clean; each item is singularly and entirely wrapped-up with plastic sheaths, which however do not form a water-proof barrier. Module transport trip to Cascina will easily have to be across mountains. Due to atmospheric pressure, function of height above sea level and weather conditions, total load onto covers and bellows can raise up to 2 t (TBC). Fixing of covers onto lips and strength of covers themselves need not to stand such load if a controlled air feeding device is connected to modules covers. Discharge of internal overpressure can be through non return valves and air filter for safety. Inlet air will have to be from a battery of clean air bottles activated by an automatic pressure sensitive valve.

Modules can be transported in groups: it is envisaged that if trucks are used then three modules can be loaded per trip.

Packed modules loaded onto trucks or wagons are also to be covered by an heavy plastic canvas of the type normally used for this kind of transport.

Bellows sections are transported to site by means of wooden boxes. Inside the boxes bellows sections are wrapped up with plastic sheaths, forming a sealed water-proof barrier. Temporary protective caps are installed to keep the inside surfaces clean.

Transport means can be trucks as well as railroad wagons, but it has to be considered that the site of Cascina is not equipped with inside railroad facilities. The closest railroad station adequate for performing the transfer of modules onto trucks is Pisa. Sea transport can also be done being the harbour of Livorno quite close to site and connected by highway. The transport system, with its details, is subject to the approval of Virgo.

31.6.3.2 The Saddles

The saddles are designed for protecting modules (their bellows in particular) from all dynamic loading due to transport causing stresses beyond an acceptable limit in any point. They should accommodate at least three modules (Standard, Initial, or Pumping, or a selection of them) for optimizing the number of transport trips. Links can also be transported onto saddles.

A number of saddles are foreseen for constantly feeding assembly site with the needed quantity of items.

31.6.3.3 Site Internal Transport

The top of the modules onto truck in transportation asset, is higher than 3.5 m from road level. This precludes from the possibility of discharging the modules close to the mid-length workshops of each tunnel because the presence of road bridges with a maximum clearance of 3.5 m.

Therefore the transportation from the stocking area and the mid-length workshops is to be done by other means.

This is in agreement with the strategy of unloading modules at the thermal insulation equipping building, which is unique for both arms (fig. 3100.5).

31.6.4 Supports

Supports are to stand mechanical loading, to allow thermal expansion of modules, within the loads acceptable by bellows and lips, and to give the possibility of realigning the tube in case of movements of the tunnel due to ground subsidence.

The mobile support is equipped with spring elements which allow the module to yield under longitudinal dilatation caused by bake out and daily temperature changes.

In order to avoid large transversal stresses onto the lip welded joints, the fixed support of one module and the mobile support of the adjacent one are mounted onto the same rigid frame. In this way they can be moved vertically together in case the tube realignment is needed. This frame is flanged to four posts, which at their turn, are bolted to the concrete floor (fig. 3100.7).

31.6.4.1 Electrical Insulation

Between modules feet and support top an electrical insulation joint is inserted. It provides electrical and thermal insulation when parts of the tube are put to different voltages to bake the tube by current flowing in its wall.

31.6.4.2 Performances

The fixed support (fig. 3100.7) is designed to stand an axial load of 3,200 kg (TBC) in both directions and a vertical load (1/2 the module weight) of about 2,000 kg.

The fixed supports of the two end modules of each section, called "superfixed", are designed to stand an axial load of 13,000 kg in both directions; other characteristics are the same as for fixed support.

The mobile support is designed to displace ±20 mm in the axial direction (with 0.5 mm maximum vertical displacement) under the load of 2,000 kg (TBC); other characteristics are as per fixed support.

The displacement range of mobile support is dictated by thermal expansion of modules at 160°C: range from of 5°C (minimum tube temperature) to 160°C is 38 mm. Such range is to be equally distributed from -19 to +19 mm to reduce the vertical displacement of top part of mobile support. Due to its design while running from -19 to +19 mm the support top part describes a curve which sagitta is 0.5 mm. Therefore the mobile support once installed is to be pre-bent of -19 mm at 5°C, or in a proportional position if pre-bending regulation is done at a different temperature.

31.6.4.3 Adjustments

The possibility of adjustment of the three support types are for assembly needs and for tube realignment.

For assembly needs the adjustments are specific of the support type. Fixed and mobile support frame can be regulated in height and transversal position before the module is put on it. Mobile support can in addition be fine adjusted vertically by ±10 mm and horizontally by ±5 mm in order to perform a careful lip joint fit-up before welding.

For tube realignment the adjustment of the support block (fixed support of one module and mobile support of the adjacent one) is made by the displacement of the entire frame, which can be moved along the vertical axis by ±75 mm.

31.6.4.4 Support interfaces

Civil works

Support bases are installed onto floor concrete slab by means of "fisher type" bolts. In the area of supports floor surface is flat and horizontal within a few mm every 2 m in all directions. Support base plates should be installed onto leveled steel plates and grouted underneath before final bolts tightening.

Modules

Modules rest onto supports just through the feet attached to the terminal rings. The boundary between supports and module is defined as the lower surface of the module feet.

31.6.4.5 Installation

Supports are to be completely assembled in their final position in the tunnel prior the proper module is laid on them.

Supports are to be completely cleaned prior to entering into the tunnel. The use of lubricants, liquid or solid or spray, is strictly forbidden. Any dirty or greasy or rusted area of supports structure is to be properly cleaned and the surface is to be reconditioned outside the tunnel.

31.6.5 Bake out

Each tube has to be heated up to 150°C under vacuum (bake out), at least each time it is evacuated, in order to eliminate the water molecule layers present on its inner surface and to reduce the water partial pressure to a negligible value. Furthermore, also during the assembly phase, each 300 m section of tube will be baked. The tube temperature must follow a cycle related to the wanted residual pressure and gas composition; 100 h at 150°C is the typical value. Moreover vacuum and mechanical resistance add constraints on temperature uniformity and increasing rate: a variation range of ±10°C and a rate of rise of 2-4°C h^{-1} (limited by the power of the installation) are taken as reference values.

Temperature in different points of the tube and its rate of change have to be monitored and automatically controlled.

The power supply, the temperature monitoring and control system, and the necessary installations are described below.

The heating power is supplied to the tubes taking advantage of the fact that they are metallic and completely welded (they are electrical conductors): an electric current will flow trough each tube heating it by Joule effect. Another solution, implying the use of electrical tape resistors wound to the tube wall, has been taken into account, tested and then discarded for economic reasons; in particular the power distribution to the heating tapes has been found remarkably expensive.

Consequently to the chosen technique a proper voltage difference must be applied to the tubes, and a return conductor of sufficiently low impedance is necessary to complete the electrical circuit. The main parameters in dimensioning the system are:

power losses through tube thermal insulation per meter of tube (see 3100.6.4.)	175 Watt m^{-1} (measured value , at 20°C room temperature)
ohmic resistance per meter of the 4 mm thick 304L stainless steel tubes	50 $\mu\Omega\ m^{-1}$ (measured value, at 150°C tube temperature)

The current effective value turns out to be I = 1870 A.

Calculations and experimental results obtained in Pisa and in LAL-Orsay clearly show that AC current is not suitable since the relevant increase of circuit impedance at 50Hz; in fact besides its small absolute value it results about 3 times higher than ohmic resistance. Furthermore AC current flows not uniformly throughout the tube causing unacceptable temperature gradients. Then DC current (10% maximum residual oscillation) has been selected.

It has to be remarked that the power density (W m^{-1}) supplied to each bellows is about 6 times higher than the one supplied to the 4 mm thick tube, due to its higher ohmic resistance (304L stainless steel, thickness 2 mm, length 0.5 m, developed length 1.8 m); then to avoid over range temperature (T>160°C) bellows thermal insulation has been specially designed, both for steady and warm-up conditions.

The return conductor shall be a 99.5% Al bar with a cross section of 15 x 160 mm^2, which dissipates a power of about 42 Watt m^{-1}. Other solutions as copper cables or steel rails have been found more expensive and not advantageous.

Taking into account all the contributions the average power density turns out to be about 270 W m^{-1}, and for each arm the needed power figures out as 0.8 MW, while the corresponding voltage drop is 430 V (70 V on return bar, 360 V on tube). Taking into account extreme values of tunnel temperature and different efficiencies and losses, the power installation for each arm will be capable of 1.2 MW. This power will heat the tunnel (400 W m^{-1}, see Virgo report VIR-TRE-PIS-3100-103), hence requiring some ventilation.

A fine dimensioning of the necessary power and current will be achieved by testing the first 300 m tube section. The relevant parts of the bake out apparatus will be ordered only after such tests.

The electrical design must take into account the human safety: proper rules (CEI 64-8, Italy) allow at maximum 60 V DC if electrical insulation is not present. To limit the max tube voltage to 60 V the power must be supplied in at least five points distributed along each arm. The actual design foresees 5 suitable AC/DC converters (55 V, 4600 A) located at Z positions 300 m, 900 m, 1500 m, 2100 m, 2700 m; each one will supply two 300 m tube sections in parallel. The tube will be insulated from ground excluding 6 points, where it will be expressly grounded, at 0 m, 600 m, 1200 m, 1800 m, 2400 m, 3000 m.

Such arrangement is still to be confirmed, since some possible compatibility problem with other instruments in electrical contact with the tube could exist. In fact, during bake out, pumping stations and vacuum devices, in addition to the ones located in the 6 grounded positions, could have to be used in correspondence of the 5 supply positions (at 55 V respect to ground).

Experimentation on this matter is actually in progress in Pisa.

An alternative design with 10 supply points per arm located at each 300 m section center (27 V, 4600 A) and 11 ground points at each 300 m section end, will allow a more standard operation of 11 pumping stations during bake out (see VIR-TRE-PIS-3100-104).

No risks for human safety arise from the magnetic field originated by the DC current, since it is far from the limit (2 T at 0 Hz frequency) imposed by CEI EN code.

About human safety it has to be remarked that bake out shall be stopped in case of people operation on the tube.

Since the tube arms will be baked not contemporary the AC/DC converters will be movable from one arm to another. They shall be placed outside the and the electrical connections shall be realized by 6 x 630 mm^2 copper cables.

The AC/DC converters will be supplied at 380 V, three phases, in part by dedicated diesel generators and, for the remaining quote (TBD), by the fixed Virgo installations.

Beyond the tube, other parts have to be heated: vacuum devices and tube links. Each separable UHV vacuum volume shall have its independent heating system.

The heating system of vacuum pumps, valves and instrumentation (see 3400 chapter) will be realized with electrical tape resistors.

The 1.2 m diameter tube links, connecting the large valves to the mirror towers and to the tube, will be also heated by electrical tape resistors.

During bake out the tube temperature has to be monitored with a precision of a few °C. Thermocouples (K or T type) have been selected among the various sensors since their wide diffusion, easiness of use and low cost. Order of 10 electrical insulated thermocouples shall be employed for each 300m tube section. The control of temperature will be achieved using one local controller unit for each power supply unit (AC/DC converters essentially, but also heating tapes on tube links and pumping stations).

All the thermocouples and the controllers will be connected by a serial bus line to a remote computer, from which it will be possible to drive the bake out changing temperature set points and control parameters. The temperature control system shall be used also during normal operation.

Many additional thermocouples, not necessarily connected to the remote computer, will be present essentially on the first 300 m tube section, to allow occasionally detailed measurements.

The bake out of each 300 m tube section during the installation phase will be performed by a AC/DC converter supplied by a diesel generator movable along the tunnel.

Another function required to the bake out system is to heat the tube in winter to avoid temperatures below +5°C. It shall be fulfilled by a single AC/DC converter placed in the center of tube (TBC) supplying 1100 A at 60 V, when tunnel temperature will be -5°C.

In this situation some equipment will be kept at a voltage with respect to ground. This is not a problem (TBC), since the permanent pumps in operation (Ti sublimators and ion pumps) should not suffer ground problems; vacuum gauges, on the contrary, will have to be operated switching off the heating system for a while.

31.6.6 Thermal insulation

A good thermal insulation will be installed on the tube external surface, about 24000 m^2, to achieve acceptable power losses during bake out. The principal technical requirements are:

- working temperature = 200°C
- indoor environment employment
- limited dust emission in tunnel.

This last requirements needs explanations: the tunnel will be not a particularly dust free environment (an airborne dust concentration of 1mg m^{-3} typical of clean workshops or country environment can be taken as reference), and in order to avoid its pollution (significant increase of dustiness) extraordinary precautions are not necessary (see also VIR-NOT-PIS-6300-100).

Felts of fibrous materials (rockwool, glasswool) have been selected for their low cost and good performances in the specified temperature range, despite their high fiber emission (6÷9 μm diameter, 10÷50 μm length; typical airborne concentration during installation less than 1 fiber cm^{-3}).

To avoid pollution of tunnel by such dust the thermal insulation will be installed on the modules in a dedicated hall, and a proper sealing sheet will be used as final layer covering the fibrous material. Then each module outer surface will be cleaned from dust with a proper plant (see 3100.6.1.) before introduction in the tunnel .

What up to now described concerns the insulation of tube stiffened part. In fact being bellows (and other minor parts as end caps, pumping stations, links) insulated only after that modules are assembled inside the tunnel, their insulation has to allow a "clean installation". The two kinds of insulation are below separately described.

The tube stiffened part will have a very thick insulation, realized with two overlapping layers to achieve high efficiency and good temperature uniformity: a power dissipation of 150 Watt per linear meter of tube (room temp. of 20°C) has been used in dimensioning.

This reference solution, well explained in a draft insulation technical specification (VIR-TRE-PIS-3100-105), includes two layers of rock wool felt (density 70-100 kg/m^3, thermal conductivity 0.045 Watt m^{-1} °C at 100°C) for a total thickness of 150 mm. The finishing layer will be realized by a thin felt (20-25 mm) of glass wool treated with thermo-hardening resins and faced on the outer layer with a foilskrim-kraft paper. Then a foilskrim kraft adhesive tape will be used to seal the joints and a zinc plated (TBD) net mesh will be used as final layer for mechanical support.

The above described solution has been experimentally tested; slightly higher power losses than estimated have been found. Hence the safe value of 175 W m^{-1} (at 20°C room temp.) has been assumed as requirement for the insulation effectiveness.

Insulation of bellows (and minor parts) will be realized with mattresses of glass-wool enveloped and quilted in an opportune cloth (Aluminum-glass cloth). The insulation of bellows will be dimensioned taking into account the higher dissipated power.

31.6.7 Assembly

The assembly activities are subdivided into Stages. Each stage includes a set of activities which result in a defined condition of the items involved. The Stages are subsequent one to each other, but only from the logical point of view and not from the planning point of view. The Stages described below are relevant to all items.

31.6.7.1 Modules and Supports preparation

This Stage includes all the works to be done prior the modules, the bellows sections and the supports are entered into the tunnel for being installed in their assigned positions.

Handling of Modules in this phase shall be done with bridge cranes equipping the yard service area (fig. 3100.5); mobile crane can be used only outside or, in case of need, inside

Hall A, after approval and under direct control of Virgo supervisor. Modules are to be handled only from the indicated lifting points and to be rested only onto their built-in feet: no other parts of the items shall be in contact with hard bodies.

Handling of Bellows Sections shall be done through lifting rings or hears equipping the protecting caps, when bellows axis is vertical; when axis is horizontal the same rings or hears may be used or the bellows can be hang by fabric slings.

Modules after arrival to site are removed from truck and stored in Hall A. Care shall be taken when removing outer canvas in order to avoid heavy contamination of modules outer sheathing.

Unpacking of modules from packing sheaths is done before bringing them in Hall B for being equipped with thermal insulation panels. Major debris from thermal insulation installation shall be removed from equipped modules prior to be transported to the "module cleaning" plant (fig. 3100.6).

Modules are then driven into Assembly building for a final overall check, mainly a verification of not having received knocks and be free of indents. The protective cover wrapped around caps are here removed, but the metallic covers are still left in place.

In the same Assembly building modules shall cue for entering into the tunnel.

31.6.7.2 Supports installation and alignment

Supports are installed prior to modules. Their position is defined with reference to the axis traced in each tunnel by the geometers. The axis is defined by means of monuments located every 300 m in correspondence to the superfixed support position of pumping modules (Fig. 3100.9). They are referred to the GPS (global positioning system) and theodolite measured monuments of whole plant.

From the "300 m" monuments 19 inter-points equally spaced at 15 m are located: they are for identifying the fixed support location of each support block modules (Fig 3100.10). Therefore the position of first support is the one of "link section" module located on tube side after the large valve DN1000. To be noted that first monument will not be 300m distant from next, but 15 m closer; more, its exact location will be defined from design position of beam splitter tower center reference. The reference marks and the axis will be used to locate the actual tube axis, in terms of lateral straightness and level (Fig 3100.10). The expected precision of traced axis from references marks is better than ±1 mm in all directions.

Support will then be installed based on such references. Base plates will first be bolted to concrete floor, then posts will be laid on them and finally the support block will be installed. The fine positioning of supports will then be executed in all three orthogonal direction: along tube axis, transversally and vertically. Precision of positioning with respect to marks on floor is expected to be better than ±1 mm in all directions. (Fig 3100.11)

Once supports are aligned the mobile part will be pre-bent. Value will be the one corresponding to average temperature of module being installed. Three supports blocks at least are expected to be installed in advance of modules.

31.6.7.3 Section assembly and welding

Modules are set down onto a dedicated trolley by the bridge cranes and are driven in the tunnel to their final destination.

Before the arrival of the module the area around its final destination is to be cleaned from minor dust by means of industrial vacuum cleaners: no brooms are allowed for this operation.

Once arrived in face of the final destination the module's bellows is compressed by means of the proper device for allowing easy assembly and fit-up.

The module is thus erected onto the supports by means of the proper device. The module alignment relies upon its manufacturing tolerances and the support alignment precision for the vertical and the transversal directions. The module axial direction precision can be improved adjusting the module final position with respect to the tunnel reference marks (Fig. 3100.12). After this operation, the erection device is removed from the area, and the alignment of the module can be checked installing the optical targets and relevant target holder onto the foreseen locations onto feet. The tolerances for alignment and the operating procedure are to be defined (TBD).

Once the alignment is checked a protective tent is positioned around the fit-up area. The facing covers of the already installed module and of the one just arrived are dismantled only when the two lips are facing and before releasing the bellows holder. Tolerances for fit-up are of the order of 0.3 mm mismatch, for performing a sound weld. The correct fit-up can be achieved operating onto the bellows compressing device and onto the screws and slides provided on the mobile support; the fixed support position shall not be modified in any case (Fig. 3100.13, 14, 15 and 16).

After the fit-up operation is completed and the lips eventually tack welded, the welding robot is installed and operated. The welding is done under the protective tent. The robot is then removed and laid down into its proper protection against dust; the protective tent may remain in position waiting for the next module.

Initial and Pumping Modules of each section receive welded End caps for section leak testing. The installation and welding of the caps are to be done under the protective tent and the fit-up procedure is to follow the indications above.

Pumps and instrumentation are installed as the Pumping Module is set in place and welded.

31.6.7.4 Section testing

Once the section is completed all welded lips are prepared for individual He testing.

The leaks found in the lip welds shall be repaired and the weld tested once more to demonstrate adequacy to UHV.

The section testing allows to verify the quality of the overall internal cleaning and the UHV level that can be reached.

After testing, the section is left under vacuum conditions (TBC).

31.6.7.5 Tube assembly

Once all 10 sections of the tube are tested they can be connected together.

Bellows sections are brought to final destination by means of the module trolley. Before carrying each of them to the final position, the two sections to which the bellows is to be welded shall be vented and the end caps nibbled off from both facing ends. Nibbling is carried out with the robot. The opened tube is thus covered by a clean transport cover. The end caps are recovered.

Once each Bellows section is brought face to its final position it is handled by means of the installation device and it is compressed by means of the proper device for allowing easy assembly and fit-up. The hard metallic covers are now removed from the Bellows section but the aluminium protection sheets are left in position. The bellows is then driven in between the two facing sections, the protective tent is put in place and the fit-up operations may be performed. One lip couple is initially fit-up, trimmed and welded; the other is similarly treated after the operations on the first is completed. Trimming is done by means of the nibbling robot to the standard welding diameter.

All the 11 bellows sections are to be installed to complete the Tube.

31.6.7.6 Tube acceptance testing

Once completed the Tube, all welded lips of the bellows sections are to be prepared for individual He testing.

The leaks found in the lip welds shall be repaired and the weld tested once more to demonstrate adequacy to UHV.

The testing also allows to verify the quality of the overall internal cleaning and the UHV level that can be reached.

After testing the entire Tube is left under vacuum conditions.

31.6.8 Test of 300 m sections

31.6.8.1 Introduction

The strategy of the assembly foresees a development section-by-section in order to start the vacuum operations as soon as possible all along the period of the whole installation, almost two years.

Once assembled, the first 300 m section is prepared for the leak search and the vacuum test. For this it is equipped with two vacuum-tight covers, lip-welded by the robot at both ends, and the proper pumping system which consists of an instrumentation group, an intermediate and a permanent pumping group, all of them connected to the section through all metal gate valves.

Given the large volume of the section, ≈340 m^3, it is convenient to establish 2 days to bring the pressure from the atmosphere down to 10^{-1} mbar. For this a movable roughing group is foreseen (see 3400.4.5.1.) to be connected to the section through a valve placed on the covers CF 63 port.

Every section is prepared for the tests in the same way as soon as assembled.

31.6.8.2 Leak and Vacuum test

The intermediate pumping group is realized by means of a hybrid 1000÷1500 l s^{-1} turbopump backed by a mechanical oil free pump, 25÷30 m^3h^{-1}. Between the two pumps, a leak detector that can detect a lowest leak rate of 5 10^{-11} mbar l s^{-1} is connected through a valve. This arrangement allows the leak detector to provide sufficient sensitivity leaving the section protected by its own vacuum system against any contamination from the leak detector, if any.

The evacuation starts with the movable roughing group. It is important to prevent any risk of contaminants, switching-on the hybrid turbopump around 10^{-1} mbar before the roughing group works close to its ultimate pressure (10^{-2} mbar). Due to high pumping speed now, the pressure should decrease in brief time in the range 10^{-5}÷10^{-6} mbar with the typical profile that depends upon the gas evolution from the inner surface of the chamber, essentially water, unless the leakage of one or more big leaks in the section determines a stop at a higher constant value of the pressure proportional to the leakage.

Anyway at this stage the leak detector vacuum system can be operated through its own vacuum pumping and the valve of connection opened.

The inspection with a Helium spray probe starts step by step from the first to the last lip-weld of the section, all of them performed during the assembly and then never tested before. Each circumferential weld is properly bagged and the individual bags are sequentially filled with Helium during the test.

If a leak is found in one lip weld, it is necessary to localize at which point of its 3.8 m length the leak is, and this can be done with the help of the He spray probe while removing the circonferential bag step by step.

Leaks from 10^{-1} mbar l s^{-1} down to possible minimum values can be found and repaired after a full section venting and a new evacuation. Smaller leaks down to 10^{-11} mbar l s^{-1} are more difficult to be evidentiated due to the high level of the total pressure in the limit of sensitivity of the leak detector.

When the pressure reaches the range of 10^{-6} mbar the system has to be heated via Joule effect at 150 ^{0}C according to the bake-out specifications.

The inspection with He is repeated when the bake-out cycle is over. Leaks down till the lowest detectable leak rate of 5 10^{-11} mbar l s^{-1} can be found. Eventual leaks can be repaired only after a full section venting and a new vacuum cycle including bake-out.

The test is finally over when the pressure and the determination of the outgassing-rate match the project requirements, namely $p<10^{-9}$ mbar and $Q<5\ 10^{-14}$ mbar l s^{-1} cm^{-2} for hydrogen. The instrumentation group contains a RGA which will be switched-on to check the actual gas composition. Without any leak, the non H_2 components of the residual gas (essentially

CO, CO_2, and CH_4) has not to overcome partial pressures of 10^{-10}mbar, to match the project requirement.

31.6.9 Leak and vacuum test of 3 km tubes

31.6.9.1 Tube Under Test

At this moment, the two large valves and the relative link-sections toward the towers (input-output) and toward the end-sections (first and tenth) are already assembled and tested as well. Therefore it will be sufficient to vent all the sections and to proceed with the insertion of the eleven bellows-sections, after cutting the lip-welds to remove the end-covers, and welding again the lip joints.

31.6.9.2 Leak and Vacuum test

The distance of 3 Km is between the two mirrors positioned in the input and in the output towers of one tube. The leak and vacuum test is performed between the two large gate valves in "closed" state, excluding the link-sections toward the towers and the towers themselves.

The evacuation starts with a movable roughing group connected to the tube-large valve link module (see 3400-4-1-1). As a matter of fact, for rough pumping, regular spacing of pumps along the tube is of no importance, and so a single movable unit, located in the central building, can operate to pump down each tube, one after the other.

As for the 300 m sections, it is important to prevent any risk of contaminants, switching-on all the hybrid turbo-pumps of the tube around 10^{-1} mbar before the roughing group works close to its ultimate pressure. The time should be again around 2 days, and again the pressure very quickly should decrease in the range $10^{-5} \div 10^{-6}$ mbar unless leakage be present somewhere. This time the leak detector is connected through the proper valve between the hybrid pump and the relative mechanical forepump of the section presenting the highest pressure.

The inspection with Helium is limited to the new lip-welds of the bellows sections starting from the closest one to the leak detector itself with the same method and sequence for sections.

Once the average pressure reaches the range of 10^{-6} mbar a complete bake-out at 150^{0}C (see 3100.6.3.) has to be performed. Before to start the heating, it is mandatory to evacuate also the two towers and the small link sections that connect the towers to the large valves. In fact this is the condition to heat the valves without any damage.

When the bake-out is over and the temperature decreased, the leak research can be pushed to find any lowest possible leak.

In the course of both pre- and post-bake outgassing rate determination, the beam tube is also tested for leakage by means of the residual gas analysis as measured by the RGA's in the sections. As soon as the total pressure measured by Penning or Bayard Alpert gauges reaches the range of 10^{-6} mbar in one section, also the relative RGA can be switched-on and the spectrum peaks can help to determine the approximate location of leakage, if any.

The tube vacuum test is over when the average pressure matches the values required by the project : $p_{ave} < 10^{-9}$ mbar and $Q < 5\ 10^{-14}$ mbar l s^{-1} cm^{-2} for hydrogen, and the residual gas composition in agreement with requirements.

31.7 Mode Cleaner Tube

The mode cleaner tube, the mode cleaner tower and the input tower constitute a special vacuum chamber isolated from the Virgo tubes and mirror towers by a window.

Putting the optical mode cleaner system into vacuum has roughly the same effect as the Virgo Vacuum system, i.e. to reduce the sources of noise which are :

- the acoustical waves,
- the thermal gradients on the optical path,

- the motion of dusts.

Vacuum contributes also to keep the optics clean.

The residual pressure allowed in the tube is 10^{-6} mbar.

The distance between tower axes is 144 m (Fig. 3100.8), the tube has a 300 mm diameter, and is composed of 24 standard modules (5.7 m long), one pumping module and 5 dilatation bellows.

One Ø 250 valve isolates the tube from the input tower.

Modules and bellows are Tig welded on site. The valves are linked to the tube by means of CF flanges with Viton gaskets. For introducing the tooling for the payload in the gallery of the mode cleaner tube there is a 5 m long dismountable tube.

The tube conductance is 23 $l.s^{-1}$ for air. The mode cleaner tube is pumped through the mode cleaner tower.

31.8 Large valves

Four large valves, at the extremities of each arm tube, allow to isolate 5 different volumes of the overall UHV system : the central part towers, the two long tubes and the two end towers. Work on every part can thus be done independently.

The nominal diameter of the valve is 1000 mm. The valve is a UHV gate valve with viton gasket for the flat. The link between valves and tube parts will be made with flanges with metal gaskets. They have to stand a 12 tons wall effect while keeping the required tightness. All the parts in contact with vacuum have to be made of stainless steel, and will have to be heated at a 400°C for the H_2 desorption, in order to reach 1.10^{-9} mbar for H_2.

Glass windows will be implemented at the center of the flats, to allow for light beam passage.

31.9 References

3100.1 M. Bernardini et al. - Virgo int. rep. VAC 010 D - 1994, Rev. 1995
M. Bernardini et al. - "Air bake-out ....", to be published on Vacuum
3100.2 M. Dialinas et al. - Virgo int. rep. - 1994
3100.3 Module tender documents. VIR-CFT-LAL-3100-113 and 115
3100.4 M. Dialinas - Tube calculation report - 1996

31.10 Figures

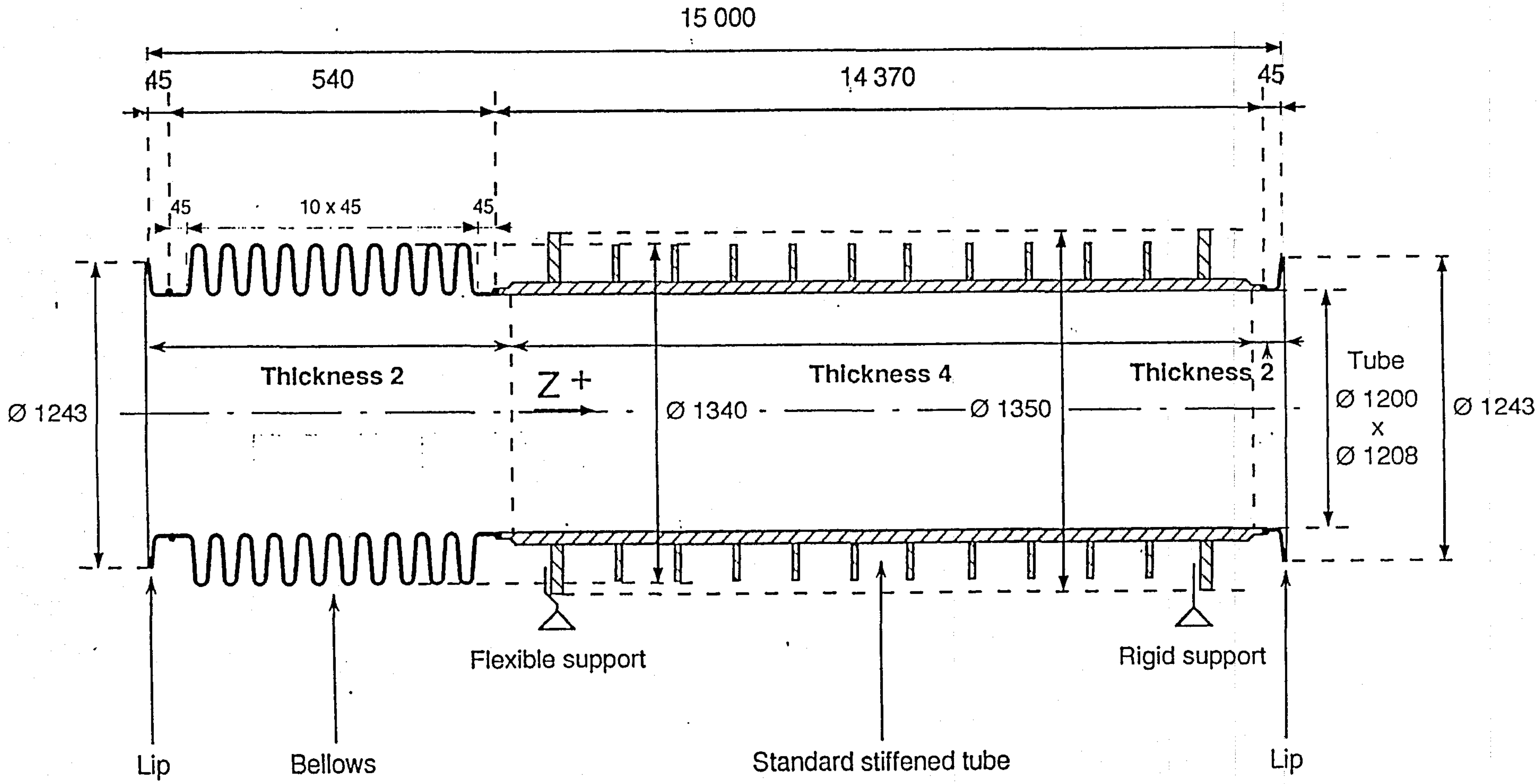

Fig. 3100.1 Standard module

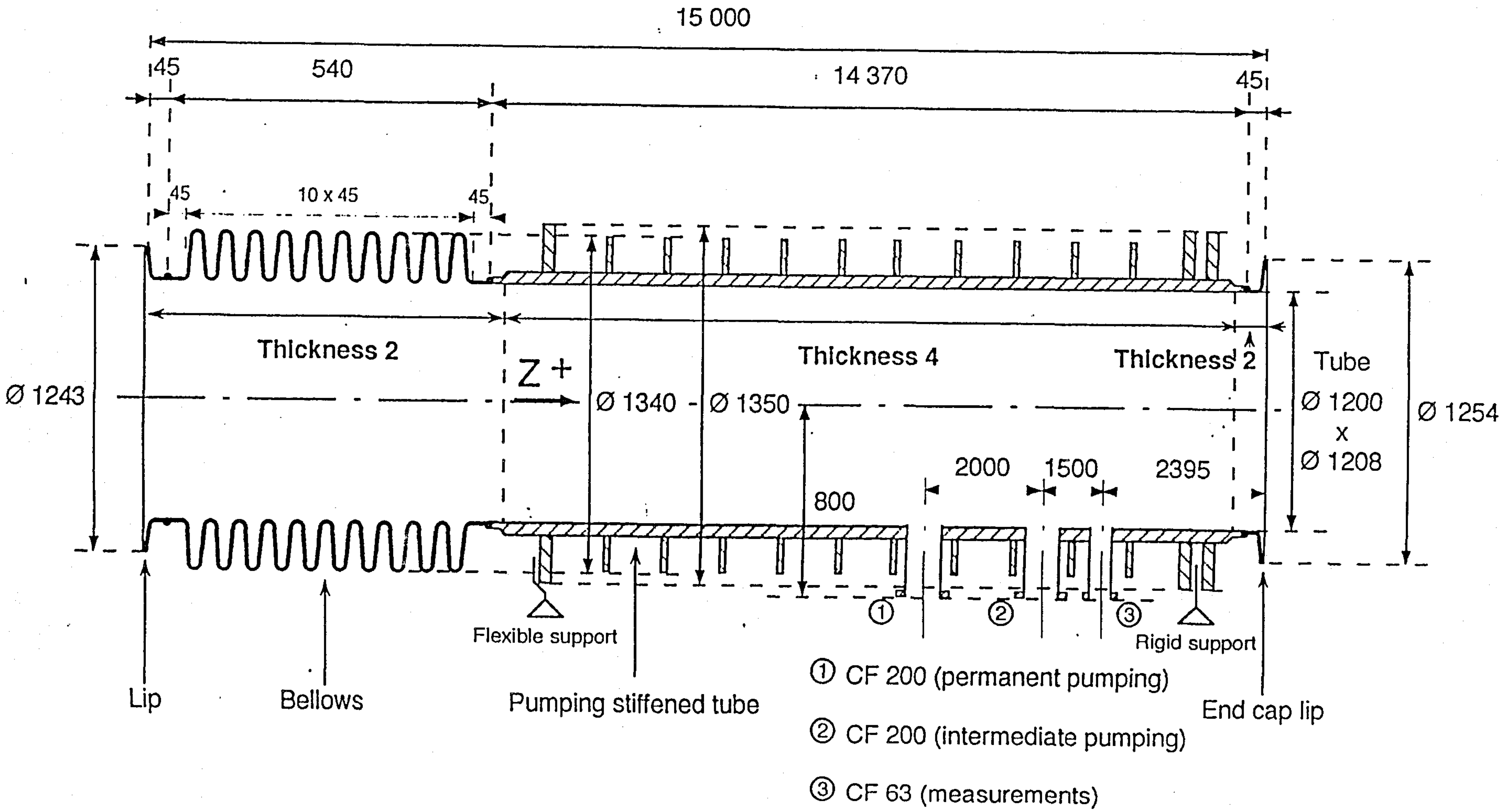

Fig. 3100.2 Pumping module

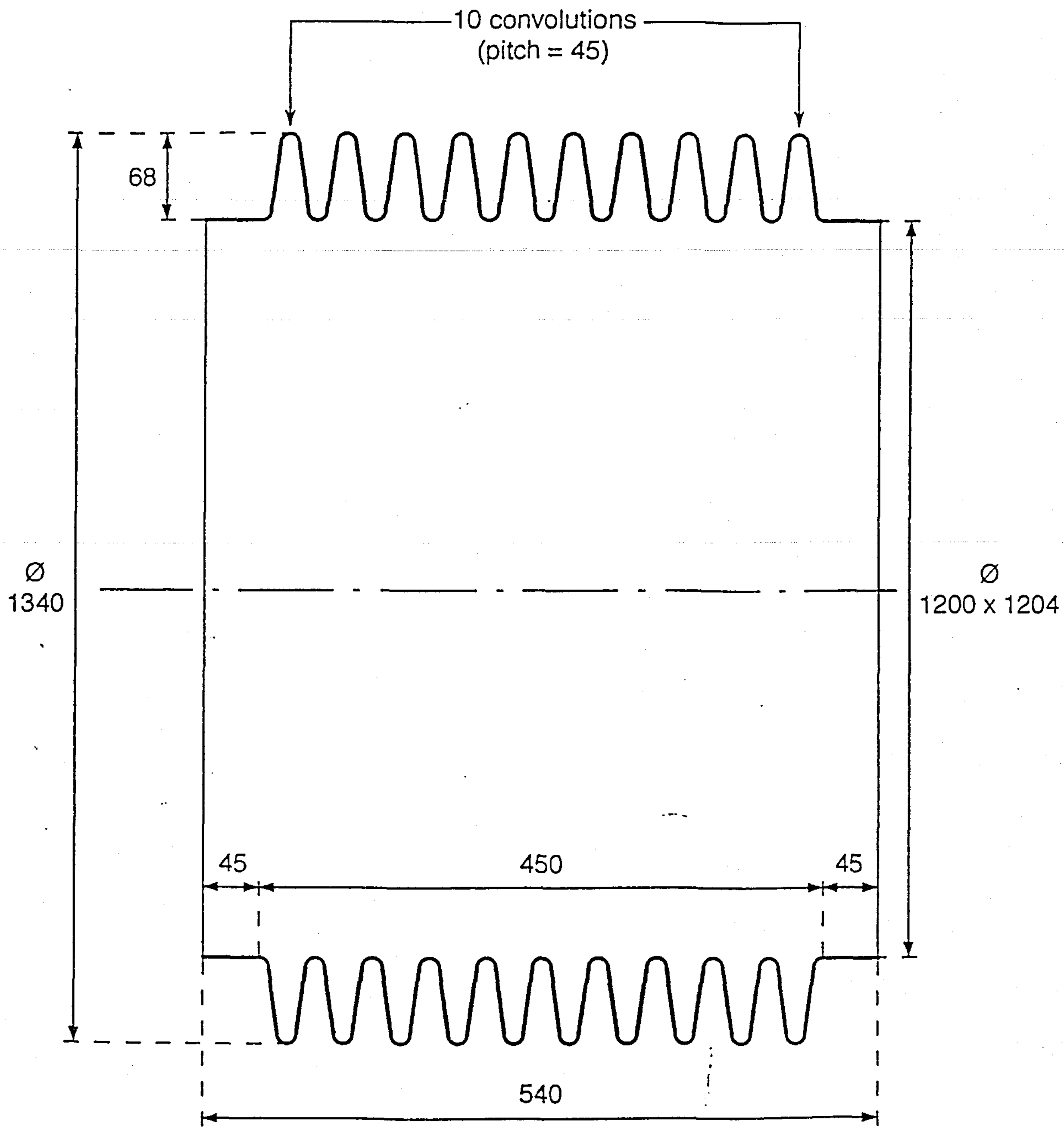

Fig. 3100.3 Bellows

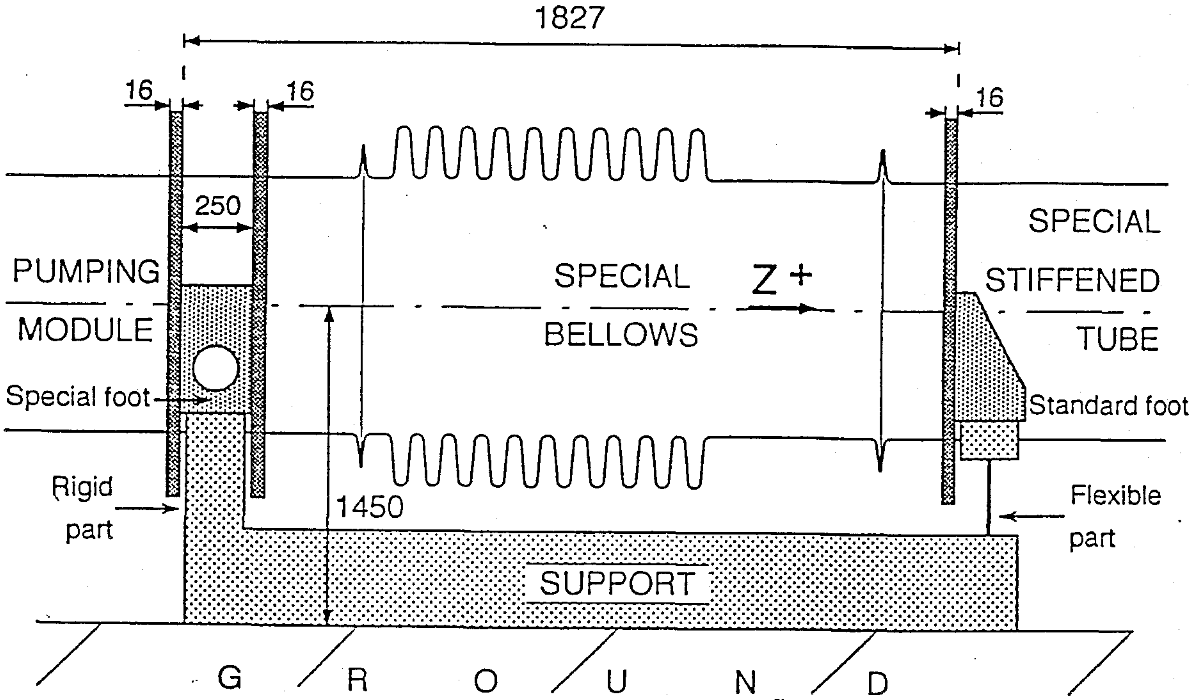

Fig. 3100.4 Feet and support conceptual scheme

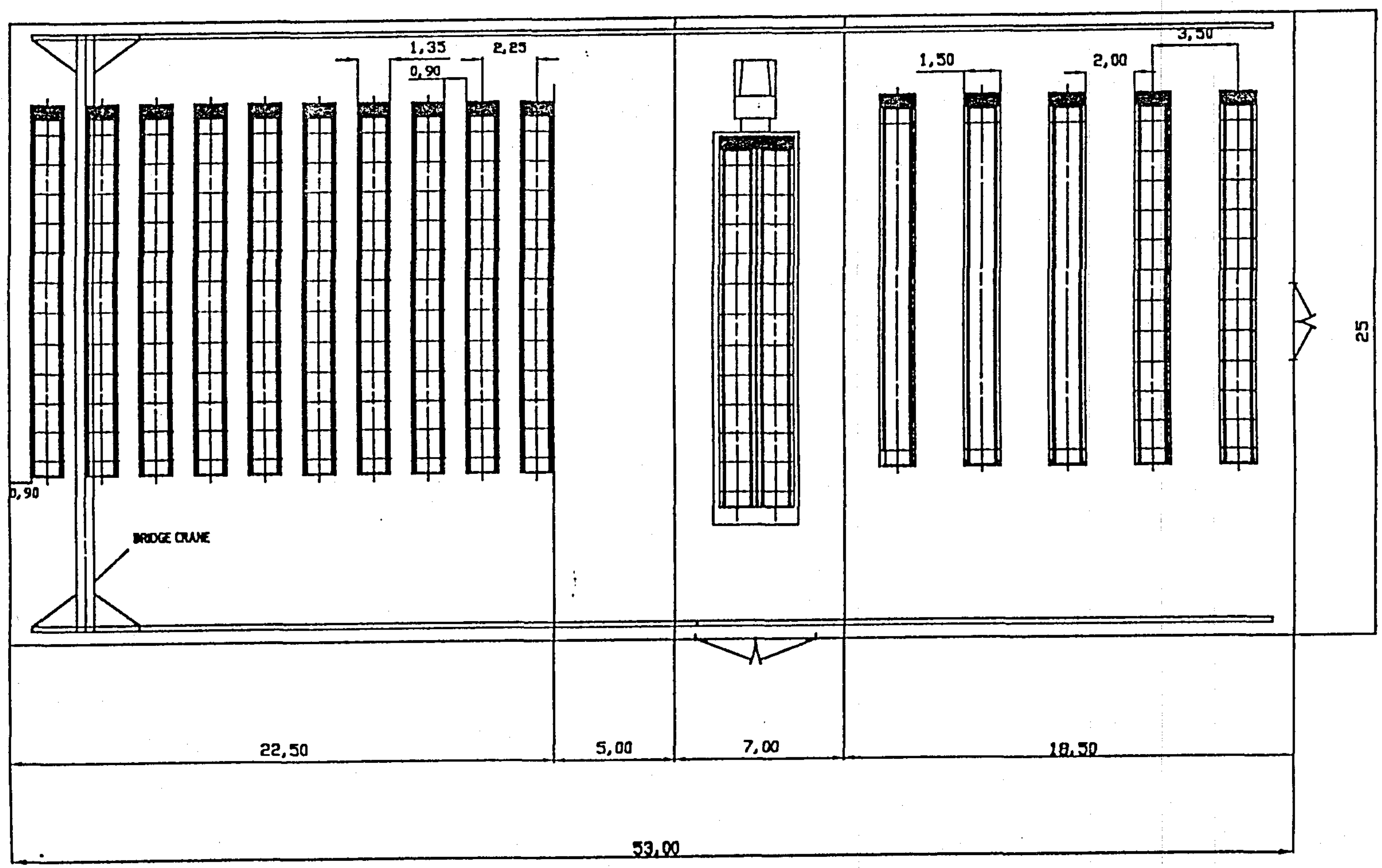

Fig. 3100.5 Building for tube modules reception and thermal insulation

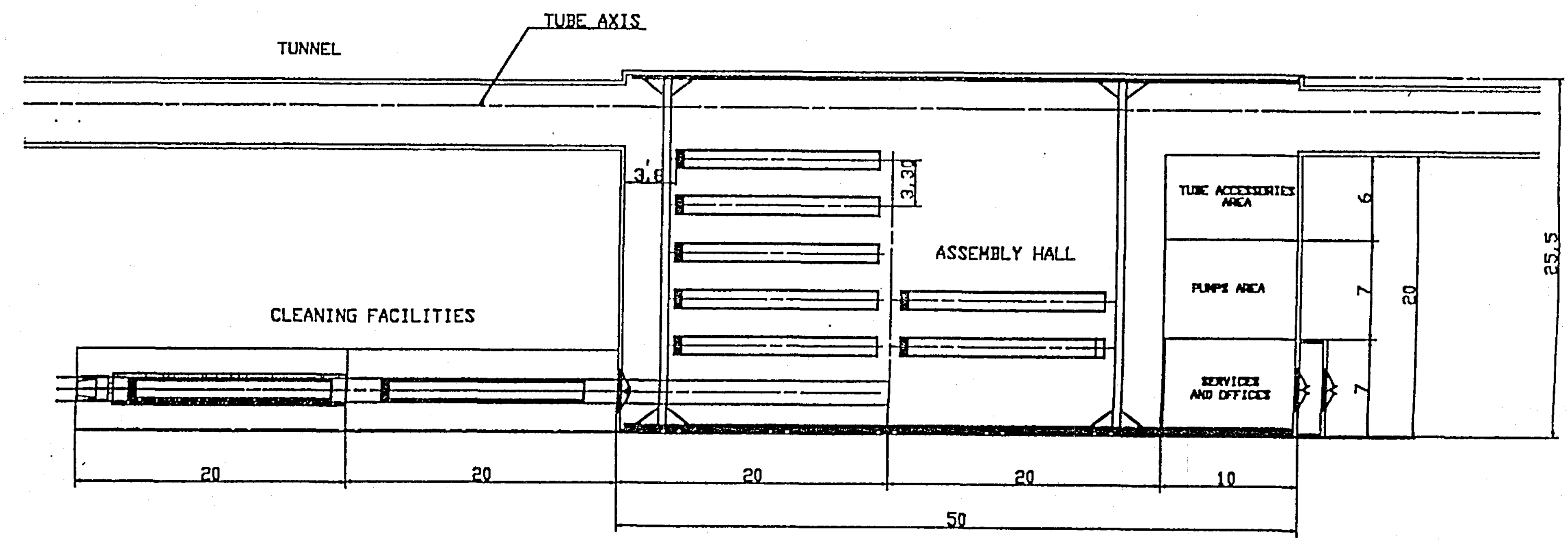

Fig. 3100.6 Tube assembly building

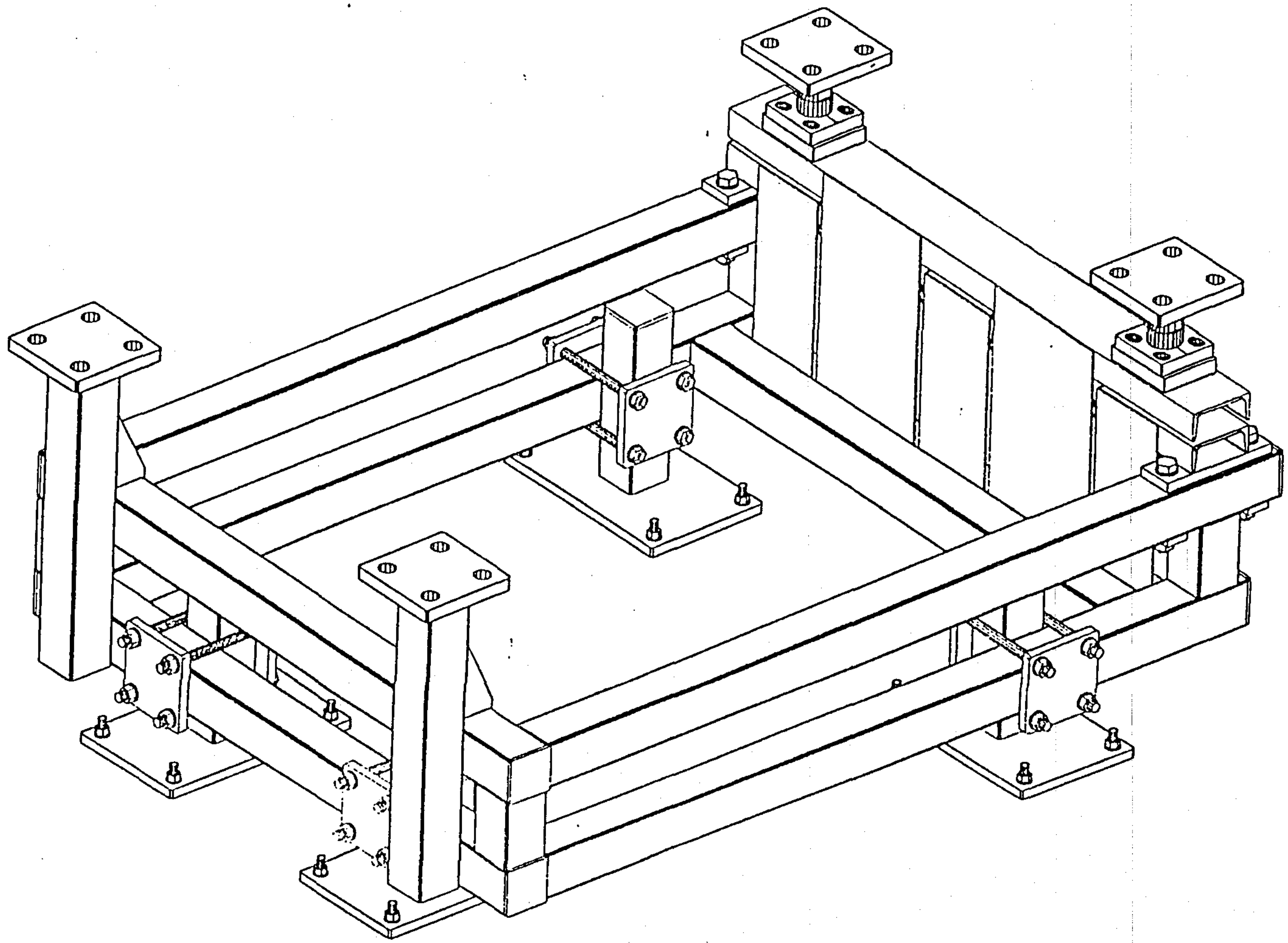

Fig. 3100.7 Tube supports, fixed and mobile

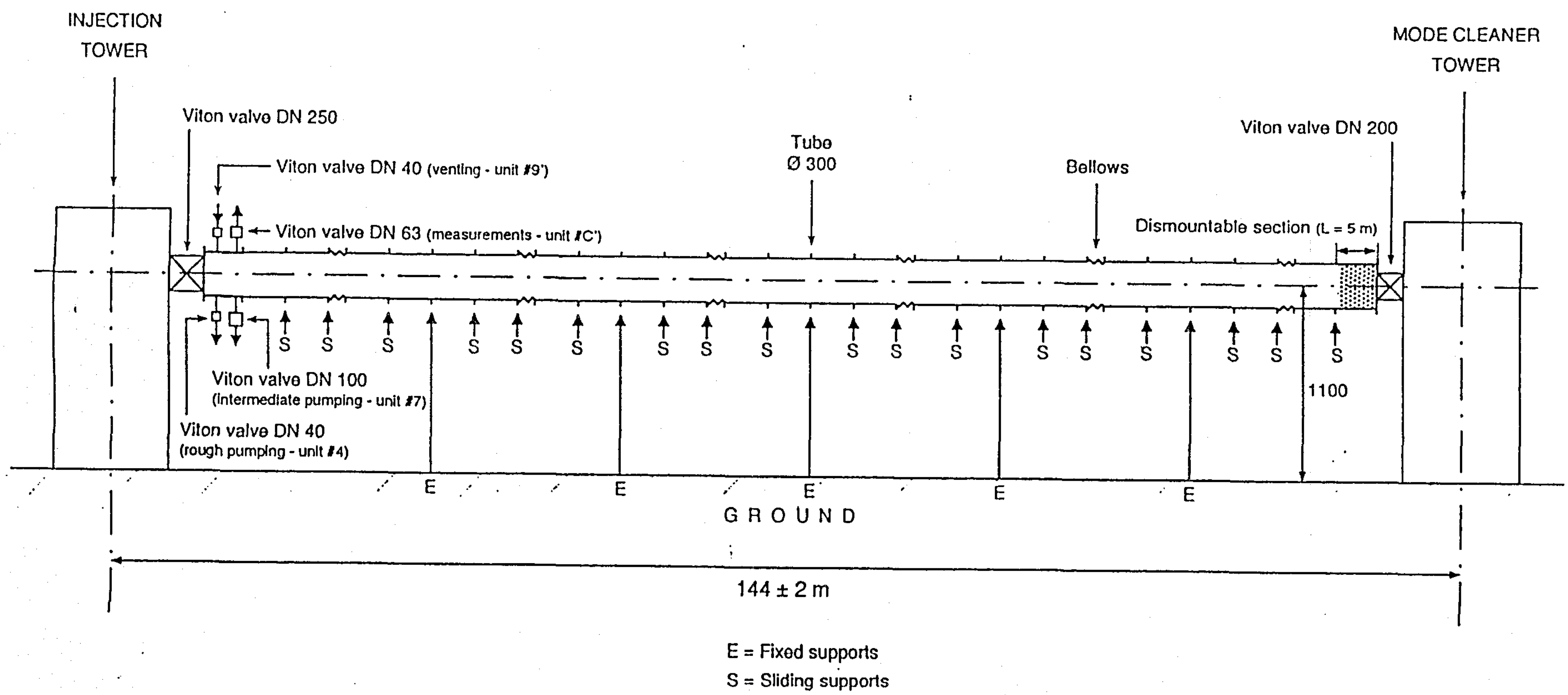

Fig. 3100.8 Mode Cleaner tube

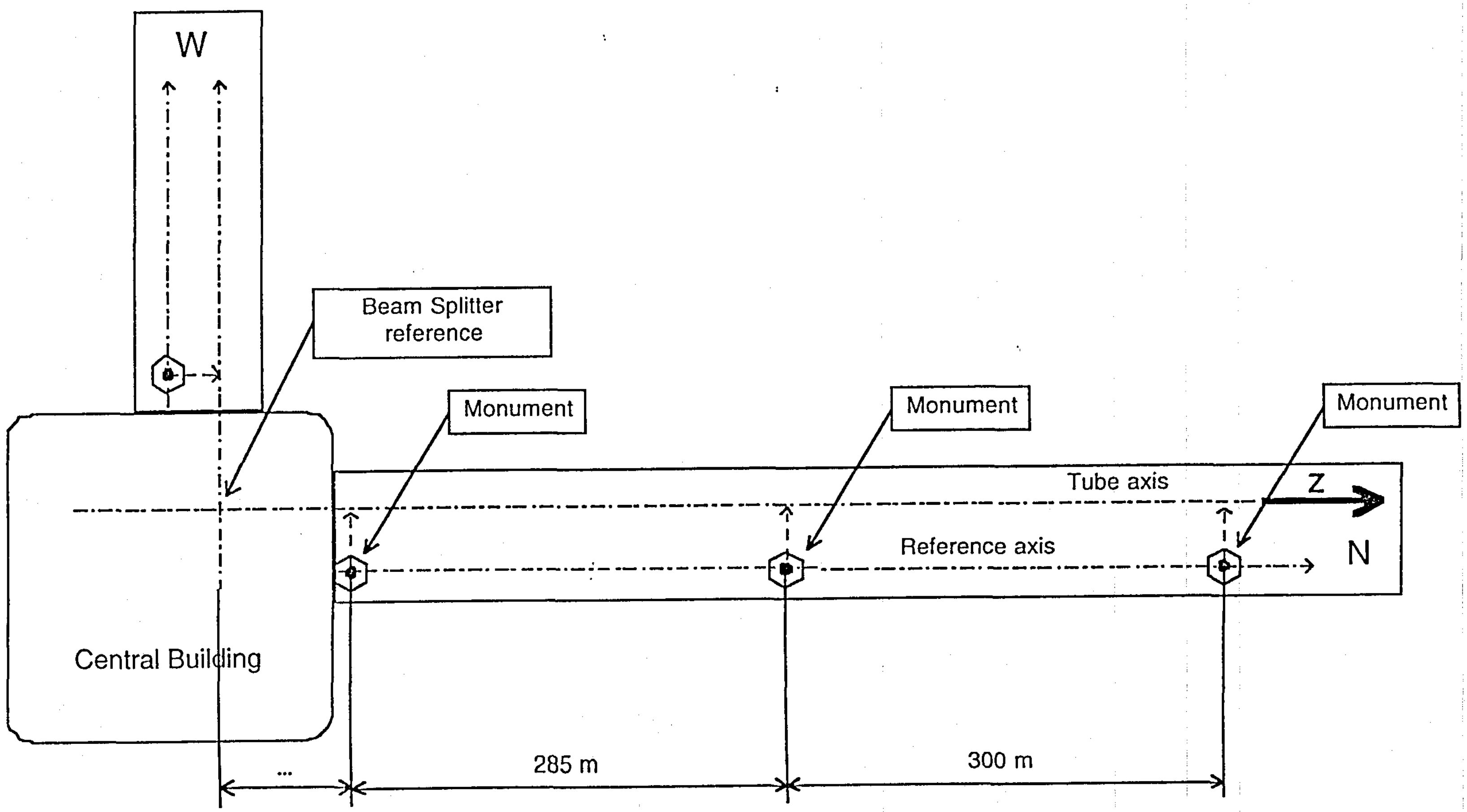

3100.9 Reference axis identification

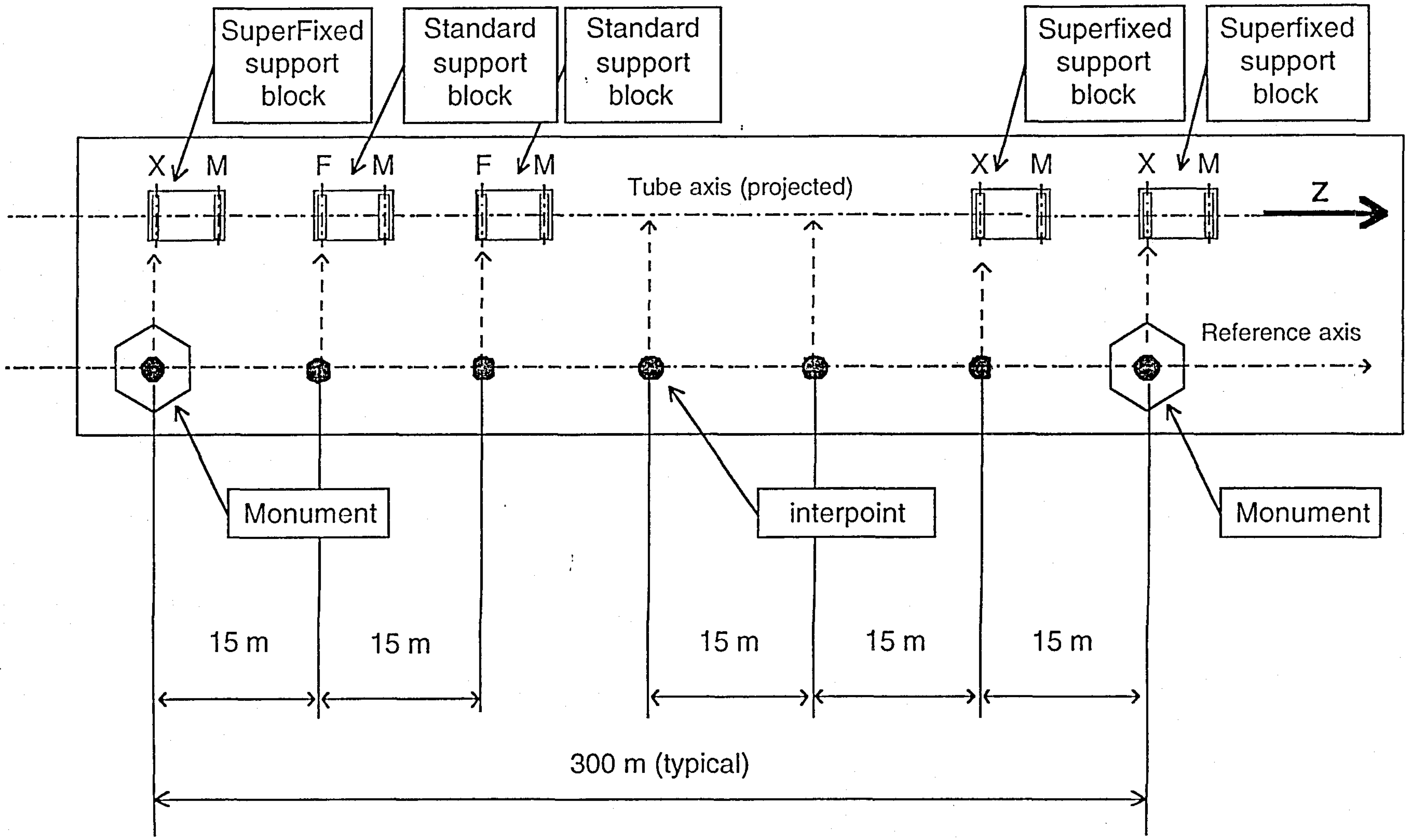

Fig. 3100.10 Support blocks position identification

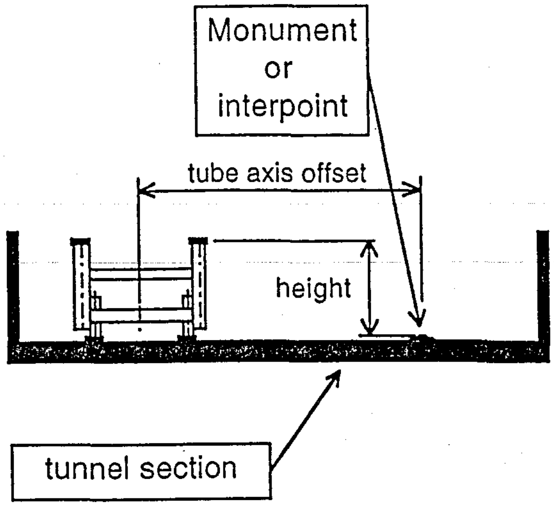

Fig 3100.11 Support alignment reference

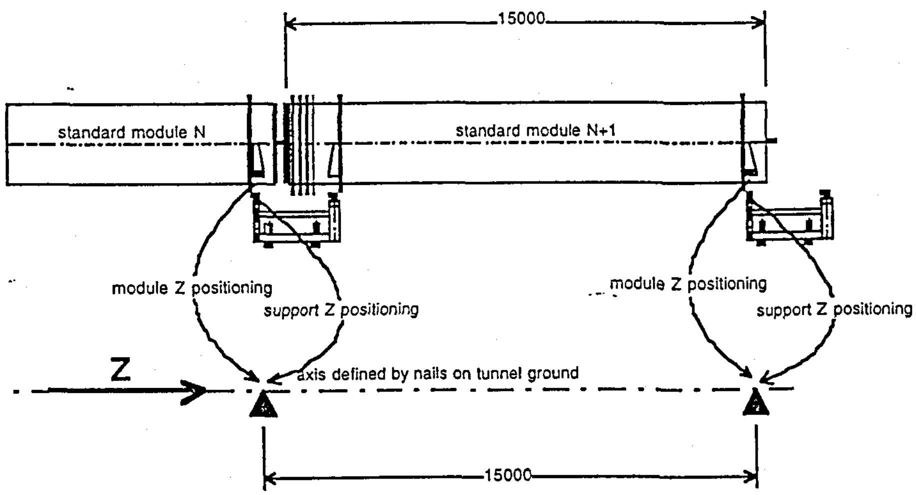

Fig. 3100.12 Supports and module positioning references

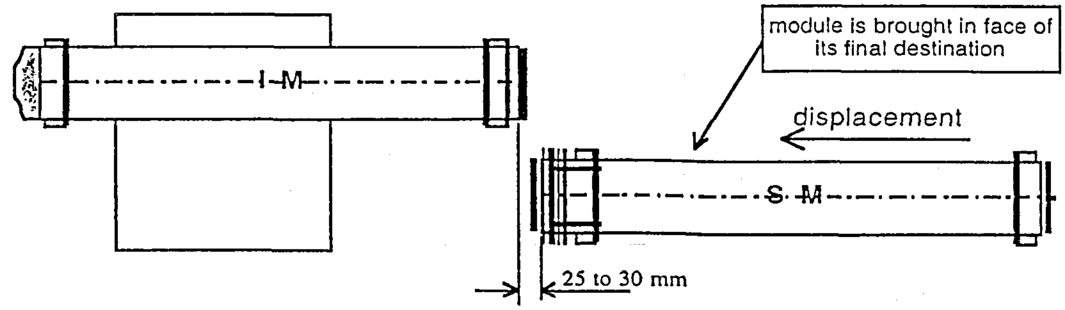

Fig. 3100.13 Modules connection (a)

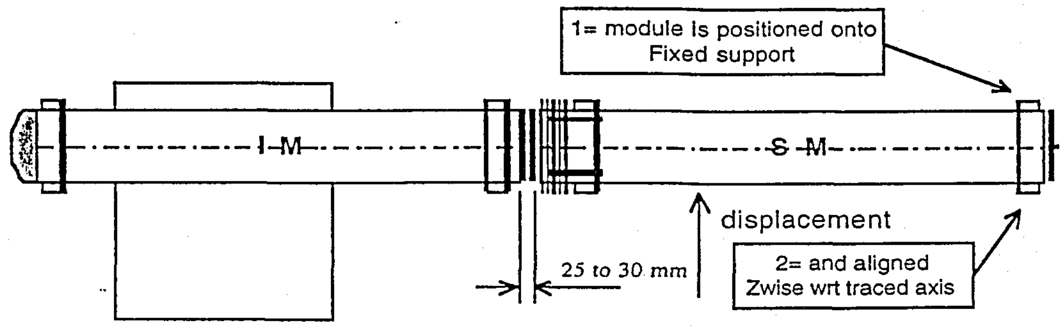

Fig. 3100.14 Modules connection (b)

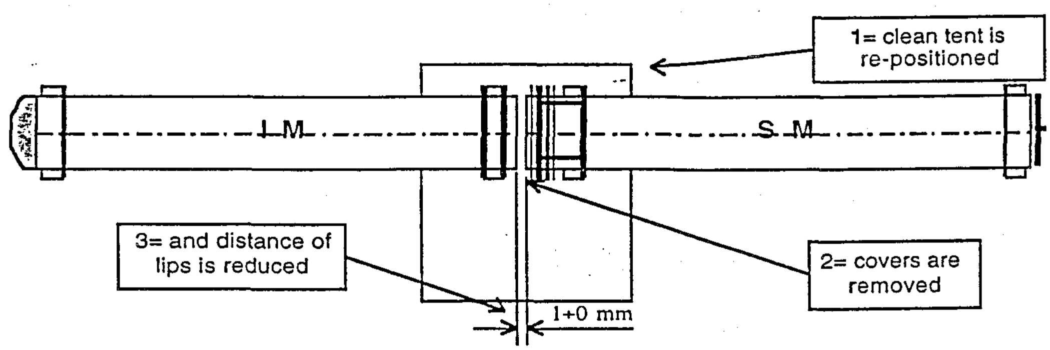

Fig. 3100.15 Modules connection (c)

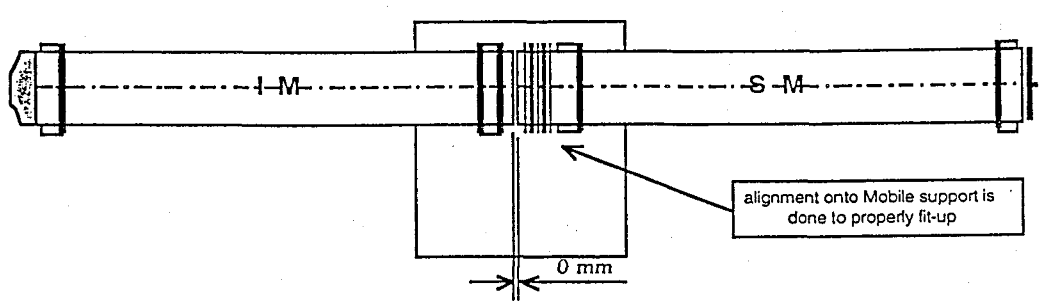

Fig. 3100.16 Modules connection (d)

32. Baffles

Table of contents

32.1 Introduction

The light scattered by diffusion off the mirrors of Virgo may be an important source of background, due to the possible recombination of scattered photons with the main beam : if these photons have been scattered by a vibrating obstacle, after the eventual recombination they may simulate an event. So these diffused photons have to be suppressed at a level such that the resulting noise be at least one order of magnitude smaller than the ultimate sensitivity of Virgo. This sensitivity, presently of $10^{-21}/\sqrt{Hz}$ at 10 Hz, can probably not be better than 10^{-23} after the improvements which can be foreseen in Virgo. So it has been decided that lowering the scattered light noise to $10^{-24}/\sqrt{Hz}$ shoud be satisfactory.

32.2 Scattered light in the long cavities

The reference solution consisting of light traps made of black glass, covering the whole solid angle, (Ref. 3200.1) which has been exposed in the 1995 Final Design, has been fully developed : a prototype has been successfully finished (with a 160° baking) and has shown that this solution is viable for Virgo.

A complete computation of the noise due to scattered light has been done analytically for all possible effects (Ref. 3200.2). In addition two detailed Monte-Carlo's have been performed for studying different baffle solutions (Ref. 3200.3) . The reference glass baffle solution has been found very efficient (noise $\sim 10^{-25}/\sqrt{Hz}$).

Nevertheless stainless steel baffles acting as deflectors rather than light traps have also been tried, and the final noise obtained is of the order of $10^{-24}\ \sqrt{Hz}$. So, taking into account the smaller cost and the larger strength of steel, it has been decided that steel baffles should replace glass except close to the mirrors, i.e. between the mirrors and the large valves, which is the most dangerous part. The spacing should follow the same rule, i.e. covering the whole solid angle.

32.2.1 Position of the baffles - Number of baffles

The whole solid angle must be covered: each baffle must be placed at the end of the shadow of the preceeding baffle on the tube, with of course a little recovering (fig. 3200.1).

The law for the z position is:

$$z_n = z_1 \left(a \frac{r}{r-h}\right)^{n-1}$$

where z_1 is the position of the first baffle and a is the coefficient for recovering, taken as 0.95.

All this geometry is symmetrical with respect to the middle of the tube.

If we want to house only one interferometer, the total number of baffles is about 90 per arm and about 120 for 2 interferometers.

32.2.2 Stainless steel baffles

It has been found that the shape minimizing the noise for these deflecting devices, is a cone with a 120° aperture angle oriented towards the nearest mirror (fig. 3200.1). The delicate point is the surface state : analytic computations have shown that the equivalent of a $1mm^2$ small mirror anywhere in the tube gives a 10^{-24} noise. This means that there should not be bright points on the surface.

The rugosity has also to be defined, since the result is sensitive to diffusion, reflectivity and absorption. These characteristics are being defined (TBD).

Another worry concerns the possible reflection on baffle edges. Even with a radius of curvature of the edge as small as $10\,\mu m$, the noise due to this kind of reflection is $\sim 6\ 10^{-25}$. A study is presently being performed in order to see whether cutting serrations on the inner edge of the baffles would solve the problem.

The possibility of mounting the stainless steel baffles at the module factory is presently being investigated. In that case, the baffles should be welded to the tube, possibly with the shape shown in fig. 3200.2.

32.2.3 Glass baffles between mirrors and large valves

The link between the mirrors and the large valves (the distance varies from 5 to 10 m) can be a dangerous part, since :

- the large valve diameter is only 1 meter and must be hidden to the scattered light.
- a bellows and vacuum ports have also to be hidden.
- the zone is close to the mirrors and the first 10 meters are quite harmful.
- in addition, if the distribution of scattered light at the emission is very peaked forward, the junction between tower and tube has to be protected.

So, two black glass light traps (fig. 3200.3), as described in the 1995 Final Design for the reference solution, will be installed in each of the mirror-tower links. These light traps can be described as follows:

A glass cone (45°) inserted in a glass cylinder allows the incoming photons to be reflected 3 times if they come from the left (on the figure), and more than 5 times if they come from the right. The reflectivity R of the glass surface has to be such that $(R)^3 \leq 10^{-6}$ which gives $<R> \leq 10^{-2}$. Geometrically, the baffle is oriented as shown in fig. 3200.1 for the first half of the tube (near the input mirror), and symmetrically with respect to a vertical plane ⊥ to the tube axis in the middle of the tube, for the end part of the tube.

A full prototype has been built and the manufacturing is now mastered.

32.2.4 Diffraction effects

The noise introduced by diffraction on the baffle edges can be quite small, provided that coherence effects due to a perfect radial geometry are broken : the beam must be slightly displaced off the tube axis (but the result is not very sensitive to the displacement) and the baffle should be slightly tilted with respect to the vertical plane, which will be done naturally by the construction imperfections.

For about 100 baffles in a arm, the noise is then $5\ 10^{-25}/\sqrt{Hz}$.

32.3 Scattered light and baffles in Central Area

Due to the number of optical components in the central area, it is impossible to compute analytically the noise due to scattered light.

A Monte Carlo has been especially developed, following the photons impiging on the different optical components in all their interactions with all the obstacles (tower body, link tubes between towers etc).

The results are exposed in ref. 3200.4.

For the construction of the interferometer, the constraints following from this study are:

- The diameter of the link tubes should be at least equal to 40 cm.
- In the 3 main towers: beam splitter, west and north input mirrors, the Ø 1000 windows seeing the beam should be covered by Ø 1200 coated glass circles with a centered Ø 200 hole (fig. 3200.4).
- In addition, in case a Ø 250 valve is used in the middle of the links, a Ø 400 coated glass circle, with a Ø 250 centered hole, should be inserted on each side of the valve.

Under these conditions, the noise in the central area is also between 10^{-24} and 10^{-25} m/√Hz at 10 Hz.

32.4 References

3200.1 V. Brisson - A solution for removing the scattered light, Virgo note 92/1
V. Brisson - Feasability of glass baffles, Virgo note 92/2

3200.2 J.Y. Vinet, V. Brisson, S. Braccini - Scattered light evaluation and calculation of the induced phase noise, Virgo note 95/26
J.Y. Vinet, V. Brisson, S. Braccini - Scattered light noise in G.W. interferometric detector : coherent effects, Phys. Rev. D54-2, 15/7/96 (1276-1286)

3200.3 a) I. Ferrante, S. Braccini - A Monte-Carlo for the calculation of noise by diffused light in the Virgo vacuum pipeVirgo note 96/18.
b) F. Bondu et E. Tournié - A Monte-Carlo for the calculation of the noise due to diffused light Virgo note (in preparation).

3200.4 S. Braccini - PhD thesis, 1996.

32.5 Figures

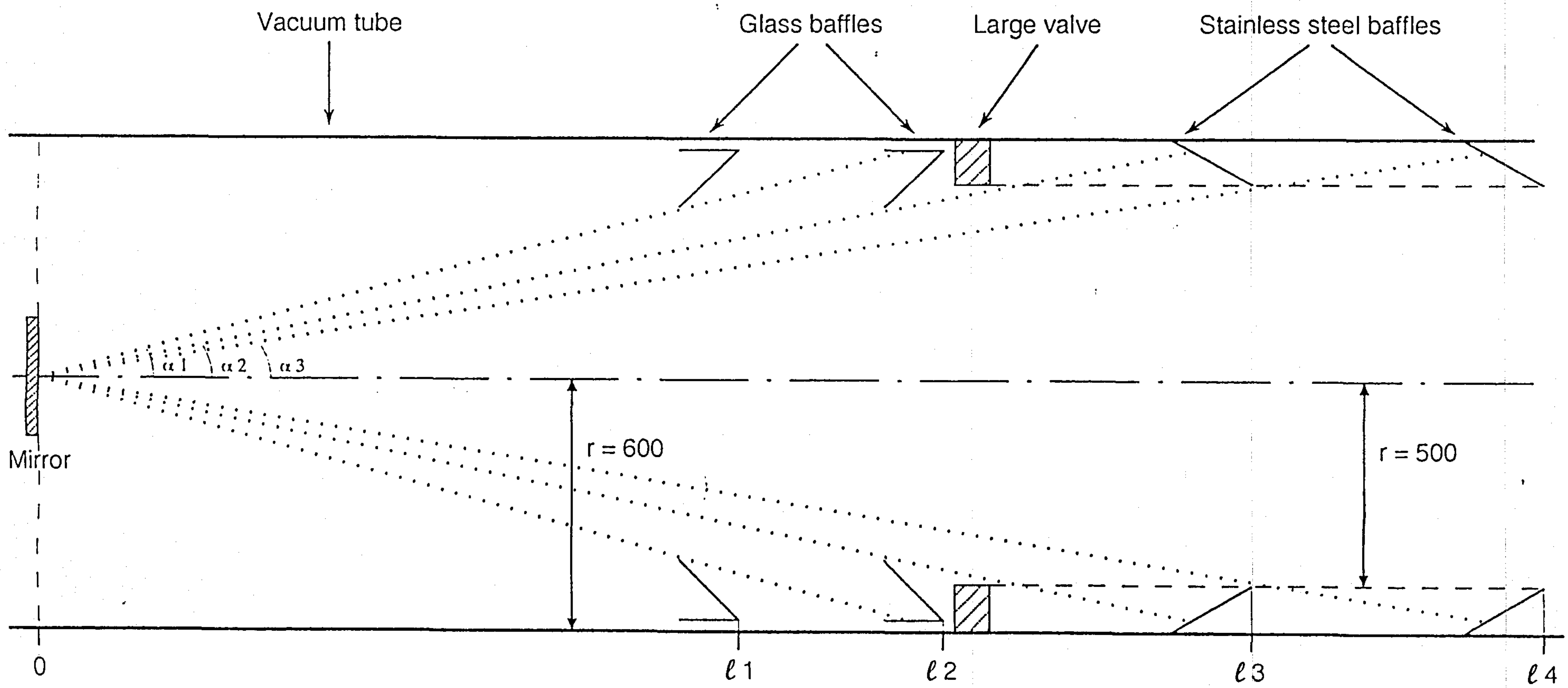

Fig. 3200.1 Working principle of baffles

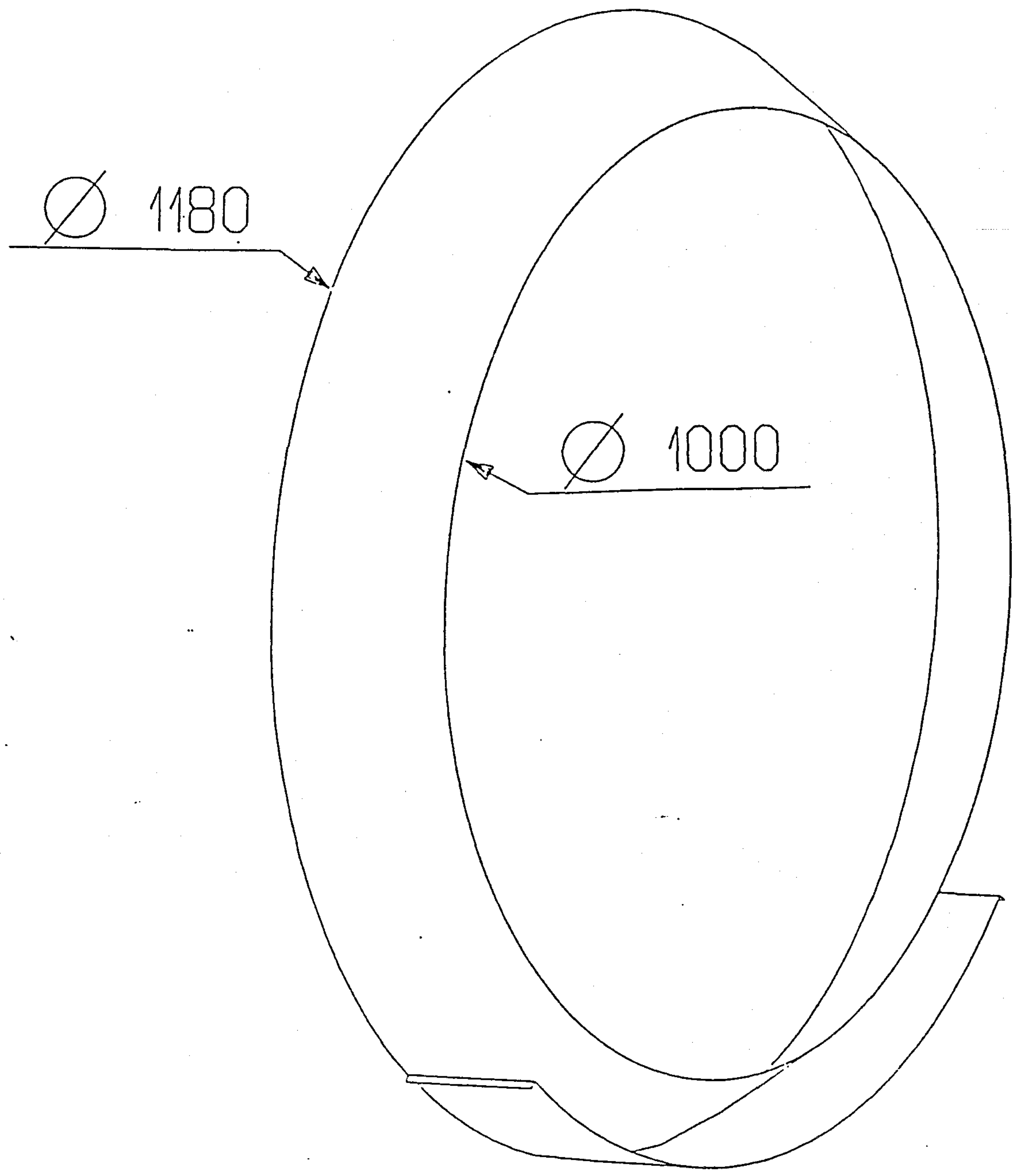

Fig. 3200.2 Stainless steel baffle

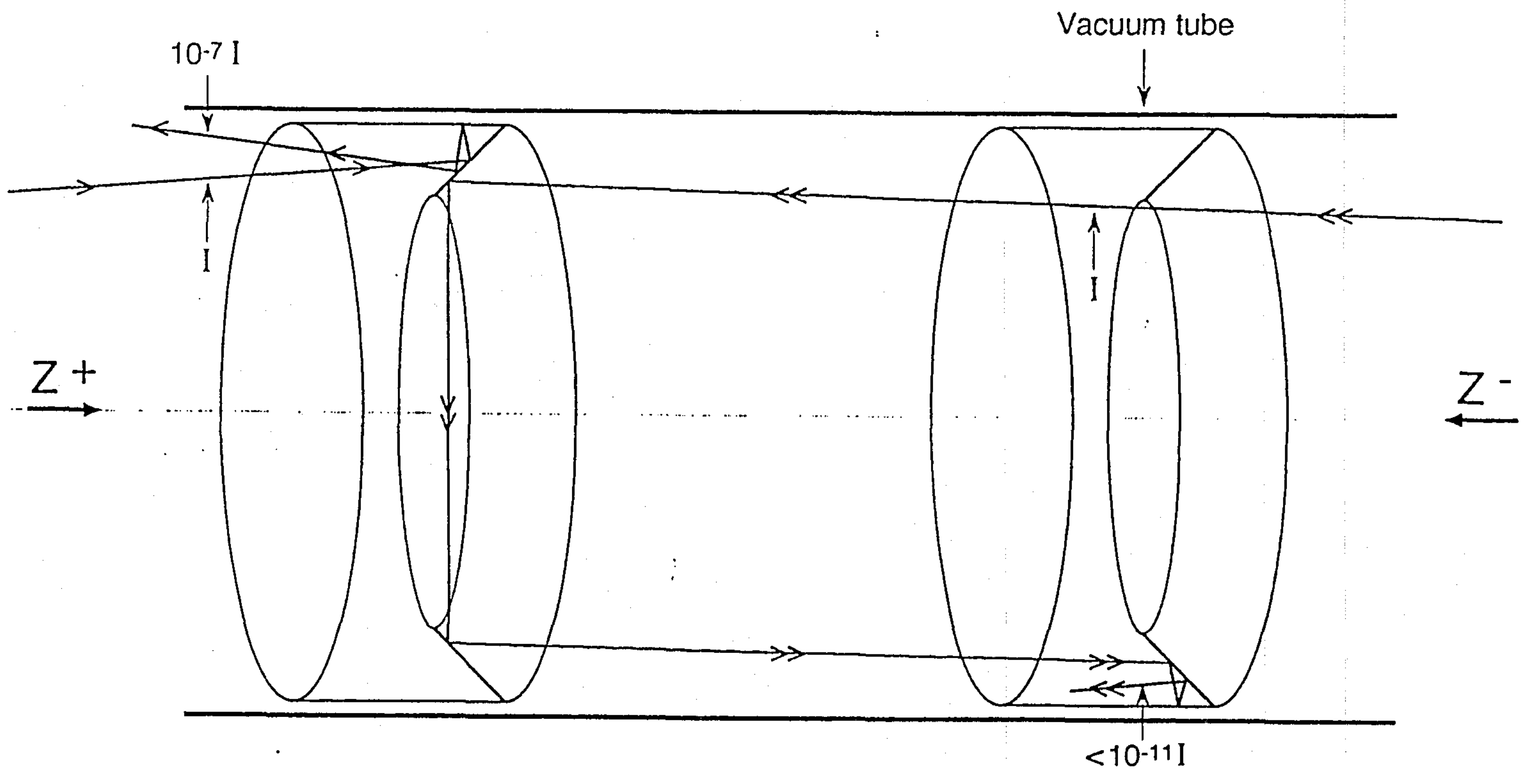

Fig. 3200.3 Glass light traps

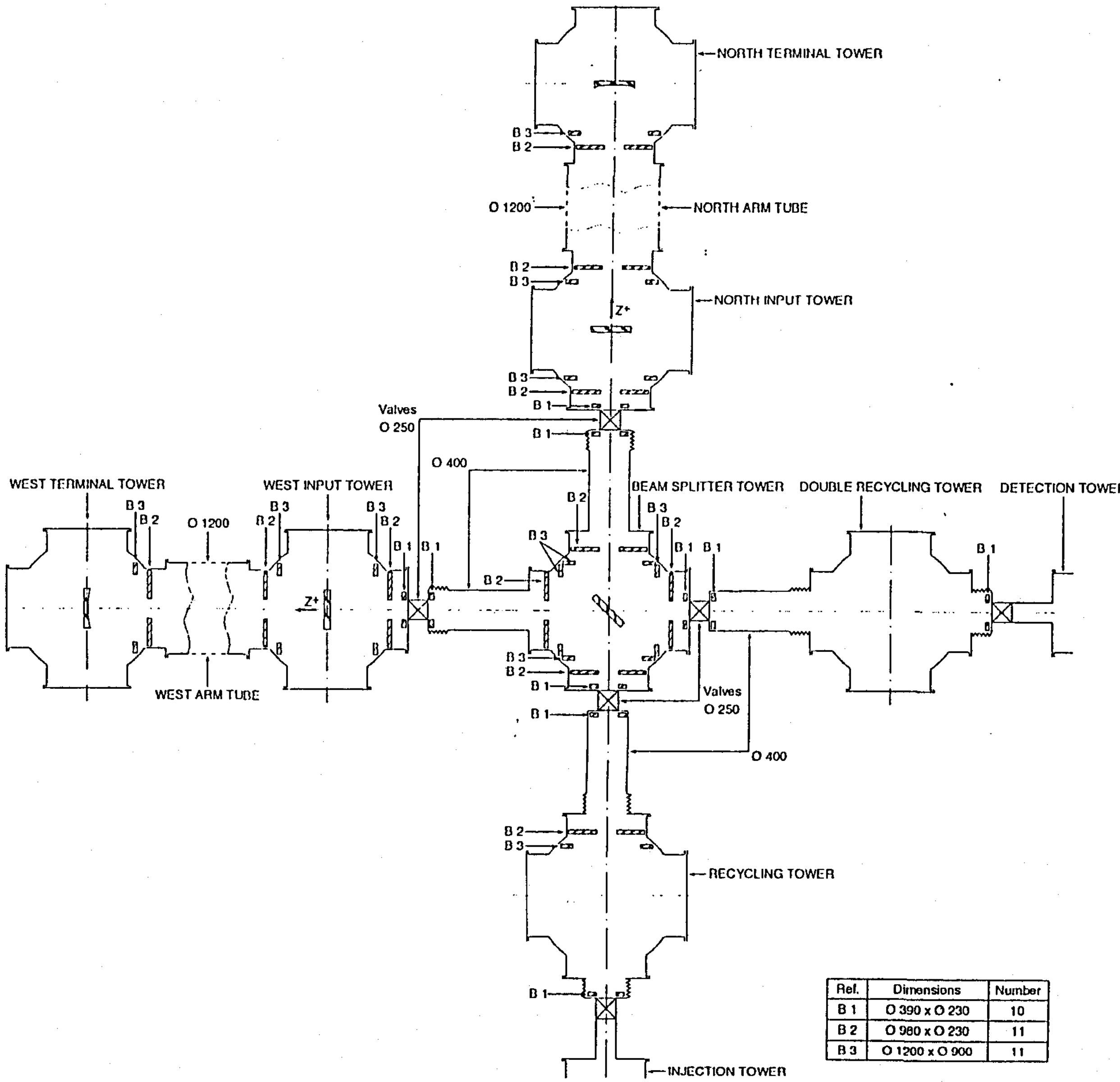

Ref.	Dimensions	Number
B 1	O 390 x O 230	10
B 2	O 980 x O 230	11
B 3	O 1200 x O 900	11

Fig. 3200.4 Glass baffles in central and terminal towers

33. Towers

Table of Contents

Introduction

Multistage suspensions are implemented in towers of various heights [fig.3300.1], depending on the locally requested seismic noise attenuation. The tower basement houses the suspended payload. It interconnects the interferometer arms, provides optical access for the component alignment and allows for the human access needed by the payload installation.

Seven towers are interlinked in the central building, three towers are linked at a distance from the central building. Towers are named according to their payload functionality [see table 3300-I]: input and detection, beam splitter, north / west input, power and signal recycling in the central building, north / west end and mode-cleaner in dedicated buildings.

In the following we review the construction design of the towers and of the central building vacuum system. The vacuum system assembly sequences are defined and a scenario for the clean installation of the interferometer components is described. The implementation of the services requested by the tower operation is sketched.

33.1 Specification

33.1.1 Experimental requirements

33.1.1.1 Tower positioning

The respective locations of the towers in the central building are determined by the details of the selected locking scheme. Provision has been made to allow for an asymmetry of up to 1600 mm between the two arms, allowing the displacement of the two input towers within +/- 400 mm. The power recycling tower can also be translated within +600 and -1000 mm.

Similarly the terminal towers positions can be adjusted within within +/- 1500 mm and the Mode Cleaner tower within +/- 2000 mm.

The beam height is set at 1100 mm relative to the building ground floor. Throughout this section, vertical coordinates (z) are given with respect to the horizontal plane which contains the beam.

As a consequence of the details of the beam propagation scheme and of the finite range of the suspension displacement mechanisms it has been decided to position the towers as shown on fig. 3300.2:

- Injection and recycling towers are translated with their links by 20 mm West with respect to the North Fabry Perot arm axis.
- Beam splitter and signal recycling towers are translated with their links by 20 mm North with respect to the West Fabry Perot arm axis. The link between signal recycling and detection towers is translated by 10 mm more, i.e. 30 mm. Detection tower is on the Fabry-Perot West arm axis.

These particular locations are accounted in the vacuum chamber design with off axed link connections as shown on table 3300-II.

The final positioning of the interferometer components is obtained in several steps:

1. Lower towers are aligned in the laboratory system using the lower tower square flange already taken as a reference for its realization at factory [fig. 3300. 4]. They are positioned within a few mm in the laboratory reference system. The horizontality of the flange is defined to .1mrad.
2. A tower is built with two vacuum compartments separated by a wall fedthrough by the suspension wire. The marionetta, hence the mirror position, is controlled accross this wall. It's geometry defines the first order position of the suspended payload. As a consequence, the wall is designed to allow for a fine tuning in position and angle with respect to the beam line.
3. Each suspension allows for the positioning of its optical component up to a few mm or mrad within the separating wall geometry.
4. The ultimate alignment is permanently updated by the control system which steers the interferometer components to a fraction of a wavelength acting on them via marionetta and reference mass.

The effective local position of a component is determined from outside the vacuum tank measuring the deflection of a well known additional laser beam. The implementation of these measurements requires the realization of optical ports pointing to the optical component. [see table 3300.II].

33.1.1.2 Decoupling from environmental noise

33.1.1.2.1 Seismic noise

One of the most remarkable and unique feature of VIRGO will be its high sensitivity for gravitational waves in a frequency band starting as low as a few Hz. This feature is achieved with the multi-stage suspensions, also called superattenuators. They reduce the seismic noise on the interferometer test mass in all the six degrees of freedom. As a consequence, the resonance frequency of the mechanical structure supporting the suspension has been pushed above 15 Hz, i.e. well above the superattenuator cutoff frequency.

33.1.1.2.2 Light losses

The light scattered off by the vacuum chamber walls or by the mirrors themselves may be an important source of background, due to possible recombination of scattered photons with the main beam. Absorbing baffles are thus foreseen inside the long arms and in the neighborhood of optical components.

The specifications on Fabry Perot optics limit diffusion losses on the coatings at the ppm level. To keep this performance, losses due to dust deposits have to be mastered at a comparable level. This consideration limits the mirror obscurancy factor (i.e. the ratio to the active surface, of the surface covered by dust particles) at the ppm level for a mirror set in operation.

Stability requirements on the index of refraction of the beam propagating medium and cleanness of the optics impose strong specifications on the vacuum chamber residual pressure. Partial pressures as low as 10^{-9} mbar for H_2, 10^{-10} mbar for other gases, and 10^{-14} mbar for hydrocarbons are required in the laser beam compartment. Such partial pressures can only be reached respecting strict cleaning procedures followed by a 150^0 C baking. Requirements are less stringent in the input, detection and Mode Cleaner tube and tanks, where partial pressures near 10^{-6} mbar are admissible.

33.1.1.3 Implementation of a calibration system

The global operation of the interferometer is monitored with an independent calibration system. It is performed using the radiation pressure produced by an additional laser beam to move a given mirror according to a well known displacement scheme. The implementation of such a system requires a set of dedicated [see table 3300-II] optical ports pointing on the selected mirrors.

33.1.2 Technical requirements

Many components are implemented in the vacuum system. Suspensions and payloads have to be installed and operated in vacuum and in clean conditions. Here we summarize the component properties to be accounted in the design of the vacuum system

33.1.2.1 Suspensions

The suspensions and the inner structures supporting them are described in the relevant sections. The suspensions contain many mechanical and electrical components, hence, in the vacuum compartment where they are installed, it will not be possible to reach a pressure lower than 10^{-6} mbar.

Suspensions will be installed on top of the lower tower; once adjusted an tested, they will be enclosed in the upper tower, sliding on the modular cylinders and the top cap.

Given the recent developments of the suspension design, the interfaces with the towers have still to be agreed (TBD).

33.1.2.2 Payloads

The payload is the interferometer optical element associated to its steering devices. The optical element is a mirror, an input or a detection bench. The 1998 optical elements being temporary, they will be adapted to their final steering devices using adhoc interfaces.

Payloads will be installed in the lower towers through the bottom port, which is accessible via the "gallery" situated in the basement of the buildings, just under the floor supporting the towers (figs. 3300.1, 3300.5).

Table 3300-I : Tower specificities

	Input & Detection	Mode cleaner	Signal recycling	Power recycling	Beam splitter	Input North & West	End North & West
Displacement range (mm)	fixed	±2000	fixed	+600 -1000	fixed	±400	fixed
Number of filters	3	3	0	5	5	5	5
Number of rings	1	1	0	3	3	3	3
Intermediate chamber	no	no	no	yes	yes	yes	yes
Weight & size (mm) of optics				750g Ø120 x30	>3.5kg Ø230 x>50	21 /42 kg Ø350 x100	21 /42 kg Ø350 x100
Reference mass	no	yes	no	yes	yes	yes	yes
Marionetta	yes	yes	no	yes	yes	yes	yes

33.1.2.2.1 "Mirror" payloads

The mirror (input/end North/West, beam splitter, power recycling) hangs on a marionetta which allows for rotations around the two axes perpendicular to the beam, and for translations along the beam line. The acting forces are generated by the current circulating through coils fixed to the last suspension stage and surrounding magnets fixed to the marionetta. A motor allows for the balancing of the marionetta. Six wires are necessary for its control.

The reference mass provides a more sensitive control on the mirror longitudinal position. It is suspended to the marionetta. It has the same mass and center of gravity as the mirror. Its cylindrical shape, which surrounds the mirror, provides also protection against dust deposits. The longitudinal correction is generated by either magnetic or electrostatic forces acting between reference mass and mirror. The necessary power is fed with 8 wires running down the suspension.

The mirror payloads being in the beam line, they follow the beam tube specifications: UHV, low outgassing rate, good mechanical behavior at 150° C, cleanness.

To respect the above mentioned specifications on optics cleanness, payloads are assembled in a clean laboratory. Accordingly, their set up in the beam line is performed in lower towers fed with filtered air.

33.1.2.2.2 Mode cleaner payload

The Mode Cleaner mirror has, in general, the same requirements as the other mirrors, but will be installed in a single compartment tower, since the Mode Cleaner cavity can run in HV (pressure $\approx 10^{-6}$ mbar).

Detailed requirements have still to be defined (TBD).

33.1.2.2.3 Input and detection benches payloads

The benches, being larger and heavier than mirrors, require special marionetta's; no reference mass is required. They will be operated in HV, in single compartment towers.

Detailed requirements have still to be defined (TBD).

33.1.3 Contingencies and flexibilities

The beam tube diameter (Ø1200mm) has been chosen to accomodate a possible second interferometer. This is not the case for the diameter of the tubes linking the towers, which has been fixed, for the first operation period, to accomodate only one interferometer.

To simplify the design and to provide some freedom at assembly, the lower tower beam linking elements will be standardized and symmetrized.

For setting up and maintenance any tower has to be accessible independently of the pressure status of its neighbouring towers, hence valves are present on the link tubes.

33.1.4 Summary and design guidelines

The above described experimental requirements and technical choices define the main characteristics of the vacuum tank design. The different outgassing rates expected from the suspensions, optical paylaods, input and detection benches dictate the tank vacuum compartment structure. The cleanness requirements on optics dictate the implementation of classified clean infrastructures inside and directly connected to the vacuum tank. The suspension weight and dimension defines the mechanical structure of the lower tower basement.

33.2 Vacuum towers design

Having made a choice for the raw material, one determines the vacuum system compartment arrangement. This defines the lower tower as the basic building module whose mechanical structure is computed according to a modelisation with the SYSTUS code. The lower tower basement and its upper tower compartment are described. The functionalities of the different towers are detailed in table 3300-I and 3300-II. The different lower tower vacuum compartments are linked together and to the 3 km arm tubes to form the beam vacuum chamber, which needs to be baked to reach its specified outgassing rate. Finally, the tower ground anchoring is described.

33.2.1 Raw material and surface treatment

The vacuum specifications defined above and the size of the vacuum chamber favour stainless steel for the choice of the chamber raw material. The 300 series of austenitic steels is the most frequently used in vacuum and cryogenic work because it is corrosion resistant, easy to work and non magnetic. The US 304L or NF Z2CN18-10 variety has been chosen.

The inner surface state of the tank is processed to limit outgassing rate and dust adhesion abrasion and electropolishing an RA smaller than 1.6 micrometer is realized. On the other hand high vacuum and cleanness specifications impose to fear hydrocarbons and dust particles in the realisation.

Tensions are relieved, hydrocarbons and hydrogen are removed by a thermal processing of the vacuum chamber. A 3 step thorough thermal processing [ref. 3300-1] of the lower tower is thus defined:

- Tension relieving: Stainless steel sheetings are air fired at 450^{0}C
- Hydrogen outgassing: Components are air fired at 400^{0}C
- Degreasing: Lower tower is baked under vacuum at 200^{0}C

After processing, the chamber is sealed and stays sealed until connection with its suspension. All vacuum components are conditioned at high temperature before being assembled in an oil free ambience. Dust particles are only tracked after reception of the complete vacuum tank, just before payload installation.

All flanges of diameter $\leq$ 250 mm are of the CONFLAT type made with 304LN stainless steel. Flanges > 250 mm can be sealed with either VITON or METAL gaskets.

33.2.2 Vacuum towers compartment structure

The highly different outgassing rates expected from suspensions, mirror paylaods, input and detection benches dictate its compartimentation. The beam compartment containing the payload is thus isolated from its corresponding suspension compartment by an intermediate vacuum chamber. Input and detection benches are isolated from the rest of the beam propagation compartment with appropriate optical windows. As the bench and suspension outgassings are expected to be comparable, they are confined in single compartments. Each of these compartments is pumped for its own.

33.2.3 Tower mechanical structure

The vacuum specifications require the construction of a tank with 15mm wall thickness fit with metallic sealings in its UHV (baked) compartment.

A more elaborate modelling using the SYSTUS code has been used to define the lower tower structure. The simulation produced distributions of static deformations and stresses under various loading conditions (tank under its proper weight at normal temperature, tank under vacuum at normal temperature, tank under vacuum at 150 °C). The model taken for baking assumes a uniform heating between the protection plate and the top of the square pedestal [fig. 3300.4]. Results of the modelling have been verified on the lower tower prototype [ref. 3300-2].

The details of the lower tower geometry have been optimized to rise the tower fundamental frequency to 27 Hz [fig 3300.3]. A collapse factor of 12.8 during baking under vacuum was obtained.

33.3 Vacuum system realisation

The interferometer vacuum tank is realized with the 3 km arm tubes and the lower towers, which link the tubes and support the suspensions. The upper vacuum compartment is a modular cylinder assembled around the suspension. Depending on the tower functionality, a mobile intermediate vacuum chamber minimizes the conductance between the two compartments.

33.3.1 Lower tower

To simplify the structure of the upper compartment, the lower tower [figs.3300.2, .4] is implemented with the intermediate vacuum chamber and the upper tower pumping ports.

It is a cylindrical tank (2000 mm in diameter, 15 mm in thickness, 2740 mm in height) welded to an upper square flange (2400mmx2400mmx60mm) which is taken as a the reference for the tank geometry. This flange has been shaped to fix the frequency of the fundamental vibration mode of the tower. Once it is fit with its various access ports, the tank is welded to a very massive 4000mmx4000mmx300mm square pedestal which rests on ground with 4 or 6 sockets (400x400x100mm^3). The pedestal, the tank, and the upper square flange are bound with 4 vertical stiffening ribs. A 20 mm thick protection plate is welded around the tank at z = 1000mm, it is the upper level of the oven used for baking.

The tank is connected to the beam tube and to the other towers with large lateral beam flanges. It is fit with optical ports to allow for alignment and calibration. It is implemented with access for pumping, clean air supply, payload introduction and installation. Technical access are available for cable and service feedthroughs. The intermediate vacuum chamber sits on the tank structure at level 1130 mm. Its steering and pumping is installed at level z = 1300 mm.

Table 3300-II: Lower tower lateral lids

	north	south	east	west
injection	DN1000.DN250 + 2 DN150	DN1000 + 1 DN200 +3DN100	DN1000.DN200 + 2 DN150	DN1000.DN250 + 2DN150
Mode cleaner	DN1200.DN200	DN1000.DN200	DN1000.DN200 + 2 DN150	DN1000.DN200 + 2 DN150
Power recycling	DN1000.DN400	DN1000.DN400	DN1000	DN1000
Beam splitter	DN1000.DN400	DN1000.DN250 20 mm off	DN1000.DN250	DN1000.DN400 20 mm off
Input north	DN1200.DN400	DN1000.DN250	DN1000	DN1000.DN150
Input west	DN1000.DN150	DN1000	DN1000.DN250	DN1200.DN400
End north	DN1000.DN400	DN1200	DN1000	DN1000
Endwest	DN1000	DN1000	DN1200	DN1000.DN400
Signal recycling	DN1000	DN1000	DN1000.DN400 10 mm off	DN1000.DN400
Detection	DN1000	DN1000.+DN63+ 2DN200+ 1DN40	DN1000. + 3DN150	DN1000.DN250 30 mm off

33.3.1.1 Lower compartment functionalities

Many access ports have to be implemented on the lower compartment. Lower compartment sealings are made with metal gaskets to allow for baking and UHV. Valve gates sealing is made with Viton gaskets for normally open gates, metal for normally closed gates.

33.3.1.1.1 Lateral beam flanges

Following the above mentioned standardization and symmetrization criteria, each lower tower is produced with 4 large orthogonal Ø1000mm apertures. Towers connected to the beam tube have one Ø1200mm flange. The necessary adaptations to the effective linking diameter is implemented on the corresponding windows as shown on table 3300-II where the different cover types are specified by their external diameter and their access flanges. Additionnal flanges are also specified when requested.

33.3.1.1.2 Access for payload installation

The bottom of the lower tower compartment is closed with a DN 2000 cover. A central DN 1000 is implemented on this cover to allow for the payload introductions. Operators use the same access to enter the tank. The lower DN 2000 cover is 195 mm high and weights 1000 kg. A DN 100 CF port is implemented for technical access.

33.3.1.1.3 Technical access

Today, there is no explicit demand for a lower compartment technical access. However, a DN 100 CF is fit on the lower cover to deserve such a purpose.

33.3.1.1.4 Lower tower/ gallery linkage

This linkage is airtight to allow a small over-pressure in the tower access gallery in order to preserve its cleanness with respect to the hall. It stands the high temperature induced by baking at 150°C. It is realized with an aluminum sheeting shape. [fig. 3300.5]

33.3.1.1.5 Optical ports

12 DN160CF optical ports pointing to the optics are implemented for alignment and calibration purpose. Injection, detection, and mode cleaner have dedicated optical windows on their lateral flanges. [figs. 3300.6, .7]

33.3.1.1.6 Clean air supply, venting, roughing and intermediate pumping

Each lower compartment is fed with a 1200 m^3/h filtered air flow. A Ø200 mm pipe leads the air from its filtering station to a DN 200 Y shaped distribution tube entering the upper part of the lower compartment just below the protection plate.[fig.3300.8]

A bypass pipe connected to the upper compartment and to the Y shaped air feeding pipe allow for air supply, intermediate pumping, venting and roughing; see also the diagrams in the pumping system section.

Roughing and venting are performed with a Ø40mm access fit between the Y shaped air feeding pipe and the upper compartment, outside the volume of the oven used for baking. Depending on the status of the Ø200mm all metall and Ø150mm Viton gate valves, venting can be done via the lower compartment and roughing on both compartments. Intermediate pumping, roughing and venting are connected through Viton gate valves.

On some towers the construction symmetry is broken by the Ø1200mm tube connection flanges. The pumping and clean air supply of the input, end and mode cleaner towers has thus to be implemented in order to fit the service distributions in the building [fig.3300.23]. Having symmetric lateral flanges, other towers are not affected by these considerations.

33.3.1.2 Intermediate vacuum chamber

The differential vacuum between suspension and beam compartments is implemented with a mobile vacuum chamber. The conductance (≈2 l/s) of the central hole allowing for the suspension wire and payload services feedthrough is thus decreased by a factor 100. [fig. 3300.9]

The intermediate vacuum chamber rests on a spacing ring which fixes the level of the separating wall. The contact area between chamber and spacing ring forms the sealing between upper and lower compartments. The corresponding area of the intermediate vacuum chamber is implemented with holes in order to pump on the sealing and thus lower its conductance. The central conductance between the two compartments is also pumped via the intermediate chamber.

As mentioned above, coils and magnets are used on either side of the intermediate chamber: coils are fixed to 4 legs penetrating stainless steel bechers resting on the separating wall of the intermediate chamber. These bechers approach closely the magnets attached to the marionetta [fig. 3300.10].

Computations performed by J.Y.Vinet [ref. 3300.3] demonstrated that the seismic noise injected in the payload suspension via the bechers is negligible provided the bechers are made with .1mm thick stainless steel and that the marionetta magnets stay at 30 mm from the becher wall. Another computation [ref. 3300.4] showed that the pressure variations induced by roughing (at 7 l/s) or venting (at 3000 mbar.l/s) are smaller than 2.2 mbar. Anyway, roughing and venting is safely performed if the intermediate vacuum chamber is lifted on purpose.

The becher must be computed to stand such a pressure difference. (TBC)

The position of the optics in the horizontal plane is determined by the location of the conductance hole. This hole is set at installation within a few mm. Small adjustments in rotation are possible at that time. The final horizontal positioning is performed once the vacuum tank is evacuated: it can be lift by 10 mm and smoothly translated in orthogonal directions with appropriate mechanisms. Lifting is essential for smooth translations. This movement has been tested on a prototype separating roof.

The intermediate chamber is submitted to the same thermal treatment as the lower tower vacuum tank. Injection, detection, signal recycling towers, as well as the mode cleaner tower don't need a differential vacuum. They are not fit with an intermediate vacuum chamber.

The operation of the intermediate vacuum chamber requires functionalities to be implemented on the lower tower at z = 1300mm [fig. 3300.11].

33.3.1.2.1 Access for pumping

There is a DN 250 mm access available for that purpose.

33.3.1.2.2 Access for translations

Translations can be induced either manually or remotely with actuators installed on 4 DN 300 ports.Translations range within +/-25mm in both directions. Commands are outside the tank, at atmospheric pressure.

33.3.1.2.3 Visual control of the suspension wire position

The wire position with respect to the conductance hole is watched with a camera installed outside the tower. The camera sits behind a DN150 mm window.

33.3.1.2.4 Thermal screening of the upper compartment

A simulation has been made to define a thermal screening which would minimize the heat radiated from the lower tower towards filter # 7 during baking.

The exact requirements for this screen have still to be defined (TBD).

33.3.1.3 Upper compartment functionalities

These functionalities are implemeted on the lower tower at z = 1300 mm, i.e.at the same level as those of the intermediate vacuum chamber, however they are in communication with the suspension compartment.[fig. 3300.11]. Sealings are realized with metal gaskets. Valves stand baking temperatures of 150°C.

33.3.1.3.1 Technical access

One DN250 port is available for technical services.

33.3.1.3.2 Pumping ports for the upper compartment

Two axial DN250 ports are available for the upper compartment permanent pumping. Moreover, a DN 150 port is fit to accomodate some upper tower emergency pumping using the lower compartment intermediate pumping. The upper tower vacuum instrumentation is fit on the DN250 flange opposite to the upper tower pumping flange.

Towers with a single compartment like input, detection and mode cleaner have only an upper pumping station. Tubing is the same as for other towers, but the intermediate pumping unit is not connected.

33.3.2 Upper tower

Its functionalities are implemented on the lower tower. It is built with a set of standard rings headed by a cupola.[fig. 3300.12]. Sealings are made with Viton gaskets.

Standard rings are about 2000 mm high with a 2000 mm inner diameter. They have forged flanges and receive either metallic or "viton" gaskets.

The exact height of the rings have still to be agreed. (TBD).

The cupola rests on the upper last ring. It is 1300 mm high and weights 1000 kg. It is also used to head directly a lower tower.

33.3.3 Central building vacuum tank

In its first version, Virgo will accomodate a single interferometer. Main building towers will thus be linked accordingly. Light loss computation favor a linking with Ø400mm tubes fit with Ø250mm valves. Diffused light is trapped with glass baffles fit in the straight links or inside the lower tower vacuum compartment. Sealings are made with metal gaskets.

Vacuum controls and UHV permanent pumping stations are implemented on the links in between the towers. Each tower, but the injection, detection and mode cleaner towers, is implemented with UHV pumping station.

33.3.3.1 Lateral window interfaces

Towers linked in the central building are connected through 12 lateral flanges. Given the off axis position of the injection and detection lines all flanges are produced with a central DN 400

CF but the beam splitter south and west, signal recycling east which are off by 20 mm and the detection west which is off by 30 mm.

The 4 towers connected to the 3km long tube are linked with flanges produced with an outer DN 1200. The 2 mode cleaner tube interface flanges have a central DN 250 /400 CF. These features are specified on table 3300-II for each tower [fig. 3300.2].

33.3.3.2 Detailed link structure

A connection between two towers has to account for:

the oven geometry,
dilatations generated by baking at 150°C: 6mm for a 3000mm long tube.
misalignment between towers: +/-5mm
mechanical tolerances on DN1000 flanges: +/-5mm in beam direction and +/-5mm perpendicular to the beam.
mechanical tolerances on the links : +/-5mm in the beam direction,
implementation of sectioning valves, glass baffles.
installation of a permanent or an intermediate tower (beamsplitter) pumping system
installation of the vacuum instrumentation of each lower tower compartment.

A link is thus build up with a bellow connected to a straight section associated to a Ø250mm sectioning valve. The valve is inside the oven. If necessary for pumping, a DN200CF port is fit on the straight sections, in between neighbouring ovens. The bellows allow for longitudinal displacements of ±40 mm and lateral displacements of ±15 mm. The end flange near the valve is freely rotating to allow an assembly with upright valves.

The outgassing of the equipments set up in the input and detection towers may prevent the achievement of the expected UHV performances in the beam line. To assert the interferometer beam vacuum chamber performance, these towers are linked across optical windows.

In conclusion, there are six different links in the central building [fig. 3300.13]. The small size and weight of their components allows for an in situ assembly.

33.3.3.2.1 Access for permanent pumping and instrumentation

Three permanent (UHV) Ti pumping stations (unit #3) are implemented on straight sections between north input-beam splitter, beam splitter-power recycling, and beam splitter-signal recycling towers. A measurement port DN63 is fit on each link straight section. A diameter 250mm access is provided for permanent pumping.

33.3.3.2.2 Sectioning valves

Assembly sealings are metallic, gate sealings are Viton and valve feedthroughs are realised with bellows.

33.3.3.2.3 Test interferometer configuration

For the test interferometer configuration, the permanent pumping station is fit on links attached on the two input towers, tube side. The standard vacuum instrumentation is fit on those links. An optical window is implemented on the end lid to allow for alignment and locking.

In the final interferometer configuration, these links are removed and replaced by Ø 1200 mm links connecting the input towers to the large valves controlling the beam tube access.

33.3.4 Beam compartment baking

33.3.4.1 Lower tower baking

The lower tower vacuum compartment is uniformly baked at 150°C surrounding it with an isolating structure blown with hot air. With the reduced space available in the tower vicinity it was found difficult to implement a dismountable structure as was done for the prototype oven. On the other hand, the suspension setting up needs the installation of an appropriate scaffolding which is also difficult to move around the towers. As a compromise, the scaffolding basement is taken as the supporting structure of the oven insulator. [fig. 3300.14]

This structure will be permanently installed. Only the insulating material and the heating elements will be moved from place to place. (TBD).

The prototype oven was operated with a flow of 2000 m^3/h heated on 20 kW resistors. The payload access cover, accessed from the gallery, is heated for its own with a 3 kW resistor.

33.3.4.2 Upper tower thermal insulation

The suspension components do not stand the baking temperature. The 50 mm (TBD) thick rock wool insulation which is part of the oven is stopped at the middle of the first ring. It may happen that the suspension needs a more efficient heat screening. (TBD).

33.3.4.3 Link baking

Baking is performed by wrapping discrete heating elements around the links and the associated instrumentation. For a wall thickness smaller than 5 mm a 16 W/dm^2 power distribution will be implemented.

33.3.5 Lower tower ground floor anchoring

The assembled lower tower, with its 4 lateral DN 1000 covers and its cupola, weights about 16540 kg.

Any tower has to be accessed or baked independently of the pressure status of its neighbouring towers. A tower is thus screwed to ground to stand pressure differences or free with respect to ground to allow for baking.

Holes are drilled in the ground after tower fine positioning and the tower is fixed to ground using those holes.

In our configuration, end towers stand the highest pressure difference. Their situation is taken as a reference for computations.

Input and end towers stand 11310 DaN induced by the beam tube vacuum. They are screwed to ground and bear on metallic plates anchored on the beam tube side [fig. 3300.15]. They are unscrewed for baking. When the tube is under vacuum, an input tower expands towards the beamsplitter tower. When it is at atmospheric pressure, i.e. the test interferometer situation, the metallic plate is removed to allow for dilatations towards the tube, bearing on spacing rods inserted between input and beamsplitter tower pedestals.

Other towers are also unscrewed for baking. Towers sandwiched between two neighbours at a different pressure are balanced with spacing rods introduced between processed and evacuated towers.

33.4 Vacuum system clean access

The payload is installed by an operator which enters the lower tower vacuum compartment. This access is implemented via an underground gallery which deserves the lower towers installed in the main building. Mode cleaner and end towers are accessed through local galleries. The vacuum tank clean access infrastructures and the payload installation scenario is reviewed.

33.4.1 A continuous clean processing line

We propose to build a continuous clean processing line [fig. 3300.16, .17] to prepare the sensitive components before their installation in the tank. The line consists of a cleaning installation, an assembly laboratory, a transfer gallery, and a tent which protects the tank access hole. Materials enter the line through a cleaning installation, people enter it via an airlock where clean clothes are weared.

After high vacuum degreasing, the requested components enter a tunnel and pass successively a washing machine followed by an oven. This devices, which can be confined with valves, are flushed with clean air or with nitrogen. Components to be cleaned are forwarded on a rolling carriage. The washing machine is a box fit with handgloves allowing for a cleaning with high pressure streams (less than 30bars). Currently used fluids are DI water or a mixture of DI water + ultra pure alcohol. The oven is able to heat at 150°C. Marionettas, reference mass, baffles, are processed through that line.

The assembly laboratory should provide a 2000mm*2000mm laminar class 100 air flow. Air is extracted through a false floor. Loads of 50 kg are handled and assembled to form payloads of 700 kg. The available height in the laminar flow is 2900 mm. Significant storage space around the laminar flow is available.

The staff airlock, the transit area between assembly laboratory and the gallery elevator are controlled class 1000 areas.

The gallery is fit with clean air piping supplying each tank access with $1200 m^3/h$ of air filtered at 99.99% DOP. During optics installation, the tank access is confined with polyan veils.

The tank itself is supplied with a $1200\ m^3/h$ air flow filtered at 99.9997% DOP. During payload installation, the tank access is always kept free to allow for an optimal air flow through the introduction hole.

The implementation of the tank clean air piping in the hall is shown on [fig. 3300.18, .19]. It is located on the pumping side. It's height is determined by the free space required by the movements of the crane. In the gallery, the tank access tent clean air piping is located on the same side wall, i.e. opposite to the elevator corner. The extraction of the air blowed through the tank and its access tent can be done either locally, below each tank, or globally at the gallery end. Unless otherwise stated it's matter of convenience. Let's recall here that the installation scenario requires a qualified cleanness only in the tank access volume in order to protect it with respect to the gallery.

33.4.2 Payload transfer system

The transfer system is a rigid gibbet made with four pillars resting on a telescopic cage. The upper part of the gibbet can thus be lowered and raised at introduction. This function is useful to limit the height of the system, specially during transport. The payload protection box slides along those pillars. The protection box is also used to block the payload during transport [fig. 3300.20].

It is clear that the payload fine tuning is made in the clean room at mounting. Then it is transported to the tower. Once hanged to the suspension, there is no more access either to the marionetta nor to the mirror.

33.4.3 Component handling tools

Special tools are needed to bring the components from the cleaning bench or transportation box (mirror) to their final position on the payload transfer system. Handling has always to be performed from below: one uses elevators rather than cranes.

The mirror transportation box has still to be agreed (TBD).

The marionetta has to go from the cleaning bench (level 1000 mm) to the payload transfer system (level 1500mm). The mirror has to go from its transportation box to the suspension wires.

The reference mass has to go from the cleaning bench to its suspension wires. It has to fit carefully the already suspended mirror. The handling tool has still to be defined (TBD).

33.4.4 Optics installation scenario

The experience gained with the tests [ref. 3300.5, .6] allows now to propose confidently a new scenario for the optical component installation. With the above proposed transfer system, any payload but the input or detection benches can be installed.[fig. 3300.17].

The operator working inside the tank is assisted by an operator resting in the gallery. Both are followed by a third operator sitting in the control room. He watches tank and gallery with TV monitors. They are linked with a free hand radio communication system.

33.4.4.1 Assembly on transfer system

The marionetta is hanged to the hook anchored in the laminar ceiling. The mirror and reference mass suspension wires are set final. The transfer cradle is presented below the marionetta sitting on the assembly chariot. The mirror, protected by its handling lids is presented to the assembly chariot. It is fixed to the transfer cradle using the front lid. Suspension wires are put in place. They are pretensioned. The rear lid is removed to introduce the reference mass. The reference mass is transfered from the cleaning bench to the assembly chariot using a special crane. Pushing the chariot, the reference mass reaches its final place where its suspension wires are put in place.

To perform these operations, the items to be assembled are presented at their final height, in order to minimize their handlings under clean conditions. Once the payload is assembled, the protection box is raised. This blocks the payload. A veil is wrapped around the box. Settings and tunings are now final.

33.4.4.2 Transfer to the tower access tent

The protected box is rolled to the elevator on the assembly chariot [fig.3300.17]. A movable arm allows its transfer from the chariot to the elevator platform fit with a telescopic cage. The elevator is lowered and rolled into the tower access tent. There, after some settling time, the payload is unveiled [fig.3300.21, step 1].

33.4.4.3 Introduction

The operator which will enter the tank dresses himself in the tank access tent. Once in the tank, he waits for the payload [fig. 3300.21 step 2]. Below the introduction hole, his partner rises the protected payload to the high position of the transfer system and actions the elevator to bring it to its final position. In this position, the tank aperture has to be clear to allow for an optimum air feedthrough. The smooth approach and guiding of the payload in between the bechers is achieved with an X.Y. rot Z positioning table. This table is qualified to operate in a class 10 clean room. The final vertical positioning is achieved by a smooth vertical movemement implemented on the introduction cage.

33.4.4.4 Fixation to the suspension wire and tool extraction

The actual height of the suspension point is to be defined (TBD). We just know that the stainless steel bechers limit possible excursions to a few mm. For that reason it's mandatory to lock the suspension ponit at its final height. It is unlocked only once the payload is in its final shape.

The operator attaches the marionetta to its suspension wire. He lets the cylindrical protection box glide along the pillars of the transfer system. The air which flushes the tower is always extracted through the introduction aperture. The transfer system can now be completely removed [fig. 3300.21, step 3, 4].

33.4.4.5 Fine tuning of the payload in the tower

Only a visual check is possible. There is no access neither to the marionetta nor to the mirror.

33.4.4.6 Baffle installation in the optics vicinity

The operator installs the baffles [fig.3300.21, step 5] around the mirror and leave the tank.

33.4.4.7 Tower closing

The transfer system is contracted to its transport position and returned to the assembly room. It comes back with the flange used to close the introduction hole [fig. 3300.21, step 6].

33.4.5 Cleanness monitoring

The final cleanness of the installed component has to be guaranteed. Of course, the best guarantee is only provided by a nearly impossible in situ measurement. In the actual scenario, the ultimate cleannes is guaranteed by:

1. an oversizing of the clean room installations. The measured safety margin is near 100.
2. a permanent monitoring of the clean installations with the particle counters.
3. the installation of witness samples on the payload. These samples are placed at the most exposed locations. They are easy to install. They are also easy to remove after installation in the tank.

33.4.6 Safety

Work in closed cavities is generally hazardous. Use of solvants in closed cavities is really dangerous. Strong safety rules apply. Acetone is prohibited.

The use of alcohol in small concentrations cannot be avoided: it is a good dust remover to be employed at the very end of the cleaning process.

The air in the tank and in the assembly room will thus be permanently monitored for its content in alcohol. Tank and gallery are also watched for their oxygen content. Operators never work alone. They are permanently in audiovideo relation with a control room.

33.5 Assembly sequences

High vacuum and classified infrastructures require some planification and care for proper implementation. Guidelines are enumerated.

33.5.1 Lower tower reception

After transportation the reception of a lower tower is made on a vacuum test (TBD).

33.5.2 Lower tower installation and linking

Once on the experimental site, the towers are put in place with rolling sockets and aligned with respect to 3 markers located on their upper flange. After positioning, they are thermally isolated from ground and tightly linked with the gallery. These links allow for baking. The oven structure is assembled around the lower tower and the tower insulation is fit.

Once linked to the clean air generators, a tower is equipped with its pumping and links. Then it is evacuated and baked for its own. This allows for its vacuum characterization before suspension installation. Once linked, the central building vacuum chamber is put in communication and its overall vacuum performance is checked. Repetitive high temperature bakings are intended to stabilise the geometry and hydrocarbon cleanness of the vacuum chamber.

33.5.3 Intermediate vacuum chamber installation

The first stage permanent scaffolding is implemented to allow for the suspension cable tray and cable laying. Cables have to be prepared when the lower towers are closed, so when the bare suspension arrive, infrastructures are ready for tests in clean conditions.

The cleanness of the central building is now under strict control. The access to the central building is reserved to authorized people.

After the cabling, lower towers are opened and one proceeds to the intermediate vacuum chamber installation. The associated mechanisms are mounted and the bechers are carefully aligned. The operation is dust protected by a tent supported by the first stage scaffolding. The lower compartment is fed with clean air to produce a small overpressure.

The reception of the vacuum chamber needs a mechanical test and a vacuum test before suspension installation. The effective conductance of the intermediate chamber is measured.

33.5.4 Suspension installation

The suspension installation follows.

A temporary scaffolding is set up. Its two parts are assembled in place. They provide access to the suspension and its related cabling. Rings are piled up. A functionality test precedes the cupola installation.

An overall interferometer alignment is still possible at this stage of the assembly. To that purpose, alignment optics are installed and tuned to operating positions. The intermediate vacuum chamber installed on the mirror towers is moved using its associated mechanisms.

After a new baking and thorough vacuum test followed by a suspension test, one proceeds with the installation of the final optics.

33.5.5 About cleaning

Clean conditions can only be met when **all necessary material conditions** are fulfilled and when **all concerned people** agree to work "clean".

Lets recall that the specifications on hydrocarbon (oil vapors) and dust contaminations have to be taken seriously and that it is well known that the easiest pollution to remove is the one which has not been made !

The building construction has to proceed as a normal construction. As a rule, one does not start any clean operation before its final reception. Any simple construction work becomes complicate once cleanness has been decided. The application of the rule requires the implementation of restricted access to the clean places. The operation of any oil vapor or dust generating device is prohibited in the controlled areas. Vacuum components are assembled in such conditions. Their assembly is not dustfree(white ambience) but oilfree(clean ambience).

The white ambience is only effective inside the lower vacuum tank compartments and in their dedicated access galeries. It can only be created when:

1. The vacuum tank is thoroughly tested for leaks.
2. All the components connected to the vacuum tank are operational (suspensions, valves, feedthroughs,..). The maintenance of the less liable parts should not break the cleanness.
3. The clean processing line is fed with clean air and overpressurized.

When these conditions are met, a thorough wet cleaning is undertaken, starting in the tank and ending in the cleaning installations at the beginning of the continuous clean processing line. After reception with the particle counters, the infrastructures are ready to operate the proposed payload installation scenario.

33.6 Guidelines for space allocation around the towers

As seen above (i.e. 3300.3.4.1), the roof of the oven supports the tower pumping units connected at level z = 1300 mm. Most of the cables exit the towers at the level of its technical port [fig. 3300.12]. As space around the towers is really scarce, another platform is implemented at the level of this technical port: it will support the cable trays being compatible with the tower insulation, the access to the technical port and to pumping units. A detailed layout of the components and cable trays fit on these levels is shown on [fig. 3300.23]. Of course, all that allows still the displacement of the suspensions with the crane and the addition of the last stage scaffolding [fig. 3300.24].

Racks for the pumping hardware are located on the pumping side on the ground floor at 800mm from the oven wall.

33.7 References

3300.1 P.Marin, Note on stainless steel processing by air firing.
3300.2 Franck Cadoux, rapport de stage LAPP, sept.1995
3300.3 J.Y. Vinet, Injection of noise through the bechers - NTS96-030
3300.4 R. Morand, A. Pasqualetti, Z.Zhang, Pressure differences in mirror tower during rough pumping and venting - VIR-TRE-PIS-3400-105.
3300.5 R. Morand, A summary of the cleanness tests performed on the lower tower prototype at LAPP - VIR-SPE-LAPP-2200-101
3300.6 R. Morand and P. Mugnier, Clean optics installation, final proposal - VIR-SPE-LAPP-2200-102

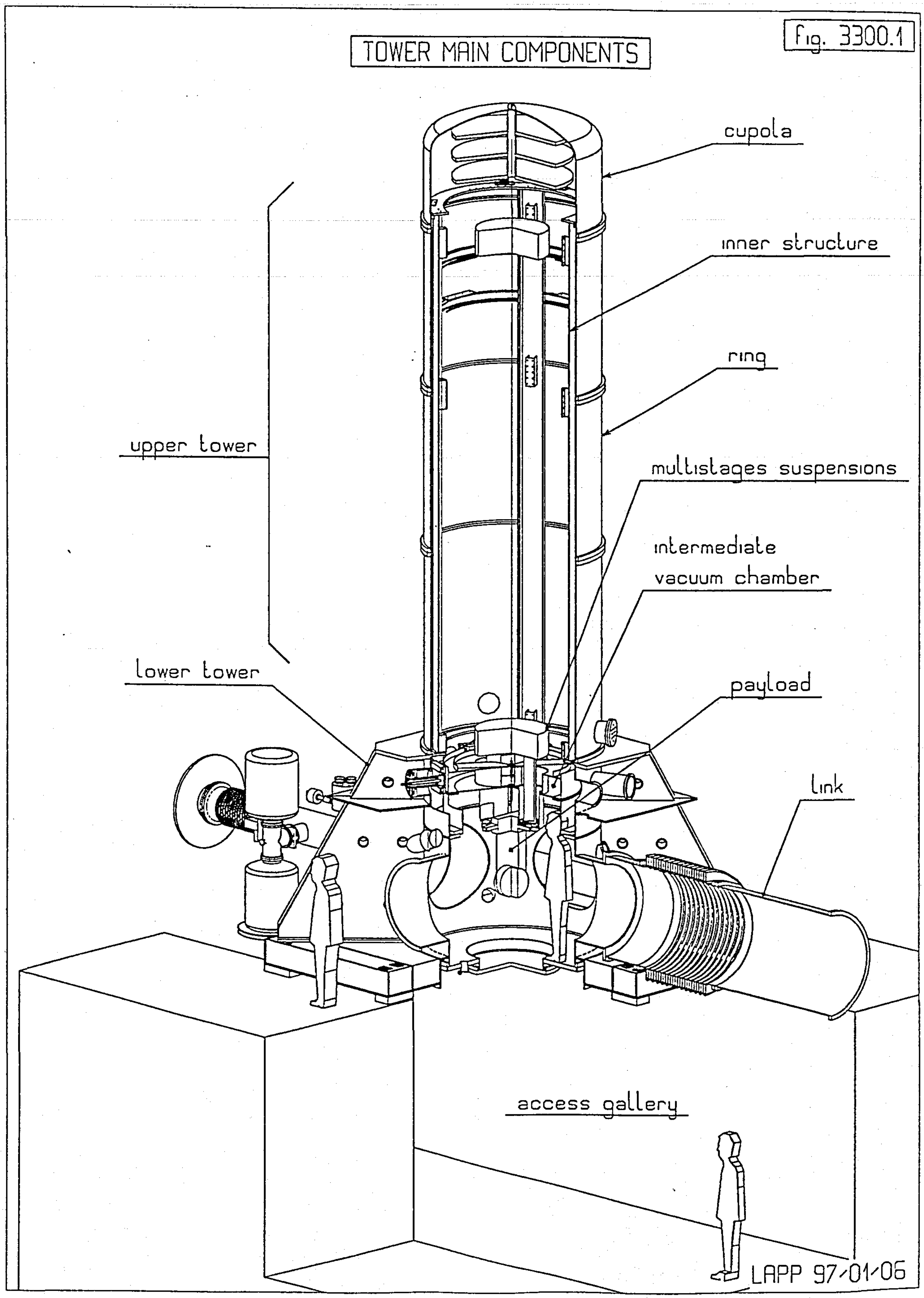

fig. 3300.1
TOWER MAIN COMPONENTS
cupola
inner structure
ring
upper tower
multistages suspensions
intermediate vacuum chamber
lower tower
payload
link
access gallery
LAPP 97/01/06

TOWER ALIGNMENT

Fig. 3300.2

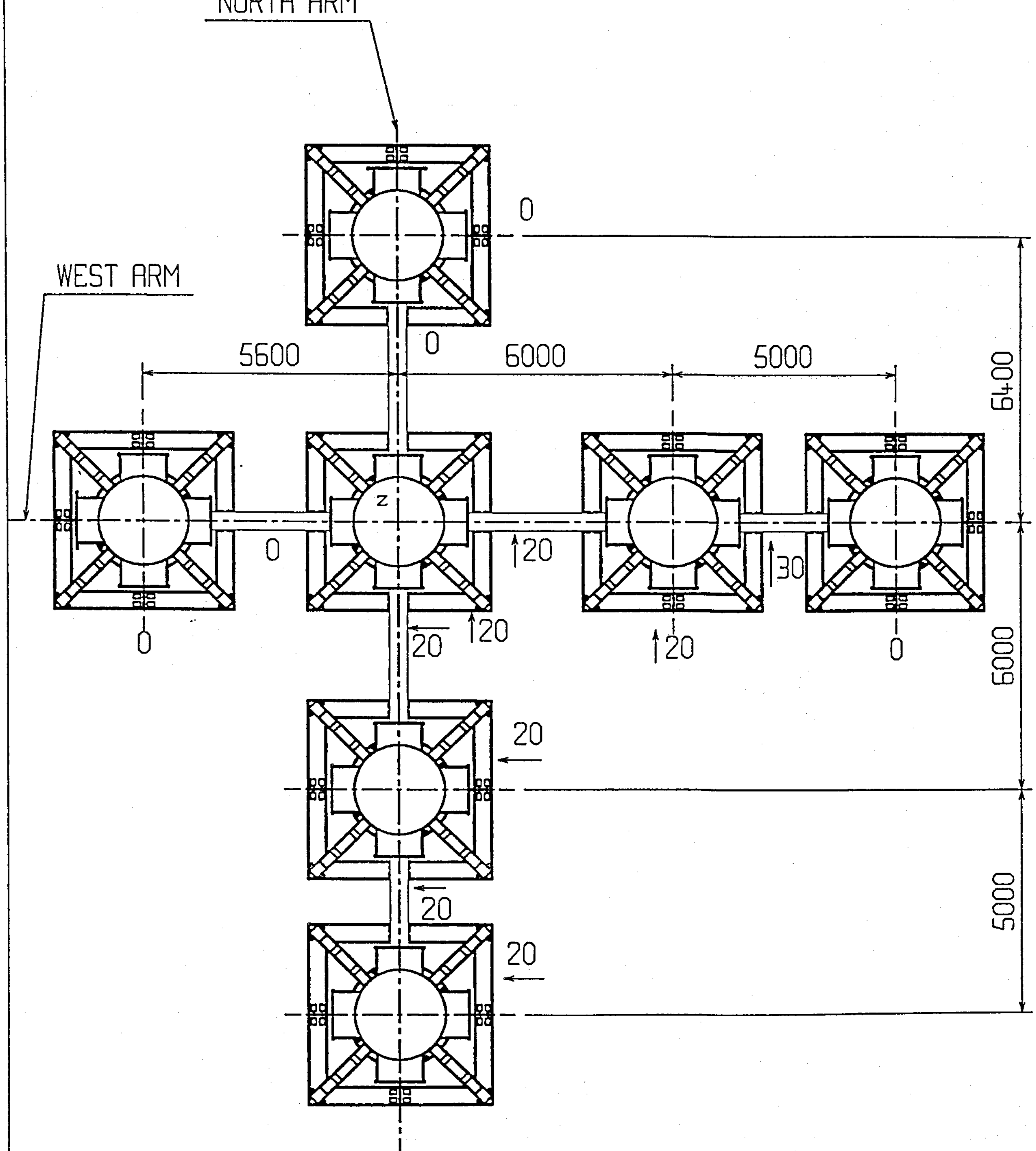

LAPP 97/01/07

Tower Fundamental Vibration Frequency for Different Geometries

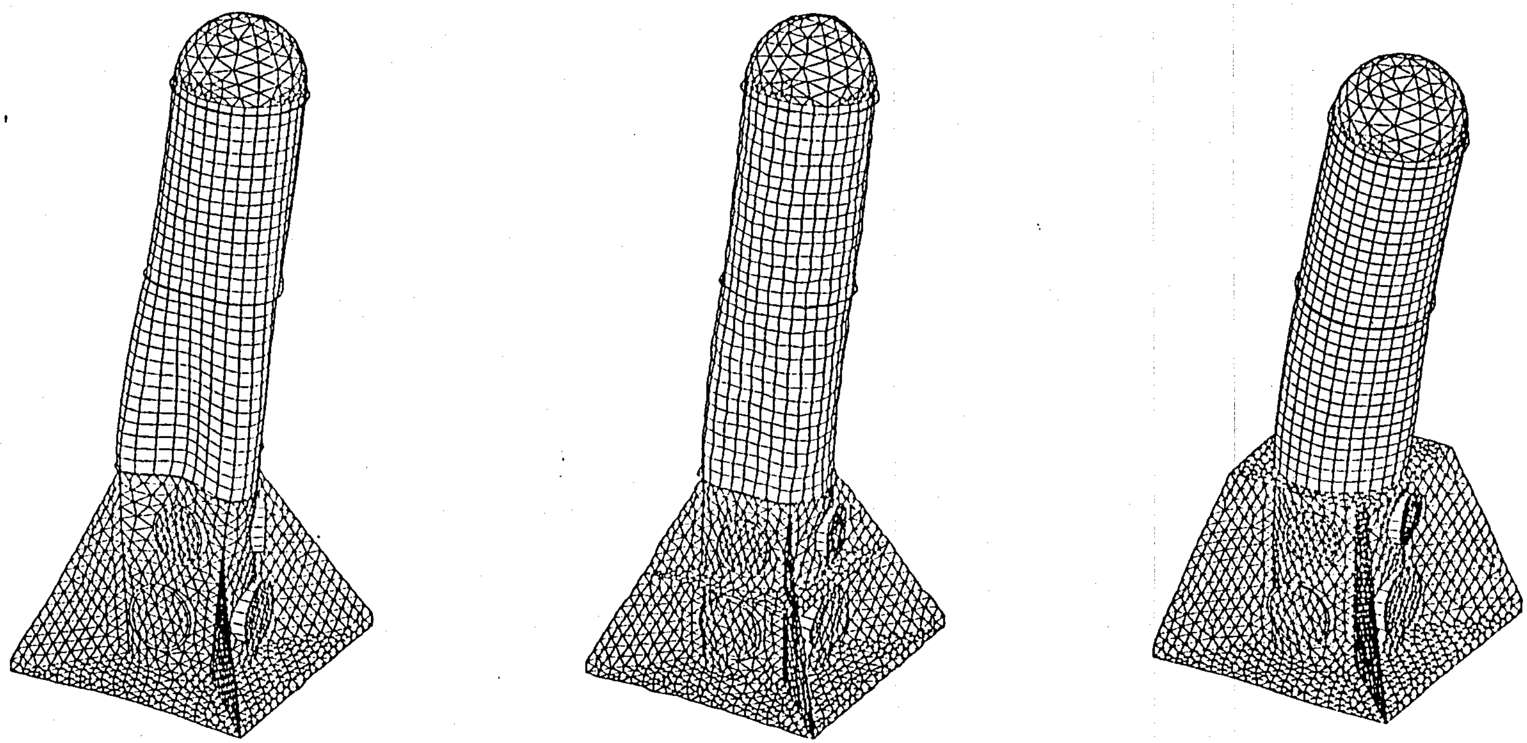

Fig. 3300.3 Tower fundamental vibration frequency as a function of its structure.

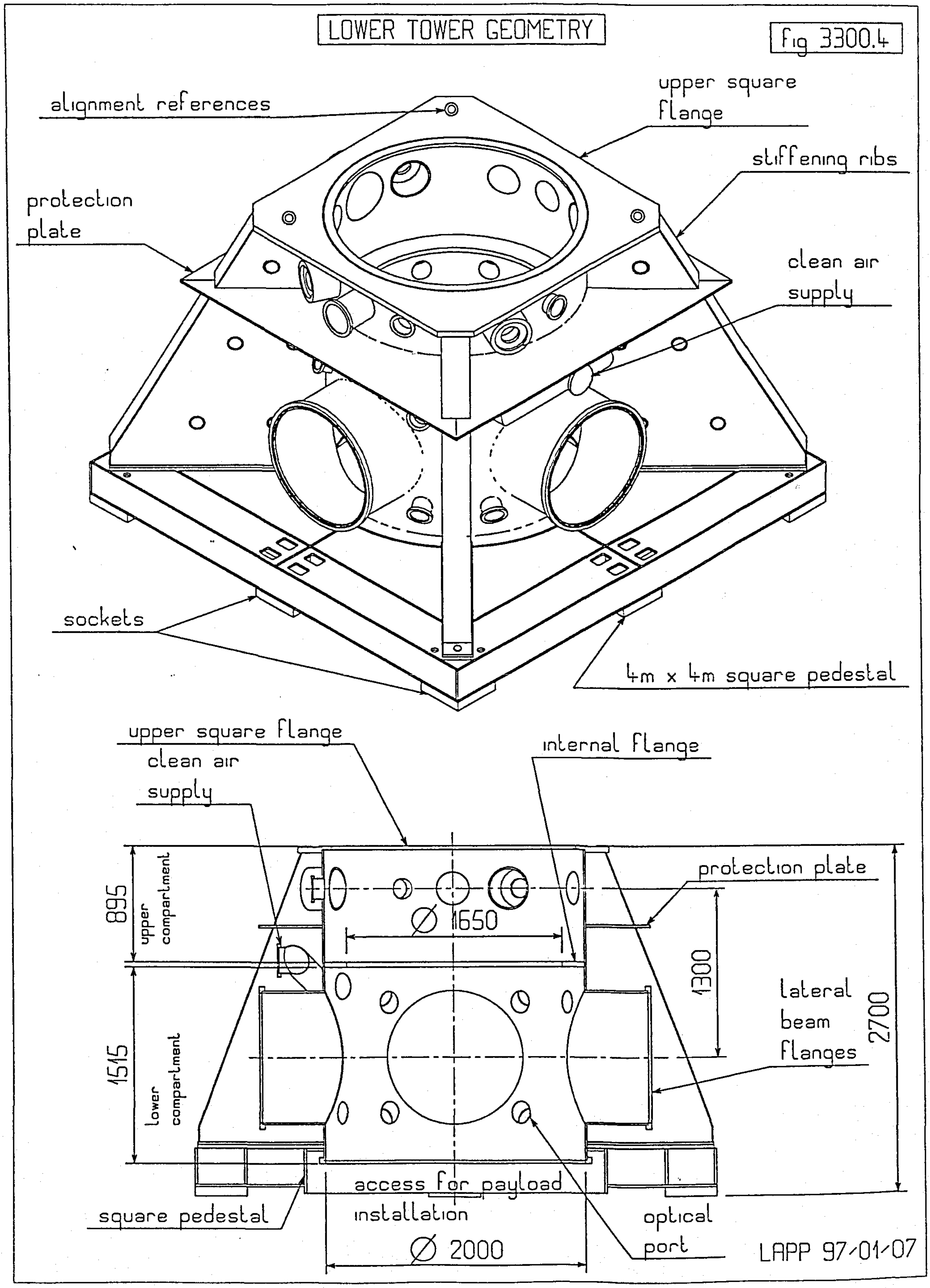

LOWER TOWER GEOMETRY
Fig 3300.4
alignment references
upper square flange
stiffening ribs
protection plate
clean air supply
sockets
4m x 4m square pedestal
upper square flange
clean air supply
internal flange
protection plate
895
upper compartment
Ø 1650
1300
1515
lower compartment
lateral beam flanges
2700
access for payload installation
square pedestal
optical port
Ø 2000
LAPP 97/01/07

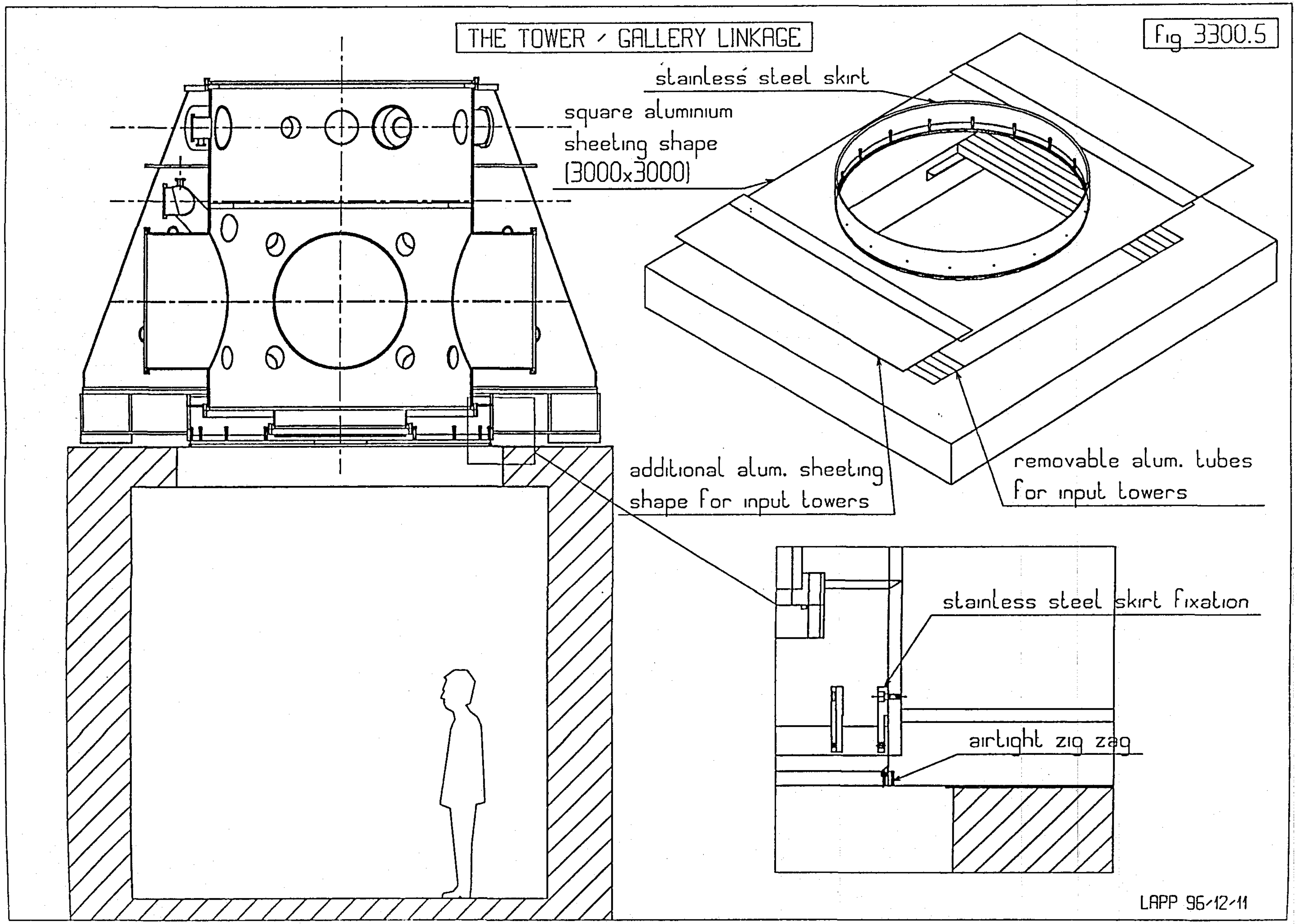
THE TOWER / GALLERY LINKAGE
Fig 3300.5
stainless steel skirt
square aluminium
sheeting shape
(3000x3000)
additional alum. sheeting
shape for input towers
removable alum. tubes
for input towers
stainless steel skirt fixation
airtight zig zag
LAPP 96/12/11

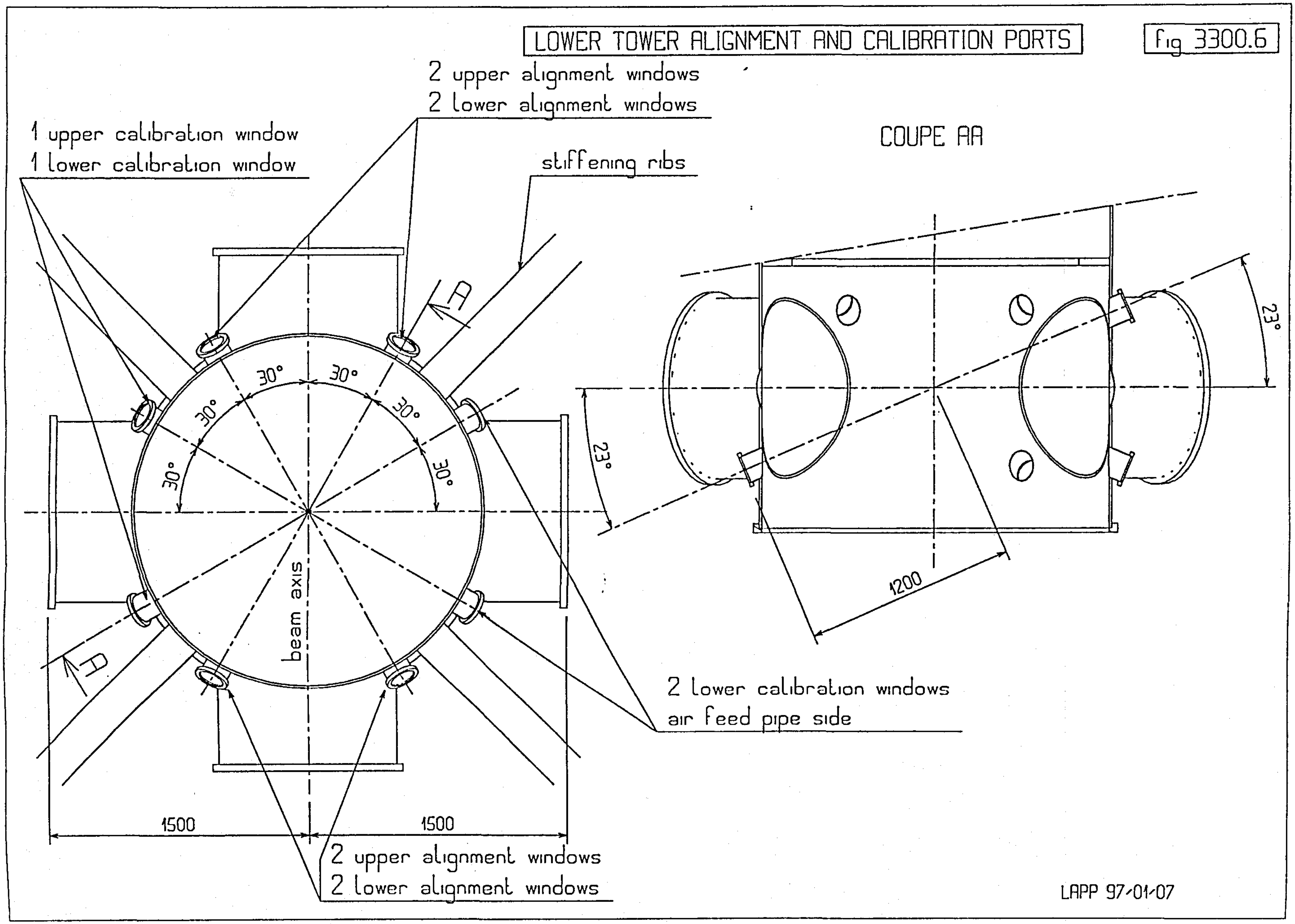
LOWER TOWER ALIGNMENT AND CALIBRATION PORTS
fig 3300.6
2 upper alignment windows
2 lower alignment windows
1 upper calibration window
1 lower calibration window
stiffening ribs
COUPE AA
A
30°
30°
30°
30°
30°
30°
23°
23°
beam axis
1200
1500
1500
2 lower calibration windows
air feed pipe side
2 upper alignment windows
2 lower alignment windows
LAPP 97-01-07

IMPLEMENTATION OF OPTICAL PORTS FOR INJECTION, DETECTION AND MODE CLEANER TOWERS.

Fig. 3300.7

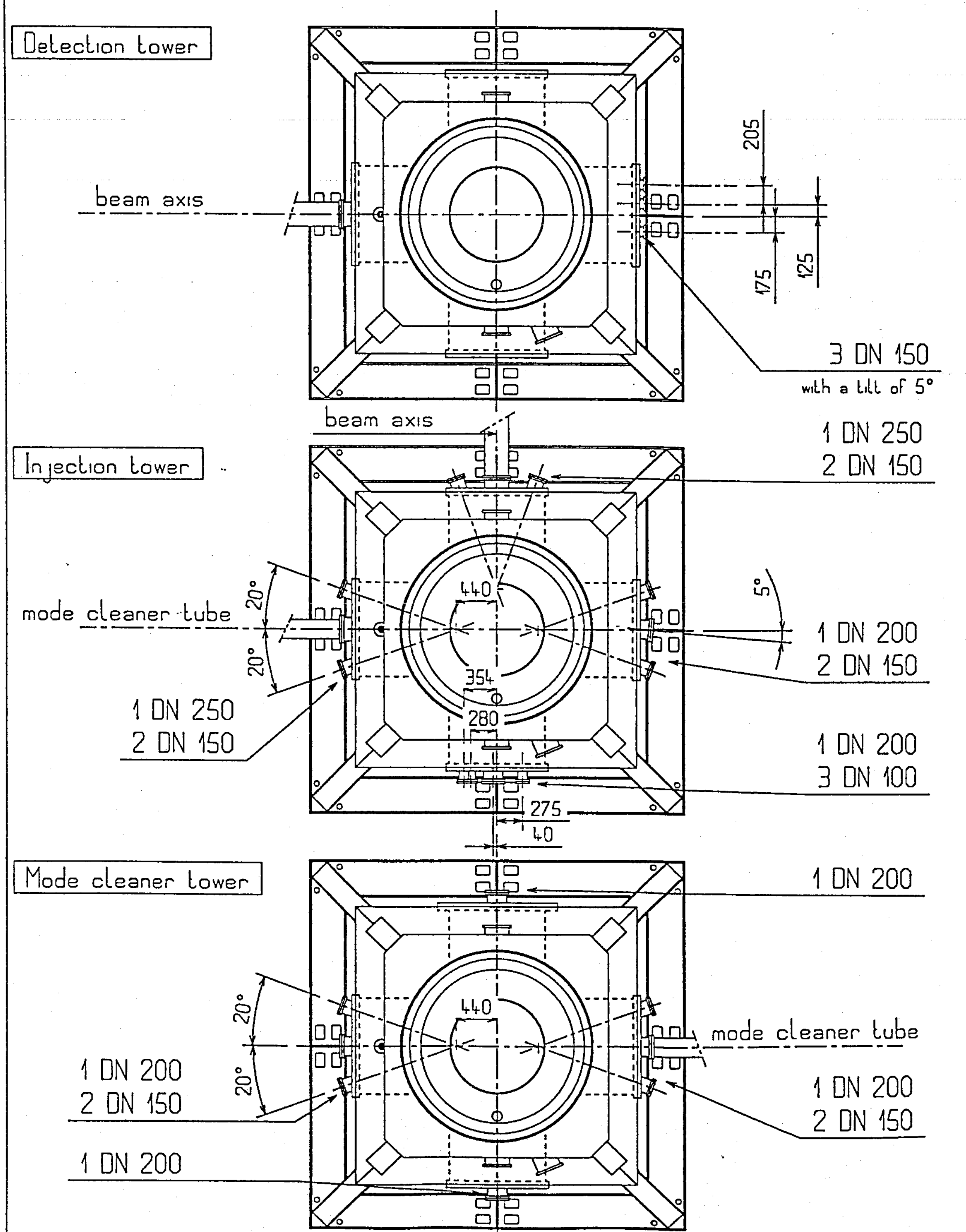

LAPP 97/01/08

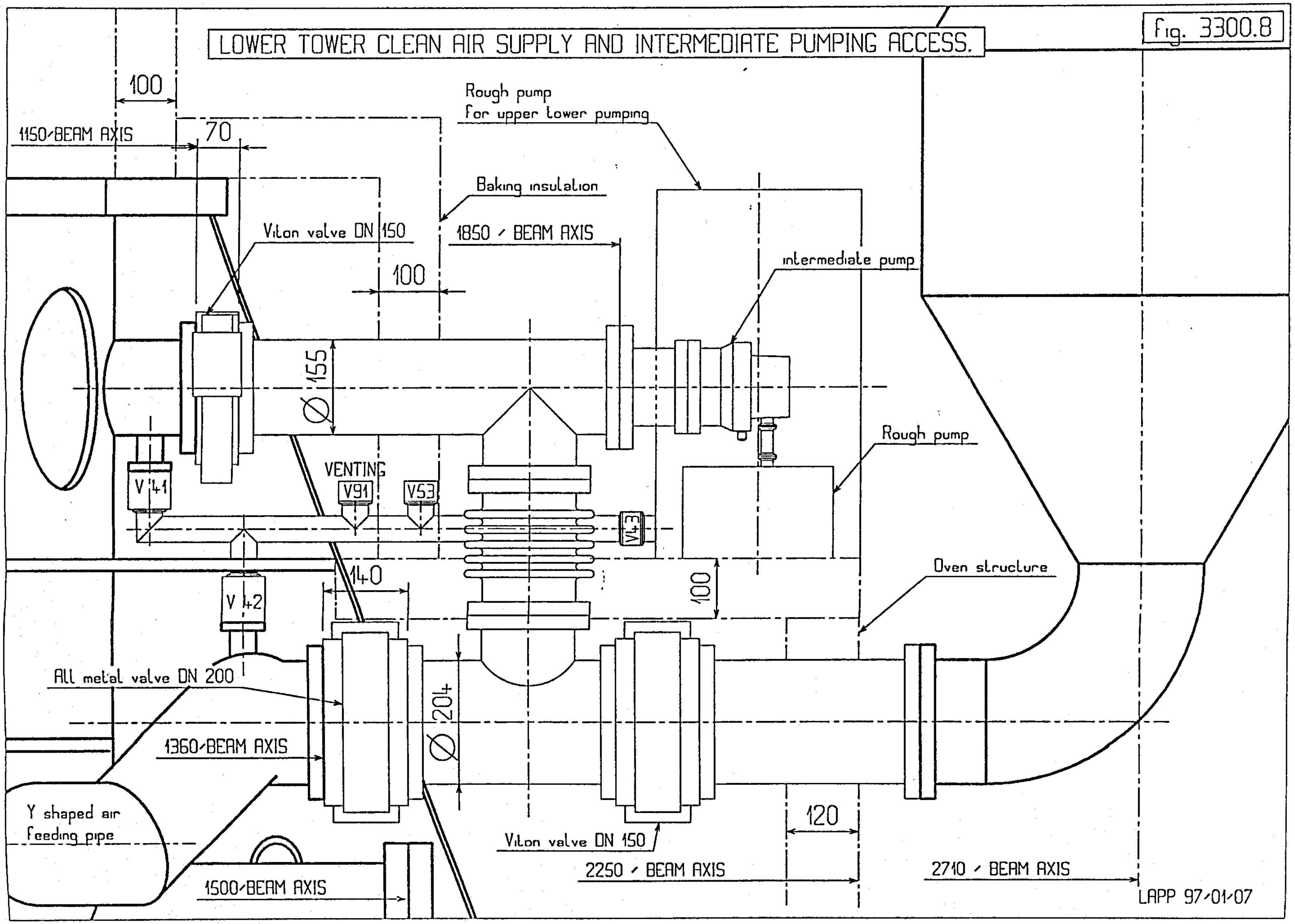

Fig. 3300.8
LOWER TOWER CLEAN AIR SUPPLY AND INTERMEDIATE PUMPING ACCESS.
100
1150/BEAM AXIS
70
Rough pump
For upper tower pumping
Baking insulation
Viton valve DN 150
100
1850 / BEAM AXIS
intermediate pump
Ø 155
Rough pump
VENTING
V91
V53
V41
V43
V42
140
100
Oven structure
All metal valve DN 200
Ø 204
1360/BEAM AXIS
Y shaped air
Feeding pipe
120
Viton valve DN 150
1500/BEAM AXIS
2250 / BEAM AXIS
2710 / BEAM AXIS
LAPP 97/01/07

Fig 3300.9

THE INTERMEDIATE VACUUM CHAMBER WITH ASSOCIATED MECHANISMS

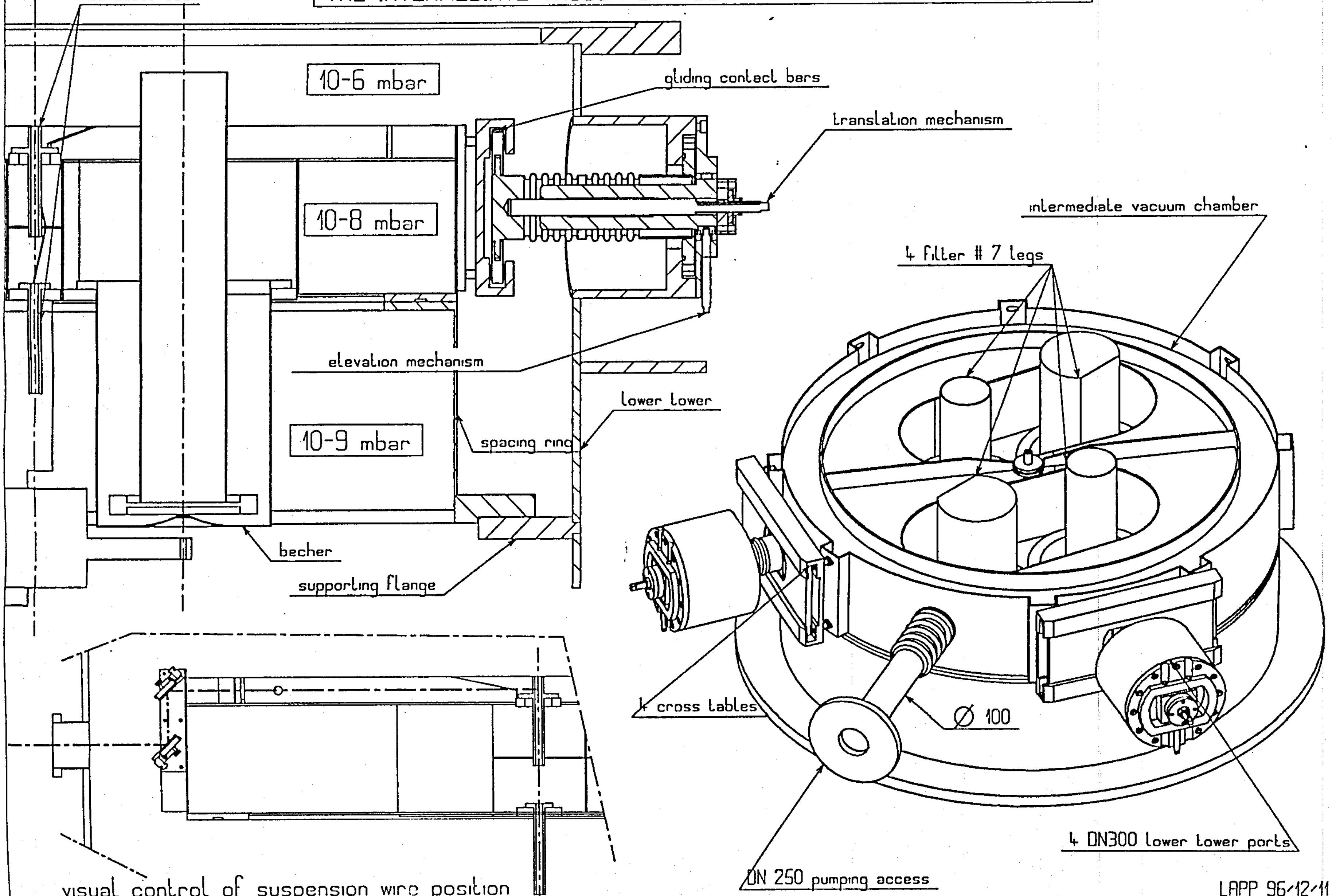

LAPP 96-12-11

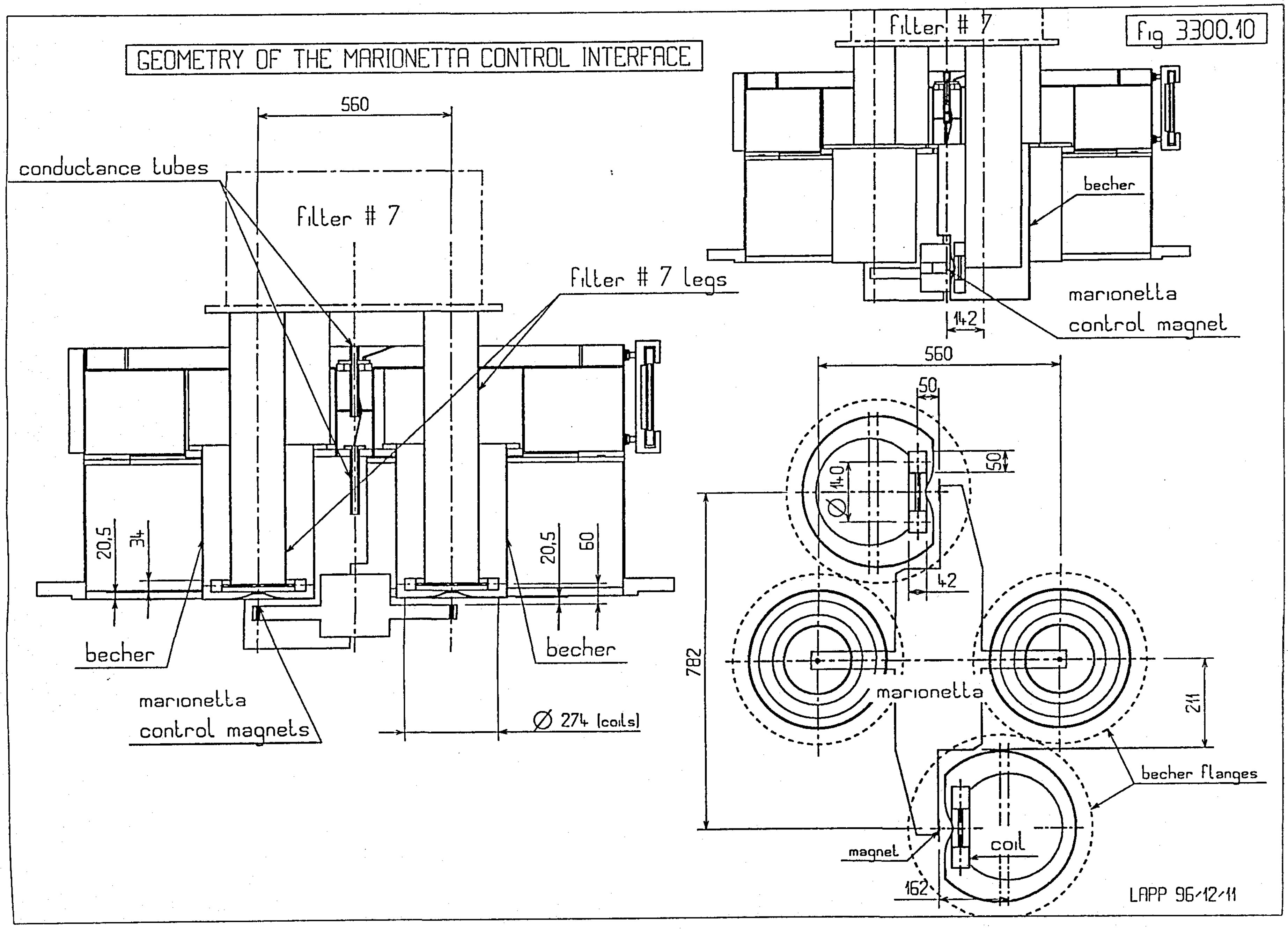
GEOMETRY OF THE MARIONETTA CONTROL INTERFACE
Fig 3300.10
560
conductance tubes
filter # 7
filter # 7 legs
20,5
34
20,5
60
becher
becher
marionetta
control magnets
Ø 274 (coils)
filter # 7
becher
marionetta
control magnet
142
560
50
50
Ø 140
42
782
211
marionetta
becher flanges
magnet
coil
162
LAPP 96-12-11

IMPLEMENTATION OF THE UPPER TOWER FONCTIONALITIES ON THE LOWER TOWER AT Z = 1300.

Fig. 3300.11

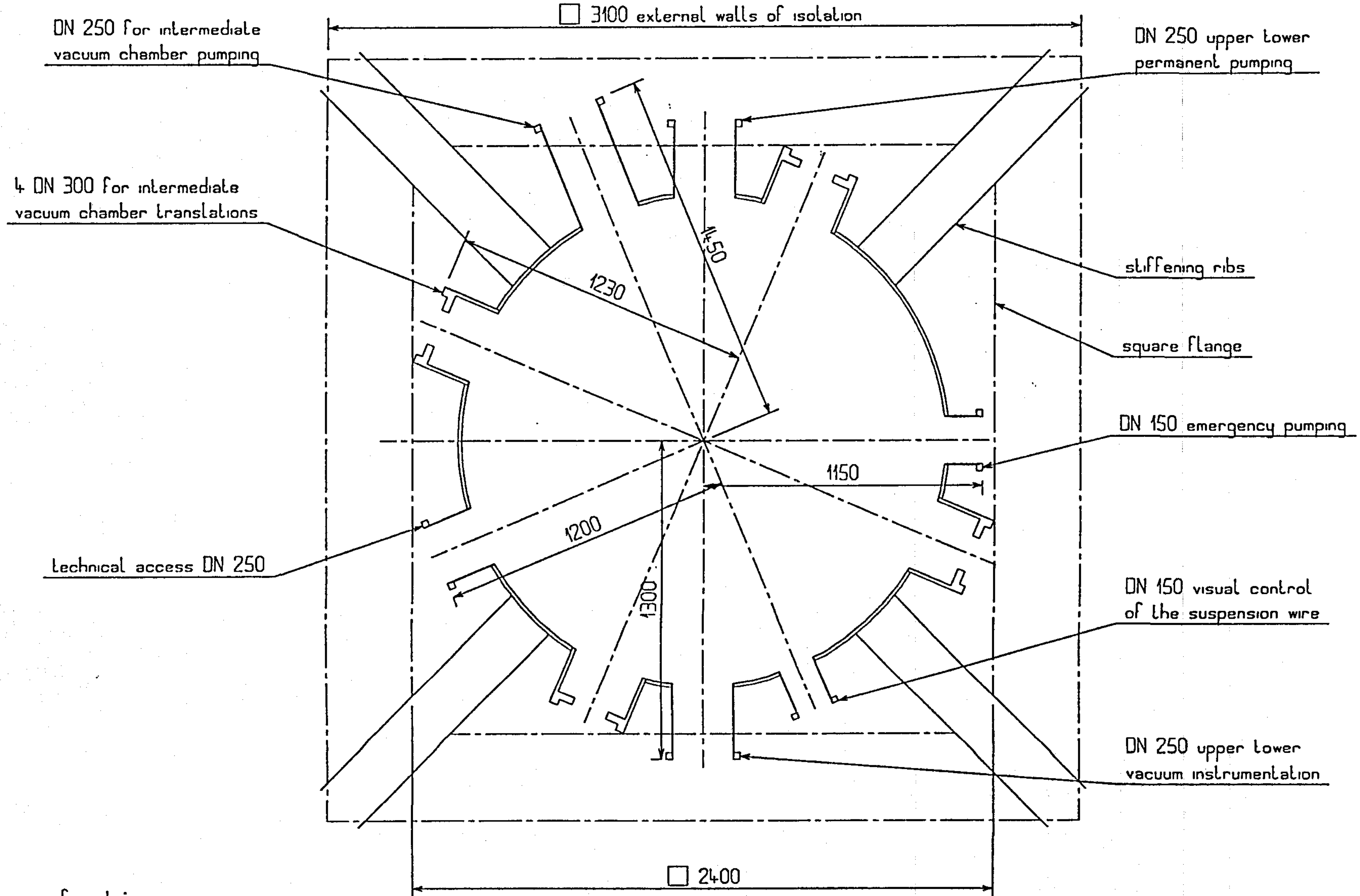

axis of parts:
1300 / axis beam

LAPP 97/01/07

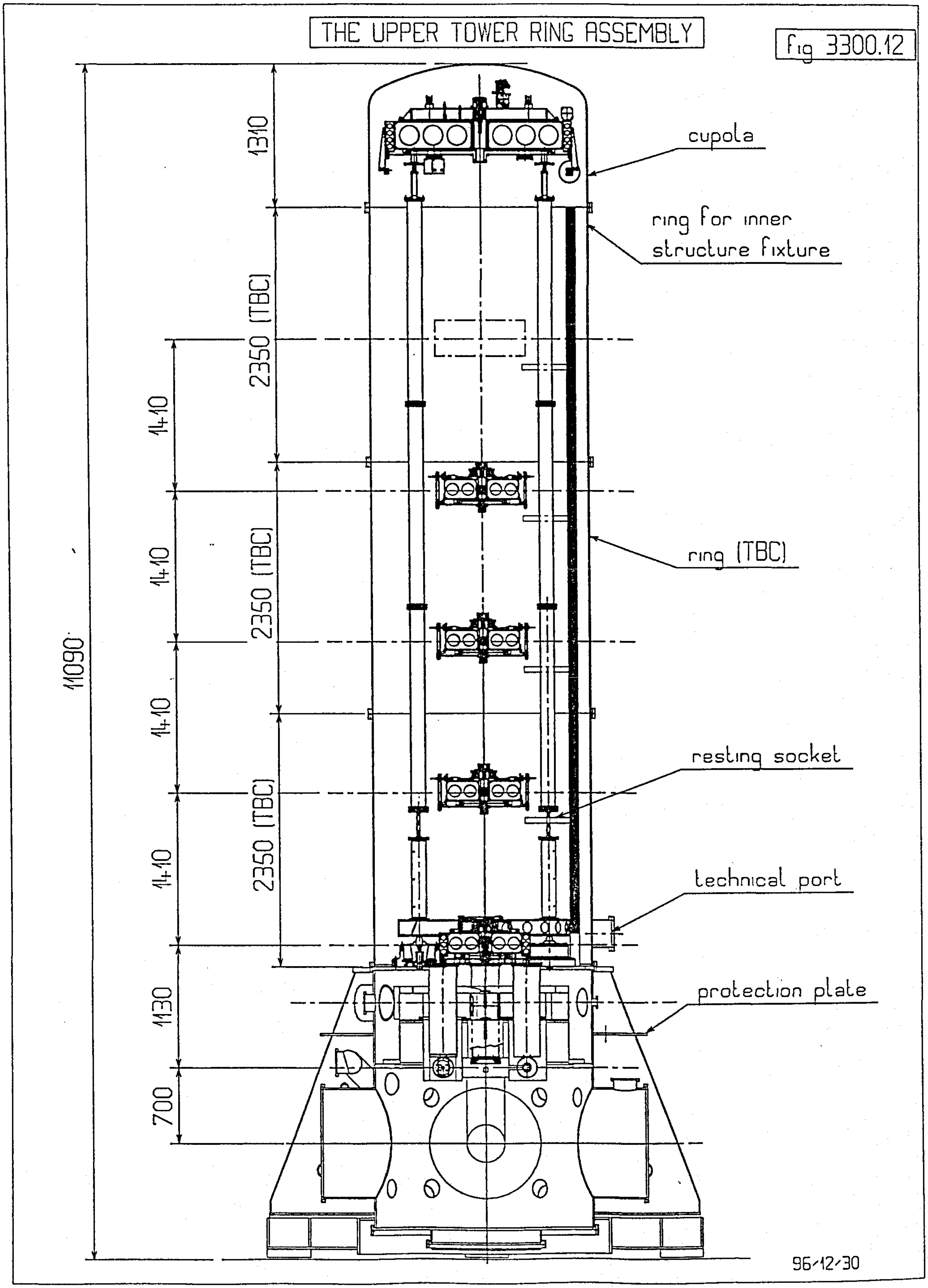
THE UPPER TOWER RING ASSEMBLY
Fig 3300.12
cupola
ring for inner
structure fixture
ring (TBC)
resting socket
technical port
protection plate
1310
2350 (TBC)
2350 (TBC)
2350 (TBC)
1410
1410
1410
1410
1130
700
11090
96-12-30

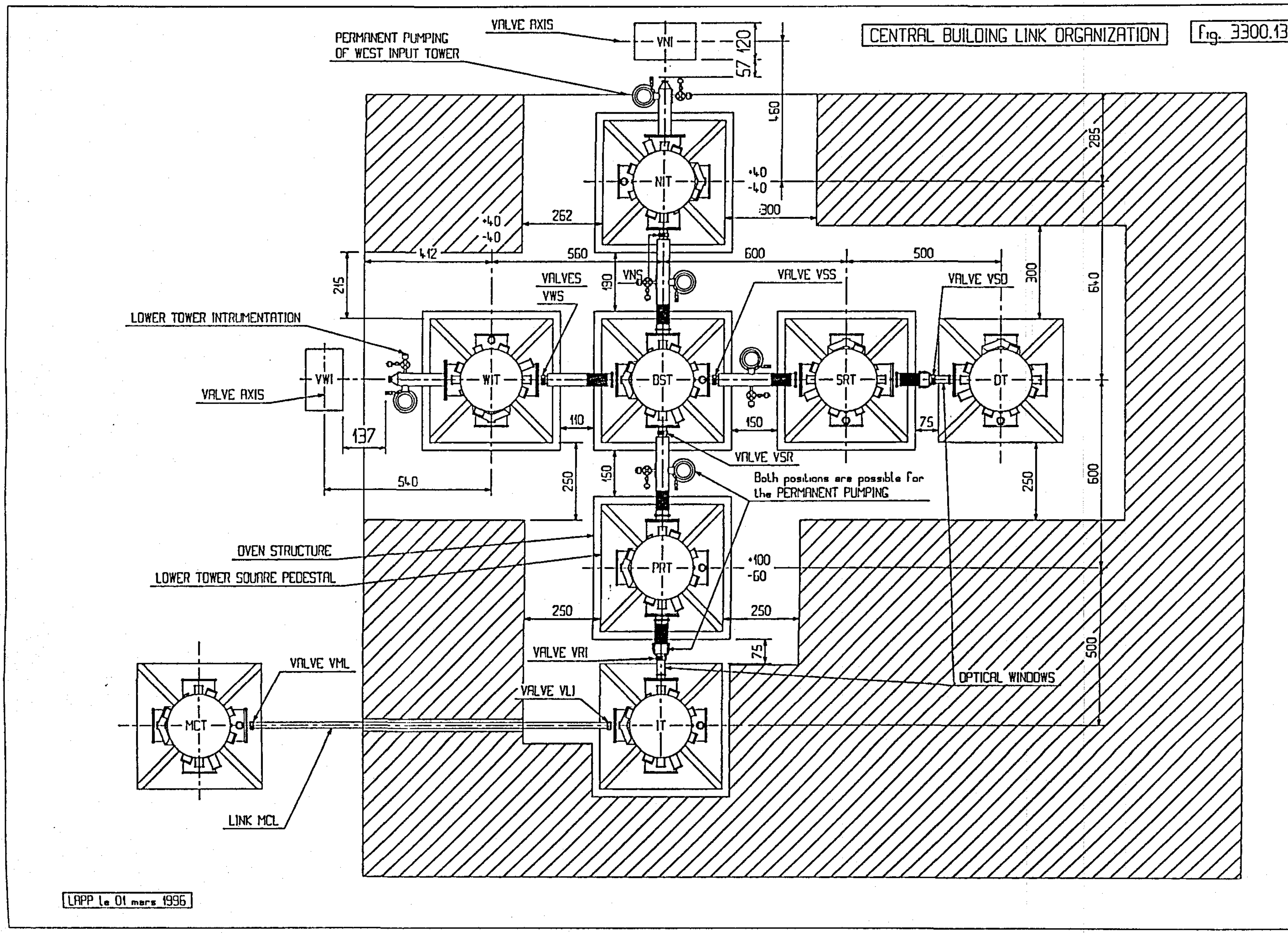

CENTRAL BUILDING LINK ORGANIZATION
Fig. 3300.13
VALVE AXIS
PERMANENT PUMPING
OF WEST INPUT TOWER
VNI
NIT
VNS
VALVES
VWS
VALVE VSS
VALVE VSD
LOWER TOWER INTRUMENTATION
VWI
VALVE AXIS
WIT
BST
SRT
DT
VALVE VSR
Both positions are possible for
the PERMANENT PUMPING
OVEN STRUCTURE
LOWER TOWER SQUARE PEDESTAL
PRT
VALVE VRI
VALVE VML
VALVE VLI
MCT
IT
OPTICAL WINDOWS
LINK MCL
LAPP le 01 mars 1996

THE OVEN / SCAFFOLDING SUPPORTING STRUCTURE

Fig 3300.14

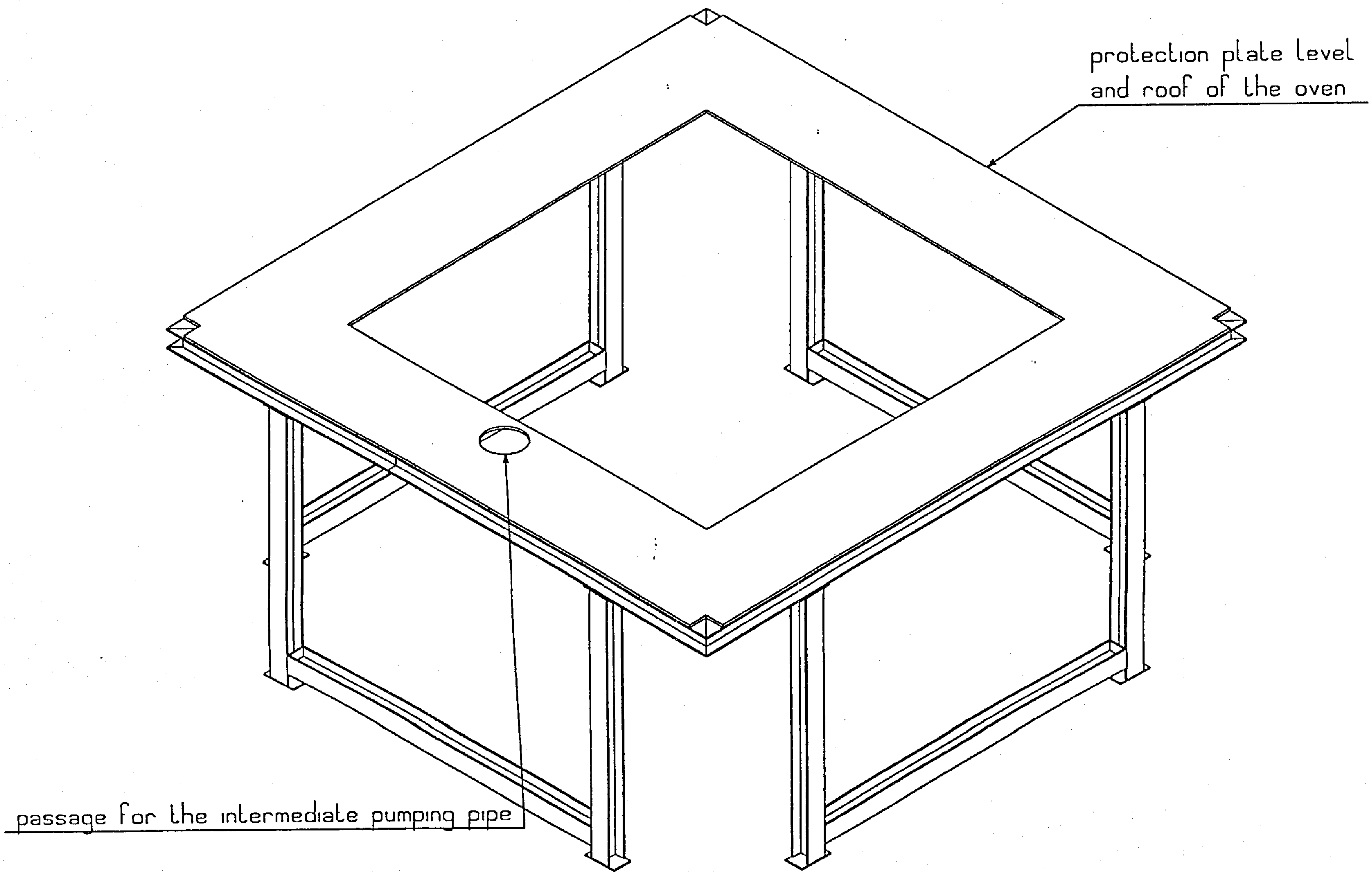

LAPP 97/01/07

THE TOWER GROUND ANCHORING

Fig 3300.15

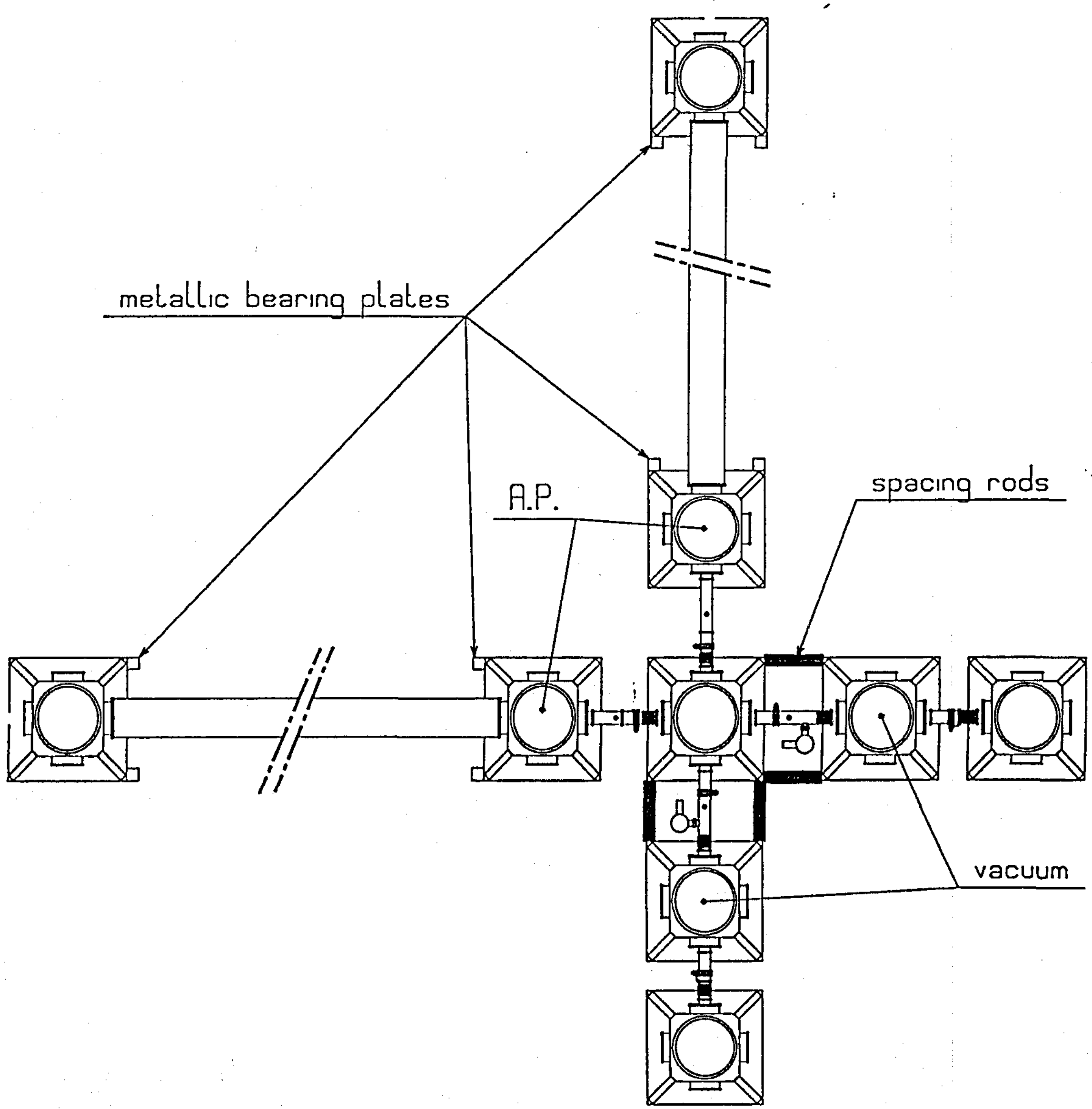

LAPP 97-01-07

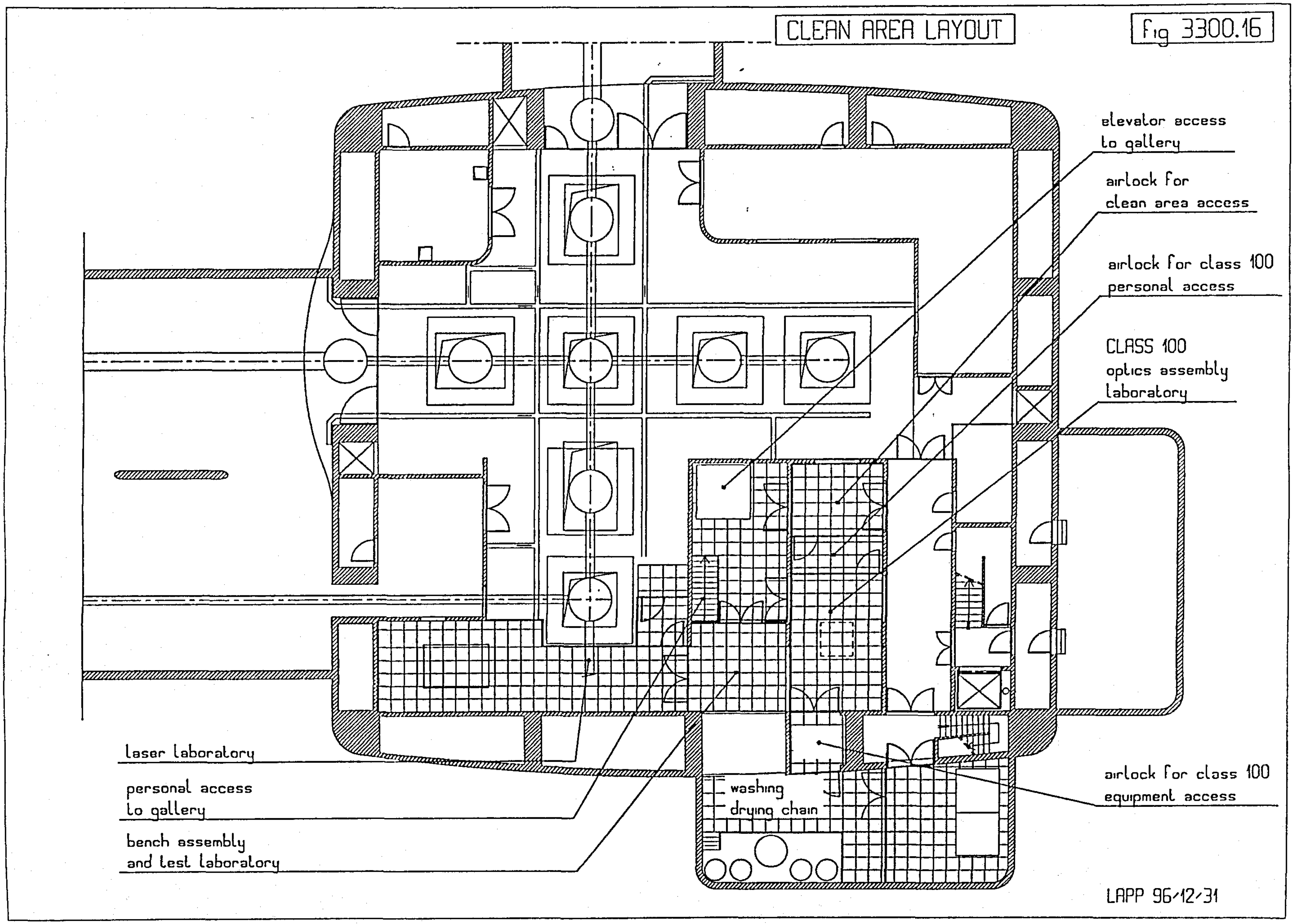
CLEAN AREA LAYOUT
Fig 3300.16
elevator access
to gallery
airlock for
clean area access
airlock for class 100
personal access
CLASS 100
optics assembly
laboratory
airlock for class 100
equipment access
laser laboratory
personal access
to gallery
bench assembly
and test laboratory
washing
drying chain
LAPP 96/12/31

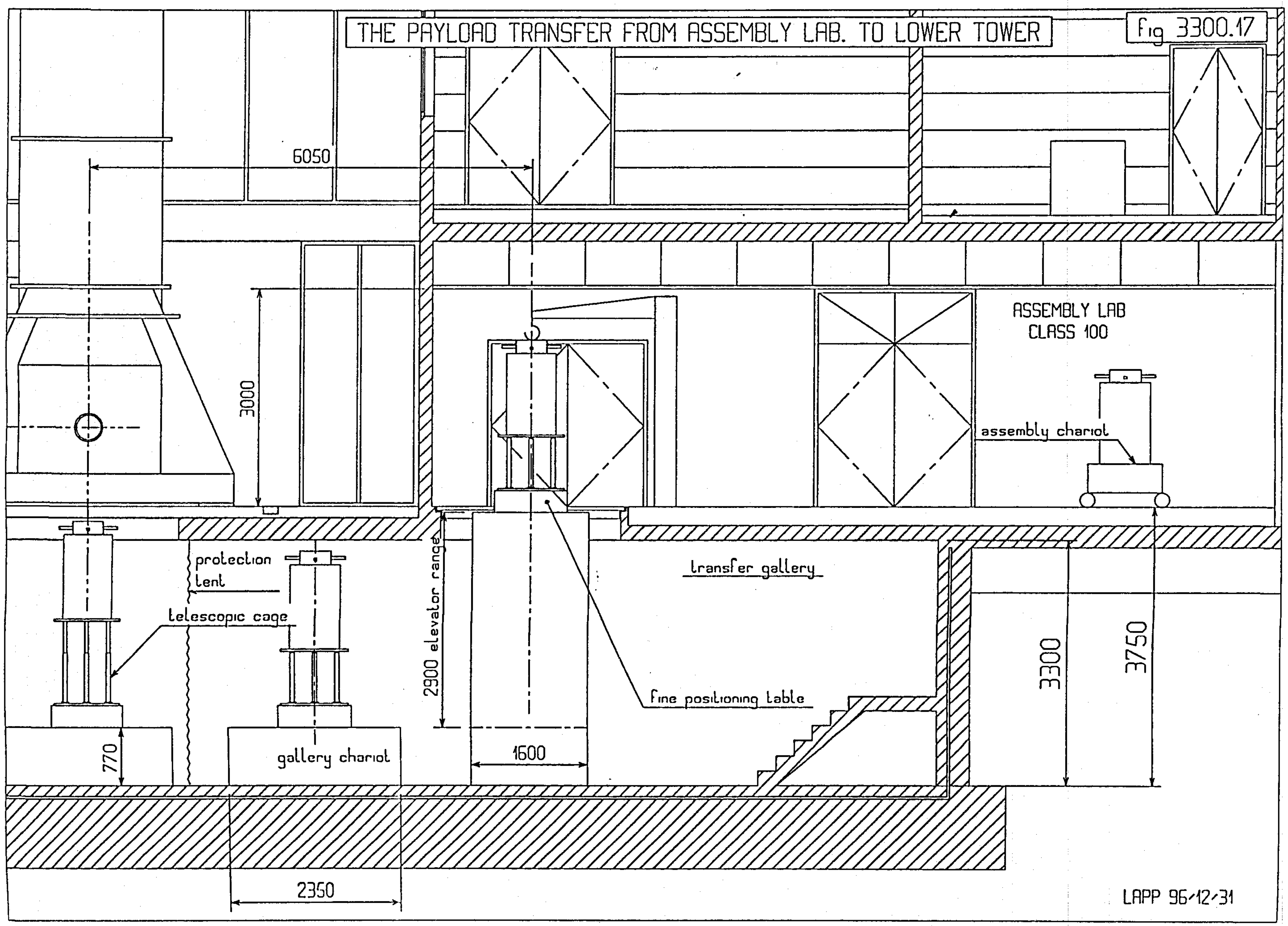

THE PAYLOAD TRANSFER FROM ASSEMBLY LAB. TO LOWER TOWER
fig 3300.17
6050
3000
ASSEMBLY LAB
CLASS 100
assembly chariot
protection
tent
telescopic cage
2900 elevator range
transfer gallery
fine positioning table
3300
3750
770
gallery chariot
1600
2350
LAPP 96/12/31

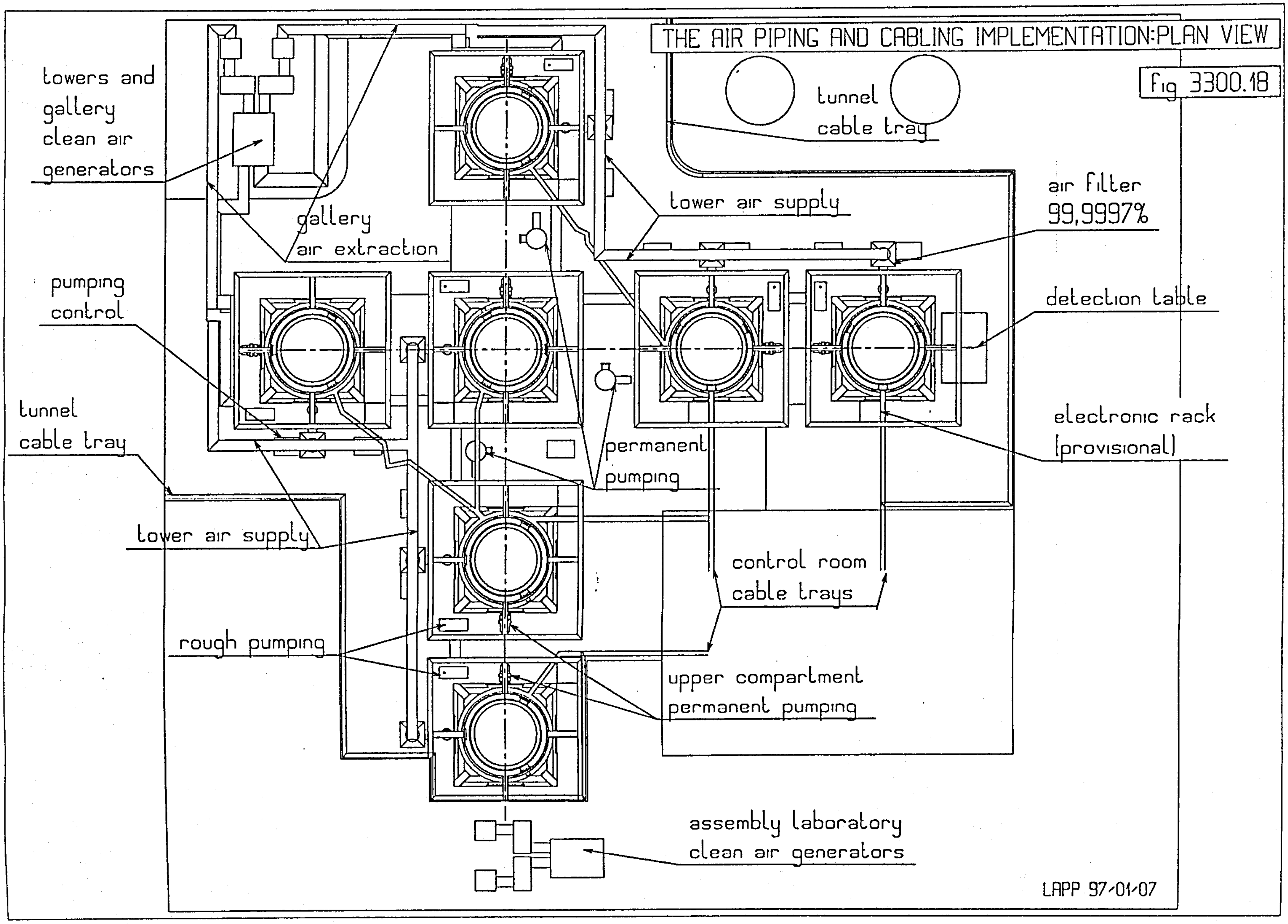

THE AIR PIPING AND CABLING IMPLEMENTATION:PLAN VIEW
Fig 3300.18
towers and gallery clean air generators
gallery air extraction
tunnel cable tray
air filter 99,9997%
tower air supply
pumping control
detection table
tunnel cable tray
electronic rack (provisional)
permanent pumping
tower air supply
control room cable trays
rough pumping
upper compartment permanent pumping
assembly laboratory clean air generators
LAPP 97-01-07

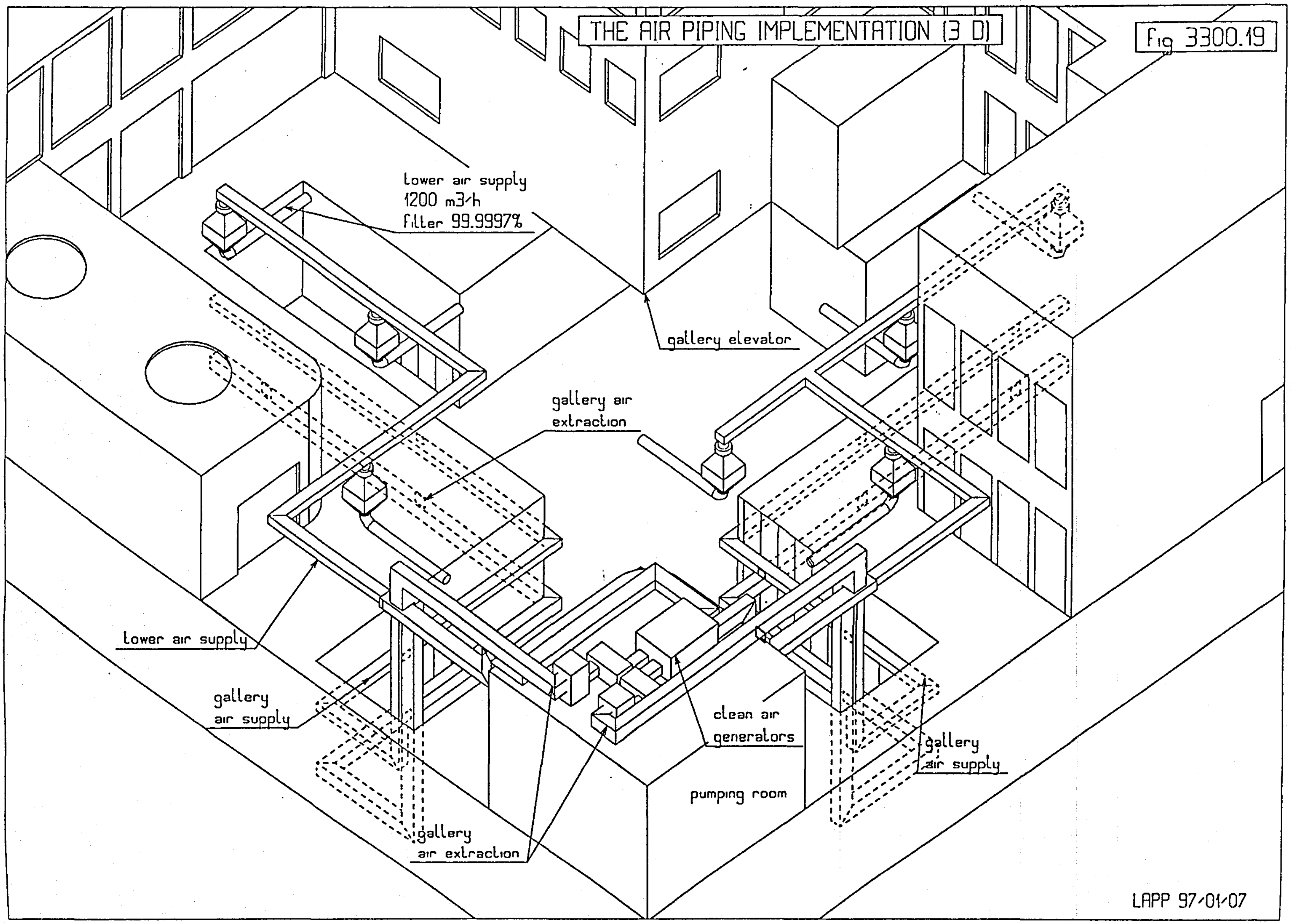
THE AIR PIPING IMPLEMENTATION (3 D)
fig 3300.19
lower air supply
1200 m3/h
filter 99.9997%
gallery elevator
gallery air
extraction
lower air supply
gallery
air supply
clean air
generators
gallery
air supply
pumping room
gallery
air extraction
LAPP 97/01/07

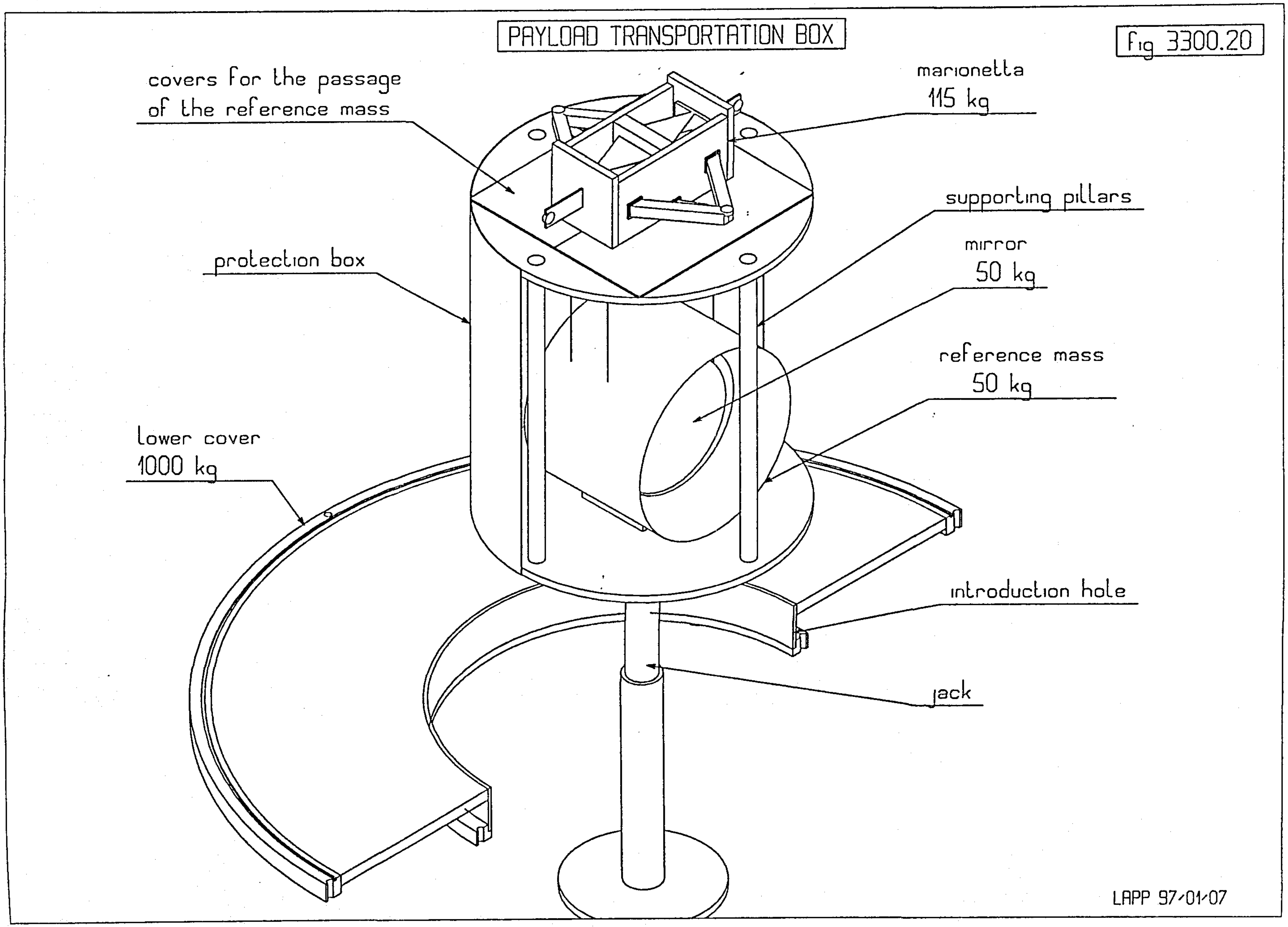
PAYLOAD TRANSPORTATION BOX
Fig 3300.20
covers for the passage of the reference mass
marionetta 115 kg
supporting pillars
mirror 50 kg
protection box
reference mass 50 kg
lower cover 1000 kg
introduction hole
jack
LAPP 97-01-07

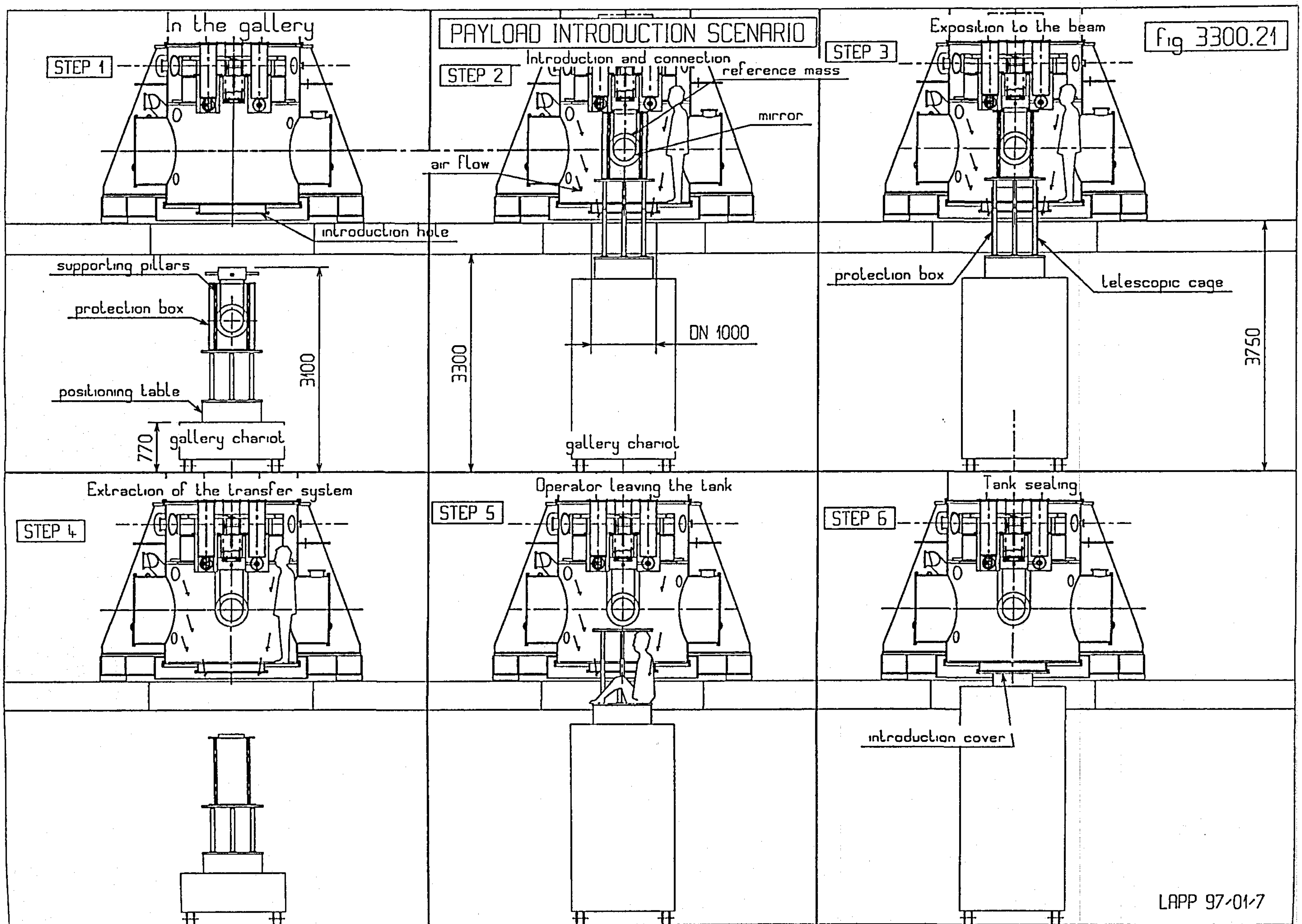

PAYLOAD INTRODUCTION SCENARIO
Fig 3300.21
STEP 1
In the gallery
introduction hole
supporting pillars
protection box
positioning table
gallery chariot
3100
770
STEP 2
Introduction and connection
reference mass
mirror
air flow
DN 1000
3300
gallery chariot
STEP 3
Exposition to the beam
protection box
telescopic cage
3750
STEP 4
Extraction of the transfer system
STEP 5
Operator leaving the tank
STEP 6
Tank sealing
introduction cover
LAPP 97-01-7

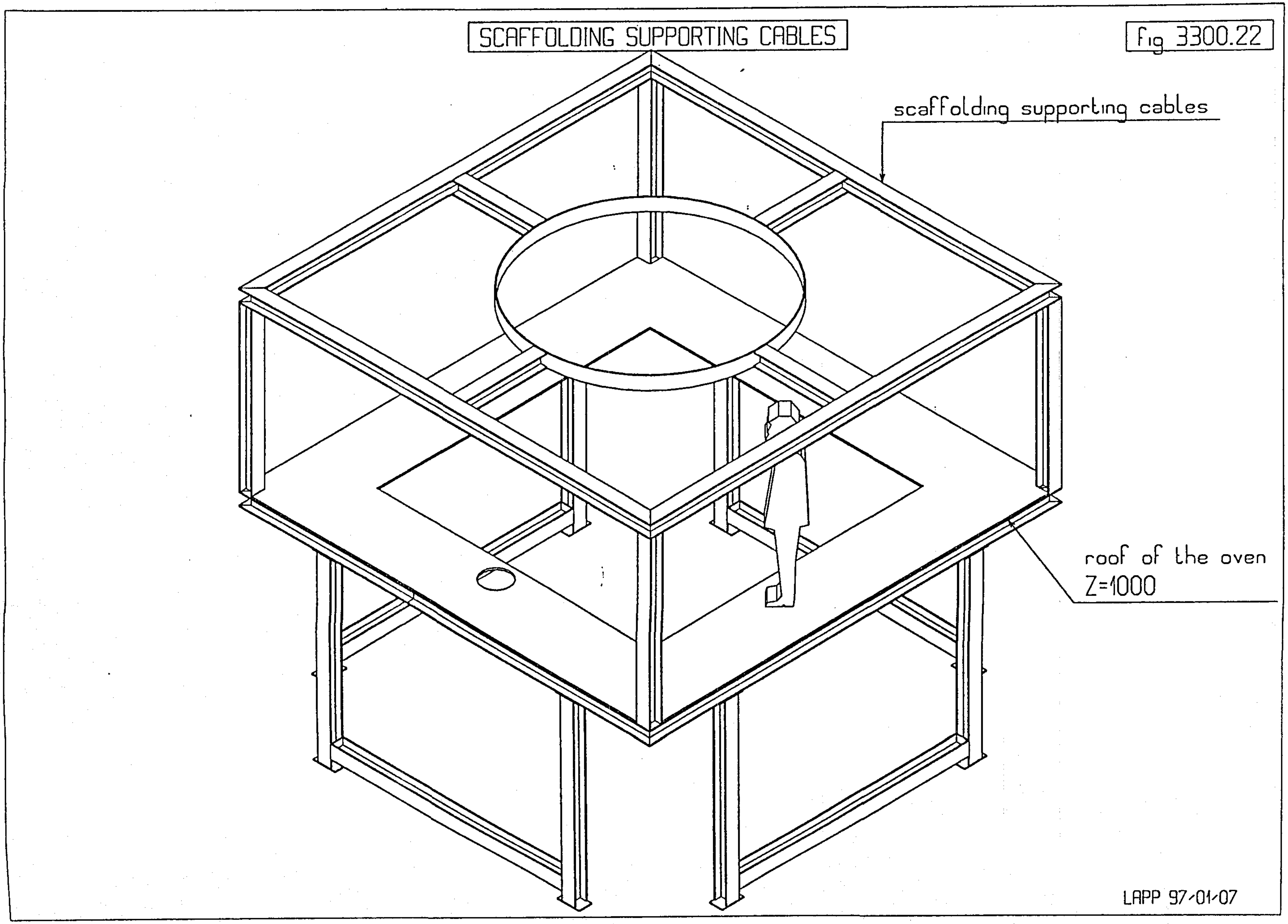
SCAFFOLDING SUPPORTING CABLES
fig 3300.22
scaffolding supporting cables
roof of the oven
Z=1000
LAPP 97-01-07

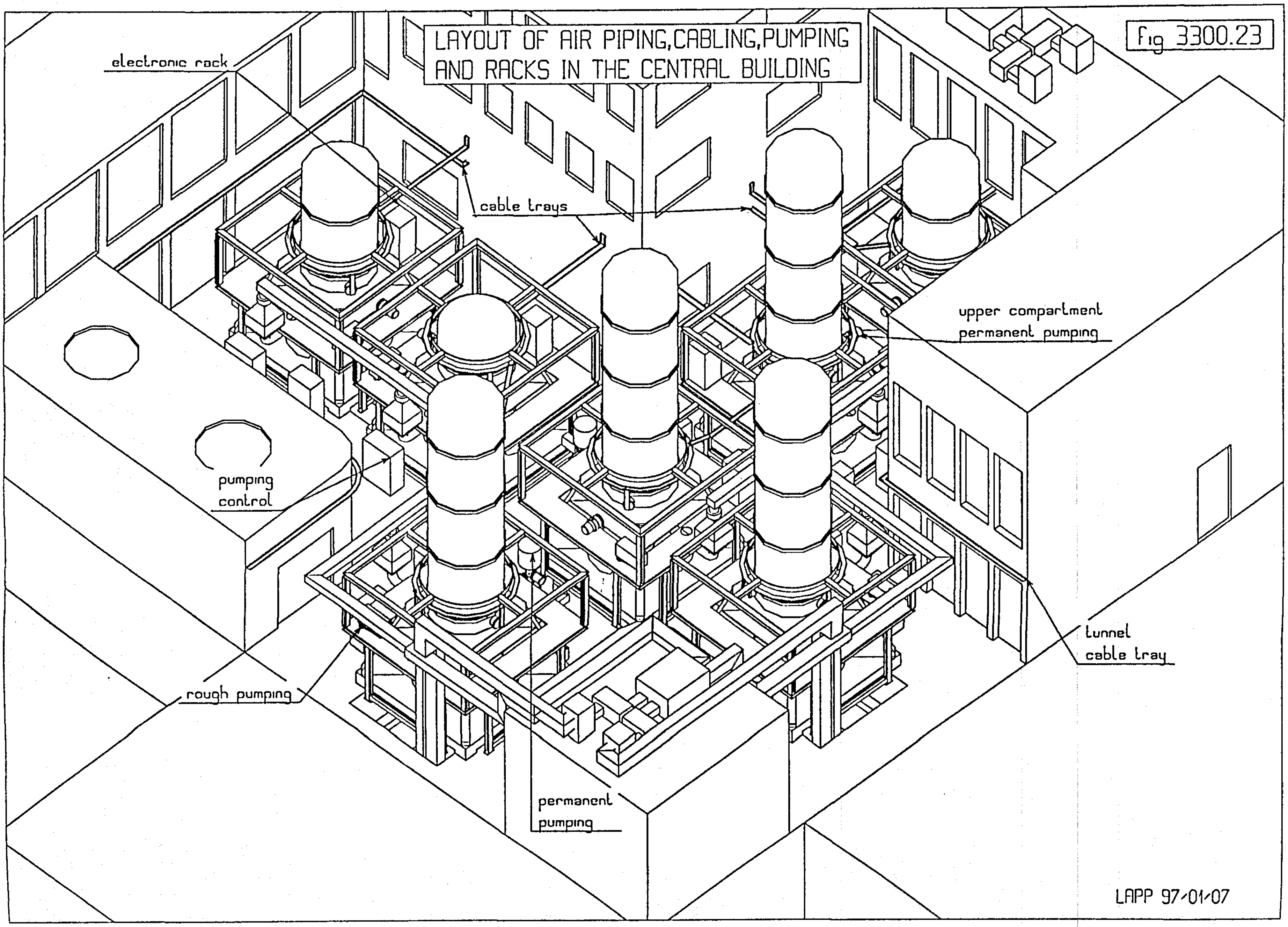

LAYOUT OF AIR PIPING,CABLING,PUMPING AND RACKS IN THE CENTRAL BUILDING
fig 3300.23
electronic rack
cable trays
upper compartment permanent pumping
pumping control
tunnel cable tray
rough pumping
permanent pumping
LAPP 97-01-07

SUSPENSION ASSEMBLY SCAFFOLDING

Fig 3300.24

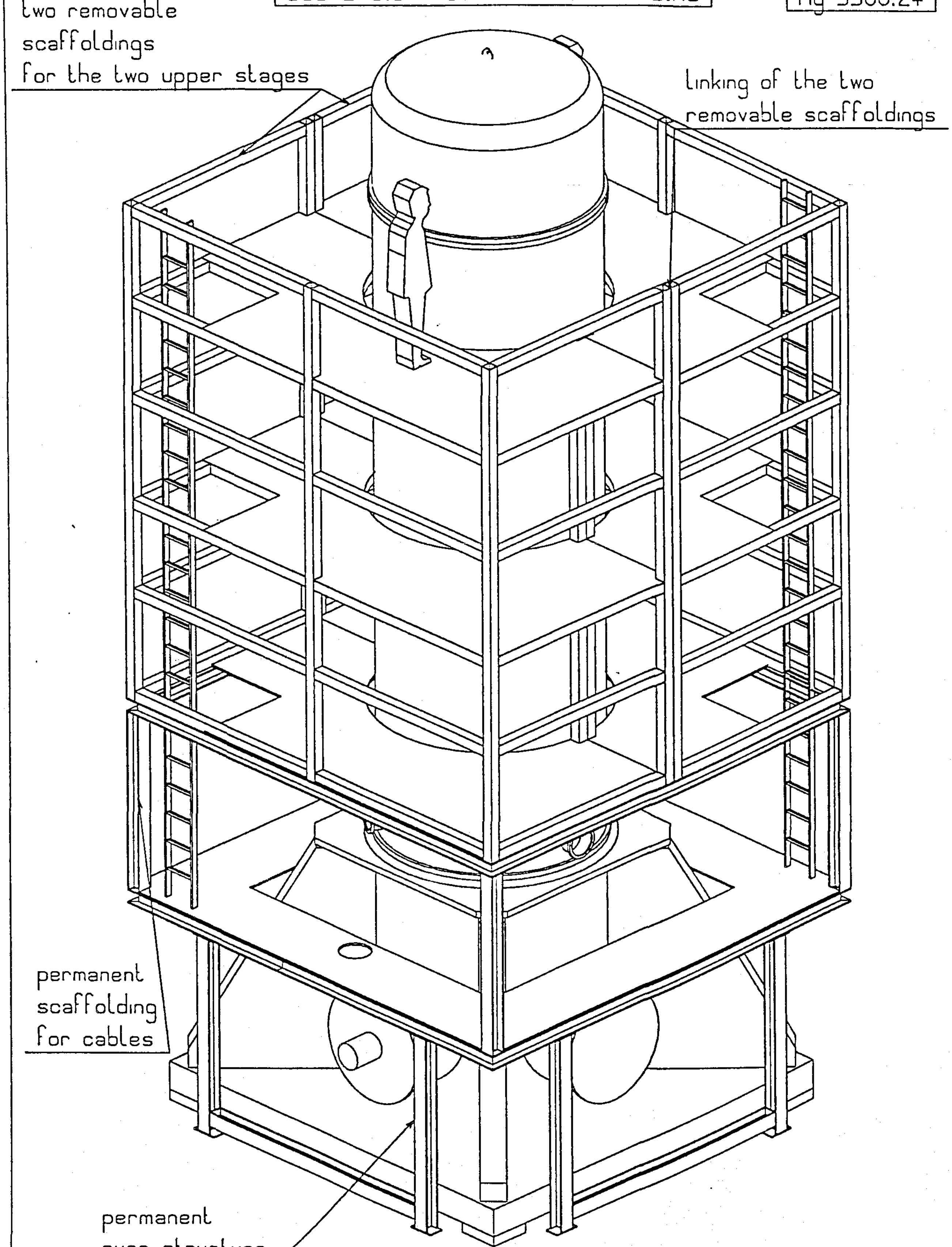

LAPP 97/01/07

34. Pumping system

Table of contents

34.1 Pumping system function and concept

The pumping system is designed to produce and monitor the vacuum for the Virgo interferometer. The main Virgo vacuum volumes are: two arm tubes, mirror towers (recycling, beam splitter, West input, West terminal, North input, North terminal and double recycling tower), single volume towers (mode cleaner, injection, and detection towers) and mode cleaner tube. Each pumping station for a volume must provide rough pumping from atmospheric pressure to 0.1 mbar, intermediate pumping down to 10^{-6} mbar and permanent pumping for required working vacuum. Gate valves separate the different large vacuum volumes, tubes and towers, to enable one to vent each large volume for interventions without spoiling the vacuum of the others.

The Virgo vacuum level is classified into two different regimes: the lower parts of mirror towers and the arm tubes in ultra high vacuum (UHV) range, the upper parts of the mirror towers, the single volume towers, and the mode cleaner tube in high vacuum (HV).

In UHV volumes, the permanent pumping is provided by titanium sublimation pump and ion pumps. In HV volumes the intermediate and permanent pumping is provided by magnetic bearing turbo molecular pump (TMP) groups.

Towers: Each mirror tower is divided into upper part and lower part by a separating roof. In order to reduce the gas transfer from the upper part to the lower part, a differential pumping system must pump the "differential volume" contained in the separating roof. A pump for emergency in the upper part is also provided for avoiding pollution of the lower part in case of stop of upper permanent pumps. The pumping system of the single volume towers is similar to the one for the upper part of the mirror towers.

The mirror towers and the single volume towers are separated permanently by glass windows so no special vacuum devices are needed for transition of the vacuum regimes.

Tubes: Since each 3 km arm tube has a huge volume (3400 m^3), the rough pump shall be able to work continuously at 1000 mbar inlet pressure and get 0.1 mbar in less than 3 days; the intermediate pumps, turbo molecular, will evacuate the tube to 10^{-6} mbar and will work during bake-out; then permanent pumps, titanium sublimation and ion pumps, will produce UHV in the tube.

34.2 Pumping system requirements

34.2.1 Gas pressure

As already said in the introduction of the Virgo vacuum system (3000.2), the targets for the average partial pressure in the Virgo UHV volume are listed in Table 3400-1. In the high vacuum volumes only 10^{-6} mbar is required.

The very low partial pressure of the hydrocarbons, 10^{-14} mbar in Table 3400-1, is required to avoid the pollution on optical components in the lower part of the mirror towers.

Table 3400-1 Required partial pressure of Virgo UHV volumes

Gas Species	Required Pressure (mbar)
H_2	1×10^{-9}
H_2O	1×10^{-10}
N_2 and CO	1×10^{-10}
CO_2	1×10^{-10}
CH_4	1×10^{-10}
Other gases	1×10^{-10}
Hydrocarbons	1×10^{-14}

34.2.2 Pumping and venting time and speed

The rough-pumping and venting speeds are chosen mostly taking into account the needed time (volume under evacuation). During bake-out, the effective pumping speed shall keep the maximum H_2O pressure lower than $5x10^{-5}$mbar. During the permanent pumping phase, the effective pumping speed of the station must ensure the required vacuum. Table 3400-2 lists the pumping speed and time requirement for each vacuum volume.

Table 3400-2 Requirements of the effective pumping speed

Volume	Pumping unit	Pumping speed ($l\ s^{-1}$)	Pumping time
Tube	Rough pumping	260	~3 days
	Intermediate pumping	5400	~7 days (bake-out)
	Permanent pumping	39000	
	Venting	100	~2 days
Mirror tower	Rough pumping	7	~12 hours
	Upper permanent pumping	1000	
	Upper emergency pumping	180	
	Differential pumping	200	
	Lower intermediate pumping	180	~7 days (bake-out)
	Lower permanent pumping	3000	
	Venting	3	~24 hours
Single volume tower	Rough pumping	7	~12 hours
	Permanent pumping	1000	
	Venting	3	~24 hours
Mode cleaner tube	Rough pumping	7	~5 hours
	Intermediate pumping	180	~4 hours
	Permanent pumping	connected towers	
	Venting	3	~5 hours

34.2.3 Measurement instrumentation

Several instruments of different ranges have to be used. Requirements on the vacuum instruments are listed in Table 3400-3.

Table 3400-3 Instruments requirements

Process	Instruments	Measurement range (mbar)
Rough pumping	Capacitance	1000-1
	Pirani	$1\text{-}10^{-3}$
Intermediate pumping and bake-out	Bayard-Alpert	$10^{-3}\text{-}10^{-9}$
	Residual gas analyzer (RGA)	$10^{-5}\text{-}10^{-11}$
Permanent pumping	Bayard-Alpert in HV	$10^{-3}\text{-}10^{-9}$
	Penning in HV	$10^{-3}\text{-}10^{-9}$
	RGA in HV	$10^{-5}\text{-}10^{-12}$
	Bayard-Alpert in UHV	$10^{-3}\text{-}10^{-10}$
	Penning in UHV	$10^{-3}\text{-}10^{-10}$
	RGA in UHV	$10^{-5}\text{-}10^{-14}$

34.2.4 Dust cleanliness

All pumps must not induce dust pollution in vacuum volumes

34.2.5 Life time

Running time of the pumping installation: 20 years

34.3 Pumping system interfaces

34.3.1 Sources of gases in the vacuum volumes

From the tests on the prototypes, values lower than 5 10^{-15} mbar l $s^{-1}.cm^{-2}$ were obtained for the outgassing rate of hydrogen from stainless steel. With a safety factor of at least 10, the figure of 5 10^{-14} mbar l $s^{-1}.cm^{-2}$ is taken as basis for the vacuum requirement to the UHV volume inner surface. This implies that all the relevant stainless steel components of the lower parts of mirror towers and tubes have to be fired in air or vacuum.

Outgassing rates and gas fluxes in permanent pumping phase used for design are listed in table 3400-4 and Table 3400-5, respectively.

Table 3400-4 Outgassing rate of materials

Material	Outgassing rate (mbar l s^{-1} cm^{-2})	gas
Stainless steel air-fired and vacuum baked	$5x10^{-14}$	H_2
Stainless steel not-air-fired and vacuum baked	$2x10^{-12}$	H_2
Stainless steel not-air-fired, not vacuum baked	$1x10^{-10}$	H_2O
Viton baked in vacuum	$2x10^{-12}$	other
Viton not-bäked in vacuum	$1x10^{-10}$	H_2O
Glass baffle in tubes	$3x10^{-13}$	H_2
Super attenuation filters in towers	$1x10^{-4}$ mbar l s^{-1}/filter	H_2O
	$2x10^{-6}$ mbar l s^{-1}/filter	H_2
	$1x10^{-7}$ mbar l s^{-1}/filter (TBC)	Hydrocarb.

Table 3400-5 Total flux per arm tube

Component	Area (cm^2)	number	total flux H_2 ($mbar\ l\ s^{-1}$)	total flux other gas ($mbar\ l\ s^{-1}$)
Tube	$1.2x10^8$	1	$6x10^{-6}$	–
Baffles	$3.3x10^6$	~100	$1x10^{-6}$	–
Tower (lower part) empty system	$4x10^5$	3	$6x10^{-8}$	–
Tower (upper to lower)		3	$3x10^{-8}$	$9x10^{-8}$
Valve Ø = 1000 (body))	$1.5x10^5$	2	$6x10^{-7}$	–
Viton gasket (Ø = 1000)	$1.8x10^3$	2	–	$8x10^{-7}$
Valve Ø = 200 (body)		28	$8x10^{-7}$	–
Viton gasket Ø = 200		20	–	$3x10^{-7}$
Valve Ø = 150 (body)		6	$2x10^{-8}$	–
Viton gasket Ø = 150		6	–	$3x10^{-8}$
Valve Ø = 63 (Body)	$5x10^3$	24	$2.4x10^{-7}$	–
Viton gasket Ø = 63	70	18	–	$2.5x10^{-7}$
Total			$<8.5x10^{-6}$	$<1.5x10^{-6}$

34.3.2 Bake-out

The bake-out for the lower part of the mirror towers and arm tubes will be carried out at 150°C for about 100 hours, in order to speed up the degassing of water from the chamber surface. Bake-out operation will produce high gas load for the intermediate pumping systems.

The tubes will be heated by Joule effect by applying electrical voltage to it (See 3100.6.4). The intermediate pumping system (TMP) and some instruments of the tubes shall work electrically connected to the tubes, then they could be at different potential respect to ground (TBC). Proper expedients will be adopted to ensure reliable operation of the pumps and instruments. In particular, more precise measurements have to be taken with a few minute interruption of the bake-out.

The pumping stations (connections, intermediate pumps, permanent pumps and measurement chambers on the lower part of the towers and tubes) are baked by heating tapes. The bake-out is controlled together with the bake-out of the volume.

34.3.3 Connection ports of pumping system

The connection port types and sizes for the pumping system to the volumes under evacuation are listed in Table 3400-6).

Table 3400-6 Connection ports to the pumping systems

Volume	Pumping unit	Connection port
Tubes	Rough pumping	CF100
	Intermediate pumping	CF200
	Permanent pumping	CF200
	Instruments	CF63
	Venting	CF63
Mirror towers	Upper rough pumping	CF40
	Upper permanent pumping	CF250
	Upper instruments	CF63
	Upper emergency pumping	CF100
	Differential pumping	CF100
	Lower rough pumping	CF40
	Lower intermediate pumping	CF200
	Lower permanent pumping	CF200
	Lower instruments	CF63
Single volume towers	Rough pumping	CF40
	Permanent pumping	CF250
	Instruments	CF63
	Emergency	CF100
	Venting	CF40
Mode cleaner tube	Rough pumping	CF40
	Intermediate pumping	CF100
	Instruments	CF63
	Venting	CF40

34.3.4 Pumping stations locations

The pumping stations for the tube shall be mounted near the fixed supports of the pumping modules to avoid large displacement induced by bake-out. The pumping system for the Mode Cleaner tube is located near the Injection tower. The pumping system location for the towers is described in section 3300.

Temperature range of the environment is listed below:

Temperature in the towers location: 20±3°C
Maximum temperature in the tube tunnel: 40°C (TBC)
Minimum temperature in the tube tunnel: -5°C (TBC)

The electrical power supply for the pumping system will be provided in the infrastructure. About 10 kW 220 VAC is the needed power for each pumping station.

If needed a small cooling unit will be installed for each pumping station.. Pumping station location and operation conditions.

34.3.5 Environmental Constraint

No polluting smokes should be rejected to outside environment from any pump.

34.3.6 Pumping system control

All the operations for the control of the tower pumping system and partially of tube pumping system, including safety and data acquisition, are computer controlled. The whole system is described in section 5000.2

34.4 Pumping system description

In order to increase the running efficiency of the antenna a few main choices were decided "a priori":

- gate valves must separate the different large vacuum volumes, tubes and towers, to enable one to vent each large volume for interventions without spoiling the vacuum of the others.
- gate valves must separate the pumping sets and the instrumentation boxes from the large vacuum volumes to allow for interventions.
- the valves to UHV volumes will have:
  - a viton gasket if normally open;
  - a viton gasket if normally closed and protected by vacuum in other side;
  - a metal gasket if normally closed and not protected in other side.

In order to reduce possible hydrocarbons pollution, rough pumps, for both roughing of the chamber and backing of the turbo molecular pumps (TMP), must be oil free at least in the process chamber, and the lubricant in the bearing box shall be protected properly; ceramic or magnetic bearing TMPs are acceptable.

The pumping system consists of several modular units of different types: 8 for pumping, 4 for vacuum measurements (called "bottles") and 2 for venting (it includes also the venting and air shower connections to towers).

34.4.1 Pumping system for tubes

Pressure stability: During the permanent pumping, the ion pumps are the only source of molecule bursts in the unit. There are many evidences that micro-objects may be expelled from ion pump electrodes. In order to minimize this effect, the ion pump is shielded from the tube by placing it after one of the Ti sublimator.

Absence of pollution: All the rough pumps will be oil-free pumps and the turbo pumps will be equipped with ceramic or magnetic bearings.

Titanium migration, if any, during a sublimation will be avoided by closing the gate valves. The absence of Ti dusts or peeling was demonstrated for typical layers, 0.1 μm thick. This figure would correspond to a 20 year pumping without venting.

Absence of mechanical vibrations: During the permanent pumping phase, the system does not generate internal vibrations.

Flexibility and easy maintenance: The gate valves insure a maximum flexibility and easy maintenance in all respects.

Pumping capacity: With one 15 g Ti ball per sublimator and 2 sublimators per 300 m of tube, the lifetime of the permanent pumping is insured for hundreds of years.

34.4.1.1 Rough pumping of the tubes: unit #1

The main specification for rough pumping concerns the absence of pollution, neither internal nor external. Internal pollution refers to hydrocarbons. For the rough pumping, regular spacing of the pumps along the tube is of no importance. A single unit, "Pumping Unit #1", located in the central building, will be used to pump down each tube, one after the other. The rough pumping must evacuate the tube from atmospheric pressure to 0.1mbar at which the intermediate turbo pumps of hybrid type can start to work. To avoid any back-stream from the rough pump system, its ultimate pressure must be 0.01mbar.

The rough pumping system is shown in Figure 3400-1: a Roots pump P11 with nominal speed 1000m^3h^{-1} is backed by a big oil-free pump P12 (250 m^3 h^{-1}). In case the ultimate pressure of the unit could not meet the requirements, a Scroll pump P13 (25 m^3 h^{-1}) (in the dot line box of Figure 3400-1) must be connected in parallel with P12 to get the correct ultimate pressure (TBC).

The pumping speed of the group and the pressure evolution in the tube are shown by dot and solid line in Figure 3400-2, respectively. The group can evacuate the tube to 0.1mbar in less than two days.

This pumping system will be controlled locally.

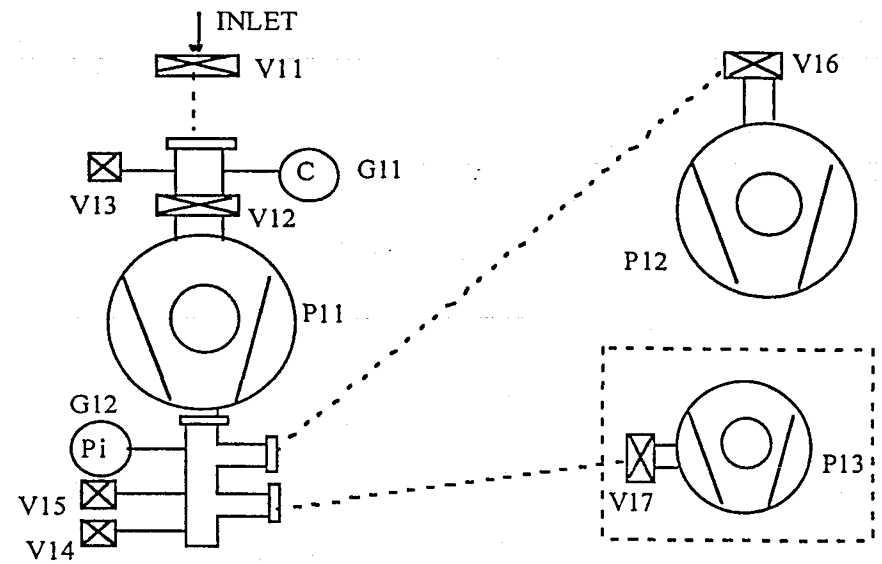

Figure 3400-1: Rough pumping for tubes: unit #1

Table 3400-7 Description of unit #1

V11	UHV Vitonl valve CF 100, Manual
V12	Viton valve ISO 100, electropneumatic
V13, V14	Viton valve KF16, manual
V15	Viton valve KF16, electromagnetic
V16, V17	Viton valve KF40, electromagnetic
P11	Roots, 1000 m^3 h^{-1}
P12	Oil-free pump, 250 m^3 h^{-1}
P13	Scroll, 25 m^3 h^{-1}
G11,G12	Pirani gauge with controller

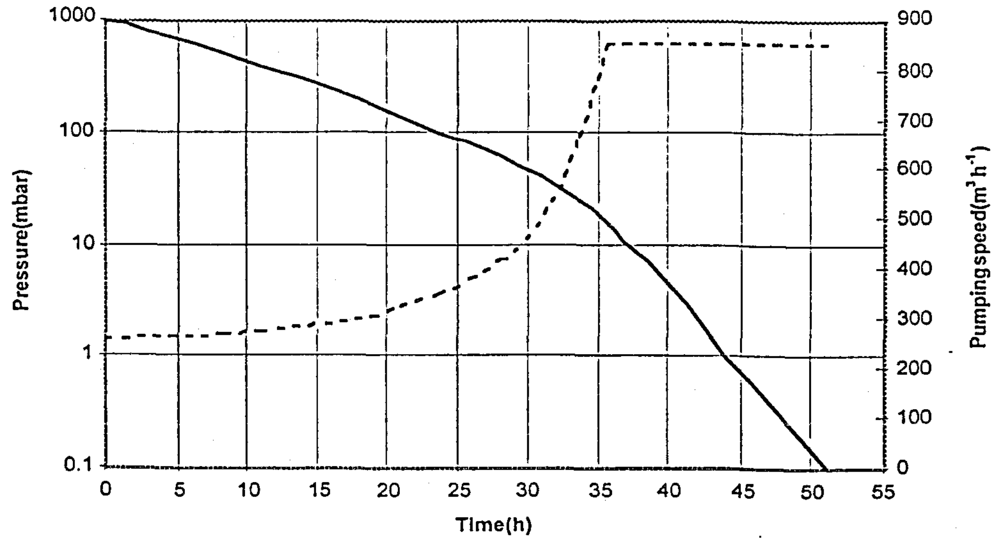

Figure 3400-2: Pumping curve for 3 km tube with the rough pumping system.

34.4.1.2 Intermediate pumping of the tubes: unit #2

The intermediate pumping system, shown in Figure 3400-3, is a typical TMP group. TMP P21 with 1000 $l.s^{-1}$ nominal pumping speed is connected to the tube via a gate valve V21 and backed by a oil-free pump (25 m^3h^{-1}) P21. A valve V23 provides a leak test port. A Pirani G22 gauge monitors the fore-line pressure, a Bayard-Alpert gauge in the front of the TMP is used to test the group itself when V21is closed and to test the pressure in tube when V21 is opened.

In order to keep maximum water partial pressure $<5x10^{-5}$ mbar during bake-out, 6 pumping stations are chosen, they are located each 600m.

Hybrid TMP will be chosen, so the pumping group can start to work at 0.1 mbar inlet pressure.

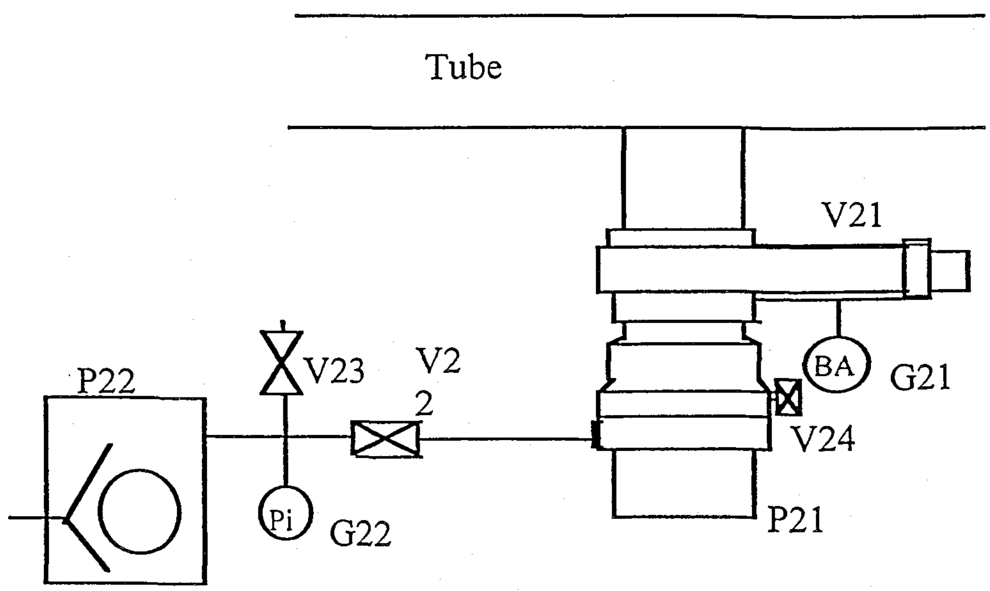

Figure 3400-3: Intermediate pumping of the tubes: unit #2.

Table 3400-8 Description of unit #2

V21	UHV Viton/metal valve CF200, electropneumatic (TBC)
V22	Viton valve KF40, electropneumatic
V23	Viton valve KF40 , manual
V24	Vent-valve, electromagnetic, KF16
P21	1000 l s^{-1} TMP ceramic bearing model with a CF 200 flange, an integrated venting valve, an air cooling system and its controller
P22	25 $m^3 \cdot h^{-1}$ dry pump
G21	B-A gauge with controller
G22	Pirani gauge with controller

34.4.1.3 Permanent pumping of the tubes: units #3

There will be 11 permanent pumping stations along each tube arm connected with a CF200 port, including one at both ends. Each pumping station has 3000 l s^{-1} effective pumping speed for hydrogen and 200 l s^{-1} for other gases provided by ion pump. The ion pump is shielded from the tube by placing it after one of the Ti sublimator. With the above conditions, one fresh sublimation per year will be sufficient.

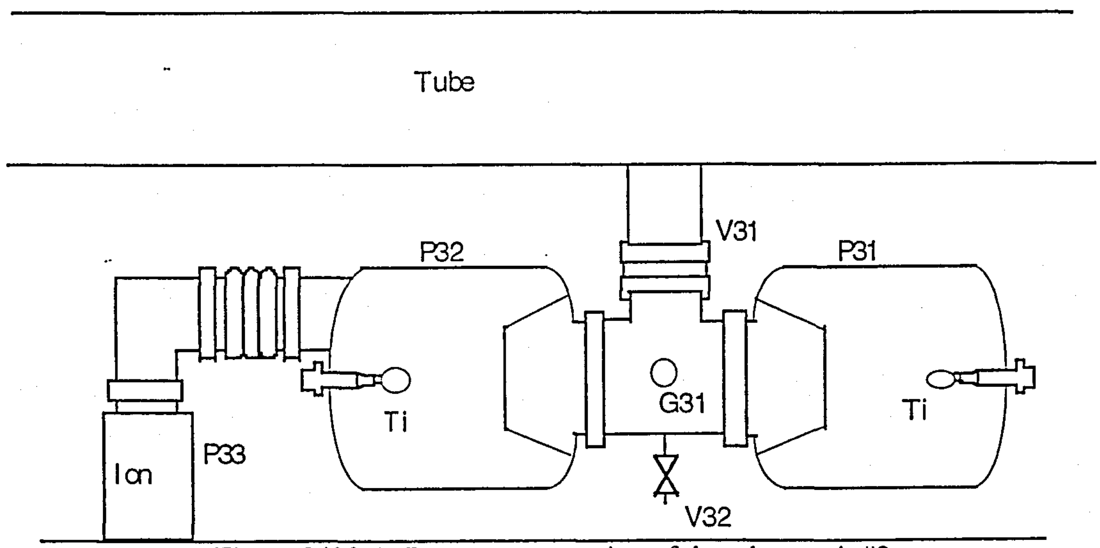

Figure 3400-4: Permanent pumping of the tubes: unit #3.

Table 3400-9 Description of unit #3

V31	UHV Viton valve CF200
V32	All metal valve CF40 for venting and rough pumping
P31,P32	Ti sublimator with the control unit; Ti pot, l=600 mm, Ø=500 mm, 1.4 m^2
P33	Ion pump, noble diode 200 l s^{-1} with its power unit
G31	Inverse Magnetron 10^{-11} mbar.

34.4.1.4 Instrumentation bottle for the tube: unit a.

This bottle is connected to the tube with a CF63 port, and it will contain an inverse magnetron gauge and a RGA to monitor continuously the pressure and the composition of gas. There will be 8 units per tube.

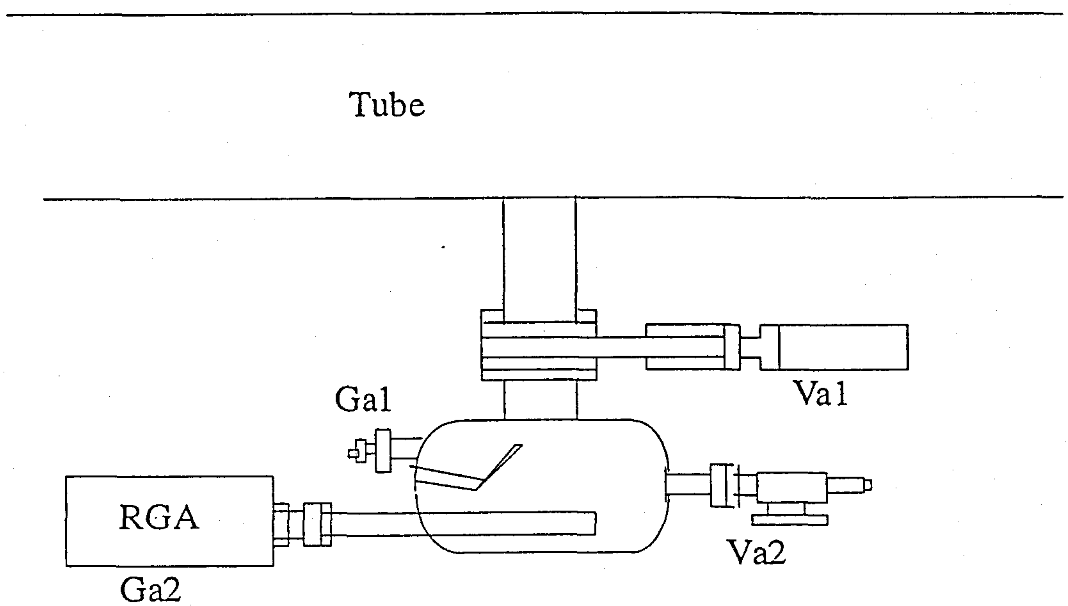

Figure 3400-5: Instrumentation bottle for the tube: unit a.

Table 3400-10 Description of unit a

	Instrumentation chamber
Va1	UHV Viton CF63 valve
Va2	All metal CF40 valve for venting the instrumentation chamber and re-evacuation.
Ga1	Inverse magnetron gauge with controller
Ga2	RGA head with controller

34.4.1.5 Instrumentation bottle for the tube: unit b.

This bottle will contain a Capacitance and a Pirani to measure the pressure during rough pumping phase, and a Bayard-Alpert gauge to monitor the pressure during bake-out. RGA will be permanently used to monitor the residual gas composition.

There will be three units located at the two ends and the center of the tube.

Table 3400-11 Description of unit b

	Instrumentation chamber
Vb1	UHV viton CF63 valve
Vb2	All metal CF40 valve for venting the instrumentation chamber
Gb1	Capacitance gauge
Gb2	Pirani gauge with controller
Gb3	Inverse Magnetron gauge with controller
Gb4	Bayard-Alpert gauge and controller
Gb5	RGA head with controller

34.4.1.6 Venting of tube: unit #9.

Concerning the huge volume of the tube only natural air can be used to vent the tube for human safety reason. Filters for dust, not for water and hydrocarbons, are required. Venting shall be finished within two-three days.

Figure 3400-6 shows the venting unit attached to the tube with a CF63 flange. A differential capacitance gauge G91 will monitor the pressure difference between the tube and atmosphere (ATM). A small rough to evacuate the un-filtered air through V92 is temporarily used. In order to vent the tube in the required time a venting filter with 360 m^3 h^{-1} flux at 1 bar pressure difference is chosen; it can remove 99.9999999% of particles whose diameter is greater than 0.003 μm; the filter chamber will be about 0.5 m in diameter and 1.2 m high. A metal net F92 works as a filter for unexpected large dimension dust swept by the venting flow.

The Joule-Thomson coefficient is 0.23 °C atm^{-1} for dry air at 20 °C, that is to say, the air temperature is about 0.23°C less after passed the filter. The effect for wet air has to be checked (TBC).

A cone is used as the venting port to reduce noise. If the cone has 100 mm in diameter in the aperture, the air speed is about 46 km h^{-1}, in the 63cm tube before the filter 115 km h^{-1}.

When the pressure in the tube approaches 1 bar, the venting flow becomes too low to reach the ATM (reference 1013 mbar). The oil-free fan shall be employed when the pressure in the tube is a few mbar less than ATM to provide higher venting pressure (a few mbar higher than ATM).

Figure 3400-7 shows a typical venting curve.

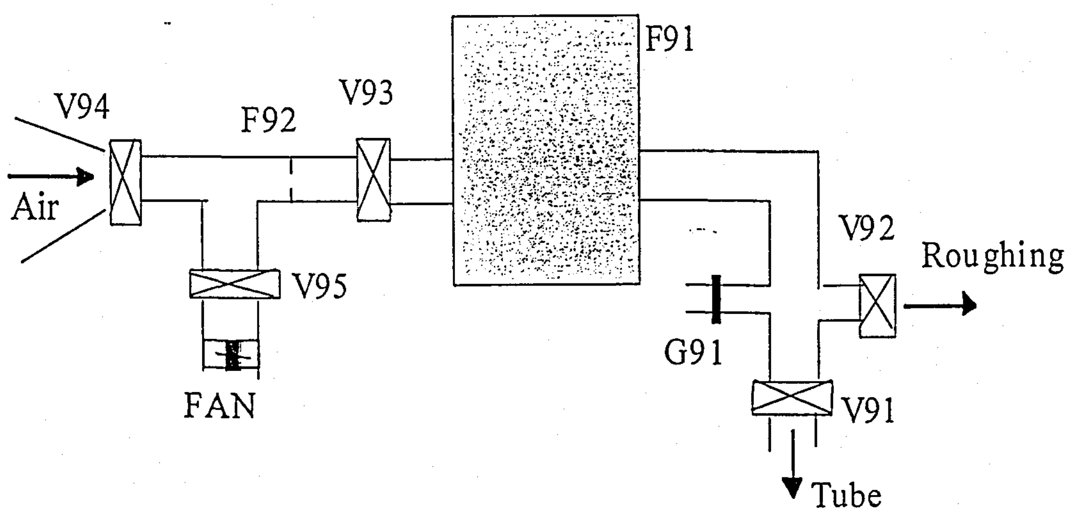

Figure 3400-6: Venting unit for the tubes: unit #9.

Table 3400-12 Description of unit #9

V91	Metal valve CF63, Manual, angle, spindle
V92	Viton valve KF40, Manual, spindle
V93	Viton valve ISO63, Manual, angle, spindle
V94	Viton valve ISO63, Manual, gate
V95	Viton valve ISO63, Manual, gate
FAN	Fan in Φ63 mm tube, ~40 W
G91	Differential Capacitance gauge, KF16
F91	Gas filter, 0.003 μm, 360m^3 h^{-1}
F92	Metal nets

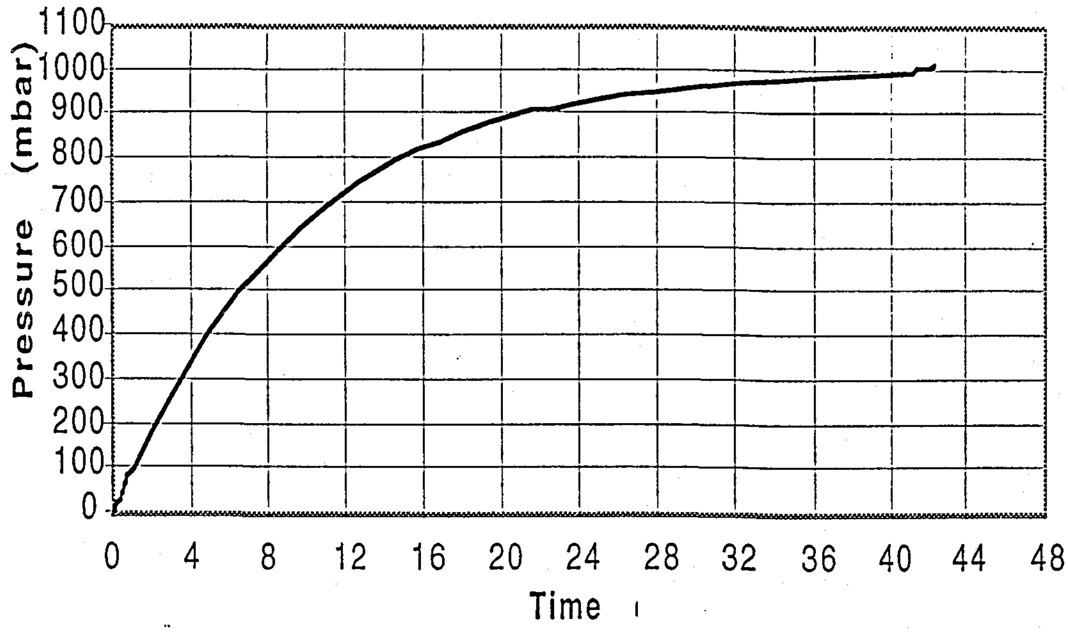

Figure 3400-7: Venting up to ATM (1013 mbar) for 3 km tube with 360 $m^3 h^{-1}$ filter. The fan provides 1020 mbar venting pressure at 1000 mbar in tube.

34.4.2 Pumping system for mirror tower

The connection between the two parts of the mirror towers is done by two cylinders, 1 cm diameter 20 cm long, with a central chamber 10 cm high for the differential pumping. This chamber is connected to a pumping group, external to the tower, via a 10 cm diameter pipe. This arrangement will reduce to less than 0.01 l s^{-1} the gas flow into the tower lower part through the central hole. The contribution from the joint of the separating roof is not measured at the moment and has been assumed to be zero, because the roof will be strictly connected to the tower wall (TBC). A value of 0.1 l s^{-1} for H_2 and 0.03 l s^{-1} for H_2O is assumed to have a safety factor of 10.

The pressure in the upper part is supposed to be 10^{-6} mbar and the residual gases to be water for 90 % and hydrogen for 10 %.

The problem of the hydrocarbon outgassing of the various components contained in the upper part of the towers is of utmost importance. Presently, it is considered from the point of view of minimizing the outgassing of the specific components. Ways to reduce its impact on the mirrors part are also investigated.

Figure 3400-8 shows the synopsis of the pumping for the mirror towers.

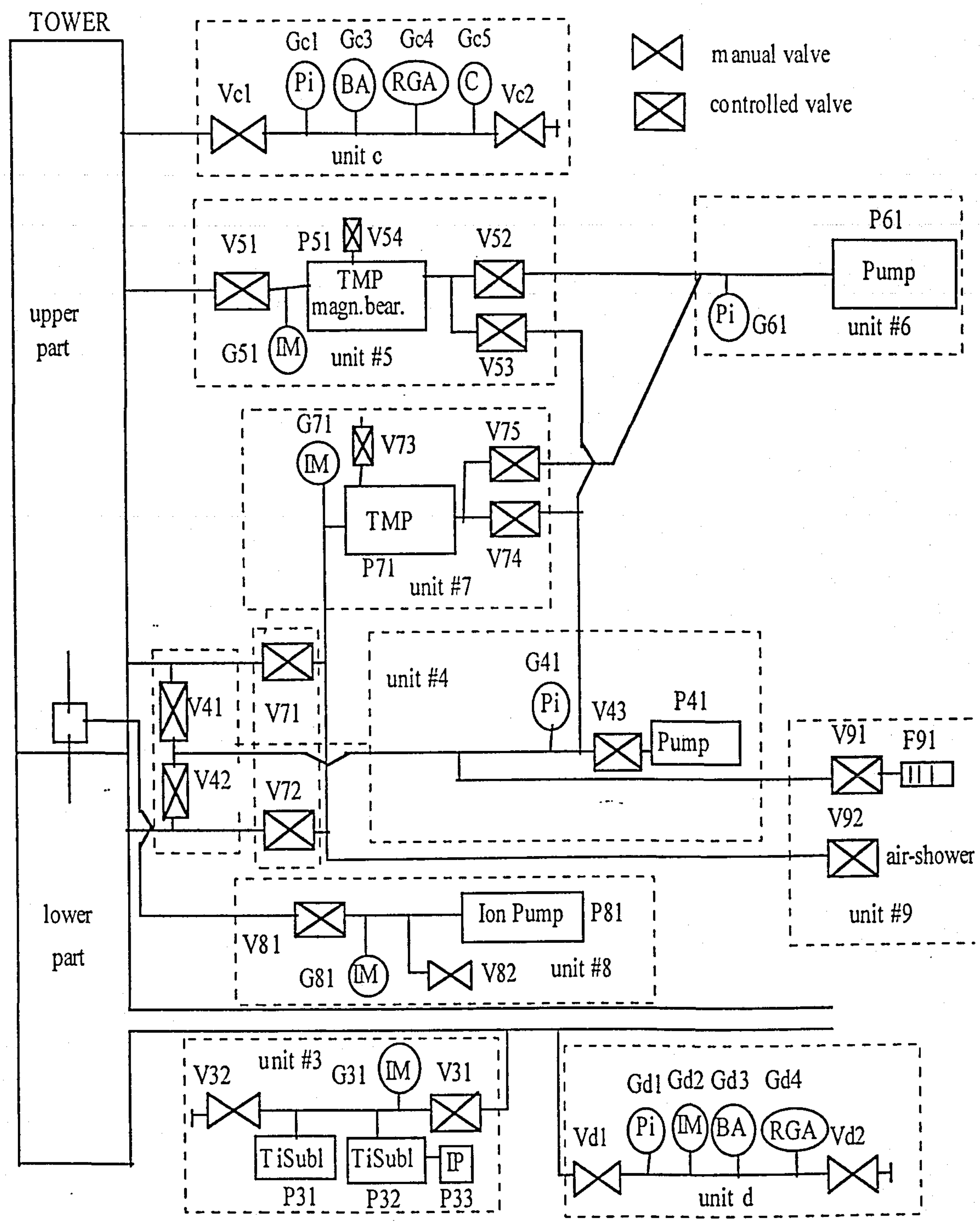

Figure 3400-8: Synopsis of the pumping for the mirror towers.

34.4.2.1 Rough pumping of the mirror tower: unit #4

During the rough pumping the two parts of the tower are connected by a 40 mm external tube to the dry pump. The valve V41 and V42 are controlled together to avoid pressure difference between two parts of the tower.

Several non turbulent cycles of pumping and venting between atmospheric pressure and 1 mbar are required in order to eliminate dusts. Such a time consuming process requires one rough pump unit per tower.

Table 3400-13 Description of unit #4

V41	Viton valve CF40
V42	Viton valve CF40
V43	Viton valve CF200
P41	25 $m^3 \cdot h^{-1}$ dry pump and its venting valve
G41	Pirani gauge with controller

34.4.2.2 Permanent pumping of the upper part: unit #5.

The upper part of the tower contains many electronic components, mechanical devices and the associated wiring, the outgassing flow of which is not completely known. For this reason it is connected to the lower part through a differential pumping system [see later] with an effective conductance lower than 10^{-2} l s^{-1} for water vapor.

To have a large safety factor about the gas flux toward the lower part a pressure of 10^{-6} mbar is required on the upper part. One assumes at the moment a total outgassing rate of 10^{-3} mbar l s^{-1}, so an effective pumping speed of 1000 l s^{-1} is therefore required. This pumping speed can be obtained using a turbo with a pumping speed higher than 1500 l s^{-1} horizontally mounted 400 mm far from the tower and connected through a 250 mm valve.

For reliability reasons (mean time before failure larger than 10 years), a magnetic bearing TMP is chosen.

The dry pump of unit #4 is also connected to the TMP outlet and it will be used as fore pump of unit #5 during the intermediate pumping. In permanent pumping conditions the unit #6 [see later] can be used as fore pump.

Table 3400-14 Description of unit #5

P51	1500 l s^{-1} TMP whit magnetic bearing, integrated venting valve, air cooling system and controller
V51	Viton valve CF250
G52	Inverse Magnetron gauge with controller
V52	Viton valve KF40 between the TMP and the unit #4
V53	Viton valve KF40 between the TMP and the unit #6

34.4.2.3 Fore pumping for upper turbo and emergency for lower bake-out fore pumping: unit #6.

A small pump is provided for the fore pumping of the upper turbo pump dedicated to the emergency pumping of the tower upper part and to the bake-out pumping of the lower part; it can also be used for the fore pumping of the large magnetic TMP [unit #5], during the permanent pumping.

This group consists of a small oil-free roughing pump and a Pirani gauge.

Table 3400-15 Description of unit #6

P61	5 $m^3 h^{-1}$ oil-free backing pump
G61	Pirani gauge with controller

34.4.2.4 Intermediate pumping of mirror tower lower part and emergency pumping of mirror tower upper part: unit #7

In case of emergency (failure of the upper TMP), unit #5 must be switched off. It is mandatory to be able to immediately switch on a temporary unit to keep the pressure in the upper part not too high. Furthermore an intermediate and bake-out pumping is needed for the tower lower part.

Both functions can be supplied by a 200 l s^{-1} Hybrid TMP model connected to the large by-pass between the two parts of the tower. Unit #4 or #6 will provide the fore pumping for .

Table 3400-16 Description of unit #7

V71	Viton valve CF160
V72	Metal valve CF200
V73	Viton valve KF16
V74	Viton valve KF25 between the TMP and unit #4
V75	Viton valve KF25 between the TMP and unit #6
P71	200 l.s^{-1} TMP whit magnetic or ceramic bearing, integrated venting valve, air cooling system and controller
G72	Inverse Magnetron gauge with controller

34.4.2.5 Differential Pumping in conductance tube: unit #8.

To reduce the gas transfer to the lower part of the tower a differential pumping system must be used. It consist of a vacuum chamber on the small conductance tube, a 100 mm tube through the tower wall, an external 100 mm valve and an ion pump 200 l s^{-1}. An Inverse Magnetron gauge to measure the pressure before switching on the ion pump and a valve for venting and external pumping completes the group.

Table 3400-17 Description of unit #8

V81	UHV Viton valve CF 100
P81	Ion pump, noble diode 200l/s with its controller
G82	Inverse Magnetron gauge with controller
V82	Metal valve CF40 for venting the ion pump

34.4.2.6 Permanent pumping of the lower parts: unit #3.

This permanent pumping unit is identical to the one used on the tubes; it will be installed on one of the links between the towers.

34.4.2.7 Venting and air shower: unit #9.

Valves and filters, connected to the roughing line between the two parts of the tower, will provide the venting, and will allow the air shower via the big by-pass. An appropriate venting procedure will be set up, in order to prevent pressure differences between lower and upper tower (TBD).

Table 3400-18. Description of unit 9

V91	Viton CF40 valve
V92	UHV Viton CF200 valve
F91	Dust Filter

34.4.2.8 Instrumentation bottle for the upper parts: unit c.

This bottle will contain a Capacitance and a Pirani to follow the tower pressure during the rough pumping, a Bayard-Alpert to measure the pressure, and a RGA will be permanently used to monitor the main gas composition.

Table 3400-19 Description of unit c

	Instrumentation chamber
Vc1	Viton CF63 valve for connecting to the tower
Vc2	Viton CF40 valve for venting the instrumentation chamber
Gc1	Pirani gauge with controller
Gc2	Capacitance gauge with controller
Gc3	Bayard-Alpert gauge with controller
Gc4	RGA head with controller

34.4.2.9 Instrumentation bottle for the lower part: unit d.

This bottle will contain an Inverse Magnetron and a Bayard-Alpert to measure the total pressure in a reliable way in the vessel; and a RGA to be permanently used to monitor the residual gas composition on the mirror and to check the efficiency of the differential pumping system.

Table 3400-20 Description of unit d

	Instrumentation chamber
Vd1	UHV Viton CF63 valve for the instrumentation chamber
Vd2	All metal CF40 valve for venting the instrumentation chamber
Gd1	Pirani gauge with controller
Gd2	Inverse Magnetron gauge with controller
Gd3	Bayard-Alpert gauge with controller
Gd4	RGA head with controller

34.4.3 Pumping system for single volume towers

The pumping system for single volume towers is simplified respect to the system of mirror towers, Figure 3400-9 shows the synopsis of the pumping system.

Rough pumping unit #4': The rough pumping is similar to the one used on the mirror tower: the dry pump is connected directly to the tower for roughing and to the turbo pump unit #5 for backing.

Permanent pumping unit #5: The permanent pumping is identical to the one used on the mirror tower upper parts.

Emergency fore pumping unit #6: The emergency fore pumping is identical to the one used on the mirror tower.

Venting unit #9': A valve and filter, directly connected to the towers, are provided for venting.

Instrumentation bottle for the tower unit c: This bottle is identical to the one used on the mirror tower upper parts. The RGA will be permanently used to monitor the gas composition on the optics.

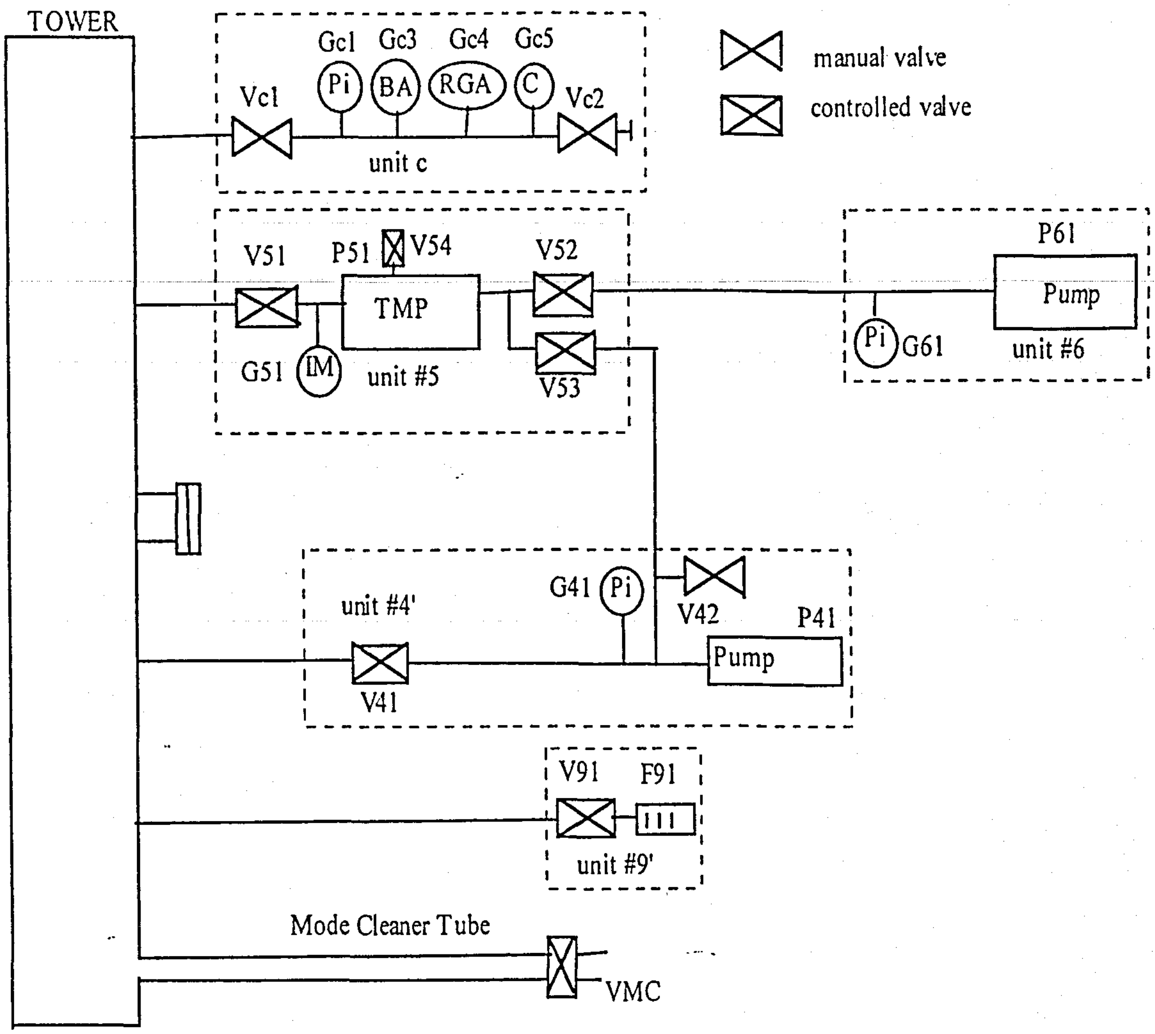

Figure 3400-9: Synopsis of the pumping of the single volume towers.

Table 3400-21 Description of pumping system for single volume towers

unit	component	description
unit #4'	V41	Viton valve CF40
	P41	25 $m^3 \cdot h^{-1}$ oil free pump and its venting valve
	G41	Pirani gauge with controller
unit #5'	P51	1500 $l\ s^{-1}$ TMP whit magnetic bearing, integrated venting valve, air cooling system and controller
	V51	UHV Viton valve CF250
	G51	Inverse Magnetron gauge with controller
	V52	Viton valve KF40 between the TMP and the unit #4
	V53	Viton valve KF40 between the TMP and the unit #6
	V54	Viton valve KF16 venting
unit #6	P61	Oil-free backing pump
	G61	Pirani gauge with controller
unit #9	V91	Viton CF16 valve
	F91	Dust Filter
unit c		Instrumentation chamber
	Vc1	Viton CF63 valve for connecting to the tower
	Vc2	Viton CF40 valve for venting the instrumentation chamber
	Gc1	Pirani gauge with controller
	Gc3	Bayard-Alpert gauge with controller
	Gc4	RGA head with controller
	Gc5	Capacitance gauge

34.4.4 Pumping system for Mode Cleaner tube

Figure 3400-10 shows the pumping system of Mode Cleaner tube.

Rough pumping: The rough pumping unit #4' is similar to the one used on the mirror tower: the dry pump is connected directly to the tube for roughing and to the turbo pump unit #7' for backing.

Intermediate pumping: A simplified version of unit #7 can provide for the intermediate pumping of the MC tube; it will consist of a 200 $l\ s^{-1}$ TMP model directly connected to the tube by a CF100 valve.

Permanent pumping: The permanent pumping of the mode cleaner tube will be achieved by the permanent pumping units of the two connected towers.

Venting: A valve and filter, directly connected to the MC tube, provide for the venting.

Instrumentation: An instrumentation bottle unit c' will monitor the pressure in the tube; the information is needed to operate the valves to the connected towers.

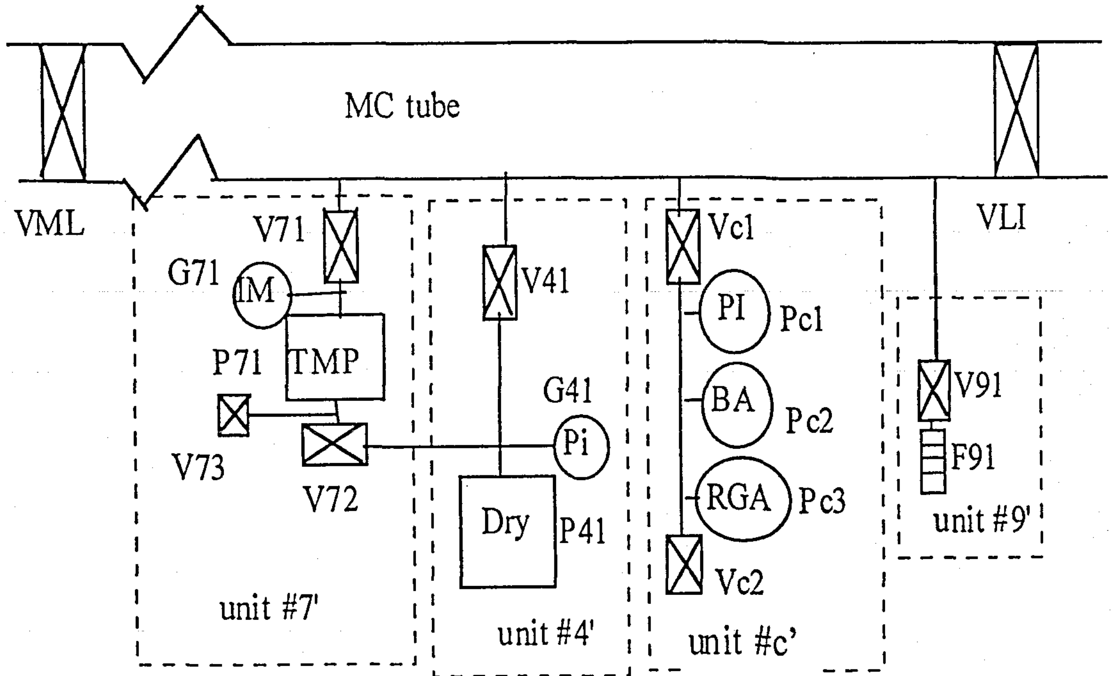

Figure 3400-10: Pumping system of Mode cleaner tube.

Table 3400-22 Description of pumping system of Mode cleaner tube

unit #4'	V41	Viton valve CF40
	P41	25 $m^3 \cdot h^{-1}$ dry pump and its venting valve
	G41	Pirani gauge with controller
unit #7'	V71	UHV viton valve CF100 to the tube
	P71	200 l s^{-1} TMP with magnetic or ceramic bearing
	G72	Inverse Magnetron with controller
	V72	Viton valve KF25 to the dry pump
	V73	Viton valve KF16 venting
unit #9'	V91	Viton valve KF40
	F91	Dust filter
unit c'		Instrumentation chamber
	Vc1	Viton CF63 valve for connecting to the tower
	Vc2	Viton CF40 valve for venting the instrumentation chamber
	Gc1	Pirani gauge with controller
	Gc3	Bayard-Alpert gauge with controller
	Gc4	RGA head with controller

34.4.5 Pumping sets for multiduty

34.4.5.1 Multiduty rough pumping: unit #10

A rough pumping set shown in Figure 3400-11 for medium volume is foreseen. It will be used for roughing the 300 m tube sections during the assembly tests, or to increase the roughing efficiency for the single volume tower tests. The pumping group will be portable: a roots pump (250 $m^3 h^{-1}$) backed by a dry pump (25 $m^3 h^{-1}$). It takes 70 hour to evacuate 300 m tube section and 5 hour for single volume towers from atmosphere pressure to 0.1 mbar.

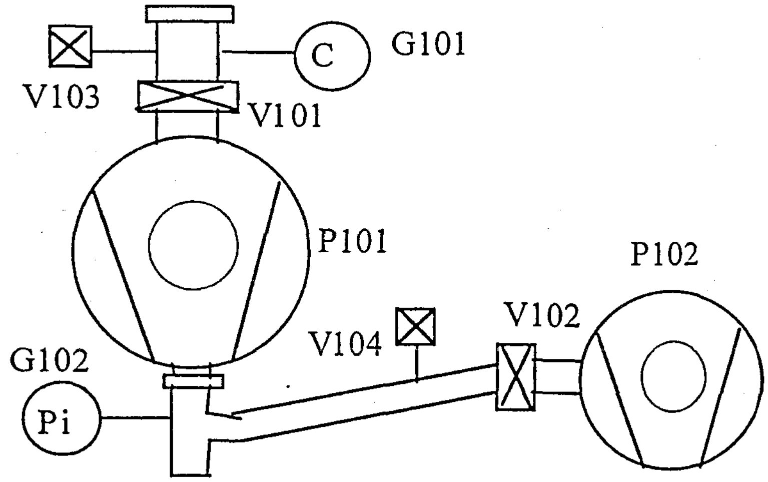

Figure 3400-11: Multiduty rough pumping: unit #10.

Table 3400-23 Description of unit #10

V101, V102	Viton valve KF40 electromagnetic
V103, V104	Viton valve KF16 electromagnetic
P101	Roots 250 $m^3 h^{-1}$
P102	Dry pump 25 $m^3 h^{-1}$
G101	Capacitance 1000-1 mbar
G102	Pirani 100-10^{-3} mbar

34.4.5.2 Pumping set for intervention on small volumes: unit #11

The intervention on some small volume chambers, such as measurement bottles and Ti sublimation pots, is foreseen without vacuum interruption to the big volumes (towers or tubes). After the intervention on a small volume, the vacuum has to be recovered by a separate pumping system shown in Figure 3400-12: a 70 $l.s^{-1}$ hybrid TMP backed by a dry pump will evacuate the volume from atmosphere to the same pressure as in the connected big volume (if UHV in big volume the intervened volume has to be baked). A RGA serves for monitoring of partial pressure during bake-out and leak-detection when the intervened volume is without RGA (Ti pots). The system must have 10^{-10} mbar ultimate pressure. At least two pumping sets are needed.

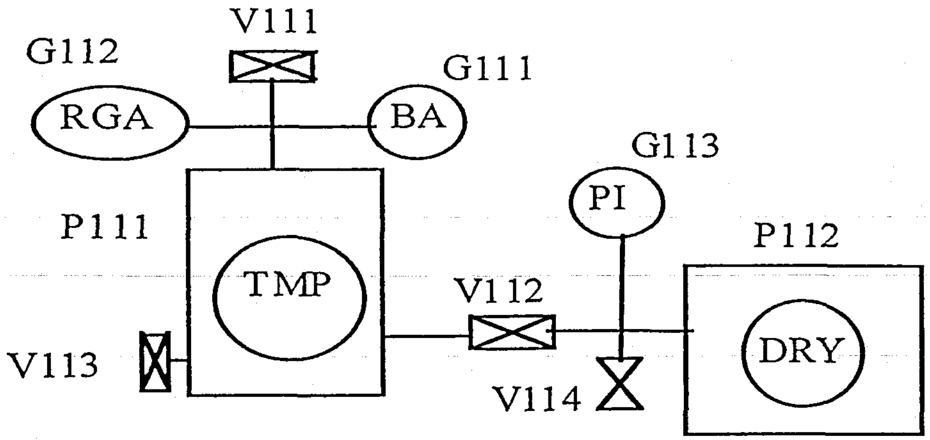

Figure 3400-12: Intervention pumping unit: unit #11

Table 3400-24 Description of unit #11

V111	UHV Viton valve CF40 electromagnetic
V112	Viton valve KF25 electromagnetic
V113	Viton valve KF16 electromagnetic
V114	Viton valve KF16, manual, spindle
P111	TMP 70 l s^{-1}
P112	Dry pump 25 $m^3 h^{-1}$
G111	Bayard-Alpert gauge with controller
G112	RGA with controller
G113	Pirani gauge with controller

34.4.6 Summary of the pumping system

The summary of the pumping system with respect to units and to components is given respectively in Table 3400-25 and 26.

Table 3400-25 Summary of pumping units

		Unit	1	2	3	4	4'	5	6	7	8	9	9'	10	11	a	b	c	c'	d
Tube	Rough pumping	1	1																	
	Intermediate pumping	2		12																
	Permanent pumping	3			22															
	Venting	9										2								
	Instrumentation	a														16				
	Instrumentation	b															6			
Mirror towers	L. permanent pumping	3			7															
	Rough pumping	4				7														
	U. permanent pumping	5						7												
	Fore emergency	6							7											
	L. intermediate pumping	7								7										
	Differential pumping	8									7									
	Venting	9'											7							
	U. instrumentation	c																10		
	L. instrumentation	d																		7
SV towers	Rough pumping	4					3													
	Permanent pumping	5						3												
	Fore emergency	6							3											
	Venting	9'											3							
	Instrumentation	c																3		
MC tube	Rough pumping	4					1													
	Intermediate pumping	7								1										
	Venting	9'											1							
	Instrumentation	c																	1	
M.D.	Rough pumping	10																		
	Intervention pumping	11																		
	Total		1	12	29	7	4	10	10	8	7	2	11	1	2	16	6	10	1	7

U:Upper part; L:Lower part; VS:Single Volume; MC:Mode Cleaner; M.D.: Multi-Duty pumping.

Table 3400-26 Statistics of pumping system components

	Item		Quantity
Gauges	C	Capacitance	17
	BA	Bayard-Alpert	36
	IM	Inverse Magnetron	57
	PI not bakeable	Pirani	40
	PI bakeable	Pirani	13
	RGA	Residual Gas Analyzer	40
Valves	Angle all metal valve CF40 man		86
	Angle all metal valve CF40 aut		14
	Angle viton valve KF16 aut		50
	Angle viton valve CF160 aut		10
	Angle viton valve CF40 aut		7
	Angle metal valve CF63 man		2
	Angle viton valve CF63 UHV man		39
	Angle viton valve KF25 aut		41
	Angle viton valve KF40 aut		11
	Gate viton valve CF100 aut		8
	Gate metal CF200 aut		7
	Gate viton valve CF 200 aut		51
	Gate viton valve CF250 aut		10
Filters	Dust filter KF16		40
	Dust filter KF 40		22
	Dust filter CF40		72
	Dust filter KF63		2
Pumps	Ion pump 200 l s^{-1}		36
	Titanium sublimator		58
	Dry pump 25 m^3h^{-1}		30
	TMP 1500 l s^{-1}		10
	TMP 100 l s^{-1}		12
	TMP 200 l s^{-1}		8
	TMP 70 l s^{-1}		2
	Roots 1000 m^3h^{-1}		1
	Roots 250 m^3h^{-1}		1
	Dry 250 m^3h^{-1}		1
	Dry 3 m^3h^{-1}		9

34.5 Operation of pumping system

34.5.1 Final pressure estimation in UHV volumes

The total outgassing in Table 3400-5 is composed of 8.5×10^{-6} mbar l s^{-1} of hydrogen and 1.5×10^{-6} mbar l s^{-1} of other gas species, mainly H_2O. Viton and upper part towers account respectively for 2/3 and 1/3 of this last figure. For hydrogen, the gate valves contribute to 20 % of the total.

For hydrogen: With a total pumping speed for the Ti sublimators of 39000 l s^{-1} (13 units), the pressure will be about 3 10^{-10} mbar . This has to be corrected for a form factor due to the tube conductance (1.5 for hydrogen and 300 m section). The hydrogen pressure is expected at all time to be lower than 6 10^{-10} mbar.

For water vapour: For water (and carbon dioxide and monoxide too) the pumping speed of ion pumps 2500 l s^{-1} (13 units) and of Ti sublimators 13000 l s^{-1} has to be considered. The pressure turns out to be $1x10^{-10}$ mbar.

The pumping speed of the wall has to be considered too. One monolayer over the inner surface of the tube would have a capacity of $4.5x10^3$ mbar l. An outgassing flux of 2.7 10^{-6} mbar l s^{-1} for water vapor would take 30 years to saturate a monolayer. One might expect water vapour molecules to be concentrated close to the towers. Even a factor of 10 would lead to a 3 year time duration. In conclusion, the $1x10^{-10}$ mbar figure above will be strongly reduced in practice.

For other species: For noble gases and methane, with a total pumping speed (for Ar) of 1400 l s^{-1} (13 units), the ion pumps should provide an extremely low pressure.

34.5.2 Search for leaks

A leak flow large enough to increase the partial pressure of gases different from hydrogen by a factor of two on one of the instrumentation stations along the tube do not perturb seriously the Virgo data taking. The gas flow of this leak will be of the order of the outgassing for gases other than hydrogen of a tube section, i.e. of the viton gaskets of the valves of a section 1 10^{-7} mbar l s^{-1}. Let us assume this leak as the typical one we are interested to detect and to localize.

The Argon partial pressure profile along the tube, (background 10^{-14} mbar) measured by the RGA of the eleven instrumentation stations, will allow us (see Figure 3400-13 leak rate 10^{-7} mbar l s^{-1} at 1300 m or 1600 m) to detect the presence of a leak and to identify its position with an accuracy or the order of 200-300 m; this means that the helium leak search will be reduced to 8-12 lip welds.

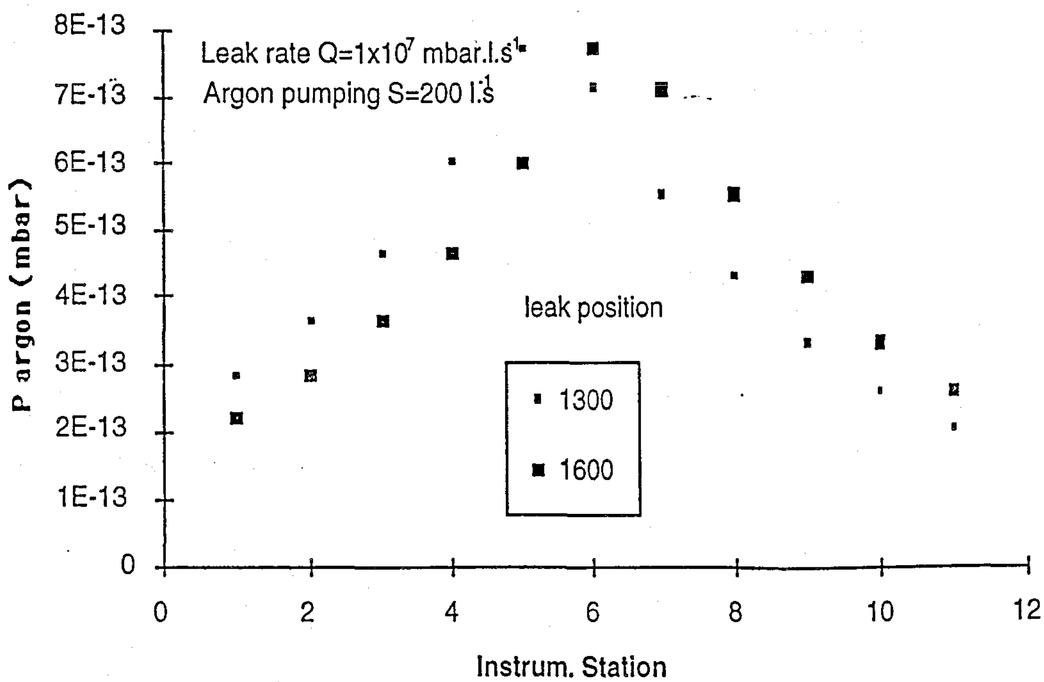

Figure 3400-13: Argon partial pressure variation profile.

34.5.3 Running efficiency of the installation

The possibility to take data continuously for very long time is one of the relevant performances we have to realize for the VIRGO detector. The pumping system has been specifically designed to require a very reduced maintenance and to guarantee the working conditions also when some of the pumping units is forced to stop by some fault.

In the UHV vacuum volumes (tubes and mirror towers lower part) the permanent pumping is done by Ti sublimation pumps and ion pumps. A fresh Ti sublimation will be done once per year and can be done without perturbing the data taking. A permanent pumping station on the tubes or on the terminal towers can be switched off without perturbing the data taking; a small perturbation will be vice versa produced if the permanent pumping station on the beam splitter tower or on the recycling towers is switched off.

The permanent pumping on the HV volumes, mirror tower upper part, single volume towers is done by magnetic bearing turbo pumps and dry pumps; these will require some maintenance twice per year. Anyway the presence of the emergency pumping groups will allow to reduce the perturbation on the data taking during the maintenance or in case of faults of the dry or turbo pumps.

The time needed for venting and evacuating again a tube or a tower is also of interest. The estimated times are reported in Table 3400-27.

Table 3400-27 Summary of operation time

Operation	Tube (hour)	Mirror towers (hour)	SV towers (hour)	MC tube (hour)
Venting	48	12	12	10
Rough pumping	48	15	15	8
Bake-out	170	170		
Total	266	197	27	18

34.6 Vacuum compatibility

The outgassing and hydrocarbon contamination budget of components to be installed inside the vacuum environment of VIRGO has a strong impact on the material selection, the cleaning, the storage, the final assembling. The specifications about the base pressure, the maximum hydrocarbon partial pressure, the total outgassing flow allowed inside the towers are described in detail above.

The Superattenuator cascade involves a large number of components of different kinds:

- metallic parts: filters body, marionetta body, cantilever springs
- cabling: for coils, for signals and power transmission
- magnets: for magnetic antisprings and mirror steering
- glues: to fix magnets
- motors: for remote positioning of parts

The general guidelines to be followed for component selection, machining, cleaning, handling and assembling are:

- every part should be made of vacuum approved materials;
- there should be no blind holes or trapped volumes in the mechanical parts;
- a component is approved if the composing materials are approved and the cleaning procedures are approved;
- a part composed of different materials should be cleaned according to the most critical material.

An extensive program of outgassing measurement has been started to qualify the components at the VIRGO contamination level. Both GEO600 and LIGO have agreed to share data and join efforts about this problem.

The measurements performed to date in the Pisa vacuum laboratory allow to assemble a Superattenuator cascade with an outgassing flow one order of magnitude below the former Final Design specifications (see note VACPISA 049).

A list of components "approved" (for UHV or HV use), "temporarily approved" and "rejected" follows, together with the reference describing the details of the measurement of the outgassing rate and composition.

34.6.1 Approved components

Approved components are the ones which are recommended for VIRGO due to their low outgassing rate and negligible hydrocarbon contamination.

- Metals (as deduced from tube measurements and literature)
    - stainless steel (304, 304L)
    - aluminium series 6000
    - OFHC copper
    - steel for cantilever blades (chromium plated, if necessary)
- Cable insulations:
    - Kapton, note VACPISA 036; suggested cleaning is ultrasonic bath in isopropyl alcohol for 15 minutes, then 120 ^{0}C baking in vacuum; FEP layer should be absent
    - alumina, note VACPISA 037; as supplied from the factory
    - Gore-tex+PTFE: suggested cleaning is ultrasonic bath in isopropyl alcohol for 20 minutes, then a few days baking at 100 ^{0}C
    - Pyre-ML: suggested cleaning as the preceding one
- vacuum sealants (to be used as glues to fix the magnets): these materials should be used in the upper part of the tower only, since there is no real way to clean them and the two base components undergo ageing.
    - VAC-SEAL, note VACPISA 048, with several days curing at room temperature; avoid contact with alcohol as suggested by LIGO experience. Moreover, there is hydrocarbon contamination above some tens degrees. It should not be used for parts baked in situ. The possibility of mechanical fixing of magnets should be considered.
- magnets, for antispring and for mirror steering
    - samarium cobalt, note VACPISA 047; suggested cleaning is baking at 150 ^{0}C. There is hydrocarbon contamination above a few tens degrees thus they should not be used on parts which must be baked in situ

34.6.2 Temporarily approved components

Temporarily approved components include either equipment built by UHV industries (e. g. feedthroughs) which is known to be good for UHV environments but has not yet explicitly tested for VIRGO contamination level or materials with good vacuum properties but not matching VIRGO requirements, thus waiting for a better cleaning method or a replacement. In the first category there are: ceramic and glass ceramic feedthroughs (Caburn/ICI and Ceramaseal under consideration) as supplied from factories; crimp contacts for electrical connections as supplied from factories; Viton for blades and cross dampers. In the second category there are the antispring magnets (ferrite Phillips Ferroxdure 330, see notes VACPISA 046 and VACPISA 050). The suggested method for cleaning is baking at 150 ^{0}C. The magnets exhibit slight hydrocarbon contamination at room temperature which becomes stronger with increasing temperatures.

34.6.3 Rejected components

The rejected components are the ones not matching VIRGO requirements, e.g. Torrseal and Krytox.

34.6.4 Motors

Motors suitable for use in UHV have been investigated. The tested samples from AML and Oriental Motors generally have a good outgassing behavior after vacuum baking but they emit some organic fragments during baking, which precludes their baking in situ. Studies are being performed to check the reproducibility of performances.

34.7 Pumping system control

It concerns the control of the whole pumping system of Virgo: Valves, pumps, gauges, RGA, and temperature during baking. It also manages all the securities.

For each pumping bench (tower or tube pumping station), there is a diskless G96 crate linked to the Slow Monitoring Network -Ethernet- (Figure 3400.14). There is one more crate with a hard disk which is used to boot all the stations. The operating System is OS9. All the Standard Software tools of Virgo are used and especially the Sequencial Language.

A local Supervisor gives the state of the vacuum of Virgo. It runs on the vacuum global workstation, in the control room. This workstation allows the access any particular pumping bench or instrument. It is also possible to link a terminal close to any bench in order to control it locally.

Each pumping sequence may be done automatically or with separate manual operations.

To secure the vacuum (especially acting on gate valves) a separate control system is foreseen; it will be able to reset the vacuum system in a safe state, even in case of power failure.

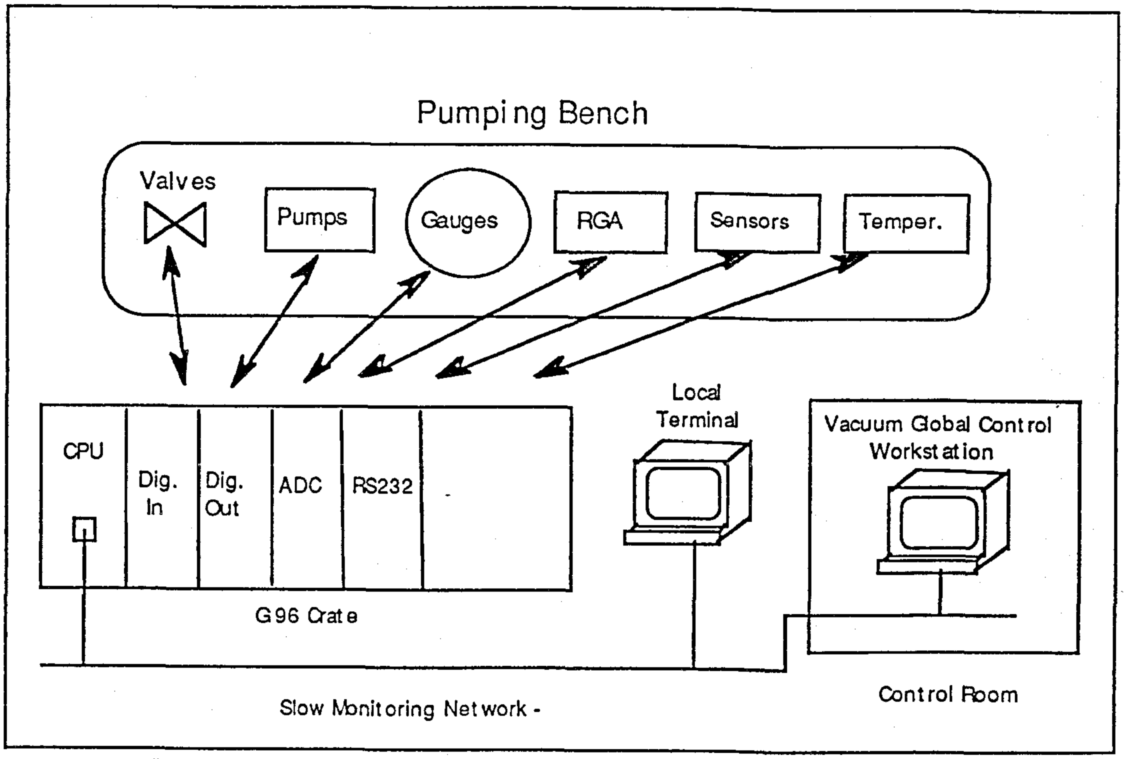

Fig. 3400-14: The pumping system control

40. INTERFEROMETER

Table of Contents

49. Suspension electronics 4900-1

40.1 Interferometer description

The interferometer is the sensitive part of VIRGO. It consists in a laser system, the input bench, which contains optics and optronics for adapting the laser beam to the interferometer, the large interferometer (mirrors and suspensions), the detection bench, which also contains optics and optronics for monitoring, cleaning and detecting the main interference signal, and all the ancillary equipment (secondary detectors for the locking and alignment servosystems, local control stations), and the calibration device(s). A major feature of the Virgo interferometer is the ensemble of " superattenuators ", the low frequency seismic isolation systems from which each sensitive component is suspended.

The main characteristics of the optical system are the following :

- The laser system consists in a high power Nd:YAG ring laser, injection-locked from a monolithic 1 Watt laser. It is actively stabilized, in frequency and in amplitude. The beam is phase modulated, to allow for a shot-noise limited detection, and filtered by transmission through a resonant (mode-cleaner) cavity. The power will be about 25W.
- The large interferometer is a Michelson interferometer, with 3 km long arms. Each arm contains a Fabry-Perot cavity of length L= 3 km. The light power is increased through the use of a standard recycling technique. The nominal values are a finesse of 50 for the Fabry-Perot's, and a recycling coefficient of 50 (corresponding to a finesse of 150 for the recycling cavity).
- These performances are obtained through the realization of very low loss mirrors, having typical surface qualities of $\lambda/300$, whose fabrication and tests are performed by the VIRGO teams.
- The main interference beam, which carries the gravitational signals, is filtered with an output mode-cleaner, and detected with an a multiple InGaAs detector of high quantum efficiency.
- All the secondary beams leaking through, or reflected by, the interferometer, are split onto two quadrant detectors and one InGaAs detector. This provides redundant information for the alignment and locking servosystem.
- We use a set of computerized CCD cameras looking inside each tower, in order to monitor the preliminary (nonlinear) alignment and to measure precisely the position of each mirror relative to its own tower and to the laser beam
- The calibration will be done by applying time-dependent forces on the mirrors, in two different ways : a magnetic force onto a set of magnets glued to the mirrors, and laser induced radiation pressure.

40.1.1 The test interferometer

By mid-98 (or about two years after the site acquisition), we will start installing a short interferometer in the central building. We call it the test interferometer. It will differ from VIRGO only by the absence of the far mirrors of the 3 km Fabry-Perot's, by a lower laser power (10W), and by the choice of the radius of curvatures and of the reflectivities of the other mirrors. The interferometer geometry will be simpler than in VIRGO, and the mirrors will be of smaller diameter. Except for that, it will provide a complete, full size, test of all the critical parts of VIRGO (suspensions, laser, benches, data management, control and alignment systems, mirror quality, data management, ...), and give some hint about the presence of unexpected noise sources.

The presence of this test bench will accelerate the commissioning of VIRGO after the end of the construction, since all the functions and components, except the final large mirrors, and the final locking and alignment procedures will have been tested.

40.2 Optical scheme and detection principles

40.2.1 Optical scheme

The central part of the antenna is made of six large size optical components (see figure 1 and table 1), they form a Michelson interferometer. The light source is an S-polarized ten watts Nd-YAG laser. The goal is to detect a differential optical length variation between the two arms, of the order of 10^{-19} m at 1 kHz. In order to enhance the antenna sensitivity, the arms of the Michelson interferometer are three kilometer long Fabry-Perot resonators with finesse of fifty, working at resonance. The whole interferometer works on a dark fringe, and light that should have escaped towards the input bench is recycled by the use of a so called recycling mirror (MR) at the input of the interferometer. The recycling mirror reflectivity factor is chosen so as to match the overall losses of the whole interferometer for an optimal efficiency of the laser injection. There is a total of ten coated surfaces, four of which are anti-reflective coatings (MR, BS, ME1, ME2).

Four substrates are crossed by the laser, three of them inside the various cavities (BS, ME1, ME2).

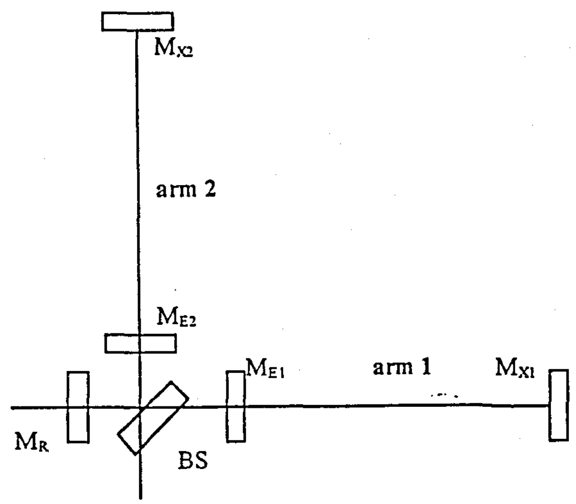

Figure 1: Virgo optical layout

40.2.2 GW detection basis

Part of the laser light is frequency shifted by the use of an electro-optic phase modulator. The frequency shift of the two sidebands is large enough to make them not resonant inside the Fabry-Perot arms and are thus insensitive to the gravitational excitation, moreover they are not resonant in the Michelson interferometer and part of the sideband energy escapes towards the detection bench. The carrier beam is resonant in the arms as well as in the Michelson interferometer. In absence of gravitational excitation the interferometer is locked on a carrier dark fringe. At the output of the interferometer the two sideband beams interfere with the dark fringe carrier beam which amplitude is proportional to the arms differential optical length variation. the optical signal is thus proportional to the gravitational signal and detection is performed at the modulation frequency.

40.2.3 Virgo sensitivity limitation by optical components flaws - simulations.

At frequencies above 500 Hz Virgo sensitivity is limited by shot noise. Any defect in the optical components will raise this limit, either by decreasing the amount of stored light inside the interferometer, by degrading the quality of the carrier dark fringe, or by making Virgo sensitive to laser frequency noise. In order to quantitatively express the effect of geometrical or other characteristics of the optical parts of Virgo a code has been written, in which real or simulated defects can be introduced, which provided the signal to noise degradation with reference to the shot noise limit of the antenna. This code is based on the field distribution projection on Hermite-Gauss basis. These functions are propagated between the various surfaces of the interferometer. Each interface is represented by matrices which acts on the various function of the Hermite-Gauss basis. This program allows to simulate various kind of defects :

- Laser defects (alignment, modes, noise...)
- Coating defects (geometrical imperfections, absorption, transmission, local defects...)
- Blank defects (absorption, local defects, geometrical distortions...)
- Thermal effects (e.g. in entrance mirrors)

This code is reliable and fast enough to be used for statistical simulations.

This last point has to be underlined because we have based our simulation programs on artificial mirrors wavefront figures based on the statistical distributions -power laws- of defects that we have experienced on test mirrors during the R and D period.

40.3 The suspension of the test masses

Gravitational waves can be detected by measuring the distance between test masses. These masses, the interferometer mirrors, need to be suspended to be as free as possible. The suspension system must:

- isolate the test mass from seismic motion
- keep low the thermal noise motion in the detection band
- allow for control and steering of the test masses to keep the best optical conditions for detection without introducing additional noise
- be compatible with the level of vacuum needed

A complete suspension chain consists, from top to bottom, of the following elements:

a movable suspension point, a chain of several seismic filters and a marionette suspending the mirror.

An inverted pendulum provides the mean to adjust the position of the suspension point relative to the supporting structure. The settings for this device are determined from the alignment error signals and the low frequency component of the locking error signals.

Then there is a chain of up to 5 seismic filters, that perform a passive mechanical attenuation in all six degrees of freedom of a rigid body. Normal motion of the filter chain can result in large oscillations bringing the interferometer away from its working point.

At the level of the marionette, mirror positioning is achieved by forces acting from a reference mass, itself suspended to the marionette. Large range longitudinal motion and angular displacements are achieved by acting on the marionette from coils suspended to the seventh filter.

40.4 Interferometer requirements

Sensitivity goal	10^{-21} @10 Hz	3.10^{-23}@100 Hz
Arm length	3000 m	
Optical requirements		
Laser wavelength	1064 nm	
Laser output power	25 W (TBC)	
Overall optical efficiency	> 40 % (TBC)	
Power recycling factor	50 (TBC)	
Cavity input mirrors	Flat, Reflectivity = 0.86 (TBC)	
Cavity end mirrors	Rcc=3450 m, Reflectivity = 0.99995	
Test masses	Low OH fused silica, R= 35 cm	
Input beam filtering	144 m mode-cleaner, finesse = 1000	
Output beam filtering	2.5 cm mode cleaner, finesse = 50 (TBC)	
Main detectors	InGaAs, efficiency > 90%	
Suspension requirements		
Seismic attenuation	at least 10^{-11} @ 10Hz	
Residual rms. motion before locking	1 µm (TBC)	
Mirror residual thermal motion	$\leq 3\ 10^{-18}$ m/√Hz @ 10 Hz	
Suspension point motion range	± 10 mm longitudinal and lateral TBC	
	TBD vertical	
Mirror orientation precision	10^{-9} radTBC	
Mirror orientation range	±0.2 mrad TBC	

41. Laser and Input Bench

Table of Contents

The sub-system is located at the input of the interferometer, it includes the realization of the laser source with its stabilizations and the input optics used to direct and to enlarge the beam to match it to the interferometer's beam size.

The laser source and stabilizations are located on at least 2 tables forming what is called here the Laser Bench, the input optics are located on a table named Input Bench, suspended under vacuum inside the injection tower.

The 3 items that will be described below are :

- the Laser Bench where the laser light is provided and located in the laser laboratory
- the Input Bench located inside the Injection tower (sometimes also called Input tower)
- the Local Controls that gather all the monitoring and controls necessary in the sub-system.

41.1 Functions and Concept

The Laser and Input Bench Subsystem is designed to produce the light power necessary for the interferometer with the stabilizations required for the expected sensitivity of Virgo as well as the beam geometry matched to that of the cavity arms. Besides that, it provides also all the monitorings and controls of the beam parameters and the automatic alignments of the cavities/beams used to achieve the different stability goals.

The requirement of high power and stability of the light source is achieved by using diode-pumped Nd:YAG lasers, and the technique of injection locking. A low power single frequency «master» laser controls a high power « slave » laser. One slave laser, or two coherently added slave lasers (TBC), will be used, depending on the necessary power and on the state of the art of high power lasers.

The achievement of laser beam stability is performed through the prestabilization and final frequency stabilization, and the power stabilization. The prestabilization of the laser is the first step of narrowing the laser linewidth using an ultra-stable short term reference cavity. The final stabilization is the one that locks the laser frequency and the interferometer resonance one to the other.

The beam jittering of the laser is cured via a passive filtering done by a Mode Cleaner, which is a resonant cavity used in transmission on the fundamental mode TEM_{00}. With a good choice of that Fabry-Perot's geometry, all the high order modes will be far away enough from the TEM_{00} one, to be reflected by this cavity, ensuring then a spatial "cleaning" of the beam. Besides that, the Fabry-Perot acts, in transmission, as a low pass filter for all the fluctuations of the laser in frequency and amplitude.

To operate all the cavities in resonance, a number of servo-loops will be unavoidable, as well as automatic alignments servo-loops of these cavities.

The SS has also the task of directing the beam to the interferometer and enlarging it from the laser's size to the interferometer's size via a number of mirrors and telescopes, each of them designed for low losses and and low extra noise.

41.2 Requirements

The requirements on the physical parameters originate from 2 sources :
- the spectral sensitivity curves of Virgo (initial and ultimate) given by the Figure **4100.1**, for which we will quote ISC (curve a) and USC (curve b) (for initial sensitivity and ultimate sensitivity curves).
- the technical limitations linked to the realization and mainly as a consequence of one chosen solution in another Sub-System, for which we will quote TLS (for technical limitations of the solution).

41.2.1 Laser Power

The accuracy of the phase measurement at the output of the interferometer is limited by statistical fluctuations or shot noise in the detection. This noise is white, but as the signal decreases with the Fourier frequency f, the phase sensitivity then varies proportionally with f, and in the case of Virgo, it becomes dominant only above 500 Hz, while below that, the other sources of noise are of various thermal origin.

To reach a strain sensitivity of $3\times10^{-23}\ Hz^{-1/2}$, 1 kW (ISC) of light should be incident on the Beamsplitter. The requirement on the laser output power depends on the recycling factor, i.e. on the quality of the large mirrors. We are presently working with the assumption that the recycling factor will be 50, which requires an effective laser power of 20 W.

41.2.2 Frequency Stability

For a given strain sensitivity goal, the frequency stability (at the entrance of the beamsplitter) is related to the expected asymmetry between the 2 arms of the Michelson. There will be a compromise between the requirements on asymmetry and on frequency stability, that depends upon the technical feasibility in one case or the other. The relation between these parameters is :

$$\frac{d\tilde{\nu}}{\nu} = \frac{\tilde{h}}{\beta}$$

where β is the asymmetry factor of the Michelson arms and $\frac{\delta\tilde{\nu}}{\nu}$ is the requested laser frequency stability at the level of the input port of the interferometer (beamsplitter).

Then for a given Virgo sensitivity goal (curve 1 of Management Plan), we plot now the requirements for different asymmetries (figure 4100.2): the upper and lower sets of curves are respectively for ISC and USC. For instance with 1% asymmetry, the lowest level to be achieved is around 10^{-6} Hz/$\sqrt{\text{Hz}}$ for the 1st generation (ISC) and this is our goal today for the laser stabilization .

41.2.3 Power Stability

The main channel through which the laser power noise may affect the Virgo's sensitivity is the finite open loop gain, or the offset, of the dark fringe control system. Again here there is a compromise between the laser stability that can be achieved and the possible residual offset. The product of the two parameters are related by :

$$\frac{d\,\tilde{P}}{P}(f)\,.\,\Phi_{offset} \le \delta\,\tilde{\Phi}_{Virgo} = \frac{2\pi}{\lambda}\,L_{total}\,.\,\tilde{h}\,(f)$$

A reasonable order of magnitude for this residual offset can be estimated to be $\Phi_{offset} \le 0.1$ mrd corresponding to a pathlength difference at the output port of $\delta_{offset} = 1.6\ 10^{-5}\,\lambda = 1.7\ 10^{-11}$m. The curve a of the Figure **4100.3** gives the level of amplitude stability requirement following the level of strain sensitivity expected for Virgo and we can see that the lowest level required is $\delta P/P \approx 3.10^{-7}/\sqrt{\text{Hz}}$ at a frequency @ 500 Hz.

The other possible cause is due to the beam impinging on a mirror causing a displacement induced by radiation pressure, which is transformed into an equivalent strain sensitivity when there is an asymmetry β between the arms: with an intracavity laser power of 15 kW, an asymmetry of 10^{-2}, tests mass of 30 kg, we get

$$\frac{\delta\tilde{P}}{P}(f) < 7\times10^{13}\,f^2\,\tilde{h}\,(f)$$

(TLS), represented by the curve b of the Figure **4100.3** : this effect is less stringent than the noise mentioned above, then the overall level of amplitude stability is dictated by the curve a at all frequencies.

41.2.4 Beam stability

The lateral or angular jitters of the beam can couple to imperfections in the interferometer and result in a phase difference at the output interference pattern. The imperfections are of many kinds: misalignments of the recombined output wavefronts in their tilts or in their curvatures, waist mismatching between the two arms, originating from residual misalignments of beamsplitter and/or test-mass themselves. The calculations have been done for a simple Michelson case [1] and extended for a recycled Michelson [2] and we summarize here the results and give the noise in term of linear spectral density. The coupling of the laser jitters $\alpha(t)$ in rd/$\sqrt{\text{Hz}}$, with the interferometer misalignments Δx (in m) gives a phase jitters

$$\delta\phi(t) = \frac{2\pi}{\lambda}\frac{1-\sqrt{R_{rec}}}{1+\sqrt{R_{rec}}}\Delta x.\ \alpha(t) = 1.23 \times 10^5\ \Delta x.\ \alpha(t)$$

with a recycling mirror of $R_{rec} = 0.92$. Again here there is a compromise between the two parameters, as their product has to be smaller than the Virgo sensitivity, i.e. when transforming this phase jitters into noise density, we get the condition that the induced phase has to be smaller than the Virgo sensitivity $\delta\tilde{\phi}_{misalign}(f) \le \text{Virgo}(f)$ (ISC and TLS). The Figure **4100.4** represents the beam jitters $\alpha(f)$ vs frequency f in the detection range (curve ***a***) and the noise due to the seismic effect on the input bench without any seismic isolation (curve ***b***). Knowing that a simple stage isolation will perform an isolation better than 10^2 around 100 Hz, we can see that the lowest jitters noise required is due to the curve a and is between 10^{-10} and 10^{-11} rd/$\sqrt{\text{Hz}}$ around 500 Hz for the beam entering the recycling cavity. With an input Mode Cleaner of a 3.10^{-3} spatial filtering effect, we get the curve ***c*** which is the requirement for the laser at the input of the MC; let's point out that the curve ***c*** is easily obtainable with a free-running laser.

41.2.5 Summary of requirements

The table below summarizes the main requirements on the laser beam

	Test interferometer	Virgo interferometer	On beamsplitter
Laser Power (ISC)	10W TEMoo	20-25W TEMoo	1kW
Frequency range	**10 < f < 100 Hz**	**100 < f < 1 kHz**	**1 kHz-10 kHz**
Frequency prestabilisation (ISC and TLS)	$10\text{-}10^3$ Hz/$\sqrt{\text{Hz}}$	0.1-10 Hz/$\sqrt{\text{Hz}}$	$\ge$ 0.1 Hz/$\sqrt{\text{Hz}}$
Power Stabilization	$< (3 10^{-3}/f^2)\ \text{Hz}^{-1/2}$	$< 3 10^{-7}\ \text{Hz}^{-1/2}$	$< 10^{-10} f\ \text{Hz}^{-1/2}$
Beam Fluctuations at the entrance of the interferometer (ISC and TLS)	$<(10^{-5}/f^2)$ rd.$\text{Hz}^{-1/2}$	$\le 10^{-10}$ rd.$\text{Hz}^{-1/2}$	$\le 10^{-13} f$ rd.$\text{Hz}^{-1/2}$

41.3 Interfaces

The interfaces are mostly between the laser bench and the infrastructure/equipment, and between the input bench and the neighboring SS, such as the suspension SS, the vacuum SS etc... For both items there are of course interfaces with the other local controls and with the global control.

41.3.1 Interface with sub-system 2100 (Central area building)

The requirements given to the central building are:

- electrical power :10 kW in continuous in the lab + 2 kW for the injection tower+ 1,5 kW around the mode cleaner tower.
- 2 access doors to the laser lab are required to have some safety lock and limited access, for security reasons.
- a double floor will be convenient to hide all the cables running around the laser bench.

41.3.2 Interface with sub-system 2200 (Clean rooms)

The requirements given to the clean areas SS concern:

- a clean laser lab (100 000 class) with an overpressure relative to the outside part.
- a "bench alignment room" in a class 1 000 or at least 10 000 if there is a local laminar flow for the alignment check of the input bench.

41.3.3 Interface with sub-system 3100 (MC tube)

The input flange of the MC tube (on the injection tower side) will be 250 mm in diameter (see Memo). The MC tube of 300 mm diameter will be evacuated via the pumping system of the MC tower.

41.3.4 Interface with sub-system 3300 (Towers)

The hanging of the input bench to the marionette is realized by the injection bench group.

As the input bench diameter does not exceed 900 mm in diameter, the installation of the input bench and mode cleaner payload in the tower needs the same lower cover of 1 m diameter, as in the standard case. The hanging of this system to the suspension inside the tower can follow the same process as the standard test-mass: the Figure **4100.9** shows the overall minimum height required for a possible protection box for the bench and its marionetta during the transportation in the gallery. (See also ref **14**): the protection box and the installation inside the tower are not planned by us now (TBC).

Due to the position of the Reference Cavity at the bottom of the Input Bench, the human access from the 1m lower cover is unfeasible so a lateral access through the 1 m East flange has been requested, giving a connection between the input tower and the sas of the laser laboratory (TBC).

In the same order, the hanging of the end mirror of the mode cleaner inside the tower is not planned by us. The procedure for hanging large mirrors should be applicable completely here (TBD).

For local control using the cameras and for auxiliary HeNe laser beams, windows are needed as shown in the **Fig.4100.5** .

As far as the windows are concerned, the distribution is the following:

- 3300 provides with all the windows in the input and mode cleaner towers, windows n° 3, 4, 5 and 6 of the Figure 4100 5.
- we provide the windows of the main input flange in the input tower (South side): these windows and their position have still to be defined.

We also provide the separation window in the link (**1** on Figure **4100.5**) between the input and recycling towers as well as the tube section containing this window, length TBD as soon as possible.

41.3.5 Interface with sub-system 3400 (Pumping)

The vacuum required in the injection tower and mode cleaner tower is the following:

- clean vacuum without hydrocarbons (TBD) and a residual pressure of $\leq 10^{-6}$ mbar.

41.3.6 Interface with sub-system 4200 (Detection bench)

We provide the detection bench SS with the modulation signal as a reference signal with the following hardware's :

- BNC output connector delivering 0 dBm of RF signal at 10 MHz (TBC), available at the level of the laser bench.
- we do not provide the cable to transport this signal outside our SS (for the demodulation of other photodiodes than D2) or to the 3 km arms.

The SS 4200 is in charge of providing the D2 photodiode for the signal detection, as this photodiode sits on the laser bench, we have to decide together the overall dimensions (TBD).

41.3.7 Interface with sub-system 4300 (Mirrors)

Mirrors of the input mode cleaner (and the spares) are coated by IPN-Lyon (see requirements in parag MC below) as well as the optical contacting of the 2 plane mirrors on the corner-cube (the mirrors substrates and the corner-cube are provided by us).

41.3.8 Interface with sub-system 4400 (Alignment)

The pointing of the laser beam into the interferometer is made in two steps:

- during the VIRGO prealignment phase (non-linear alignment SS), the Input Bench as a whole **cannot be moved**, as it is resonant with the Mode Cleaner cavity, but signals to orientate the beam can be applied to the picomotors carrying the input telescope, without any harm for the Mode Cleaner lock (which allows the transmission of the beam to the interferometer).
- during the interferometer autoalignment (linear alignemnt SS), where it is a matter of smaller dynamic range, correction signals coming from automatic alignment can be applied (TBD), if necessary, to orientate the Input Bench through its marionetta coils (within a small dynamic range the lock and the autoalignment of the Mode Cleaner can be kept locked).

This is the interfacing we propose to the SS 4400 and we need to check out together if the resolution and dynamic range of our transducers match the alignments request (TBD).

A "screen" is planned after the last mirror of the IB at the 4400 SS request. There is room for such a device on the IB, but nevertheless we will need to have more details on that screen (beginning of 97) in order to finalize the clamping of it on the bench.

41.3.9 Interface with sub-system 4700 (Last stage suspensions)

Mechanical interface: the SS 4700 will provide the marionettas for input bench and mode cleaner: it is different from other marionettas, since the input bench must be controllable in all six degrees of freedom, which necessitates 8 coils each.

SS 4700 provides the coils and the magnets (TBC).

The coil drivers are furnished by 4100 (TBC).

It would be convenient if the force of one coil onto a magnet (Ø 10 mm, thick 4 mm) with 23 mm µmetal extensions on both sides (who provides them? TBD) can be around 0.6 N/A (this is the number obtained for the MC prototype coils defined in [3]).

The marionetta serves at the same time as a shield against dust coming from the upper suspension, which might spoil the cleanliness of the suspended optics. The wires between marionetta and suspended mass (3 for IB and 2 for MC) are also provided by 4700, they are made out of Marval 18 alloy in 1 mm diameter and 827 mm in total length (821 mm between the nail heads). The clamps of these wires on the IB are designed and provided by us.

Electrical interface: there will be about 25 cables running from the input bench to the marionette and to the top. The clamp position of the wires have to be on the bench (TBD by us) and somewhere on the suspension (TBD by 4700).

41.3.10 Interface with sub-system 4900 (Suspensions electronics)

The MC local mass control system will mainly act on the marionetta, but due to the limited dynamic range (< 1 mm) for translations, slow drifts need to be corrected by acting on the upper suspension point (available degrees of freedom: x, y, z, θ_y). This necessitates an interaction with the Suspension electronics SS. An offset for moving the suspension point by ± 10 mm in x and z and a few mm in y directions can be added to the local control of the suspension point; moreover, a rotation around θ_y can be done. For this purpose, the action of the local control is transparent for the user. The bandwidth is 10 Hz.

Hardware: there will be two separate VME crates for each of the two masses (IB and MC far mirror); the first controls the coil currents on mass and marionette and reads the camera image (item 4140 below). The second one controls the movements of the upper suspension point.

The correction signals will be calculated by a local or "global" (within the MC context) control system (item 4140); all signals below a certain limit frequency (e.g. 100 mHz) will go to the mass suspension point. In practice, the whole correction signal will be sent to crate 2 by a digital optical link (x, y, z, θ_y=4 signals), but only the low frequency part will contribute to the suspension point movement; the two cutoff frequencies for marionetta (high pass) and suspension point (low pass) must of course agree. Trigger signals corresponding to the sampling moments will be provided to crate 2 by cable.

41.3.11 Interface with sub-system 5100 (Global control)

A global error signal for the beam linear alignment is needed, since the local control short and long term precision might not be sufficient for the VIRGO data taking phase (see also interface 4400).

- Data of the control system are sent to the slow control frame builder through the standard Fb...Cm messages requests.

The foreseen signals transmitted are : DpsDc (DC power of the laser), mod 2 (modulation index for the signal detection).

Servos-status and status of components giving an alarm if out of range value.

- Data of the fast acquisition (10 kHz) will be obtained in a specific VME crate under the LAPP responsibility. Analog signals to be read are delivered by the subsystem : DpsAc (noise power of the laser), SphEr (frequency noise of the laser), D2 (a or b) (error signal from recycling cavity).

- Precise signals exchange with subsystems marionette, suspension, interferometer are defined
above in paragraphs 4100.3.4, 4100.3.5, 4100.3.7.

- Error reporting is done via the error-logger system. The list of signals giving Alarm (with the severity level) is exposed in detail in the note [4].

41.4 Selection of solutions

- Choice of laser: the light will be generated by high power Nd:YAG lasers, this choice has been dictated by the expected efficiency, stability, and reliability of this kind of lasers, mostly when pumped by laser diodes.

- Choice of multistage frequency stabilization: the final stability required is about 10^7 below the level of usual laser including Yag lasers. Knowing that it is impossible nowadays to perform servo-loops with such high gain at 500 Hz, we choose to achieve the stabilization in 2 steps; the 1st is the prestabilisation which reduces the laser fluctuations to those of a short term rigid reference cavity; the 2nd is the final stage which locks the laser to the interferometer and brings it at the required level.

- Choice of using input mode cleaner: the beam geometry required is about 10^3 times better than the normal jitters presented by any stable laser beam, and the best way to reach the desired beam stability in position and geometry is to pass it through a resonant cavity, named as mode cleaner. Then it is known that a mode cleaner with the adequate characteristics, will filter out the residual beam jitters and bring it down to the required level. Furthermore it could help filtering the HF noise of the laser, anyway we will take it into account when estimating for the prestabilization level required.

41.5 Detailed description

For feasibility, maintenance and cost reasons, the components which are not due to stay in vacuum and/or seismically isolated will be located on the **laser bench** which consists on 2 tables or more (TBC) in the laser laboratory (Figures **4100.6 and 4100.7**). They are :

- the lasers
- the necessary phase modulators (there will be 2 at minimum). We provide the cable and the demodulation electronics for the signal of photodiode D2 as it is used by us for the locking of the laser on the interferometer.
- the optical isolators between lasers and interferometer.
- the beam monitoring by CCD cameras
- the photodetectors for active frequency stabilization including D2
- the quadrant photodiodes for the auto-alignments to reference cavity and mode cleaner
- the matching optics between the laser bench and the input bench.

The components that should be under vacuum for cleanliness and acoustic noise reasons will then be sitting on the **input bench** (Figure **4100.8**) that will be suspended inside the injection tower :

- the reference cavity
- the mode cleaner (input mirrors on the input bench suspended inside injection tower and curved end mirror suspended inside mode cleaner tower)
- the input matching optics (laser beam to interferometer beam)
- the power stabilization photodetector

If we anticipate and state that the input bench is carrying also the reference cavity (RC) as well as the mode cleaner (MC), the **alignment** of the laser beam coming from the laser bench to the input bench (IB), carrying one of these critical cavities, is due to match their alignment requirements. We have then two choices which are whether to align to the RC cavity or to the MC cavity. If we also state that there is another system to realign the beam on the input bench to match the MC, then it is simple to decide that the RC is reference for the input bench. So the laser bench is aligned to the RC by some automatic beam positioning sitting on the laser bench (named ABP 1) and the beam on the IB is aligned relative to the MC by another ABP named APB 2 sitting on the IB. Then finally the beam coming out from the IB is aligned relative to the Virgo interferometer by another ABP named APB 3 positioned after the MC.

The subsequent mode matching for the mode cleaner is done by a telescope sitting on the laser bench. The mode cleaner mirrors themselves are controlled only locally, and steered only during the phase of initial alignment. The input matching optics matches the beam exiting from the MC to the interferometer. Its mirrors can be steered, too, for automatic alignment of the beam to the interferometer if necessary (TBC). Their distances can be controlled in order to choose the waist position.

The power stabilization of the laser will use a photodiode sitting on the Input Bench hit by a small fraction of the main beam transmitted by the Mode Cleaner (to take advantage of its low-pass filtering) through a leak of a HR mirror for instance. The feedback will be done on the laser diode current directly either on the power supplies or on the diodes directly. We have chosen not to feedback on the laser beam in order to avoid extra optical transducer.

41.5.1 Laser bench

41.5.1.1 Laser bench function and concept

The laser bench includes the following functions :
- to produce a 10W power laser with 2 or more lasers (for test interferometer) in a TEM_{00} polarized mode
- active stabilization of laser in frequency and in power (prestabilisation and final stage stabilization)
- phase modulate the laser for the signal detection

All the components including the lasers will be sitting physically on a laser table, rigidly connected to it. To avoid optical feedback into the high power laser we will use as far as possible, interfaces at Brewster angle and reflective optics instead of refractive optics.

41.5.1.2 Laser bench detailed description

- Power : the requirement of power combined with the level of stability needed is very stringent for one single laser as no such laser does exist today. But thanks to the use of recycling cavity in Virgo which allows us to expect a recycling gain of the order of 50-100, the demand on incident laser power is now 10-20 W. Besides that the recycling gain is inversely proportional to the total losses so the mirrors technology will determine later on what recycling factor will be possible. Meanwhile our strategy for the laser power is the following: we will first develop a laser of 10W for the 98's test interferometer and experiences its reliability. That experience and the mirrors state-of-art will determine then what will be the final laser power required.
- Injection locking : to solve the problem of compatibility with frequency stabilizing a laser and keeping its high output power, we use the following process which is first to injection lock a high power laser (called slave laser) by a low power laser (called master laser) and then to frequency stabilize the beam of the high power laser by acting on both the master laser and the slave laser.
- The master laser is a diode-pumped commercial laser with an output power of 700 mW for the test interferometer.
- The slave laser is a slab laser pumped by fiber-coupled diodes chosen for their easy collimating beam and their easy maintenance possibility (a change of one diode could be done without stopping the whole laser).
- Prestabilisation: the 10W laser will be frequency stabilized on the reference cavity **RC** (which is sitting on the input bench and described below) with a feedback onto the master laser pzt and to the external phase corrector **EO2** sitting on the laser bench.
- Modulation frequency for signal detection: a modulation frequency at **F2** $\approx$ 6.25 MHz (TBD) is applied on the same phase modulator **EO2**.

41.5.1.2.1 Master laser

It is a commercial Nd:YAG diode-pumped built in the technology of monolithic piece (MISER), single frequency operating and delivering more than 700 mW. The monolithic technology makes the laser intrinsically ultrastable and the use of two laser diodes for pumping the Nd:YAG insures the continuous operation (the failed laser diode might be replaced while the other one keeps operating).

The power is adequate for injection locking of a high power laser of a few tens of Watts. The cavity is formed by the crystal itself and the frequency tuning of the laser is done in the slow range by a thermal control of the crystal while the fast part (up to 30 kHz) is done by a pzt bonded on the crystal (first resonance frequency around 50 kHz, sensitivity $\geq$ 4 MHz/Volt)

The laser beam is elliptically polarized, there is a need of a quarter wave plate and a half waveplate to match its polarization to that of the phase modulator and of the high power laser.

The delivered beam is slightly asymmetric, so the matching optics between the lasers have to take it into account.

A servo-loop (named **SOr**) using 25 mW of light on photodiode **Dro** is used to kill the relaxation oscillation of the laser at 600 kHz.

41.5.1.2.2 Slave laser

The 10W laser is the result of a collaboration between B.M.I. company and SPI Orsay group and is running in Orsay since October 96. The details on the mechanical construction can be found in the laser technical doc., B.M.I. 19/04/95. The main features sketched on **Figure 4120.1** are:

- Nd:YAG Xtal: 5x5x76 mm Nd:Yag zigzag slab with end faces cut at Brewster angle in order to minimize thermal induced birefringence effect (10 internal reflections)
- transverse pumped on one side pumped by 10 fiber coupled diodes
- collimation from the fibers beam by a cylindrical lens of 2.5 mm in diameter giving a horizontal gain profile of 1.5 mm (FWHM) in width.
- presence of induced thermal focal length in the vertical plane of more than 1m and 0.24m in the horizontal plane (for 68W of pump power).
- heat is evacuated via the upper and lower faces in contact with a gold coated copper bloc which temperature is controlled by 4 Peltier elements and servoed by one PID servo element (PID: Proportional Integrator Derivator), the Peltier elements are cooled by a close circuit water flow.
- Cavity: it is a X-shaped ring cavity, 3 flat mirrors, one concave of 0.75 m focal length, this insures a radius mode in the slab of 430 microns (horizontal) and 860 microns (vertical), for the optimum stable mode. One of the plane mirror serves as output coupler with 10% transmission.
- mechanics of the cavity: all the mirrors are clamped on Zerodur in order to get rid of the frequency drift due to thermal expansion of the cavity (reduced in this way down to 2-3 MHz/°C).
- pzt transducers: 2 flat mirrors are glued on a piezo actuators for frequency control, a slow one (Physik Instrument) with a sensitivity of 33 Å/V or 3.6 MHz/V (-1000V/+200V) and a flat response up to 28 kHz (+6 dB amplitude), and a fast one with a sensitivity of 3 Å/V or 0.4 MHz/V and a flat response up to 200 kHz.
- Fiber coupled pumping Diodes: the ten diodes lie on Peltier elements cooled by a close circuit water flow, the Peltier are fed by a PID servo element (Proportional Integrator Derivator), which allows to set the temperature of the diode digitally via the local controls. The characteristics of the diodes are given hereafter: output power of 10W for 23.5A under 1.8 Volt (nominal current is 28A, i.e. 12W output), spectral linewidth HWHM $\leq$ 3 nm, running temperature according the diode ranges from 17 to 30°C, at 808 nm for optimum Nd:YAG absorption, $d\lambda/dT$= 0.3 nm/degree, output fiber NA= 0.2 and fiber diameter is 500 µm. The diodes are coupled with secondary fibers (numerical aperture of 0.2, diameter of 600 microns) which are connected to the laser head.
- thermal control of the laser is done via Peltier elements, the sensitivity is 500 MHz/°C, the dynamic is larger than 10 GHz, the bandwidth is smaller than 1 Hz.
- performances: TEM_{00} mode operation is achieved by using a diaphragm inside the cavity, however a slight contribution of TEM_{01} remains; by using a spatial filter the TEM_{00} component can be extracted, giving then 9W output power for a effective pumped power of 60W (optical efficiency of 15%); both vertical and horizontal waists are located on the output coupler and equals 515 microns and 233 microns respectively (radius at 1/e2). The M^2 parameter is lower than 1.2 for both directions.

The strategy of our high power laser is quite clear: we use an efficient laser at 60% of the nominal power (reached with 120 W of diode pumping) to prevent maintenance problems. This means that we can afford to have up to 4 laser diodes failed before stopping the laser operation, besides the fact that using the laser diodes far from their nominal current will lengthen their lifetime.

41.5.1.2.3 Injection locking

The principle of this servo named **SLi** has been described in the FD v.0 (1995). Herewith are the characteristics of the main components:

- Electronic: the photodiode **Dil** used is a InGaAs cell which feeds 1kΩ in DC and 7 kΩ in AC, it is shot noise limited at less than 1mW incident (photodiode Dil on the scheme). The servo transfer function is $1/f^4$ from DC to 8kHz, and $1/f$ above 8 kHz; the error signal **LSPz** is feedback to the 3 transducers described above. Photodiode **Dbw** monitors the injection locked status and acts as a trigger to relock automatically the servo **SLi**.

The incident power needed on the photodiode **Dil** is determined according to the level of the sidebands used and the specifications in terms of frequency stability. From the development studies [5], we need 4.10^{-4}W, and a modulation index of 0.024 radians to achieve the stability of a standard Lightwave laser ($\frac{10\text{kHz}}{\text{F}}\sqrt{\text{Hz}}$). The expected locking range is 1-2MHz (output coupler transmission of 10%, free spectral range of 517 MHz, ratio of master laser power to slave laser power is 0.06).

41.5.1.2.4 Optical components

Waveplates at the output of the master laser converts and adjust the elliptical polarization to a linear one in order to send 25 mW into the photodiode Dro (the relaxation oscillation servo of the master laser) from the input polarizer of Faraday 1 (Figure **4100.6**).

Faraday isolator 1 is a TGG crystal surrounded by Brewster dielectric filters forming the polarizers; it protects the master laser against the feedback of the slave laser when it is not injection locked.

Details on the specifications for the Faraday (1 and 2) and their measured performances can be found in the internal note [6].

The lenses in front of the EO1 are cylindrical (0.25m and 0.34 m focal length) and achieve the matching between master and slave laser.

EO1 is the electro-optic crystal which generates the **F1** sidebands used in the Pound-Drever scheme of the injection, the prestabilization, and the mode cleaner lockings; it is made of a pair of LNO at Brewster angles and the modulation frequency is around 11 MHz such that the sidebands are reflected by all the cavities involved in the above mentioned servo-loops.

EO2 is the same kind of electro-optic used for the phase correction of the prestabilization loop **SFr** and used simultaneously (TBC) to generate the sidebands of the signal modulation called **F2**.

ABP1 is the auto beam positioning serving to realign the beam from the laser bench to the Reference cavity sitting on the input bench (see also alignment strategy below) and is fed back by the error signal coming from the autoalignment of the **RC**, named here **ARc**.

An off-axis mirrors telescope (3 mirrors TBC) of magnitude 10 will be used to match the laser beam to the MC waist.

41.5.1.2.5 Frequency prestabilisation

The level required for the prestabilisation depends upon the final stage loop gain and the filtering encountered by the beam transmitted by the mode cleaners and the recycling cavity before reaching the beamsplitter. Starting from an average asymmetry of 1%, we have calculated the level required for the prestabilisation stage (see details in note PJT 93-009), which is at the same time the level of absolute stability required for the reference cavity (see reference cavity below).

The Figure **4120.2** gives the requirement of prestabilization (see also note PJT 94-036) for different asymmetries in the initial and ultimate sensitivity requirements (see results in PJT 95-025).

41.5.1.2.6 Power stabilization

The power stabilisation servo loop **SPo** reduces the amplitude noise of the light as far as possible in the frequency region of interest of the Virgo experiment, that is 10Hz - 10kHz. The goal for this noise reduction is shown in Fig 4100.2. At present this loop has a unity gain frequency of around 38kHz. It also is responsible for maintaining the average power level of the slave laser as seen after the modecleaner, to a level specified by the user.

The loop consists of a detector (Detector **Dps**) operating under vacuum mounted on the input bench, a PID or Servo Unit, and a control unit (Laserdiode Controller) which is an interface between the Servo Unit and one of the laser diode arrays of the slave laser (Figure **4120.3**) :

- The detector **Dps**.samples a small proportion of the light after the modecleaner (30mW), using a photodiode of type RMP 16A-030 (equivalent to Hamamatsu G5832-03).
- The Servo uses the outputs of **Dps** to produce control signals which are then applied to the slave laser via the laserdiodes to regulate the average output power as seen after the modecleaner, and to reduce the amplitude noise down to or below the specified levels.
- The Laserdiode Controller is an interface between the Servo Unit and one array of five laserdiodes which drive the slave laser. Its mode of operation is to bypass a small amount of current away from the laserdiodes and in this way to change the laserdiode current. While this task is in fact achieved by a simple Darlington transistor arrangement, it is extremely important to ensure that no dammage results to the laserdiodes, as they are very sensitive to reverse voltages. Consequently the Laserdiode Controller includes a safety network which prevents the application of reverse voltages to the laserdiodes, and short-circuits any applied signals in the event of laserdiode power supply shutdown.

Operation :

The DC output of **Dps** is directly compared with a reference signal in order to give a DC error signal (Signal **SPoEr**) which is later used to regulate the average power of the laser as well as to provide general stabilisation at frequencies below 10Hz. The AC output of **Dps** without any processing, is literally the AC error signal. These two error signals are then added together at the input of a high gain amplifier. (Note that it is at this stage where the simulation of the modecleaner two low pass filters with poles at 500Hz takes place, at the input of the high gain amplifier. For operation with the real modecleaner, the capacitors of these filters must be disconnected using the on-board switches provided).

Following this are several stages of filtering giving the necessary roll-offs in order to maintain high gains in the lower frequencies of interest, while allowing the gains at higher frequencies to be reduced to manageable levels. There is also an integrator operating in the region below 50Hz to give precise locking to the external reference signal.

Finally the output stages produce two correction signals for the Laserdiode Controller and laserdiode power supply respectively: the Fast and Slow Correction Siganls. The Slow Correction Signal is produced by integrating the Fast. This has three important advantages. Firstly, the average level of the Fast Correction Signal is maintained at zero (the middle of its range) thus insuring that the Laserdiode Controller stays at the centre of its operating regime under normal operation. Secondly, the Slow Signal contains all the DC correction information and is thus an indication of the DC adjustment performed by the power stabilisation system (Signal **LDsPl**). Thirdly, this arrangement allows a convient way of predicting an immanent delock by sensing when the Fast Correction Signal moves away from zero volts (Delock signal **SPoSt**).

Vacuum compatible photodetector **Dps** :

For a more detailed description of the design and function of the electronics of this detector, see ref [13]. To facilitate the use of this detector under vacuum, the circuit board containing the photodiode is mounted in a specially made stainless-steel box (Figure **4120.4**), with an Indium jount to render it air-tight, the photodiode being accessed via a sealed window. Normal atmospheric pressure is maintained inside the box to faciliate the cooling of the electronic components.

The detector is mounted on the Input Bench, and receives light from the mirror M4 via a matching lens of 22.5 cm focal length, inserted 20 cm in front of the detector. The detector has an active area of diameter 3mm. In order to allow for alignment error or small fluctuations in the beam position, the beam is focussed down to roughly half the size, being 1.6mm.

Design Strategy :

Since the power stabilisation loop will be the last loop concerning the laser control to be activated in any normal activation sequence, it is important that this unit remains "transparent" until the time of activation, to avoid interference with the laser or other servo units. Also in the possibility of computer or hardware failure, the resulting ramifications should to be kept to a minimum. To these ends, the following design strategy has been adopted :

- when the servo unit is deactivated, either locally or by local controls, or disconnected from its power supply, all outputs return to zero volts, returning it to its normal bias level of 50%, and thus leaving the laser power at the level predetermined by the main laserdiode power supply, be that locally or remotely selected.
- the reference level for the laser power is not taken uniquely from local controls, but is given by a combination of a multi-turn potentiometer found on the front panel of the Servo Unit which sets the average power (nominal level 10W) and an external signal derived from control command allowing an adjustment of 1W either side of the average level. In this way, if this external signal is disconnected or there is a computer failure, the laser continues to function, and its output power returns automatically to the predetermined average level, dictated by the local potentiometer.

41.5.1.2.7 Laser Table Mechanics

The requiirements on the laser table (TLS) are the following :

- mechanical induced tilts on the beam smaller than 3.10^{-8} rd/$\sqrt{}$Hz around 100 Hz
- mechanical induced distortions on the optics should not misalign the beam
- minimum of seismic isolation (see below)
- some rigidity of the table and the optical mountings but no stringent conditions on thermal stability (induced beam waist displacements are small compared to the Rayleigh range of the MC cavity).

Description of the laser table :

- it is a TMC optical table: 0.2mx0.9mx1.5m, 216 kg. The first and main mechanical resonance is located around 200 Hz, the damping for this resonance provides an amplification factor Q smaller than 14 for the deformation of the table (14 is a typical value given by the manufacturer).
- the power spectrum density (psd) of the table deformation $\delta(f)$ expresses like

$$Q(f).\gamma(f).\ \frac{1}{(2\pi f)^2}\ ,$$

where f is the Fourier frequency, $\gamma(f)$ the psd of the perturbation expressed in m.s^{-2}/$\sqrt{}$Hz (mainly seismic or acoustic noise). The associated tilt is then $\delta(f)$ /0.75 radians, and since we consider the first resonance $\delta(f)$, the maximum deformation raises at half length of the table.

- Seismic noise induced tilts: in the Orsay laboratory $\gamma(f)$ has been found to be less than 5.10^{-5} m.s^{-2}/$\sqrt{}$Hz [7], so the induced tilt is 0.4 nrd/$\sqrt{}$Hz. This is anyway below the specification on the whole frequency range.
- Acoustical noise induced tilts: let's assume a level of 50 dBa/$\sqrt{}$Hz (standard lab normal

level), this means a pressure of 0.0085N/√Hz on the surface of the table; it leads to an acceleration of the table of $\frac{0.0085\text{N}}{216\text{kg}.(2\pi f)^2}$/√Hz in case of a table lying on rigid feet and of $\frac{0.0085\text{N}}{216\text{kg}}$ /√Hz if the table is lying on a piston isolators (free mass). At 200 Hz, for the rigid feet we obtain a tilt of 10^{-16} radians/√Hz; and a tilt of 0.46 nrd/√Hz for the spring feet. In both cases we are well below the specifications for the allowed tilt at the input bench entrance.

41.5.1.2.8 Alignment & matching LB/RC

Alignment: the beam leaving the laser bench will be automatically aligned to the reference cavity sitting on the input bench (servo ARc) via the pzt-mounted-mirrors named ABP 1 sitting on the laser bench. The misalignment of the RC due to slow drifts can be critical as it can change the prestabilization level.

Matching: of the beam to the **RC** achieved via a two fixed lenses-telescope placed in front of the RC (see Figure **4100.8**). This matching of the RC is not very critical as the level of light needed in the RC is less than 5 mW.

This strategy implies that seen from the laser bench, the RC is used as reference position for the input bench.

41.5.1.2.9 Last stage of frequency stabilization

The signal coming from the reflection of the whole interferometer, is seen by photodiode D2 and will be demodulated before amplification, filtered and added to the error signal coming from the reference cavity (prestabilization loop). Then the width of the reference cavity is the allowed dynamical range of the detuning between the laser frequency and the interferometer frequency. This range is today around 12 kHz which is much more than what any phase corrector could have. Of course the transfer function of this last stage has to be defined coherently with the locking group and the global control SS **[16]**. This loop can have a maximum bandwidth of 15 kHz (about one third of the free spectral range of the interferometer). An analog servo-loop is planned and being developed today in the SS, but a digital servo-loop which can be demonstrated to have this bandwidth should be more flexible in term of adaptation of transfer function compatible with the locking purposes. An agreement with Virgo-Napoli is underway which results in an implementation and test of such a digital filter in the laser system built in Orsay.

41.5.2 Input bench

41.5.2.1 Input bench function and concept

The input optics are sitting under vacuum on the suspended Input Bench (**IB**) and serve 2 purposes : filter spatially the beam and stabilize its position with the Mode Cleaner (MC) and yield the necessary movements to align the beam to the axis of the interferometer.

The **IB** supports the Reference Cavity (RC) which acts as a mechanical reference for the frequency prestabilization and the input-output plane mirrors of the mode cleaner.

The MC is a three-mirror cavity used in transmission, in a ring shape configuration, and has its two input-output plane mirrors forming a corner-cube and sitting on the Input Bench, while the far curved mirror is suspended alone about 144 m away on an axis perpendicular to that of the corner-cube.

The **IB** and the Mode Cleaner far mirror (Mmc) are 2 masses suspended in 2 separate towers connected together by the Mode Cleaner tube which is 144 m long. For each mass, local controls based on position memory readouts are implemented and are used for damping the pendulum oscillation and making the pre-alignment of the **MC** cavity by moving the mass in all degrees of freedom. Both of them will be done by action on the 8 coils implemented around the marionetta of the **IB** and the **Mmc** (TBC) or on coils implemented on the lower part of the towers (TBD).

Once the cavity aligned, the **MC** is brought into resonance with the axial position of **Mmc** (a Pound-Drever error signal is used) by feedback possibly on some coils (TBD) located behind the mirror (TBD).

Then the automatic alignment (based on H.Ward's technique) of the **MC** starts to run with a correction signal applied to the **Mmc** marionetta 8-coils, in order to avoid reintroduction of seismic noise during operation..

41.5.2.2 Input bench detailed description

It is a table suspended inside the injection tower where we can find the following optics:

- 1 transmitting plane mirror giving 10^{-3} of the light to the **RC**
- 2 plane mirrors of **APB 2** serve to fold the beam to the **MC** corner cube and mounted on pzt in order to do the auto-alignment of the beam to the MC cavity and fed back by error signals from servo **AMc**
- the corner-cube carrying the two input mirrors of the **MC**
- one plane mirror to fold the output beam of the **MC** to the telescope and transmitting 3.10^{-3} of the light to the power stabilization photodiode **Dps**
- the final telescope formed by two off-axis curved mirrors used to match the beam to the interferometer; they are mounted on pzt and can serve for the pre-alignment of the beam (**APB 3**) to the interferometer as well as auto-alignment if necessary and if they don't bring extra noise
- not seen on the **IB** is the end curved mirror of the mode cleaner **Mmc** to which we will refer when talking about **MC** alignment, controls, etc...

41.5.2.2.1 Reference cavity : optical parts

The stability of the cavity is coming from the thermal noise considerations and the induced seismic noise on the internal modes. A detailed discussion can be found in the Virgo note PJT 93-009 and summarized hereafter. To keep the thermal noise low, the internal mode resonant frequencies must be above the detection range as well as its internal Q sufficiently high (Q > 10^4). The first condition can be fulfilled with a judicious shape, while the second one is performed with a high Q (and good thermal stability for long term operation) material (see Figure in FD 95).

To avoid acoustic noise and dust pollution of the mirrors, the cavity sits in a clean vacuum chamber so the mounting should be designed in order not to increased the rms. motion of the cavity.

Besides that there is an optical consideration concerning the finesse of the **RC** which should be high as far as possible to lower the shot noise limit of the prestabilization around $10^{-4}\,\mathrm{Hz}/\sqrt{\mathrm{Hz}}$ with 1-2 mW of light.

The beam entering the **IB** is matched to the **MC** waist of 4.9 mm, then a-2-lenses telescope is used on the beam derived to the **RC** to reduce its size to of that of the 0.286 mm waist of the **RC**.

The constraint for this telescope are mainly mechanics for distances "laser-first lens" and second lens- mirror" and optical for the distance L_1L_2

The optical parameters are:

RC waist = 0.286 mm
MC waist = 4.9 mm
L_1L_2 = 437,7 mm
L_1 focal length = -70 mm
L_2 focal length = 500 mm

Near the input mirrors cavity, 2 mirrors have been installed in order to take the beams coming from the reflection and transmission of the cavity outside the injection tower on the detectors table.

41.5.2.2.2 Reference cavity : mechanical parts

The cavity is put inside a vacuum housing, evacuated by a small ion pump. This housing is necessary to keep the cavity clean from dust contamination on mirrors. The ion pump will be mantained to evacuate separately the RC during the first tests, to keep the mirrors of the cavity clean in case of possible contamination of the input tower. Figure **4130.1** shows the mechanical drawings.

41.5.2.2.3 Mode cleaner: optical parts

The MC should fulfill the following criteria:
- spatial filtering efficiency meaning a transmission ratio between the high order and the fundamental modes smaller than 10^{-3}
- frequency filtering efficiency as a low pass filter for the laser noises, we can choose a pole ≤ 500 Hz giving an attenuation of at least 10 at 5 kHz
- used with the whole laser power, it should avoid thermal effects, meaning that the absorbed light should not exceed a few tens of mW; of course this will depend on the coating technology and on the laser power planned in the future
- as a cavity used in transmission, its efficiency should be more than 95%
- used to pass the signal modulation, its free spectral range has to be a sub-multiple of the modulation frequency F2
- furthermore to avoid light feedback into the laser, it should be a three-mirror ring-shape cavity.

With all these conditions taken into account (see [8]), the solution adopted today is:

length L_c: 144m, free spectral range =
beam waist at input mirrors: 4.9 mm $2 L_c$
beam size at end mirror: 11 mm
mirrors diameter: 80 mm (TBC)
end mirror curvature: 181m
corner cube angle: 90°-1'

The 2 plane mirrors are optically contacted on the corner cube (**Figure 4130.2**) sitting on the IB and the concave mirror suspended inside the mode cleaner tower 144 m away (± 2m).

Because the mode cleaner is a low pass filter at 500 Hz (f_p) for laser noises, the finesse F of the MC will be around 1000 meaning a high reflective end mirror (r_1) and a reflectivity of 0.997 (r_2, r_3) on «s » polarization for input mirrors

$$F = \frac{\pi\sqrt{r_1 r_2 r_3}}{1 - r_1 r_2 r_3}$$

The figure 4130.3 gives the drawing of the corner cube, which is made of Silica. A spare piece exists in Zerodur. The mechanical support of the corner cube is a simple plate clamped to the IB, the corner cube is sitting on top of three thin cylindrical rods used as a simple stage isolation for the MC (see mechanical isolation of IB). A cover will be put around to protect it from contamination during the prealignment phase.

The far-mirror mass Mmc can be clamped in some ways (TBD) to a larger mass in order to use for it the same marionette as the standard test-mass. In the same way the use of a reference mass is also possible (TBC), mostly when it can help controlling the position of the MC length in the locking purpose.

41.5.2.2.4 Matching optics for the interferometer

The waist of the beam entering the interferometer (matched to the FP cavities) should be located at the input mirror of the FP with a size of about 20 mm. Due to the large confocal parameter of 2310 m in Virgo, the tolerance in position of this waist is about ± 100 m for a loss level compatible with the estimated optical losses of the recycling cavity.

To match the beam coming out of the MC and entering into the interferometer, an Input Telescope (ITC) should be designed that match the following requirements. To avoid spurious reflection backward into the laser, the telescope is a reflective type, dealing with off-axis mirrors; it should introduce low beam distortion i.e. the induced aberration loss should be smaller than 10^{-3}.

The following 2-mirrors off-axis telescope has been designed for the test interferometer :

length of telescope = 549 mm
first mirror radius of curvature = 3380 mm at incidence angle 4°
second mirror radius of curvature = - 2300 mm at incidence angle 4.9°

The two incidence angles ensure a compensation of astigmatism; the tolerances on the radius of curvature is around 10^{-3} corresponding to a deviation between $\lambda/10$ to $\lambda/20$ which is probably easy to achieve; the tolerance on the length of the telescope is ± 1 mm which gives loss smaller than 10^{-4} in the matching.

These two mirrors will be mounted on 3-axis pzt motors (APB 3) serving for their fine alignment and auto-alignment of the interferometer if necessary.

41.5.2.2.5 Input Bench Mechanics

The mechanical design of the **IB** and its components is governed by the mechanical and thermal induced fluctuations of the bench. These are translated in terms of phase fluctuations at the input of the interferometer. This phase noise has to be compared to the requirements of the laser phase noise given in the Figure **4120.2**. Knowing that any path length fluctuation $\delta\tilde{L}\,(F)$ is equivalent to a laser frequency fluctuation $\delta\tilde{\nu}\,(F)$ as $\delta\tilde{\nu}\,(F) = \frac{2\pi}{\lambda} F.\, \delta\tilde{L}\,(F).$, let's examine the noise encountered by the **IB** and each component sitting on it.

When the usual seismic noise on $10^{-6}/f^2$ m/√Hz impinges on the Reference Cavity, we get the curve a of the Figure **4130.4**, which is well below the requirement (curve c). So there is no need for seismic isolation of the RC except to avoid excitation of mechanical resonances of its support.

For the Mode Cleaner, any length fluctuation is enhanced by a factor which is equal to the number of round trips of the beam multiplied by the low pass transfer function of the MC. For a finesse of 1 000 and a pole frequency of 500 Hz, the $10^{-6}/f^2$ m/√Hz seismic noise induced fluctuation is given by the curve b of the same Figure. One can see that above 100 Hz there is a need of some seismic isolation for the MC, for instance a simple pendulum at 1 Hz will be enough for the suspension of the IB, even for the ultimate Virgo (curve e).

The Figure **4130.5** shows the drawings of the IB as it has been realized today in Alplan chosen for its low Q value, the mechanical resonances have been found between 500 Hz and few kHz with measured Q smaller than 500.

If the MC input mirrors block is rigidly connected to the bench, it will add its thermal noise to that of the bench and the resulting noise is plotted on the Figure **4130.6** in comparison with the laser requirement at the output of the mode cleaner. The straightforward conclusion is either to have a low Q material (Q<100) or a block's shape giving a mechanical resonance outside the detection range (≥ 10 kHz). This is the reason why the two plane mirrors of the MC is rigidly clamped (optical contact) to a corner cube of Silica (Zerodur is better in terms of low Q) with a shape designed to have the lowest resonance around 9 kHz. Furthermore to lower the influence of this thermal noise, the corner cube sits on 3 rods designed to act as isolation above 50 Hz. Then the calculation shows that now the equivalent frequency noise plotted on Figure **4130.7** is well below the requirement.

Mode Cleaner cavity	Frequency Pole 500 Hz few ppm loss optics	Length = N times 12m	1-stage suspension	clean vacuum ≤ 10^{-6}mbar
MC Input corner-cube	1st resonance ≥10kHz		additional isolation on the **IB**	
Input telescope	reflective optics	induced low loss aberration	low beam distorsion optics	
Input bench **IB**	Q < 1000 mechanics		1-stage suspension	clean vacuum ≤ 10^{-6}mbar
Reference Cavity **RC**	high finesse ≥ 30 000	few ppm loss optics		
RC mechanics	1st resonance ≥10 kHz	Q > 10 000	zero expansion material	clean vacuum ≤ 10^{-6}mbar

Table 4100.2 : Specifications of the main components of the Input Bench.

41.5.2.2.6 Auto-alignment of cavities

The automatic alignment of the 2 cavities used in the SS will be achieved using a differential phase sensing technique, which was proposed and experimentally demonstrated by the Glasgow gravitational wave group[0] . The technique is an extension of the Pound-Drever modulation scheme for locking the length of a cavity to the frequency of a laser. In both cases, (Figure **4130.8**) the incident laser beam is phase modulated at a high frequency (e.g. around 10 MHz), and the light reflected from the cavity is observed with a photodiode; the information contained in the photocurrent is extracted by demodulating with the modulation frequency. In the first case a simple photodiode is used, while the second one needs two quadrant photodiodes, one in the near field, and the other one in the far field (with a lens).

The principle of this technique can be understood as follows (for simplicity, only one lateral dimensional is considered). In the case of simple frequency locking, the light reflected directly at the cavity entrance mirror (including the modulation sidebands) interferes with the light having entered the cavity and being transmitted back through the cavity entrance mirror (indirect reflection, containing only the carrier); the demodulated signal contains information about the frequency error, coming from the dephasing between the two interfering components, which depends on the detuning. In the case of a misalignment, the beam incident on the cavity can be decomposed with respect to the cavity reference system in terms of the Hermite-Gaussian cavity eigen modes U_n. Especially, an only slightly misaligned (mismatched) beam can be represented as a simple superposition of low-order modes:

beam error	*eigen mode decomposition (phase)*
lateral misalignment (shift)	U_o & U_1 $(0°)$
angular misalignment (tilt)	U_o & $U_1(90°)$
waist size mismatch	U_o & U_2 $(0°)$
waist position mismatch	U_o & $U_2(90°)$

In general, the U_n will have different resonant frequencies, so only the U_o will enter the cavity and resonate; the other modes are reflected off the entrance mirror. So the direct

[0]E. Morrison, B. J. Meers, D. I. Robertson, H. Ward, "Automatic alignment of optical interferometers", Appl. Opt. 33, 5041 (1994); E. Morrison, B. J. Meers, D. I. Robertson, H. Ward, "Experimental demonstration of an automatic alignment system for optical interferometers", Appl. Opt. 33, 5037 (1994)

reflection off the cavity entrance mirror (R_1) contains the original U_o and $U_{1/2}$ contributions, including the modulation sidebands, whereas the part transmitted back through the cavity entrance mirror (the "indirect reflection", R_2) contains only the U_o part. The total reflected beam will thus consist of two beams: the unaltered (misaligned) incident beam plus a fundamental beam U_o aligned with the cavity axis. The beat of both gives:

1. The beat of the fundamental part (U_o) of R_1 with R_2 gives the information about the frequency error between laser and cavity

2. The beat of the first order contribution U_1 of R_1 ("misaligned part") with R_2 gives a two-lobed beat signal, which can be detected with a symmetrically split photodiode (for both lateral dimensions: quadrant photodiode) to yield information about the misalignment. According to the type of misalignment (lateral shift or tilt, which determines the relative phase between U_o and U_1), the beat note occurs in the near field or in the far field of the reflected light.

Thus, in order to obtain the required informations, 3 photodiodes are necessary:

1. A quadrant diode looking at the light reflected from the cavity for obtaining informations about the beam tilts
2. A quadrant diode in the focus of a lens collecting the light reflected from the cavity for obtaining informations about the lateral beam shifts
3. An ordinary photodiode for obtaining informations about the frequency deviation of the laser (this might be replaced by the sum of the 4 quadrants of photodiode 1).

41.5.2.2.7 Position measurements of IB and Mmc masses: position memory readout

The reading of the mass position/orientation of the **IB** and the **Mmc** uses the position memory based on CCD cameras [9], read out by computer (Annecy camera [VIRGO note PJT 92-032]).

The Fig.**4130.9** shows the 1st scheme where one CCD is used to image the mass carrying 4 reference marks: during the phase of initial alignment, when the mass is still strongly misaligned, if the mass moves in x or y direction, or turns around the z axis, the images of the marks 1 and 2 move accordingly on the camera, which gives informations on these 3 degrees of freedom. For measuring z, the perspectivic change in the distance between the images of mark 3 and 4 is used, which leads to a small precision for this variable. The uncertainty in z will be partially transferred to the measurement of x due to the angle γ under which the mass is seen. Then an appropriate combination of the position of the 4 images on the CCD allows to determine the 6 degrees of freedom of the mass position with a high dynamic range in θ_x and θ_y

Then a finer alignment can be done with additional two lasers and an auxiliary mirror as shown in Figure **4130.10**: they are arranged in such a way as to create two light spots on the camera. The beam of laser 1 is folded, so its spot on the camera does not change with z. It thus gives a precise information on θ_x and θ_y. For measuring z, laser 2 is used. Due to the camera lens, laser 2 is not sensitive to mass rotations.

It might be useful to switch between the two modes of measurement according to the state of alignment and the desired precision.

The following tables show the theoretical and experimental performance of the position measurement system. The position was measured at 30 Hz, integrating over 1/60 s; the rms. noise is the variance of 30 consecutive points.

Theoretical performances

	half dynam. range coarse	fine		rms. noise (1/60 s) coarse	fine	
x	10	10	mm	6	0.2	μm
y	9	9	"	0.15	0.15	"
z	18	9	"	11	0.2	"
θ_x	40°	3 mrad		40	0.08	μrad
θ_y	40°	3 mrad		30	0.07	"
θ_z	25°	25°		15	15	"

Measurement results (table top experiment)

		rms. noise fine exp.	fine theor.	coarse exp.	coarse theor.	drifts fine	drifts coarse
x	μm *μm/√Hz*	0.15 *0.02*	0.2 *0.026*	11 *1.4*	6 *0.8*	3	50
y	- " -	0.3 *0.04*	0.15 *0.02*	0.4 *0.05*	0.15 *0.02*	4	10
z	- " -	0.15 *0.02*	0.2 *0.026*	20 *2.6*	11 *1.4*	5	200
θ_x	μrad *μrad/√Hz*	0.2 *0.026*	0.08 *0.01*	60 *8*	40 *5*	12	150
θ_y	- " -	0.07 *0.009*	0.07 *0.009*	60 *8*	30 *4*	12	200
θ_z	- " -	15 2	15 2	30 *4*	15 2	70	75

41.5.2.2.8 Position controls of IB and Mmc masses

The position controls of these 2 masses concern:

- their damping
- their pre-alignment relatively to each other
- the **MC** resonance lock
- the **MC** automatic alignment

The 2 first items take correction signals from position memory readout to feedback on each marionetta's coils, the **MC** resonance lock uses the Pound-Drever correction signal to feedback to the 2 coils behind the **Mmc** mass and the autoalignment is performed by Ward's technique and correction signal fedback to the **Mmc** marionetta's coils.

<u>1. Damping</u>: in order to correct pendular movements/slow angular drifts, mass position and orientation $(x, y, z, \theta_x, \theta_y, \theta_z)$ are measured at a rate of 30 or 60 Hz by the camera scheme. They are then communicated from the camera readout program to the coil control program, which computes the correction current. This is done using a digital filter, which compensates the mechanical (pendulum) and electronic transfer function of the system in order to achieve a stable feedback loop. The filter algorithm used **[10]** simulates an analog filter, for which the parameters (gain, delay, position of poles and zeroes) can be entered on-line by the user; the advantage is a more intuitive filter design, facilitating the optimization of the loop behavior. However, this requires a sampling speed sufficiently high with respect to the unity gain frequency of the feedback loop, in order to make sure that the approximations made are valid.

2. Pre-alignment: according to the experience gained with the MC prototype at Orsay, the mechanical prealignment of the marionetta might be difficult if one demands better than 1 mrad. So let's put ≤2 mrad as the angular prealignment precision requirement (q_x, q_y, q_z) and as requirement for the long-term prealignment stability against drifts etc. due to thermal expansion, aging of components, relaxation of constraints (e.g. rotational constraints in the wire supporting the marionetta!) etc.

3. MC lock SMc: the frequency difference between laser and mode cleaner resonance is measured with the Pound-Drever technique, and a correction signal is applied to the MC far mirror at a rate of > 100 Hz, possibly to the marionetta coils (TBC). A detailed discussion of the MC locking can be found in **[11]**. Here we give a short overview. The task of the mode cleaner locking system is to ensure:

1) a good transmission by keeping the mode cleaner resonant, i.e. keeping the difference between laser frequency and mode cleaner resonance frequency low. Not more than 0.5% of the incident laser power should be lost (reflected) due to bad locking, so the laser frequency must stay well within the MC resonance bandwidth.

2) low phase fluctuations at the output, in order to fulfill the specifications for the residual laser frequency noise. This necessitates reducing the residual mass movements.

3) a constant transmission for avoiding output power fluctuations; this necessitates keeping the fluctuations in the aforementioned difference frequency low.

So one sees that it is necessary to have a good agreement between the laser frequency and the mode cleaner resonance frequency. The difference between both can be measured with the Pound-Drever technique.

Specifications: from these three conditions, the following specifications for the relative deviation z of the MC length from resonance can be derived **[11]**:

$$\tilde{z} < \begin{cases} 2.5\cdot10^{-12}/(f/\mathrm{Hz})^{0.8} & (10\ \mathrm{Hz} < f < 400\ \mathrm{Hz}) \\ 3\cdot10^{-9}/(f/\mathrm{Hz})^{2} & (400\ \mathrm{Hz} < f < 10\ kHz) \end{cases} \frac{\mathrm{m}}{\sqrt{\mathrm{Hz}}},$$

$$z_{rms} < 20\ \mathrm{pm}\ (100\ pm)\ .$$

These values determine the required performance of the feedback system.

Figure **4130.11** shows the effect of various noise sources in terms of displacement noise spectral density (m/$\sqrt{\mathrm{Hz}}$; mass displacement relative to resonance), and the noise limits due to the permitted residual amplitude and frequency noise of the MC output beam (see **[11]** for the detailed discussion). The open and closed loop cases are shown. Mechanical transfer functions are simplified. For the feedback, a unity gain frequency F_O of 100 Hz was assumed, with an open loop gain going like $1/f^3$ up to $f_0/3$ and $1/f$ above.

As one can see, the amplitude and frequency noise specifications are fulfilled even when no superattenuator chain is used (2- instead of 5-stage pendulum). No reference mass is needed from a noise point of view; the locking coils, acting directly on the mass, can be fixed on the ground, without compromising the laser stability at the output due to seismic noise transmitted by the coils. Moreover, the noise specifications are satisfied also in the open loop case; thus the task of the locking is limited to keep the rms. deviation small (requirement 1.) by reducing slow movements.

As can be seen from Figure **4130.11**, seismic and laser frequency noise dominate the spectrum at low and high frequencies (above and below 3 Hz), respectively. Therefore it is sufficient if the loop design is made to suit these two noise sources.

Laser frequency noise: Supposing that below a frequency f_o the locking loop corrects the deviations $\Delta\nu$ from resonance by acting on the mirror position, one obtains for the servo loop unity gain frequency f_o > 0.08 Hz. The open loop gain must increase to low frequencies at least like the laser frequency noise, i.e. a simple integrating loop with a sufficiently high f_o is generally appropriate. Thus, the frequency fluctuations of the prestabilized laser pose no severe constraints on the locking loop.

Seismic noise: Comparing the residual rms. mass displacement noise (without resonances) with the allowed value, one sees that the gain of the feedback loop must be $4\cdot10^4$ at 1 Hz, which requires a unity gain frequency at least two orders of magnitude higher than the seismic noise cutoff frequency (f_o > 100 Hz). Taking account of the resonances requires a gain about 10 times higher than above. If between the resonance and the unity gain frequency two decades are available, then the open loop transfer function must have a $1/f^4$ behavior up to f_o /3 and $1/f$ above.

Drifts: An open loop gain of $4 \cdot 10^8$ is needed at 10 µHz for correcting slow drifts; these very low frequency corrections go to the suspension point control system.

Dynamic range: The DAC dynamic range is given by the fact that on one hand a sufficiently large number of resonance peaks must be covered, mostly for facilitating the lock acquisition, on the other hand a high resolution within the peak of a resonance fringe is required for locking. The DAC resolution resulting from the dynamic range and the digitization noise added to the correction forces is 18 bit. If this causes a problem, then the locking signal can be split, the fast part going to the mass, and the slow one to the marionetta. Locking by acting uniquely on the marionetta would require a too high coil current at high frequencies.

4. MC automatic alignment AMc: the alignment error uses the Ward technique (described above) and the correction signal is applied to the MC far mirror (TBC) and ABP2 (TBC).

Considering the relative alignment of the two flat **MC** mirrors fixed, there are 4 degrees of freedom which may need alignment correction. Possible feedback strategies are discussed in [12]; the **IB** orientation cannot be used for the **MC** alignment, since it will probably be controlled by the interferometer autoalignment in order to steer the beam properly into the interferometer. The beam coming from the laser bench is rigidly coupled to the **IB** by its autoalignment to the reference cavity (**ABP 1**); thus, all rotations of the **IB** will change the direction of the beam into the mode cleaner. This necessitates a correction with an angular alignment (θ_x and θ_y) of the MC curved mirror. The remaining two degrees of freedom, due to a non-perfect rigid coupling of the beam to the bench (bench deformations...), can be corrected by acting on **APB 2**. So the autoalignment correction signal has parts going to the mode cleaner far mass and to APB 2.

It is theoretically sufficient to have a slow feedback in order to correct misalignments caused by drifts. However, perturbations and/or autoalignment corrections might excite pendular motions of the mass, and thus it is probably better to take a fast feedback which covers also the pendulum frequencies in the range of 1 Hz [12].

5. Magnets-coils specifications: for correcting the mass positions, there will be magnets mounted on the marionetta, on which forces can be applied with electromagnets (coils). For fast corrections (locking, z direction), forces must act directly on the mass itself. The coil currents are controlled by programs running on a VME CPU via DACs.

Mass position corrections may come from different sources:

- Operator commands during the phase of initial alignment (manual, but computer aided);
- Action of the feedback responsible for the damping of pendular movements (during manual alignment)
- z correction signal coming from the locking system
- angular correction signals coming from the autoalignment system

Once the mechanical prealignment is made with the required precision, the residual misalignment of the marionetta orientation must be corrected with a current in the coils on the marionetta. The maximum current foreseen in the MC prototype coils is 1 A; therefore, the coil drivers (amplifiers) are designed for that current, so it would be good to keep 1A as maximum coil current if one wants to keep the same amplifiers for the test interferometer. One must be able to easily cover the whole prealignment uncertainty range, without saturating the coils. In order to have some margin for additional corrections necessary e.g. during damping, the requirement for the possible angular correction using the coils is 5 mrad (q_x, q_y, q_z) with 1 Amp. It is possible that the q_y drifts will be larger than 2 mrad, but the coil force in this direction should not be a problem. The translation sensitivity in x and z depends on the weight of the marionetta+bench. In order to have sufficient force for fast damping, locking etc., the sensitivity should not be less than 1/3 of the MC prototype values, so the specification is 0.1

mm for 1 A for x and z. No specification is given for y, since that depends on the superattenuator blade stiffness.

This table gives the MC prototype values for displacement/rotation sensitivity for comparison.

x	0.5 mm/N	0.3 mm/A
y	0.2 mm/N	0.12 mm/A
z	0.5 mm/N	0.3 mm/A
q_x	150 mrad/Nm	18 mrad/A
q_y	3000 mrad/Nm	360 mrad/A
q_z	150 mrad/Nm	18 mrad/A

41.5.3 Local controls

The laser bench delivers a high power laser beam which characteristics have to be monitored permanently with a low frequency rate. This laser beam originates from a certain number of lasers (master laser, slave lasers, laser diodes for the pumping), and in order to observe the operation conditions and the aging of the lasers, there is also a need to monitor and control the operation of parameters such as currents, temperatures, powers, pzt voltages, photodiodes signals, etc...

To match the above mentioned requirements the lasers are stabilized to each other and to the resonant cavities RC and MC in a logical order. Therefore the servos sequence has been precisely defined in order to start and stop the servos and to give alarms to prevent to taking into account false events.

These topics also named *local controls* involve many items that have to be specified clearly in order to be sure that the laser stability's requirements are matched for the whole sub-system. If we consider that the IB and the MC are two suspended masses, the task of the local control is to measure and correct the position and orientation of these 2 masses with respect to a local reference system. Together with the MC cavity control, which controls of the MC mass relative to the IB mass, it will work also during the prealignment phase. The local control is necessary for:

- the prealignment : the local control allows reading and correcting the mass position in order to achieve the right orientation for the MC resonance.
- the mass local readout : the mass position is continuously monitored (or stored once after the first alignment is finished) and, in case of a fault (out-of-lock condition...), the last position can be read and restored, thus avoiding a complete start from scratch.
- damping of the pendular motions : the pendulum Q should be reduced to quite close to unity in order to avoid excessive mass movements, which disturb the prealignment and cause fluctuations of the beam position/angle after the mode cleaner, even while MC cavity control (longitudinal locking/autoalignment) is working.

In the case of the IB, the local control system can be active even after alignment (during normal operation); it then receives the positioning commands from the MC cavity control (locking and autoalignment systems) either from a local reference system or the operator.

41.5.3.1 Function and concept

The control command of the Laser and Input bench has to define hardware and software components used to command the running of the Lasers and optical components of the input-bench and Mode-Cleaner to get the beam to the Interferometer. All these tasks act as a whole system called « Beam Source » since correlations between components are mandatory. The final task resides in the Servo-control which is the purpose of Beam Source.

The functionnalities of the Control Command are :

- Commands of components : ON/OFF state of power supplies - ON/OFF state of analog or digital servo-loops - ON/OFF running of sensors.
- Monitoring of signals and hardware parameters
- Checking the validity range of parameters and according to specifications validation of alarms.
- Control of the whole Servo either in user-mode or in automatic mode
- Reporting to the General Virgo Control the states of Beam Source, the signal values, the alarms with a severity level.

The components of Beam Source Control System are :
. Lasers : Master, Slave, Diodes
. Mass control : Input bench, Mode Cleaner
. Reference Cavity, frequency pre-stabilization
. Mode Cleaner, pre-alignment, lock, auto-alignment
. Laser power stabilization.

The concepts used to perform Beam Source Control Command are :
. the frame work of Client-Server of Virgo
. the specifications and structure of the Supervisor to build a Local-Supervisor to control a set of servers - taking into account the multi-client requirements.
- the independence (or the modularity) of components as well for the hardware as for the software design
- A hierarchical analysis to design the architecture of the system owing to explicit correlations between components of the servo-loops system.

41.5.3.2 Detailed description

41.5.3.2.1 Hardware components :

The list of signals is given by components. The naming convention is the definitive one and will appear as such in the Data-Base. The list contains the usage of signals for what concerns the monitoring. See also ref. [4].

41.5.3.2.2 Hardware architecture :

The list of VME crate together with the signals sharing is as follow :
a) Crate « laser » :

- CPU : CES (or CETIA)
- status register : StR-1 (M-module)

signals : LDSlri, LDSti, LDFi, LDAji (i=1,2 ; j=1,6)
- status register : StR-2

signals : LDSlri, LDSti, LDFi, LDAji (i=3,4 ; j=1,6), LSF, SPolr
- status register : StR-3

signals : SPoSt, SLiSt, SOrST, SFrST, SPhST
- ADC - 1 et 2 (M-module) 12 bits

signals : LDIi, LDTtj, (i=1,4 ; j=1,12)
- ADC 3 et 4

signals : LDWi (i=1,20)
- ADC 5 à 7

signals : Dsl, Dbw, Dil, DpsDc, DrØ, Drc
LSPz, SLiPz, SFrPz
SLiEr, SpoEr, SFrEr
LSTe, LMId, LDSp1,2, LMDTd1,2, LMTy
- Interface RS485 (M-module MEN-M17)

signals : LDTei, LDTj, LDPej (i=1,4 ; j=1,20), LDTe, LSTj, LSPoj (j=1,2), LSTe, LSTc
- DAC (M-module) 12 bits
signals : LDIci, LDTci, SpoPc, LSTc (i=1,4)
- command Register : CdR (M-module MEN-M29)
signals : LDCri (i=1,4)
SPoCr, SLiCr, SOrCr, SFrCr, SPhCr
- gate-timer (M-module)

b) Crate « ARC » auto-alignment Rc

- CPU : CES (or CETIA)
- ADC (M-module) 12 bits
signals : ARcQi (i=1,8)
ARcQs, Mod1
- command register (M-module)
signals ARcCr
- DAC (M-module) 12 bits
signals : PaRci (i=1,4)
- status register (M-module)
signals : ARcSt
- gate-timer (M-module)

c) Crate « AMC » auto-alignment MC

- CPU
- ADC (M-module) 12 bits
signals : AMcQi (i=1,8)
AMcQs/Dlmc, Dmc, SMcEr
- command register
signals : AmCr, SMcCr
- DAC (M-module)
signals : PaMci (i=1,4)
- status register (M-module)
signals : AMcSt, SMcSt
- gate-timer (M-module) / ou timing (LAPP)
- DOL to MMC-2 : to DAC BMci

d) Crate MMC-1 (building MC)

- CPU : CES
- gate-timer (M-module)
- camera (LAPP)
- Dol to MMC-2

e) Crate MMC-2 (building MC)
- CPU
- DOL-1 from MMC-1
- DOL-2 from AMC
- DAC-m (M-module)
signals : BMci (i=1,8)
- DAC-z (M-module)
signals BMcj (j=1,2)
- Logic (M-module)
signals : IN : synchro MMC-1, AMC, SMcCr, AMcCr
OUT : Trigger DAC-m,-z

f) crate MEB (possible modifications)
- CPU
- DAC (M-module)

signals : Bbei (i=1,10)
- gate-timer (M-module)
- DOL from « interferometer »

g) crate acquisition Fast LAPP → (possible configuration)
- CPU
- TIMING
- ADC 18 bits (LAPP)

signals : DpsAc, SphEr, D2 (a or b)
- DOL to « interferometer »

The labeling of cables will follow the naming conventions and will be through patch panel near the crate.

41.5.3.2.3 Software architecture:

The Beam Source control command is implemented as a local supervisor. From a user point of view the activation of Beam Source trough the Supervisor-call appears as a graphical page showing the status of components and current values of some important parameters.

The design uses the client-server protocol providing the Master-Slave quality of the relationship. To serve the supervisor requirements a Finite State Machine is installed to control the required status of the various processes.

As a master the overall (not detailed) states required are :
- installation of servers (fork, status,...)
- configuration of servers from Data Base
  from User requests
- activation and/or sequence of individual components
- pre-running phase
  - Master
  - Slave
  - Diodes
  - Analog servo-loop
  - Damping
- running phase and servo-sequences

The error reporting is done via the error-logger standard including the ALARM levels. (as defined by requirements listed above 4041.2.1). The log file of all servers and Beam Source Supervisor is implemented with the Virgo-log file package.

41.5.3.2.4 List and functionnalities of Beam source Servers :

* « Lasers » Server : control of Master, Slave, Diodes
- localization CPU crate LASERS.Name : to be given
- functionnalities :
  . initialization
    - Cm, Db, Ep, Log, Scope, LocMon
    - Db access
    - VME modules

  . Interrupt validations - command validation

  . Running mode (possible link to Lasers-Client)

  . Active mode acquisition - on interrupt receipt
    - readout
    - specifications on parameters (checks, calculations)
    - monitoring : filling histos (local histos)

  . Active mode scope on request

- gate-timing setting
- readout - share memory filling

. Reset state
. Stop state
. Active mode any : check status on interrupt requests
- specific action : El update
. Active mode : Fb requests
signals sent to Fb slow monitoring
(list to be confirmed : DpsDc
some status like servos status, and status of signals generating ALARM.

* « CPM » server Control position mass
  - localization CPU crate MMC-1.name : to be given
  - functionnalities
    .initialization : Cm, Db, EC, Log, Scope, LocMan
    . Db access (filters parameters)
    . VME modules
    . shared memory (GX)
  - semaphore validation
  - running mode : servo
    . calculations servo-loops
    . writing DOL
  - running mode : scope - simultaneously with mode servo
    . writing shared memory scope
  - error reporting
  - reset state
  - stop state
  - dialog state with CPM-Client (filters, reference...)

* « CLM » server Control Local Mass
  - localization CPU crate MMC-2.name : to be given
  - initialization - Cm, Db, EP, Log
    - VME modules (DAC, DOL, logic-module)
  - interrupt receipt from DOL
  - running :
    . reading DOL
    . writing DAC
  - error reporting
  - reset state
  - stop state
  - (dialog state with CLM-client to be confirmed)

* « GX » server Galaxie process - Mass position measurements
  - localization : CPU crate MMC-1
    CPU crate MBE
  - functionnalities : see LAPP notes

* « AA-RC » Server - auto-alignment reference cavity
  - localization : CPU crate ARC name : to be given
  - functionnalities (not yet detailed design)
    . initialization : Cm, Db, El, Log
      VME module
    . interrupt receipt
    . running mode
      - resdont ADC
      - calculations servo-loop
      - writing DAC

. status and command control
. reset state
. stop state
. error reporting
. dialog state with AA-RC client

* « AL-MC » server - alignment and lock mode cleaner
- localization : CPU crate AMC name : to be given
- functionnalities :
  . initialization — Cm, Db, EP, Log, Scope; VME modules; Db access
  . dialog state with AAMC client : - filters parameters - calibration - command
  . interrupt receipt
  . running mode (frequency ~ 400 Hz)
    - reading ABC
    - calculations servo-loop
    - writing DAC (ABP) and DOL (BMci)
  . error reporting
  . reset state
  . stop state

* « CPBE » server - control position input bench
- localization : CPU crate MBE name : to be given
- functionnalities :
  . initialization : Cm, Db, El, Log, Scope; Db access; VME modules
  . dialog with CPBE client (like CPM)
  . interrupt and semaphore validation
  . running mode : servo
    - calculation servo-loop
    - writing DAC
  . running mode : scope
  . error reporting
  . reset state
  . stop state
  . running mode : interferometer to be designed

* « Beam Source Fast Acquisition » to be designed by LAPP.

41.5.3.2.5 Software implementations Beam Source Supervisor :

The figures **4100.6-8** shows the implementation of sensors and active components along the beam. A tentative design of a graphical-page to control Beam Source is shown in Figure **4140.2**. The definitive control-page will benefit from the Mode-Cleaner test (30m length) done at LAL-Orsay. In this page all boxes are « actives » click to get informations concerning the chosen component. Some of active boxes will be able to activate the specific client of a Server providing the Master-delegation if requested by USER. Such client process have to link to FSM if either is called through the Supervisor or activated as stand alone during a phase of tests of the main Virgo Supervisor. By the way the implementation of partitioning has to be done through a shell-like process as foreseen for the Supervisor.

41.5.3.2.6 Software implementations Beam Source Servos :

The control of the different servos of Beam Source follows the requirements of sequence analysis. Some of servos such as SOr, SLi, SFr and SPo are performed in analog electronic devices and one has only to know their status. The others servos : ARc, SMc, AMc and the MBe, MMc dampings (called SDM) are done by computer via a digital conversion of error signal and an analog conversion of the signal correction. The sequencing will be done by a « smooth » user choice of automate from the graphical interface. In a later step some automatic modes could be implemented specially for SOr, SLi and ARc, SMc, AMc. The user's inputs cannot be avoid for the so-called « Pre-alignment » which requires a visual observation of the beam by video-camera.

The fig **4140.3** shows a tentative presentation of the active graphical page of the Servo-Control.

It is foreseen to implement Servos-Control as a super-server able to access directly the status Register and command Register needed to control the system and requesting informations useful to the user.

The definitive implementation will benefit from the Mode Cleaner test done at LAL-ORSAY.

41.6 Separation windows

41.6.1 Function and concept

A separation window is used to differentiate the ultra-high vacuum (10^{-9} mbar) in the central part of the interferometer from the normal vacuum (10^{-6} mbar) of the IB and input mode cleaner. It is inserted in the links localized close to the input and recycling towers, mounted on tube sections mechanically compatible with the links.

In order to get low insertion loss it will be made out of Silica, with the optical specifications matching the requirements of induced low noise in the laser beam .

41.6.1.1 Requirements of Input window

The Input Beam Window is inserted just at the output port of the injection tower and will be crossed by the full laser beam having the stability requirements described above. So the constraints on that IBW come from the fact that it should induce no degradation of the prestabilized laser frequency after the mode cleaner (meaning we can tolerate additional fluctuations up to 10^{-2} Hz/Hz in the low frequency range up to 100 Hz) see also ref[**15**].

The requirements of the output window has TBD taking into account the possible noise induced by the scattering effects (ref Ligo).

41.6.1.2 Selected solution

The solution takes into account the studies described in ref [**17**] of all the possible losses induced by mechanical as well as optical effects. The typical criteria is insertion loss $\leq 10^{-3}$.

The Figure **4130.12** shows a drawing of the tube portion including the window : it is without AR coating near the Brewster angle (53±1°), the residual reflected beam from that window position is of the order of 0.0005-0.001 and can be used either to monitor the beam at the input or to send an extra beam for the bench alignment purposes.

The window will be clamped on both sides by viton o-rings, thus can stand vacuum on both sides of it in case of opening of the tower benches or the recycling towers.

The window will be screwed on an internal tube cut at Brewster angle, which is itself clamped on a small portion of link which length is 560 mm from the SS 3300. Besides that due to the presence of viton o-rings we would like this window-link to be as far as possible from the baking system, so as close as possible to the towers (TBC).

Window size : ϕ 200mm x 20mm

The input beam for the test interferometer will be around 7 mm in diameter and 15 mm for the Virgo interferometer. The window can fit more than 8 times the final beam size in the vertical direction and more 12 times the same beam size in the horizontal direction.

41.7 Laser and Input Bench assembly

41.7.1 Laser Bench assembly

The laser bench assembly will be mostly done in the lab before moving on site. For the transport, the most fragile optical components will be removed, as well as the laser head which will be dismounted in order to avoid damaging of the laser crystal. All the mechanical mounting will be clamped on the table and the laser beam axis will be referenced by a certain number of iris. The optical parts will be transported in a clean air tight box.

All the detectors localized on the laser bench should be removed in order to avoid cabling fractures.

On site the re-positioning of all the removed optics will be done with an auxilliary low power Yag laser, as well as the detectors.

41.7.2 Input Bench assembly

The IB will be prealigned mechanically in the labo before moving on site. An air tight box has been designed specifically for the transportation of the IB, which will sit on 4 legs with the RC screwed internally and externally, in order to avoid strong misalignments in case of mechanical schocks. The optics of the MC will be transported separately to the other mirrors; all of them in a clean box .

On site the repositioning of the optics on the IB will be done also with an auxilliary laser in a clean room (class 1000) or under a laminar flow to avoid contamination of the MC optics.

The introduction of the IB and [illegible] with these components protected in a housing which will be removed after the complete installation of the IB. Figure 4130.14 is a view of the IB inside the injection tower.

41.7.3 Sub-system assembly

As soon as the laser beam will be available from the laser bench, it will be sent into the input tower to match the axes defined by the interferometer and MC axes. The axes are defined on the IB relaltive to some local reference of the tower itself which has TBD with the SS Geometry facility. The beams reflected by the IB will help the positioning of the outside photodetectors and cameras.

List of References

[1] A.Rudiger et al. Optica Acta (1981)

[2] P.Hello, E.Calloni, meeting Virgo 1995

[3] H. Heitmann, "Détails sur les bobines du Mode Cleaner", internal note Orsay, (29.06.1994) (about the MC prototype coils)

[4] C.N.Man, Ph.Heusse: Control-Command of the SS Laser and Input Bench (v.5), 20/2/97

[5] Orsay internal note, F. Cleva:"Evaluation of ultimate performances of the slave cavity servo", 20/11/94

[6] Orsay internal note, F. Cleva:"Isolateurs de Faraday VIRGO 97&99 - Solutions", 25/07/95

[7] VIRGO NTS95-011, "Acousto-optic effects in air", F. Cleva, J.P. Coulon

[8] Orsay internal note: C.N.Man : "Mode cleaner specifications (1) and (2)", 8-28/3/95.

[9] H. Heitmann, "Measurement of position and orientation of the input mode cleaner masses", VIRGO note NTS96038 (18.6.1996)

[10] R. Chiche, "Note à propos de la technique d'implantation du correcteur numérique équivalent à partir de la définition d'un correcteur analogique", internal note Orsay (07/1995)

[11] H. Heitmann, "Longitudinal control of the VIRGO mode cleaner", internal note Orsay (10.07.1996)

[12] H. Heitmann, "Some points on mode cleaner lock & autoalignment", internal note Orsay (4.10.1996)

[13] M.Taubman, Orsay internal note, 3/97

[14] C.N.Man, VIR-MEM-LAS-4100-105

[15] A.Brillet, "Action of a window on a laser beam" 1994

[16] M.Barsuglia, Locking meeting minutes, Pisa 1995.

[17] F.Cleva, P.Mugnier, 30/10/96

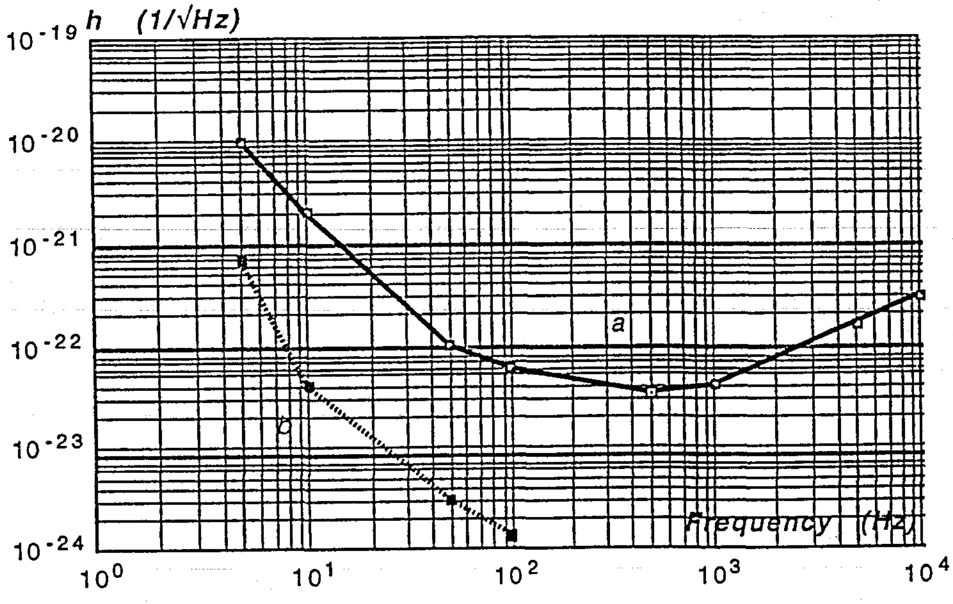

Figure 4100.1 : Initial (curve a) and ultimate (curve b) sensitivity curves of Virgo vs frequency

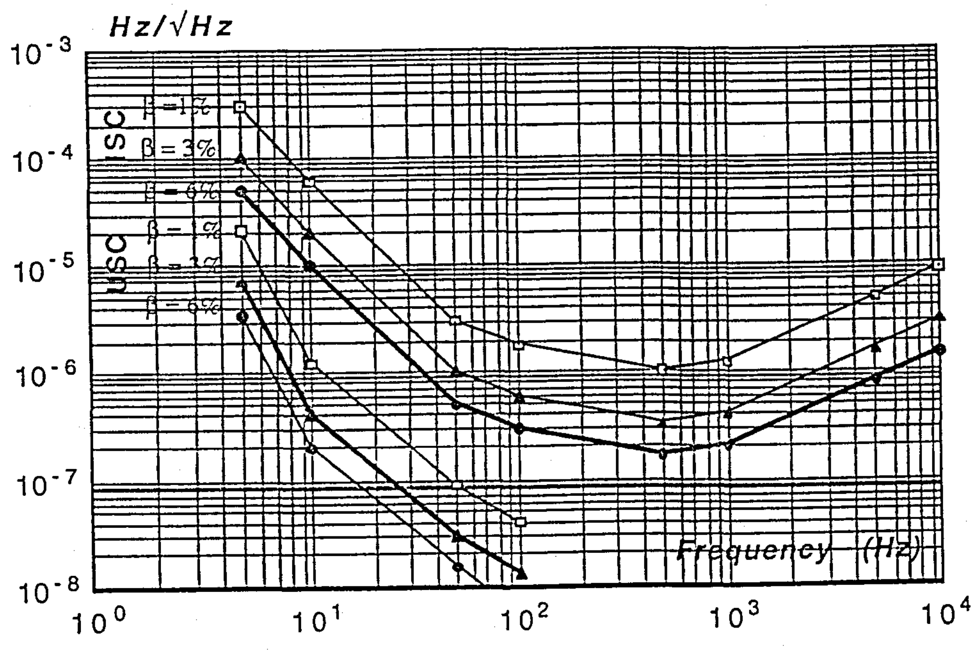

Figure 4100.2 : Requirements for laser frequency stability at the input of the interferometer for different asymmetries (1%, 3%, 6%) and for the two cases ISC (upper sets) and USC (lower sets).

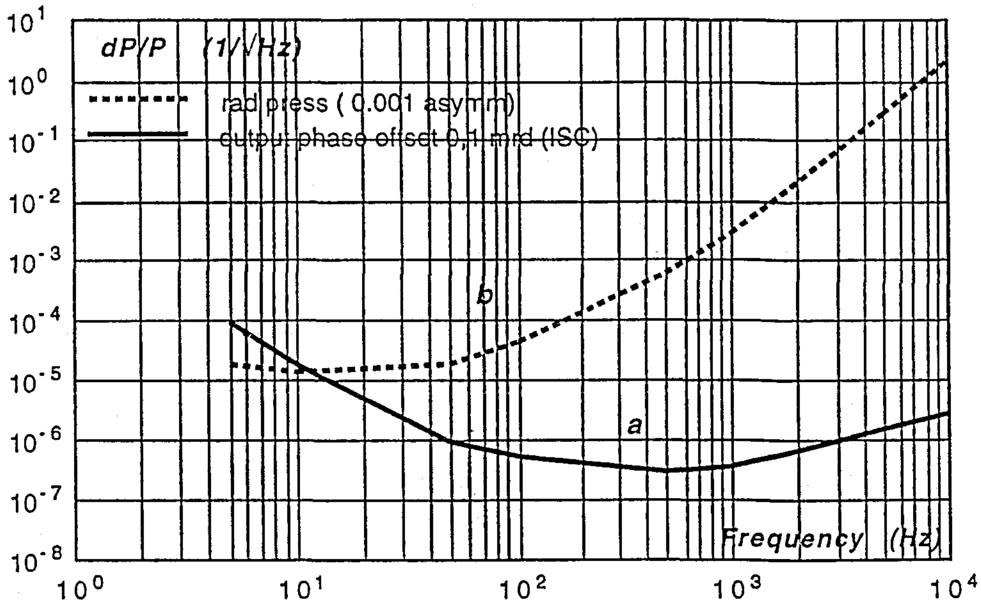

Figure 4100.3 : Requirement on relative amplitude stability, curve *a*: due to an output phase offset of 3 mrd, curve *b*: due to radiation pressure on test-mass with an asymmetry of 10^{-3}.

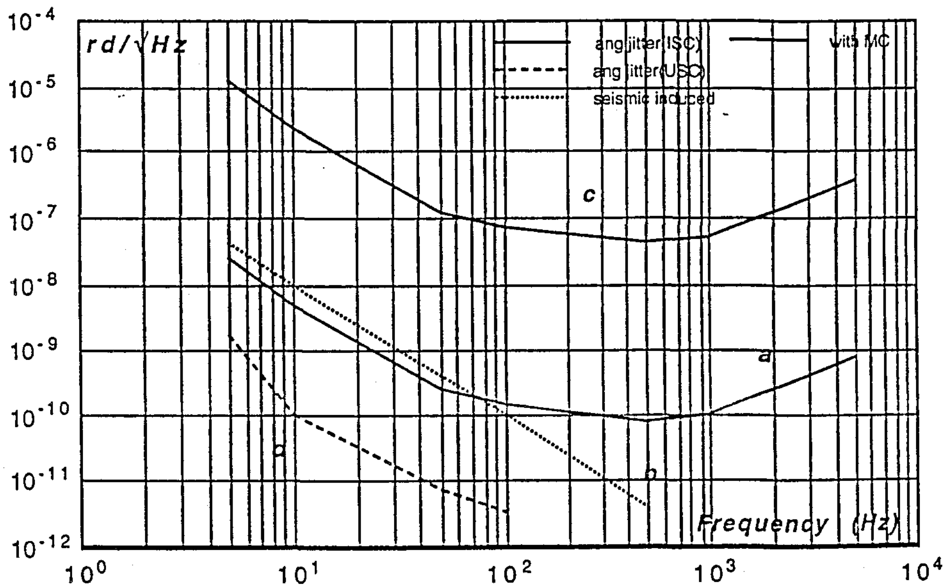

Figure 4100.4 : Curve *a*: Residual jitter of laser beam required at the exit of the Input Bench coupled with an Interferometer misalignment of 10^{-9} rd (3μm over 3 km). Curve *b*: Effect of the seismic noise on the Input Bench (without any seismic isolation) in terms of tilt . Curve *c* : Residual jitters of laser beam required at the input of the Mode cleaner with a filtering factor of 3.10^{-3} .

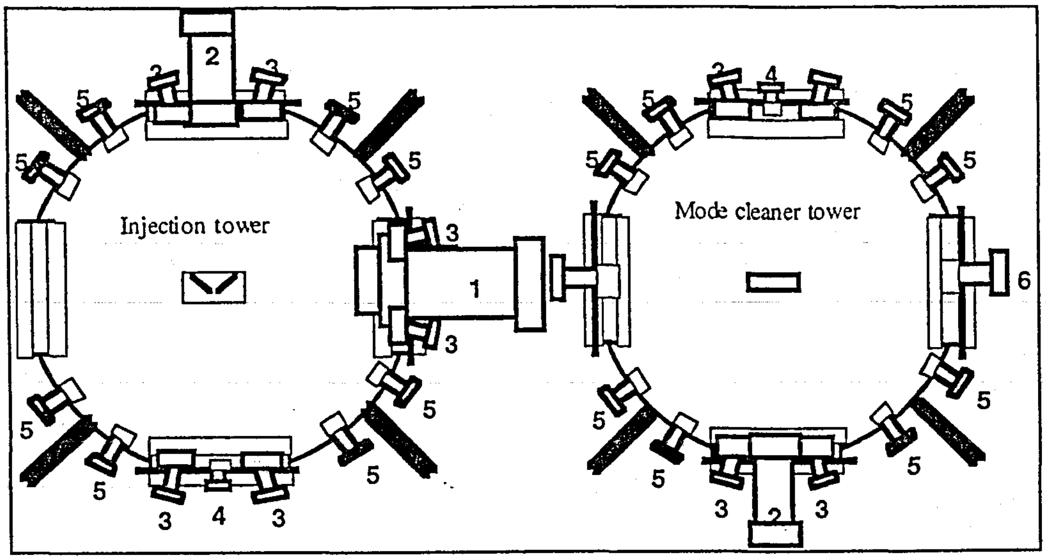

Figure 4100. 5 : Position of windows required on the injection and mode cleaner towers:
1: link between injection and recycling towers; **2**: MC tube; **3**: Windows Ø 150 for cameras etc., ±15° from axis, 5° additional tilt for avoiding perpendicularity (AR coated; in the flange); **4**: Window Ø 100 for auxiliary HeNe beam (AR coated) (MC axis; in the flange); **5**: Windows in the lower tower itself (above/below paper plane)(diam.). Not all of these openings will contain windows; **6**: Lateral windows Ø 200.

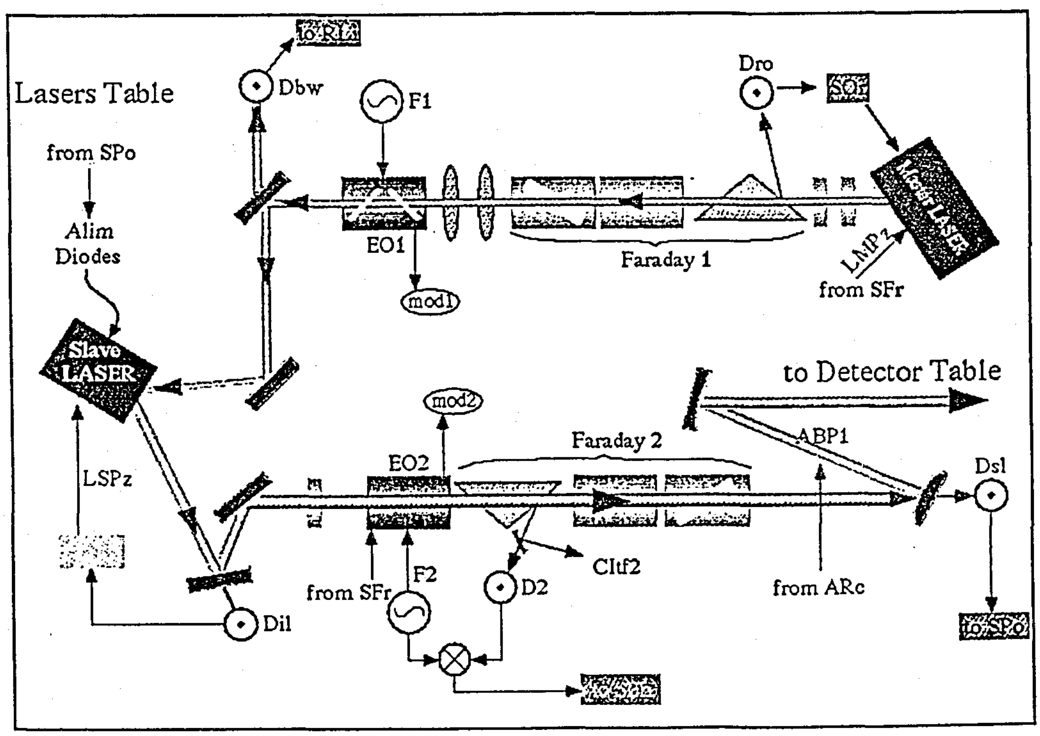

Figure 4100.6:Schematic of the laser table containing the lasers, the modulators, and the telescope to match the beam to the input bench. This table is part of the Laser Bench .

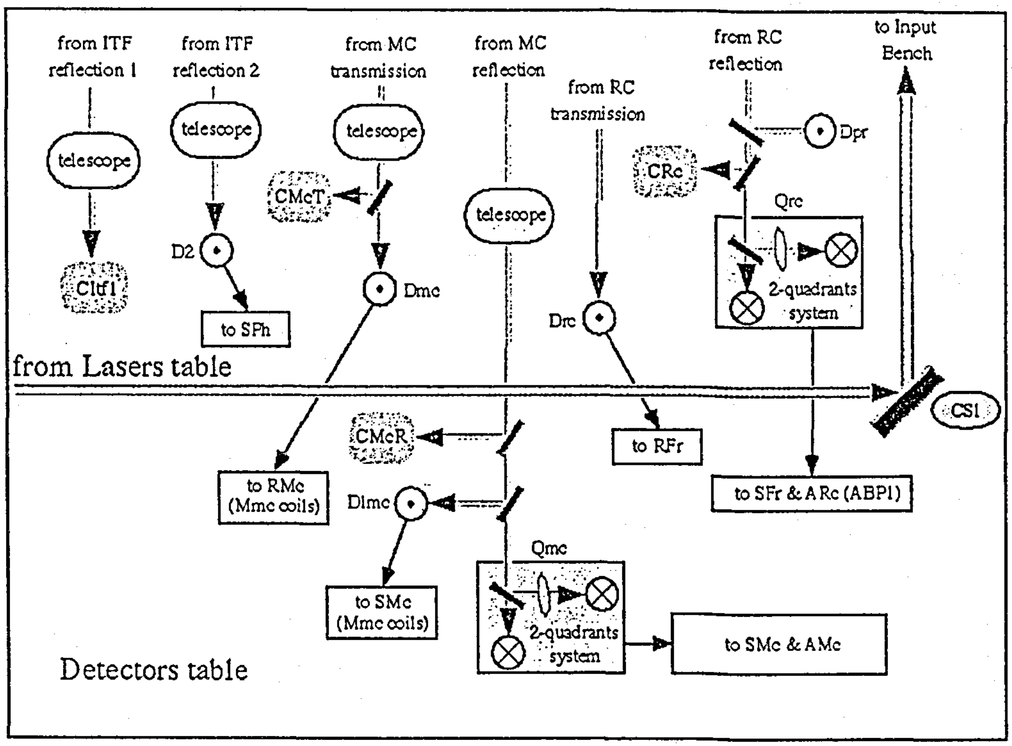

Figure 4100.7 : Schematic of the detectors table containing the detectors and cameras for beams coming back from the input bench. This table is part of the Laser Bench.

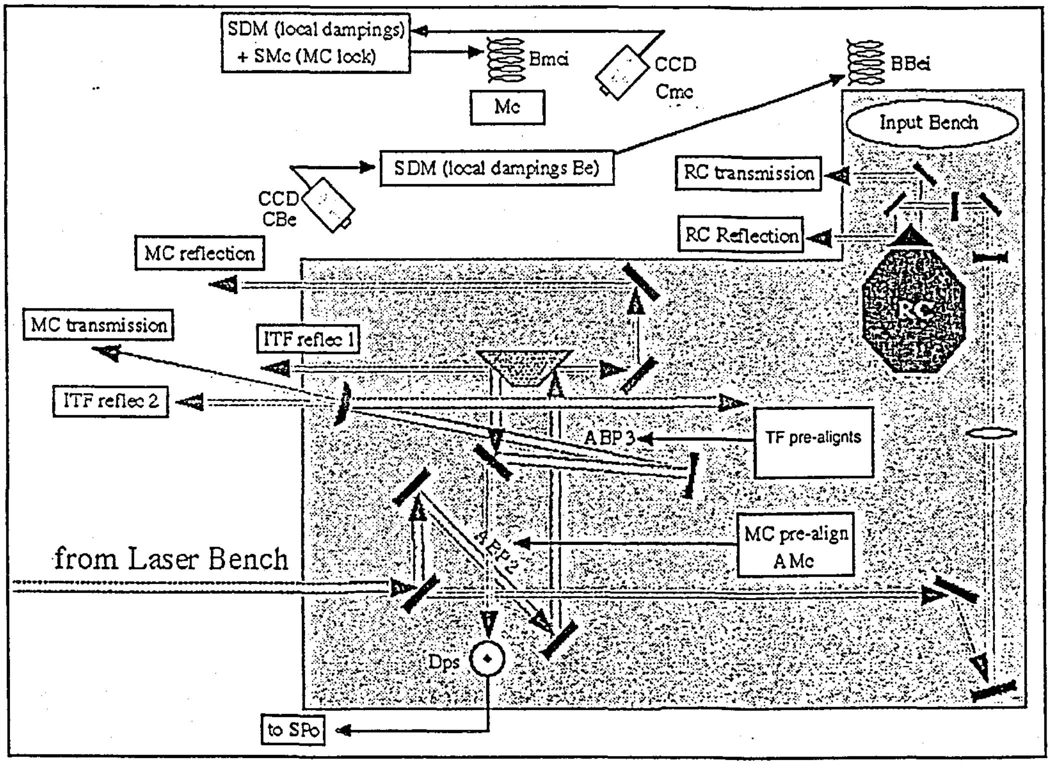

Figure 4100.8 : Input Bench schematic: the dashed zone represents what is physically inside the injection tower.

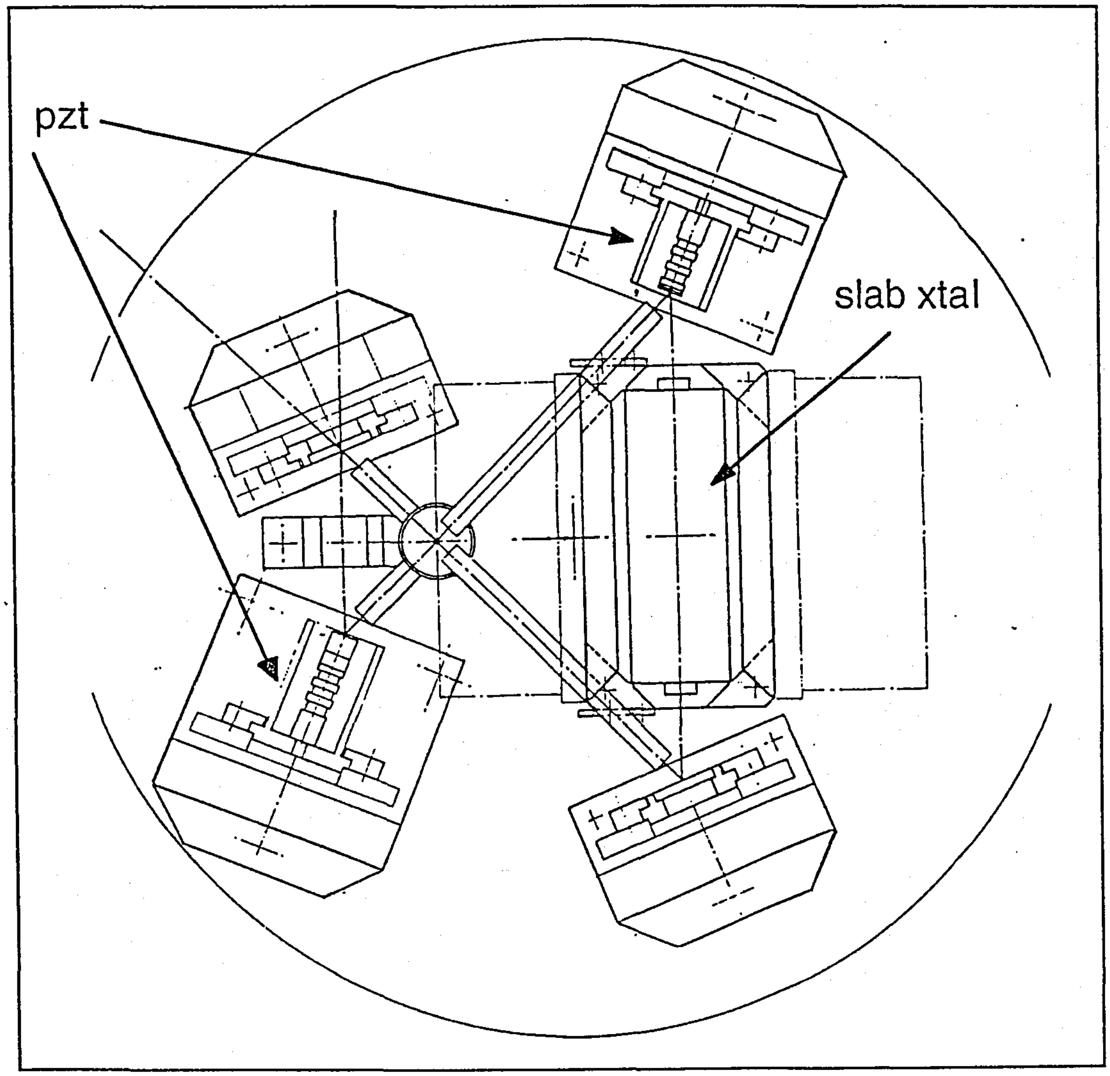

Figure 4120.1 : Slave 10W laser in a ring shape cavity with 4 mirrors, 2 of them mounted on pzt transducers.

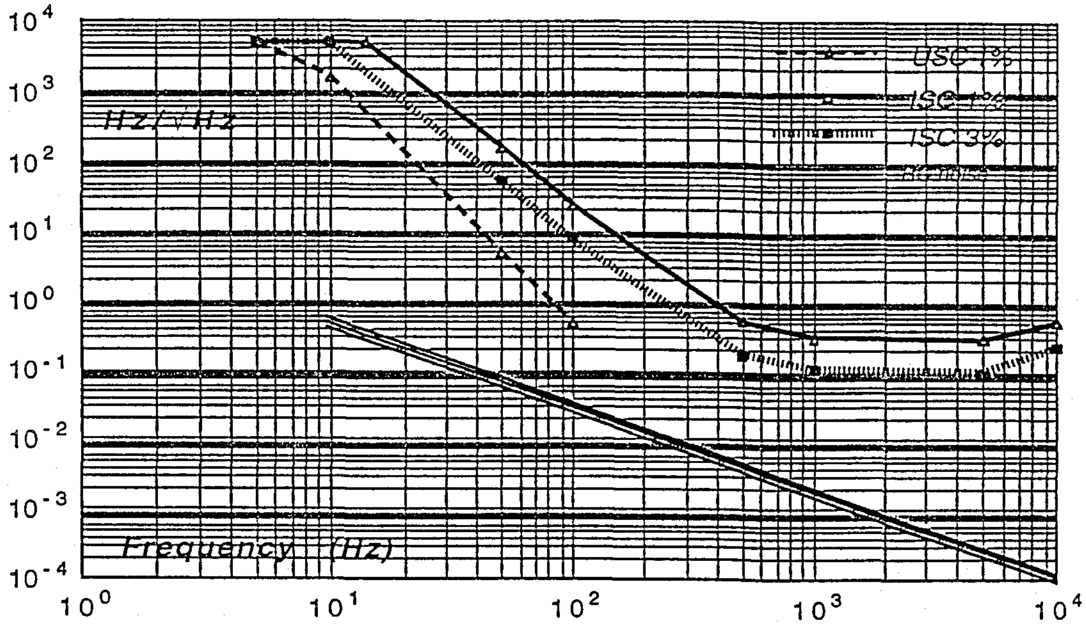

Figure 4120.2: Laser Frequency prestabilization (Hz/√Hz) requirements for initial (ISC) and ultimate (USC) sensitivities with the following assumptions: MC cavity is a pole filter at 500 Hz, recycling cavity is a pole filter at 5 Hz, the asymmetry is X%. The line at the bottom represents the noise measured on the RC used for Virgo.

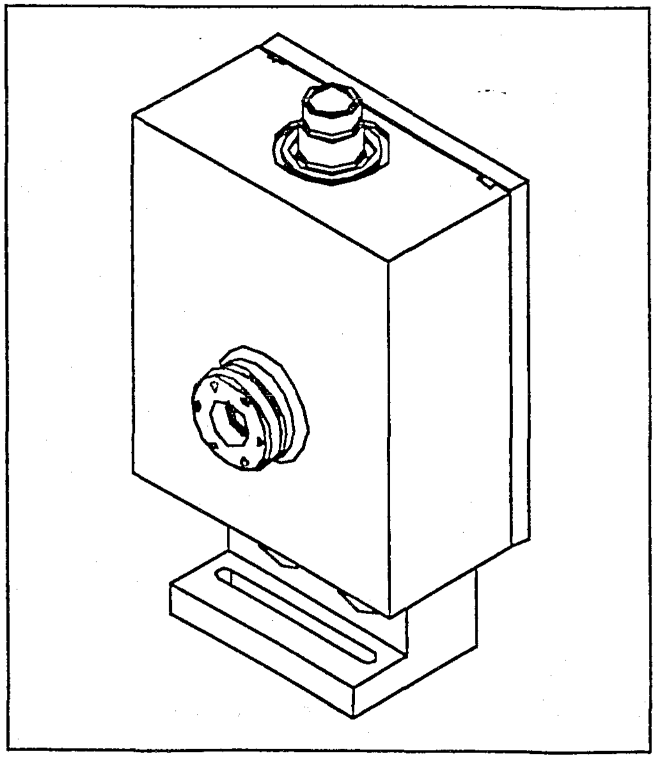

Figure 4120.4 : vacuum compatible box containing the power stabilization photodiode Dps clamped on the Input Bench.

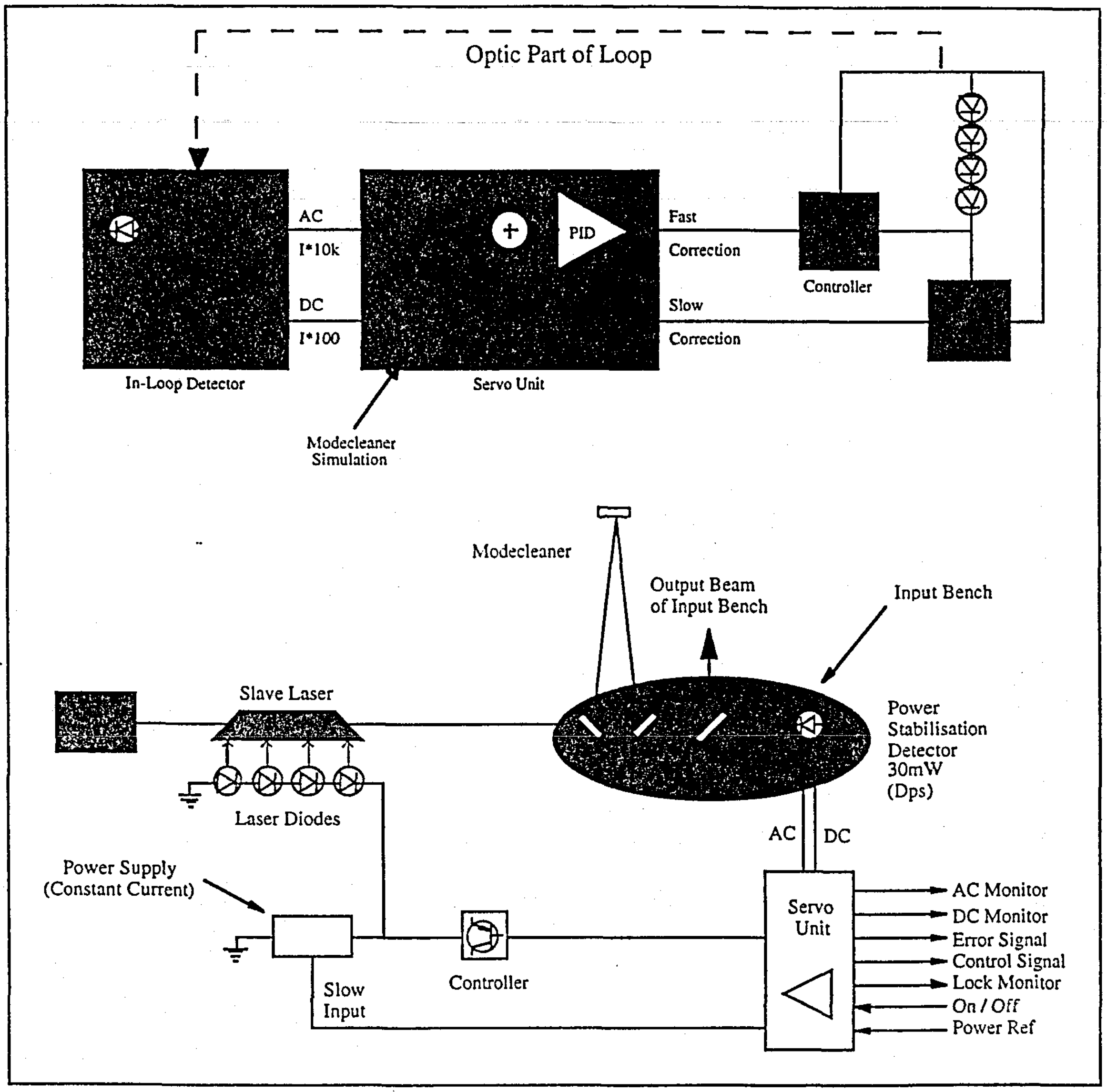

Figure 4120.3: Power stabilization Servo-loop. Upper part is the block diagram. Lower part is the physical implementation of the different parts of the loop.

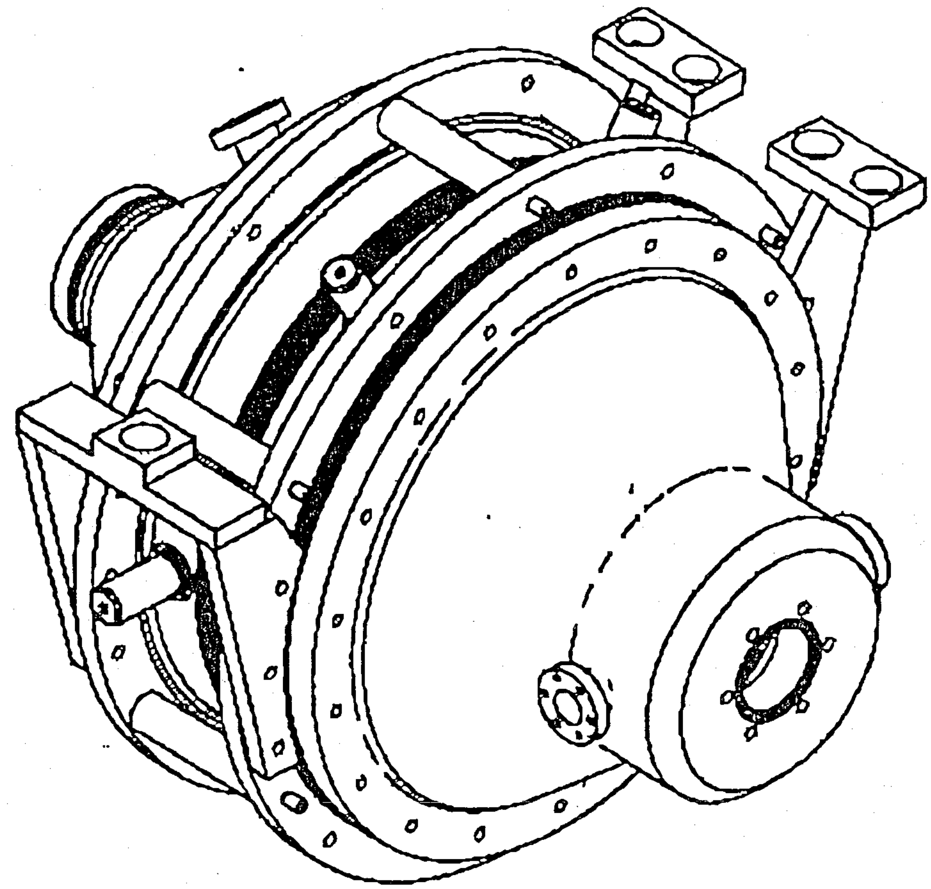

Figure 4130.1 : Refrence cavity vacuum housing to be clamped at the bottom of the Input Bench.

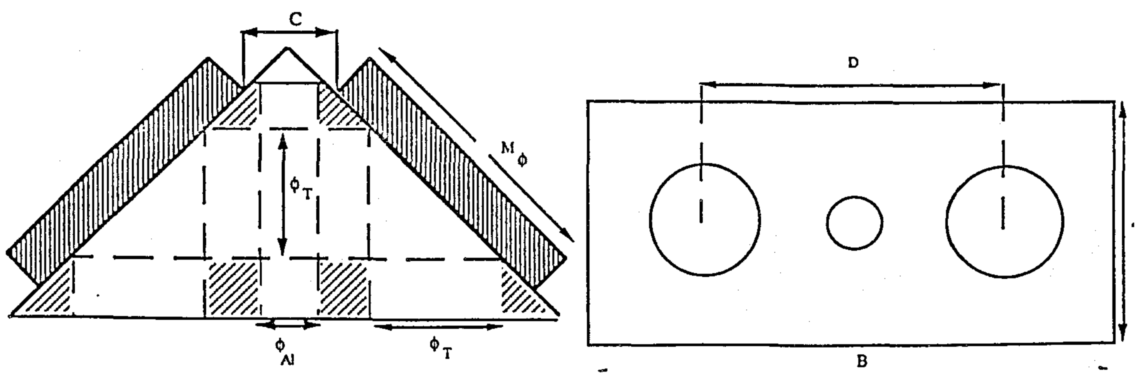

Figure 4130.2 : Corner-cube served to hold the two input plane mirrors of the MC (dashed rectangles): the overall dimensions is 180 mm over 108 mm in thick, 3 holes are drilled inside for the beams , the central hole being used for the MC prealignment with a visible light; the separation between the beam axis is around 90 mm.

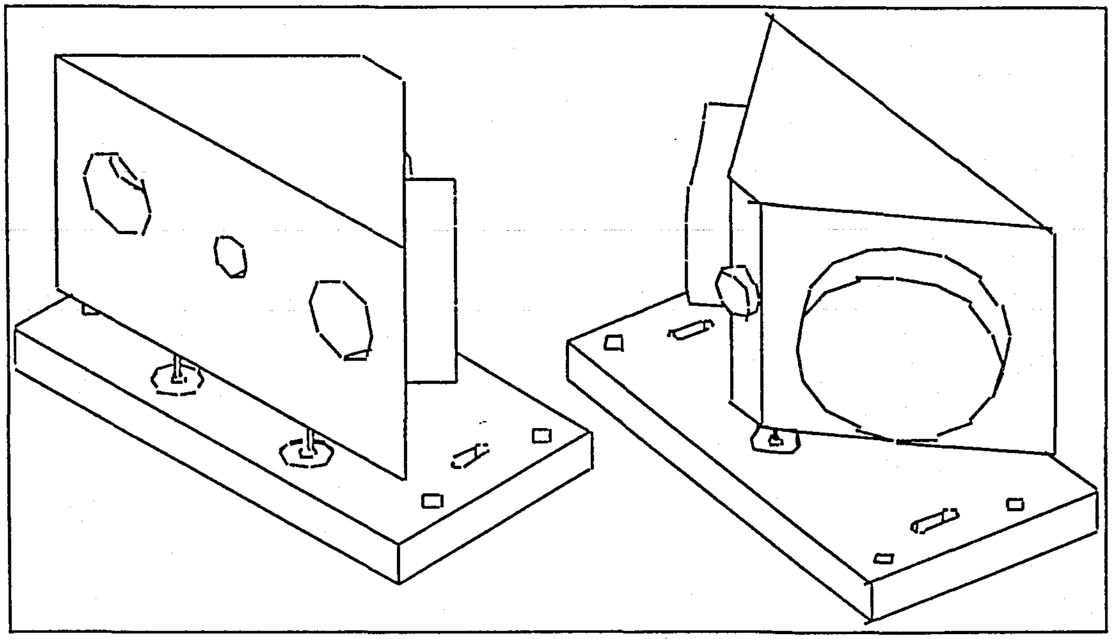

Figure 4130.3 : Corner-cube made of Silica sitting on 3 rods and a Silica basement.

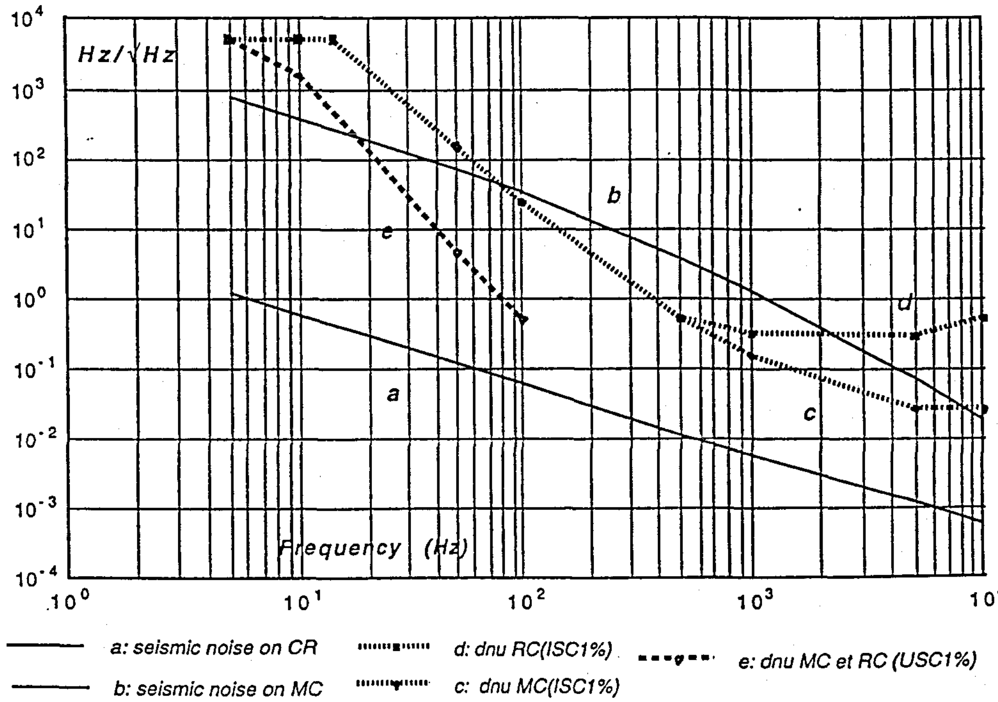

Figure 4130.4 : Seismic noise effect on the non isolated Reference Cavity (curve a) , on the Mode Cleaner (curve b), translated in terms of laser frequency noise. Curve a has to be compared to the requirement for the prestabilization (curve d for ISC and e for USC), and curve b to the laser noise at the input of the recycling cavity (curves c and e).

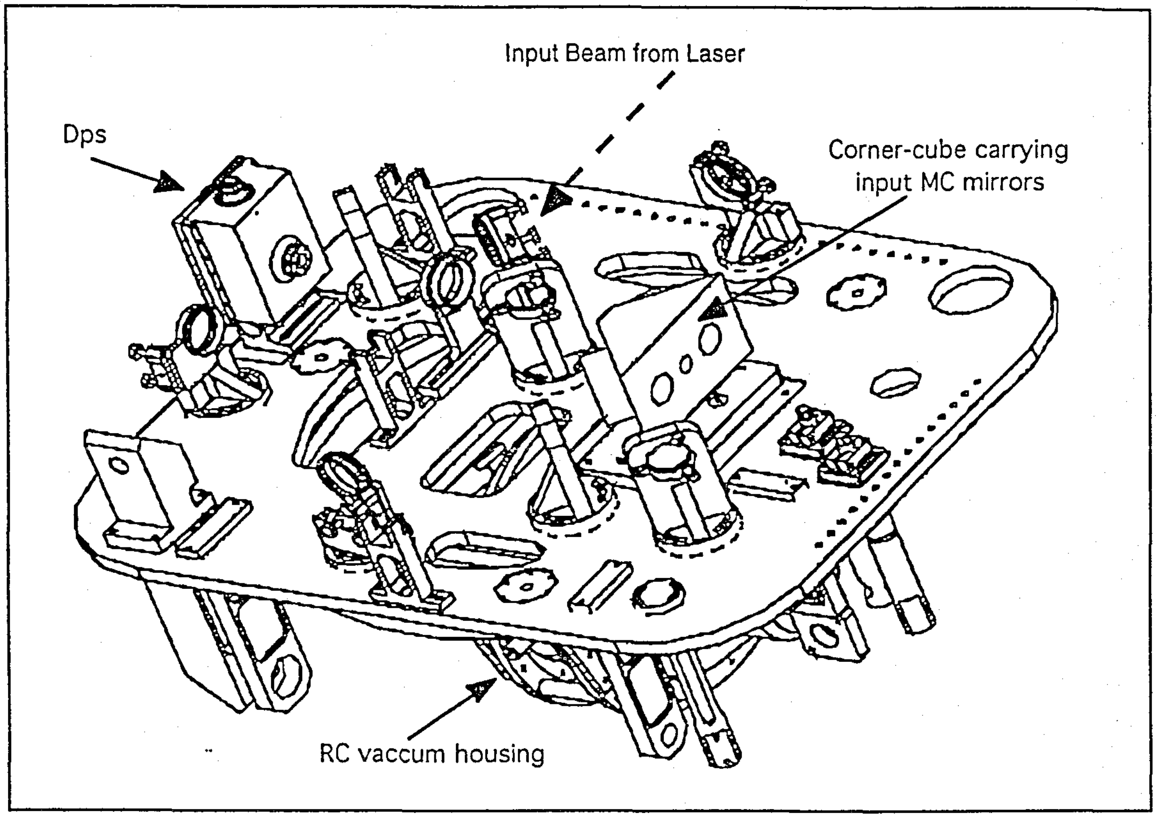

Figure 4130.5 : Input Bench mechanics

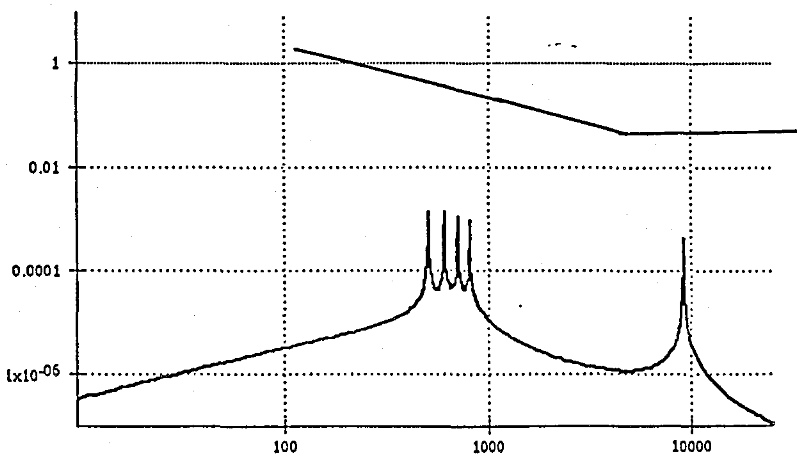

Figure 4130.6 : Equivalent frequency fluctuation (Hz/√Hz) induced by the thermal noise of the input MC mirrors of mass M=1 kg, Q=100, (5kHz) and by the IB (4 resonances between 100 and 400 Hz). The upper curve is the Virgo requirement on the laser noise after the MC.

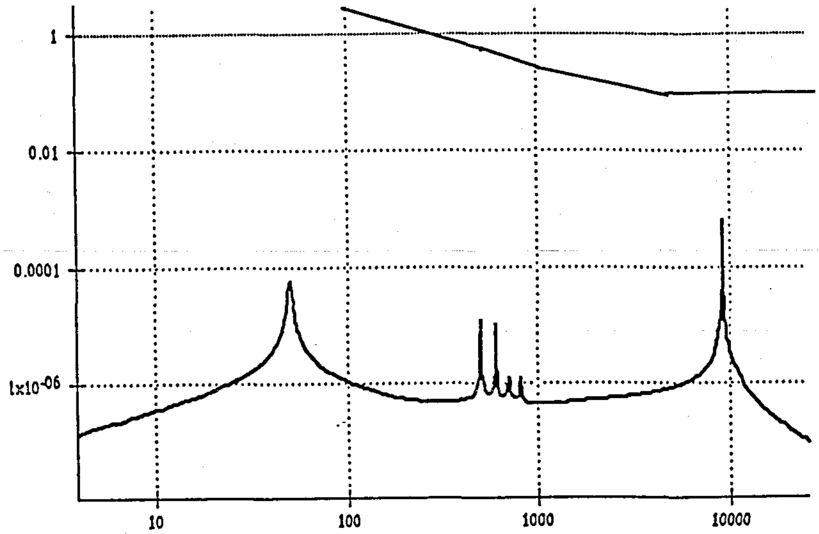

Figure 4130.7 : Equivalent frequency fluctuation (Hz/√Hz) induced by the thermal noise of the input MC mirrors of mass M=1 kg, Q=100, (9 kHz) and by the IB (4 resonances between 500 and 800 Hz). The corner cube of the MC is 1 kg with a Q of 1000 and isolated from IB by a simple stage of 50 Hz with Q of 1000. The upper curve is the Virgo requirement on the laser noise after the MC.

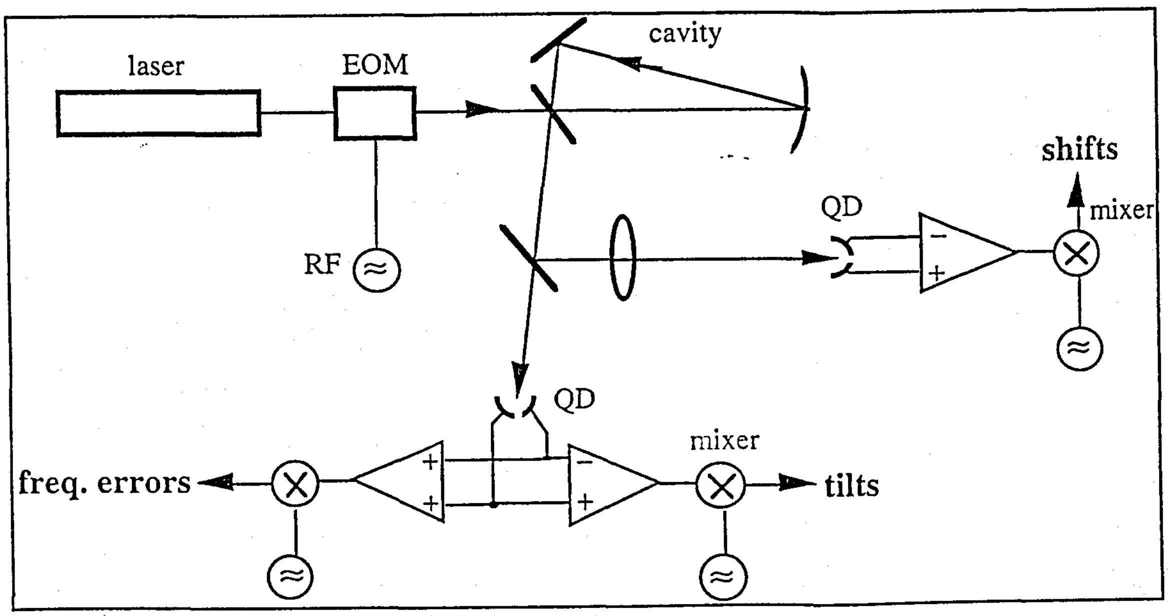

Figure 4130.8 : Typical setup for measuring the alignment (and frequency) errors of a laser with respect to a cavity.
EOM=electro-optical modulator; QD=quadrant photodiode; RF=radio frequency generator.

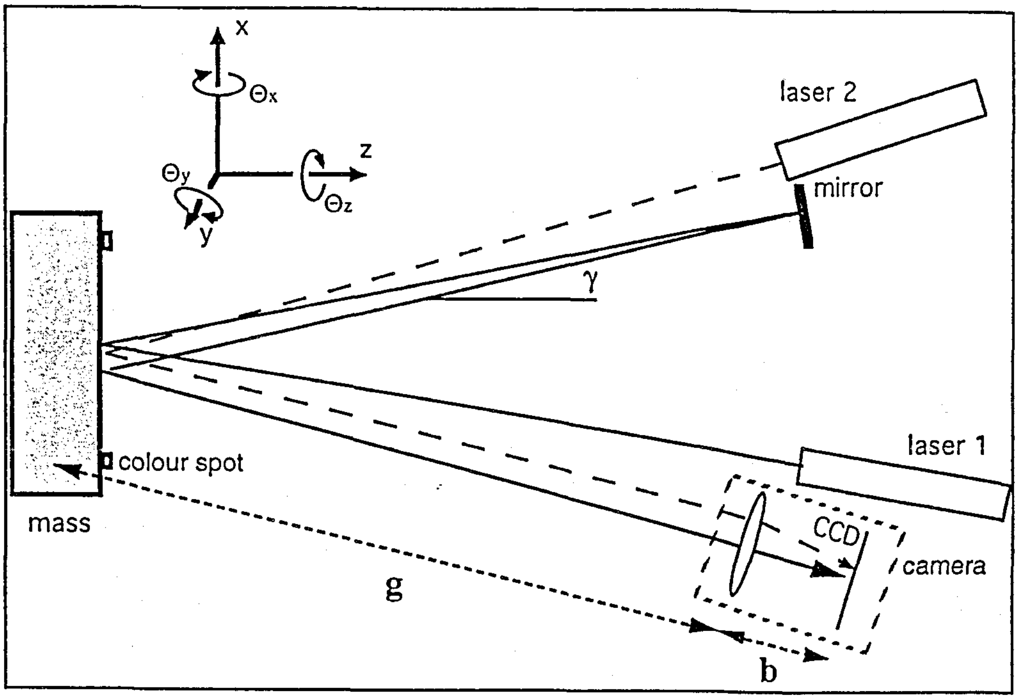

Figure 4130.9: Optical scheme for determining the mass position with a CCD camera. The spot generated by laser 1 serves for determining θ_x, θ_y; the image of the two points on the CCD gives x,y and θ_z; , laser 2 gives informations on z..

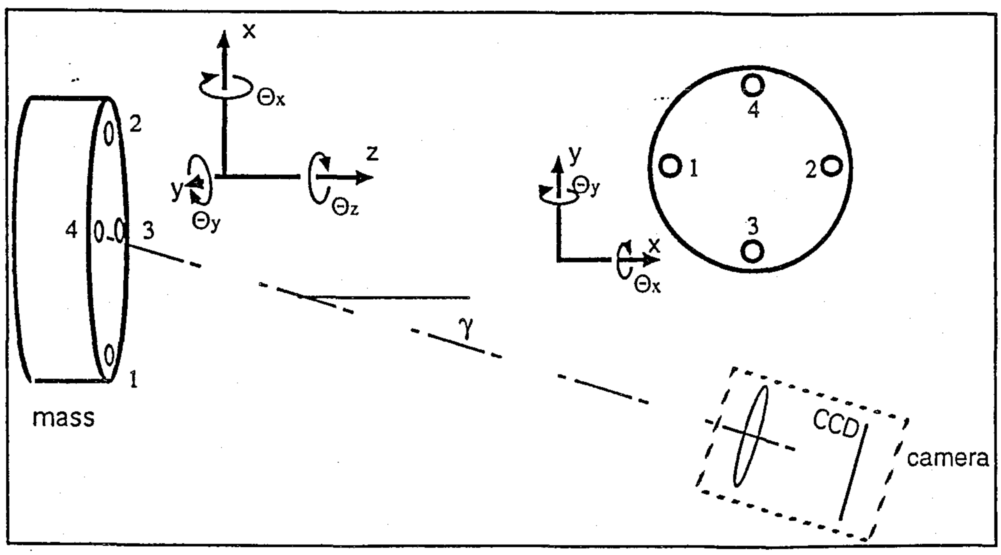

Figure 4130.10: Camera scheme for determining the mass position without lasers, seen from above.

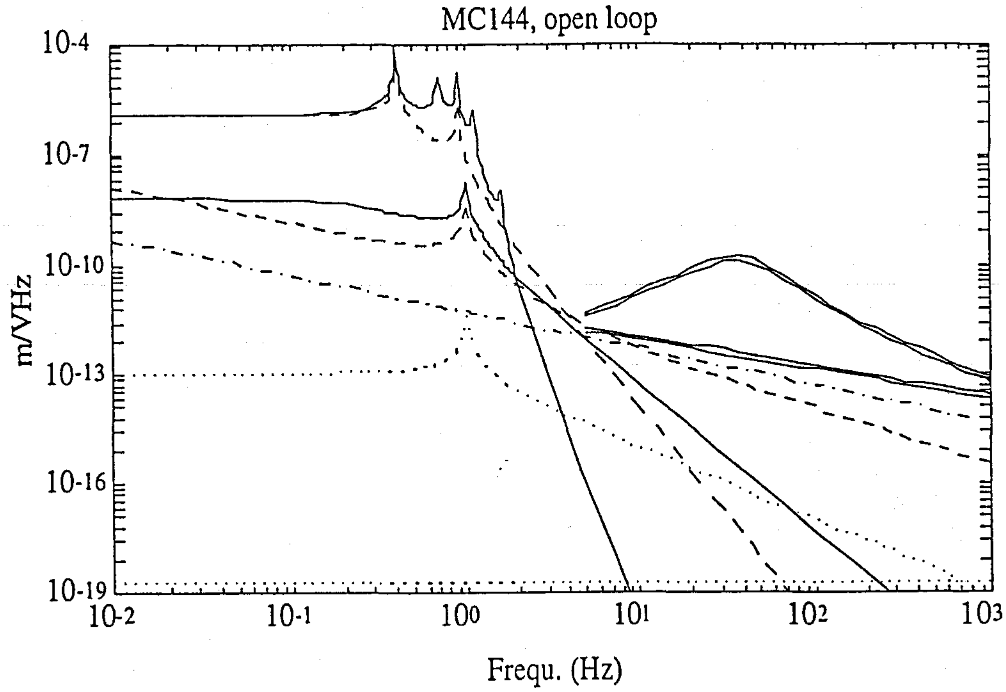

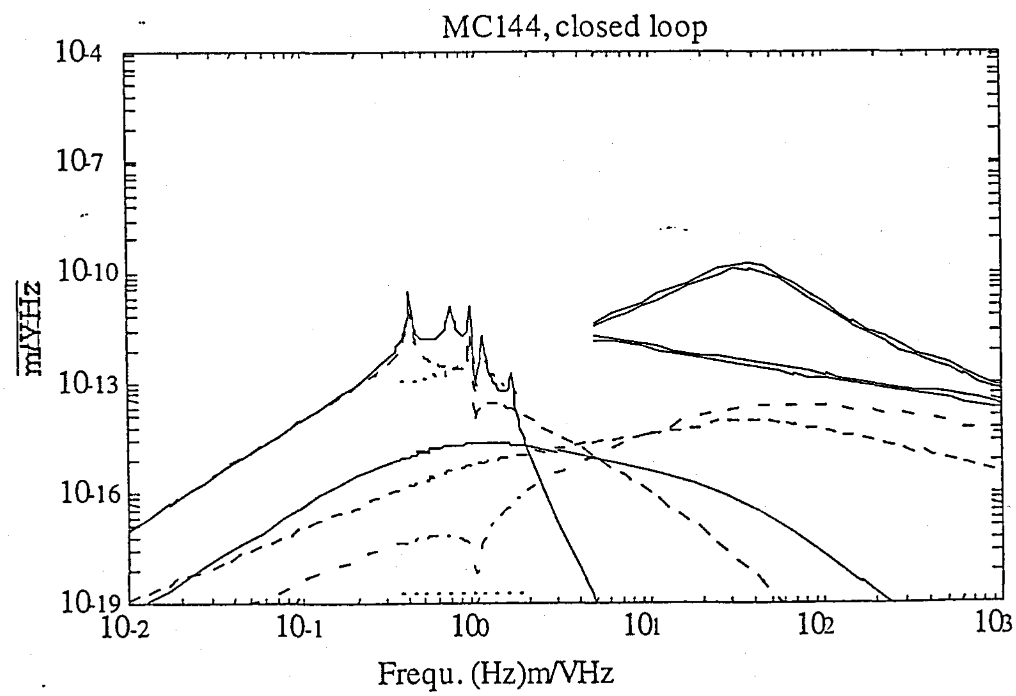

Figure 4130.11: Noise sources acting on the mode cleaner in terms of equivalent relative mass displacement spectral density ($m/\sqrt{Hz}$). Dotted: shot noise (lower) and DAC digitization noise (upper). Dash-dotted: laser frequency noise. Solid: seismic noise transmitted by the suspension (upper), seismic noise transmitted by locking coils fixed to the ground acting on the mass (lower). Dashed: current noise of the coil amplifier (lower) and suspension seismic noise without 3-stages superattenuator (upper). Double lines: mass displacement noise limits coming from the required frequency (upper) and amplitude stability (lower) of the MC output beam.

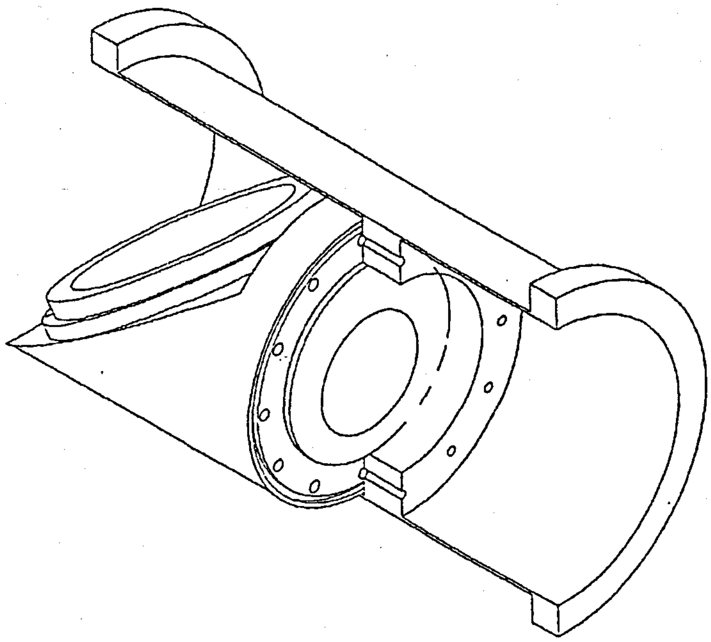

Figure 4130.12 : View of the portion of tube containing the separation window between the input tower and the links going to the power recycling tower.

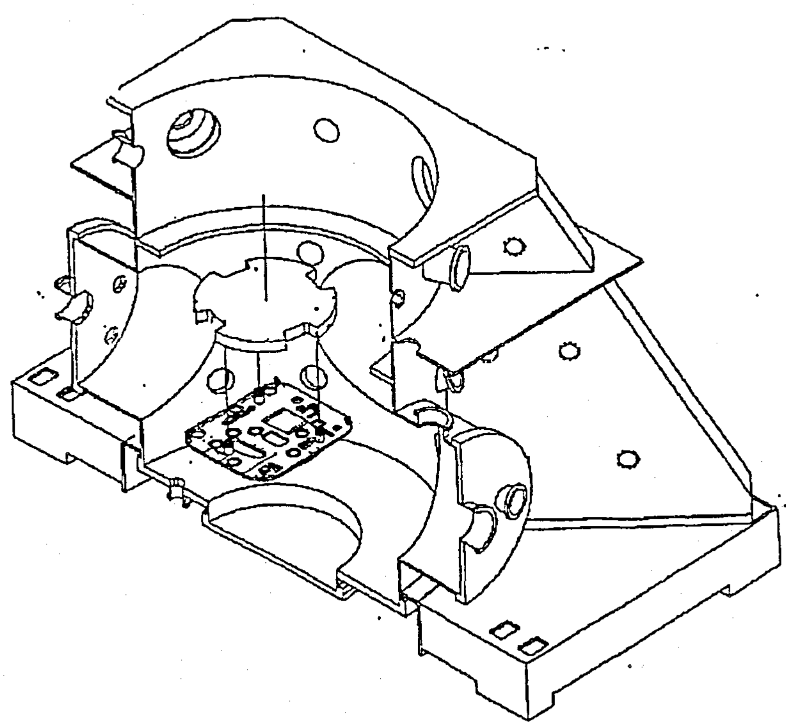

Figure 4130.14 : View of the input bench suspended to its marionetta inside the input tower.

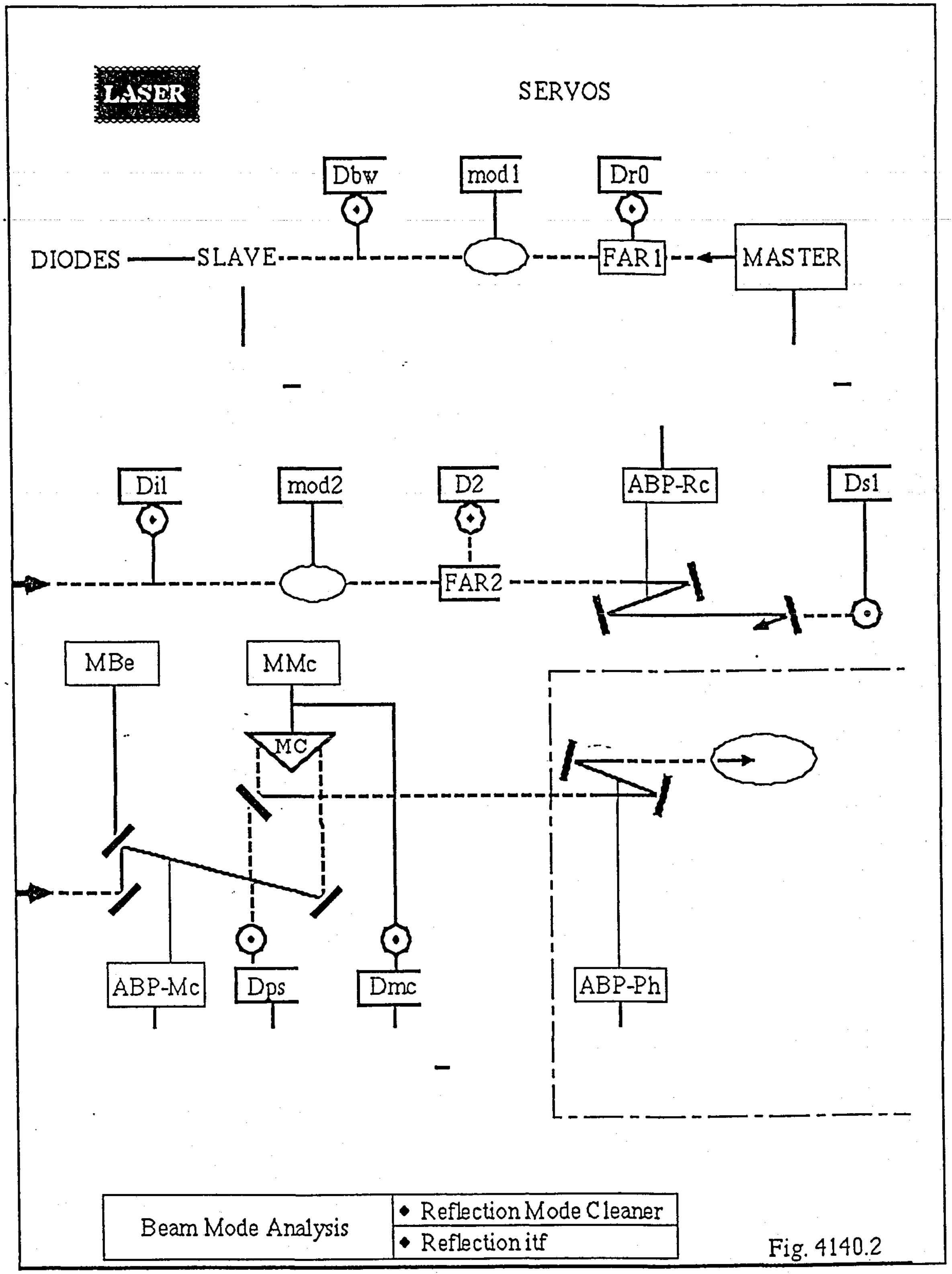

Fig. 4140.2

Fig. 4140.2

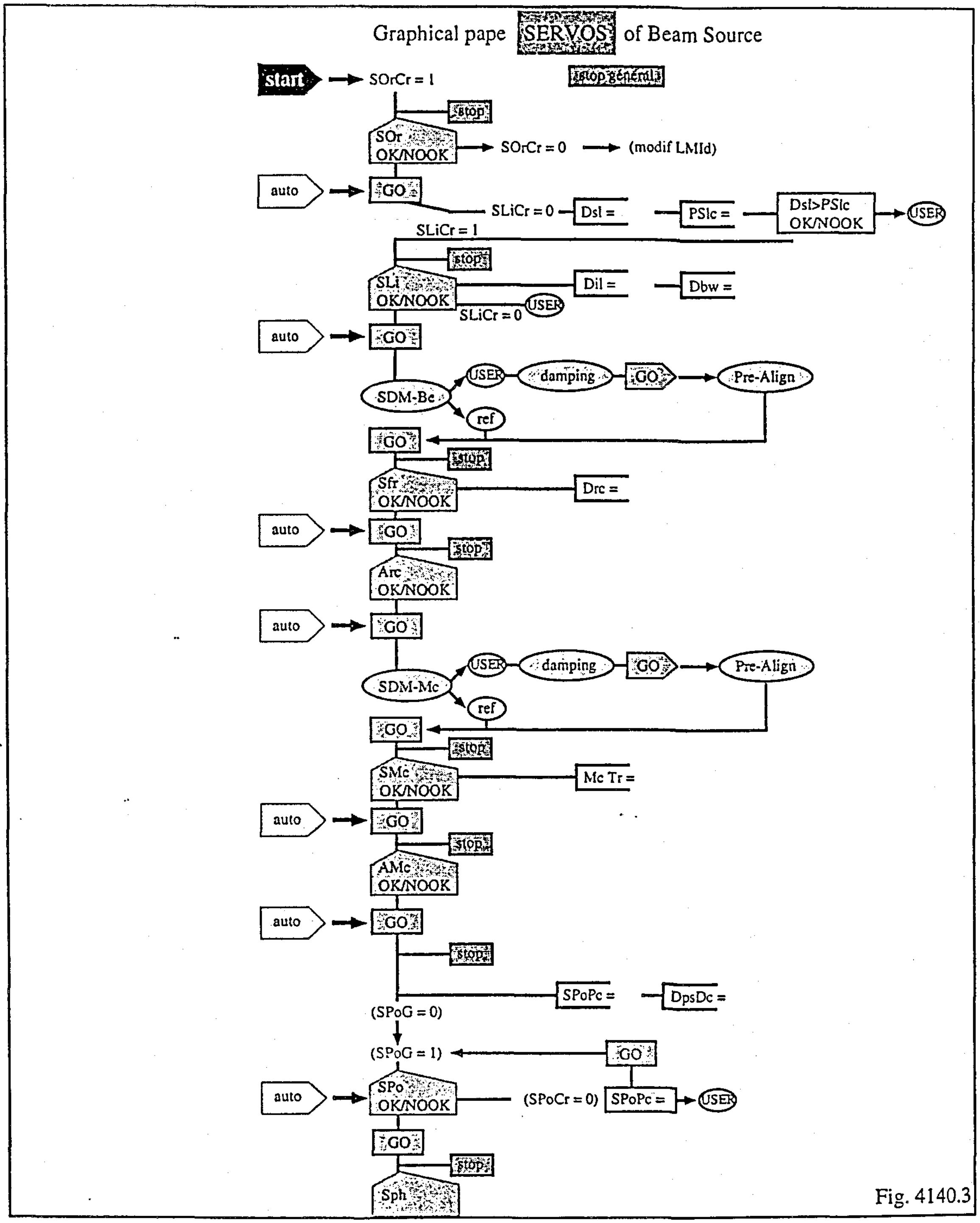
Graphical pape SERVOS of Beam Source
start
SOrCr = 1
stop général
stop
SOr OK/NOOK
SOrCr = 0
(modif LMId)
auto
GO
SLiCr = 0
Dsl =
PSlc =
Dsl>PSlc OK/NOOK
USER
SLiCr = 1
SLi OK/NOOK
Dil =
Dbw =
SLiCr = 0
SDM-Be
damping
Pre-Align
ref
Sfr OK/NOOK
Drc =
Arc OK/NOOK
SDM-Mc
SMc OK/NOOK
Mc Tr =
AMc OK/NOOK
SPoPc =
DpsDc =
(SPoG = 0)
(SPoG = 1)
SPo OK/NOOK
(SPoCr = 0)
Sph
Fig. 4140.3

Fig. 4140.3

42. Detection bench

Table of Contents

The detection bench sub-system is divided in the following three items [1]:

- 4210 Output Optics
- 4220 Photodiodes
- 4230 Signal read-out

42.1 Detection bench function and concept

The detection bench main functions are the following:

- 'Dark fringe' beam extraction: it consist in providing all the optics required to extract and filter the 'dark fringe' beam at the interferometer anti-symmetric port;
- 'Dark fringe' signal detection: it concerns the detection of the gravitational wave signal which is carried by the 'dark fringe beam' at the interferometer main output;
- Locking signals detection: it consists in the detection of all the beams coming out of the interferometer and used to control the longitudinal position of the suspended mirrors.

The 'dark fringe' beam is the beam obtained from the interference between the two beams reflected from the two arms of the interferometer and traveling from the beam-splitter towards the so called detection tower. This is the beam carrying the interferometer main output signal i.e. the one directly related to the gravitational wave signal.

Figure 4200.1 shows the 'dark fringe' beam as well as the beam coming from the north arm and reflected from the beam splitter second face toward the detection tower. Due to their relatively big size (19.8 mm) and to the beam-splitter geometry [2] the two beams are partially superposed and they form an angle of 3.6 mrad.

Some optics (output optics) is required in order to spatially separate the two beams. Once separated the two beams have to be detected by some appropriate photodetectors. To this purpose the output optics should reduce the beams size to a dimension compatible with the photodetectors size.

The detection of the 'dark fringe' beam requires some signal-to-noise ratio considerations.

As explained in the 4000 chapter the interferometer phase difference is measured by detecting the power amplitude at the frequency of modulation. The best phase sensitivity one can reach with a Michelson interferometer is given by the following expression:

$$\delta\varphi = \sqrt{\frac{2h\nu}{\eta P}}\ \mathrm{Hz}^{-1/2}$$

where P is the amount of light impinging on the beam splitter (1 kW for VIRGO), $h\nu$ is the photon energy (0.85 eV for λ=1.064 μm) and η the photodiode quantum efficiency. As a consequence the photodiodes quantum efficiency should be as high as possible. Nevertheless since the VIRGO sensitivity is shot-noise limited only above a few hundreds hertz its impact on the overall sensitivity is limited to this part of the spectrum.

The previous expression assumes a perfect fringe contrast at the interferometer output port. In practice the exact shot noise level and so the phase sensitivity will depend on the average amount of light impinging on the photodetector i.e. on the fringe contrast C.

Figure 4200.2 shows the phase sensitivity normalized to the best sensitivity as a function of the modulation depth m. The various curves correspond to different values of the contrast defect (1-C). The graphs shows that it always exists an optimum modulation depth which maximizes the sensitivity but, as the contrast defect increased, the S/N at the maximum get smaller. In addition to this, as the contrast defect increases, the required modulation depth increased.

The exact value of the interferometer contrast is unknown at present since it will depend on the amount of wave front deformation introduced by the various optical components. Optical specifications for the mirrors have been calculated in order to obtain a contrast of the order of 10^{-2} [3]. This level of contrast will reduce the phase sensitivity by about 50%.

It is possible to improve the contrast by spatially filtering the output beam before the photodiodes. To this purpose the optics at the interferometer output should include some spatial filtering of the 'dark fringe' beam.

The detection of the dark fringe beam and of the beam reflected from the second face of the beam splitter do not provides enough signals to lock the whole interferometer. The locking of the interferometer requires the detection of the following beams (see figure 4200.3):

- the 'dark fringe' beam (beam 1 in figure 4200.3)
- the beam reflected from the north arm and deflected by the beam-splitter second face towards the interferometer output port (beam 5 in figure 4200.3)
- the beam reflected from the recycling mirror and extracted at the input bench (beam 2 in figure 4200.3)
- the beam transmitted from the end mirror of the North cavity and extracted at the North end bench (beam 7 in figure 4200.3)
- the beam transmitted from the end mirror of the West cavity and extracted at the West end bench (beam 8 in figure 4200.3).

For all these beams two (for redundancy) or more photodetectors have to be used in order to measure the signal amplitude at the modulation frequency (in phase and in quadrature with the modulation signal) as well as the DC power impinging on the photodetector.

Once amplified all this signals have to be digitized with a system of ADC's. The digitized signals are then provided to the global control and to the data acquisition sub-systems.

42.2 Requirements applicable to the detection bench

The main requirements for the detection bench sub-system concern the detection of the dark fringe beam: it is required that the read-out system allows to measure the signal at the modulation frequency with a shot noise limited sensitivity.

- The output optics should separate the two beams at the interferometer output port. Then it should reduce their sizes to about 1 mm so that the two beams will fit in the photodiodes area.
- The requirements for the 'dark fringe' beam filtering is to reduce the total amount of light on the 'dark fringe' below 1 Watt (carrier + sidebands). This value corresponds to a contrast defect of the order of 10^{-4} (assuming a power of 1 kW impinging on the beam-splitter)
- In order to maximize the phase sensitivity, the photodiode quantum efficiency should be a high as possible. A value of 0.85 (already measured) will allow to maintain the spectral sensitivity at 92% of the optimum one.
- The photodetectors should measure the signal at the modulation frequency with a shot-noise limited sensitivity. The signal-to-noise ratio (shown in the previous figure) as well as all the AC and DC signals amplitude have been evaluated assuming 6.27 MHz as modulation frequency and 0.8 m as interferometer asymmetry. Nevertheless the photodiodes should be able to measure signals up to a frequency of the order of 10 MHz (TBC).
- The total DC power impinging on the photodiodes should also be measured. This measurement should be done on a 0 to 10 kHz frequency span.
- The photodiodes electronics front-end should have a high dynamic range in order to deal with the big dynamic range of the input signal. A well defined requirements is missing since a higher gain of the locking loop gain can reduce the signal dynamic range. The expected order of magnitude is from 10^7 to 10^8 $\sqrt{\text{Hz}}$.
- For all the photodiodes the in-phase signal, the in-quadrature signal and the DC signal should be sampled with a 20 kHz sampling rate and sent to the DAQ sub-system.
- All these signal have to be sent to the global control at a 10 kHz rate in real time.

42.3 Detection bench interfaces

42.3.1 List of interfaces

Interface name	Concerned sub-system	Interface description
Detection tower input window:	WBS 4100	(see § 4200.5.1.1)
Detection tower output windows:	WBS 3300	(see § 4200.5.1.1)
Suspended bench wires:	WBS 4700	(see § 4200.5.1.2)
Beam-splitter geometry:	WBS 4300	(see § 4200.5.1.3)
Bench position control:	WBS 4900	(see § 4200.5.1.4)
Mode-cleaner coating:	WBS 4300	(see § 4200.5.1.5)
External bench optical implementation:	WBS 4400	(see § 4200.5.1.6)
Beams profile monitoring:	WBS 5200	(see § 4200.5.1.8)
Suspended bench cabling:	WBS 4700	(see § 4200.5.1.9)
Photodiodes D2 and D2':	WBS 4100	(see § 4200.5.2.3)
Photodiodes D7 and D8:	WBS 4400	(see § 4200.5.2.3)
Digitized signals for locking:	WBS 5100	(see § 4200.5.3.1)
Digitized signals for DAQ:	WBS 5400	(see § 4200.5.3.1)

42.4 Selection of solutions

InGaAs photodiodes are known for being the most sensitive photodetectors at 1.06 µm. They have been proposed for the VIRGO detection system since the first VIRGO proposal [4].

Several commercial InGaAs Photodiodes have been tested at LAPP in the past years [5,6,7]. As the dimension of the photodiodes is increased the capacitance also increases thus decreasing the bandwidth. On the other hand greater dimensions allows to deal with more light power. The use of 3 mm diameter photodetectors is a good compromise. Test done at LAPP shows that these photodetectors are able to detect a power of 100 mW (this level of power is above the constructors specifications). To deal with more power, more photodetectors can be used in parallel.

The 3 mm diameter Hamamatsu photodetectors fulfill the VIRGO requirements in terms of bandwidth (10 MHz) and quantum efficiency (85%). To guarantee this quantum efficiency Hamamatsu is able to provide the photodetectors with anti-reflection coating on both the window and the detector. The possibility of using these photodetectors at higher frequency has not been demonstrated yet.

For the test interferometer all the photodetectors will be placed outside the vacuum tank [8]. If needed the photodiodes used to detect the 'dark fringe' beam will be placed inside the detection tower.

Each photodiode output signal will be digitized using a 16 bits ADC. The ADC's read-out system will be based on a VME architecture.

The design of the 'dark fringe' beam filtering has not been frozen yet. The use of a short optical cavity is the solution offering the best performance. A very short cavity is required if one wants to transmit the carrier and the two modulation sidebands in the same Airy peak. The main critical drawback is the great sensitivity of the interferometer output signal to the cavity length vibrations (at the level of 10^{-16} m/$\sqrt{\text{Hz}}$ @ 100 Hz). One prototype have been built and is under test since one year in Annecy [7].

The use of a system made by one or two diaphragm may be a possible backup solution. The comparison between the two system depends on the origin of the contrast defect. If the wave front deformations give mainly rise to low order transverse modes in the 'dark fringe' beam, the optical cavity solution seems the more appropriate.

The use of a Fabry-Perot cavity as spatial filter requires that the output optics used to separate and filter the two beams at the interferometer output port, will be isolated from seismic and acoustic perturbations. To this purpose these optics will be fixed on a suspended bench placed inside the detection tower.

The amount of seismic isolation required depends on the transmission of vibrations from the top of the suspension to the suspended bench and from the bench to the Fabry-Perot cavity. If 1% of the bench residual vibrations is transmitted to the Fabry-Perot than a two stages super-attenuator will guarantee the required isolation. The use of a three stages suspension (including the filter #0) will allows to have a larger security factor for future development.

42.5 Detailed description

The detection bench sub-system has been divided in the following three items [1]:

- 4220 Output Optics:
  It includes the optics required to extract the two beams at the interferometer output port. The output optics main function is to separate the two beams and to reduce their sizes. In addition the dark fringe beam has to be spatially filtered.
- 4220 Photodiodes:
  It concerns all the photodetectors required for the detection of the beams used to lock the interferometer. It includes the analog electronics required to demodulate and filter the signal at the modulation frequency. It also includes the electronics necessary to read the DC power impinging on the photodetectors.
- 4230 Signal read-out:
  It includes the system required to digitized all the photodiode signals. It also takes care of providing them to the DAQ and to the global control.

42.5.1 Output Optics

42.5.1.1 Overview

The output optics is located inside and behind the detection tower.

All the optics inside the tower is fixed on a suspended optical bench. The bench is suspended to a marionette through three wires (figure 4200.4). The marionette is itself suspended to a three or two stages suspension (TBD). The whole system is kept under vacuum at 10^{-6} mbar.

All the optics outside the tower is located on a commercial optical bench (0.9x2 m^2) placed behind the detection tower (figure 4200.5). The beams go from the suspended bench to the external bench passing through 3 CF150 windows placed on one of the tower lateral cover.

The optics general implementation on the benches is shown in figure 4200.6. The two beams coming from the beam-splitter goes through a telescope that separate the two beams and that reduce the beam waist to about 1 mm. We will refer to the 'dark fringe' beam as beam #1 and to the beam-splitter secondary beam as beam #5.

After the telescope the Beam #1 is separated by a splitter in two parts.

Most of the Beam #1 (98% TBC) is reflected towards the mode-cleaner system. The beams transmitted and reflected by the mode-cleaner are sent outside the tower towards the D1 and D1'' photodiodes. These photodiodes are both placed on the external bench. A very small fraction of these beams are sent to two CCD cameras for control purposes.

A small fraction (2% TBC) is transmitted by the splitter and then reflected by a small mirror towards the external bench. This part of the beam reach the D1' photodiodes placed on the external bench and it is used for lock acquisition purpose. A small fraction of the beam is sent to a CCD camera for control purposes.

The Beam #5 is also separated in two parts by a splitter.

Most of the Beam #5 (90% TBC) is transmitted by the splitter and then reflected by a small mirror towards the external bench. This part of the beam reaches the D5 photodiodes placed on the external bench and it is used for locking purpose. A small fraction of the beam is sent to a CCD camera for control purpose.

About 10% (TBC) of the light is reflected towards the bench position sensors. This system uses two quadrants placed on the suspended bench to align the bench with the interferometer output beam.

All the optics will be mounted at a height of 100 mm respect to the bench. As a consequence the bench will be located 100 mm below the VIRGO beam axis.

42.5.1.2 The suspended bench

The suspended bench (see figure 4200.7) is made from a piece of aluminum alloy (Alplan) machined in an octagonal shape (950 mm external diameter). The top plate is 10 mm thick. Several ribs 50 mm high and 10 mm thick are machined below the top plate. An aluminum plate 10 mm thick is screwed below the ribs in order to add mass and rigidity to the bench. The total bench mass is 60 kg (optics not included).

The possibility of placing the D1 photodiodes on the suspended bench is kept for the future. In this case the additional mass will be compensated by replacing the lower plate with a smaller (and so lighter) plate.

A grid of M6 holes are machined on the top plate in order to fix the optical components. Three larger holes are also machined on the top plate in order to add (if necessary) some optical elements below the table.

42.5.1.3 The telescope

Due to the different beam geometry (the beam waist is 3.25 mm for the test interferometer and 19.8 mm for VIRGO), the telescope used for the test interferometer cannot be the same used for the complete interferometer. Nevertheless the beam dimension after the telescope will be the same (1 mm) so that the following optics can also be the same.

The design of the VIRGO telescope has not been definitely frozen yet. The present solution foreseen the use of a confocal doublet formed by two lenses [9,14] with focal lengths equal to 2m and 10 cm respectively. The use of lenses eliminate any astigmatism effects. A small prism placed on the first lens focal point separates the two beams. Due to the long focal length of the first lens, two folding mirrors will be necessary to fit the telescope on the suspended bench.

The use of mirrors instead of lenses allows to reduce the number of optical surfaces but involve some not negligible astigmatism and spherical aberrations [10] on the output beam. The possibility of using astigmatic optics remains to be investigated.

The telescope [11] for the test interferometer (see figure 4200.8) will also be a confocal doublet. The reduced dimension of the beam waist at the telescope input (3.25 mm) allows the use of two spherical mirrors in this case. The two focal lengths will be 1 m and 0.3 m respectively. This solution reduces the number of optical surfaces since no folding mirror is needed. The two beams will be separated by a prism placed about 77 cm after the second mirror.

42.5.1.4 The bench position sensors

A small fraction of the Beam #5 is used to align the suspended bench on the interferometer output beam [12]. The Beam #5 position and angle will be read by two quadrants placed at two different distances from the telescope (see figure 4200.8). The EGG YAG-444A-4 quadrants have been selected to this purpose.

In order to maintain the dark fringe beam aligned with the output mode-cleaner the bench position has to be controlled with an rms. precision of the order of 600 μm and the bench alignment has to be controlled with an rms. precision of 0.5 μrad [7]. These requirements are related to mode-cleaner alignment.

For the test interferometer the input beam waist is smaller by a factor of 6. As a consequence these requirements are a factor of six more strict for what concerns the position, but they are a factor of six less strict for what concerns the angles.

In both cases (VIRGO or test interferometer) the beam #5 displacement at the level of the quadrants should be controlled with a precision of the order of 10μm [12].

The EGG quadrants will be placed on the bench under vacuum. Only four resistors (one for each element of the quadrant) will be placed under vacuum. The remaining part of the electronics read-out will be outside of the vacuum system near the detection tower.

The quadrants output signals will be digitized by a system of ADC's located in the suspension control crate. These digitized signals will be used to control the bench position with the digital control system developed by the Pisa group (interface with WBS 4900).

42.5.1.5 The mode-cleaner

As already said in the 4200.4 section of this chapter, the mode-cleaner system is still in an R&D phase. This section describes the present solution.

The mode-cleaner is a short (25 mm) monolithic triangular cavity (see figure 4200.9). The cavity is a small piece of silica having three faces polished and coated. One of the faces is spherical with a radius of curvature equal to 0.3 m. Three prototypes have been built. They have all been coated (at IPN Lyon, interface with WBS 4300) in order to have a finesse of 50.

As a consequence of the difference between the silica index of refraction and the vacuum, the mode-cleaner input and output beam are affected by a strong astigmatism. Two solutions have been studied to match the cavity waist. The first one consists in using cylindrical lenses while the second one foreseen the use of two small prisms. The solution using two 10 mm prisms is shown in the figure 4200.9 and will be soon tested at LAPP.

This solution correspond to the bench implementation shown on figure 4200.8. A lens is used to focus the beam on the mode-cleaner with the right dimension.

Two small mirrors, mounted on remotely adjustable optical mountings, are placed between the lens and the mode cleaner in order to help the mode-cleaner alignment.

The mode-cleaner length is controlled through a thermal actuator made by a Peltier cells [7]. The error signal is obtained by modulating the cavity length with a small piezoelectric pushing on the top of the cavity. The signal at the modulation frequency (of the order of 10 kHz) will be extracted by looking at the DC outputs of two or more of the D1 photodetectors. The feedback will be operated using a digital control system.

42.5.1.6 The external bench

The external bench will be a commercial 0.9x2 m^2 optical bench. In order to keep enough space between the external bench and the wall of the suspension assembly hall, the bench will be partially mounted on the tower base (see figure 4200.5).

All the photodiodes and cameras required to detect and monitor the beams #1 and #5 will be fixed on the external bench.

Some space is kept free in order to accommodate the quadrants used by the linear alignment system (interface with WBS 4400). The exact locations of the quadrants as well as the required optics still remain to be defined in agreement with the WBS 4400 sub-system.

42.5.1.7 Output optics control

It consists of one VME crate containing the digital electronics required to control the mode cleaner as well as the pico-motors used to remotely align some of the mirrors placed on the suspended bench. This same crate may be used to accommodate the boards used to read the CCD cameras (interface with WBS 5200) placed on the external bench.

A second crate is required to accommodate the analog electronics used to amplify the quadrants outputs. This same crate will accommodate the analog electronics needed to detect the mode-cleaner output signal.

42.5.1.8 Output optics test

A laser will be placed on the external bench in order to test the component located on the suspended bench inside the detection tower.

The laser output beam is separated in two parts (see figure 4200.10). One is sent towards the mode-cleaner system in order to test the correct functioning of the mode-cleaner control system. In order to have enough power impinging on the mode-cleaner, one of the splitters under vacuum will have to be rotated. The second part of the beam is sent towards the bench position sensors in order to test the correct functioning of the two quadrants.

The laser test placed on the external bench will not allow to test the entire bench but only two of the main elements. The possibility of a complete test done by injecting two light beams at the telescope input is currently being studied.

42.5.1.9 Suspended bench cabling

The cabling has not been definitely frozen yet. This section describes the present solution.

It is foreseen to have six remotely controlled optical mounts. Two of them are equipped with 3 pico-motors while the other fours uses only 2 pico-motors. One short pulse (few ms) with 300 volts amplitude is provided to the pico-motor to make one step. One should remark that these motors will only be used for the initial alignment and to compensate some slow drift. No voltage need to be applied when the motor is at rest. The total number of cables required to this purpose is around 28. Two 16 wires flat cables are foreseen at present.

The two quadrants need 5 wires each. The use of one shielded 16 wires flat cable if foreseen at present.

The mode cleaner system will need at least 6 wires: 2 for the piezoelectric, 2 for the Peltier cells and two for a thermometer. One additional shielded 16 wires flat cable may guarantee the required flexibility for future upgrades.

The present solution foresees to clamp the cables to the suspension wires of the bench and attach them to the marionette (interface with WBS 4700). The cables will then travel along the suspension up to the top of the tower.

42.5.2 Photodiodes

42.5.2.1 Overview

The photodiodes location is shown in the figure 4200.11. Photodiodes D1, D1', D1'', and D5 are located on the bench behind the detection tower. Photodiodes D2 and D2' are located on the laser bench near the injection tower (interface with WBS 4100). Finally photodiodes D7 and D8 are located behind the North end tower and the West end tower respectively (interface with WBS 4400).

Since the total amount of power is limited to 100 mW per photodiode, a different number of photodetectors will be needed for each beam. In order to reduce the impact of failures it is foreseen to use at least two photodetectors on each beam.

The amount of power impinging on each photodetector depends on the light interference condition and will be drastically different during the lock acquisition process and once the interferometer is locked. Since the locking acquisition process has not been completely defined yet, the exact amount of power impinging on each photodetector are only very roughly known. Nevertheless for construction purposes the total number of photodetectors has been evaluated and the foreseen solution is described in this section.

42.5.2.2 The photodetector D1

Assuming 1 kW of power stored inside the recycling power, an asymmetry of 0.8 m, a modulation frequency of 6.25 MHz and a contrast defect of 10^{-4} (after the beam filtering), the optimum modulation depth turns out to be around 0.4 (see figure 4200.2). In these conditions the amount of DC power impinging on the D1 photodetector is of the order of 0.7 W. The amount of power at twice the modulation frequency (12.5 MHz) will be around 0.65 W. The peak power approaches 1.4 W. The use of 16 photodetectors will allow to deal with this power.

The detector arrangement is shown in figure 4200.12. Fifteen 50% splitters are used to divide the beam in sixteen parts. The photodiodes are placed in order to be all at the same distance from the first splitter. In this configuration, the use of only one lens in front of the first beam-splitter allows to focus the beam on all the photodetectors at the same time.

All the photodetectors are mounted on an individual support which allows to center the photodiode on the light beam and that places the photodiodes at about 10 cm above the bench (see figure 4200.13).

42.5.2.3 The other photodetectors

42.5.2.3.1 Photodiode D1'

The amount of power carried by the 'dark fringe' beam during the lock acquisition process (when the interferometer is not locked on the 'dark fringe' yet) will not be the same one has when the interferometer is locked. In addition to this the output mode-cleaner is not expected to be locked during the lock acquisition process. To deal with the locking acquisition process a small fraction of the 'dark fringe' beam is extracted before the mode-cleaner and is sent towards the D1' photodetectors. Two photodiodes will be used to this purpose.

42.5.2.3.2 Photodiode D1''

A big fraction of the 'dark fringe' beam is reflected by the mode-cleaner. The exact amount will depend on the fringe contrast before the mode-cleaner. The reflected light is detected by the D1'' photodetectors. This beam will be used only from mode-cleaner monitoring purpose. Two photodiodes will be used.

42.5.2.3.3 Photodiode D2

When all the interferometer is locked, the light is resonant in the recycling cavity. If the recycling cavity gain is optimized (TBC), only a very small fraction of the light coming from the laser (10 W for the test interferometer and 20 W for VIRGO) will be reflected by the recycling mirror towards the D2 photodiodes. In practice the exact amount of light impinging on the D2 photodetectors will depend on the fringe contrast of the recycling cavity i.e. on the beam matching and on the matching between the recycling mirror transmission and the interferometer losses one will be able to achieve. From this point of view the situation is similar to what happen on the D1 photodetector.

The difference is that this beam will mainly be used for laser frequency stabilization (interface with WBS 4100 and Locking group) in 5 Hz to 15 kHz range (TBC) and the required sensitivity is below [13] the one required for the D1 photodetector. As a consequence the detection of all the light will not be required. The fraction of light used to this purpose is TBD. The present solution foreseen the use of two photodiodes.

42.5.2.3.4 Photodiode D2'

The amount of light on the D2 photodetector will increase during the lock acquisition process as it happen for D1. As for the D1' photodetector the D2' will be used for locking acquisition purposes. The fraction of light used is TBD. The present solution is to use two photodiodes to this purpose.

42.5.2.3.5 Photodiode D5

The expected amount of light impinging on the D5 photodetector is of the order of 50 mW. This value assume 1 kW of power inside the recycling cavity and 10^{-4} [14] as reflection coefficient for the beam-splitter second face. It is foreseen to use two photodiodes.

42.5.2.3.6 Photodiodes D7 and D8

The expected amount of light transmitted through the Fabry-Perot end mirrors is of the order of 0.75 W. This value is calculated assuming 1 kW inside the recycling cavity, 50 for the Fabry-Perot finesse and 50 ppm for the end mirror transmission [14]. To deal with such a power 8 photodetectors would be required. The sensitivity required on these signal has not be specified yet (interface with Locking group). As a consequence it is not clear what fraction of light will be used (TBD). The present solution foreseen the use of 2 (TBC) photodiodes.

If required these photodetectors will be delivered for the test interferometer. In this case the total amount of power will be about 30 times lower. The use of two photodiodes will be more than enough to detect such a power.

42.5.2.4 Photodiodes electronics: overview

This section and the following two are dedicated to the analogue electronics and cabling which will be implemented in order to transform the photodiodes current into a suitable signal ready to be digitized. The modulation frequency, envisaged in this reference solution, is 6.27 MHz it might be increased to 12 or 18 MHz, note that a change of frequency imply some hardware work on this system and therefore is an important operation which cannot be envisaged without some preparation.

The dark fringe beam is expected to contain the following power distribution :

~ 0.7 W @ DC
~ 0.6 W peak @ 2 Fmod
~ 0.1 W peak @ Fmod [15]

The interferometer's beams to be detected are used either for the signal detection or for the interferometer locking. The general principle is to organize the beams geometry in order not to exceed 100 mW of light peak power per diode. Taking into account a quantum efficiency of 0.85 for the photodiodes, i.e. a conversion factor of 0.73 A/W, this implies a maximum current of 75 mA peak per channel, the number of channels depending of the beam power.

Each electronics channel associated with one photodiode contains :

- one DC channel with a bandwidth of about 50 kHz
- two AC channels with demodulated and filtered outputs in phase and in quadrature with respect to the frontal modulation
- one AC test output
- one DC bias for the photodiode

42.5.2.5 Electronics design

The schematic diagram of one electronics channel described below is given in figure 4200.14.

42.5.2.5.1 Dynamic range

For each photodiode, the peak current is 80 mA and the average current 40 mA. This induces a shot noise current of 110 pA/√Hz. The useful signal at Fmod corresponds to a peak current of about 4.5 mA. The useful dynamic range is then given by :

$4.5\ \text{mA} / 110\ \text{pA}/\sqrt{\text{Hz}} = 4.10^7\ \sqrt{\text{Hz}}$

42.5.2.5.2 Fmod component filtering and DC channel

In order to reduce the dynamic range to its useful value, the 2 Fmod component must be filtered and brought to a value below the Fmod component.

To achieve this filtering, we use a short-circuited cable tuned to the modulation frequency ($L = \lambda_{mod}/4$) so that the cable presents a high impedance at Fmod and a short circuit at 2 Fmod. This cable is terminated by a capacitor ensuring the high frequency short circuit in parallel with a current amplifier which provides the DC output

To ensure a safety factor on the attenuation of the 2 Fmod component, a notch filter at this frequency is placed at the input of the amplifier.

42.5.2.5.3 Noise Considerations

A 50 Ω resistor is placed at the input of the amplification stage to match the 50 Ω cable transporting the signal from the photodiode. The electronics components should not add noise in order to keep the shot noise limited detection. The voltage induced by the shot noise across the 50Ω resistor is about 5 nV/√Hz. Measurements have shown that the input equivalent noise of the electronics is 1.6 nV/√Hz [6].

42.5.2.5.4 Frequency response

The equivalent circuit of the photodiode is a parallel capacitor and a series resistor. The frequency limitation of the system is made by the photodiode itself and the input impedance of the readout circuit (50Ω). However, the detection channel could be used even at a higher frequency than the photodiode cut-off frequency. The signal and shot noise will be reduced by the same amount, so the signal to noise ratio will not be affected, provided the shot noise remains above the electronics' noise.

42.5.2.5.5 Amplification

An amplification is necessary to bring the Fmod signal at the maximum level allowed by the mixer (0.9 V peak).We have chosen a CLC 425 operational amplifier for its low noise and high speed characteristics :

noise voltage	:	1.05 nV /√Hz
GBW product	:	1.7 GHz
DC offset	:	100 μV typ.
gain	:	10 to 1000
power supply	:	+/- 5V

42.5.2.5.6 Demodulation

The output of the amplifier feeds the mixer's RF inputs through a 3 way power divider :

one way for the in-phase detection
one way for the quadrature detection
one way for the test channel

The demodulation reference is supplied by the modulator. It is divided by a 90° splitter in order to achieve the in-phase and quadrature demodulation's. The absolute phase of the LO signal can be adjusted to take into account all the phase lags between the modulator and the mixer.

The demodulators are double balanced mixers with a LO level of +13 dBm and a maximum RF level of +9 dBm. Their dynamic range have been measured to 4.10^7 √Hz and just matches the specifications.

42.5.2.5.7 Output filtering

The IF outputs of the mixers are connected to a low pass filter which eliminates all the frequency components above 20 kHz.

Then, a second order lead compensator filter is placed to compress the dynamic range of the signal and makes it fit into a 16 bits ADC. This filter has a low cutoff frequency at 0.25 Hz and a high cutoff frequency at 25 Hz.

Finally, the gain of the stage is adjusted to match the full scale input level of the ADC's.

42.5.2.5.8 Bias Voltage of the photodiode

The reverse bias voltage is driven by an external DAC. The DC current and the applied bias voltage are measured by two dedicated circuits, the output ports of these circuits are connected to a multiplexing system which allows a channel by channel visualization of current and voltage and to direct these information's towards the acquisition system ADCs. The bias voltage is applied to the photodiode by a triaxial cable. This system allows to apply the reverse bias voltage and to transport the signal with a single cable. This same system will allow to automatically turn the bias voltage off if the current flowing through the photodetector increases above a given threshold.

42.5.2.5.9 Implantation

All the electronics described above for one channel, is implanted on a VME like printed circuit board. No processor or fast digital electronics will be installed on these analog crates.

42.5.3 Signal read-out

42.5.3.1 Overview

The photodiodes signals are converted using low noise ADC's (ADC5020 from Analogic) sampled at 20 kHz. These ADC's are installed on VME boards which provide the readout facility. They include an inboard FIFO and a private bus which allows to read a full VME crate in a single bloc transfer at a user defined frequency (10 kHz in our case).

Given the size of the A/D converter a maximum of 32 channels could be fitted in one VME crate. Therefore, three crates are foreseen for the readout of the in-phase, quadrature and DC signals for all the photodiodes in the central building. One crate will be enough for each end mirror building.

There will be one CPU per VME crate reading at 10 kHz, all the channels, doing calibration, unwhitening and summing the twin channels, sending the result to the global control (at 10 kHz) and to the Data Acquisition through Digital Optical Links. The detailed crate/channels assignment is TBC

42.6 Detection bench assembly

42.6.1 Output optics assembly and installation

The suspended bench will be clean, assembled and pre-aligned at LAPP. During this phase the bench is also suspended and balanced by adding some small masses at the appropriate places. The bench will be then shipped to Cascina inside a protection box ensuring a minimum level of cleanness (TBD).

Once received in Cascina, the bench will be installed in the benches lab using a chariot. Here the precise alignment will be done using a Nd:YAG laser and some movable diaphragms. The laser will be located on another small bench placed near the first one and the light will be sent from one bench to the other using a fiber (TBC).

The marionette will be then assembled on the bench using some specific support attached to bench edge. It is assumed that the marionette has been previously suspended and balanced separately (interface with WBS 4700). The cables coming from the bench are then clamped to the three suspension wires and connected to the connectors fixed on the marionette.

Once the cabling is completed, the correct functioning of the electrical components located on the bench (piezoelectric, thermometer, Peltier cell, quadrants and the pico-motors) will be tested. This operation will need some electrical equipment like one oscilloscope and one crate (TBC).

The marionette will be then suspended to a small clean forklift through a wire similar to the one used to hang it to the last stage of the super-attenuator and the supports attached to the bench edge are removed. The balancing of the whole payload is checked by rising it with the forklift.

The marionette is then placed again on the support and the payload is ready to be installed inside the tower. Using the chariot and the elevator the payload is transported in the gallery below the detection tower and placed on the 1 m diameter tower lower cover. An elevator is then used to transport the payload inside the tower (see figure 4200.15).

The bench supporting feet are then installed inside the tower (see figure 4200.15). The marionette is hanged to the super-attenuator and the cables coming from the top are connected to the connectors attached on the marionette. The elevator goes down slowly until the marionette suspension wires is under tension. The supports attached to the bench edge are removed (protection against the falling of the marionette remains to be defined).

The first test of the bench will be done by resting it upon the supporting foots. To this purpose each foot is equipped with some adjustable screw. Test beams are then injected from the external bench (already installed) and the correct functioning of the elements placed on the bench and of the cabling is checked.

The bench is then suspended again and the correct functioning of the position control system using the cameras and the quadrants is checked. The bench is then ready to be used under vacuum.

42.6.2 Photodiodes assembly and installation

The photodiodes will be tested together with their electronics at LAPP.

Once shipped to Cascina the photodiodes will be installed on the appropriate benches. For what concern D2, D2', D7, and D8 the installation will be done together with the people responsible of the input bench (interface WBS 4100) and of the end benches (interface with WBS 4400).

The exact location of the analog electronics remains TBD.

42.6.3 Signal read-out assembly and installation

The VME crates with their ADC's, CPU and DOL will be set up and tested at LAPP. Then they will be shipped at Cascina installed in their assigned rack (in the data acquisition room for the central building TBC) and connected to the photodiodes signal outputs.

List of References

[1] VIRGO WPD Work Package Description (unpublished)

[2] J.Y.Vinet; 'Splitter', VIRGO note PJT94-16 (1994)

[3] P.Hello; 'Modele physique et simulation de l'antenne interferometrique gravitationelle VIRGO' PhD thesis, Orsay (1990)

[4] The VIRGO collaboration; VIRGO proposal (1989)

[5] B.Caron et al.; Photodiodes selection for VIRGO detector, the first step', Nuclear Instruments & Methods in Physics Research A 360 (1995) 379-384

[6] A.Dominjon et al.; Detection diodes: the second step', VIRGO note NTS95-009 (1995)

[7] A.Dominjon; 'Recherche des ondes gravitationelles: etude et conception de l'ensemble de detection du signal', PhD thesis, Annecy (1996)

[8] R.Flaminio; 'Do we really need to put the photodiodes in vacuum ?', VIRGO note NTS96-035 (1996)

[9] A. Dominjon et al.; 'Detection bench telescope', VIRGO note NTS95-020 (1995)

[10] R.Flaminio, V.Sannibale; 'Spherical aberrations of a gaussian beam produced by mirror and lenses', VIRGO note NTS96-029 (1996)

[11] V.Sannibale; 'The VIRGO 1998 Detection Bench telescope', VIR-NOT-LAP-1390-069 (1996)

[12] V.Sannibale; 'The VIRGO detection bench position sensor' (in preparation)

[13] see chapter 4100 of this document

[14] The VIRGO collaboration; 'VIRGO final design version 0' (1995)

[15] B.Caron et al.; 'A preliminary study of the locking of an interferometer for gravitational wave detection', LAPP-EXP-96.04 (1996) (to be published on Astroparticle Physics)

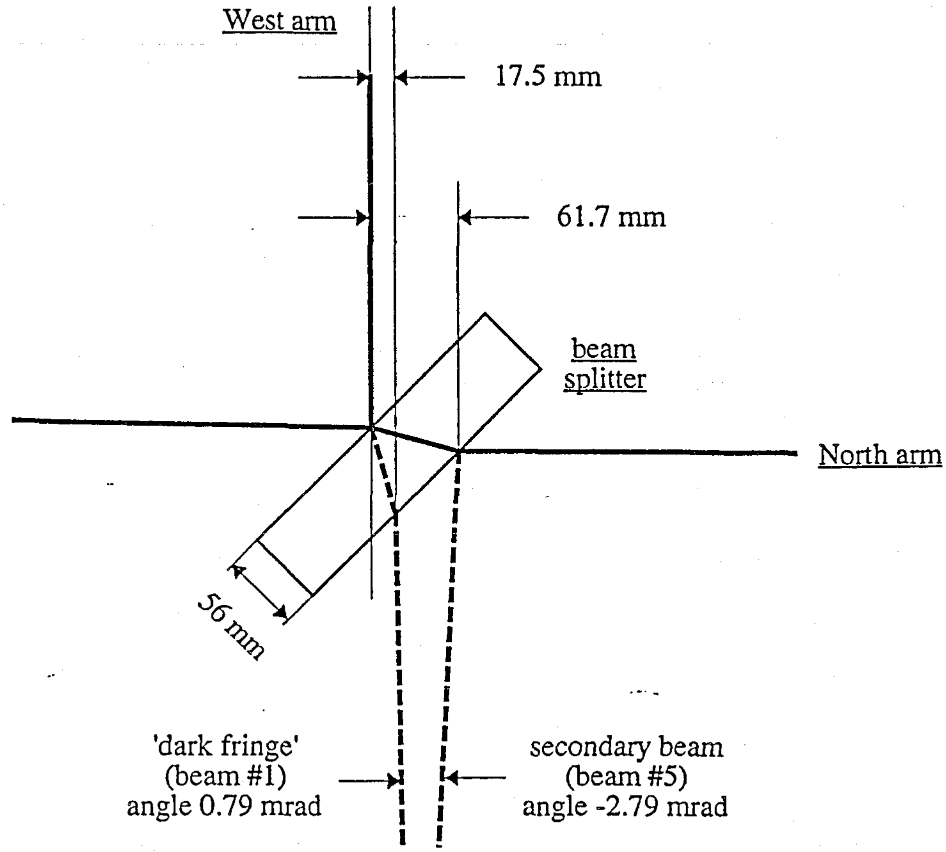

Fig. 4200.1 View of the beam-splitter area from the top. The dark fringe beam and the secondary beam propagates in the direction of the detection tower.

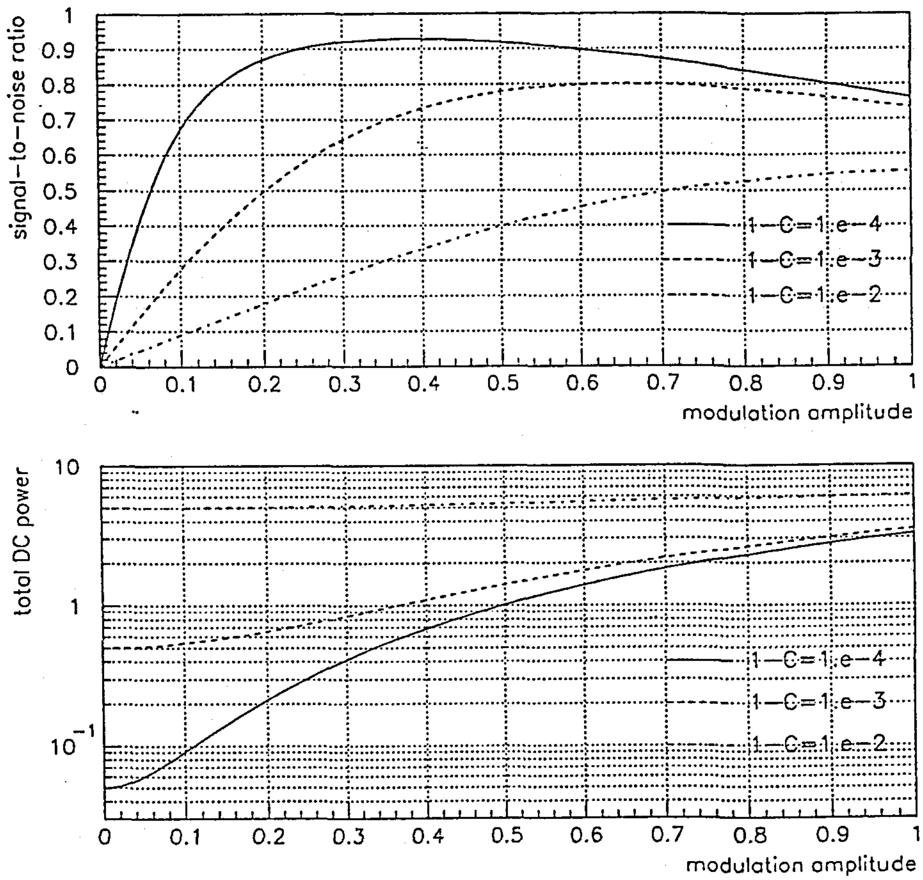

Fig. 4200.2 a) The phase sensitivity normalized to the best sensitivity is shown as a function of the input modulation amplitude. The three curves corresponds to three different values of the contrast defect. b) For the same three values of the contrast defect, the DC power on the 'dark fringe' is shown as a function of the modulation amplitude.

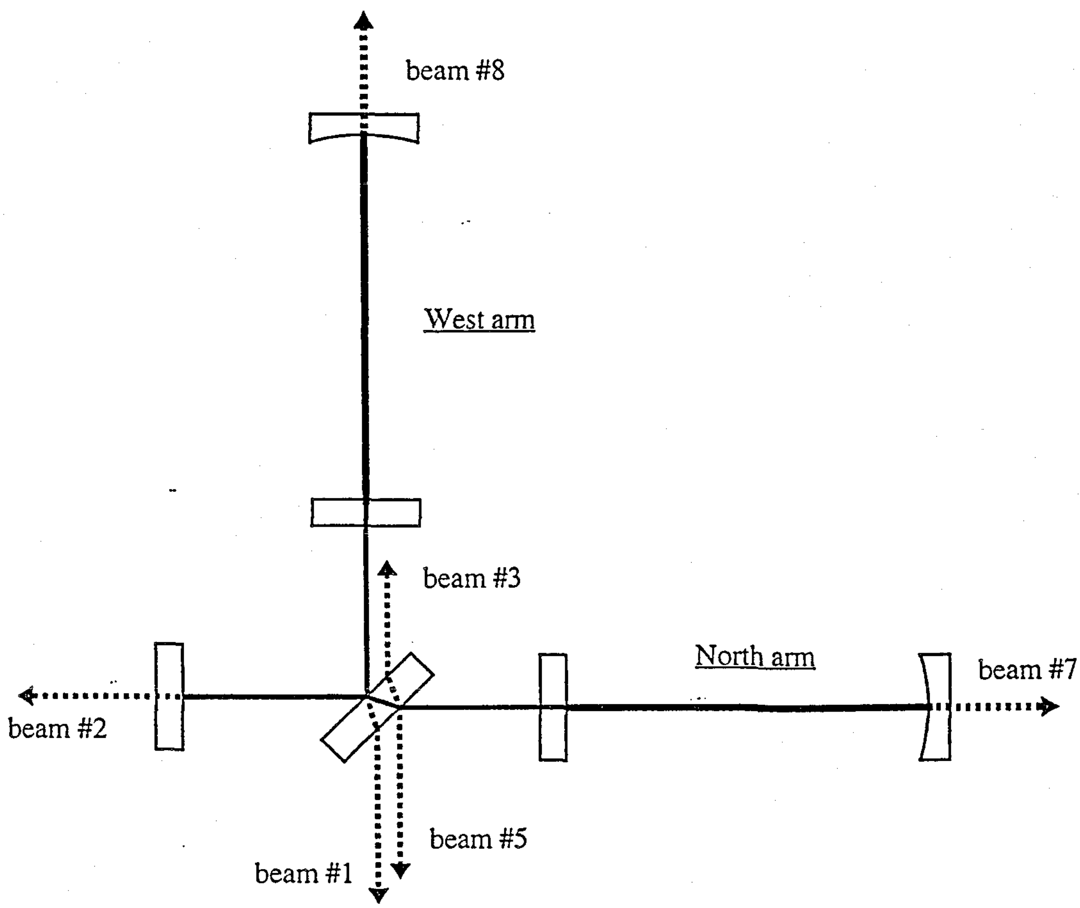

Fig. 4200.3 Schematic view of the interferometer. The beam numbering correspond to the one used in the text. The same numbering will be used for the photodetectors.

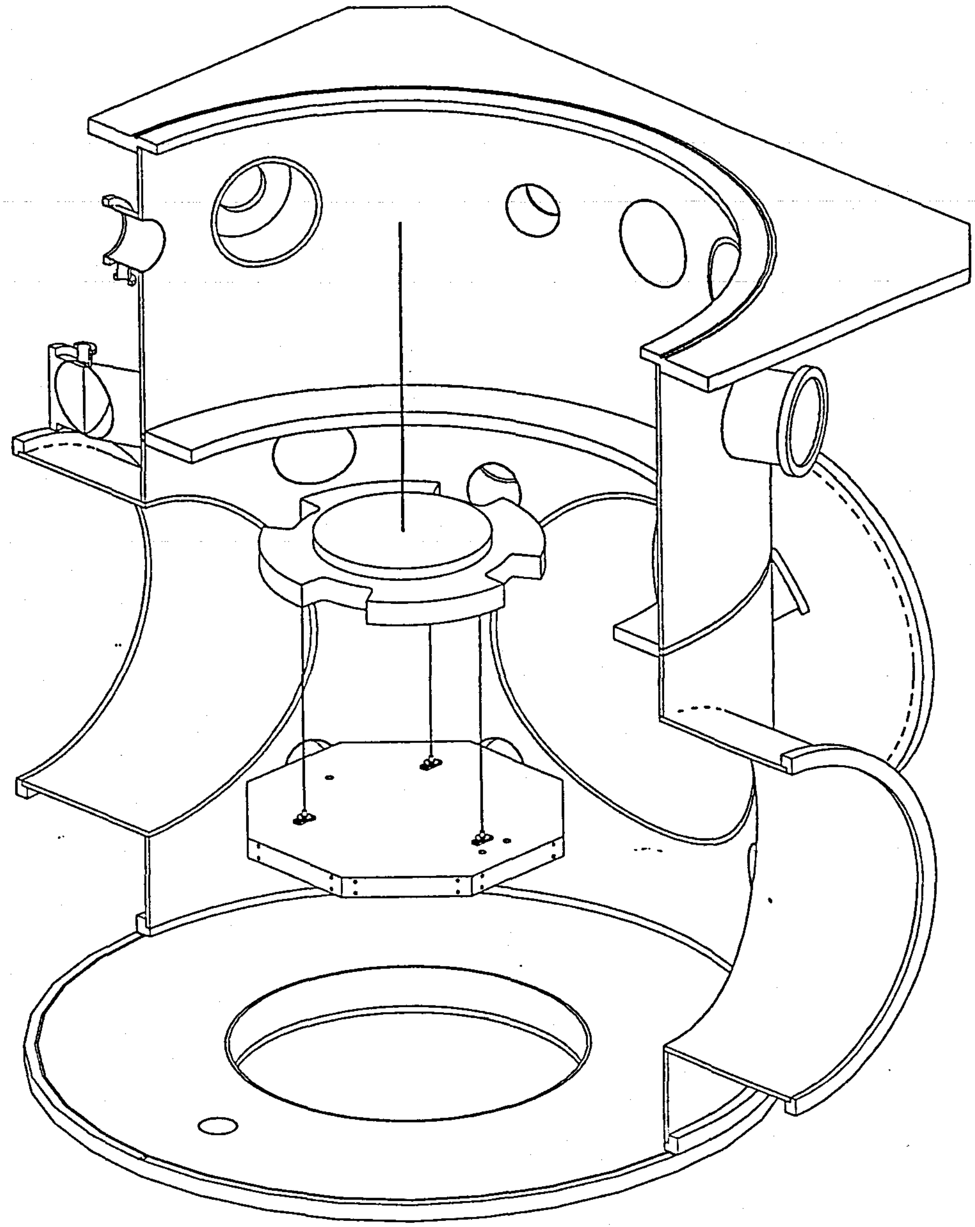

Fig. 4200.4 Perspective view of the bench suspended to the marionette inside the detection tower.

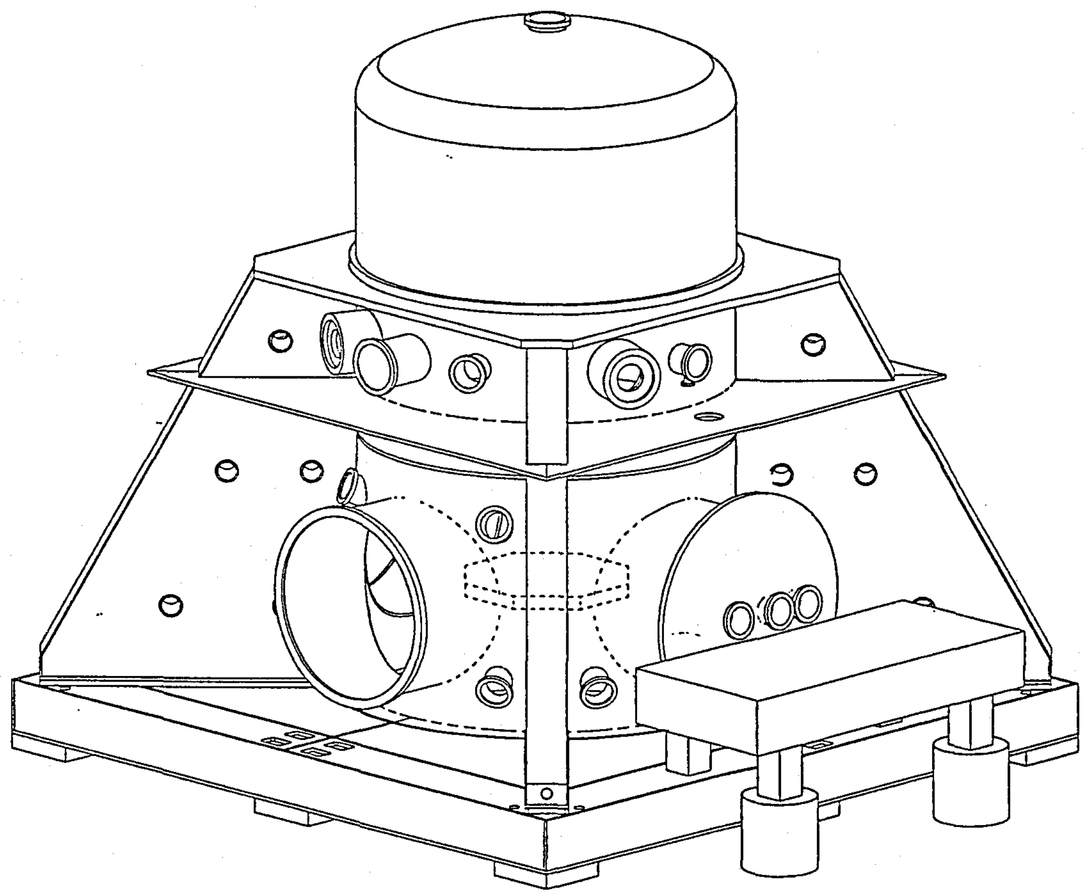

Fig. 4200.5 View of the detection lower tower. The external bench will be placed behind the tower and it will be partially mounted on the tower base.

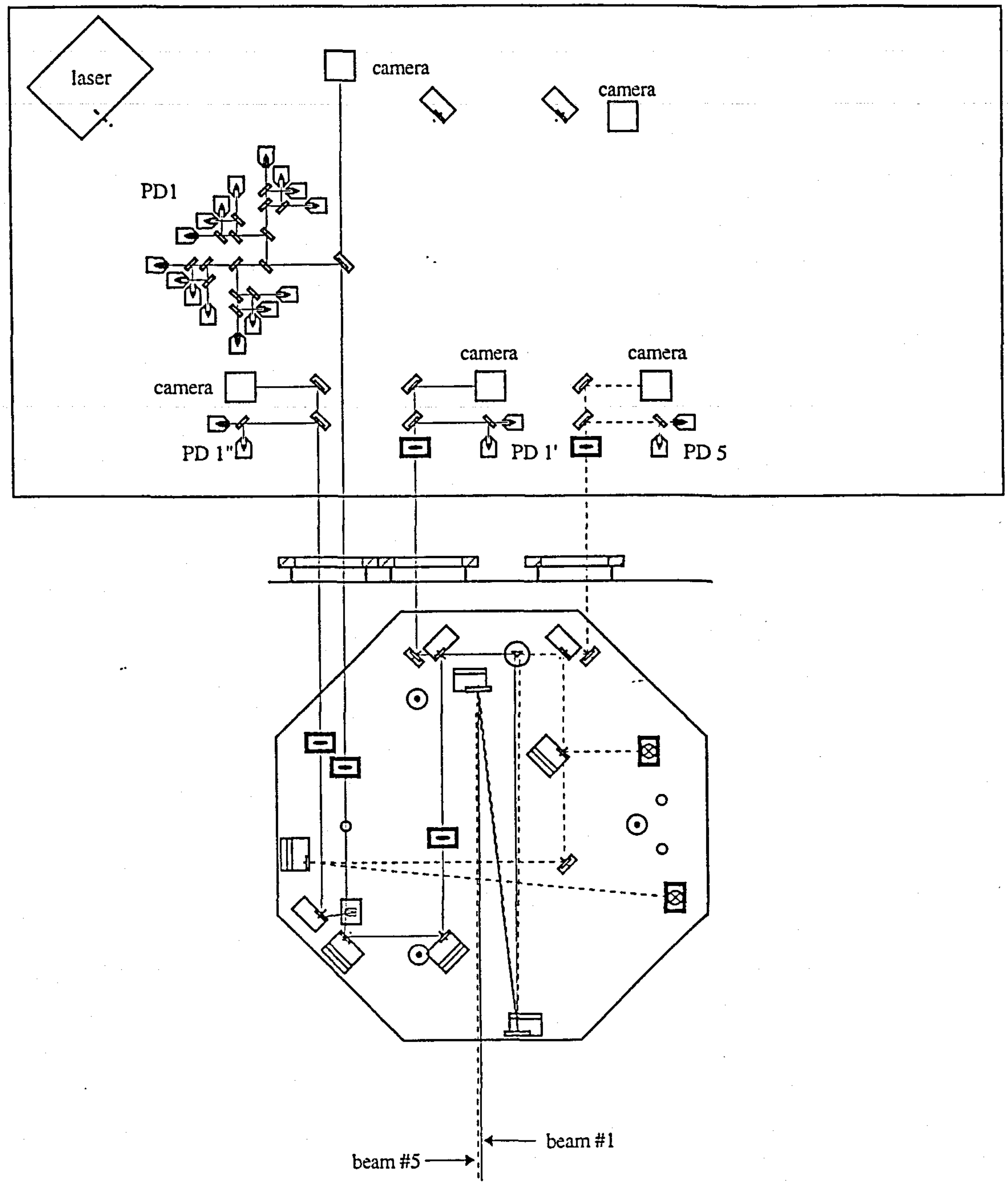

Fig. 4200.6 General implementation of the optics on the suspended bench and on the external bench. Beam #1 refers to the dark fringe while beam #5 refers to the beam-splitter second face reflection.

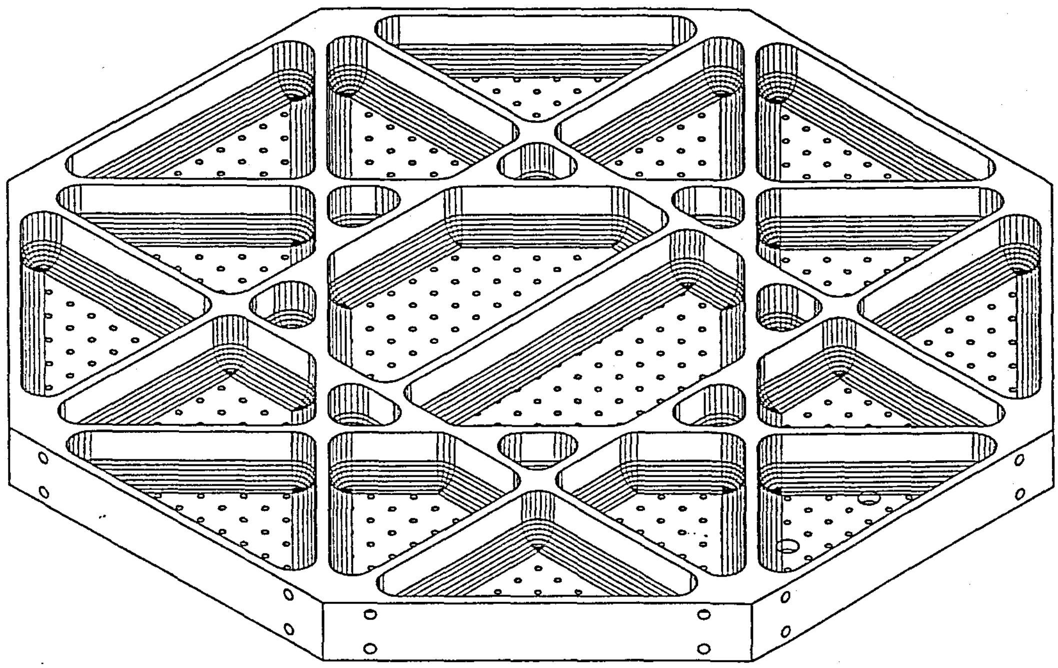

Fig. 4200.7 Mechanical structure of the suspended bench. The bench is machined using an aluminum alloy.

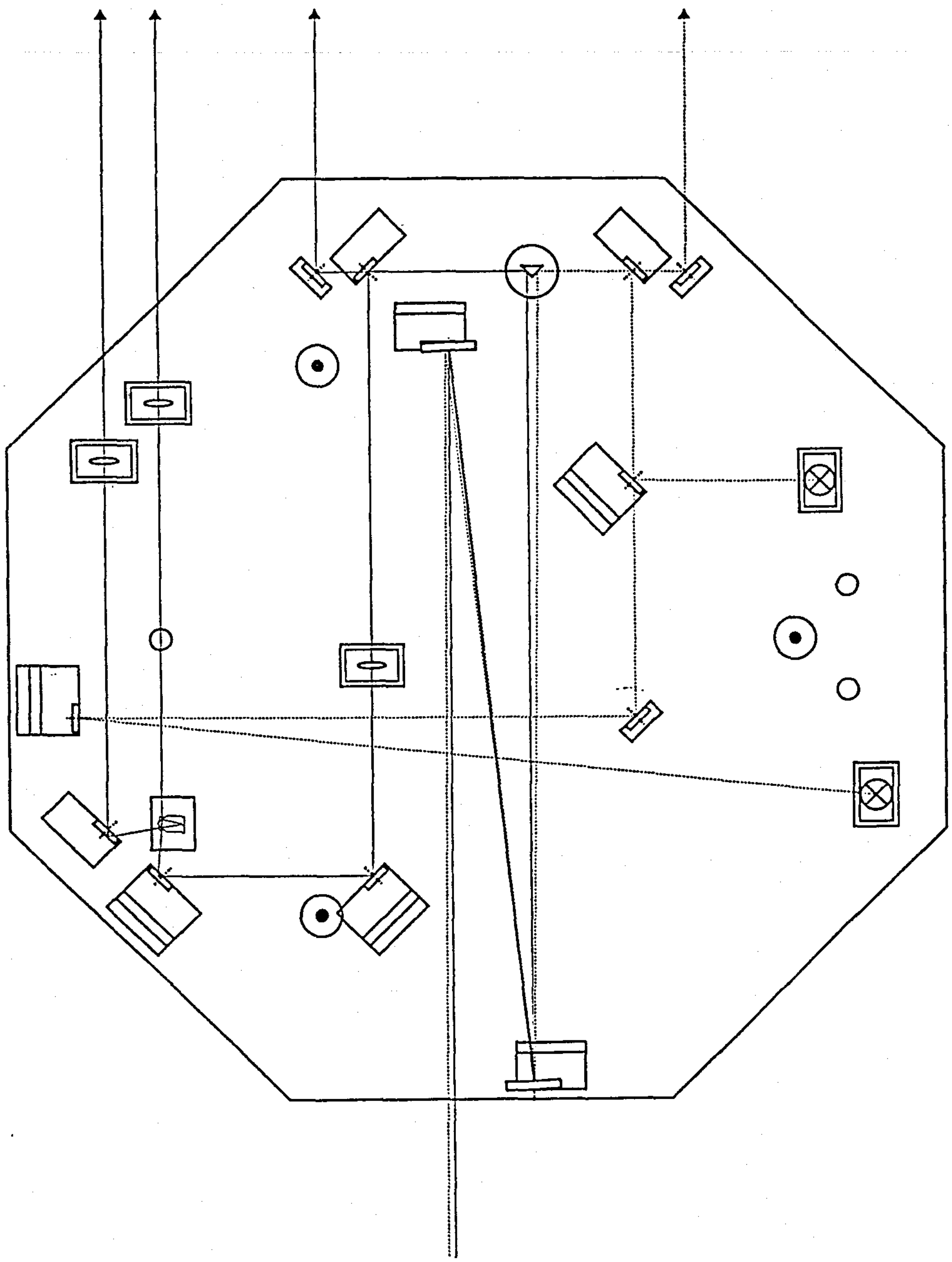

Fig. 4200.8 Optics implementation on the suspended bench. Some of the mirrors are mounted on remotely adjustable support.

a)

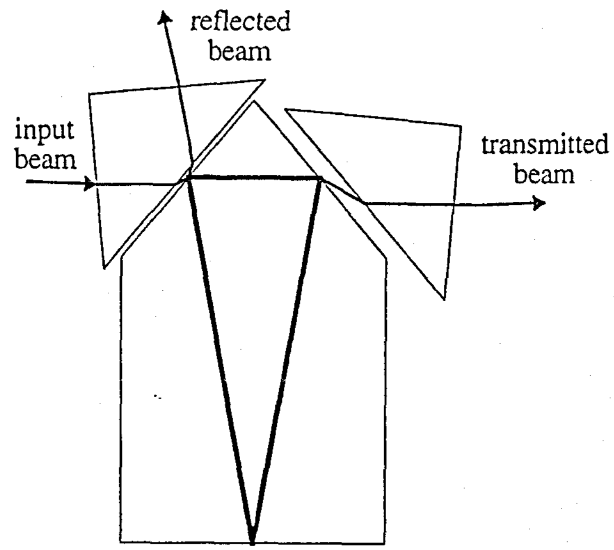

b)

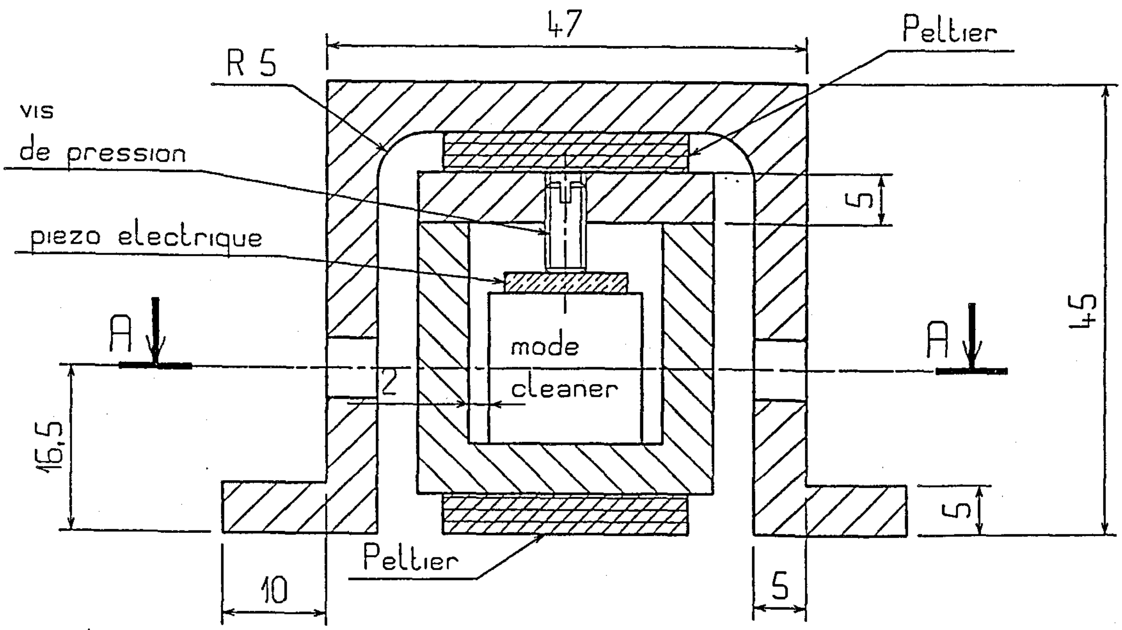

Fig. 4200.9 a) View of the output mode cleaner prototype. b) View of the mode-cleaner length control system. The error signal is obtained by pushing on the top of the mode cleaner with a small piezoelectric. Two Peltier cells are used to change the cavity temperature and so the cavity optical length.

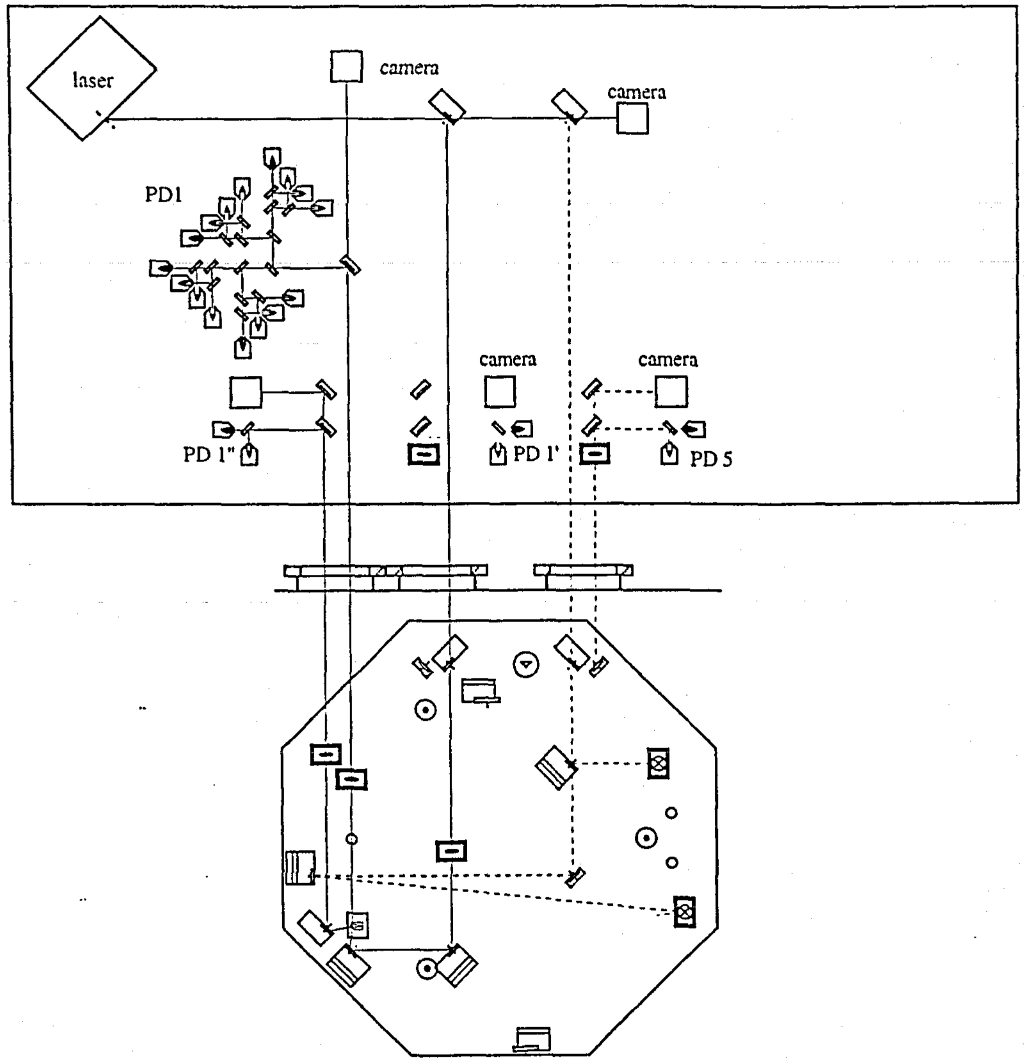

Fig. 4200.10 Test of the suspended bench: using a laser located on the external bench, two beams are injected inside the tower through the tower lateral windows.

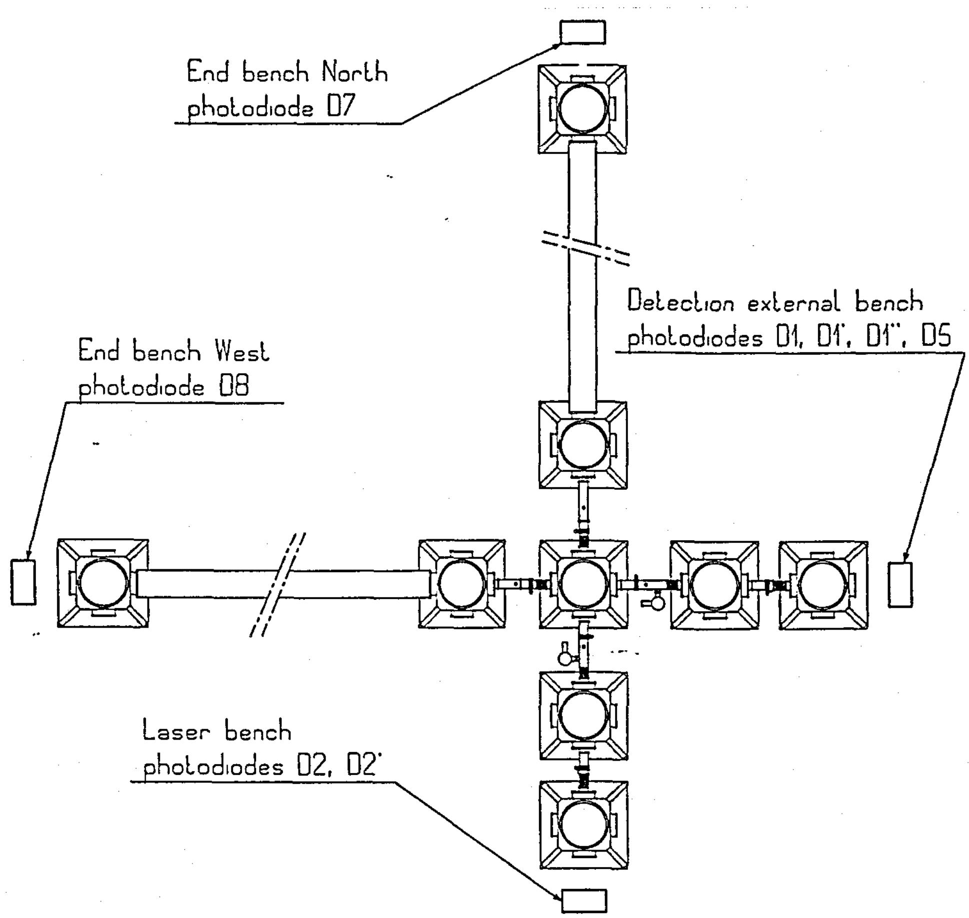

Fig. 4200.11 Location of the photodetectors used for the interferometer control.

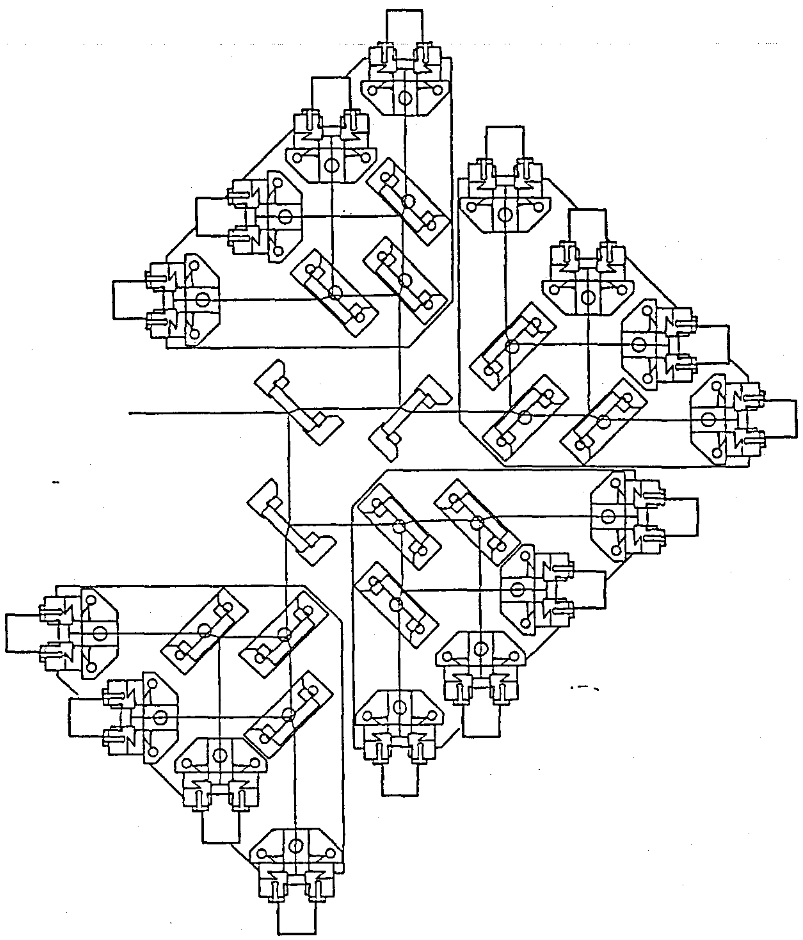

Fig. 4200.12 The photodetector D1. The incoming beam is separated in sixteen parts using fifteen splitters and sixteen photodiodes are used in parallel. One single lens placed in front of the splitters allows to focus the beam on the photodiodes.

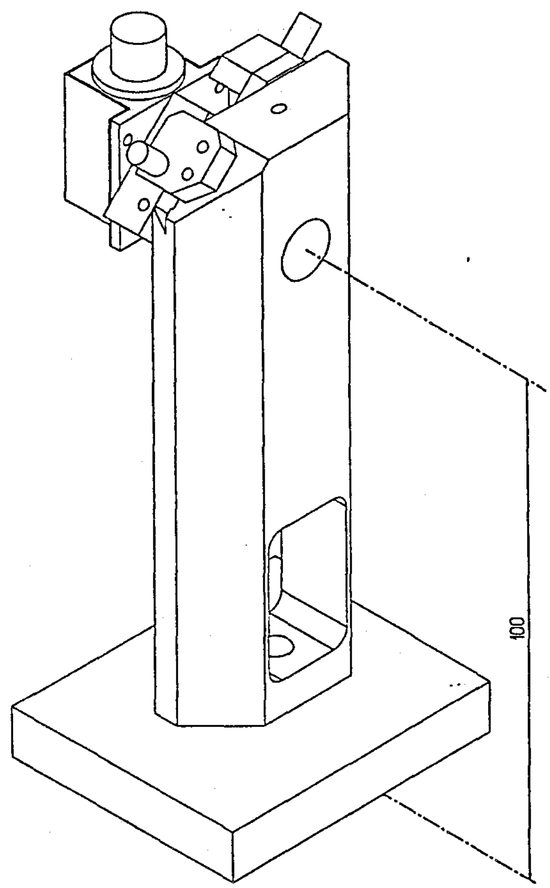

Fig. 4200.13 Perspective view of the photodiode support. The photodiode is located 10 cm above the bench.

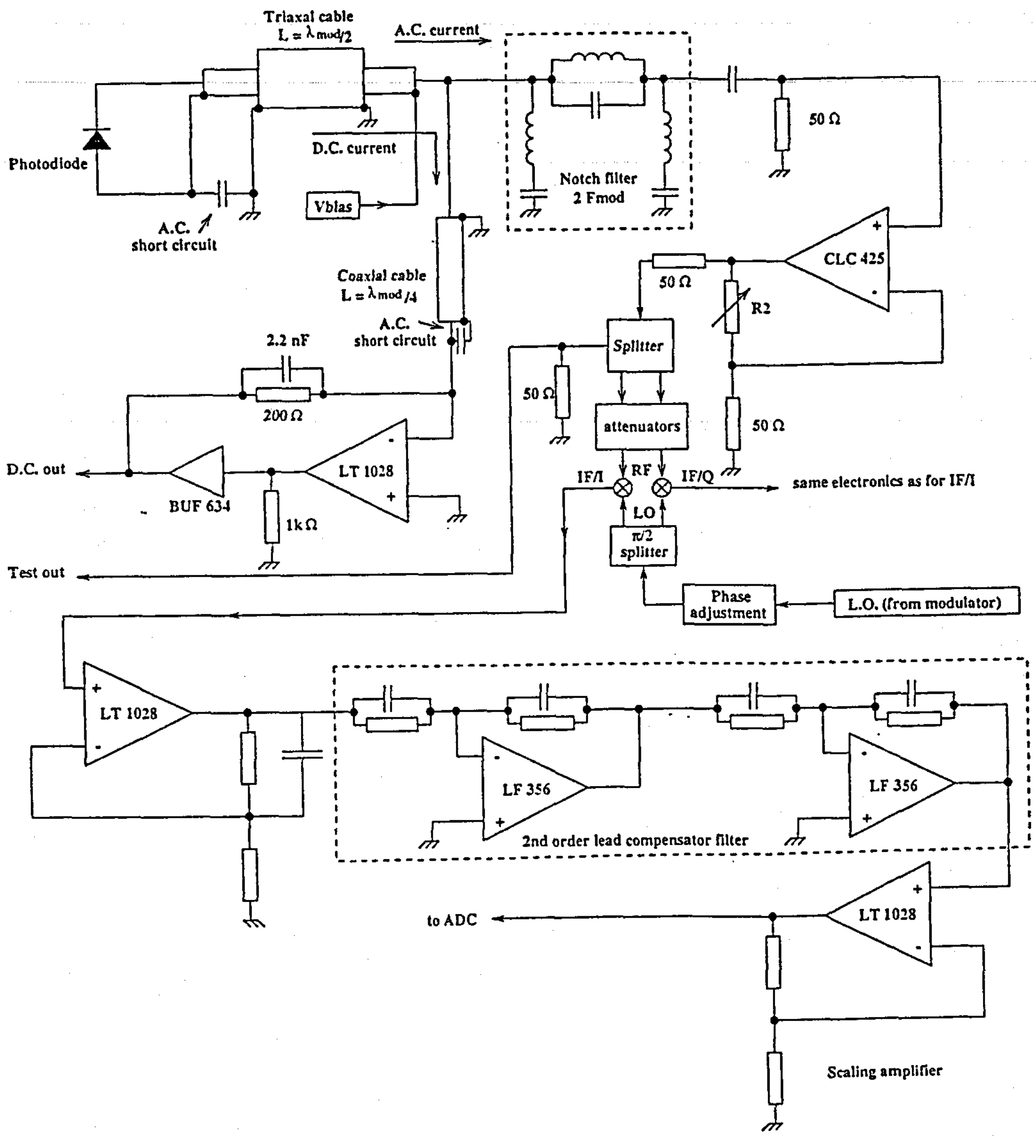

Fig. 4200.14 Schematic diagram of one electronic detection channel.

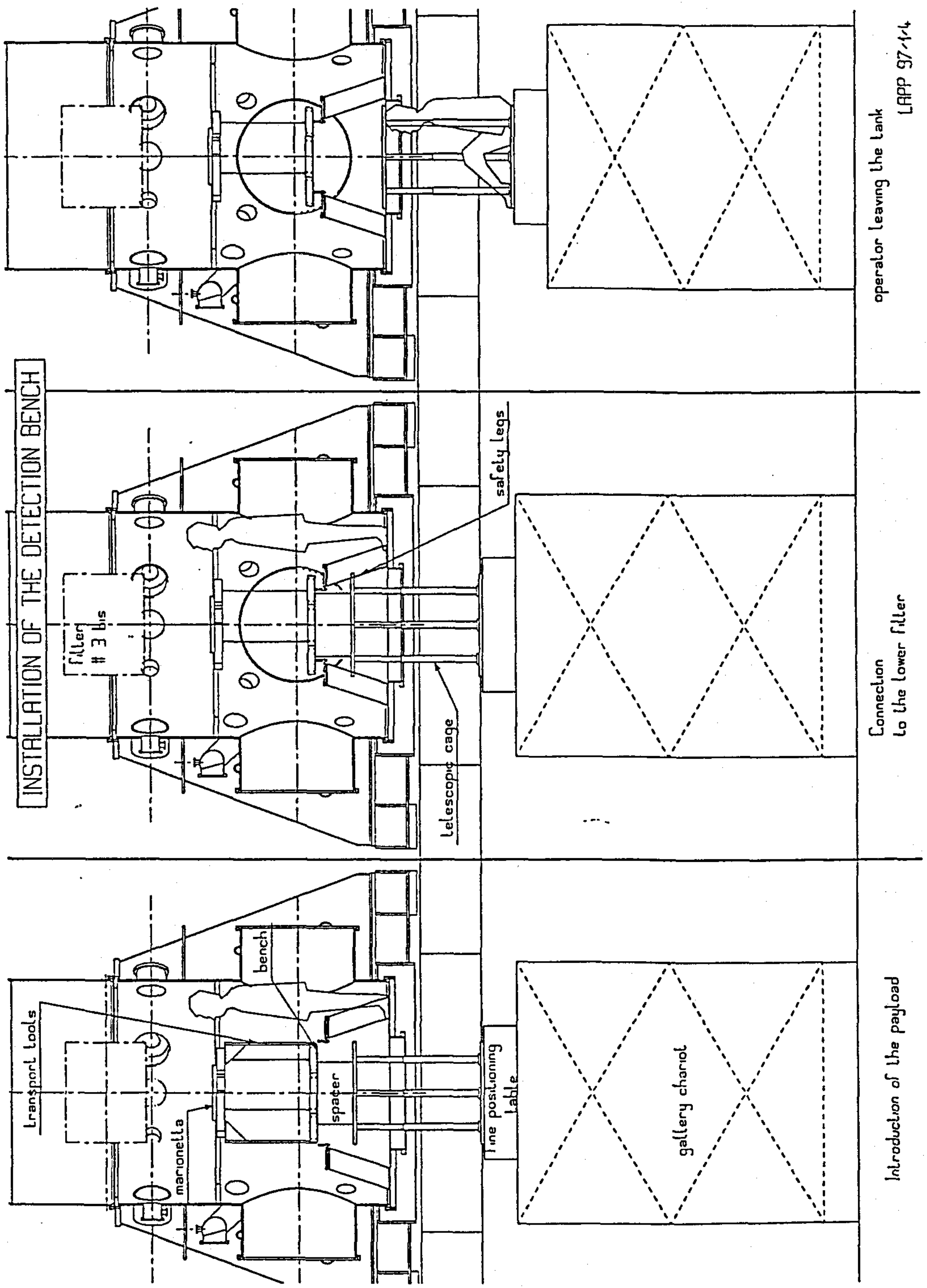

Fig. 4200.15 Scenario for the installation of the suspended bench inside the detection tower.

43. Large Mirrors

Table of Contents

43.1 Mirrors requirements

43.1.1 Test interferometer

It has been decided to build a short interferometer in 1998 to test all the sub-systems of Virgo. The interferometer is a simple Michelson formed by the recycling mirror M_R, the beam splitter and the input mirrors M_E. Different solutions concerning the size and the shape of the optical components have been studied; the chosen solution uses small substrates of 2 inches diameter (except for the beam splitter) instead of large substrates. Thus, the components can be made in the present D.I.B.S. coater in Lyon.

The requirements of the test interferometer components are summarized in the table 1 below. The substrate quality must be the same to the one we are using at the moment. The losses (absorption + scattering + wavefront losses) should be lower than 10 ppm.

The coating of the curved substrate (input mirror) is in fact not a technical problem. The problem is the feasibility for the polisher to obtain a substrate with the desired curvature R and with a good accuracy (the accuracy on the radius of curvature is ± 2-3%).

Table 1 : Virgo test interferometer optical components requirements

Component	M_R	M_{E1} , M_{E2}	B.S.
SUBSTRATES			
Material	SUPRASIL 312	SUPRASIL 312	SUPRASIL 311 sv
Diameter (mm)	50	50	230
Thickness (mm)	20	20	55
Shape Side 1	Flat	Concave R = 93 m	Flat
Shape Side 2	Flat	Flat	Flat
Wedge	0.3 +/- 0.075 mrad		1+/- 0.075 mrad
Incident angle	0°	0°	45°
Losses (abs.= scat.)	1 ppm		
Substrate Surface Deformation	compatible with coated surfaces requirements		
COATINGS			
Coating diameter (mm)	40	40	50
Losses (abs. = scat.)	1 ppm		
Coating Side 1 (S polarization)	AR $R<10^{-3}$	HR. $10^{-5}<T<10^{-4}$	T = R = 0.5 +/- 0.005
Coating Side 2 (S polarization)	R = 0.985		AR $R<10^{-3}$
Surface Deformation Side 1	TBD	TBD	λ/70 rms. on Ø = 7 cm*
Surface Deformation Side 2	TBD		TBD

* assuming a roughness power law $z(f)\propto f^{1.7}$:where z is the height [m] and f the spatial frequency [m^{-1}]

43.1.2 The Virgo interferometer

The requirements for Virgo optical components are listed below (Table 2).

Table 2 : Virgo optical components requirements

Component	M_{X1} , M_{X2}	M_{E1} , M_{E2}	M_R	B.S.
SUBSTRATE S				
Material	HERASIL 1 TOP	SUPRASIL 312 sv	SUPRASIL 312 sv	SUPRASIL 311 sv
Diameter (mm)	350	350	120	230
Thickness (mm)	200	100	30	55
Shape Side 1	Concave R = 3450+/- 100 m	Flat	Convex R = 4-5 m	Flat
Shape Side 2	Flat	Flat	Flat	Flat
Wedge		TBD	N/A.	1 +/-0.075 mrad
Incident angle	0°	0°	0°	45°
Substrate Surface Deformation	compatible with coated surfaces requirements			
COATINGS				
Coating diameter (mm)	280	100	100	200
Coating Side 1 (S polarization)	H.R. R>0.99995 T > 10 ppm	AR $R<5\times10^{-4}$	AR $R<5\times10^{-4}$	T = R = 0.5 +/- 0.005
Coating Side 2 (S polarization)		R = 0.88	R = 0.92	AR $R<10^{-3}$
Side 2 surface pairs equality	TBD	$\Delta R< 0.001$	N/A.	N/A.
Losses (abs. = scat.)	<5 ppm	<5 ppm	TBD	TBD
Surface deformation Side 1	$\lambda/120$ rms. on $\varnothing$ = 10 cm*	TBD	TBD	$\lambda/70$ rms. on $\varnothing$ = 7 cm*
Surface deformation Side 2	TBD	$\lambda/120$ rms. on $\varnothing$ = 4 cm*	$\lambda/70$ rms. on $\varnothing$ = 4 cm*	TBD

* assuming a roughness power law $z(f)\propto f^{1.7}$
where z is the height [m] and f the spatial frequency [m^{-1}]

The ESPCI group will be in charge of testing the quality of the large optical pieces which are passed through by the light beam and which will be used in the final antenna. The main test will be : homogeneity of the refractive index, local defects, birefringence, absorption losses for the silica substrates. Direct contact with European and American glass companies will continue during the various phases of the project in order to get state of the art materials.

To be able to realize such large samples, new facilities have to be built in Lyon.

At first, a new plant must be built with all the facilities needed for the process (clean areas class 1, D.I. water, gas).

Secondly, a new large coater must be designed to be able to coat such large samples. The cleanliness of the large substrates before deposit is also a crucial point. So, a new large wet cleaning machine is needed.

At last, a new metrology, a handling and packaging method have to be developed for the large components.

Concerning the metrology, the major task of the ESPCI group is to build the corresponding equipment to be installed in Lyon with a scale matching the Virgo mirrors. If most of the difficulties have been overcome, there is still work on the wavefront control which will be coupled to the large coater where the corrective coating will take place and which will take advantage of the handling and moving systems of the coater.

43.1.3 Present results

Table 3 : Virgo final optical components and test coatings performances

Component	M_{X1} , M_{X2}	M_{E1} , M_{E2}	M_R	B.S.
SUBSTRATE S				
Diameter (mm)	N/A.		230	
Thickness (mm)	N/A.		56	
Wedge	N/A.		1 +/- 0.2 mrad	
Substrate optical thickness homogeneity	N/A.		<λ/200 rms on 10×10 cm^2	
Point defects	N/A.		not visible in the B.S. volume	
Birefringence	N/A.		<0.7 mrad on 2×2 cm^2 (center)	
COATING				
Coating Face 1 (S polarization)	H.R. R>0.99995 on 20 cm^2 T > 10 ppm		AR $R<10^{-3}$ on 20 cm^2	
Coating Face 2 (S polarization)	AR $R<10^{-3}$		N/A.	
Scattering	1 ppm on 5 cm^2			
Absorption	1 ppm on 5 cm^2			
Surface Deformation Face 1 coated Pick to valley (nm)	14 nm on 70 mm diameter			

43.2 General Description

43.2.1 Virgo optical components

43.2.1.1 Substrates

As it is mentioned in the Virgo requirements, the nature of the bulk material of all the optical components has been chosen:

- SUPRASIL 311 SV form Heraeus for the beam splitter
- SUPRASIL 312 SV from Heraeus for the input mirrors and the recycling mirror
- HERASIL 1 TOP for the end mirrors.

The blank material for the Virgo interferometer will be ordered at the beginning of 1997.

The beam splitter has already been purchased because it will be used in the 1998 test interferometer. The polishing was made by Research Electro-Optics (R.E.O.). This silica substrate has been tested at ESPCI : the requirements on the birefringence, on the flatness seem to be satisfied.

Except for the beam splitter, the choice of the polisher has not yet been done. A list of the manufacturers capable of doing micropolished substrates can be performed : the French companies REOSC, SFIM and SAGEM, R.E.O., PERKIN-ELMER, ITEK OPTICAL from the Litton group, ZEISS. For this part, a call for tender will be done.

Because the polishing quality has a strong influence on the scattering level, we have fixed very strict requirements on the polished surfaces :

* RMS roughness : < 0.4 Å (measured with the "Micromap" system)
* Surface deformation : < 10 nm rms.

We have tested the polishing quality of 1 inch silica substrates coming from the french companies mentioned above.

Some of them are able to obtain on 1 inch diameter the requirements on the microroughness. But, unfortunately, there is still some big defects (scratches) which are detrimental to the scattering level. These defects are totally absent on the REO substrates up to a diameter of 80 mm.

Moreover, there is always an interrogation point concerning the polishing delay. We do not know at the present moment if it can be respected.

The ESPCI group is in charge of the large polished substrates control to see if the specifications and the requirements are respected : homogeneity of the refractive index, birefringence, absorption losses of the silica but also control of the microroughness and the flatness.

To avoid problems of manipulation by too many people, it will be easier and safer in the future to do these controls in Lyon, near the large coater and the cleaning station, because all the infrastructure (essentially the white rooms) will be in place.

If the polishing requirements are not satisfied, a new polishing will be asked.

43.2.1.2 Coatings

After having checked that the substrates have the good specifications, we have to prepare them for the coatings.

* Because of their weight, new tools have to be developed to handle them the right way. To do so, we will get informations from people who are used to manipulate large telescope components (REOSC, MATRA, SESO).

* Concerning the cleaning, a prototype of a wet cleaning station is under test. A lot of technical problems have occurred leading to a waste of time. Thus, we are still waiting to perform some tests to validate the process. Nevertheless, we have learned a lot and it will be easy to avoid these problems for the future large cleaning system which is the only way to clean big substrates.

The cleaning station needs ultra pure water which is heated during one part of the process. A special care should be taken for a high power line of the ultra pure water heater; indeed, this equipment will need about 200 kW for a very short time.

* The optical losses (Absorption + Scattering + Wavefront losses) of each Virgo component must be lower than 10 ppm..

The scattering will be measured on the real pieces (a new sample holder will be purchased for the CASI).

The absorption will be measured on small test samples which will be put on several places of the coater sample holder. A reflection and transmission measurement will also be performed.

* A large oven will be purchased to stabilize thermally the mirrors.

* Before shipping the coated components, they will be cleaned once more and packaged in a box that will conserve the cleanliness of the sample during the transportation. We have already realized some metallic boxes which gave good results.

43.2.2 Deposition process

The technology required for the Virgo optical components coatings, whose specifications are very severe, is the one used in the gyrolaser applications: the reactive Dual Ion Beam Sputtering (D.I.B.S.). The deposition technique leads to dense (near bulk density) and very stable films (no columnar microstructure).

43.2.2.1 D.I.B.S. deposition process

In the D.I.B.S. process, we use a broad-beam Kaufman ion source or equivalent which generate a spatially well defined , monoenergetic (between 700 and 1300 eV) and positive ion beam to sputter the material (Target) we want to deposit. This beam (argon ions or noble gas ions) is neutralized a hot tungsten filament or others electron sources such as a plasma bridge neutralizer or an hollow cathode.

The neutralization has two purposes. At first, it prevents the substrate and the target from discharge as we are using dielectric materials. Secondly, it prevents beam spread by repulsion between ions. The sputtering ion beam has an elliptical cross-section to minimize the ellipticity of the beam footprint of the tilted target.

The planar sputtered target (Silicon dioxide, Tantalum, Tantalum pentoxide) is tilted so that the ions coming from the source are incident at an angle of approximately 60° to maximize the sputtering yield of the target. The purity of this target is a crucial point and it should be as high as possible to prevent the layers from contaminations.

A second ion source, directed to the substrate, is used to control the stœchiometry of the growing film with oxygen ions. This source is equipped with an appropriate grid to permit the generation of low energy ions (50-100 eV).

An other important point in the D.I.B.S. process is the size of the coater where the base pressure ranges from 10^{-7} to 10^{-8} Torr : the box coater has to be large to prevent contaminations from interactions between ions and the walls. Thus, the size should be well adapted to the diameter of the substrate.

Moreover, the chamber geometry must be designed to avoid gas phase interactions for a given working pressure (between 1.10^{-4} to 4.10^{-4} Torr). So, the atoms sputtered from the target reach the substrate with a very low energy loss.

43.2.2.2 D.I.B.S. process justification

A comparative study (Electron gun evaporation, Ion assisted deposition, R.F. diode deposition) has been done and it has shown that only the D.I.B.S. process is able to provide very low losses.

The losses are due to absorption and scattering : the absorption can be reduced between 5 to 15 ppm for all the techniques but the scattering remains high (100 - 300 ppm) for these techniques except for the D.I.B.S. (5 - 50 ppm). This latter point is the key of our choice. By decreasing the losses, higher reflectance values are achievable.

Moreover, the layers realized with the D.I.B.S. technique have special properties which result from their very low porosity : we can mention for example a high thermal stability, scratch and flux resistance.

As the deposition speed is low (a few Å/s), it is easier to monitor the thickness homogeneity, to control the growing structure and the layer composition. Nevertheless, to be able to obtain low loss samples, the environment around the deposition chamber must be very clean to keep the dust particles to a minimum : the elaboration, the characterization, the transportation and the mounting of the Virgo components has to be done in clean conditions, typically in class 10 or better.

43.2.3 State of the art

Until now, we have undertook a R&D study to improve all the performances of our coatings. Moreover, the ESPCI group develops tools to allow optimizing the coatings fabrication in order to reach the required goals.

To be able to do that, some equipments have been built or developed to characterize :

- the scattering and the transmission value (CASI scatterometer @1064 nm from TMA).
- With this system, mappings are also possible. To do accurate and sensitive measurements, a clean environment (class 1) has been required.
- The absorption (photothermal absorption measurement system @1064 nm)
- The cleanliness (particle counter); this point can also be evaluated with a scattering measurement. The two methods are totally complementary and very sensitive.

43.2.3.1 The scattering level

Over the entire surface of the sample, we have reached @1064 nm an average scattering level close to 1 ppm on 80 mm diameter mirrors (0.6 +/- 0.1 ppm). Thus, all the eventual point defects are included. Consequently, this is a very realistic value. This improvement (about 20 times compared to the best available performance 5 years ago) is due to several factors.

The first one is the use of new micropolished silica substrates from REO (Research Electro-Optics) which have neither scratches nor digs (the RMS microroughness is lower than 0.3 Å).

The second factor of improvement is linked to a new cleaning technique which guarantees a very low particles contamination level. But, to preserve the cleanliness, all the sample manipulations must be done under class 10 or better environment : this is a crucial point.

43.2.3.2 The absorption level

The mirror absorption level @1064 nm is now 0.5 +/- 0.1 ppm on 80 mm diameter. To reach this low value, an improvement of the deposition process has been done to reduce the layer contaminations which controls the absorption level. To converge and find the best solution, some S.I.M.S. (Second Ion Mass Spectrometry) and E.D.S. (Energy Dispersive X-ray Spectrometry) analyses have been done routinely.

43.2.3.3 Centering of mirrors and AR coatings

A multidielectric mirror only reflects the light on a small domain of wavelength (typically 200-250 nm wide) with a high efficiency. The middle of this band corresponds to the centering wavelength which must be 1064 nm in our case. The centering of the coating at the good wavelength (1064 nm) is another important point we have studied. It is directly related to the absolute thickness of each layer. It controls the optical performances of the coating and, particularly, the transmission loss of the mirror.

A new centering method has been developed which allows us to guarantee now a difference between the experimental and the desired centering wavelength of less than 5 nm. Thus, the transmission variation is quite negligible.

The problem of centering is more critical for AR coatings, because the number of layers is less and the useful bandwidth is smaller.

Thanks to very low absorption and scattering losses, high reflectance values can be achieved (R>99.995 %) and, for antireflective coating, we can also have good optical efficiency ($R<10^3$) if we monitor precisely each monolayer.

43.2.3.4 The thickness uniformity

The coating homogeneity is critical for the wavefront preservation in the interferometer. This point is evaluated with a ZYGO Mark IV xp (λ = 633 nm) which is now in Lyon. This system has been tested preliminarily at ESPCI. It has been demonstrated that the reproducibility of the measurement is 4 nm if great care is taken in the positioning of the optical piece.

A simulation program has been developed to optimize the thickness distribution of the coatings by changing the sample holder and the target angles. Moreover, a new sample holder, which has a planetary motion, has been built. This leads to an homogeneity on monolayers of 8.10^{-3} on 2 inches. On 80 mm diameter mirrors, a uniformity of $\lambda/40$ (λ = 633 nm) peak to valley on 25 mm and $\lambda/10$ peak to valley on 70 mm has been reached (note : this value has not been obtained with the best angle conditions).

Moreover, with the ZYGO Mark IV, we have evaluated the mechanical stress of our coatings which has an important role on the wavefront shape.

43.2.4 Coater : Technical description

In order to minimize the asymmetry between the arms of Virgo, the large coater must be able to coat two 350 mm diameter silica substrates at the same time. The two components must have the same optical properties which satisfy the Virgo requirements.

We have defined the needs and the technical specifications concerning the two following parts :

- Sample holder, target holder
- Vacuum chamber

After a first call for companies able to do the work (September 1996), a first choice has been made. Then the definitive call for tender will be done for these two parts. We will follow up the realization of each part.

In the following paragraphs, we make a technical description of the main parts which compose the large coater.

a) The shape of the coater has not yet been frozen : it can be a cylinder or a parallelepiped (2.5 - 3 m). The first solution is the best to reduce the weight of the system : it can be decreased by a factor of 30 %. Nevertheless, we are used to work with parallelepipedic coaters and we have a great skill on this kind of systems. Moreover, it is easier to install all the coater parts in such a vacuum chamber.

b) Presently, we are using an ion source with hot filaments. It cannot be the same in the future coater because of the short filament lifetime ($\approx$ 30 hours). Indeed, in the large coater, the process will last at least one hundred hours.

The solution of this problem is to use a Radio-Frequency (RF) ion source. But our main interrogation is to know if this source is able to work hundreds of hours without any drop out. Thanks to R.E.O. informations, we know that, on the one hand, the Oxford source does not work well during a long time and that, on the other hand, REO people are very satisfied with the IonTech RF ion source.

Moreover, people from Ion Tech told us that they solved that by putting a third grid on their source to protect the two active grids.

There is another alternative to the RF source : this is the Hollow Cathode. It has been demonstrated (R.E.O.) that the couple Hollow Cathode (to sputter) and the Plasma Bridge Neutralizer (to neutralize the beam) is working well during very long runs. The drawback of the Hollow Cathode is that the spare parts are very expensive and that they must be changed very often.

Then, it seems reasonable to choose the IonTech RF ion source.

The sources size will be quite small (about 20 cm) because larger sources (40-50 cm) are not enough reliable and also because they are only used for etching. These sources will be water cooled.

We are developing a new coating simulation program to determine the number of ion sources in the large coater. A real coating in the future large coater can be simulated; thus, if the deposition rate with one source is too small, two sources will be eventually used in parallel to obtain process time which are acceptable.

c) Concerning the targets, their size should be the double of the source size (about 40 cm). In our small coater, high purity targets are used (99.99 %). It should be the same quality for the larger ones. We have to check if the target manufacturer can provide high purity materials, whatever the size we will choose, to minimize the layers contamination.

d) The primary vacuum (up to 10^{-2} Torr) will be achieved in 30 minutes with two oil free groups (roots + dry pump); the base pressure (about 10^{-7} Torr) will be obtained in 4 hours with two cryopumps. These calculations have been done for a 2.5 meters cubic chamber.
The chamber walls are electropolished; the coater will also have double walls to make the cleaning of the system easier. At last, to suppress water vapor in the chamber, a Polycold™ will be used in vacuum.

e) To control the process in-situ, we will only use a quartz balance which is a very reliable system. In our present chamber, we are using only one quartz. Probably, in the future coater, several quartz, put at different places of the coater, will be used to increase the accuracy of the control.

f) A general control command system, which controls in real time the entire deposition process, will be purchased. This kind of system is already manufactured by some companies and it is working well.

g) On one door of the coater will be placed the robot which will support the silica substrates. It will have an "intelligent" robotic motion. The final scheme of this system will depend on the result that we will get with the small robot and also on the capability we will have to transpose the technology used for the small robot to the large one.

The procedure that will be used to achieve to the wavefront specifications is this one :

* The multilayer coating will be realized and will be stopped at the right moment before the end ((HB)n H 0.7B).

* Then, the sample will be annealed before making the wavefront metrology (indeed, the major part of the layer stress will be relaxed).

* Then a small correction will be done to planarize the surface by adding a very thin SiO_2 layer.

At this moment of the deposit, it will not be necessary to anneal again the sample to compensate the absorption increase due to the corrective layer.

43.2.5 Wavefront correction

The wavefront preservation is a priority at the moment because the Virgo requirements on the maximum wavefront deformation are not yet satisfied. A simple planetary motion is not enough.

That is why a small robot has been built. To pilot this system, a software has been developed to allow any movement of the substrate. Moreover, the maximum size of the substrates that can be coated is 100 mm diameter.

An other advantage of this system is that the distance between the substrate and the target is greater. This is a more favorable case to homogenize the layer thickness.

Nevertheless, this system alone is not sufficient to reach VIRGO requirements. The use of masks between the substrate and the target is a solution : it gives good homogeneity results on monolayers (for example, homogeneity of 6.10^{-3} on 80 mm diameter for SiO_2 monolayers). But to reach the Virgo requirements, a planarization method must be used.

The principle of this method, called 'Corrective Coating Treatment', is to add a small amount of SiO_2 (maximal thickness 900 Å) through a hole (square, circle) on the last SiO_2 layer of the multilayer stack. This treatment is possible thanks to our small robot.

The addition of silica produces a phase retardation . We follow the phase variation with the Zygo interferometer to find a wavefront shape as plane as possible. The correction is fully automated thanks to a software we have developed.

The first results obtained are hopeful : on a 80 mm diameter mirror, the wavefront goes from 40 nm to 14 nm peak to valley.

To validate this method, we checked that the absorption and the scattering losses are not locally deteriorated by the deposition of a small amount of SiO_2 on the last layer. It has to be emphasized that the correction must come after the thermal treatment of the sample : indeed, it stabilizes the optical performances and relaxes the constraints which modify the wavefront.

The addition of silica also modifies the residual transmission of the mirror. The transmission increase can be compensated by increasing the number of doublets of the multilayer stack.

The same principle will be used for the large mirrors in the future large coater.

43.3 Metrology

43.3.1 Goals

The aim of Virgo metrology is :

* To help to improve the fabrication process during the R and D period of the project (for instance to reduce scattering and absorption losses, residual stresses in the coating, etc...) ;

* To settle a set of -mostly new- set ups for measuring with the required high level of accuracy the performances of the mirrors (See table 1 and 2: substrates and coated optics) ;

* To establish a simulation code able to provide the signal to noise degradation level with reference to shot noise by taking into account the actual mirrors characteristics.

43.3.2 Blanks Metrology

43.3.2.1 Silica Absorption

In order to avoid thermally induced wavefront distortions in Silica the absorption level must be maintained to a level of the order of 10^{-6} cm^{-1}. A quasi collinear Mirage bench (photothermal deflection) have been constructed and coupled to a powerful (30 W) cw Nd-YAG Laser.

The noise of this set-up corresponds to a absorption level of 10^{-7} cm^{-1} and reach the required Virgo goals.

Herasil 311SV and 312SV (Special Virgo) were found to be in the range 1ppm/cm, the main factor of absorption in silica is due to OH content which has been reduced to a concentration level lower than 50 ppm by atmosphere controlled preparation and probably by further annealing.

43.3.2.2 Bubbles and Local Defects

After polishing there is a need to explore the full volume of the optics which will be crossed by the laser beam in the Virgo interferometer.

The scanning system uses two non parallel split laser beams, balanced in power, which cross the optical pieces and are alternatively set on and off. The scattered light associated with one beam at a specific point is recorded with a photomultiplier and correlated with the signal corresponding to the second beam.

Lock-in detection provides a clear "signature" of such correlated signals with exhibits equal amplitude and opposite sign. The spatial shift between these signals provides the information of the scatterer position in depth. The magnitude of the signal provides the order of magnitude of the scatterer cross section.

43.3.2.3 Birefringence

The birefringence of the optical pieces crossed by the beam is responsible of losses which affects the sensitivity of the antenna when its level is larger that 10^{-4} rd/cm.

It is worth underlining that the companies which provides silica can only guarantee a birefringence "lower than 10^{-3} rd/cm" because they do not have instruments sensitive enough to characterize it at a lower level.

The bench we have built uses the same scanning system of the mirror (horizontal) and of the measuring bench (vertical) which is used for local defects and wavefront distortion. The principle of the measurement is to add to the static birefringence which has to be measured, a controlled periodic birefringence induced by a photoelastic modulator. Between cross polarizers DC and AC signals (lock-in detected) allow a precise measurement of the phase shift between the two orthogonal polarisations associated to the polarizer and analyzer.

We perform two measurements by rotating (45°) the bench in order to get a map of the birefringence value and of the directions of the principal axes. The sensitivity is better than 10^{-4} rd/cm.

43.3.2.4 Wavefront control in transmission

The optical pieces which must be controlled in transmission (beam splitter and input mirrors) being parallel plates, their translation do not introduce any rotation of a probe beam crossing them. So the probe beam deflection can only be due to the gradient of the optical path distribution.

Usually in order to reconstruct the wavefront one has to integrate the measurement along e.g. a diameter. This integration introduces cumulative errors which reduce the accuracy of the measurement.

Because such measurement carries more information than required for a simple integration, it is possible to use an iterative algorithm (close to the one used in the Shack-Hartman and adaptive optic control interferometers) which does not propagate the errors.

The accuracy over 100 cm^2 is $\lambda/65$ pv which is enough for the optical pieces mentioned above.

43.3.2.5 Surface polishing and scattering

The scattering will be controlled either by a direct measurement of the scattered light angular distribution or by direct measurement of the roughness the corresponding instruments will be described in the next part (coated optics).

43.3.3 Coated Optics Metrology

43.3.3.1 Absorption

Since the beginning of the R & D of Virgo, few "mirage benches" have been used to control the absorption level of various coatings made either by the best companies in the field or by the Virgo group in Lyon (SMA). For coated silica the sensitivity with one watt of power on the coated surface is of the order of a few (typically 5 to 8) 10^{-9} (a few parts per billion of the incident power left in the coating) which is enough not only for measuring the required losses (1 ppm) but also to check the homogeneity of such absorption losses.

43.3.3.2 Reflection coefficients homogeneity and equality

As mentioned before in the description of the interferometer, the symmetry of the two arms is an important goal for Virgo.

Moreover working at the dark fringe imposes a good homogeneity of the reflection coefficients of the mirrors (mainly the input mirrors). The required sensitivity is of the order of 10^{-4}, which excludes any kind of direct photoelectric measurement.

For this reason, we have built a differential measurement bench in which a beam strikes alternatively the surface under examination and a reference surface whose reflection coefficients are close. The differential signal reflects the difference between the two coefficients (typically less than 1%) and a measurement in the 10^{-2} range is enough to reach the required sensitivity (we have reached 5 10^{-5} with a small scale set-up during the R & D period).

43.3.3.3 Wavefront in reflection

During the R & D period two systems were used :

- A commercial Fizeau interferometer @0.633 μm has been extensively used to improve the fabrication process (mainly in term of residual stresses which distort the surface) and to validate the "corrective coating" approach for the Virgo mirrors.
- A slope based system working by scanning the mirror surface and using a reference beam for compensation of the tilt of the scanning system gave the required sensitivity for the small optics of the test interferometer (less than 10 nm over 10 cm).

For the large mirrors of Virgo two solutions are currently explored in parallel in order to avoid any risk in such a crucial measurement :

- Commercial Fizeau (or equivalent system) @1.06 μm exists and can handle (without expanders) 15 cm diameters optics. With such systems and a careful calibration of the reference surface (using e.g. multiple 3-flats methods) we can achieve the required λ/100 pv sensitivity. Such system providing a fast control will be used for finalizing the corrective coating procedure @1.06 μm.

- A slope based system which is an improved version of the one describe above, will be used with a new improved algorithm which does not propagate the errors. Let us underline that for a system working in reflection only one slope direction can be made independent of the scanning system and the Shack-Hartman algorithms are no longer able to provide the proper results.

43.3.3.4 Roughness and local defects

The quality of the coating has been improved so much during the R&D period that structural imperfections are now at undetectable levels, so the scattering is now only due to local defects which can be induced during the polishing period or during the coating deposition period.

For this reason VIRGO needs a tool which allows a complete mapping of the substrates and coated optics with a few picometers in sensitivity.

Such instruments start to be commercially available and will be used in VIRGO in 1997.

44. Alignment

Table of Contents

44.1 Alignment functions and concept

The non-linear alignment, starting from a mechanical pre-aligned state (order of a millimeter), has to bring the interferometer mirrors in a coarse aligned state (at the level of a few microradians), sufficient to start the longitudinal locking.

After this is achieved, the linear alignment can start and should be able to reduce the alignment errors of each mirror down at the nanoradian level.

The system of position memories, based on the use of small auxiliaries lasers and CCD cameras, will continuously monitor the position of the mirrors in six degrees of freedom with an accuracy sufficient to bring back the interferometer, if for any reason the locking is lost, in a state where longitudinal locking and linear alignment can be started again.

44.2 Requirements applicable to alignment

Requirements for the Non linear alignment and related position memory system:

The requirements concerning the position of the optical elements of the interferometer after the non linear alignment phase are the following: $\theta_{x,y,z} = 2\ 10^{-7}$ rad, x and y $= 1\ 10^{-4}$ m and z= $1\ 10^{-6}$ m.

Requirements for Linear Alignment :

The system shall be able to detect misalignments of any Virgo mirror of the order of 10^{-10} rad/$\sqrt{\text{Hz}}$.

44.3 Alignment interfaces

44.3.1 List of alignment interfaces

The alignment sub-system will have physical interfaces and/or interactions with the following sub-systems :

1- Towers (3300)
2- Laser & input bench (4100)
3- Detection bench (4200)
4- Mirrors (4300)
5- Global control (5100)
6- Data acquisition (5400)

44.3.2 Interface with sub-system 3300

The towers will be equipped with the specific optical benches of the position memories. The installation will be performed in Cascina just after the tower delivery on site. For the non linear alignment procedure one auxiliary window for each end tower is requested to monitor the direction of the interferometer beam transmitted by the end mirrors.

44.3.3 Interface with sub-system 4100

Following the proposed non linear alignment procedure of the bench, we will look at the reflected light from the recycling mirror onto a diaphragm screen set in vacuum on the input bench.

The set-up foreseen for the linear alignment requires the use of a pair of quadrant photodiodes on the beam reflected by the recycling mirror. These photodiodes, together with the associated telescopes, will be placed on the laser bench, on the beam from the interferometer transmitted by one of the mirrors constituting the input telescope.

44.3.4 Interface with sub-system 4200

A pair of quadrant photodiodes will be placed on the bench located in air after the detection bench on the beam reflected by the second surface of the beam-splitter.

44.3.5 Interface with sub-system 4300

The mirrors will be equipped with four spots on the border out of the coated surface. These spots will be used for the position memories.

44.3.6 Interface with sub-system 5100

The global control will receive the digitised data of the quadrant photodiodes through the data acquisition, and has to reconstruct from them the misalignments of the mirrors. The linear alignment group will provide all the informations required to perform this reconstruction.

44.3.7 Interface with sub-system 5400

Each of the 8 quadrant photodiodes (4 pairs) used for linear alignment, will produce 8 output signals to be read by ADCs :
- one per each quadrant directly,
- vertical and horizontal differences, demodulated in-phase and in-quadrature.

For all these signals, a reasonable sampling rate can be ≈ 100 Hz.
The data acquisition group will be responsible for the acquisition of these signals.

44.4 Non linear alignment

44.4.1 Non linear Alignment function and concept

The pre alignment (initial alignment or non-linear alignment) is the procedure through which the Virgo interferometer is set in the range of operation of the control feedback (linear). The non-linear alignment is likely to be a crucial procedure which must be carefully designed to drive the interferometer set-up to the operating point. Then the occurrence of the pre alignment procedure in the sequence of passes of the Virgo setting-up is just in the middle between the geometric positioning and the automatic operation. Other items are closely related to the design of the pre alignment of the interferometer as follows:
- aspect ratio, size and design of mirrors (M_i; i=0,...,4) and reference masses (RM_i; i=0,...,4)
- control system of the marionette
- position monitoring and memory
- UHV compatibility.

The proposed procedure has to match all the requirements related to the above me mentioned items. The goal of the non-linear alignment is to bring the Interferometer to a level good enough to allow the linear alignment to start. This means that the angular errors of the mirrors have to be smaller than the angular divergence of the beam θ=17 µrad.

44.4.2 Non linear Alignment detailed description

The following hardware will be required in order to perform the pre alignment procedure

- 2 screens outside the vacuum.
- 1 screen/diaphragm on the injection bench.
- 4 sets of scattering spots on the FP mirrors.
- 4 blue lamps.
- 7 CCD cameras.

Two screens should be placed after the far mirrors of each FP, outside the vacuum. A camera will look at the spot on this screen due to the beam transmitted by the FP end mirror with respect to suitable reference markers. This requires that the far mirror of each FP has to have some finite transmittivity (for example 10^{-4}) constant over the mirror useful aperture. This requires vacuum window having the same diameter as the portion of the back side of the far mirror that can be seen through its reference mass (minimum diameter 20 cm). It is important to design a rigid stand for the these screens, steady with respect to the vacuum chambers (and then to the towers).

A screen (with a camera to look at it) on the injection bench with an aperture for the beam. This will detect the position of the beam reflected by the interferometer and will also protect the injection bench from the reflected beam when the misalignment is large. The design of the screen and the definition of the material is still matter of discussion. The screen surface will be machined in such a way to form a net which will be used to localise the spot from the data of the camera images. It has been proposed also to spray the surface of the screen with a material that re-emits the Nd-Yag laser light.

The four spot detection scheme developed at LAPP and tested by H. Heitmann is suitable to be implemented in the pre alignment hardware equipment. A good contrast must be reached using lamps equipped with infrared filters that permit to detect the position of the spots using the cameras.

- C_{M0} mounted on the recycling mirror tower, pointing at the rear face of the reference mass of M0;
- C_{M1} mounted on the near mirror tower along FP1 (see figure), equipped with a lens and monitoring M_1;
- C_{M3} mounted on the near mirror tower along FP2 (see figure), equipped with a lens and monitoring M_3;
- C_{M2} mounted on the far mirror tower along FP1 (see figure), equipped with a lens and monitoring M_2;
- C_{M4} mounted on the far mirror tower along FP2 (see figure), equipped with a lens and monitoring M_4;
- C_{S0} mounted on the injection bench tower, pointing at the diaphragm screen S_0;
- C_{S1} pointing at the screen outside the tower of FP1's far mirror;
- C_{S2} pointing at the screen outside the tower of FP2's far mirror.

It has been said that the angular divergence of the beam is $\theta_\infty = 17$ µrad.

Then, the CCD cameras have to monitor the spots of scattered light with the following precision:

- C_{M0}, $C_{S0} = 1$ mm
- C_{M1}, C_{M2}, C_{M3}, $C_{M4} = 1$ cm

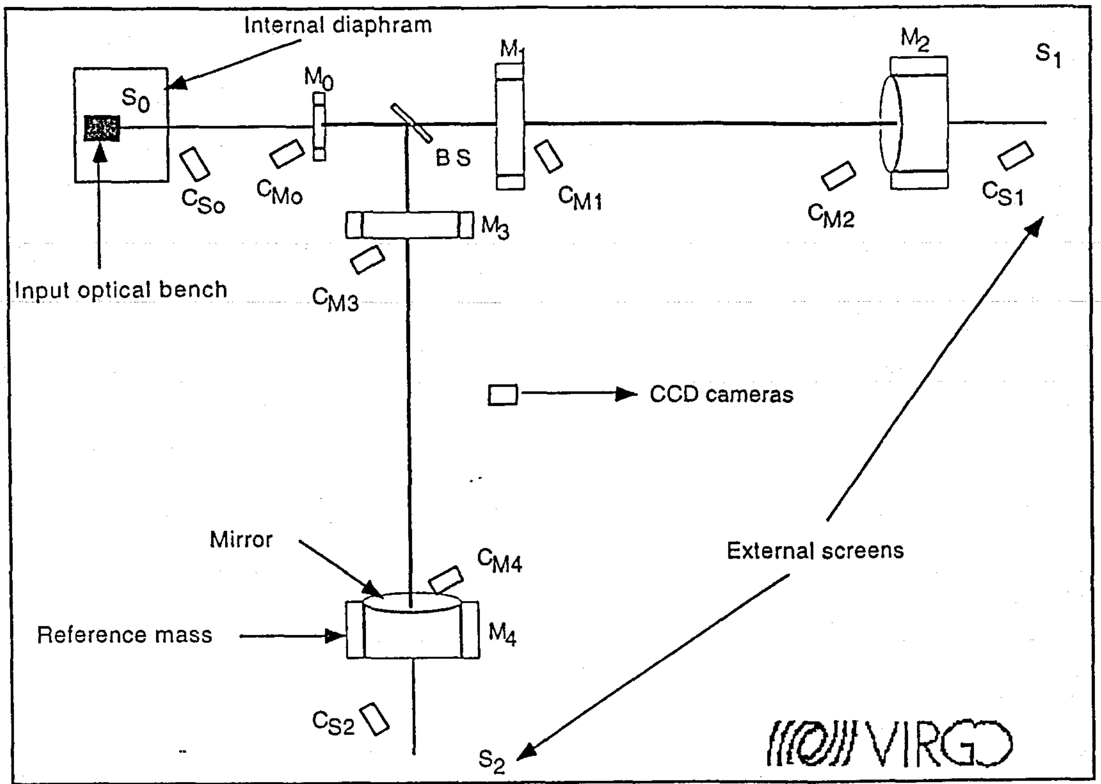

Figure 4400-1

The requirements for the calibration of movements (coarse) and for the optical memories (fine) are summarised in table 1. If these requirements are met, the accuracy on the alignment of all optical elements at the end of this non-linear procedure, should be of one or few μrad, thus allowing the automatic alignment to start.

	Range	Sensitivity	Step number
Injection			
Coarse	> ± 25 mrad	166 μrad	2
Bench			
Fine	± 200 μrad	3.3 μrad	5
Coarse	>± 25 mrad	166 μrad	3
M_0			
Fine	± 200 μrad	1.0 μrad	8
Coarse	> ± 25 mrad	100 μrad	11
Beam Splitter			
Fine	± 100 μrad	< 3.3 μrad	12
Coarse	> ± 12 mrad	80 μrad	4
M_1, M_3			
Fine	± 100 μrad	~1.0 μrad	8
Coarse	> ± 1 mrad	50 μrad	6
M_2, M_4			
Fine	± 100 μrad	<3.3 μrad	6

Table 1

44.4.3 Procedure

The first operation is the alignment of the injection bench. To do this it is important to centre first the beam onto the power recycling mirror M_0. This mirror is supposed to be surrounded by a reference mass RM_0 which has the same shape and size as the FPs' RMs. Suitable markers applied on the side of RM_0 facing the injection bench (rear) must diffuse λ=1.06 μm light or detect by screen remission in order to detect the injected beam when the bench is rotated about θ_x θ_y axes.

- **STEP 1**: Scan with the input bench centring the beam onto M_0 referring the beam spot to suitable markers on RM_0.

⇒ INPUT BEAM CENTRED ON M_0

In order to perform the alignment of the bench the reflected light from M_0 can be detected onto the diaphragm screen S_0 and to discriminate among the spots which are displayed there it is crucial to misalign the FPs' mirrors avoiding spurious reflections from the other optical elements of the interferometer.

Taking into accounts the distance between M_0 and each near mirror NM (M_1,M_2) and the full diameter (coated + uncoated) of M_0 we get the following request about the needed angle of misalignment:

θmisNM ≥ 5 10^{-3} rad

this angle must be compared with the largest mechanical rotation allowed by the coil-magnet configuration on the marionette and with the room available between the marionette itself and the roof that separates the UHV from the HV spaces. We have:

θ max. = 2 10^{-2} rad

According to the specifications of the electromagnetic actuators which act on the arms at the top of the marionette, in order to avoid the thermal noise due to the current driven into the coils, few t urn coils have been designed (coils with a number of turns N=400, a mean radius of the coil r =80 mm and made with a cooper wire of a diameter of 1 mm).

Then, considering the momentum of inertia of the marionette (for the torsional mode), an unreasonably high current should be applied to the coils (~ 20 A). There are two solutions to overcome this problem:

a) use of the motorised rotation stage which acts on clamping point of the marionette's cable of suspension.

b) use of another couple (at least one per marionette arm) magnet-coil actuators exerting a stronger force. According to the design of the UHV roof hypothesis b) seems more feasible.

Similarly we can deduce the misalignment required for the far mirror FM (M_2,M_4), getting $\theta_{mis}{}^{FM}$ ≥ 20 μrad. In this case the constraint is not crucial first because the FPs of the interferometers elements at this stage are supposed to be rather far from the aligned position, second being the required misalignment (20 μrad) attainable within the dynamics of the designed magnet-coil actuators.

- **STEP 2** Misalign near and far mirrors.

The first element which reaches a rough alignment is M0. This can be done by monitoring with camera C_{S0} C_1 the spot on screen S_0, due to the beam reflected by M_0, which must be driven into the diaphragm. The angular scan of M_0 is obtained by moving M_0's marionette.

- **STEP 3** Scan M_0 looking with C_{S0} at the spot on S_0, find the right position, leave it misaligned.

⇒ RIGHT POSITION OF M_0 STORED

At this point a rough alignment of M_1 is reached following the spot of the reflected beam onto S0. Since M1 has been previously strongly misaligned, its position must be followed by means of the position memory system in the four-spot configuration of monitoring (see H. Heitmann). The system measures the position of the mirror with respect to the tower. The following two situations c an take place:

a) at the beginning of the procedure M_1 is already very misaligned and the reflected beam are already laying outside the field of M_0 and then it do not appeared onto screen S_0;

b) during the misalignment of M_1, driving the spot outside S_0, the position memory system (camera CS1 (C3)) records the angular scan path and then the position can be recovered.

We remark that it is supposed that the actuators of the marionette must be calibrated allowing to drive the marionettes to the wanted positions.

- **STEP 4** Angular scan of M1 monitoring the reflected beam on screen S_0 by means of C_{S0}, find the aligned position and leave it misaligned.

⇒ RIGHT POSITION OF M_1 STORED

The lens system in the injection bench can be used for the fine alignment of the injected light once the beam is found onto screen S_1. Since S_1 is supposed to be steady with respect to the tower where the far mirror M_2 is housed, the position of the beam onto the mirror can be deduced by correlating the images of screen S_1 and to those from the front face of M_2.

- **STEP 5** Fine angular scan (telescope) of the injected beam monitoring the spot on screen S_1 by means of camera CS_1 (C_4)

⇒ BEAM CENTRED ON M_2, INJECTION BENCH ALIGNED

- **STEP 6** Angular scan of M_2 to monitor and record the aligned position on screen S_0. Leave M_2 misaligned.

⇒ RIGHT POSITION OF M_2 STORED

The FP cavity M_0-M_1 driven to the resonance and the transmitted light spot on screen S_1 is monitored. This technique allows to optimise the alignment of M_0 (and M_1) along the injected light. These movements can be obtained using the weak magnet-coil pairs installed onto the marionette of the NM.

- **STEP 7** Drive M_1 (and M_0) to the stored position, look at the spot due to the transmitted light from cavity M_0-M_1 on screen S_1 and optimise the alignment.

⇒ RIGHT POSITION OF M_0, M_1 STORED

- **STEP 8** Misalign M_0, M_1, M_2.

An angular scan of the BS is required to reach a rough centring of the beam on S_2. In this case since the beam is supposed to be already centred along the line M_0-M_2 and the correct position of M_0 is supposed to be known.

- **STEP 9** Angular scan of BS monitoring the spot on screen S_2 with camera C_{S2}

⇒ BEAM CENTRED ON M_4

Then, similarly to STEP 6,

- **STEP 10**. Angular scan of M4 monitoring the spot on S_0. Leave it misaligned.

⇒ RIGHT POSITION OF M_4 STORED

- **STEP 11** Angular scan with M_3 to monitor the spot on S_0.

Again, the light transmitted from the short FP (M_0-M_3) can be used to optimise the position of M_3 (M_0 is now fixed).

- **STEP 12** Restore the correct position of M0. Align finely M_3 monitoring the spot on S_2.

⇒ RIGHT POSITION OF M_3 STORED

- **STEP 13** Restore aligned position of M_1, M_2, M_4.

⇒ RECYCLED FP-INTERFEROMETER ALIGNED

44.5 Linear Alignment

44.5.1 Linear Alignment function and concept

The linear alignment will make use of 8 quadrant photodiodes placed in pairs on the beams transmitted by the Fabry-Perot's, on the beam reflected by the recycling mirror, and on the beam reflected by the second surface of the beam-splitter. The two photodiodes of each pair will be located at values of the "Guoy phase" different by 90°. To achieve this, each photodiode will use a telescope of 2 lenses with adjustable positions.

Each photodiode will provide directly coupled signals from each of the 4 quadrants : they will be used as a check of its correct functioning, as a measurement of the average power and to determine the average position of the beam. In particular, from the quadrant photodiodes placed on the beam transmitted by the two Fabry-Perot's, it will be possible to extract the "average" alignment of the two arms of the interferometer and thus to act on the beam-splitter and on the direction of the beam leaving the injection bench, in order to maintain fixed the average position of the interferometer.

For the detection of the misalignments of the mirrors one with respect to the other and with the direction of the input beam, we will make use of the left-right and up-down differences between the quadrants, demodulated in-phase and in-quadrature. The 8 quadrant photodiodes will thus provide a total of 32 of such differences (16 in horizontal and 16 in vertical). For each direction, the angular positions of the 5 mirrors of the interferometer, can be deduced from the 16 signals with a χ^2 minimisation procedure. In order to optimise this reconstruction of the mirrors angles, the laser beam has to be modulated at a frequency such that both sidebands resonate in the recycling cavity and one of them resonates in the FP's as TEM_{10}.

44.5.2 Linear Alignment detailed description

44.5.2.1 Geometrical Considerations

In ref.[1] it is shown that the effective optical length of a FP-cavity depends on the deviation angles $\theta_{1,2}$ of the two terminal mirrors $M_{1,2}$ from the conditions of perfect alignment. This can be seen in a greater detail by considering both the finite size of the mirrors and the positions of their rotation centres. Let us consider fig. (4400-2), where:

- $\theta_{1,2}$ are the mirror deviation angles;
- $a_{1,2}$ are the mirror half thicknesses;
- L is the separation between the two centres of masses;
- l is the actual length of the cavity;
- R is the curvature radius of the mirror M_2 (3450 m);
- $l_0 = L - a_1 - a_2$ is the optical length in condition of perfect alignment (2988 m).

With simple geometrical considerations one can show that the actual length of the cavity can be written in the following way

$$l(t) = l_0 + (R + a_2)[1 - \cos(\vartheta_1 - \vartheta_2)] - L(1 - \cos\vartheta_1) \qquad (4440.1.1)$$

By taking a series expansion up to second order in $\theta_{1,2}$, this equation reproduces the expression given by eq. (1) of ref. [2]:

$$l(t) \approx l_0 + \alpha\vartheta_1^2 + \beta\vartheta_2^2 + \gamma\vartheta_1\vartheta_2 \qquad (4440.1.2)$$

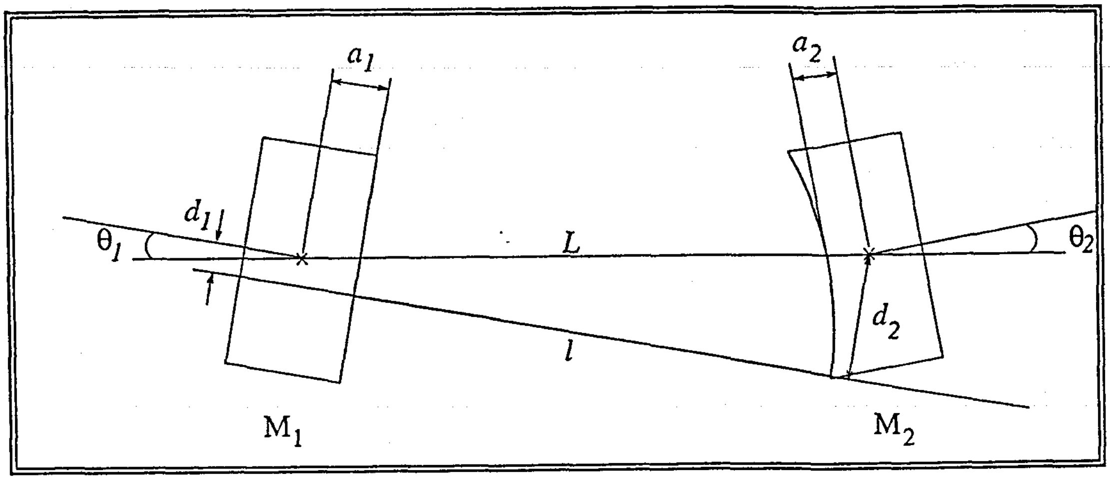

Figure 4400-2

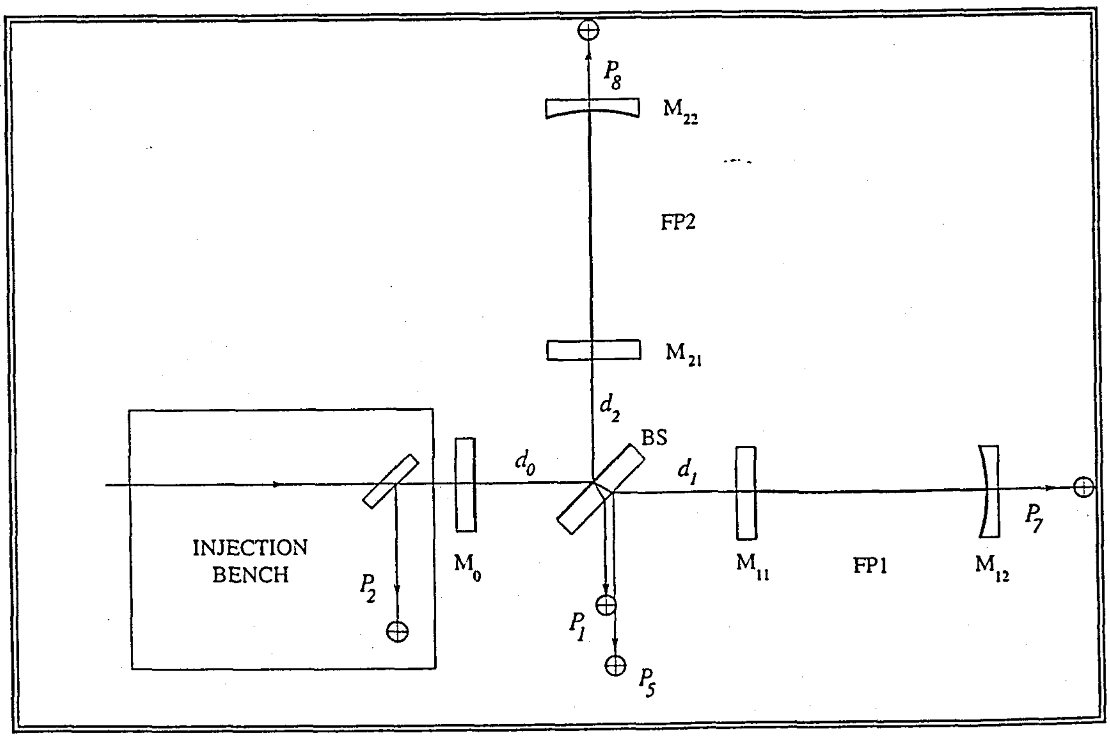

Figure 4400-3

where

$$\alpha = \frac{1}{2}(R + a_2 - L),\ \beta = \frac{1}{2}(R + a_2),\ \gamma = -2\beta \qquad (4440.1.3)$$

44.5.2.2 Sensitivity Requirements

Terrestrial gravitational wave detectors will monitor l(t) only at frequencies above 10 Hz, whereas the alignment errors $\theta_{1,2}$ are dominated by static *(offsets)* or slowly varying components (below 10 Hz). Faster angle fluctuations, at frequencies within the observation band, are considerably smaller.

Let us suppose that the angular fluctuations of the two terminal mirrors can be described in the time and frequency domain, in the following form

$$\vartheta_k(t) = \vartheta_k^{(0)}(t) + \eta_k(t) + \varepsilon_k(t)$$

$$(k=1,2) \qquad (4440.2.1)$$

$$\overline{\vartheta}_k(f) = \vartheta_k^{(0)}\delta(f) + \overline{\eta}_k(f) + \overline{\varepsilon}_k(f)$$

where $\vartheta_k^{(0)}$ are the static angular offsets and

$\overline{\eta}_k(f) \neq 0, \qquad 0 < f \leq \omega$

$$\omega \approx 10\ Hz \qquad (4440.2.2)$$

$$\overline{\varepsilon}_k(f) \neq 0, \qquad f > \omega$$

$$\int_{-\omega}^{\omega} |\ \overline{\eta}_k(f)\ |^2\ df >> \int_{-\infty}^{+\infty} |\ \overline{\varepsilon}_k(f)\ |^2\ df \qquad (4440.2.3)$$

i.e. the low–frequency component carries substantially more spectral power than the high–frequency component. The Fourier transform of eq. (1.2) follows from the convolution theorem

$$F(f \otimes g) = F(f) \cdot F(g), \qquad (4440.2.4)$$

and is given by

$$\overline{l}(f) = l_0\delta(f) + \alpha(\overline{\vartheta}_1 \otimes \overline{\vartheta}_1) + \beta(\overline{\vartheta}_2 \otimes \overline{\vartheta}_2) + \gamma(\overline{\vartheta}_1 \otimes \overline{\vartheta}_2) \qquad (4440.2.5)$$

After some algebra, eq. (2.5) can be reduced to the form

$$\overline{l}(f) = \sum_{k=1}^{2}[\overline{d}_k^{(0)}(\overline{\varepsilon}_k + \overline{\eta}_k) + \overline{d}_k \otimes \overline{\varepsilon}_k(f)] + \alpha[(\overline{\varepsilon}_1 \otimes \overline{\varepsilon}_1) + (\overline{\eta}_1 \otimes \overline{\eta}_1)]$$

$$+\beta[(\overline{\varepsilon}_2 \otimes \overline{\varepsilon}_2) + (\overline{\eta}_2 \otimes \overline{\eta}_2)] + \gamma[(\overline{\varepsilon}_1 \otimes \overline{\varepsilon}_2) + (\overline{\eta}_1 \otimes \overline{\eta}_2)] \qquad (4440.2.6)$$

where:

$$\overline{d}_1^{(0)} = 2(\alpha\vartheta_1^{(0)} - \beta\vartheta_2^{(0)}), \quad \overline{d}_2^{(0)} = 2\beta(\vartheta_2^{(0)} - \vartheta_1^{(0)}) \qquad (4440.2.7)$$

and no assumption has been made. However, since the angular fluctuations can be considered as purely stochastic processes, the correlation functions of the last three terms of eq. (2.6) can be neglected and this expression simplifies into

$$\overline{l}(f) = \sum_{k=1}^{2}\{\overline{d}_k^{(0)}\overline{\eta}_k(f) + \overline{\varepsilon}_k(f) \otimes [\overline{d}_k(f) + \overline{d}_k^{(0)}\delta(f)]\} \qquad (4440.2.8)$$

The two quantities $\overline{d}_{1,2}(f)$ are the moment arms separating the perturbed optical axis from each mirror's centre of rotations and are given by

$$\overline{d}_1(f) = 2(\alpha\overline{\eta}_1 - \beta\overline{\eta}_2), \quad \overline{d}_2(f) = 2\beta(\overline{\eta}_2 - \overline{\eta}_1) \qquad (4440.2.9)$$

Two specific cases can be considered:

a. The alignment errors are determined only by static and/or slowly varying angular displacements (below 10 Hz) due to long-term thermal drift and seismic vibrations combined with the low-pass filtering action of the suspensions. In this case $\overline{\varepsilon}_{1,2} \approx 0$ and eq.(2.8) becomes

$$\overline{l}(f) = \sum_{k=1}^{2}\overline{d}_k^{(0)}\overline{\eta}_k(f) \qquad (4440.2.10)$$

b. In the general case where $\overline{\varepsilon}_{1,2}(f) \neq 0$, the high frequency components of l(f) will be coupled to the effect of the low-frequency noise. This can be seen as follows. Let us put

$$\overline{A}_k(f) = \overline{d}_l^{(0)}\delta(f) + \overline{d}_k(f) \qquad (k=1,2) \qquad (4440.2.11)$$

and let us take the square of eq.(2.8) for f >> 10 Hz ($\overline{\eta}_{1,2} = 0$). The expressions of the two diagonal terms become (k=1,2)

$$[\overline{\varepsilon}_k \otimes \overline{A}_k(f)]^2 = \int_{-\infty}^{+\infty} \overline{\varepsilon}_k(f')\overline{A}_k(f-f')df' \int_{-\infty}^{+\infty} \overline{\varepsilon}_k(g')\overline{A}_k(f-g')dg'$$

$$= \int_{-\infty}^{+\infty} \overline{\varepsilon}_k(f')\overline{\varepsilon}_k(f'+x)dx \int_{-\infty}^{+\infty} \overline{A}_k(f-f')\overline{A}_k(f-f'-x)df' \qquad (4440.2.12)$$

where x=g'-f'. In absence of any correlations among the values of A(f) calculated at different frequencies, one has

$$\int_{-\infty}^{+\infty} \overline{A}_k(f-f')\overline{A}_k(f-f'-x)df' = \Delta f \ \langle \overline{A}_k^2 \rangle \delta(x) = \Delta f \ (\overline{d}_k^{(0)^2} + \sigma_{d_k}^2) \ \delta(x) \qquad (4440.2.13)$$

where σ_{d_k} are the RMS-values of the $\overline{d}_k(f)$ of eq.(2.9).

For the same reason, the two non-diagonal terms vanish and the expression of $l^2(f)$ reduces to

$$\frac{\overline{l}^2(f)}{\Delta f} = \sum_{k=1}^{2} \overline{\varepsilon}_k^2(f) \ (\overline{d}_k^{(0)^2} + \sigma_{d_k}^2) \qquad (4440.2.14)$$

where the contributions of the two mirrors can be assumed to be approximately equal. This expression can be compared with eq.(14) of ref.[2] and it's worthwhile to notice that the $\overline{d}_k$ RMS-values entering the latter, appears to be multiplied by an extra factor 2, which, apparently, is unjustifiable.

The first case shows that, at least in principle, the offset contributions appearing in eqs.(2.8) can be trimmed down to zero by applying a periodic torque to the mirror and by monitoring the corresponding variations of the optical length of the cavity. Moreover, measurements performed on the superattenuators and estimates of the thermal noise indicate that:

- the low frequency angular noise is dominated by the suspension noise, that is concentrated in the region below 1 Hz and has a total RMS-value of about $2.5 \cdot 10^{-5}$ rad;
- the high frequency (> 10 Hz) component of the spectrum is dominated by the thermal noise that is estimated to be $2 \cdot 10^{-17}$ $rad/\sqrt{Hz}$ at 10 Hz and $3 \cdot 10^{-20}$ $rad/\sqrt{Hz}$ at 100 Hz.

The RMS-value of the angular noise at low frequency would cause

$$d_1^{RMS} = 9 \ cm \qquad d_2^{RMS} = 12 \ cm$$

in each direction. Following (2.14), this would give a limit of $h = 1.4 \cdot 10^{-21} \ /\sqrt{Hz}$ at 10 Hz. For the sensitivity limits of

$$h < 10^{-22} \ /\sqrt{Hz} \ \text{ at } 10\,\text{Hz} \qquad (4440.2.15)$$

$$h < 10^{-23} \ /\sqrt{Hz} \ \text{ at } 100\,\text{Hz}$$

the 10 Hz region is the most demanding and the d_i^{RMS} comes out to be about 1 cm. To achieve this, the RMS-value of the low-frequency angular noise must be reduced down to 10^{-6} rad.

44.5.2.3 The Fabry-Perot Alignment

The methods of D.Z.Anderson and H.Ward [3,4] have been originally suggested for the alignment of one single Fabry-Perot (FP) and no attempt has ever been made to extend this procedure to the case of a complete Michelson Interferometer (MI). In both these methods the beam is frequency modulated and, in the Anderson scheme, the modulation equals the frequency difference between the TEM_{00} and TEM_{10} modes $\Omega / 2\pi = 19.1 \ KHz$. The alignment information is related to the detection of the TEM_{10} components, in phase or in quadrature, with the main TEM_{00}. All these details have been widely discussed elsewhere [1,3,4].

In the case of a single FP, the knowledge of a tilt and/or displacement of the optical axis, is sufficient to identify the mirror that caused it. But this is not true for a complete MI, where a misalignment signal measured behind one FP, will not be sufficient to single out the mirror(s) that caused it. In order to disentangle the information, more measurements are needed. In ref.[1] we initiated to consider the complete Michelson Interferometer where the beam splitter and the recycling mirror remained perfectly aligned. With the Anderson method and under some simplifying assumptions, we reached the following conclusions :

1. the left/right or up/down asymmetries, measured behind the terminal mirrors of one of the two FP's, yields direct information of the tilt of the FP-cavity axis, but its displacement appears always in a linear combination with the displacement of the other FP-cavity;
2. this cross-talk between the two arms couples the two displacements only. Neither angle/angle nor angle/displacement couplings are predicted;
3. the coupling effect for the displacements is very close to one;
4. with a maximum power of 10 mW impinging on the quadrant photodiodes, the limits imposed by the shot-noise would be :

$$\frac{\alpha}{\vartheta_\infty} = 9.9\cdot 10^{-7} / \sqrt{Hz}$$

$$\frac{a}{w_0} = 3\cdot 10^{-8} / \sqrt{Hz} \qquad (4440.3.1)$$

where α and a refer to the optical axis of the FP-cavities.

44.5.2.4 Alignment of the Full Interferometer with the Anderson Method

In order to obtain a better approximation, we removed two of the limitations that affected the results of ref.[1], i.e. :

1. the recycling mirror was kept "fixed" in a perfectly aligned condition;
2. the FP-reflectivities for the resonant (β) and non-resonant (γ) frequencies

$$\beta = \frac{|R_1 - R_2|}{1 - R_1 R_2} \qquad \gamma = \frac{R_1 + R_2}{1 + R_1 R_2} \qquad (4440.4.1)$$

were both assumed to be equal to 1 ($T_2 = 0$).

With the values

$$R_1^2 = 0.882\ , \qquad T_1^2 = 0.118$$

$$R_2^2 = 0.9999\ , \qquad T_2^2 = 10^{-4} \qquad (4440.4.2)$$

taken from ref.[4], one has instead:

$$\beta = 0.99841\ , \qquad \gamma = 0.999997 \qquad (4440.4.3)$$

and even if tiny, this difference can play a significant role. By limiting ourselves to consider only the horizontal plane, we have to measure the 2-displacements ($a_{1,2}$) and the 2-angles ($\alpha_{1,2}$) of the FP-cavity axes and the angle of the recycling mirror (ϑ_0) : in total five unknown quantities. Three quadrant photodiode will be sufficient to disentangle the problem: two located right behind the two terminal mirrors, and a third on the injection bench, to measure the component reflected back from the recycling mirror (see fig.4400-3). However a further fourth photodiode can be used to measure the component reflected from the uncoated part of the beam splitter: this is not necessary but can add an important extra piece of information.
Given a complete set of mirror misalignments, the equilibrium condition among the three electric fields impinging upon the recycling mirror, imposes the following relation :

$$\overline{E}_3 = T_0 \overline{E}_1 + i R_0 \overline{E}_2 \qquad (4440.4.4)$$

where:

- $\overline{E}_1$ is the external incident beam;
- $\overline{E}_2$ is the beam impinging on the recycling mirror after a complete round trip in the interferometer;
- $\overline{E}_3$ is the beam leaving the recycling mirror for the tour of the interferometer;
- R_0 and T_0 are the amplitude reflectivity and transmittivity of the recycling mirror, respectively.

According to ref.[5], the reflectivity and transmittivity of the recycling mirror will be assumed to be:

$$R_0^2 = 0.92\ , \qquad T_0^2 = 0.08 \qquad (4440.4.5)$$

After some tedious algebra, eq.(4.4) drives to the misalignment signals expressed in terms of the misalignments specified for each mirror.
The left/right power components transmitted behind the two terminal mirrors are (+=left, -=right):

$$P_{7,8}^{L,R} = \frac{P_{inc}T_0^2T_2^2F}{4(1-\beta R_0)^2}[J_0^2 \pm \sqrt{\frac{2}{\pi}}\frac{J_0J_1}{1+\gamma R_0}(A_{7,8}\ \cos\Omega t + B_{7,8}\ \sin\Omega t)$$

$$+\ O(\alpha_{h,k}^2, a_{h,k}^2, a_{h,k}\alpha_{h,k})] \qquad (4440.4.6)$$

where P_{inc} is the incident laser power and

$$A_{7,8} = [(\beta-\gamma)R_0 - 2]a_{1,2} - (\beta+\gamma)R_0 a_{2,1}$$

$$B_{7,8} = [2-(\gamma+\beta)R_0]\alpha_{1,2} + (\beta-\gamma)R_0\alpha_{2,1} + 4\gamma R_0\vartheta_0 \qquad (4440.4.7)$$

$$F = \frac{T_1^2}{(1-R_1R_2)^2}$$

By neglecting the higher order terms, the left/right asymmetry, which is free from systematic errors, is given by:

$$\Sigma_t^{FP_{1,2}} = \frac{left-right}{left+right} = \sqrt{\frac{8}{\pi}}\frac{J_1}{J_0}\frac{1}{1+\gamma R_0}(A_{7,8}\ \cos\Omega t + B_{7,8}\ \sin\Omega t) \qquad (4440.4.8)$$

The component reflected from the recycling mirror (P_2) and its asymmetry are:

$$P_2^{L,R} = \frac{P_{inc}}{2(1-\beta R_0)^2}[(\beta-R_0)^2J_0^2 \pm \sqrt{\frac{2}{\pi}}\frac{J_0J_1T_0^2(\beta+\gamma)}{(1+\gamma R_0)^2}(A_2\ \cos\Omega t + B_2\ \sin\Omega t)$$

$$+\ O(\alpha_{h,k}^2, a_{h,k}^2, a_{h,k}\alpha_{h,k})] \qquad (4440.4.9)$$

$$\Sigma_r^{Rec} = \sqrt{\frac{2}{\pi}}\frac{J_1}{J_0}\frac{T_0^2(\beta+\gamma)}{(\beta-R_0)^2(1+\gamma R_0)^2}(A_2\ \cos\Omega t + B_2\ \sin\Omega t) \qquad (4440.4.10)$$

where:

$$A_2 = (R_0-\beta)(1+\gamma R_0)(a_1+a_2)$$

$$B_2 = [(R_0+3)(1+\gamma R_0) - 2(\gamma+\beta R_0^2)](\alpha_1+\alpha_2) \qquad (4440.4.11)$$

$$+4R_0[\gamma\beta - 2 + R_0(2\beta-\gamma)]\vartheta_0$$

The component reflected by the uncoated face of the beam splitter (P_5), and its asymmetry are:

$$P_5^{L,R} = \frac{P_{inc}T_0^2}{4(1-\beta R_0)^2}[\beta^2J_0^2 \pm \sqrt{\frac{2}{\pi}}\frac{J_0J_1(\beta+\gamma)}{1+\gamma R_0}(A_5\ \cos\Omega t + B_5\ \sin\Omega t)$$

$$+\ O(\alpha_{h,k}^2, a_{h,k}^2, a_{h,k}\alpha_{h,k})] \qquad (4440.4.12)$$

$$\Sigma_r^{FP_1} = \sqrt{\frac{2}{\pi}}\frac{J_1}{J_0}\frac{\beta+\gamma}{\beta^2(1+\gamma R_0)}(A_5\ \cos\Omega t + B_5\ \sin\Omega t) \qquad (4440.4.13)$$

where:

$$A_5 = \beta[(\beta R_0 - 2)a_1 - \beta R_0 a_2]$$

$$B_5 = \{\alpha_1[2\beta - 2\gamma(1-\beta R_0)(2+\gamma R_0) - \beta^2 R_0(1+\gamma R_0)] \qquad (4440.4.14)$$

$$+\alpha_2 R_0[\beta^2(1+\gamma R_0) + 2\gamma^2(1-\beta R_0) - 2\beta\gamma] + 4\beta\gamma R_0 \vartheta_0\} / (1+\gamma R_0)$$

Finally, the beam going toward the fringe detector P_1 has not been considered because, under these approximations, it contains information on the misalignments only at the second order level.

In all these expressions, displacements and angles are always measured in units of beam waist ($w_0 = 1.98 \cdot 10^{-2}\ m$) and angular divergence ($\vartheta_\infty = 1.7 \cdot 10^{-5}\ rad$).

Moreover, for the sake of simplicity, we have assumed that:

– the propagation phases in the recycling cavity are the same for all the beams,
– the beams are either on-resonance or perfectly off-resonance in the FP's, (4440.4.15)
– only the resonant beams are transmitted by the FP's.

With these approximations, a first numerical evaluation is reported in Table I. With the values $J_1^2 = 10^{-2}$, $\Omega / 2\pi = 19.1\ KHz$,the table shows the contributions that every angular misalignment gives to the in phase/in quadrature components of the asymmetries.

All the coefficients of Table I, as well as in Tables II and III, have been calculated for $\vartheta_i = 10^{-2}$.

The ϑ_i variables expressed in units of the beam angular divergence, have the following meaning:

- ϑ_0 is a tilt of the recycling mirror M_0,
- $\vartheta_{11,12}$ are tilts of the ($M_{11,12}$) mirrors that produce a displacement a_1 and a tilt α_1 of the FP_1 cavity axis, according to [$a_0 = w_0 / \vartheta_\infty = 1.16 \cdot 10^3\ m/rad$]

Beam		θ_0	θ_{11}	θ_{12}	θ_{21}	θ_{22}
$\Sigma_t^{FP_1}$	sin	$1.58 \cdot 10^{-3}$	$3.45 \cdot 10^{-5}$	0	$-6.33 \cdot 10^{-7}$	0
	cos	0	$3.187 \cdot 10^{-4}$	$-2.444 \cdot 10^{-3}$	$3.052 \cdot 10^{-4}$	$-2.34 \cdot 10^{-3}$
$\Sigma_t^{FP_2}$	sin	$1.58 \cdot 10^{-3}$	$-6.33 \cdot 10^{-7}$	0	$3.45 \cdot 10^{-5}$	0
	cos	0	$3.052 \cdot 10^{-4}$	$-2.34 \cdot 10^{-3}$	$3.187 \cdot 10^{-4}$	$-2.444 \cdot 10^{-3}$
Σ_r^{Rec}	sin	$-3.71 \cdot 10^{-3}$	$-3.95 \cdot 10^{-5}$	0	$-3.95 \cdot 10^{-5}$	0
	cos	0	$6.352 \cdot 10^{-4}$	$-4.87 \cdot 10^{-3}$	$6.352 \cdot 10^{-4}$	$-4.87 \cdot 10^{-5}$
$\Sigma_r^{FP_1}$	sin	$1.61 \cdot 10^{-3}$	$-5.33 \cdot 10^{-5}$	0	$1.65 \cdot 10^{-5}$	0
	cos	0	$3.327 \cdot 10^{-4}$	$-2.551 \cdot 10^{-3}$	$3.052 \cdot 10^{-4}$	$-2.34 \cdot 10^{-3}$

Table I

$$a_1 = \frac{l_0 - R}{a_0}\vartheta_{11} + \frac{R}{a_0}\vartheta_{12}, \qquad \alpha_1 = \vartheta_{11} \qquad (4440.4.17)$$

- $\vartheta_{21,22}$ are tilts of the ($M_{21,22}$) mirrors that produce a displacement a_2 and a tilt α_2 of the FP_2 cavity axis, according to :

$$a_2 = \frac{l_0 - R}{a_0}\vartheta_{21} + \frac{R}{a_0}\vartheta_{22}, \qquad \alpha_2 = \vartheta_{21} \qquad (4440.4.18)$$

Some immediate comments to these results are:

- ϑ_0 induces only sin-components (angles)
- $\vartheta_{12,22}$ induce only cos-components (displacements)
- $\vartheta_{11,21}$ induce both sin and cos-components but to a much smaller extent

Moreover:

- ϑ_0 acts on P_7 in the same way as ϑ_0 acts on P_8
- ϑ_{11} acts on P_8 in the same way as ϑ_{21} acts on P_7
- ϑ_{12} acts on P_8 in the same way as ϑ_{22} acts on P_7
- ϑ_{11} acts on P_2 in the same way as ϑ_{21} acts on P_2
- ϑ_{12} acts on P_2 in the same way as ϑ_{22} acts on P_2

as it must be expected from the symmetry of the problem: the two FP's are specularly located with respect to the plane of the beam splitter.

44.5.2.5 Achievable Accuracies

The expressions (4.6, 4.9, 4.12) for the power detected by the quadrant photodiode, are always of the kind

$$P^{L,R} = P_0 \pm P' \sin(\Omega t + \varphi) \qquad (4440.5.1)$$

where

$$P^L + P^R = 2P_0 = P_{Tot} \qquad (4440.5.2)$$

$$\langle P^L \rangle = \langle P^R \rangle = P_0 \qquad (4440.5.3)$$

The asymmetries of eqs (4.8,4.10,4.13) are defined in terms of the quantities (5.1)

$$\Sigma = \frac{P^R - P^L}{P^R + P^L} = \frac{P'}{P_0}\sin(\Omega t + \varphi) \qquad (4440.5.4)$$

and the corresponding errors

$$(\Delta\Sigma)^2 = \frac{4}{(P^L + P^R)^4}[(P^R)^2(\Delta P^L)^2 + (P^L)^2(\Delta P^R)^2] \qquad (4440.5.5)$$

will be calculated on the ground that both P^L and P^R are only affected by the shot-noise associated to their mean value ($= P_0$).Therefore assuming a quantum efficiency =1, the shot-noise errors $\Delta P^{L,R}$ are given by

$$\Delta P^{L,R} = 6.11 \cdot 10^{-10}\sqrt{P_0} \quad (W/\sqrt{Hz}) \qquad (4440.5.6)$$

and eq.(5.5) becomes

$$\Delta\Sigma = 6.11 \cdot 10^{-10}\sqrt{\frac{1+\Sigma^2}{P_{Tot}}} \qquad (4440.5.7)$$

Finally, since it is always $|\Sigma| << 1$ and assuming that the maximum power tolerated on the photodiodes is 10 mW, the minimum asymmetry that can be appreciated is

$$\Delta\Sigma = 6.11 \cdot 10^{-9} \qquad (4440.5.8)$$

As shown in table I, there are eight available signals of the five independent variables $\vartheta_0, \vartheta_{11}, \vartheta_{12}, \vartheta_{21}, \vartheta_{22}$, so there are several possible systems of five equations that can be solved to deduce the values of the angles. Not all the possible choices are equivalent; actually not all the signals are independent. For example, the $\Sigma_r^{Rec}(\cos)$ equation is proportional to the sum of $\Sigma_t^{FP_1}(\cos)$ and $\Sigma_t^{FP_2}(\cos)$ equations.

It can be seen that a good choice (others choices are equivalent) is the system made of equations $\Sigma_t^{FP_1}(\sin)$, $\Sigma_r^{Rec}(\sin)$, $\Sigma_r^{Rec}(\cos)$, $\Sigma_r^{FP_1}(\sin)$, $\Sigma_r^{FP_1}(\cos)$. Taking into account the shot-noise limitation, given by eq.(5.8), one can reconstruct all the angular misalignments with the accuracies shown in the first column of table IV.

Beam		θ_0	θ_{11}	θ_{12}	θ_{21}	θ_{22}
$\Sigma_t^{FP_1}$	sin	$1.483 \cdot 10^{-3}$	$-3.728 \cdot 10^{-5}$	$5.662 \cdot 10^{-4}$	$-7.161 \cdot 10^{-5}$	$5.627 \cdot 10^{-4}$
	cos	$3.809 \cdot 10^{-4}$	$2.900 \cdot 10^{-4}$	$-2.304 \cdot 10^{-3}$	$2.785 \cdot 10^{-4}$	$-2.201 \cdot 10^{-3}$
$\Sigma_t^{FP_2}$	sin	$1.483 \cdot 10^{-3}$	$-7.170 \cdot 10^{-5}$	$5.634 \cdot 10^{-4}$	$-3.739 \cdot 10^{-5}$	$5.670 \cdot 10^{-4}$
	cos	$3.814 \cdot 10^{-4}$	$2.785 \cdot 10^{-4}$	$-2.201 \cdot 10^{-3}$	$2.900 \cdot 10^{-4}$	$-2.304 \cdot 10^{-3}$
Σ_r^{Rec}	sin	$-3.910 \cdot 10^{-3}$	$-1.839 \cdot 10^{-4}$	$1.144 \cdot 10^{-3}$	$-1.830 \cdot 10^{-4}$	$1.137 \cdot 10^{-3}$
	cos	$7.796 \cdot 10^{-4}$	$5.774 \cdot 10^{-4}$	$-4.575 \cdot 10^{-3}$	$5.775 \cdot 10^{-4}$	$-4.575 \cdot 10^{-3}$
$\Sigma_r^{FP_1}$	sin	$1.517 \cdot 10^{-3}$	$-1.240 \cdot 10^{-4}$	$5.591 \cdot 10^{-4}$	$-5.471 \cdot 10^{-5}$	$5.636 \cdot 10^{-4}$
	cos	$3.842 \cdot 10^{-4}$	$3.048 \cdot 10^{-4}$	$-2.408 \cdot 10^{-3}$	$2.764 \cdot 10^{-4}$	$-2.201 \cdot 10^{-3}$

Table II

The same calculation can be repeated by removing the approximations (4.15) used to construct table I and introducing the arm-length difference of 0.8 m requested by the longitudinal locking scheme [6] ($d_0 = 6.0\ m,\ \ d_1 = 5.6\ m,\ \ d_2 = 6.4\ m$). The results are reported in table II and do not show any significant variation. Again, the detector signals have been omitted because they are extremely small. The symmetry properties are substantially maintained and the values of the σ's, reported in the second column of table IV, remain almost the same.

So far the modulation frequency has been always kept at the value of 19.1 kHz, but nothing forbids to add to this frequency an integer number n of c/2L of the Fabry-Perot (50.166 kHz). In particular with n=125, the modulation frequency is 6.2898 MHz, which is very close to the optimal value for the longitudinal locking of 6.29032 MHz. Indeed, with the recycling cavity only 9 mm longer, the frequency for the longitudinal locking will coincide with the one for the alignment.
Therefore with the values :

$$\Omega / 2\pi = 6.289840\ MHz$$

$$d_0 = 6.009\ m,\ \ d_1 = 5.6\ m,\ \ d_2 = 6.4\ m \qquad (4440.5.9)$$

one obtains the results shown in table III.
Since now the side bands resonate in the recycling cavity, it is not surprising that these results are sensibly better than those reported in tables I,II. Furthermore, it is worthwhile noticing that at this high frequency value, also the detector (P_1) starts exhibiting sizeable signals. However its contribution has not been included in the results of table IV, which summarises the accuracy levels that are achievable in the 3 cases we have examined.
On the experimental side the use of one single high frequency modulation is highly desirable : the results obtained indicate that this possibility is not out of reach.

Beam		θ_0	θ_{11}	θ_{12}	θ_{21}	θ_{22}
$\Sigma_t^{FP_1}$	sin	$-3.975 \cdot 10^{-4}$	$-7.558 \cdot 10^{-5}$	$2.274 \cdot 10^{-3}$	$4.613 \cdot 10^{-4}$	$-2.114 \cdot 10^{-3}$
	cos	$-4.625 \cdot 10^{-4}$	$9.881 \cdot 10^{-4}$	$7.509 \cdot 10^{-5}$	$-5.180 \cdot 10^{-4}$	$-4.837 \cdot 10^{-5}$
$\Sigma_t^{FP_2}$	sin	$-4.423 \cdot 10^{-4}$	$5.133 \cdot 10^{-4}$	$-2.097 \cdot 10^{-3}$	$-8.088 \cdot 10^{-5}$	$2.259 \cdot 10^{-3}$
	cos	$-4.179 \cdot 10^{-4}$	$-4.664 \cdot 10^{-4}$	$-2.716 \cdot 10^{-4}$	$8.935 \cdot 10^{-4}$	$2.783 \cdot 10^{-4}$
Σ_r^{Rec}	sin	$-1.959 \cdot 10^{-2}$	$1.200 \cdot 10^{-2}$	$1.155 \cdot 10^{-3}$	$7.103 \cdot 10^{-3}$	$1.443 \cdot 10^{-3}$
	cos	$4.473 \cdot 10^{-2}$	$-2.206 \cdot 10^{-2}$	$1.500 \cdot 10^{-3}$	$-2.409 \cdot 10^{-2}$	$1.224 \cdot 10^{-3}$
$\Sigma_r^{FP_1}$	sin	$-2.308 \cdot 10^{-2}$	$1.371 \cdot 10^{-2}$	$-3.300 \cdot 10^{-3}$	$9.964 \cdot 10^{-3}$	$3.040 \cdot 10^{-3}$
	cos	$6.279 \cdot 10^{-3}$	$-1.517 \cdot 10^{-3}$	$3.909 \cdot 10^{-3}$	$-5.161 \cdot 10^{-3}$	$-2.071 \cdot 10^{-3}$
Σ^{Det}	sin	$-5.660 \cdot 10^{-6}$	$-4.167 \cdot 10^{-3}$	$2.496 \cdot 10^{-2}$	$4.161 \cdot 10^{-3}$	$-2.491 \cdot 10^{-2}$
	cos	$5.541 \cdot 10^{-6}$	$4.080 \cdot 10^{-3}$	$-2.443 \cdot 10^{-2}$	$-4.073 \cdot 10^{-3}$	$2.439 \cdot 10^{-2}$

Table III

	$19.1\ KHz$ with (4.16)	$19.1\ KHz$	$6.289\ MHz$ with (5.9)
$\sigma(\theta_0/\theta_\infty)$	$3.0 \cdot 10^{-8}$	$3.0 \cdot 10^{-8}$	$3.5 \cdot 10^{-7}$
$\sigma(\theta_{11}/\theta_\infty)$	$7.0 \cdot 10^{-7}$	$6.0 \cdot 10^{-7}$	$3.3 \cdot 10^{-7}$
$\sigma(\theta_{12}/\theta_\infty)$	$3.6 \cdot 10^{-7}$	$2.5 \cdot 10^{-7}$	$1.3 \cdot 10^{-7}$
$\sigma(\theta_{21}/\theta_\infty)$	$2.4 \cdot 10^{-6}$	$2.0 \cdot 10^{-6}$	$3.7 \cdot 10^{-7}$
$\sigma(\theta_{22}/\theta_\infty)$	$4.8 \cdot 10^{-7}$	$4.0 \cdot 10^{-7}$	$1.4 \cdot 10^{-7}$

Table IV

From table IV, we see that the shot-noise limits the reconstruction of the angles of the FP mirrors at most to $4 \cdot 10^{-11}\ rad / \sqrt{Hz}$, leading to a RMS-value which is much smaller than the value of $10^{-6}\ rad$ required in section 2.

44.5.2.6 Conclusions

We have demonstrated that in the Anderson scheme, the alignment problem is over determined with the five indicated quadrant photodiodes. Moreover this amount of information can be substantially doubled by adding an extra photodiode on each beam. As a matter of fact one could take advantage of the different dephasing effect that the $TEM_{00} - TEM_{01}$ modes undergo in their spatial evolution. This means that measurements of the $TEM_{00} - TEM_{01}$ mixtures at two different dephasing values (typically 0° and 90°) yield two independent informations. This requires only to locate the two photodiodes at a known separation, or to use a telescope.

An accurate analysis of this extra possibility is presently under study. For the time being we strongly recommend the presence of two quadrant photodiodes per beam line, except the main interference beam (P_1) (for a total of 8 quadrant photodiodes), in the final VIRGO experimental set-up.

44.6 Position memories.

44.6.1 Position memories function and concept.

During the interferometer normal operation, the six degree of freedom co-ordinates defining the position of each optical element (both mirrors and benches) will be monitored continuously and recorded with a sampling time much lower than for the g.w. data.

If the locking point of the interferometer is lost, these data will be necessary to move the optical elements to positions where the linear alignment procedure can be restarted.

See also chapter 41.5.2.2.2 (Mode Cleaner controls and alignment).

44.6.2 Position memory detailed description

This requirement gives the constraints on the sensitivity of the monitoring apparatus that should be used:

$\theta_x = 2\ 10^{-7}$ *rad*

$\theta_y = 2\ 10^{-7}$ *rad*

$\theta_z = 2\ 10^{-7}$ *rad*

$x = 1\ 10^{-4}$ *m*

$y = 1\ 10^{-4}$ *m*

$z = 1\ 10^{-6}$ *m*

where z is the optical axis of one arm of the interferometer.

Moreover, the monitoring apparatus will be in place permanently. Thus, the stability of the system over a long time of observation is crucial. Concerning the measurement bandwidth, we can accept an integration time in the range of 0.1 - 1 s.

A scheme for such a monitoring, operating in principle with only one camera, has been proposed and tested on a table top experiment by C. Drezen and H. Heitmann [1]. This method can be implemented in the VME based imaging system, developed at LAPP [2], by means of which the commercial CCD camera EG\&G-Reticon M9256 has been interfaced and calibrated. The system has been upgraded with the camera EEV CAM 17 - GEC.

In [1] it is noticed that, in order to achieve a first alignment of the mirror, a camera with lens which monitors the position of four coloured spots is sufficient. However, the best resolution on θ_x, θ_y and z , can be reached using two laser beams (one direct and one folded) and a camera without a lens.

Thus, we propose a solution which, for each optical element to be monitored, implies the use of

a) two cameras, one with and the second one without lens
b) two laser beams
c) one lamp
d) an auxiliary mirror.
e) four point markers on the mirror surface out of the coated zone. The overall measurement scheme we propose is in figure 4400-4.

These components will be placed in front of the two windows of each tower forming an angle of 30 degrees with the optical axis of the mirror. These windows (figure 4400-4) are located on the tower side that permits to look at the coated surface of the optical element and will be completely dedicated to this purpose. The use of other windows is precluded by the use of a reference mass (see Section Marionette and Reference Mass).

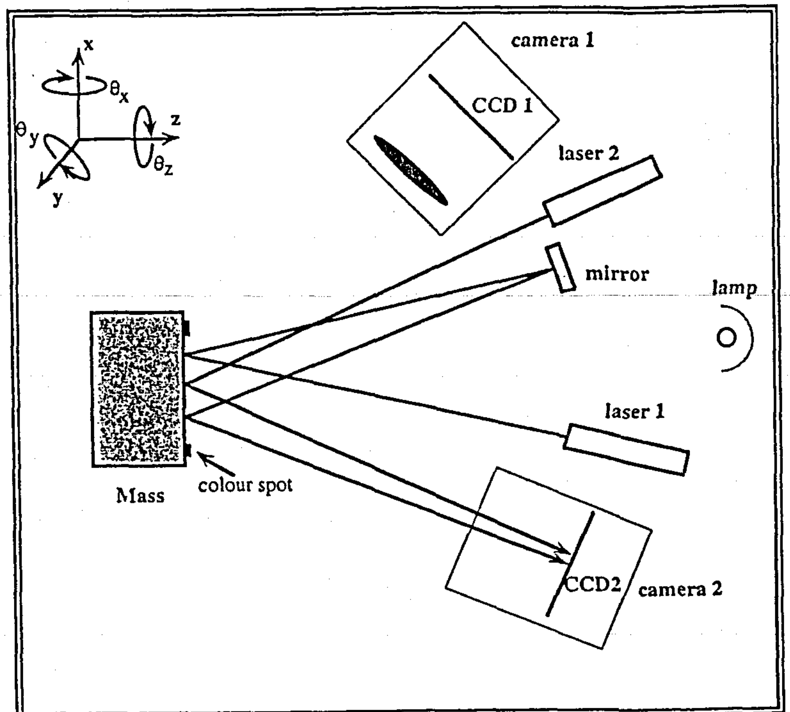

Figure 4400-4 Scheme proposed for determining the mass position.

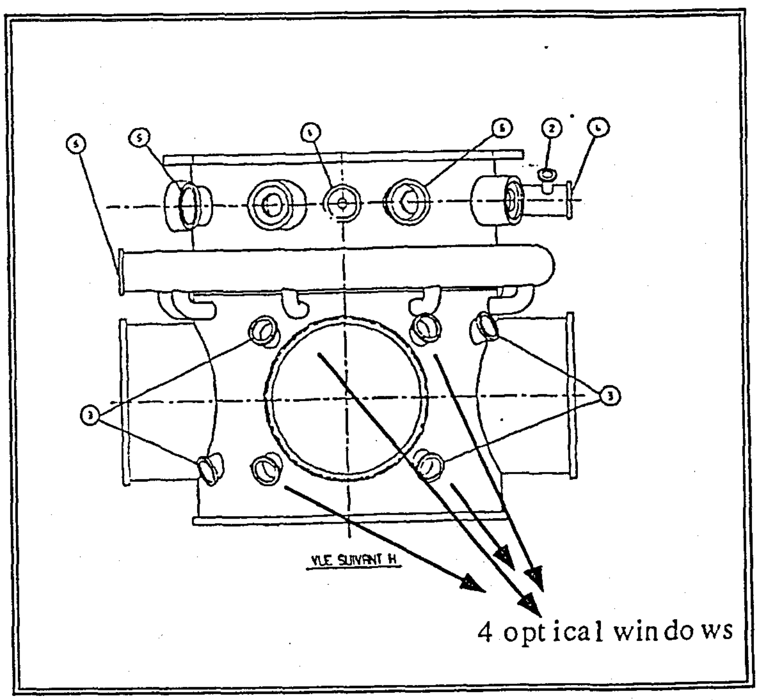

Figure 4400-5

In the case of the beam splitter we plan to look still to the coated side of the element using the two windows at 15 degrees.

The overall scheme of the cameras used to monitor the positions of the six mirrors of VIRGO is in figure 4400-6 where also the positions of the camera used for the non linear alignment are shown.

Each measuring system (lasers and cameras) will be attached to the structure of the towers by supports which will comply to the following specifications:

- The supports must not have mechanical resonances at frequencies lower than 100 Hz
- Their design should insure the possibility to remove the elements from the towers before out gassing
- The positioning of each element should be reproducible within 0.1 mm, in order to facilitate re calibration of the measuring apparatus after every assembly.

Care will be taken to isolate all measuring apparatus from the acoustic noise in the environment and from the fluctuations of air refraction index which could limit their sensitivity.

References section 44.5

[1] D.Babusci , H.Fang, G.Giordano, G.Matone, V.Sannibale, LNF-94/027(IR), Virgo note PJT 94-017 (1994)

[2] S.Kawamura and M.E.Zucker, Appl. Opt., 33 (1994),3912

[3] D.Z.Anderson, Appl. Opt., 23 (1984), 2944 and N.M.Sampas and D.Z.Anderson, Appl. Opt.} 29 (1990), 394

[4] E. Morrison, B.J. Meers, D.J. Robertson and H. Ward, Appl. Opt., 33 (1994), 5041

[5] C.N.Man, Virgo note PJT 94-024 (1994)

[6] R. Flaminio and H. Heitmann, Virgo note PJT 93-021 (1993)

References section 44.6

[1] H. Heitmann, Virgo Notes, 21.4.1994, 11.8.1994, 9.1.1995.

[2] A. Bazan et al., Astroparticle Phys. 2, 229 (1994).

[3] H. Heitmann, Virgo Note NTS 96038

[4] C. Drezen, H. Heitmann, F. Ricci, Virgo Note NTS 96072

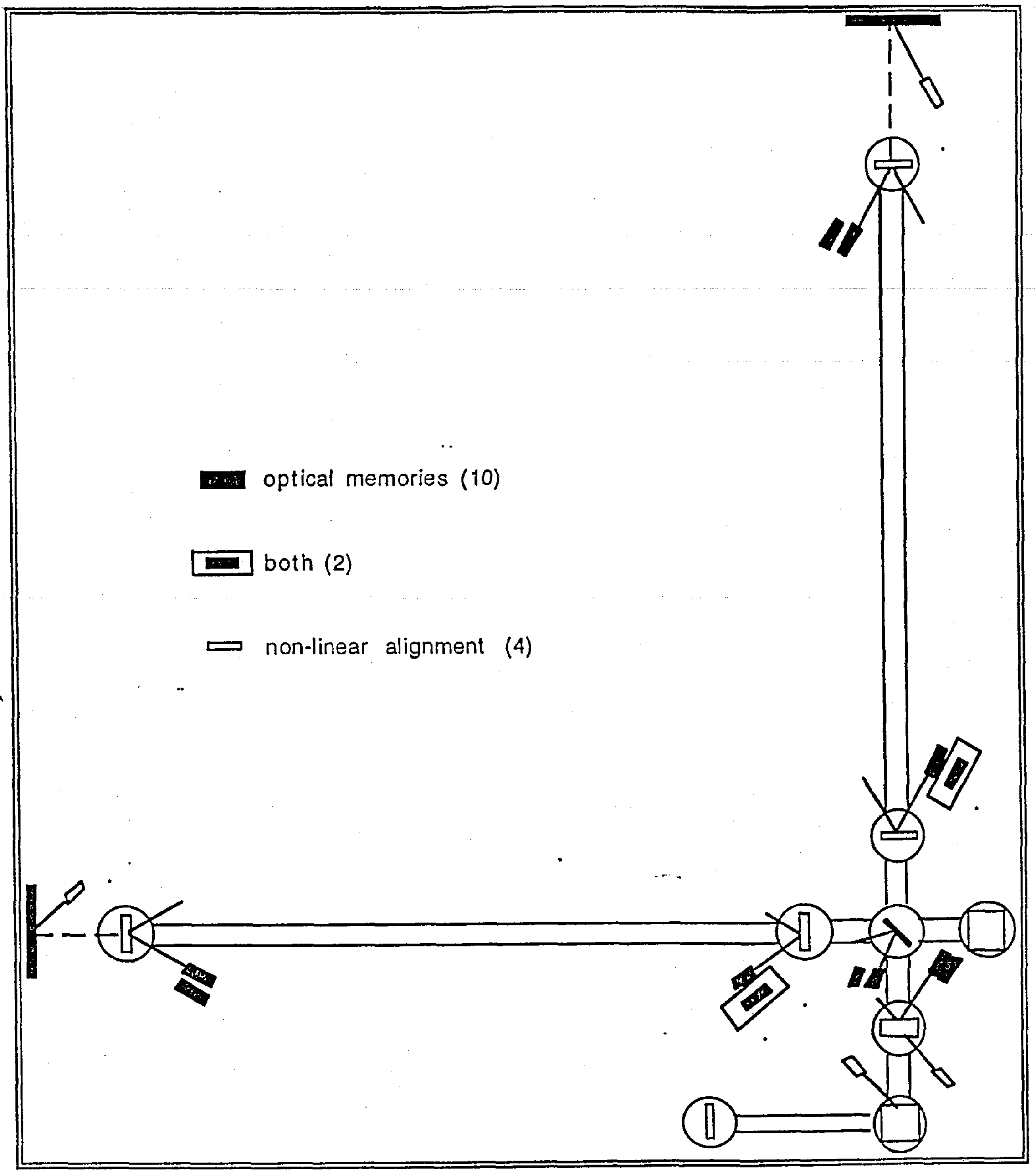

Figure 4400-6

45. Calibration

Table of Contents

45.1 Calibration function and concept

The purpose of the calibration of an apparatus is to provide the tools needed to convert the measured data to a physical quantity which is in our case the metric perturbation **h** induced by a gravitational wave. The first obvious way to do it is to use our detailed knowledge of the various components of the interferometer (laser power, conversion factors for the photodetectors, interferometer transfer function,...). This process relies on a precise determination of the detector calibration constants and on a detailed deconvolution which, taking into account optical transfer function and the locking system of the interferometer, is a non-trivial operation. Therefore, to gain confidence in our data we will use an independent system to calibrate the interferometer. By calibration, we mean the injection of a signal of known amplitude and phase, which mimics, as well as possible, the effect of a gravitational wave by moving one mirror and the study of the corresponding signal in our recorded data.

The calibration will be used for at least two different goals. The first one is a general study of the VIRGO sensitivity. In this mode we should be able to apply periodic or non periodic signals with an amplitude and a frequency which could be changed by few orders of magnitude in order to study the full bandwidth of VIRGO. The other mode of operation is a permanent monitoring of the VIRGO interferometer. In this case, we will apply a set of periodic signals of well known amplitudes and very stable frequency. In this mode, we will check the stability of the interferometer and of the data acquisition system.

To move the mirrors we will use two different methods. One is to push the mirrors with the standard coils located on the reference masse but driven by an external signal. The other one is the push the mirror with the radiation pressure from an additional laser beam driven also by an external signal. In addition to the software used to operate these calibration devices we need the software used to extract the calibration constant and the software needed to use this information to recompute **h** (**h** reconstruction). Therefore, the calibration is subdivided in the following items:

- a stand alone signal generator of arbitrary waveform, with an accurate timing
- two light generators to push the input cavity mirrors including the electronics and the mechanical supports
- all the needed VME electronics and software to run the calibrators.
- the software to extract the calibration constants
- the VIRGO reconstruction software, i.e. the software to compute h from the raw data (TBC).

45.2 Requirements

The signal generator should be able to provide a signal at 20 kHz with an absolute timing better than 5 μs (a fraction of the sampling frequency).

The transducer should have enough power to produce a visible signal on the VIRGO output. Its fluctuations should not introduce noise in the VIRGO sensitivity.

The control software should provide any shape.

45.3 Selection of solutions

This calibration signal should produce a mirror displacement of well known amplitude and time dependence. This means we should know the force applied on the mirror and the mechanical transfer function. The calibration signals will be applied to the two input cavity mirrors located in the central building. This choice gives us the opportunity to already install on the test interferometer the final solution. We could also send the calibration signals on both arms with a single signal generator.

The principle of the calibration is to have a system as independent as possible from the VIRGO control system. Of course, the calibration signal should not induce additional noise like seismic noise or electromagnetic noise. Two different ways of pushing the mirrors have been selected :

- Forces using the locking actuators
- The radiation pressure from an additional laser beam

45.4 Detailed description

45.4.1 The signal generator

The signal is generated by a DAC triggered by an GPS clock. The DAC (ADAS 704) has 4 outputs channels of 16 bits with independent FIFO of 32 kwords. The data are provided by a VME CPU running in real time the SIESTA environment in order to provide any signal shape. The VME crate will be located in the data acquisition room in the central building. The clock will be independent of the VIRGO timing system in order to check its validity (hardware and software).

A summary of the status of the signal generator which includes the definition of the generated signal and the signal phase at some well defined time will be sent to the slow monitoring system.

45.4.2 The coils driver

The calibration signals used to drive the coils of the reference masses will be sent to the suspension control using coaxial cables with BNC connectors (±10V TBC). Then they will be locally added to the locking signals.

45.4.3 The laser diodes

The principle of this method is to move the mirror by the pressure of radiation of a source of light with a modulated power. This method is able to produce any kind of waveform very easily. The implantation is presented by figure 4500.1. Let's now review the light parameters.

45.4.3.1 Laser wavelength

Given our mirror coating, the choice of the wavelength is connected with the choice of the angle of incidence. As figure 4500.2 shows it, when the angle of incidence increases, the area with large reflectivity is shifted to smaller wavelength (0° is for normal incidence). The easier solution for the mechanical point of view is to use angle of incidence of 30° or 60°. In order to avoid any confusion with the main laser beam we will use a wavelength of 860 nm for the calibration laser and therefore we will use the 60° optical port.

45.4.3.2 Laser power

If we take a laser of power $P = P_0\cos(\omega t)$, hitting a mirror of mass M of reflection R with an angle of incidence i, the mirror motion is, above the pendulum frequency (a few Hz given the suspension design) :

$$x(t) = P_0\cos(\omega t)R\cos(i)/(Mc\omega^2)$$

As an example, if we want a displacement of $x = 10^{-17}$m, at 100 Hz, with M=21kg, R=.95, i =62° the needed laser power is: P = 110 mW (taking into account a factor 2 to generate a 55 mW cosine wave).

To get a better determination of the needed power, we compute the needed power to produce a displacement equal to the noise for one second of integration. The result is presented by the figure 4500.3 assuming a mass of 21 Kg and an angle of incidence of 62°. One can see that a 1W laser is enough to cover most of the frequency range. This correspond to a typical laser diode. It is also interesting to notice that a 1 W laser would provide a large signal in the 10-100 Hz where we could have problem to reach our design sensitivity in the beginning of the VIRGO running.

This low power compared to the main beam power (about 10 kW in the cavity) shows that no thermal problem on the mirror surface is to be expected. This low power combined with the fact that the calibration light has a different wavelength and is not modulated at high frequency removes any concern about diffused light going into the main beam.

The selected laser diode is a 5W diode from Spectra Physics with an 5 m long optical fiber connected to a beam expander. The resulting beam as a 2 cm diameter.

45.4.3.3 Optical layout and laser monitoring

Three small optical tables will be attached to the towers to hold the optical components. They will be the same as the ones used for the position memories. During the tower bakeout, the components installed on these tables will be removed.

The laser power will be monitored by two photodiodes collecting the input and the reflected beam. One of these signals will be recorded by the standard data acquisition system. The beam alignment will be checked by a quadrant photodiode looking at the transmitted beam. A 16 channels ADC will be used to collect these signals. The calibrator control CPU will perform these monitoring.

45.4.4 Calibration software

During special runs, we will sweep a sine wave or introduce a white noise to measure the transfer function. The calibration software will use these data to extract and parametrize this transfer function (TBC). A few permanent sine waves of small amplitude will be used to monitor this transfer function. The resulting value will be archived in a database.

45.4.5 Reconstruction software (TBC)

The reconstruction software will use the parametrized transfer function to compute in the time domain the h reconstructed values starting from the photodiodes signal. This software has to be studied in collaboration with the locking group.

45.5 Calibration interfaces

The interfaces are the following :

With the suspension control (WBS 4900): two coaxial cables with BNC connector are provided for the coils calibration signals.

With the tower (WBS 3200) : the calibration optical tables are attached on the tower. Three windows are needed on each input tower with the corresponding space.

With the Data Acquisition system (WBS 5400) : the four analog signals sent to each calibrator are recorded by the general DAQ. The status information which includes the parameters of the generated signals is sent to the slow monitoring frame builder.

With the VIRGO software : the reconstruction program will work on frames and will have the standard (SIESTA like) interface to the main program.

List of Figures

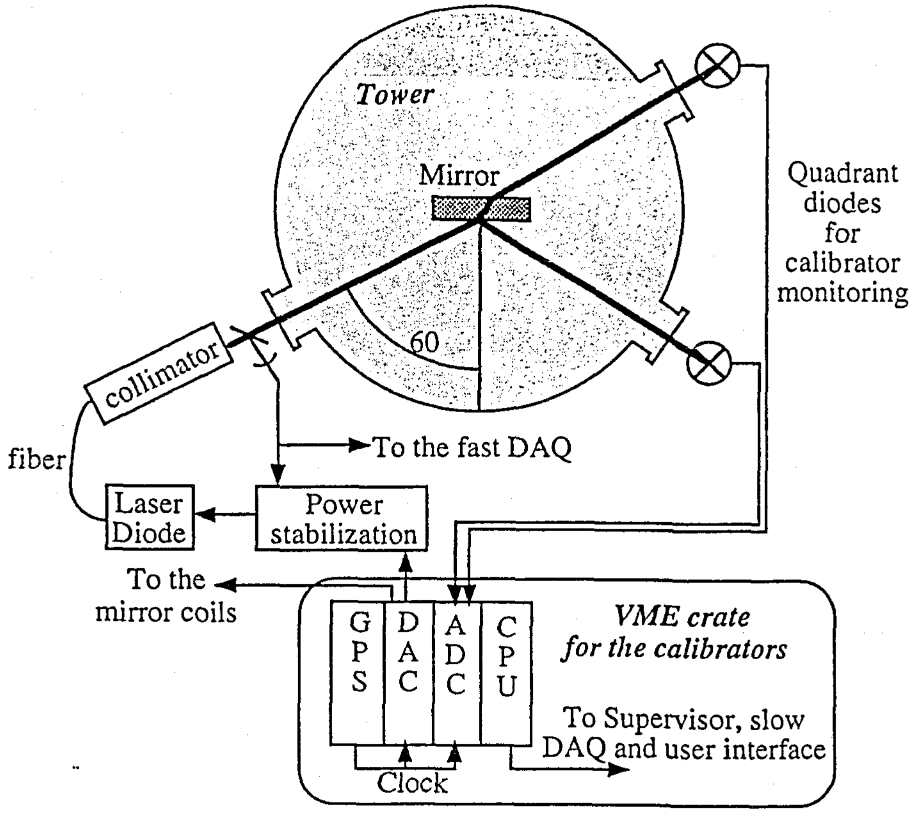

Fig. 4500.1

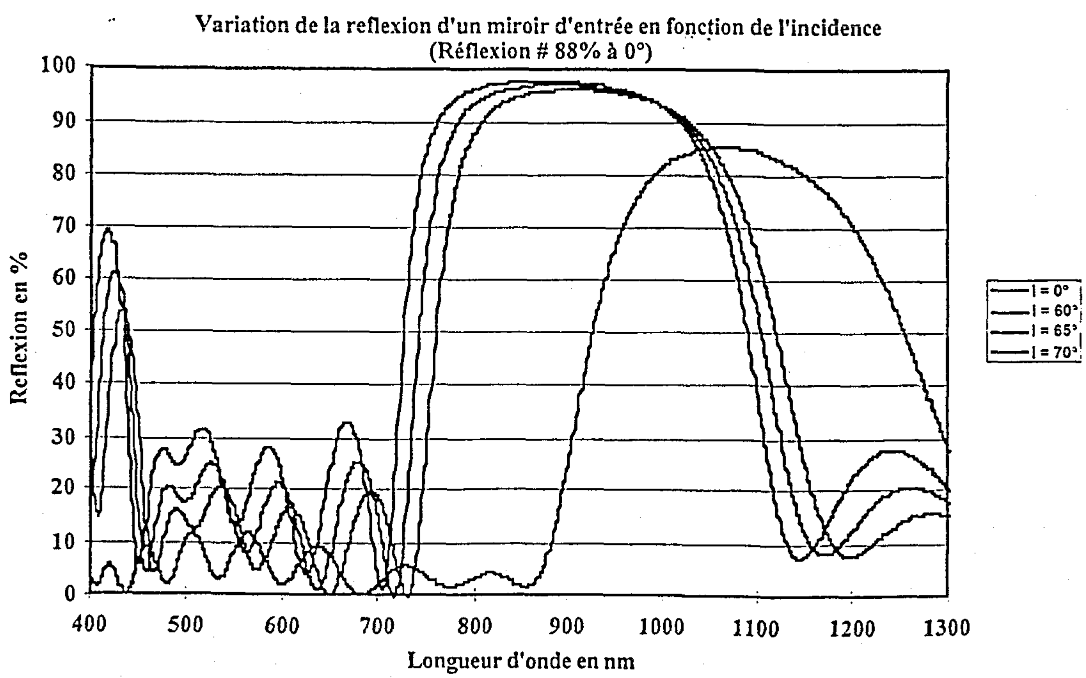

Fig. 4500.2

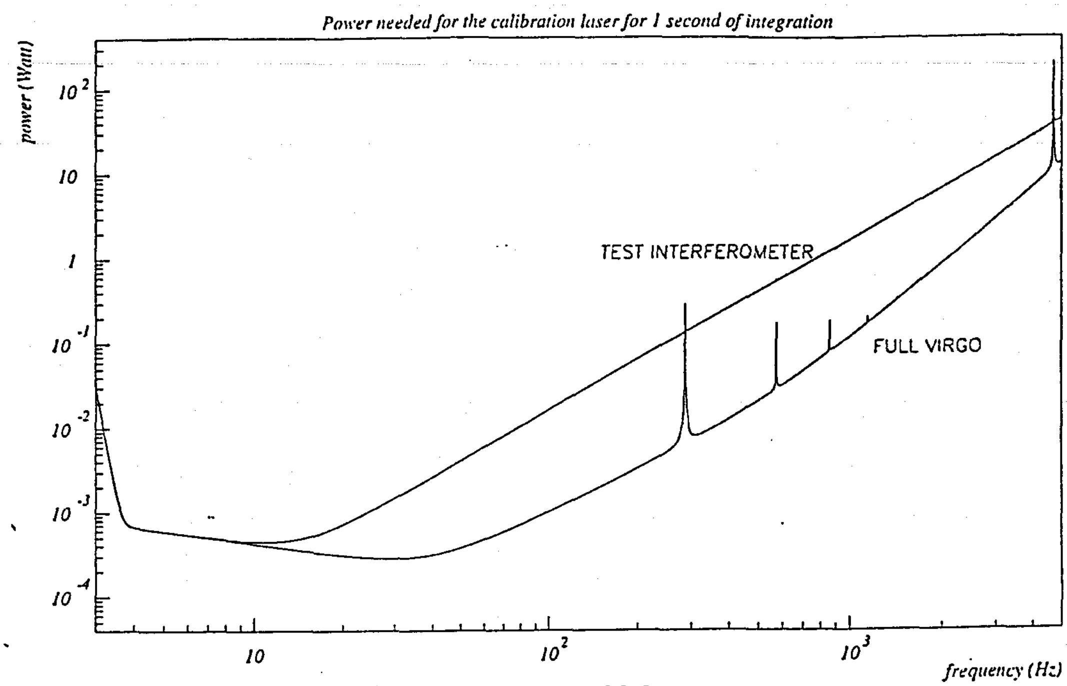
Power needed for the calibration laser for 1 second of integration
power (Watt)
10^2
10
1
10^{-1}
10^{-2}
10^{-3}
10^{-4}
10
10^2
10^3
frequency (Hz)
TEST INTERFEROMETER
FULL VIRGO

Fig. 4500.3

46. Suspension system

Table of Contents

46.1 Introduction

The test masses used in VIRGO have to be sufficiently decoupled from environmental perturbations so that gravitational waves are not masked by local effects. The suspensions for the VIRGO mirrors are designed to deal with the two main sources of noise in position while ensuring reliable operation of the interferometer. The resulting requirements and the working principles of the suspensions are shortly described below.

The first source of noise is the motion of the ground itself, the seismic noise. On the site of Cascina it is well described by a position noise spectrum [1]

$$\tilde{x}(\nu) = 10^{-6} / \nu^2 \mathrm{m} / \sqrt{\mathrm{Hz}} \qquad 4600.1$$

for frequencies above a few Hz. Attenuation for this noise to the required level is achieved by a cascade of mechanical filters. These are essentially harmonic oscillators with a low resonant frequency.

A damping mechanism is necessary to limit the oscillation amplitude at resonance frequency to keep the interferometer on its working point.

The other relevant source of noise is the thermal bath the mirrors are in equilibrium with. For any mechanical degree of freedom an amount of energy kT is stored between kinetic and potential energy, resulting in what is commonly called thermal noise. Although the amount of energy stored can be reduced only by working at low temperature, it is possible to confine most of the resulting motion in a frequency range where in any case VIRGO would not be sensitive.

A fundamental limitation comes from local gravity effects due to fluctuatons in the density of the surrounding matter. These have been estimated to account for a position noise of the order of

$$\tilde{x}(\nu) = 6 \cdot 10^{-16} / \nu^4 \mathrm{m} / \sqrt{\mathrm{Hz}} \qquad 4600.2$$

Severe constraints must be met by the suspension system in order to ensure a reliable operation of the apparatus. The mirror position should be controlled over a suitable range of frequencies to keep the interferometer on its working point. This requires a huge dynamic range: while the mirror motions due to the signal are of the order of 10^{-18} m there can be at low frequencies motions of the order of the mm due to daily ground displacements. Not only would these take the interferometer away from the ideal detection conditions but they would cause the passage through several fringes during data taking with severe consequences on operation efficiency. Up conversion of this low frequency motion can introduce further noise in the sensitivity band.

To apply corrections without introducing further noise is done as follows. Only the "fast" corrections are applied to the mirrors while the slower ones come at some point in the attenuation system. For the latter the mechanical filters attenuate the high frequency components which would fall within the VIRGO sensitivity range while transmitting the required low frequency motion. Large offsets to the nominal position are applied at the suspension point of the filter cascade.

The last important requirement for the suspension system is that it has to be compatible with the vacuum level required by the experiment. This gives constraints to the overall outgassing rate and on the presence of hydrocarbons that can deteriorate the mirror coatings.

The principle of the attenuation mechanism has been thoroughly tested experimentally and several computations predict the behaviour of the system, The sensitivity needed to measure the noise that the suspension will introduce can be achieved by suspending to an attenuation chain an optical cavity fed by an highly stabilised laser. This device is essential to the understanding the various causes of noise in Virgo as it can allow to single out the contribution of the suspension and allow to improve in the long term the sensitivity.

A complete suspension chain consists, from top to bottom, of the following elements: a movable suspension point, a chain of several seismic filters and a marionetta suspending the mirror. An elastic structure based on the principle of the inverted pendulum determines the position of the suspension point relative to the tower. The settings for this device are determined from the alignment error signals and the low frequency component of the locking error signals. Then there is a chain of five seismic filters, that perform a mechanical attenuation in all six degrees of freedom of a rigid body.. Each filter has its own height control so that the spring softening device stays on the right position. According to the requirements for the reference configuration two kind of suspension chains are used, a complete one with five filters and a short one with only two filters.

The stage on top of the inverted pendulum is equipped with accelerometers and shadowmeters to reduce the movement induced by the ground that will excite the normal mode oscillations of the structure. Damping forces are applied to the inverted pendulum and vertically on the suspension point by coils.

There are a few variations at the level of the last suspension stage, the marionetta, to take care of the mirrors and of the injection and detection benches with the same system.

Table 1. Suspension structure. The height is from the floor to the suspension point and doesn't include therefore the tower cover.

Position control	Mar. wgt kg		Filters	Height m	Total wgt kg
FP near	80	Mar.+Ref.Mass	5	10.430	1037
FP remote	80	Mar.+Ref.Mass	5	10.430	1058
Beam Splitter	80	Mar.+Ref.Mass	5	10.430	1021
Recycling Mirror	80	Mar.+Ref.Mass	5	10.430	1021
Mode Cleaner End Mirror	60	Mar.	2	6.436	TBD
Input bench	80 TBC	Mar.	2	6.436	TBD
Detection bench	80 TBC	Mar.	2	6.436	TBD

46.2 Suspension system requirements

46.2.1 Functionality and payload

The various elements of the interferometer are all suspended by means of a superattenuator. However the requests on position noise depend on the specific function of each optical element and are part of the interferometer design (see chapter on interferometer optics). They are summarized in table 2, *where no safety factor is included.*

Table 2.Position noise requirements for the optical elements without safety factor.

Device	Residual motion along beam		
	at 10 Hz RMS	at 100 Hz m/sqrt Hz	m/sqrt Hz l=10-6 m
Fabry-Perot Mirrors	3 10-18	10-19	6 10-6 l
Beam Splitter	10-16	3 10-18	2 10-4 l
Recycling Mirror	10-14	3 10-16	2 10-3 l
Mode Cleaner End Mirror	TBD	TBD	TBD
Input bench	TBD	TBD	TBD
Detection bench	TBD	TBD	TBD

While the requirements within the frequency band of VIRGO sensitivity are fulfilled by the suspensions, the low frequency displacements must be corrected by an active feed-back system.

The weight to be carried varies in a significant way from element to element. Optical requirements and thermal noise considerations lead to different mirrors in the Fabry-Perot interferometers. The far mirrors can be massive to reduce thermal noise while the near mirrors are the result of a compromise between light transmission and thermal noise.

The injection and detection benches carry relatively complex optical systems under feed-back control. The displacement requirements come from possible Doppler shifts. The same can be said for the mode-cleaner end mirror.

Position and orientation of all elements have to be controlled as part of the overall interferometer locking scheme. The position noise introduced by the actuators has to be below the nominal VIRGO sensitivity. The requirements on suspensions are summarized in table 3.

Table 3. Requirements on residual motion.

Suspension	Payload kg	Size cm	RMS position residuals transverse m	RMS position residuals angular rad
FP near	21	35	10^{-6} TBC	10^{-7}
FP remote	43	35	10^{-6} TBC	10^{-7}
Beam Splitter	6.4	23	10^{-6} TBC	10^{-7}
Recycling Mirror	0.750	12	10^{-6} TBC	10^{-7}
Mode Cleaner End Mirror	0.750 TBC	12	10^{-6} TBC	10^{-7}
Input bench	80 TBC	80	10^{-6} TBC	10^{-3}
Detection bench	80 TBC	80	10^{-6} TBC	10^{-3}

46.2.2 Temperature stabilisation

Residual motion, even at low frequency, is a concern. Since low resonance frequencies are achieved by forces with different behaviour with position the system is expected to be more sensitive to temperature variations. Displacements of 1 mm/degree can be expected at the mirror level. Moreover the system may go out of its optimal tuning, as discussed in the standard filter description. A temperature stability of $\pm$ 0.1 degree (TBC) is required to ensure correct operation of the suspensions.

46.2.3 Vacuum compatibility

Refractive index variations due to pressure fluctuations are a source of noise in the optical length measurement. The residual H_2 pressure to be achieved in Virgo is of 10^{-8} mbar and the elements under vacuum have to be compatible with the pumping rate of the installed system (see the chapter on the vacuum pumping system). In addition the partial pressure for hydrocarbons has to be less than 10^{-13} mbar so that the reflective coatings do not loose their properties. To achieve this the suspension towers are divided into an upper and a lower part separated by a conductance pipe for the supporting wire. The conductance is 1 l/s for water. In this configuration the components in the upper tower part should have an overall outgassing rate compatible with a residual pressure of 10^{-6} mbar at a pumping speed of 500-1000 liters/s. In addition the outgassing rate for hydrocarbons should be less than 10^{-10} mbar liters/s assuming 1 l/sec conductance from upper to lower part of the tower also for hydrocarbons.

46.2.4 Bakeability

The suspension system should be able to stand a temperature of 80 degrees which is expected during the baking of the towers lower parts.

46.3 Suspension interfaces

The suspension system has a number of sensors to monitor its state and a number of actuators to achieve, directly indirectly, mirror positioning. External information needed to position mirrors comes from the interferometer error signals, local postition monitors and commands to define the behaviour of the digital filters that synthetize force signals. Suspension electronics (4900) takes care of this, producing currents that feed the control coils and stepping motors.

46.3.1 Interface with towers

The internal support structure must fit the tower basis and must hook to the tower rings.
Baking of the tower lower part causes high temperatures to be achieved in the upper part, where some elements cannot reach high temperatures.

46.3.2 Interface with local electronics

Cables for LVDT, stepping motors and control coils must be connected to the local electronics. Since in the present design no active element stays inside the vacuum system connections will mostly be analog and have to be noise-free. This is true in particular for signals acting on mirrors, where soldering is mandatory. The detailed description of the signals is available in the cabling sub-subsytem description.

46.4 Detailed description

The solution adopted for the VIRGO suspensions is a sophisticated mechanical structure, called Superattenuator, able to filter the seismic noise down to frequencies of a few Hertz (fig. 4600.1).

The suspension consists in a cascade of massive pendula 1.2 m each connected one to the other. The working principle relies on the fact that for frequencies above the resonances of the system each stage can be seen as a filter attenuating a signal by a factor

$$A(\omega) \propto \frac{\omega_0^2}{\omega^2} \qquad 4600.4$$

as is well known from the behaviour of a driven harmonic oscillator. In this way the use of pendulum properties results in an attenuation of the position noise from the suspension point to the swinging mass.

It turns out that due to uncontrollable couplings between the pendular and other degrees of freedom it is necessary to attenuate also rotations and the motion in the vertical direction. Rotational degrees of freedom are taken care of with high moments of inertia and short lever arms for torque application. This is achieved by having the connections at the filter level very close one to the other. The resulting resonance frequencies are of the order of 1 Hz.

In the vertical direction a similar result is achieved by suspending the next element of the chain through springs. However the resonant frequency of the system is be high if the Superattenuator is to be sustained with an acceptable elongation. To reach also in this case a low resonant frequency these springs are ``softened" around the working position by means of a force increasing locally with displacement.

The solution adopted for the seismic filters uses magnets in a repulsive configuration that move transversally to their magnetic field.

The attenuation of the seismic noise has been studied experimentally. This result doesn't take into account further attenuation that can be achieved using the system designed to damp normal mode oscillations.

46.4.1 Mechanical filters

46.4.1.1 Mechanical filters function and concept

As discussed above, each mechanical filter is designed to reduce the transmission of mechanical vibrations in all degrees of freedom. The mechanical filter (Fig.4620.1) is essentially a rigid steel cylinder suspended as close as possible to its center of mass by a piano steel wire (about 1 m long and with a diameter of few mm). The filter supports the load of the lower stages through a converging set of triangular cantilever blade springs. The base of each triangular blade is clamped to the outer circumference of the bottom of the filter body. The tip of each blade of the filter is attached to a vertical central column through a 1 mm diameter piano wire. The central column can move only in vertical as its movements in any other direction are prevented by two systems of four centering wires mounted on the top and on the bottom of the filter body. The next mechanical filter is attached to the central column through another piano steel wire. In other words, the moving part of the filter, formed by the blade springs, the central column and the crossbar, acts as a vertical spring suspending the lower stages. In this way a chain of vertical pendula able to attenuate the seismic vibrations also in the vertical direction is achieved. In order to attain the attenuation performances discussed in the previous §, each mechanical filter must have the frequency of the vertical and horizontal pendulum below 0.5 Hz [1]. This condition guarantees that all the vertical resonances of the chain are below 3 Hz. The internal resonances of the filter structure must be at high frequency (well above the seismic noise region). When necessary, special dampers will be used to suppress the spurious peaks induced in the mechanical transfer function by the internal resonances of the filter.

As illustrated in Fig.4620.2, the blades are pre-bent to a rest position with a single radius of curvature. They return to be straight and horizontal under load. A vertical spring return force acts on the load suspended from the blade's tip as it moves from its equilibrium position. What determines the vertical frequency f_v of the filter is the stiffness of the blades ring k_v:

$$f_v = \frac{1}{2\pi}\sqrt{\frac{k_v}{M}} \qquad 4620.1$$

where M is the mass of the load suspended from the central column. The advantage to use blade springs is that they are able to support large loads with a small stiffness and exhibit only high frequency internal modes. k_v is limited by the equilibrium condition

$$k_v \cdot y_0 = M \cdot g \qquad 4620.2$$

where y_0 (Fig.4620.2) represents the vertical displacement of the blades' tip from the rest position to their new equilibrium position. As the load is fixed, the blade stiffness can be minimized by building long blades or highly stressed blades. In order to lower the vertical stiffness (and thus the vertical frequency) it would be necessary to have filters of larger diameters. Practical limitations force the use of filters with diameters less than 1 meter. The elastic limit of steel fixes the lower limit of the stiffness obtainable for blades. As a result, only a vertical resonant frequency of 1.5 Hz in each stage of the superattenuator can be achieved, well above the goal of 0.5 Hz. A vertical frequency below 0.5 Hz can be obtained by "softening" the vertical blade springs around their working point by means of the magnetic system indicated in fig. 4600.2 (antispring).

The working principle of the magnetic antispring can be explained considering the system of fig. 4620.3: two permanent magnets, aligned facing each other, with opposite horizontal magnetic moments (namely in a repulsive configuration) and constrained to move only along the vertical axis. When the magnets are perfectly aligned (Fig.4620.3.a) the repulsive force has a zero vertical component. If one of the magnets is moved in the vertical direction, a vertical component of the repulsive force appears. For a vertical relative displacement (Δy), small with respect to the separation (d) of the magnets effective centers and to their transverse dimension, the vertical component (F_y) of the repulsive force is proportional to Δy:

$$F_y = F_0 \cdot sin(\alpha) \approx F_0 \cdot \Delta y/d \qquad 4620.3$$

where F_0 denotes the modulus of the repulsive force and $\alpha \approx \Delta y/d$ is the angle in Fig.4620.3.b. This arrangement is thus equivalent to a vertical spring with a negative elastic constant (antispring) whose modulus is F_0/d and with the rest position where the magnets are perfectly faced.

The antispring effect is achieved on the mechanical filters by mounting two matrices of rectangular brick magnets on the top of the filter body, facing two back to back matrices fixed to the crossbar of the central column (Fig.4620.4). Since the central column is attached to the blades'tip and holds the wire of the suspended mass, the magnetic matrices on the crossbar are solidal to the lower attenuator stage. In other words, a vertical antispring force acts between the blade filter and the load. This force is in parallel with the spring force of the blades and neutralize it. The effectiveness of the antisprings in reducing the main vertical resonant of each filter well below 0.5 Hz has been proved on prototypes [2].

In order to tune the vertical position of the moving part of the filter so as to place the magnetic matrices one in front of the other, the inclination of some cantilever blades can be varied by a system of setting screws (Fig.4620.1). The number of adjustable blades on each stage depends on the total number of blades used on that stage (see Table 4). Recent studies on the thermal stability of the mechanical filters [3,4] have shown that the sophisticated hydraulic bellows system [5] used to tune the inclination of the adjustable blades during the data taking can be eliminated. The fine tuning of the vertical position of the central column will be performed without opening the vacuum tower by changing through a stepping motor the inclination of a small blade connected through a steel piano wire to the crossbar. This system is named "fishing rod" and it is driven by a feed-back loop. The vertical position of the moving part of the filter is detected by measuring the vertical position of the crossbar with respect to the filter body by an LVDT (Linear Variable Differential Transformer) sensor, whose description is given in the next §. This system should be able to tune the vertical position of the moving part of the filter with a precision of few microns.

46.4.1.2 Mechanical filters detailed description

On the basis of the description provided in the last §, the following breakdown structure for the mechanical filter has been performed: 1) Filter body (and its components), 2) Blades, 3) Antisprings, 4) LVDT sensor, 5) Dampers, 6) Fishing rod, 7) Centering system and 8) Suspension wires.

46.4.1.2.1 Filter body

The filter body is a stainless steel AISI 304L cylindrical element of about 800 mm diameter and 200 mm height (Fig.4620.5). It is a cylindrical drum closed on the bottom and top by two lids stiffened by 12 internal ribs. Clamps for holding a maximum of twelve blades are welded on the outer diameter of the cylinder. The components attached to the filter body and the corresponding materials are listed in [6]. Studies on prototypes attested the good mechanical performances of the filter body [7], allowing to finalize its design.

46.4.1.2.2 Blades

The steel blades of the mechanical filters [5,8,9] have a thickness of 3.5 mm, a length of 345.4 mm, while the width of their base changes according to the load to be supported (see Table 4). The triangular shape gives the blades a rest and stressed shape with a single curvature radius and allow to distribute uniformly the stress in the material under load. Bending curvature and dimensions are such that in a loaded cantilever the internal stress is always kept below 2/3 of the elastic limit. Recent studies [10] have shown that the Marval 18 steel has to be used to avoid creep in the blades. This material will replace the C70 stainless steel, used in the first prototypes. The following thermal treatment of the Marval 18 has provided the best results in terms of creep: solubilization at 825 ^{0}C for 1 hour under vacuum (or in neutral environment), natural cooling at room temperature and aging at 480 ^{0}C for 16 hour. Starting from this raw material, the blades will be constructed following the design of Fig.4620.2. All the blades will be protected from rust formation with a thin layer of nickel. The blades under load exhibit a 1.5 Hz pendulum mode and the first flexural mode at about 100 Hz.

In Table 4 the main characteristics of the blades mounted on each filter of the chain are reported. A full characterization of the mechanical performances of the cantilever blades has been given in [5,8,9]. The blades have been heated under load at 80^{0}C without significant effects in their mechanical performances. Future tests should allow to identify the maximum baking temperature tolerated by the blades under stress.

46.4.1.2.3 Antisprings

Each of the four magnetic matrix mounted on the filter (Fig.4620.4) is made of two or four lines of Philips ferroxdure (FXD 330) magnets (6 x 2 x 1.5 cm^3) producing a nominal magnetic field of 0.36 Tesla in the direction parallel to the 1.5 cm dimension [11]. Each line of magnets in the matrix has the sense of the magnetic field opposite both to that of the neighboring line, in the same matrix, and to that of the line facing on the opposite matrix. This configuration allows to minimize the total magnetic dipole of the system, reducing the coupling with the external magnetic field [12]. The number of magnets in each line is decreased from the top to the bottom filter to match roughly the need of antispring elastic constant. 24 magnets per matrix will be used on the first filter, 20 on the second one, 16 on the third one and 12 on the fourth one. Fine tuning of the antispring force is obtained by setting the horizontal separation of the magnetic matrices. A vertical frequency of 0.4 Hz on the filter can be attained with a separation between the magnetic matrices of about 1 cm. The supports (Fig.4620.4) will be made of Titanium, a material showing the same thermal dilation coefficient of the magnets. A full characterization of the antispring system (dependence on the positioning, on the temperature and on the number of magnets) has been given in [2,13]. This work has shown that large tolerances are allowed in the assembly of the antispring matrices. The main problem arises from the strong dependence of the permanent magnetic field on temperature. In order to keep the magnetic matrices aligned within the vertical working range (about one hundred of microns), it is necessary to reduce the filter thermal swings, stabilizing the temperature of the VIRGO towers. A thermal stabilization of few tenths of degree peak to peak is necessary [14].

Both the magnets and the titanium supports exhibit good vacuum performances. The glue proposed for attaching the magnets on the supports is VAC-SEAL [15]. This glue has shown a very low outgassing rate. The mechanical performances of this glue have not been still certified and other cheaper glues are also under test.

Table 4: Main specification of the mechanical fitlers for a complete chain

Filter	1	2	3	4
Total load (Kg)	729.3	597.6	469.6	354
Fixed Blades n.	8	6	4	4
material	Marval 18	"	"	"
width (mm)	137	136	134	132
flexural length (mm)	354.5	354.5	354.5	354.5
thickness (mm)	3.5	3.5	3.5	3.5
load per blade (N)	691	614	607.5	595.8
curv. radius (mm)	461	461	461	461
stress (N/mm^2)	787	783.9	787.2	783.7
stiffness (N/m)	5327	4733	4683	4593
Adjustable Blades n.	4	4	4	2
material	Marval 18	"	"	"
width (mm)	120	120	120	120
flexural length (mm)	354.5	354.5	354.5	354.5
thickness (mm)	3.5	3.5	3.5	3.5
load per blade (N)	543	543	543	543
curv. radius (mm)	461	461	461	461
stress (N/mm^2)	787	783.9	787.2	783.7
stiffness (N/m)	5327	4733	4683	4593
Suspension Wires				
material	Marval 18	"	"	"
load (N)	7147	5856.5	4602.1	3469.2
length (mm)	1993.8	993.8	993.8	996.3
diameter (mm)	3.25	3.0	2.5	2.25
stress (N/mm^2)	861.5	828.5	937.5.	872.5

46.4.1.2.4 LVDT sensor

The design of the LVDT sensor is reported in Fig.4620.6. A 10 kHz AC-signal flows in the internal coil, while the external coil, which is the passive element, is composed of two parts wound in opposite direction (clockwise and anti-clockwise). When the external coil moves with respect to the symmetric position ("zero position") the combined output signal at the passive coil extremities is proportional to the difference between the signals induced on either of its two parts. A 10 kHz signal, whose amplitude is proportional to the relative displacement between the two coils, is induced on the passive elements. The electronic performances and the vacuum compatibility of the materials have been validated and the final design of Fig.4620.6 has been frozen.

46.4.1.2.5 Dampers

The first flexural mode of each blade (around 100 Hz) can be suppressed by attaching at the point of its maximum oscillation, close to the center of the triangular surface, a short viton rod (3 cm long and with a diameter of 5 mm) with a light mass (5 grams) located near its other extremity (Fig.4620.7). The mass oscillates in the vertical direction inducing a flexure of the viton rod with opposite phase to that of the blade's displacement. The frequency of the viton oscillator can be tuned on the blade's first flexural mode by varying the position of the mass along the rod. In this way, the energy of the blade flexural mode is transferred to the dissipative viton oscillator and a strong attenuation is obtained.

A similar solution has been designed for suppressing a resonant mode involving the crossbar. This internal mode is due to the fact that the suspension wire connecting the crossbar to the next filter acts as a spring. The resonance, around 60-80 Hz, is suppressed by using an iron cylindrical mass of 2.5 kg resting on three viton columns at the center of the crossbar (Fig.4620.8). The mass oscillates in the vertical direction while the viton columns act as damping springs. The length of the columns is chosen to tune the damping system on the frequency of the crossbar mode.

Attenuation performances of the dampers on the blades and on the crossbar have been measured, obtaining in both cases a reduction of the peak of the transfer function of more than one order of magnitude [16]. These results are satisfying and have been obtained within tolerances of about 1 mm both in the positioning of the mass of Fig.4620.7 and in the tuning of the length of the three columns of the crossbar damper (Fig.4620.8). The exact frequency of the internal resonances of the filter depends on the precise structure of each stage and a fine adjustment of the dampers will be necessary during the construction phase.

46.4.1.2.6 Fishing rod

The system must be able to tune the position of the crossbar with a precision of few microns and with a dynamic range of few mm. The fishing rod prototype depicted in Fig.4620.9 has still to be tested. The proposed Marval 18 triangular blade has a width of 40 mm, a flexural length of 248 mm, a maximum load of 20 N, a curvature radius of 469.2 mm, an internal stress of 330.7 N/mm^2 and a stiffness of 402.5 N/m. The blade is connected through a Maraging H steel wire (0.6 mm diameter and 200 mm length) to the crossbar. The proposed motor is a commercial stepping motor, which will be chosen on the basis of the mechanical and outgassing tests.

46.4.1.2.7 Centering wires

The centering wires are made of Marval 18 steel in order to avoid creep problems. They will be protected from rust formation with a thin layer of nickel. All the centering wires will be set at a frequency 200±50 Hz. In this condition, the tension of the wires is sufficient to keep the central column aligned and it is small enough to avoid overstress (and thus creep) inside the material. This frequency must be stable on the long term in order to avoid mechanical vibrations induced by yielding of the wires. For this reason the end of each of the 8 centering wires is strongly clamped in a mandrel, whose mechanical performances have been validated [17].

46.4.1.2.8 Suspension wires

Recent studies [18] have shown that use of Marval 18 steel wires is mandatory to minimize the creep processes and hysteresis effects in the suspension wires. This material will replace the C70 steel. The suspension wires have a "double nail head" obtained by center-less griding of a larger diameter of the piano wires. The nail head is mounted inside a screw head by means of a split cup washer. The resulting wire headings are then simply screwed in two tapped bridges attached to the upper and lower suspension points of the lower and higher filters.

The distance between the attach points of the two wires is only 5 mm in order to keep the rocking frequency of the filter below 1 Hz. In Table 4, the features of each of the suspension wires are reported. The chosen diameters of the suspension wires allow to have all the rotational frequencies of the chain below 1 Hz.

46.4.2 Inertial Damping

46.4.2.1 Inertial damping function and concept

Once suspended to the Super-Attenuator the mirrors will oscillate at low frequency (about 0.2 Hz) with an amplitude of the order of ten micron. This oscillation is maintained by the seismic noise injected at the suspension point and its amplitude is determined by the quality factors associated to the normal modes of the suspension. In order to keep the interferometer optical cavities at resonance this residual motion has to be reduced by several orders of magnitude.

By applying a feedback force proportional to the velocity one performs a "viscous" damping reducing the quality factor of the normal modes.

In the reasonable hypothesis that the residual rms displacement of the mirror is mostly due to the lowest frequency normal mode (where all the SA stages are moving like a single pendulum) it is simple to evaluate the effect of a viscous damping system. For a pendulum having f_0 as resonant frequency and Q as quality factor one has

$$x_{\mathrm{RMS}} = \tilde{x}(f_0)\sqrt{\frac{\pi f_0 Q}{2}}$$

where $\tilde{x}_s(\nu)$ is the seismic noise spectral density. Assuming $\tilde{x}_s(\nu) = 10^{-6} / \nu^2 \mathrm{m} / \sqrt{\mathrm{Hz}}$ (eq.1), a quality factor of 60 and a resonant frequency of 0.23 Hz (the values measured on the first SA prototype), the rms displacement of the mirror is about 80 microns, which would give difficulties in locking the interferometer. By achieving a Q of 0.5 the residual rms displacement becomes 8micron.

This quantity is low enough to make the interferometer work (assuming that the locking system is able to cope with mirror displacements up to 10 micron).

A residual displacement x_RMS=3.4 micron has been achieved in the suspension prototype developed in the last years in Pisa.

The viscous force applied on the top stage of the SA may not be sufficient to reduce the displacement under a few micron. The measurement of the displacement is performed with respect to a grounded noisy structure: by increasing the gain loop of this cooling system, the top stage shall be locked to the grounded structure, short-circuiting theinverted pendulum.

Moreover when forces are applied to the top stage to damp it, vibrations are induced in the structure supporting the actuators and the sensors. These vibrations can generate oscillations in the feedback system, thus limiting the bandwidth of the damping system and so the resulting gain.

It is foreseen to further reduce the rms displacement below 1 micron by performing a measurement not referred to a noisy structure but to an inertial frame instead by means of acceleration sensors. Four such devices are installed on the top stage (three horizontal and one vertical acceleration sensors) while two others are on thebottom ring sensitive to rotation acceleration. Signals are produced that measure motion with respecto to an inertial frame. These signals can be used to apply appropriate forces through magnet-coils pairs. In this way not only the resonant motion can be damped but a higher reduction of the low frequency level of the displacement can be achieved.

46.4.2.2 Inertial damping detailed description

Inertial damping is achieved by means of accelerometers and LVDT that generate signals to be used to compensate the position of the suspension point.

46.4.2.2.1 Horizontal accelerometers

Horizontal accelerometers are based on a mass suspended by means of a low resonant frequency spring system. A feed back loop keeps the mass on a reference position. Acceleration is derived from the correction signal applied to the accelerometer.

46.4.2.2.2 Vertical accelerometers

The vertical accelerometer is based on the same principle as the horizontal one. The mechanics is different to achieve a low resonant frequency while compensating for the acceleration of gravity.

46.4.2.2.3 Rotation accelerometers

Rotation accelerometers use the same elements as the horizontal accelerometers but instead of a mass the sensitive element is a rod allowed to turn around an axis.

46.4.3 Filter 7 (or steering filter)

The last filter of the chain, historically called filter 7, holds the coils that steer the marionetta and the injection and detection benches. It must be able to exert forces and torques on the marionetta to set the mirror longitudinal and angular position. Such an action will cause a recoil of the filter and the system filter7+marionetta will have a dynamics similar to the one of two masses held by a sprint and must be taken into account whendesigning the feedback control.

To reduce the power dissipateed in the steering coils mechanical offsets of the filter position have been included. The rest angular position of filter 7 with respect to the conductance bechers and the angular position of the marionetta have to be adjusted. Furthermore the angle the filter makes with the vertical has to be adjusted as well.

During the baking process of the tower lower part the legs will be heated as well. The filter must be designed to resist to the temperature it will reach during baking. Calculations are in progress to determine the temperature distribution in the whole chain.

46.4.3.1 Filter 7 detailed description

Filter 7 consists in a modified standard filter body to allow for vertical rotation of the filter itselfwith respect to the suspension and of the wire suspending the marionetta. Two vacuum compatible ceramics ball bearings allow for rotation, steered by two stepping motors.

Balancing of the filter is achieved by means of a plate that acts as counterweight on the top of the filter body. The position of the plate can be adjusted in the x-y direction by stepping motors. It is foreseen to perform these adjustments quite unfrequently and outside data taking periods.

The legs and coils have to be connected in a sufficiently rigid way not to introduce further resonances in the system. This is achieved with an additional plate bolted to the filter body.

A drawing of filter) is shown in figure 4640.1

46.4.4 Top Stage

46.4.4.1 Top stage function and concept

The motion at frequencies below the first resonance frequency of the superattenuator have to be achieved by moving the suspension point. The top stage lays at the top of the metal support structure of the towers. It defines the average position of the whole SA at the level of a few micron while carrying the whole weight (about 1 ton)

The requirement for smooth motion with a large load over a large range leads to a system moving in elastic regime. This is achieved by building a structure hereby called Filter 0 that rests on three beams. These beams 6 meter high are fixed to a ring by means of elastic joints. A large motion at the top results in a small deformation of the joint. A relevant consequence is that the elastic recalling force on Filter 0 can be small, leading to low resonance frequencies of the system.

The ring is itself supported by piezoelectric feet that maintain it horizontal. Noise in the motion comes in priciple only from internal friction in the metal of the joints. This allows to move the suspension point smoothly during data taking to compensate for slow ground motion.

Horizontal motion is obtained with stepping motors working under vacuum that push and pull Filter 0 supporting the suspension point. Finally a mechanism raises and lower the superattenuator by means of a screw.

A drawing of the whole system is shown in fig 4.

All these motions are remotely controlled but an offset can be applied at assembly time to the position around the vertical axis. All stepping motors have an absolute position readout to allow for reliable operation when the tower is closed.

The vertical lift contains a recirculating ceramicball bearing that can work under vacuum.

46.4.4.2 Support structure function and concept

The support structure holds the safety rings for the seismic filters. In addition they hold the coils and stepping motors of the top stage. Finally they bring the cables to the top of the suspension chain.

46.4.4.3 Top stage detailed description

The top stage consists in an elastic structure resting on a rigid ring. The ring itself is kept horizontal by an active feedback on angular position. By keeping the resonance frequency of the structure below 100 mHz a significant attenuation in the horizontal direction is achieved. This results also in low forces that need to be applied to compensate for the ground slow motion.

A simple inverted pendulum is made of a light vertical stick fixed on ground by means of an elastic joint. A weightat the top of the stick is source of a vertical force. For small angles the restoring moment is given by

$$M = -(k - mgl)\theta$$

where m is the mass at the top of the stick, l is the length, k is the elastic constant of the joint and θ is the angle of the inverted pendulum with respect to the vertical. The resonance frequency can be brought to zero by increasing the weight.

Practical realisation requires to take into account the stick moment of inertia and to allow for tolerances in the joint elastic constant. A system made of three inverted pendula supporting a table is more complex and prototypes have been developed to understand the dyynamics in detail and to measure seismic attenuation.

The resulting design consists in a support ring that is kept horizontal by means of three piezoelectric feets. This ring supports the elastic joints, that apply their restoring momentum at the "percussion point" of each stick, using rotation inertia to improve seismic attenuation. With a rigid connection of the top table to the three sticks the torsional resonance frequency is much higher than the pendulum ones. The top table is therefore suspended by means of wires: a torsion of the system is achieved by inclination of the sticks only without torsion of the elastic joint.

To achieve attenuation in the vertical direction too the top table has metal springs to support the suspension point, the resulting structure being similar to a standard filter, but of a larger size (Filter 0). This filter is suspended at the top extremity of the legs by wires. The reason is that a rigid structure at the top would make the system more stiff.

LVDT provide a position measurement of filter 0 with respect to the safety structure (see 4650) which supports also coils and stepping motors for positioning the suspension point.

46.4.5 Cabling

46.4.5.1 Cabling function and concept

The cables are used for the electrical connection between the equipment inside the towers and the one outside. Inside the tower these cables go down along the suspension to reach all filters, the marionetta and the reference mass, or the optical table . Therefore they must be selected taking into account their vacuum compatibility, seismic isolation compatibility, electrical compatibility (currrent intensity, impedance, cross talk, etc.). Besides they should not introduce additional noise, for example by rubbing one against the other.

Table 5 gives the number of cables needed for a full tower before any optimization. These cables have a typical length of about 10 m.

Table 5. Cables in each tower.

Purpose	Number
Readout signal	30
Position control	36
Power for position control	86
Driving signal	30

46.4.5.2 Cable description

The various cables are described below.

46.4.5.2.1 Signal cables

These cables bring back the signals from the accelerometers and the LVDT. The signal is modulated at a driving frequency around 50 and 20 kHz respectively . The dominant noise is thermal noise in the coils.

46.4.5.2.2 Control cables

These cables have to supply the currents to the coils that produce electromagnetic forces on the following elements:
- top stage
- accelerometer mass
- marionetta and benches
- mirror through the reference mass

The cables that go to the mirror coils are particularly sensitive to noise: they must not pick up any signal that would create a displacement above the residual mirror motion.

46.4.5.2.3 Power cables

These cables power the several stepping motors and the piezoelectric feet. They should be shielded not to induce signals on other cables, especially the control ones.

46.4.5.2.4 Driving signal cables

These cables provide the driving signal for the LVDT on the suspension and inside the accelerometers.

46.4.5.2.5 Top stage support ring and piezoelectric feet

The supporting ring is a structure with diameter 1800 mm (TBC) which rests on three piezoelectric feets. The lowest resonance frequency has been calculated to be above 80 Hz (TBC). These are the actuators that allow to keep the ring horizontal, contrasting ground tilt motion. Only part of the force needed is supported by the piezo crystals, an elastic metal cup providing the necessary additional force (see fig.4650.3).

46.4.5.2.6 Top stage legs and elastic joints

Contact between the legs and the elastic joint has to be at some distance from the extremity to minimize seism effect at the top. This leas to the bell at the leg bottom, with the elastic joint at the clapper place.

The elastic joints are a critical item of this component. If they are fabricated with too low an elastic constant the system can be unstable. The current design foresees a nominal resonance frequency of 100 mHz, with the possibility to lower it either passively by adding weight at the top or actively by positive feedback on Filter 0 position.

46.4.5.2.7 Filter 0

Filter 0 isbased on a standardbody structure, but with a larger diameter. In addition the filter is suspended by the sides to the legs by short wires that don't introduce any unwanted rigidity in the system.

Fig. 4650.4 shows a drawing of filter 0 inside the tower cap.

46.4.5.2.8 LVDT and actuators

Position with respect to a structure connected to the ground is measured by means of LVDT. This information, together with the low frequency component coming from the locking and local alignment is used to compensate long term ground motion. The LVDT have a diameter of 50 mm (TBC) and a useful range of +/- 20 mm (TBC). The position noise is 10-10 m/sqrthz.

To avoid high dissipation in vacuum there are two kinds of actuators. For AC motion coils are used togenerate a magnetic field gradient causing a force on permanent magnets. For slw and DC offsets a stepping motor pushes or pulls a wire connected to the filter 0, displacing thus the equilibrium position of the system.

46.4.5.3 Support structure detailed description

The support structure is made of three beams with a C profile connected by rings. The structure is modular so that assembly of the superattenuator can be performed by working at ground level. Suitable bolts connect the structure to the viroles.

46.4.6 Tools

46.4.6.1 Tools function and concept

Special tools have been developed to allow te production and check of the suspension elements.

46.4.6.2 Tools detailed description

Tooling is required for the mass production of the suspension elements. In particular tools for testing ans assembling the filter elements are required, together with a facility that allows cleaning for vaccum compatibility the assembled elements.

46.4.6.2.1 Metal spring test

Each metal spring undergoes mechanical and thermal treatment. The resulting elastic constant has to be measured and the uniformity of strain has to be verified by an hydraulic machine capable of applying a known stress. Metal springs can be also cycled to check further their mechanical properties.

46.4.6.2.2 Suspension wire test

The suspension wires must be checked by plotting stress-strain curve that allow to extrapolate to the yield and breaking points. All wires have to be checked, since they undergo a treatment to produce nail-heads at theit extremities.

46.4.6.2.3 Test bench for filter and damper tuning

A test setup with two filters and a tunable mass must be available to tune a seismic filter with its real load. This will allow to tune the metal spring and crossbar dampers and to measure for reference purposes the filter to filter transfer function.

The setup must allow to work without soiling the filter, since such a tuning will be one of the last operations before storage for assembly.

46.4.6.2.4 Washing machine

An ultrasonic cleaning machine with a vessel diameter of 1250 mm is being purchased. It will allow cleaning of a whole assembled seismic filter and of several other parts (for example metal baffles). The procedure is bieng defined, with the purpose that cleaning must aim to remove grease residuals that would otherwise influence the vacuum quality.

46.4.7 Storage and transport

46.4.7.1 Storage and transport function and concept

The prodcution of the suspension elements is a complex pipeline. Local storage and transport facilities are needed to synchronize production with asembly on site.

46.4.7.2 Storage and transport detailed description

It is intended to store tested clean elements in protection cases to allow for transportation to Cascina and direct assembly on site.

46.4.8 Transfer function measurement

46.4.8.1 Function and concept

The problem of the measurement of the transfer function (TF) of the last stages of the Superattenuator (SA) was discussed in a workshop dedicated to this subject [19].The idea is to send a light beam on the suspended mirror from the outside of the vacuum tank and to recover the mirror displacement (when subjected to a known excitation) by looking at the reflected light with a suitable optical device. The first motivation for building such a device is the characterization of the final stages of the suspension, including the transduction efficiency of the magnetic coils used for the locking and alignement servoloops. This is necessary in order to design the loop filters itself. In particular it is necessary to measure the mechanical transfer function of the system for forces applyed on the marionetta or directly on the mirror from the reference mass; what is actually measured is the displacement induced on a suspended Virgo test mass, when exited with a known force with the loop coils (or better when a given signal is feed to the coil driver).

For this measurement a dedicated interferometric device will be used. The main requests on the characteristics of this device can be summarized as follows:

1) It must be operating outside the vacuum tower to avoid any interference with the operation of VIRGO.
2) It must be "portable" in the sense that it could be necessary to dismount it sometime since it will use some windows that could be used also for other purpose (calibration, optical memories,...).

The measurement of the transfer function will be performed in on site in Cascina for all the suspension chains before the operation of the central interferometer to verify that the systems behaves according to the design and to defyne the actual location of mechanical poles and zeroes in order to design the proper loop filters to lock the interferometer. During Virgo operation in principle an indipendent TF measurement in not necessary because Virgo itself is of course sensitive enough to measure the transfer function of the suspensions, but the device should be ready to repeat the measurement all the time that it will be necessary, in particular if for some reason the interferometer gets unlocked and the TF of some of the suspension need to be veryfied.

It seems that the most convenient think is to have a system for TF measurement permanently mounted on each tower at least at the beginning of the operation of the central interferometer, also if this is in principle not strictly necessary duting routine VIRGO operation.

46.4.8.2 Detailed description

46.4.8.2.1 Principle of operation

The principle of operation is simple; the device is a michelson interferometer with folded optical paths; one of the beams is folded several times on a suspended platform (SP) where all the mirrors of one arm, the beam splitter and other optical components are mounted. On the same bench are also placed the detection photodiodes and the laser source.

The second beam of the interferometer enters the vacuum tank through one of the windows which are on the lower part of the towers (see section 3300) and it is reflected by the VIRGO test mass toward another windows. At the output window is placed the end mirror, also mounted on a suspended platform, which reflects the beam back to the test mass and to the beam splitter to interfere with the beam of the rigid arm.If the beam incises on the center of the surface of the test mass a longitudinal displacement of the mass along the Virgo optical axis gives an optical path change, while an angular displacement only induces (at first order) a beam rotation.

The displacement of the test mass induced with the loop actuators will then be measured as a phase signal in the Michelson interferometer. For the measurement of the angular displacements a small fraction of the beam reflected by the VIRGO test mass will be deviated with a beam sampler (mounted on the SP); the position of this beam will be measured with a PSD (position sensing device) or a quadrant photodiode, placed in the focus of a lens to be not sensitve to lateral beam displacements.

The use of a folded optical path allows to have almost egual armlength in both the arms of the interferometer, reducing the effect of laser frequency noise.

All the optical components of the interferometric device will be suspended because the main limitation on the sensitivity will by imposed by seismic noise. Due to the position on the tower of the optical ports, the optical path will not be laying in the orizontal plane. In particular the windows are looking at the test masses with an angle in the vertical direction of $\pm$ 23°, and the beams will be oriented accordingly. As a consequence the device will be sensitive to both horizontal and vertical seismic noise and we will need to use a 3-dimensional seismic isolation sistem.

6 coils properly placed exerting forces on 6 magnets mounted on the SA will be used as actuators for normal mode damping as well as for alignement and locking.

46.4.8.2.2 Specifications

The specifications for transfer function measurement are reported in a Virgo note devoted to this subject [20]; here we report the conclusions.

The frequency interval for the transfer function measurement should be large enough to permit a good knowledge of the suspension response within at least twice the frequency band of the servoloops used for the locking and alignement of VIRGO. The present estimation is that a bandwhidth of 100 Hz should be sufficient.

The specification on the sensitivity of the device (in our case a suspended interferometer) is fixed by the amplitude of the test mass displacement and then depends on the point where to apply the force, on measurement frequency. Also the integration time is important to define the S/N ratio. In any case the detection sensitivity will be limitated by the residual seismic noise of the SP and a one stage 3-dimentional seismic attenuator with resonance frequency of the order of one Hz (TBC) shoul be enough to give a good S/R ratio at all frequencyes with a reasonable integration time.

For what concerns angular displacement there is not the necessity of a very sensitive device since the alignement feed-back of VIRGO should be very simple and should operate only at very low frequency.

46.4.8.2.3 Prototype system

A prototype suspended interferometric device has been realized at the Napoli INFN section and is presently under test. In figure 4690.1 is shown the optical setup on the suspended platform. The light source is a single mode He-Ne laser and the optical path of the rigid arm is folded in order to have e total length of two meters. The platform is suspended to a 0.5 meter long pendulum and vertical isolation is provided by rubber springs.

A very simple DC detection scheme is used with the interferometer locked on the slope of a fringe; the error signal is provided by the difference of the currents of the two output photodiodes. One of the mirrors of the rigid arm is mounted on a PZT transducer that will be used for calibration. The interferometer is locked on the fringe by reacting on the SP, in this way the SP is forced to follow the SA motion. The measurement of the SA motion is then provied by the actuating signal of the servoloop.

The prototype will be tested by measuring the transfer function of the two stage suspensn of the 3 m interferometer operationg in Napoli. It will also be used to measure the TF of a SA prototype when it will be mounted in Pisa.

The main difference between the prototype suspended interferometer and the final ones that will be used for the actual suspensions in Cascina is the fact that the prototype operates just in front of the test mass and then the beam is reflected normally. As a consequence a second suspended mirror is not necessary and the whole optical path is in the horizontal plane. For this reason the final suspension will be different and probably blade springs will be used for all the degrees of freedom (TBD) in order to achieve a more compact system.

On the other side the princilple of operation, the electronics and the optical set-up (with an armlength of about 3 m) should be almost the same.

List of References

[1] R.Del Fabbro: 1994, "Superattenuator dynamics" (VIRGO Internal Report, NTS 006 - 1994).

[2] S.Braccini et al.: 1996, "Extending the VIRGO detection band down to a few Hz: metal blade springs and magnetic antisprings" (VIRGO Internal Note, VIR-NOT-PIS-1390-068), submitted to Nucl.Instr.Meth.

[3] S.Braccini, C.Casciano, R.De Salvo, F.Fidecaro: 1996, "On the stability of the superattenuator" (VIRGO Internal Note, NTS 031 - 1996).

[4] S.Braccini, C.Casciano, R.De Salvo, F.Fidecaro: 1996, "Elimination of the hydraulic adjustment of the filter suspension offset" (VIRGO Internal Note, NTS 026 - 1996).

[5] S.Braccini et al., Rev. Sci. Instrum., 67 (8) (1996) 2899.

[6] A.Gaddi , F.Raffaelli: 1996, "Standard filters specifications" (VIRGO Internal Note, VIR-SPE-PIS-4600-105).

[7] S.Braccini, C.Casciano, R.De Salvo, F.Paoletti, F.Fidecaro: 1996, "Evidence of creep in the superattenuator mechanical filters" (VIRGO Internal Note, NTS044/1996).

[8] Pisa VIRGO group: 1994, "Seismic isolation: the use of blade springs" (VIRGO Internal Note, PJT 094/008).

[9] Pisa VIRGO group: 1994, "Blade springs: transfer function measurement performed on a two stage suspension" (VIRGO Internal note PJT094/009).

[10] S.Braccini, C.Casciano, R.De Salvo, F.Paoletti, F.Fidecaro: 1996, "The microcreep problem in the VIRGO mechanical attenuators" (VIRGO Internal Note, in preparation), to be submitted to Nucl.Instr.Meth.

[11] Datasheet of Ferroxdure 330 (FXD 330) in the "Handbook of Philips Components", 1991.

[12] "Electromagnetic Noise", Appendix to the VIRGO Final Conceptual Design, 1992.

[13] S.Braccini, Thesis, Scuola Normale Superiore, 1996, Pisa, Italy (To be published in the "Collections of the Scuola Normale Superiore").

[14] S.Braccini, C.Casciano, R.De Salvo, F.Fidecaro: 1996, "Temperature stabilization requirement of the VIRGO towers" (VIRGO Internal Note, NTS 032 - 1996).

[15] M.Bernardini, C.Bradaschia, H.B.Pan, A.Pasqualetti, R.Poggiani, Z.Zhang: 1996, "Outgassing measurement of VAC-SEAL vacuum epoxy" (VIRGO Internal Note, VACPISA 048 P).

[16] S.Braccini, C.Casciano, R.De Salvo: 1996, "Blades and crossbar dampers" (VIRGO Internal Note, VIR-NOT-PIS-4600-108).

[17] S.Braccini, S.Malik: 1997, "Role of the centering wires in determining the main resonant frequency of the mechanical filters" (VIRGO Internal Note, VIR-NOT-PIS-4600-112).

[18] S.Braccini, R.De Salvo, G.T.Feng: 1997, "Mechanical properties of the mechanical filters suspension wires" (VIRGO Internal Note, in preparation).

[19] Minutes of the workshp on Transfer function measurement; Orsay March 23th 1995.

[20] virgo note VIR-NOT-NAP-4600-....

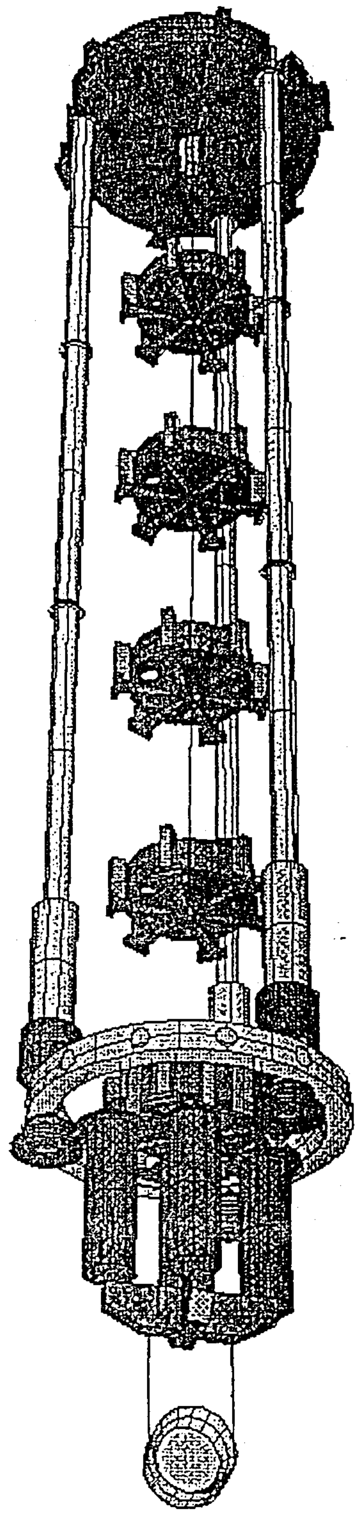

Fig. 4600.1: The superattenuator.

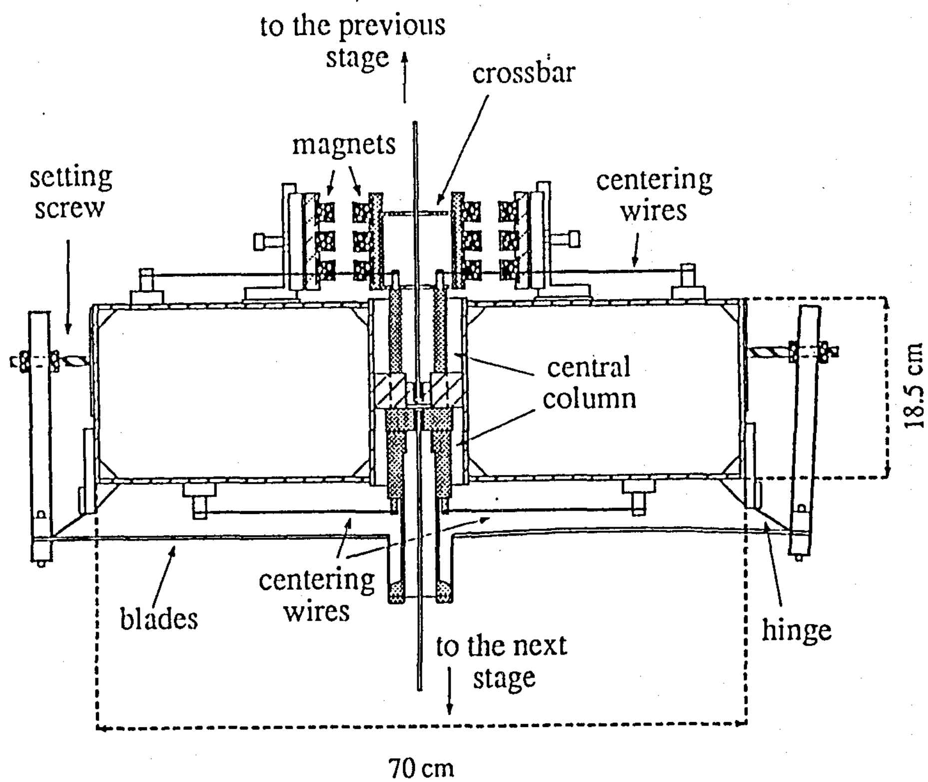

Fig.4620.1 - Side view of the superattenuator mechanical filter.

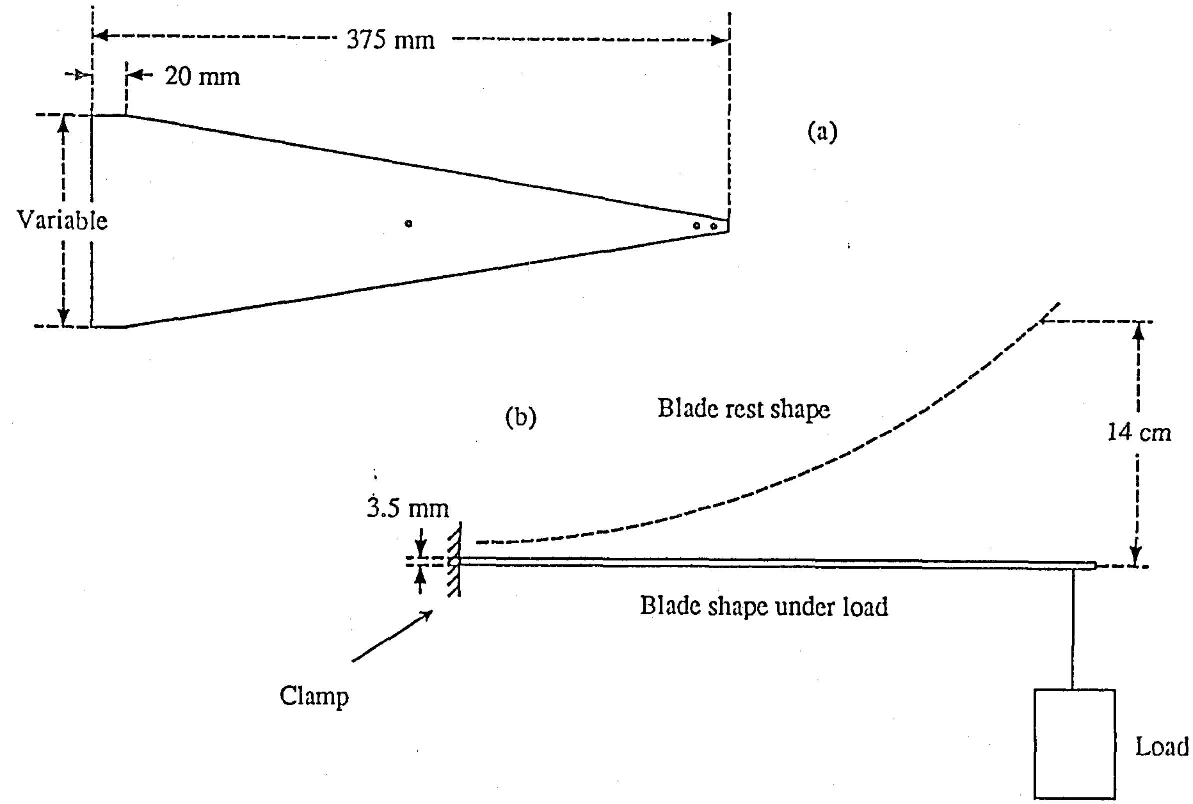

Fig.4620.2 - Plan (a) and side (b) view of a triangular pre- bent cantilever blade. Once loaded with the nominal weight the blade assumes a straight horizontal shape. The pendulum oscillation of the loaded blades is around 1.5 Hz.

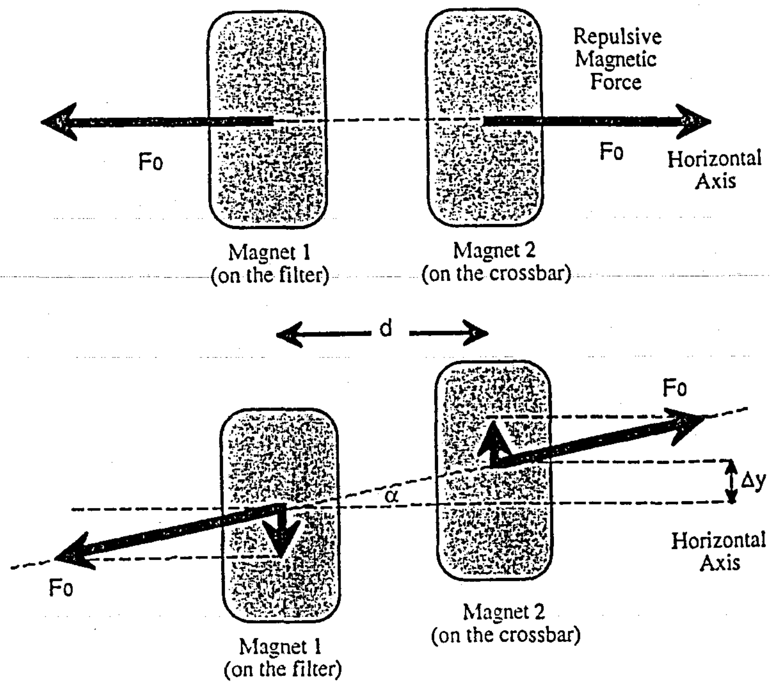

Fig.4620.3:
Working principle of the antispring system. As the magnets are moved one respect to the other in the vertical direction, a vertical component of the repulsive force appears.

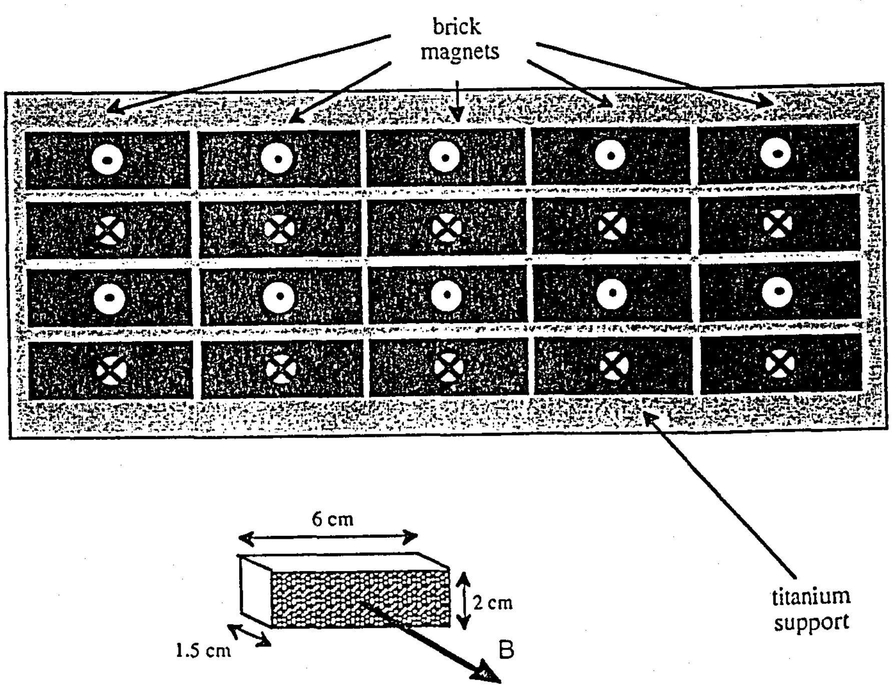

Fig. 4620.4 - One of the four magnetic matrices mounted on the filter.

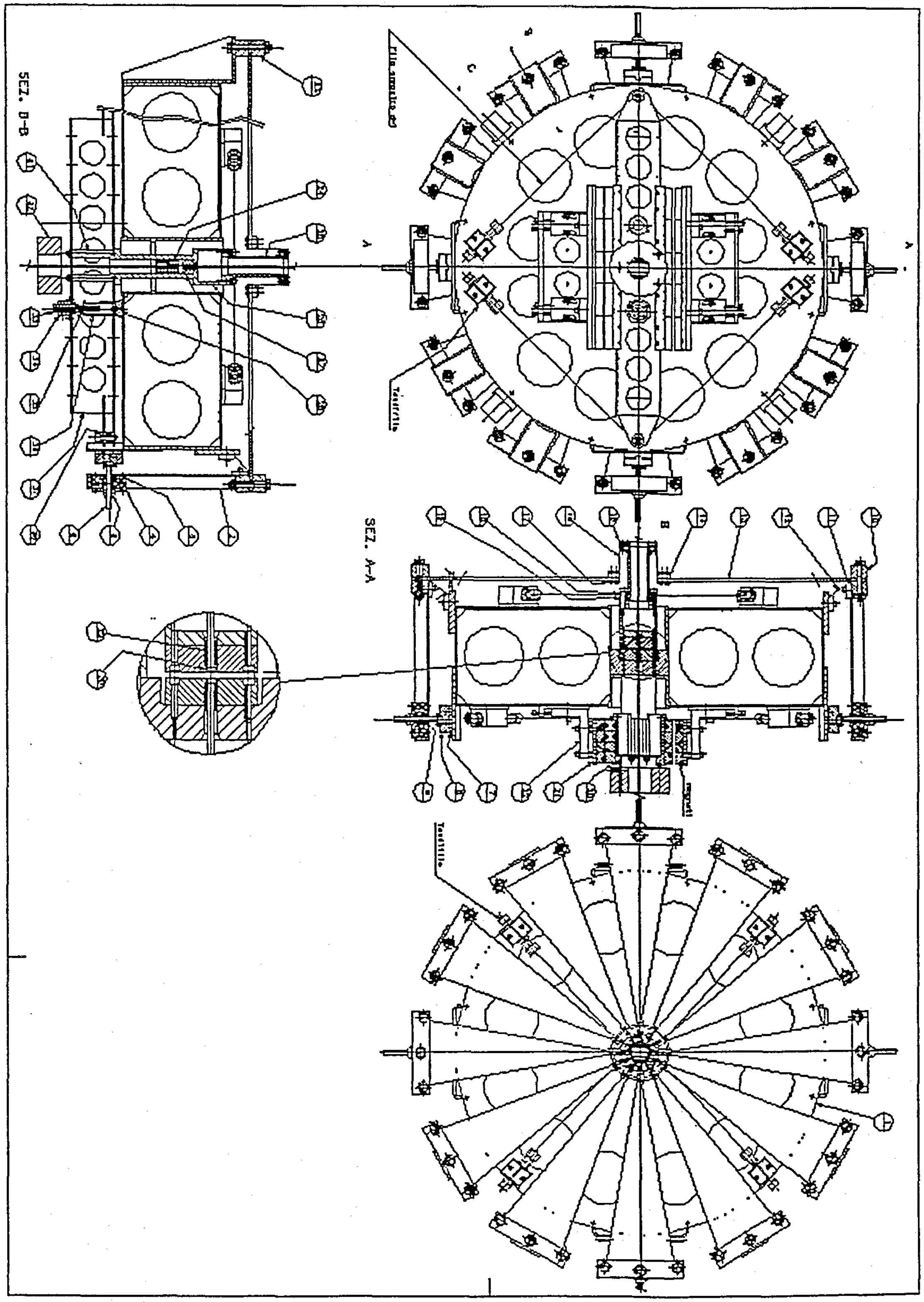

Fig.4620.5 - Diagram of the body of the mechanical filter.

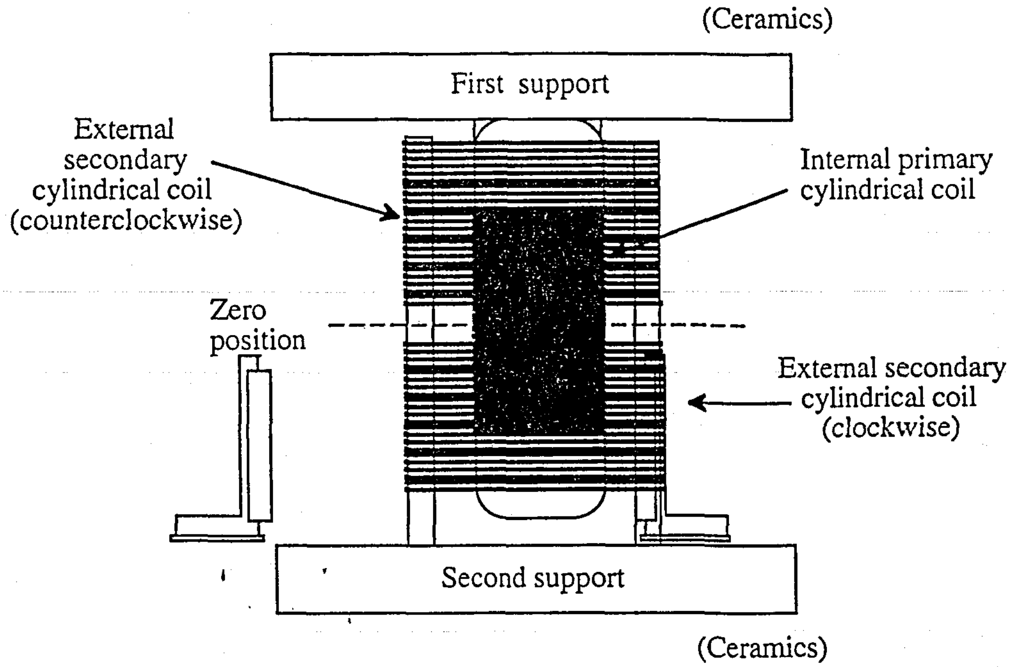

Fig. 4620.6:
.. The LVDT sensor used to measure the vertical position of the crossbar with respect to the filter body.

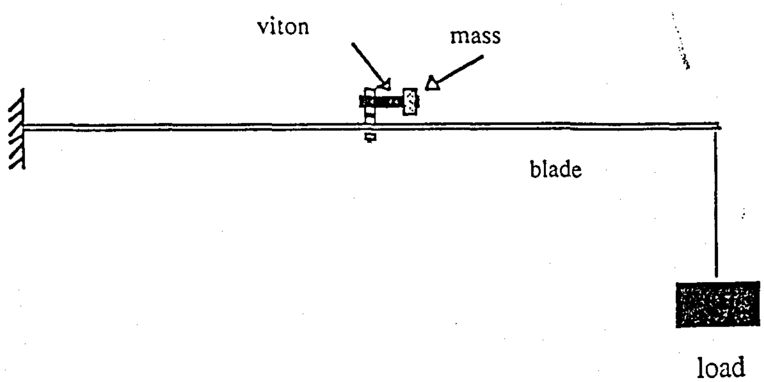

Fig.4620.7:
The damper mounted on each blade to suppress its first flexural mode (around 100 Hz).

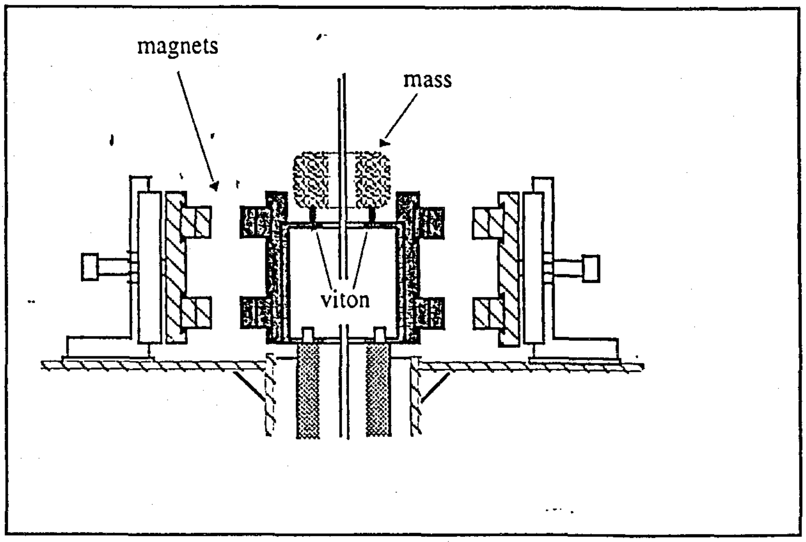

Fig.4620.8 :
The damper mounted on the crossbar. The oscillator, formed by the mass and by the three viton legs, absorbs a large fraction of the energy of the crossbar mode once its resonant frequency is tuned on the internal resonance of the filter. Also visible are the rows of magnets.

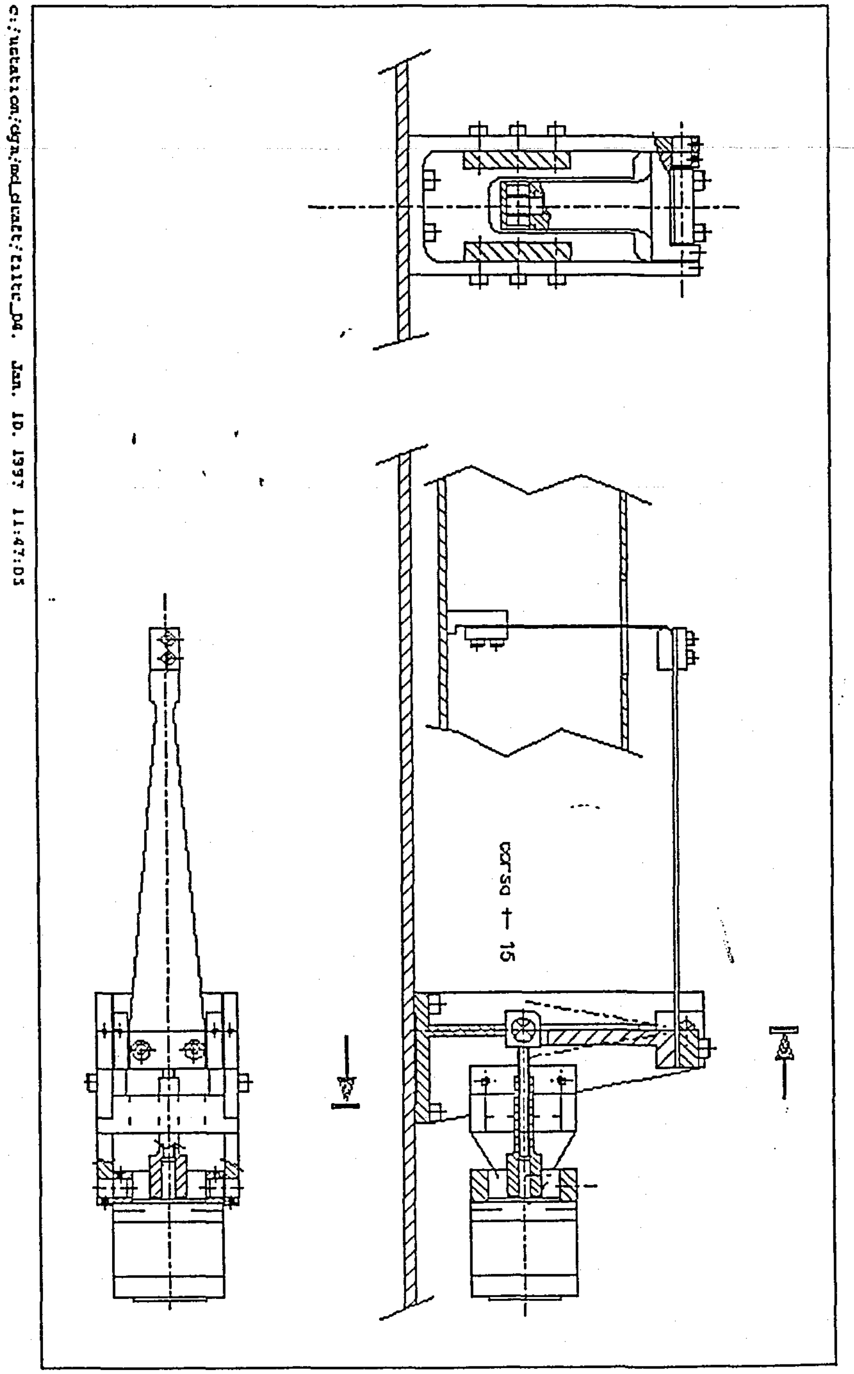

Fig. 4620.9: Design of the "fishing rod": the stepping motor changes the inclination of the blade, tuning through a piano wire the position of the crossbar.

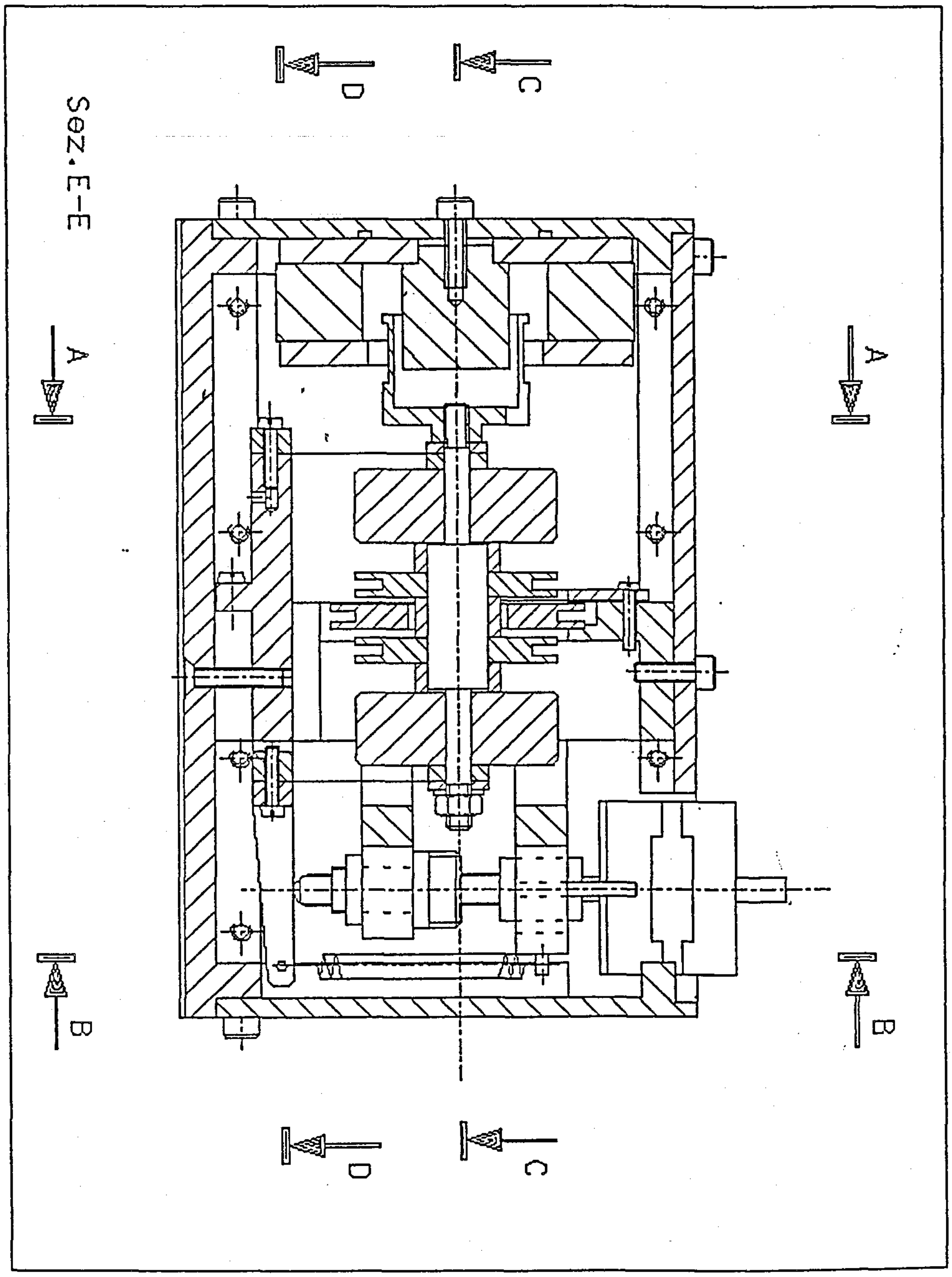

Fig. 4630.1: Horizontal accelerometer.

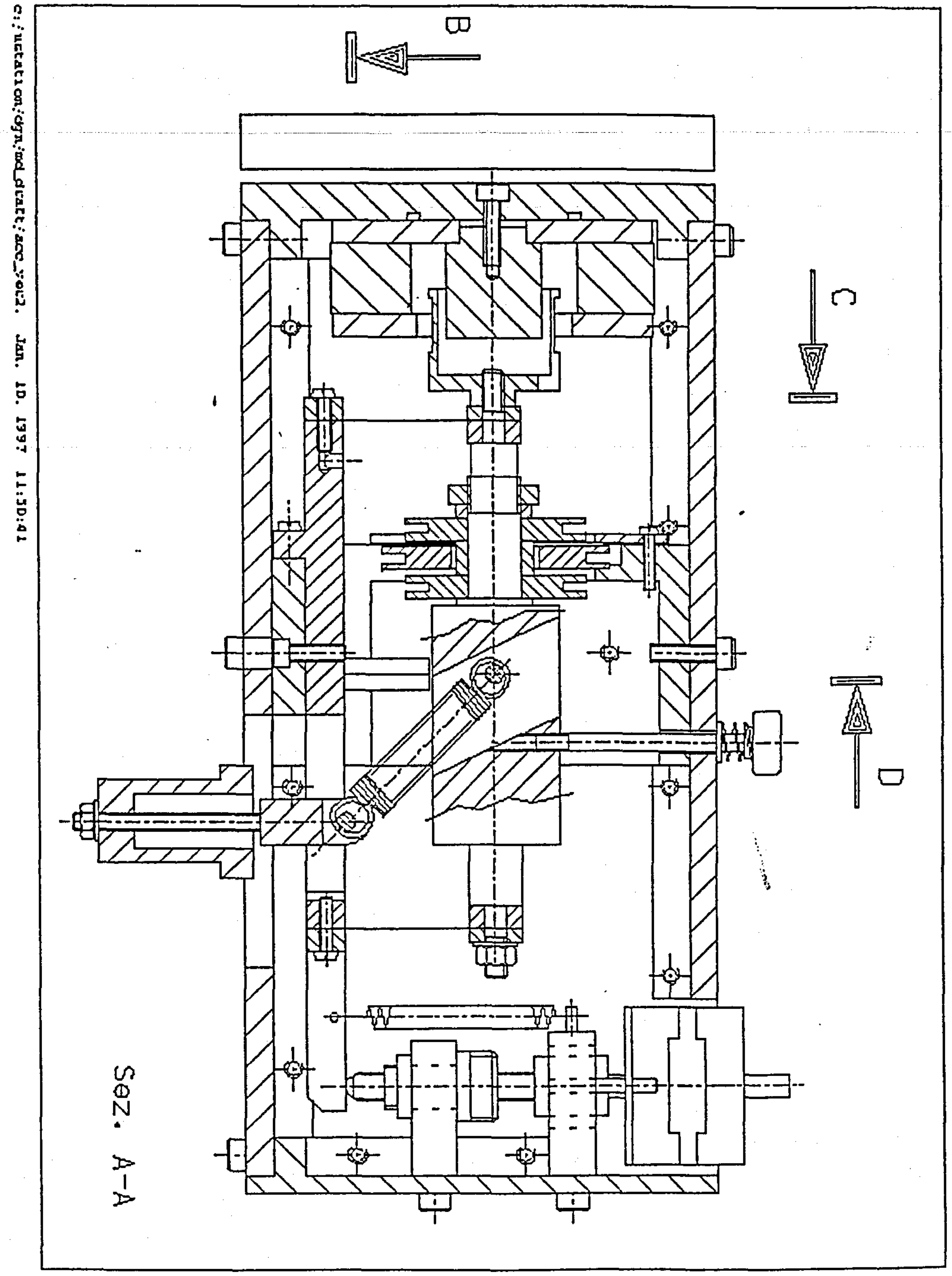

Fig. 4630.2: Vertical acceleometer.

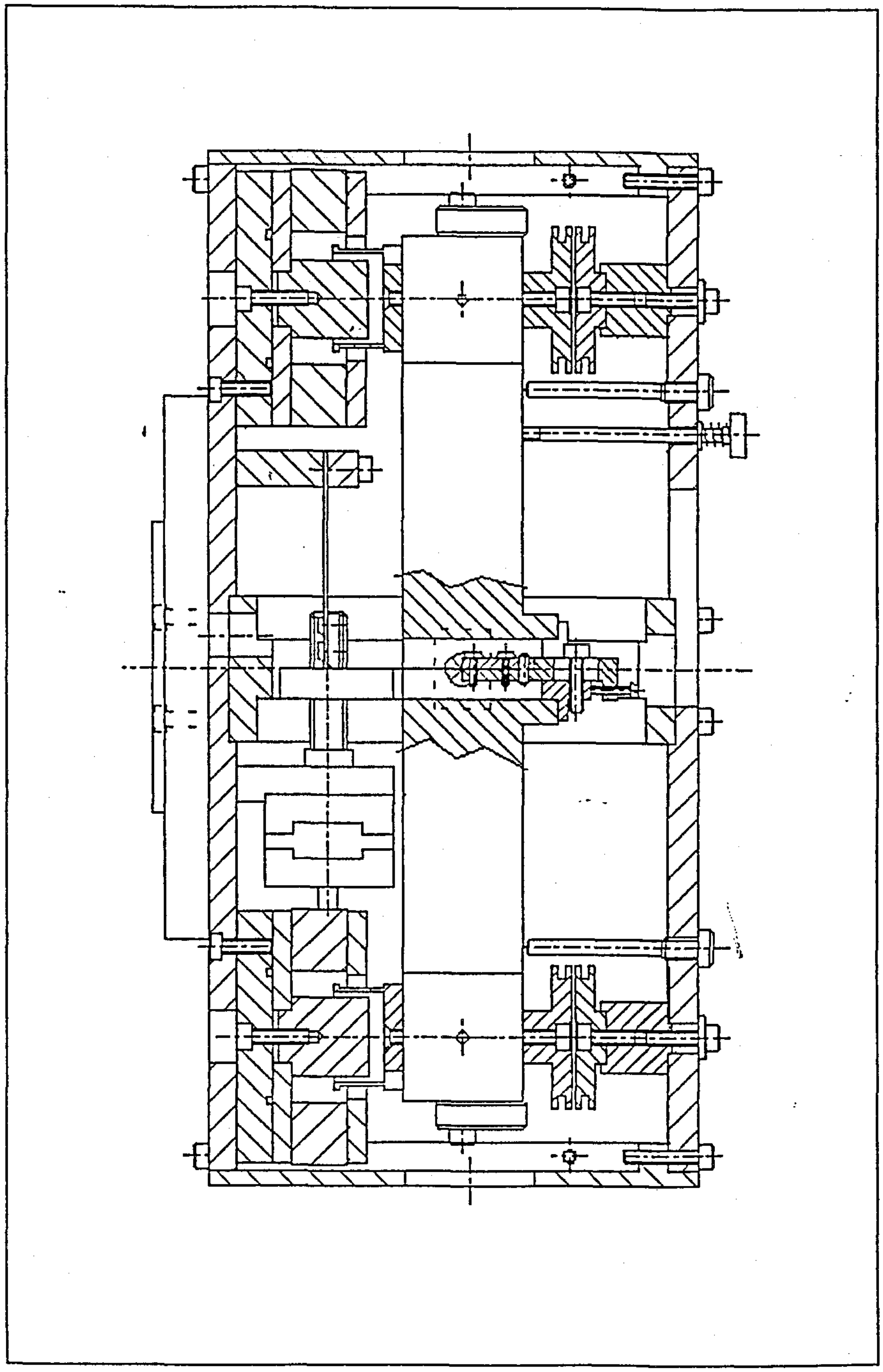

Fig. 4630.3: Rotation accelerometer.

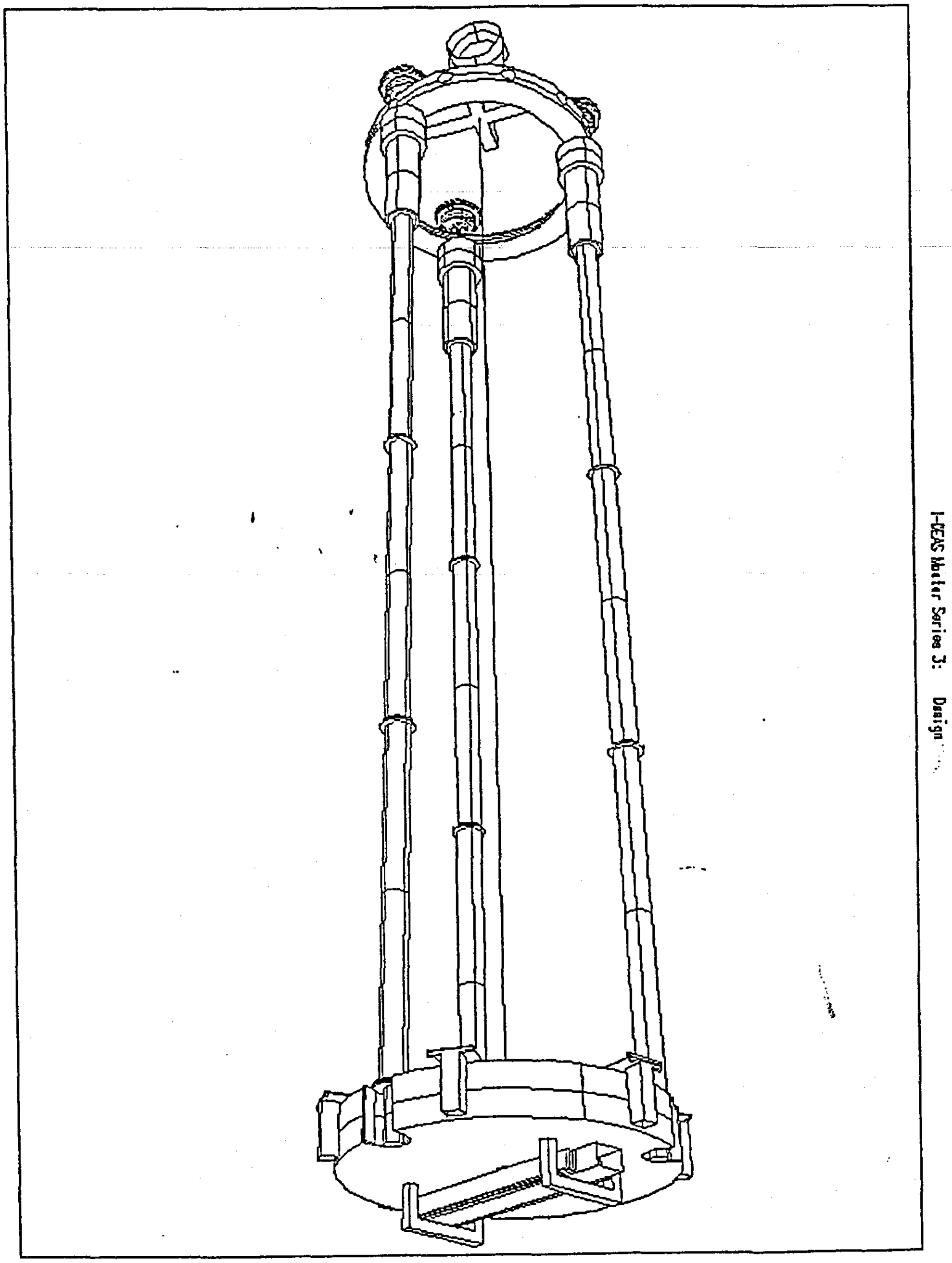
I-DEAS Master Series 3: Design

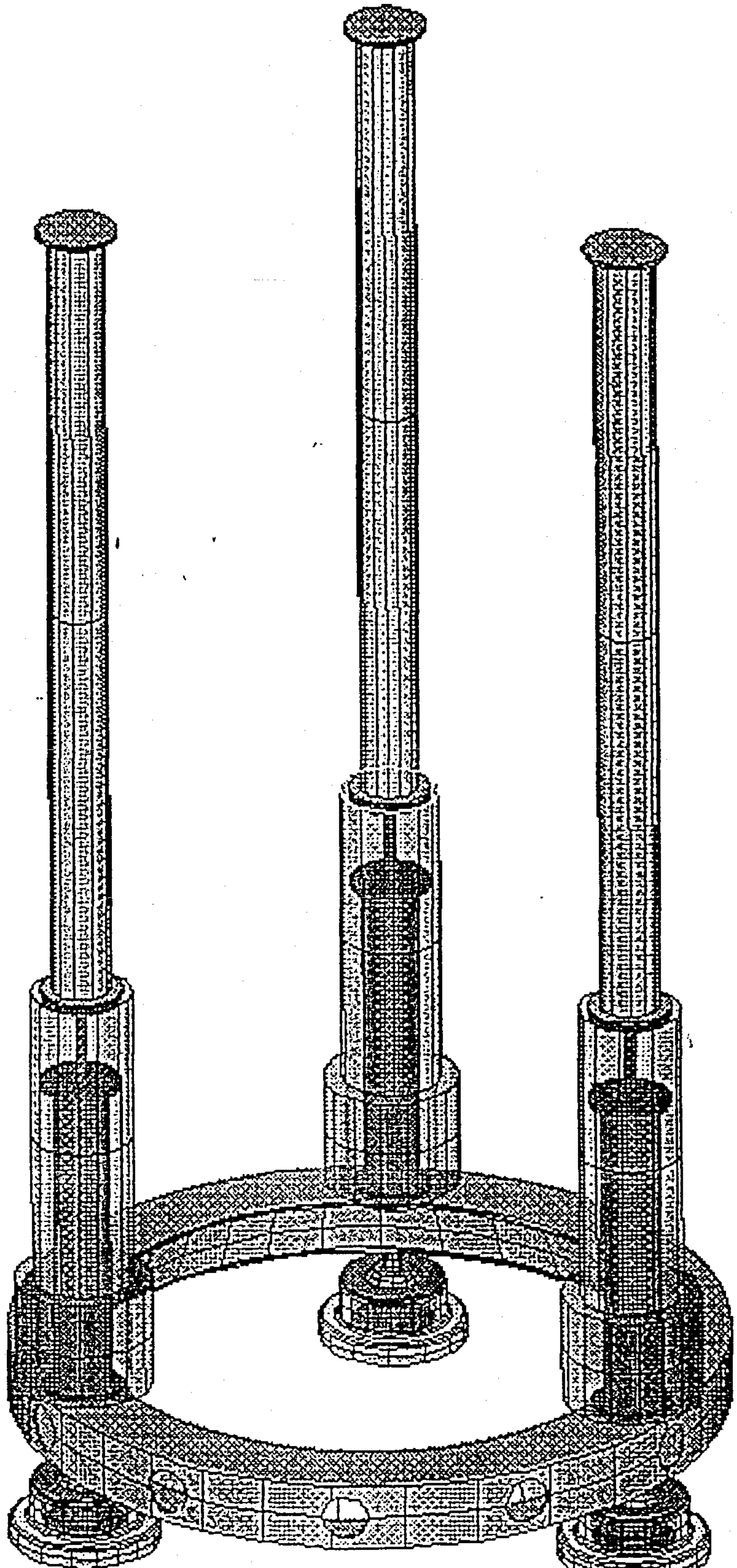

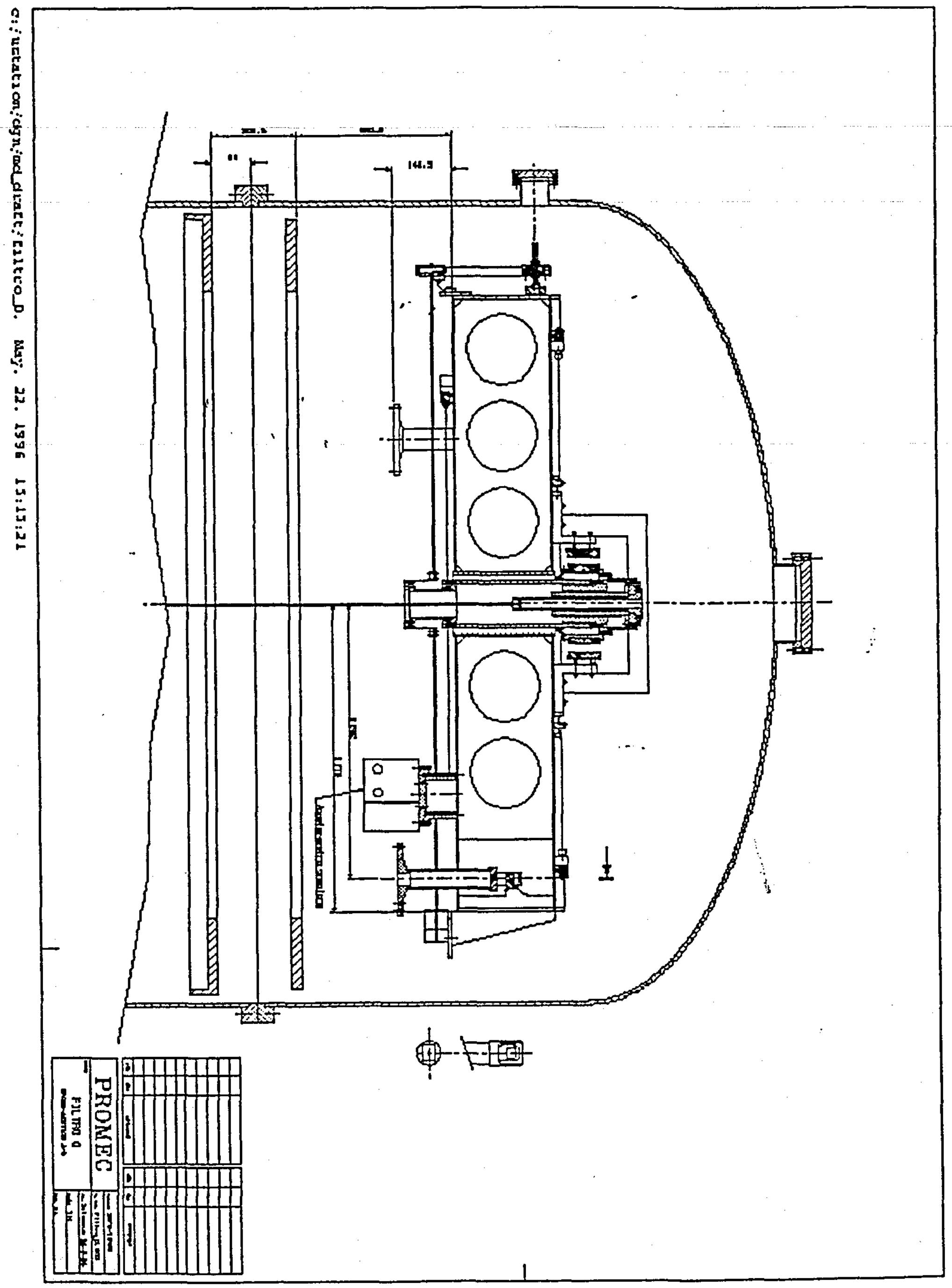

Fig. 4650.4: Filter 0, side view.

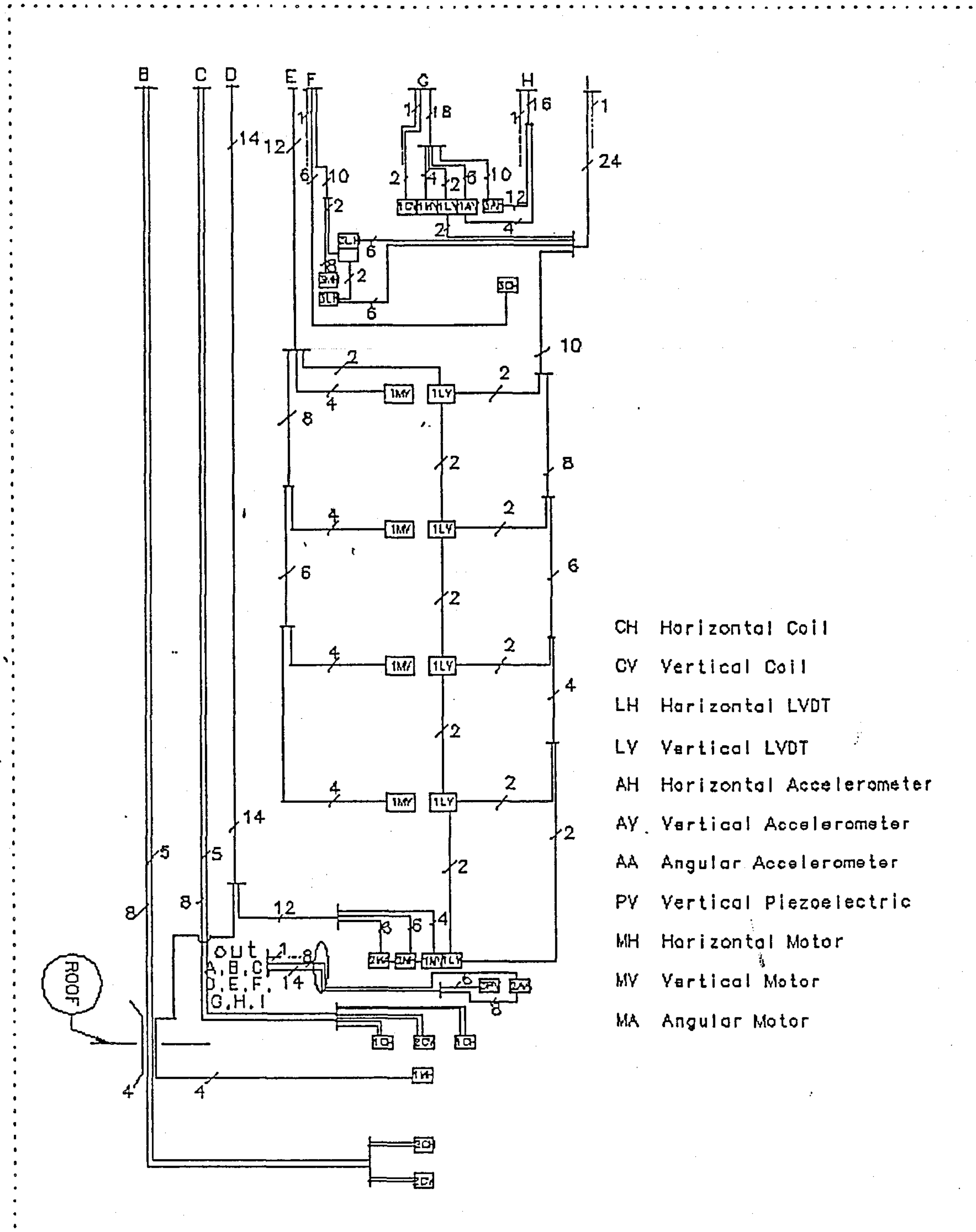

Fig. 4660.1: Cabling scheme of a full tower.

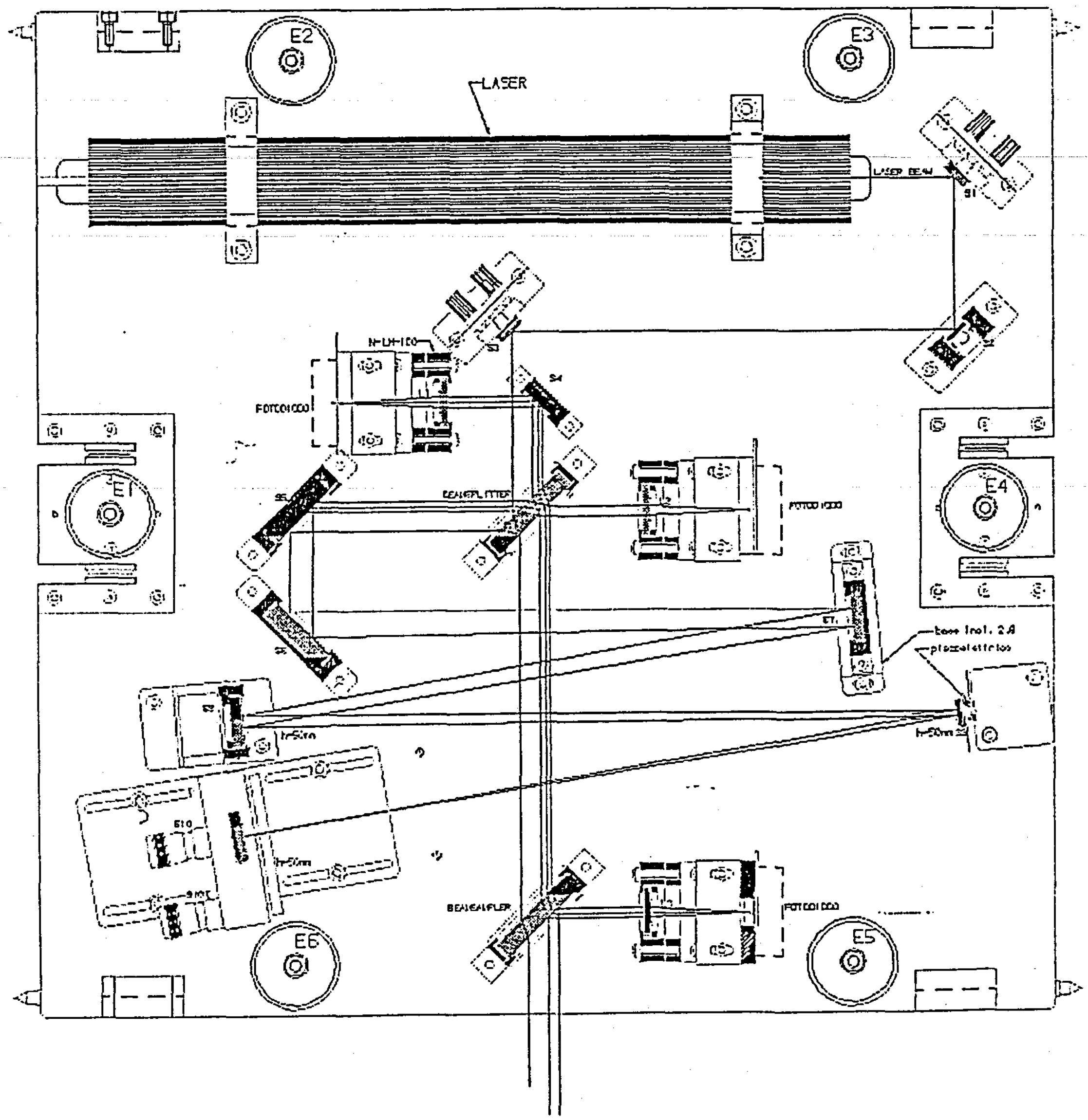

Fig. 4690.1: The transfer function measurement interferometer.

47. Last stage suspension

Table of Contents

47.1 Last stage function and concept

The last stage elements main functions are the following:

- Steering the optical components for locking the interferometer
- Alignment in DC of the test masses and of the optical benches.
- Compensation of the remnant seismic noise below 1 Hz.

47.2 Requirements for last stage elements

The main requirements for the Last Stage sub-system are:

- Tilt remotely the marionetta by 0.3 mrad in order to align the interferometer
- Steer the optical elements located in the UHV, lower part of the towers.
- Provide a further attenuation stage from external seismic noise.
- The resonance frequencies of the last stage elements must be as high as possible
- High Vacuum compatibible: the design and materials used for marionettas, motors, coils and reference masses must be compatible with the high vacuum (10^{-8} mb) of the lower parts of the towers.
- Clean Room (class 1) compatibility
- Easy implementation of the procedure for positioning and tensioning the wires for suspending the mirrors.

47.2.1 Last stage interfaces

List of interfaces

Interface name	*Concerned sub-system*	*Interface description*
Clamps and wires	WBS 4800	(see § 4700.4.1)
Suspension mechanics:	WBS 4600	(see § 4700.4.1)
Suspension electronics	WBS 4900	(see § 4700.4.1)
Alignment:	WBS 4400	(see § 4700.4.1)
Mirrors:	WBS 4300	(see § 4700.4.1)
Input Bench:	WBS 4100	(see § 4700.4.1)

47.3 Detailed description

47.3.1 Marionetta for Mirrors

This kind of marionetta has been designed to suspend the input and far mirrors, the recycling mirror, the beam splitter and the mode cleaner.

The design has been made in such a way to have a structure with the highest rigidity in the allowed space (see fig. 4700.1). The overall mass of the complete last stage system (marionetta+test mass+reference mass), is chosen to be close to one SA stage mass (160 kg).

The weight of the marionetta for the mirrors in the current design is 85 kg. The material is AISI 304, which has optimal characteristics both for UHV and clean room compatibility.

The marionetta must be suspended at the center of mass to minimize the momentum producing rotations. Moreover, the horizontal plane containing the center of mass must allow the clamping of the suspension wires for mirrors and reference masses.

The arms of the marionetta are used to support magnets (10 mm diameter, 4 mm thickness, .25 T magnetic field) which are driven by the magnetic field provided by external coils suspended to the last stage of the SA.

The marionetta provides a rotation angular range of ± 2mrad and a pointing accuracy of 1μrad.

One the lower section of the marionetta is a load positioned by a UHV compatible stepper motor, which allows to tilt the marionetta by 0.3 mrad, for the initial alignment of the interferometer.

47.3.2 Reference masses

Small ac corrections to the test mass position and the feedback signals from the control are applied directly to the test mass from four coils on a reference mass suspended to the marionetta, thus having the same seismic isolation of the test mass.

The reference mass must have the centre of mass coincident with that of the test mass, and a mass at least equal to the test mass, and its shape has been studied so to provide a further protection of the optical elements from dust.

Four models of reference masses are needed, according to the mirror dimensions and chracteristics:

- Input mirrors Reference Masses,
- Mirrors Reference Masses
- Recycling mirror Reference Mass
- Beam Splitter Reference Mass.

Currently, a model of reference mass cast in Al alloy has been built, susitable to be used for the input mirrors. A detailed study is being carried out to determine if it is necessary to use a dielectric material to strongly reduce the contribution of Foucault currents

47.3.3 Marionettas for input and detection benches

The input and detection benches will be suspended to a marionetta which shall have the following characteristics:

- Overall mass of the same order of the benches.
- Shape which permits to protect the benches from dust coming from the SA.
- Possibility to suspend the benches with 3 or 4 wires.
- Mechanical prealignment better than 2 mrad ($\theta_x\theta_y\theta_z$).
- Angular corrections of 5 mrad around all three main axis ($\theta_x\theta_y\theta_z$).
- Displacement corrections of 0.1 mm in x, z and y.

The marionetta suspending the benches is shown in fig. 4700.3. It is built in the same material of the two benches (Alplan Al alloy) and has a circular symmetry with dimensions which allow to protect almost all the surfaces of input and detection benches from dust coming from the SA elements. For the prealignment of the marionetta two motors are used which move two 100 g masses on the barycentral horizontal plane in perpendicular directions. The fine control of position is provided by 8 coils which act on magnets (10 mm diameter, 4 mm thickness, .25 T magnetic field) on the marionetta. The coils have 1000 turns of 1 mm diameter copper wire on a mean diameter of 80 mm for a length of 50 mm, with a maximum current of 0.5 A.

LIST OF FIGURES

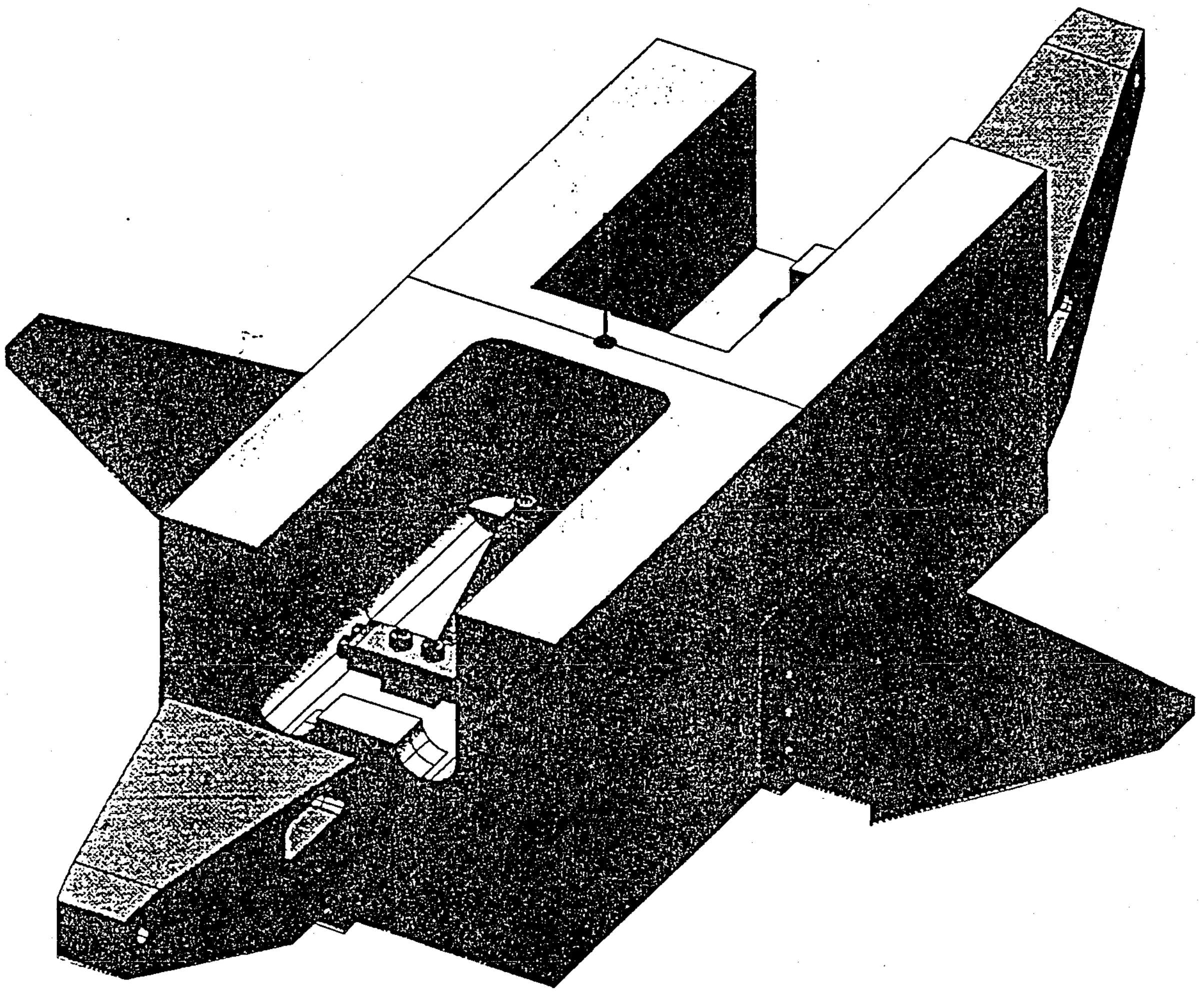

Fig. 4700.1

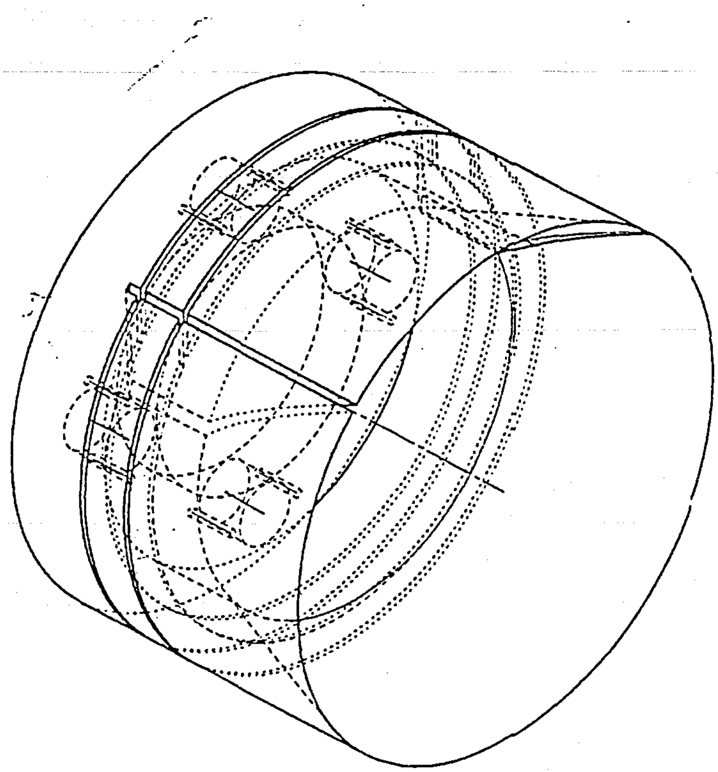

Fig. 4700.2

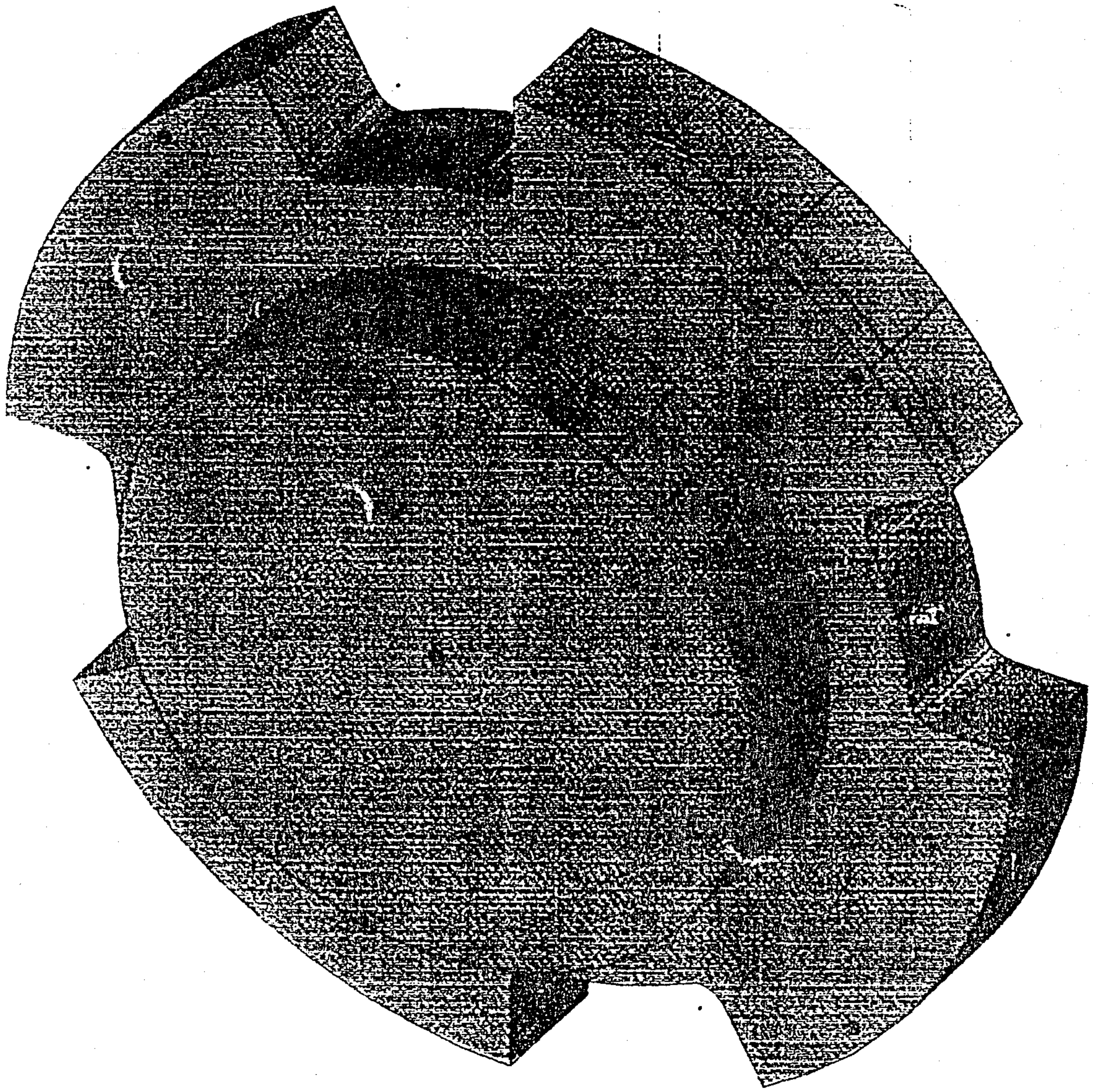

Fig. 4700.3

48. Clamps and wires

Table of Contents

48.1 Overview

The test mass or end mirror of the gravity wave interferometer is a monolithic piece of fused quartz that is suspended as a pendulum. The design of this pendulum must allow the position of the mirror to be controlled to a high accuracy. The mechanical losses of the pendulum must also be small so that the resultant off-resonance displacement thermal noise is small too. The final design must take into account the actual suspension of the mirror, the type of material that suspends the mirror and the manner in which these pieces are fastened.

The Virgo mirrors will be suspended from the *Marionetta* by two wires forming each a single loop around the mirror lower surface. This avoids the use of any fixed mechanical contact on the mirror which might reduce the mirror quality factor by post-production machining. With this solution, the true contact points between the wires and the mirror surface will be limited to a short part of the wire touching the mirror itself. The rest of the wire will not play an important role from the point of view of wire-mirror friction.

The use of two wires allows the tilt of the mirror about the horizontal axis perpendicular to the optic axis to be controlled by the suspension point of the pendulum-hence, the term *marionetta*. One drawback of this scheme is that it raises the frequency of the tilt motion about this axis. This can couple vertical motion into horizontal motion and add noise to the gravity wave signal.

The off-resonance thermal noise displacement is proportional to the square root of the pendulum loss angle

4800. 1

$$\sqrt{\langle x(\omega)^2 \rangle} \propto \sqrt{\phi(\omega)}$$

The loss angle is related to the pendulum quality factor Q by:

4800. 2

$$Q \equiv \frac{1}{\phi(\omega_0)}$$

Therefore, we must reduce $\Phi(\omega)$ (or increase the Q) to reduce the thermal noise effect. The actual loss angle $\Phi(\omega)$ can be expressed as the sum of three different contributions:

1. the effective pendulum loss angle $\Phi_p(\omega)$
2. the energy loss Φ_{clamp} due to a *stick-and-slip* process between the suspension wire and the clamp
3. the residual gas damping Φ_{gas}

The measured Q can be expressed as

4800. 3

$$Q \equiv \frac{1}{\phi(\omega_0)} = \frac{1}{\phi_p(\omega_0) + \phi_{clamp} + \phi_{gas}}$$

A maximisation of Q requires the minimisation of the three different contributions.

For the pressure maintained in the Virgo vacuum system ($\approx 10^{-6}$ *Pa*), the residual gas contribution to the quality factor Q is negligible ($Q_{gas} \approx 10^{11}$) and the main process limiting the Q of pendulum will be given by $\phi_p(\omega_0)$ and ϕ_{clamp}.

48.1.1 Requirements for clamps and wires

The requirements for the last stage, from the point of view of the mirror suspension performance and thermal noise reduction, are quickly summarised in the following list

- the pendulum quality factor must be high: $Q \geq 5 \times 10^5$
- the mass normal mode quality factor should be $Q_{mirror} \geq 1 \times 10^6$
- the suspension wire violin frequency mode as high as possible
- the mirror should hang safely
- the suspension wire properties must be stable in time
- the suspension wires should stretch as little as possible during the initial Virgo baking treatment (TBQ).

48.2 Wires

48.2.1 Overview

The suspension wires are an important consideration in the final design since they play a crucial role in determining the thermal noise performance of the pendulum. The contribution of the loss angle $\phi_p(\omega)$ to the effective pendulum Q is given by

4800. 4

$$\phi_p(\omega) = \phi_w(\omega) \frac{1}{L} \sqrt{\frac{EI}{Mg}} \equiv \phi_w(\omega) K$$

where ϕ_w is the loss that characterises the material and is independent of the geometry of the pendulum suspension wire, L is the length of the pendulum wire, E is the Young's modulus, I is the moment of inertia of the wire cross section and K describes the dependence of the loss on the pendulum geometry.

The lowest violin mode frequency (which should be maximised) is given by

4800. 5

$$f_1 \approx \frac{1}{2L} \sqrt{\frac{Mg}{4\pi \rho r^2}}$$

where ρ is the mass density of the wire material.

Since the mass of the mirror is fixed from other design considerations, the only parameters to be optimised are the wire material ($\phi_w(\omega)$, E) and thickness ($I = \pi r^4/4$). It is clear that a thin wire with a low loss is the best choice. The diameter of the wire can only be made as thin as the material strength allows.

The choice of wire material, from the point of view of the inherent loss, is a bit more difficult. If the wire is carefully prepared in a way that eliminates imperfections such as impurities and structural irregularities, the inherent loss in the material itself can be bound by using thermo-elastic damping as a lower limit. In this case, a thinner wire reduces the effect of thermoelastic damping in the frequency band below 100Hz.

48.2.2 Description

From the reasons described previously, the best choice is a wire with a high breaking load and low loss angle.

Table 4800. 1 presents a list of material characteristics tested in Perugia. From this table, it is evident that C85 piano wire is the best current solution for Virgo mirror wire suspensions.

A wire diameter of 0.20mm has been chosen for the 21 Kg mirror and 0.30mm for the 42 Kg mirror. This gives a safety factor of 65% which is adequate given the results of tests performed. The lowest violin mode frequency is greater than 300 Hz.

Another important consideration is the anelastic stretching of the wire when it is loaded with the mirror mass and thermalised at the Virgo baking temperature for a long time period. A *C85 0.2 mm* diameter wire, loaded with a *5 Kg* mass and maintained at 150°C in vacuum for one week, shows *2.3 mm* of permanent elongation. The elongation shows a logarithmic dependence in time (creep effect). Because of this stretching effect, it is necessary to use, for the mirror suspensions, only pre-heated wires. A wire heated for one week, shows, after another week of baking, a residual elongation less than *0.3 mm*. No residual creep effect has been detected in that wire after twenty days at 35°C with a sensor having a resolution better than *0.0005mm*.

Table 4800. 1 Wire loss angle and breaking load test results

Wire Material	ϕ_w (10^{-4})	diameter (mm)	Breaking Load (Kg)	Normalised Break. Load (Kg/mm²)
AISI 302 (Fe/Cr18/Ni8)	33	0.25	8.5÷9.5	170÷210
AISI 316 (Fe/Cr18/Ni8/Mo3)	20	0.25	8.5÷9.5	170÷210
INVAR (Fe64/Ni36)	29	0.25	< 5	< 102
ALUCHROM (Fe70/Cr25/Al5)	8	0.25	< 5	< 102
CHROMALOY (Fe75/Cr20/Al5)	-	0.25	< 5	< 102
C75	5.4±1	0.50	*6.5÷7.8*	*134÷160*
C85 (r = 0.1mm)	**6.0±1**	**0.20**	**8.5÷9.5**	**270÷300**
Straight Piano Wire (Goodfellow, AISI 316)	20÷23	0.30	12	170
Titan	20	0.25	-	-
Tungsten	14	0.25	11÷12	224÷244

48.2.3 Specifications

Considering that C85 piano wire is an easy material to find and to handle, it has been chosen as the reference solution (two piano wire loops, with length *2.2 m* and diameter $d=0.2$ *mm* and $d=0.30$ *mm*, for the light and heavy mirror, respectively); however, several studies are in progress to verify some interesting alternatives.

Table 4800. 2 Wire Specifications

Material	C85 Piano Wire
Breaking Load (Kg/mm²)	*250÷300*
Wire diameter for the 21Kg mirror	*0.2mm*
Wire diameter for the 42Kg mirror	*0.3mm*
Wire length (one loop)	*2,2m*
Wire residual elongation in baking (150°C per 1 week)	*0.3mm*
Wire residual creep effect at 35°C	*no evidence (<0.0005mm per 20 days)*
Wire loss angle	6×10^{-4}
Pendulum *Q* in a full scale prototype with spacers	5×10^{5}

48.2.4 Marionetta-Wire clamps

48.2.5 Overview

To minimise the clamp energy loss, it is very important to decrease the *stick-and-slip* friction between the suspension wire and the clamp itself. The easiest way to reach this goal is to increase the squeezing pressure exerted by the clamp on the suspension wire.

From several tests performed by the Perugia group and reported in Figure 4800. 1, it is clear that by increasing the clamping pressure, we obtain an increment of the pendulum Q and, consequently, a decrement of the energy loss ϕ. In Figure 4800. 1, the Q and the ϕ of a small pendulum prototype, made by a *0.4 mm* diameter piano wire with a length ranging between *200 mm* and *300 mm* and with a mass of *762 g* attached to the lower end of the wire, is plotted versus the squeezing torque applied to a group of four screws on the clamping head of the pendulum. By increasing the torque, we increase the clamping pressure. The different curves shown in Figure 4800. 1 refer to different clamp materials. Aluminium, stainless steel and tool steel have been tested. There seem to be no evident differences between the behaviour of the different materials tested. Tool steel has been chosen to build the part of the clamp where the suspension wire touches the clamp surface. This avoids surface damage to the clamp after several squeezing and dismounting procedures.

48.2.6 Specifications

The reference technical drawing for the mirror and reference mass clamps is showed in Figure 4800. 2. This clamp is designed to be directly mounted on the *marionetta* and to host the mirror and reference mass wires. It is completely made in steel with four tool steel inserts.

If the reference solution for the *marionetta* is modified to include two blades to suspend the mirror (in order to lower the vertical resonant frequency), a backup solution for the clamps is ready (Figure 4800. 3). In this case, any mass attached to the blades on the *marionetta* must be kept small so that the internal normal modes of the blade are at high frequencies outside of the gravity wave detection band. For this reason, the clamp will be made of aluminium.

48.3 Mirror - Wires spacers

48.3.1 Overview

The *marionetta*-wire clamps test showed the importance of decreasing the *stick-and-slip* process to improve the quality factor of the pendulum. A similar process is foreseen in the point of contact of the suspension wires with the lateral mirror surface. In fact, several test performed on a full scale prototype with two wire loops simply cradling the mirror showed a very poor Q (10^4-10^5) and a strong amplitude dependence. To reduce this effect different solution have been tested.

The solution that gives very good results with a minimal change to the configuration is shown in Figure 4800. 4 (B); two cylindrical spacers, located in the equatorial plane of the mirror, kept in position by the wire tension give a Q of about 5×10^5 for the pendulum mode with a very small amplitude dependence.

48.3.2 Specifications

The spacer characteristics are to be confirmed after their effect on the mirror internal Q has been tested. The current solution is listed here:

- cylindrical spacers
- $r = 0.25\ mm$ (TBC)
- $h = 10\ mm$ (TBC)
- in aluminium or quartz (TBC)
- kept in position by the wire tension.

48.4 Interfaces

• Mirror construction	4300
• Position control	4920
• Marionetta and reference mass	4720

48.5 Future developments

A high pressure locking of the suspension wire is the easiest way to reduce the *stick-and-slip* process inside the clamp, but not the most efficient. We are investigating the possibility of producing a new generation of "monolithic" suspensions where the wire and the clamp are produce in a single piece, without the use of any mechanical connection or soldering procedure. In fact, by constructing a wire with a large cylindrical head, it is possible to lock the suspension to the support frame in a very rigid manner that almost completely removes any clamp loss. This has been tested in Perugia with a small "monolithic" prototype made by a short $80\ mm$ steel strip linked to two big cylindrical heads. The "monolithic" prototype Q behaviour has been compared with a strip pendulum with the "usual" clamp and thus, the usual clamp energy dissipation. The suspension strip also has been squeezed by using small cylinders inside the clamp to localise the pressure to the contact lines between the strip and the small cylinders themselves. This configuration decreases the effect of the *stick-and-slip* process inside the clamp. The results obtained show a much lower ϕ for the "monolithic" pendulum at all the squeezing torques tested $\phi_{monolithic}\approx3\times10^{-4}$, $\phi_{strip}\approx1.5\times10^{-3}$. The technological problem that must be solved in order to use this "monolithic" pendulum as the Virgo suspension geometry is to find a technique to construct "monolithic" wires instead of strips with a length of *700 mm* or more. Some preliminar prototypes have been developed and tested in Perugia.

A promising enhancement of the "monolithic" solution is to use amorphous quartz to construct the suspension wire and heads. In this case, it is possible to build long wires and to fuse them directly to the heads. The problem with this process is the intrinsic fragility of the quartz wire in presence of humidity and its stability over long time periods. Some prototypes tested in Perugia showed very good ϕ values.

Table 4800. 3 Monolithic samples

Wire prototype	ϕ_w (10^{-4})	Note
Monolithic steel strip	0.2÷0.4	Mounting problems anisotropic behaviour
Monolithic steel wire	0.2÷0.4	Surface damage ⇓ Low breaking load (44 Kg/mm^2)
Monolithic quartz wire	0.03÷0.06	Under development

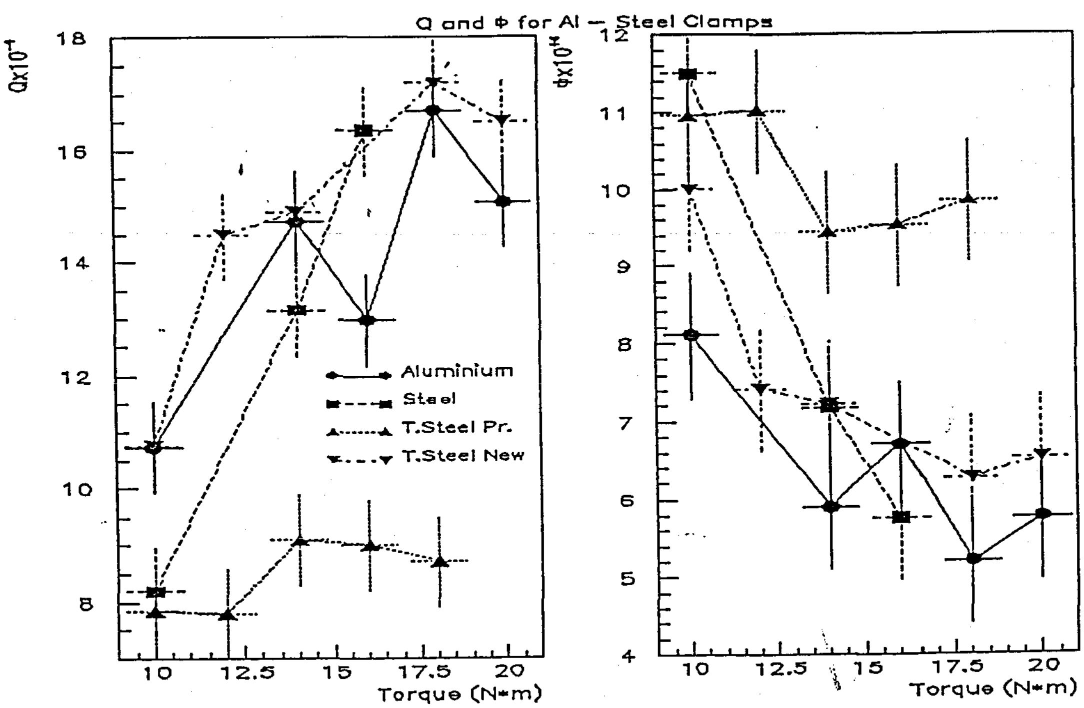

Figure 4800. 1: Small pendulum prototype: piano wire suspension with clamps made of different materials

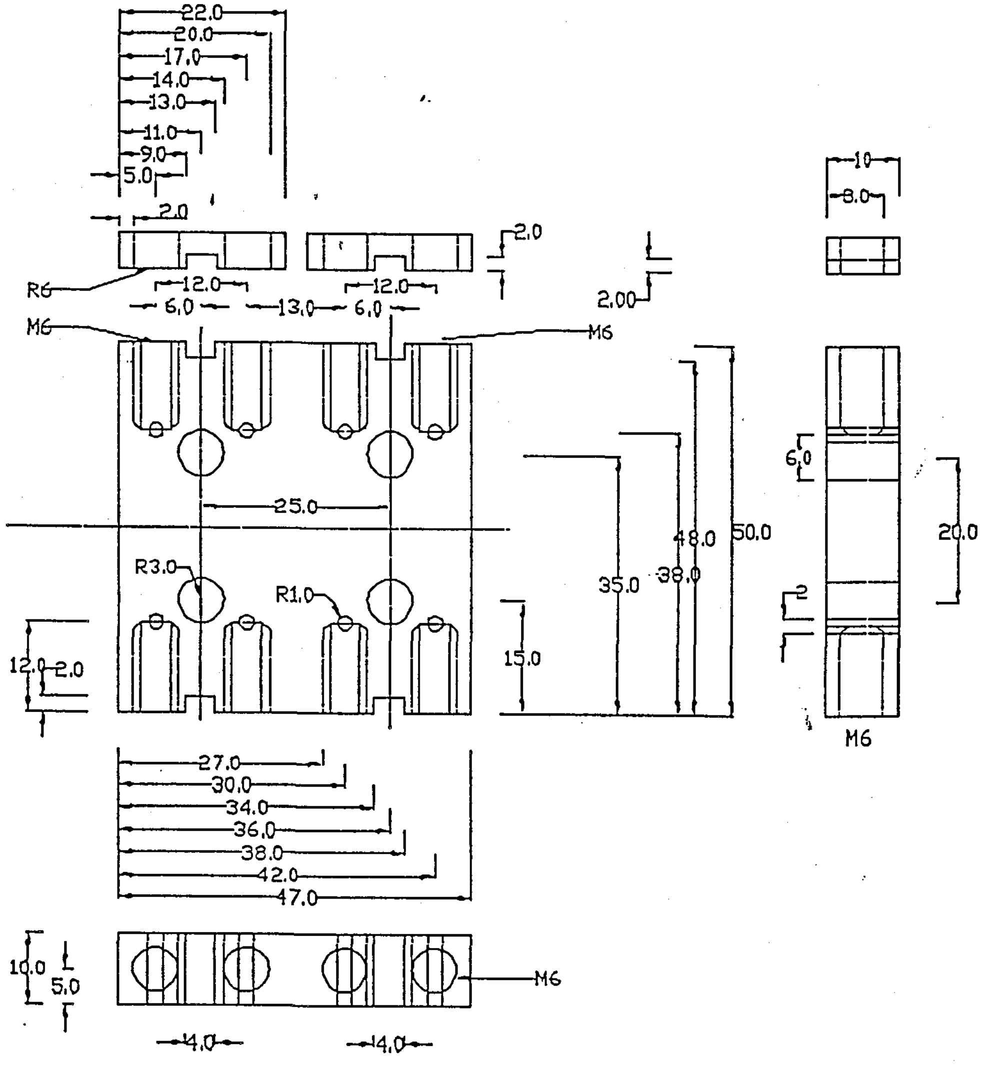

Figure 4800. 2: Clamp Reference Design

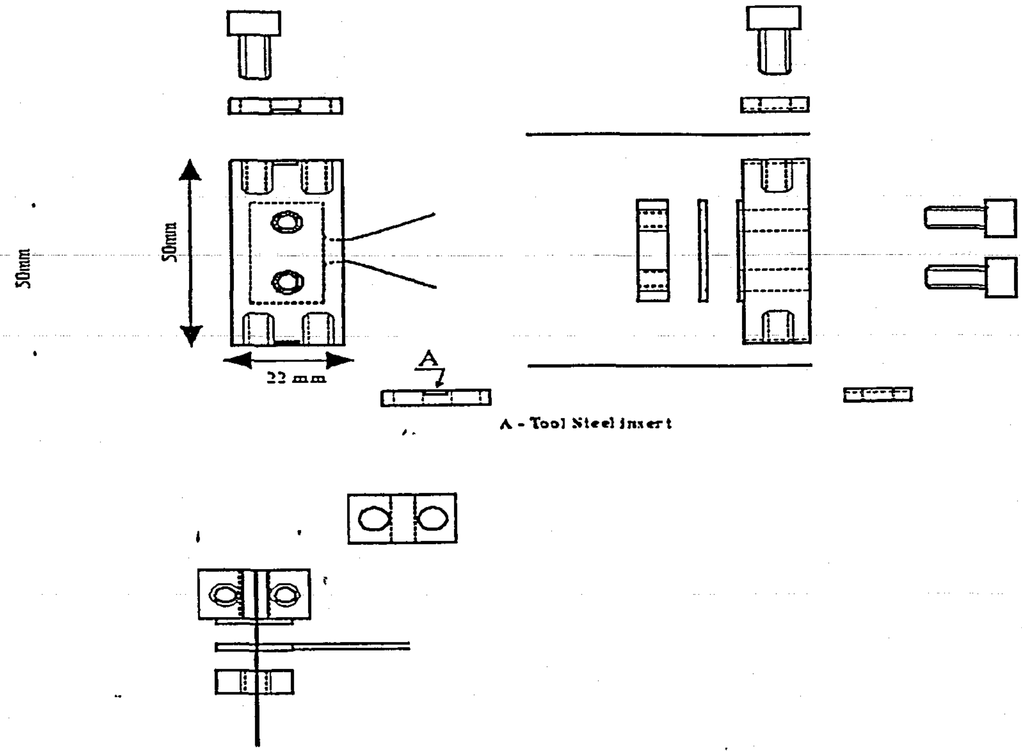

Figure 4800. 3: Suspension wire clamp backup design

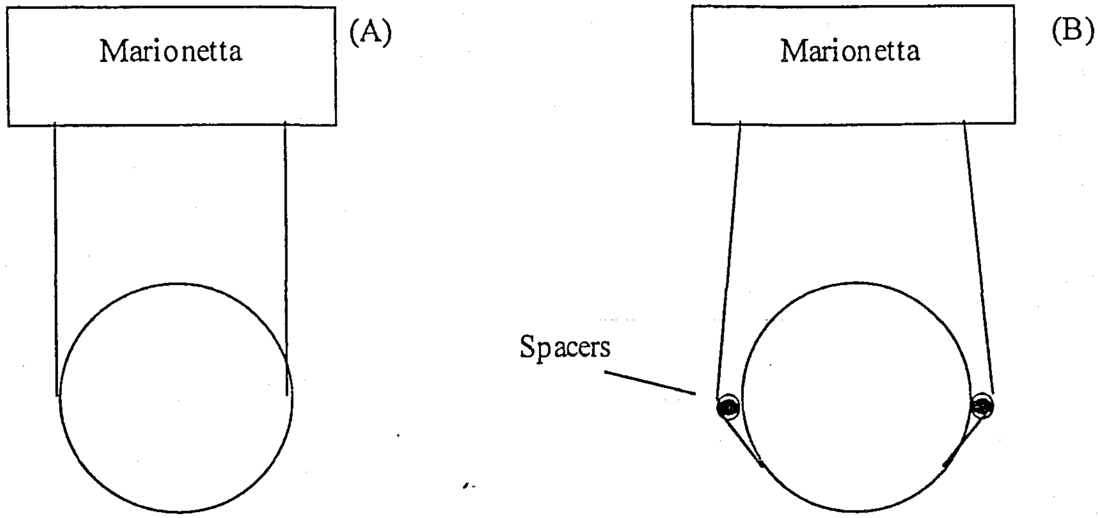

Figure 4800. 4: Mirror hanging without (A) and with (B) spacers

49. Suspension Electronics

Table of Contents

49.1 General Description

The suspension control system can be divided into four main parts:

1. Active damping of suspensions .
2. Suspended masses position control.
3. Super Attenuators internal status monitoring and correction.
4. Interface between the S.A. control system and other VIRGO sub-systems.

Fig. 4900.1 shows the schematic structure of the control system for a generic suspension.

49.1.1 Active damping of suspensions

The S.A. has been designed to reduce the suspended masses spectral displacement in the VIRGO sensitivity frequency range. An active reduction of the masses rms displacement, located at the S.A. normal modes frequency, is necessary in order to reduce the dynamic range and the required bandwidth of the VIRGO locking system. The specification concerning the mirrors displacement are the following:

- Spectral displacement lower than 10^{-18} m $Hz^{-1/2}$ at frequencies higher than 3 Hz.
- Rms displacement lower than 1 μm on a time scale of 100 seconds.

To achieve the rms displacement requirement a sophisticated digital control system has been designed and built. A Digital Signal Processor, under control of a VME CPU, elaborates signals coming from position and acceleration sensors, located on top of the S.A. and tilt sensors located on the bottom of the pre-stabilization stage. Then the DSP drives coil-magnet pairs on top and piezo actuators located under the pre-stabilization stage legs. Fig. 4900.2 shows a block diagram of the damping strategy implemented with the DSP. The DSP devoted to the damping system reads signals coming from sensors located on Filter Zero. PH1, PH2 and PH3 are LVDT position sensors which measure the relative displacement between Fiter Zero and Tower. AH1, AH2 and AH3 are acceleration sensors which measure the absolute acceleration of Filter Zero. The DSP combines these signals making a projection towards the three main longitudinal modes (x, y and q_z) of the pre-isolation system (Inverted Pendulum), performs the required compensation and finally feeds back to the IP using magnet-coil pair actuators (CH1, CH2 and CH3). Sensors PV1 and AV1 provide signals proportional to the vertical motion of Filter Zero crossbar. The DSP computes corrections and acts on the crossbar with CV1. T1 and T2 are tilt sensors located on the lower ring supporting the IP legs. Signals coming from T1 and T2 are used to reduce the tower tilt with a control loop which uses piezoelectric actuators located under the ring

49.1.2 Suspended masses position control

The required dynamic range for the suspended masses position control is very large (about 10^{15} $Hz^{1/2}$). To achieve this requirement the correct mirrors position will be set acting on three different points in the S.A chain.:

- the suspension point (pre-stabilization stage),
- marionetta (from "filter 7")
- mirror (from "reference mass").

In Fig. 4900.1 the subdivision of control forces is shown. Three independent filters acting on the three control stages are implemented in the DSP devoted to the position control. High resolution digital to analog converters and low noise coil drivers are necessary. A DSP processor under control of a VME CPU computes the forces to be applied on each point in order to obtain the desired displacement.

49.1.3 Super Attenuators internal status monitoring and correction

Each filter in the S.A. chain needs a very low frequency control of the anti-spring magnets position. This control is achieved reading the relative displacement between filter and cross bar. Stepping motors located on the filter itself will eventually correct the position. A similar adjustment system is foreseen on the marionetta stage. These low frequency controls are provided directly by the VME CPU.

49.1.4 Interface between the S.A. control system and other VIRGO sub-systems

The Suspension Electronics has direct interfaces with the Global Control, Alignment, Data Acquisition and Monitoring sub-systems. The Suspension Electronics system receives data from Global Control and Alignment through fast optical links read by the DSP board; the S.A. status is sent to the Data Acquisition and Monitoring through both fast links and Ethernet connections. The Suspension Electronics system is in charge for the development of the software for the data exchange running on its hardware.

49.2 Hardware Description

The typical hardware configuration for the SA damping is shown in Fig. 4900.3. It is composed by a NIM crate containing sensors and actuators conditioning and driving electronic modules (coil drivers, accelerometers, position sensors and low frequency modulation carrier sources) and a VME crate where the processing units are located.

The DSP board interfaces to the VME bus, to the VSB bus and to another local I/O extension bus named VBeX. The VBeX bus is used for communications between the DSP board and ADC/DAC boards and it is mapped on VME P2 connector. The bus connected to P2 can be software selected. Any conflict between VBeX and VSB modules is avoided dividing the address space into two different regions. ADC and DAC boards interface to the VME bus, used for initial boards setup, and to the VBeX bus. The single connection with the timing board is the trigger signal (the trigger signal starts the data conversion and generates an interrupt request on the VBeX bus). A Digital to Optical conversion board can be addressed by both the DSP and the CPU in order to allow fast data transfer to/from the VIRGO frame builder.

Two different mechanisms are foreseen for the communication between CPU and VME. The first one is an access to the DSP memory through the VME bus using the DSP board Host Interface. This fast interrupt mechanism (only two instruction are inserted in the program flux) allows the CPU to write into the DSP memory and it is used for the program downloading, to start/stop the program itself and for the "on the fly" upgrade of computational parameters. The second communication mechanism is mainly used for monitoring purpose. The DSP board writes the signal to be monitored into a dual port memory board using the VSB bus in block transfer mode. The CPU reads those data using the VME bus in order not to generate conflicts with the DSP.

<u>Timing summary</u>

600 → 800 ns to read 6 channel on the VBeX bus.

600 → 800 ns to write 6 channel on the VBeX bus.

1 → 2 ms to write data on the DOL board (VSB Block Transfer).

1 → 2 ms to write data on the RAM board (VSB Block Transfer).

1 → 2 ms to read data from the RAM board with the CPU (VME Block Transfer).
5 ms ADCs conversion time.
1.2 ms DACs conversion time.

About 40 ms available for DSP operations (800 instruction) with a sampling rate of 20 kHz (single sample delay between input and output).

49.2.1 Digital Signal Processor Board

The VME Digital Signal Processor board, fully developed in the I.N.F.N. Labs in Pisa, has been designed for the Virgo payloads position control and for the S.A. normal modes damping. The main features of this board are the following:

- One Motorola DSP96002 processor running at up to 40MHz giving a peak processing rate of 60MFLOPs (30 MFLOPs sustained).
- Large high speed memory array. Up to 256kWord of local SRAM Zero Wait State.
- Standard VME A24 D32 Master/Slave interface supporting VME Block Transfer (DMA) for rapid VME data transfers. Direct access to the DSP Host Interface to efficiently transfer data at high speed.
- Standard VSB master interface.
- Local I/O expansion bus VBEx (24 data bits, 6 address bits) providing a real time communication path with ADC and DAC boards.
- OnCE port for DSP96002 debugging compatible with Motorola software tools.
- RS232 serial port.

49.2.2 ADC616b

The ADC616b is a 6 channels 16 bit ADC board that interfaces both to the VME bus and to the VBeX local I/O bus. The card has been fully designed and developed in the I.N.F.N. laboratories in Pisa.

The ADC616b uses the ANALOG DEVICES AD7885 analogue to digital converter, which is a 16-bit monolithic converter with internal sample-and-hold. The maximum throughput rate is 166 kSPS achieved using a two pass flash architecture. The power supplies required from the backplane are +12 V, -12 V and +5 V.

ANALOGUE INPUTS

Each ADC input has its own anti-aliasing filter module. The input impedance is 100 kΩ and the input voltage range is 10 Vpp (-5 V → +5V).

BOARD PROGRAMMING

The ADC616b board is programmed only through the VMEbus. The following features can be programmed.

<u>Sample Clock Source Register</u>
Internal (Clock Master) or External (Slave)

<u>Sample Clock Rate Register</u>
The internal 24 MHz crystal frequency is divided by the 16 bit number written in the sampling frequency on board register.

<u>ADC Channel Enable Mask Register</u>
Each channel can be enabled using an 8 bits register. Even if the channel is not enabled, the conversion take place anyway. This register is used only when the board is read in BT.

<u>FIFO Enable Register</u>

The FIFO memories can be enabled or not depending on the status of a mode register (8 bit).

Downscaling Set Register
The on board adder can be programmed using an 8 bit register. The register contains the number of samples to be averaged (-1 => 255 to divide by 256) (the maximum number of averaged samples is 256). The output of the adder is a 24 bits data (sign extended to 32 bits for the VMEbus) and can be read both from the VME bus and from the VBeX bus. Since the result of an average of 4 16 bits samples is on 18 bits, when FIFOs are enabled and the number of averaged samples is greater than 4 only the 18 most significative bits are available.

Interrupt Request Generation
When the VMEbus is selected an interrupt request can be generated on IRQ1..7. When the VBeX bus is selected only one level of interrupt request is available. The interrupt request is generated:

- When the programmed number of averages has been made.
- When the 6 ADC channels conversion starts.
- When the FIFO is "almost full" (programmable).

DAQ Synchronization
The ADC616b board can perform a synchronized samples averaging. The adder result is fed to the output (or to the FIFO memories) in correspondence with a double width clock pulse. When clock master the ADC616b board supplies this sync pulse every 1/M clock pulse, where M is the programmed number of samples to be averaged. When slave the board automatically computes the number of averages in order to be synchronized with the master card. This feature produce an uniform signals sampling other than a synchronized data acquisition.

BLOCK TRANSFER

The ADC616b board supports standard block transfer from the VMEbus. When the FIFO memories are enabled, it is possible to transfer 256 byte from the addressed channel otherwise, when the FIFO memories are not enabled, the 6 ADC channels (or only the enabled channels) are read starting from the first one. Using the BT daisy chain cabled on P2 it is possible to read more than one board in block transfer.

ADC NOISE

In a sampling AD converter the noise is made up of sample-and-hold noise and a/d converter noise. The sample-and-hold section contributes 85 uV rms and the ADC section contributes 98 uV rms. These add up to a total rms noise of 120 uV rms. Fig. 4900.4 shows a histogram plot for 5000 conversions of a dc input using the AD7885 in the ±5 V input range. The analog input was set close to the center of a code transition. All code other than the center code are due to the ADC noise. In this case the spread is six codes. The noise rms value can be calculated from the standard deviation estimation. We obtain:

$$n_{rms} = \sigma \frac{V_{pp}}{2^{16}} = 120\ \mu V$$

Dynamic Performance And Effective Number of Bits
For the dynamic measure of the ADC noise we used a 9.8 Volt peak to peak sine waveform. Before entering the ADC this signal has been filtered with a 3rd order Butterworth low pass filter with a cut frequency of 4*f0, where f0 is the sine wave frequency, in order to reduce the source noise. The digital signal has been elaborated by a numerical notch filter and then converted by a 20 bit DAC to perform the noise analysis with a spectrum analyzer. There is not a significative change of the noise level changing the sine wave frequency until this frequency reaches about 200 Hz. Above this limit, the noise increase with the sine wave frequency. Fig. 4900.6 shows the measurement result for a 120 Hz sine wave. The straight line is the average

noise spectrum density used in the following calculations (1.6 uV $Hz^{-1/2}$). The Signal to (Noise+Distorsion) Ratio is about 89.89 dB. This ADC is equivalent to an ideal ADC having

$$N = \log_2\left(\frac{V_{rms}}{n_{rms}}\right) = \log_2\left(\frac{V_P/\sqrt{2}}{\tilde{N}\sqrt{B}}\right) = \log_2\left(\frac{5/\sqrt{2}}{1.6\cdot 10^{-6}\sqrt{10000}}\right) = 14.43 \text{ bits.}$$

Note: a standard way to compute the effective number of bits is $N = (SNR - 1.76) / 6.02 = 14.64$

49.2.3 DAC820c

The DAC820c is an 8 channels 20 bit DAC board that interfaces both to the VME bus and to the VBeX bus. The card has been fully designed and developed in the I.N.F.N. laboratories in PISA. The DAC820c board uses the ANALOG DEVICES AD1862 digital to analogue converter which is a low-noise, low-distortion 20 bit audio converter. The maximum throughput rate of this chip is about 800 kHz.

ANALOGUE OUTPUTS

Each DAC output has its own filter module. The cut frequency is 20 kHz. The output voltage range is 10 Vpp (-5 V $\rightarrow$ 5 V).

DAC NOISE. Harmonic Distorsion and Signal to Noise Ratio

Total Harmonic Distorsion (THD) can be measured using the technique shown in Fig. 4900.7. The 20 bit DAC is driven with a 20 bit digital sine wave having a frequency of 156.25 Hz. The DAC update rate is 20 kHz. The FFT Spectrum Analyzer (Ono Sokki CF-6400) performs a 4096 point FFT of the filtered signal and computes THD and Signal to Noise Ratio (SNR). The Signal to (Noise+Distorsion) Ratio is about 106 dB. This DAC is equivalent to an ideal DAC having

$$N = \log_2\left(\frac{V_{rms}}{n_{rms}}\right) = \log_2\left(\frac{V_P/\sqrt{2}}{\tilde{N}\sqrt{B}}\right) = \log_2\left(\frac{5/\sqrt{2}}{2\cdot 10^{-7}\sqrt{10000}}\right) = 17.43 \text{ bits.}$$

49.3 Software Description

49.3.1 Advanced Damping Toolkit (ADT).

The ADT software has been developed to produce an highly optimized code for the DSP's control system without requiring a deep knowledge of the hardware implementation. In fact, the user of the existing software is, in general, a specialized one who knows exactly the DSP hardware, furthermore the software is frequently designed for a set of configurations and not for all.

ADT software solves all this problems. ADT's users can produce, essentially without an accurate knowledge on how his digital filter is implemented into the DSP's system, highly optimized code using a graphical description of what the DSP have to do. Furthermore, this implementation is no more correlated to the particular hardware choice, so it is possible to use the same user program with different hardware configurations.

This software satisfies the following general requirements: portability; user friendly interface, a Client/Server structure and finally a "protected" interface to the hardware system. The protected access to the processes that are running on the DSP's system plays a fundamental role during the setup phase when it will be necessary to fix the control loops parameters.

To assure nice GUI (Graphical User Interface), easy portability and Client/Server structure we have chosen:

- ANSI C.
- UNIX-Like OS with XWINDOWS SYSTEM MANAGER.
- TCP/IP as transmission protocol.

The GUI is based on a public domain library, XFORMS, that runs on at most all the UNIX-Like systems including the Lynx-OS system. It is based on XWINDOWS and is written in standard ANSI C language. At the moment the ADT software can run on the following platforms:

- LynxOS 2.2 /m68k
- IBM-RS6000
- PowerPC /AIX
- Linux
- Linux/i386
- Linux/alpha
- Linux/m68k
- Linux/sparc
- MkLinux/PowerMac X11R6.1
- Sun
- SunOS
- Solaris
- Dec-Alpha (OSF1 V2 & V3)
- HP/HP-UX
- OpenVMS /Alpha

49.3.2 The graphical user interface

Unfortunately, the implementation of a GUI for programs is in general a time consuming process. In the last few years a number of packages have appeared that help build up graphical user interfaces in a simple way. ADT software uses a public domain library (Forms Library) to build the GUI. The Forms Library contains a large number of pre-defined objects, such as buttons, menus, sliders etc. The interactive GUI builder bundled with this library can be used to generate all the geometry and C code needed, and in general it is not necessary to write additional C code to make a nice-looking GUI. The application program has a large amount of control over how objects are drawn on the forms. It can set color, shape, text style, text size, text color, etc. In this way forms can be fine tuned to programmer's liking, furthermore special goodies are built-in to perform common task in the application program, like select a file name, ask questions etc. In this way, the application programmer can concentrate his own work on designing the handler functions and on the real core of the software project. The Forms Library can be used both in C and in C++ programs. The library uses only the services provided by the XLIB and should run on all workstations that have X installed on them.

49.3.3 The internal structure of adt software

The ADT software was designed to use its own library and to be easily scaleable for future needed, i.e. change in the hardware setup, etc. For this reason we have maintained an high level of modularity in writing the code. The internal structure of this tool is sketched in Fig. 4900.10.

The Design unit takes its graphical input from a schematic entry and performs the error check, the extraction of the Netlist file, and the simulation of the control loops using external data (simulated or real).

The Kernel unit is the core of the ADT software. It performs the compilation and the downloading tasks. The compilation translates the Netlist information into binary code that the download module send to the VME CPU trough the network. This unit also coordinates the communications between the other units and DSP's control system building up the required protected access to hardware system.

The third unit is the Monitor. The tasks are the probe positioning on the schematic and the analysis of the information to make graphics, FFT and Transfer Function of the signals taken from the DSP's control system.

The Tool unit is an advanced area in which the user can build its own ADT library using the Library Designer tool, or design his own special digital filter using the Digital Filter Designer. Finally, ADT software has provided, also, of the Bitmap Vector Creator tool that can be used to build a vectorial description of the library object's icon.

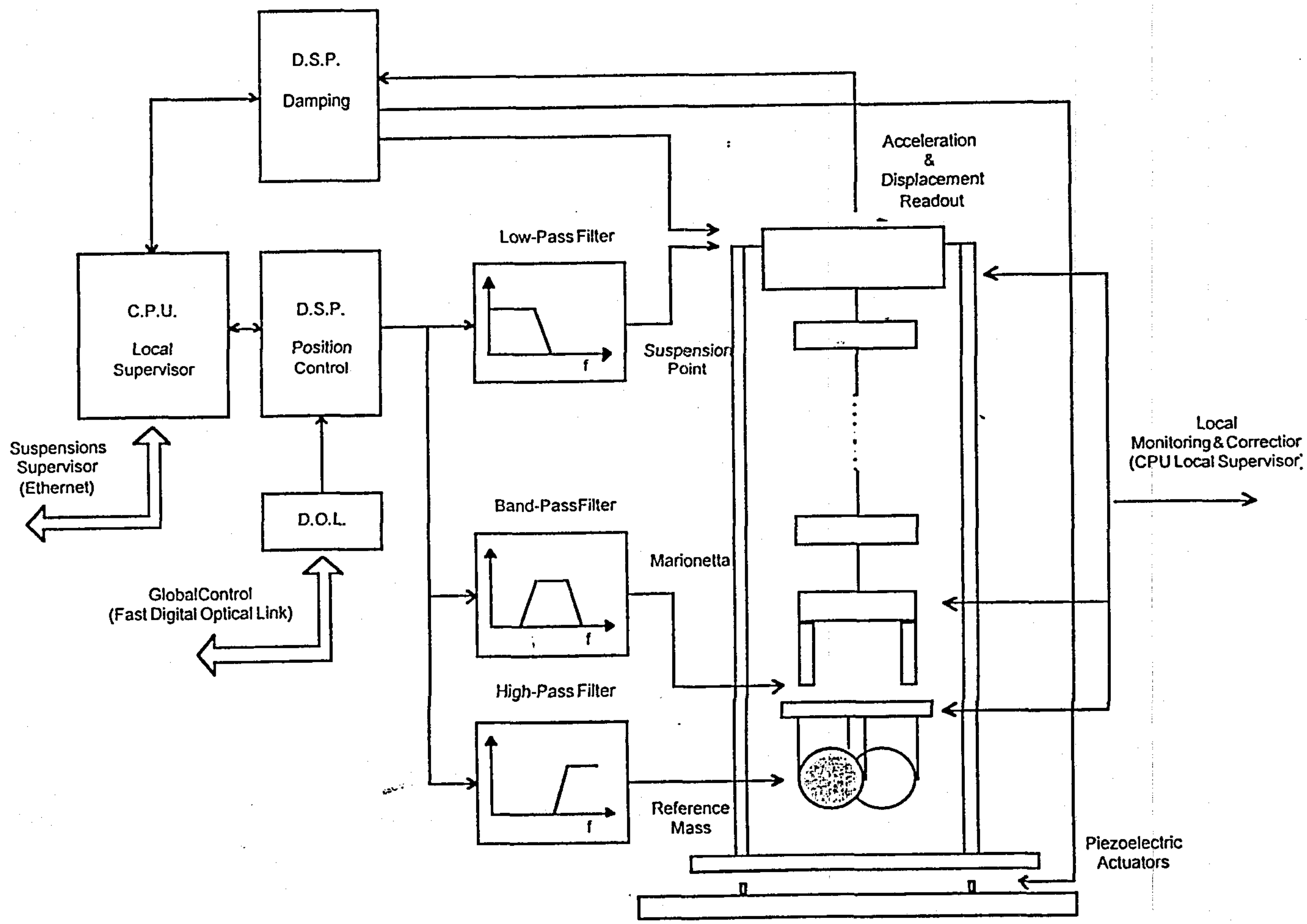

Fig. 4900.1 Suspension Control

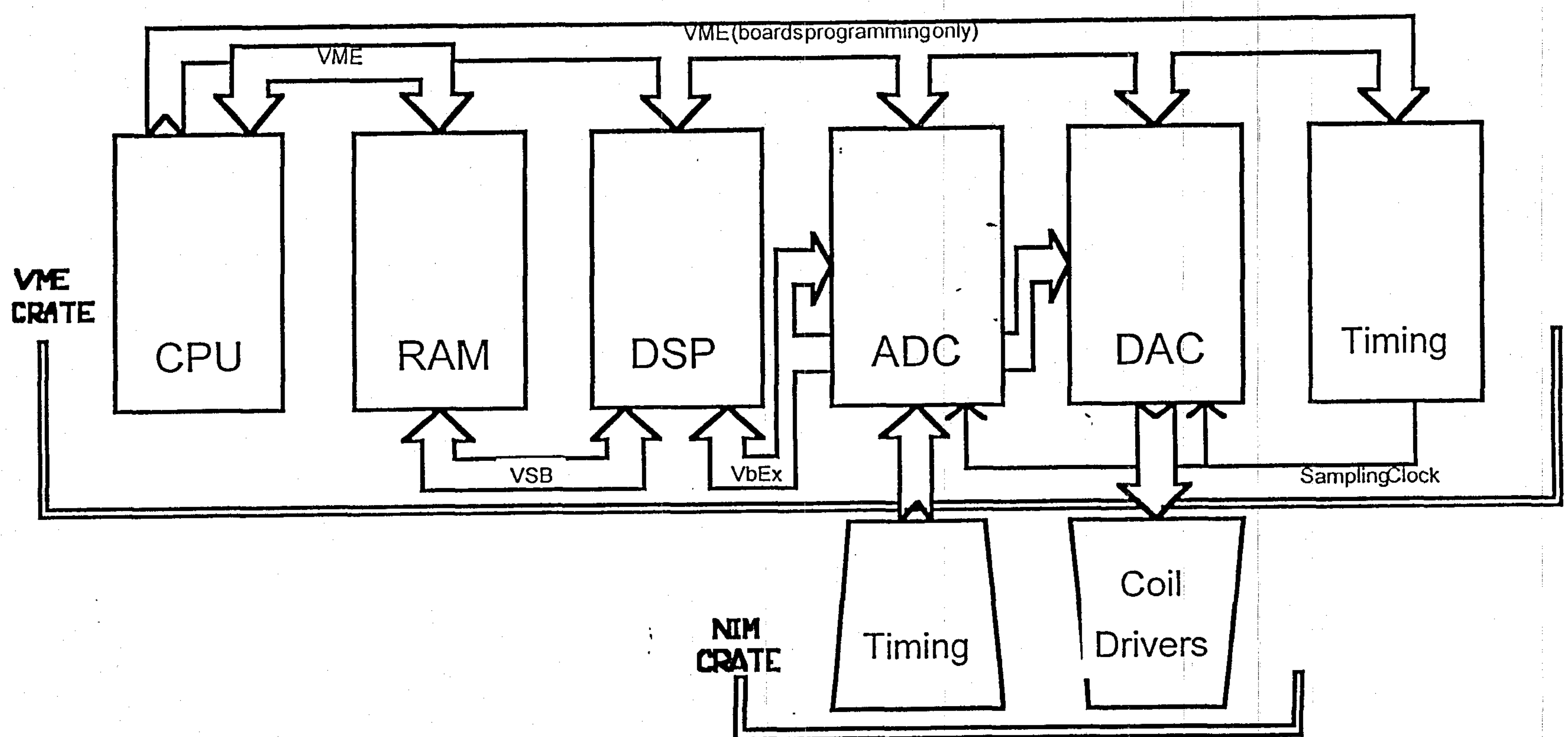

Fig. 4900.3 Standard suspension control crates: electronic devices for local controls

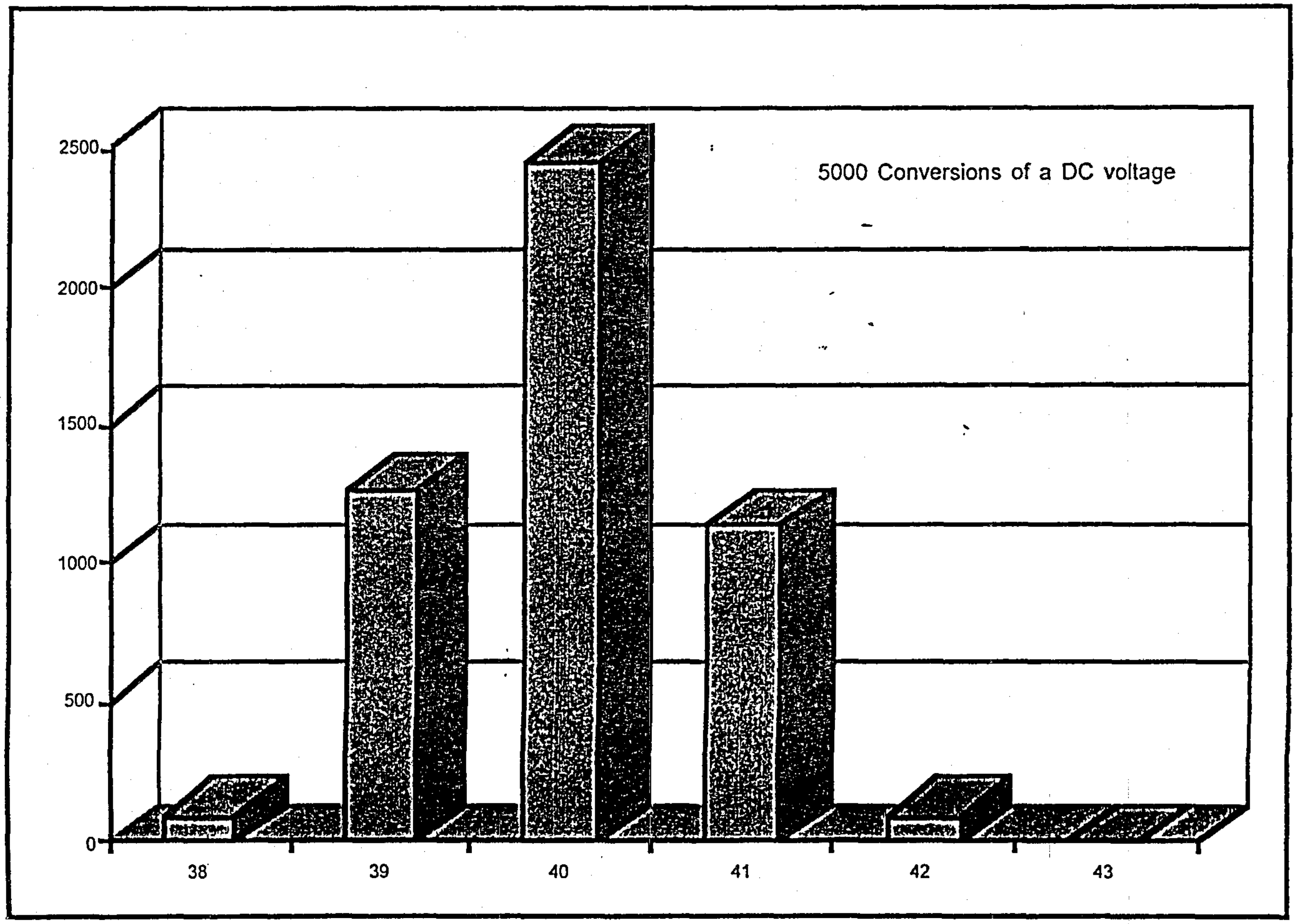

Fig. 4900.4 Histogram of 5000 Conversions of a DC Input ($f_s = 20$ kHz)

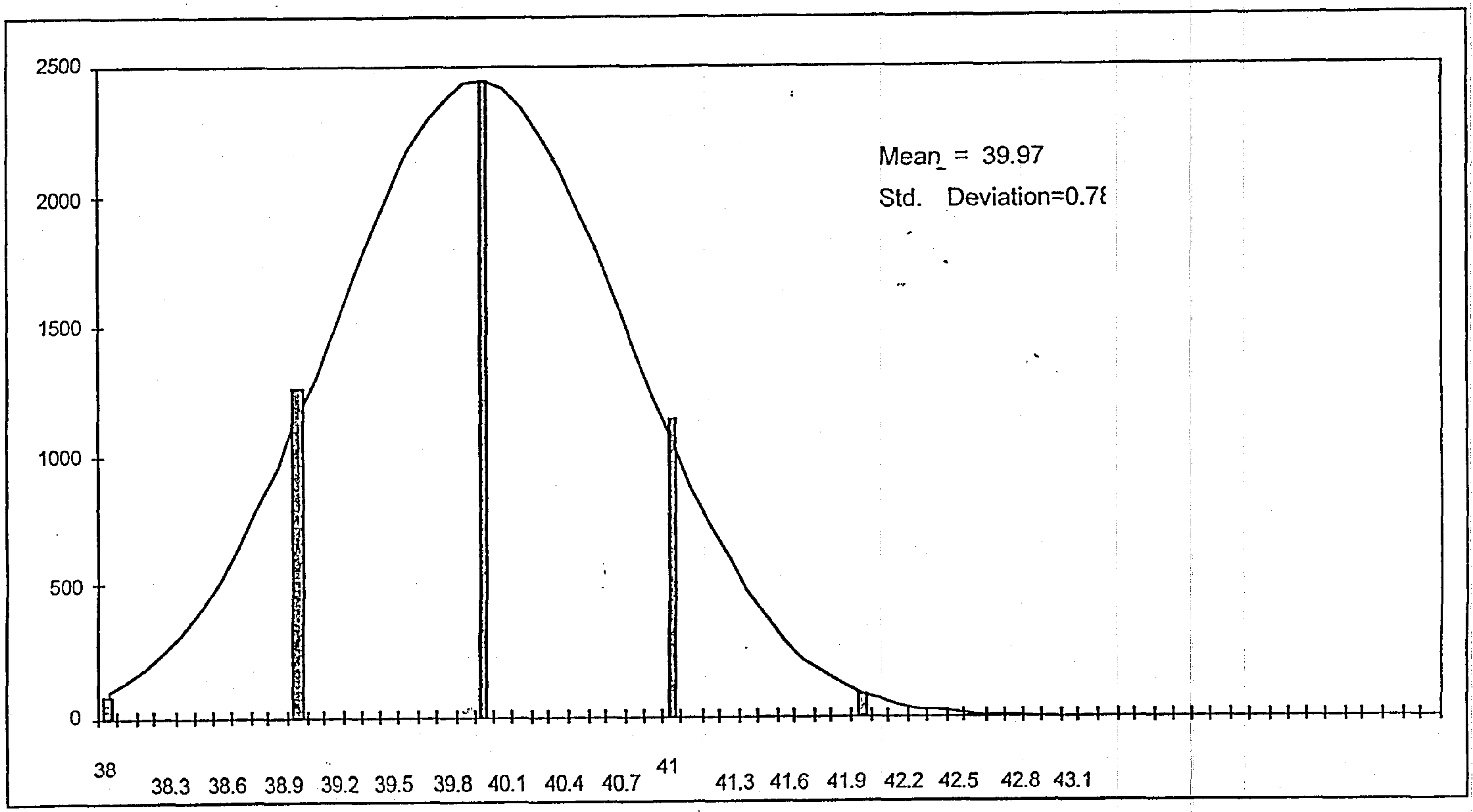

Fig. 4900.5 Mean Value And Std. Deviation Estimation

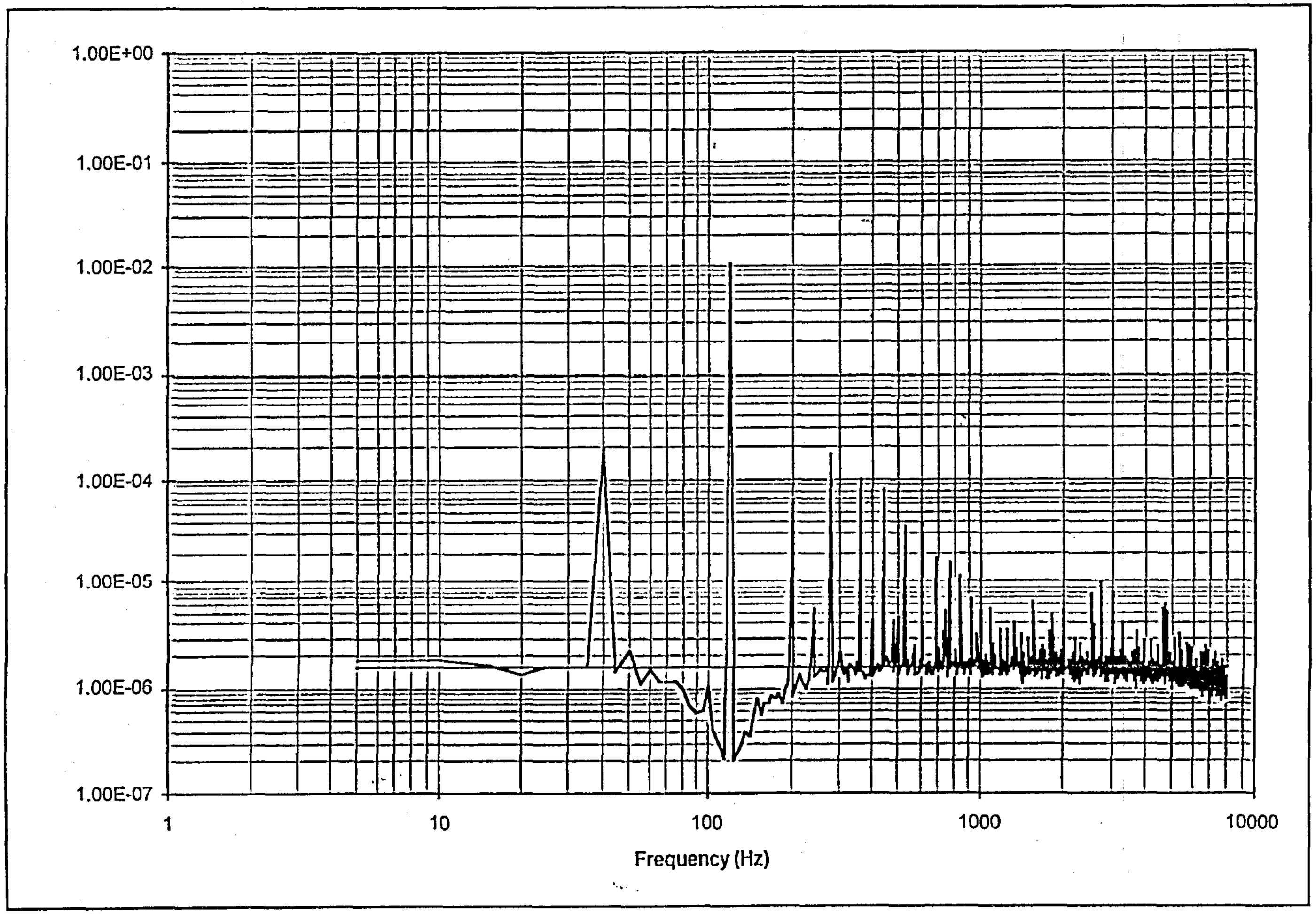

Fig. 4900.6 Noise Power Spectrum Density

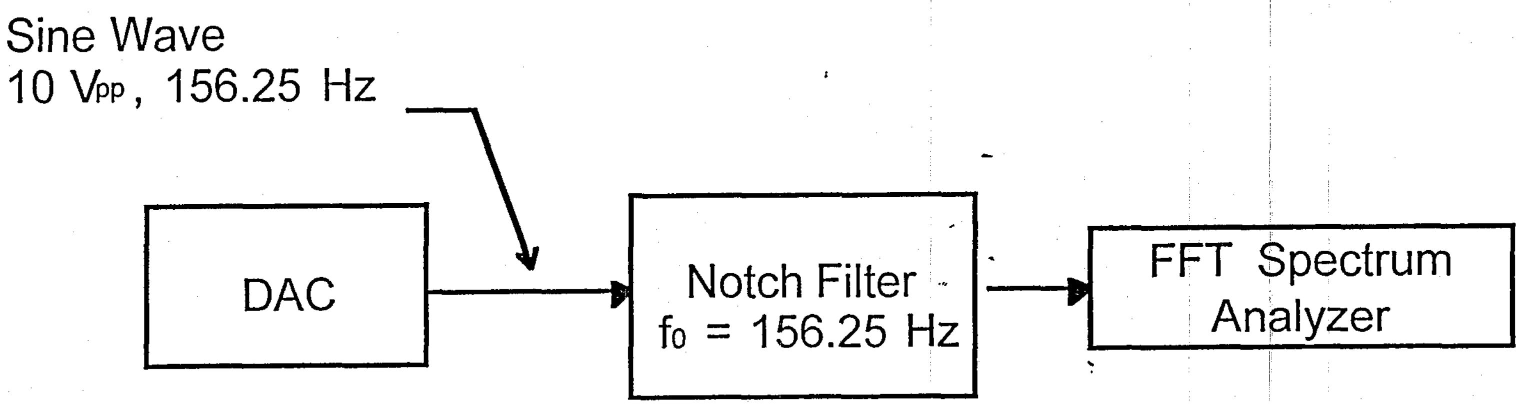

Fig. 4900.7 Total Harmonic Distortion (THD) measurement setup.

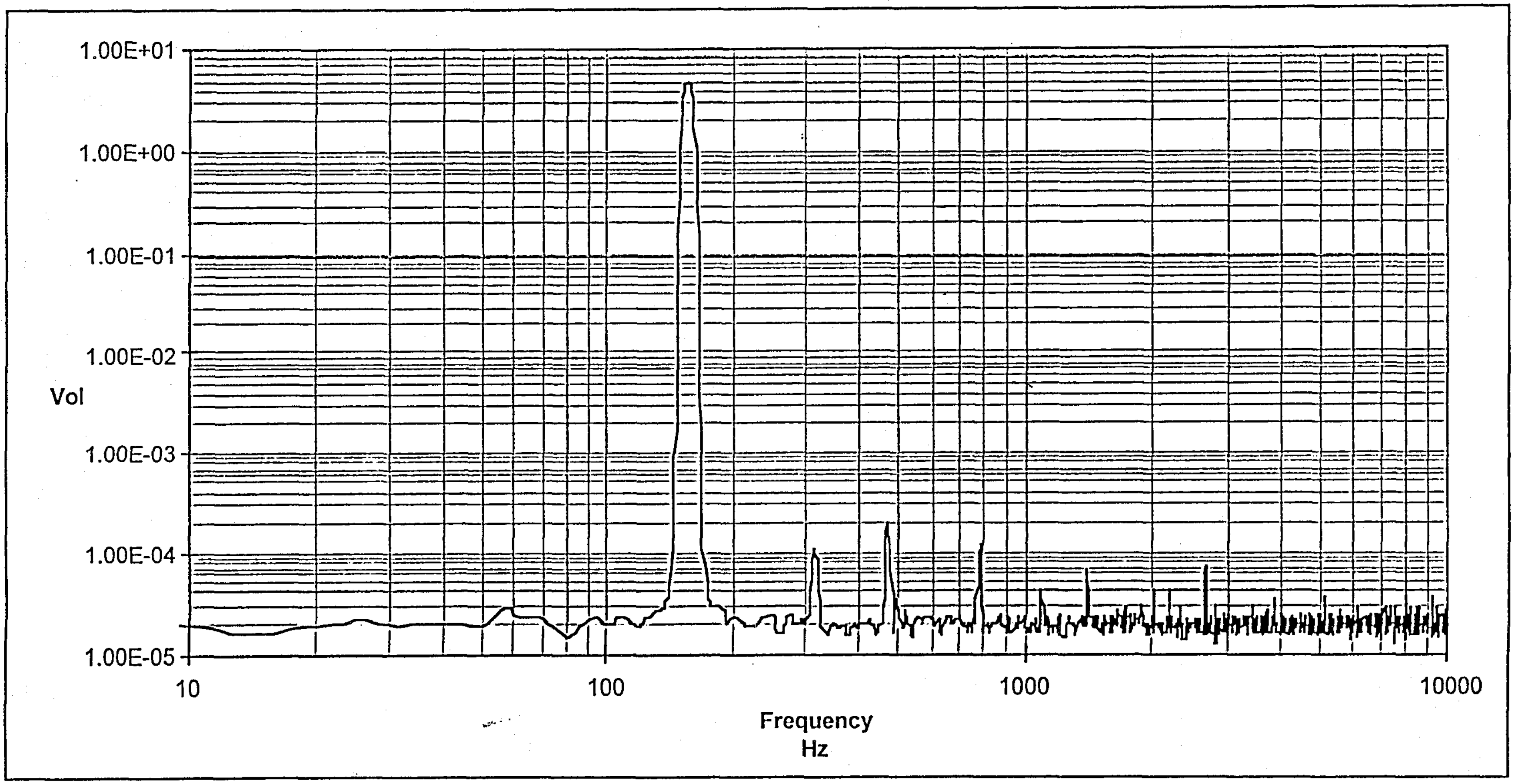

Fig. 4900.8 Noise spectra without notch filter

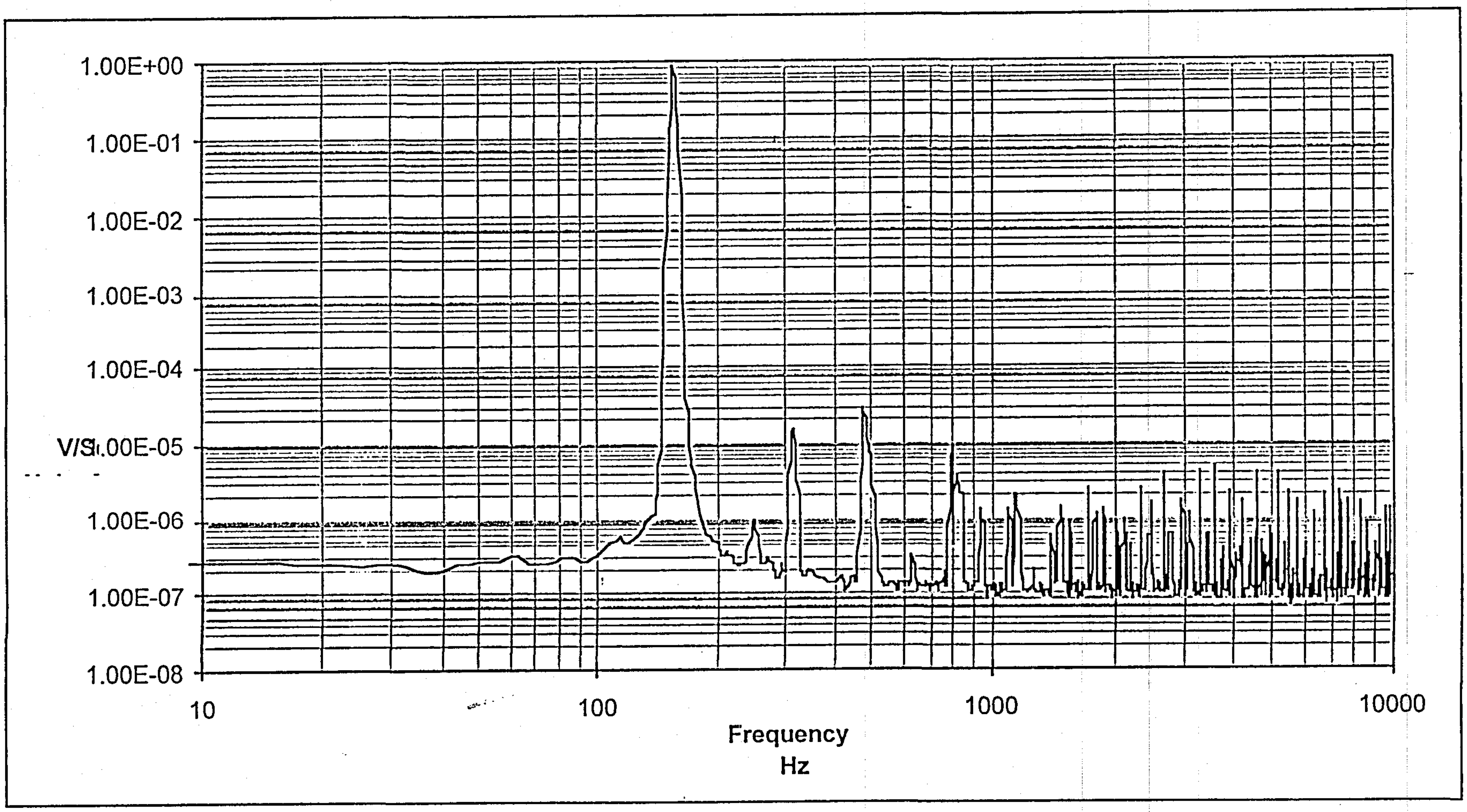

Fig. 4900.9 Noise spectra divided by the filter transfer function

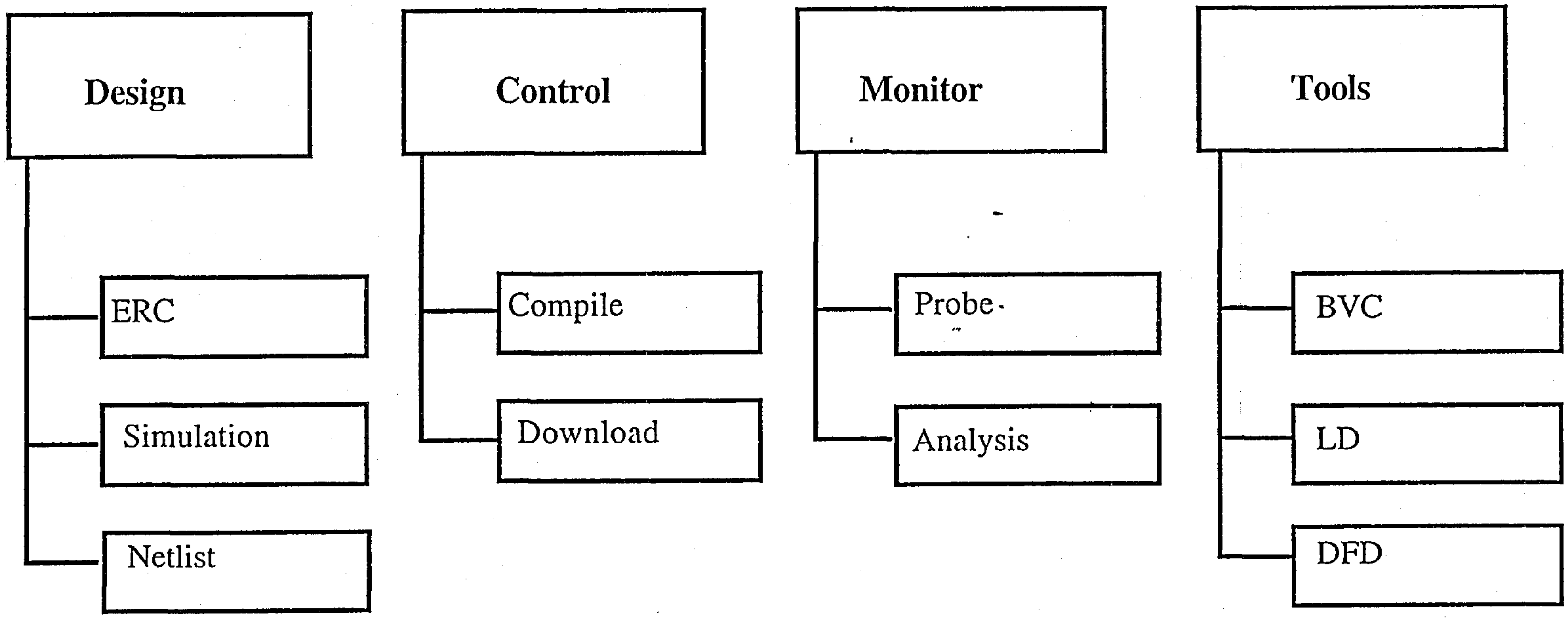

Fig. 4900.10 The internal structure of ADT software. Each unit is linked to its own module. Each module performs a well defined task.

50. ELECTRONICS AND SOFTWARE

Table of Contents

50.1 System description

This chapter describes all the needed activities starting from the output of the local electronics up to the data ready to be analyzed for Gravitational Waves search. It covers three fields :

- The online activity. It concerns the controls of the interferometer, the acquisition, online processing, and monitoring of the data produced by the various detectors or control process.
- The detector simulation activity. It concerns the generation of gravitational events like coalescent binaries, pulsars, supernovae and the simulation of the response of the interferometer to such signals and to all possible noises.
- The offline activity. It concerns the basic tools for the refined analysis of the large amount of collected data.

A coherent view of all these activities will help optimizing the design, the commissioning, the running and the understanding of the first results produced by the interferometer.

50.2 System requirements

The main requirements for the online system are :

- a real time control system running at 10 kHz with fast decision taking processes and correlation capability all over the site,
- a data acquisition system with a maximum sampling frequency of 20 kHz and a maximum data rate up to 10 MBytes/s (typical data rate = 1MBytes/s),
- full data archiving,
- data selection and tools to provide reduced data set for the data analysis,
- a dead time between the user interface and the real time process lower than one second,
- a system easy to reconfigure and to use on small test bench,
- test capability at all levels,
- software reusability.
- Good reliability and maintainability

50.3 General description

50.3.1 The online Architecture

The various active parts of the detector which produce digitized information or 'data' are represented on figure 5000.1. Most of the signals produced by the different sensors are processed by a layer of local controls which compute and apply local corrections to keep the controlled elements (laser, mirror, vacuum pump,...) within a given set of tolerances. These controls produce data like status information or feedback values. Several local controls may be supervised by a higher level control, the Global Control, in charge of the locking and the alignment.

The data generated by these detectors and controls (the 'raw data') are collected by a local readout process, concentrated and structured by a Frame Builder and written to tape (Data archiving). They are processed ('reconstructed') to convert ADC counts and feedback signals to an h value, and 'filtered' to reduce their amount to a level manageable by the offline analysis. The data quality is permanently monitored by surveying the noise level and a known signal produced by a calibration device stimulating permanently the interferometer as a gravitational wave would do it. Finally, the 'filtered' data are sent to a storage and distribution system which is the experiment front end for the offline analysis. The system provides also tools for histogramming and data editing (including monitoring data).

All these controls are coordinated by a Supervisor and synchronized with a central Timing system.

50.3.1.1 The architecture

The interferometer is kept at its working point by a set of controls which process data provided by sensors and adjust accordingly its main components : the laser, the two mirrors of each Fabry Perot cavity, the end mirror of the mode cleaner, the recycling mirror, the beam splitter, the injection and detection benches.

The architecture of the control and read out systems has to account for the large distances which may separate two components. To preserve flexibility in the interferometer setting up, the control systems are organized as much as possible into independent units in charge of the adjustment of a well defined component. They are run locally in standalone mode and accessed remotely by some high level control process. Similarly, the readout systems are implemented into independent units in charge of the concentration of the data produced near the components located in a same building : end mirror West and North, mode cleaner, and main buildings. A central data acquisition system, located in the control room, collects and assembles these data before writing them to tape.

The knowledge of the precise timing of the various measurements and actions performed around the interferometer is one of the key points of its operation as a gravitational wave detector. This is implemented with a central timing system, located in the control room, and set up to distribute a well defined clocking sequence all over the site.

50.3.1.2 The hardware options

To achieve a few kHz bandwidth on the interferometer sensitivity, one has to design its various servo loops with a much higher bandwidth in the range of 10 kHz. As a consequence, one has to implement the system with 'fast' sensors, processors and actuators connected with 'fast' links. To execute the various feedback loops within a constant time the system has to be built with conflict free accesses.

Sensors, processors, and their actuators sampled at those high rates are thus implemented within the commercially available VME standard. High transfer rate digital servo loops are implemented with a dedicated bus. Conflictual bus accesses are avoided by housing only exclusive controls in the same crate. To keep proper track of all the measurements only digital information can be exchanged. Higher level control processes transfer their information from building to building via a Digital Optical Link (DOL). Short distance transfers between different controls are performed through mirrored memories connected on a local bus or using a DOL.

The environment status is generally measured with sensors sampled at a low rate. They are thus implemented in VME or G64, depending on their availability and cost. They are read out by slow monitoring systems and the data are exchanged using a dedicated ETHERNET network (the slow monitoring network) extending all over the site.

The data sampled at high rates are collected by the local fast readout systems. Then they are transferred to the main control room by a digital optical link.

All the processors are networked via ETHERNET or FDDI and accessible for control and file exchange by all workstations. Figure 5000.2 shows the networking which has to be implemented between the main building, an end mirror building and the control room. The basic rule is that hardware links are used for all real time connections while computer networks are used for state control and for slow monitoring.

The use of standard hardware is mandatory since it allows easy reconfiguration and long term maintenance.

50.3.1.3 The software options

The steady operation of the interferometer is implemented in the context of distributed processing synchronized by a 'central' timing system. The various control processes are designed as standalone tasks getting data from a dedicated local sensor and/or from another control process. The different readout tasks are organized to operate under the mastership of a central DAQ task.

Each control process (fig. 5000.3) is a server built in the framework of the client-server model. It is a real time program usually running on a VME CPU. It has direct access to the hardware required by its functionality (typically ADC's, servoloop,...). It should be able to run and to deal with its possible error conditions, minimizing its access to the computer network. For fast control proccesses, only data for test, configuration parameters and status information should be exchanged using the computer network.

The user interface (a client of the control process) configures the server and/or monitor and displays the data provided by the server. Several user interface clients can be simultaneously used to monitor its information, but only one client at a time (the master client) has the privilege to configure a server. Possible conflicts are locally solved using standard rules and information provided by the online database. The user's interfaces are run on workstations and they do not need to be real time.

The Cm library is used for ALL the communications between processes on the computer network. This package provides platform independent communications tools and access to the processes using logical names. The correspondence between logical names and physical addresses is provided by the Cm name server. This server is needed for all applications using cm and therefore it should always be running. There is a unique Cm name server for the experiment.

To provide an easy control of all the process by a single user interface (The supervisor) all the running servers are able to respond to a standard set of messages. These messages allow the supervisor to control the basic server operations and some monitoring facility. The list of the standard messages is given in the standardization section (5200)

The stable state is reached when the server and its hardware are operated in a mode which allows stable data taking. Running is for the cases where the system tries to reach the stable case like pumping down, trying to align, to lock,... Several running levels could be specified.

All the parameters needed to run a server are stored in configuration files which could be stored locally, by the server, or by the Online Data Base. These configuration files are just an ASCII text to allow easy understanding and debugging. In fact one of the main tasks of the user interface is to be an intelligent configuration editor. The Online Data Base stores also all the information about privilege access to the server. This is done by using the machine name and the user account as selection parameters.

The error logger is the last server which should always be running. It collects the information and error messages from all the process. The error display is the error logger client which provides the tools to select and display error messages collected by the error logger.

50.3.1.4 Security

It is important to be able to protect the hardware against any kind of wrong action. We first have to remenber that the hardware is connected to a VME CPU which runs the server. The first protection will be to limit the number of accounts on these processors. Then the server is driven by a client which runs on a different computer. Since all connections use Cm, the next protection will be the limitation (using domain name for instance) of computers able to be connected to the name server. The Cm connection will also provide the user name for the client. Therefore we can restrict the connections to a limited number of accounts run on a limited number of workstations. The server will get these informations from the online data base. When two clients want to control the same server, the server will ask the online data base to decide which one has the highest priority. If the connection with the data base is not possible, the first connected client will have the priority.

50.3.1.5 The Slow monitoring network organization

The slow monitoring network is designed to control and collect data from Slow Monitoring Station (SMS). A SMS is a standalone system which controls some hardware and which provides a small amount of data with no precise timing information (the foreseen timing accuracy is 1 second). A typical SMS is a Tube control station which controls a pumping station.

A SMS follows the standard software rules. It is a server with user interface run on different machines (see figure 5000.4). The data read by the SMS are formated and sent to the frame builder on its request once per frame. The frame builder will send these data to the data distribution and the archiving system even if the fast data acquisition is not running. The history of the parameters can be displayed on a workstation using the Data display and the data distribution systems. For this data collection the SMS has to be able to answer to standard Cm messages described in the standardization section (5200)

To preserve the network bandwidth, a dedicated network is used for the slow monitoring. The only connected CPU's on this network are the SMS, the needed workstations to run the user interfaces and the fame builder.

50.3.2 The control of the interferometer

50.3.2.1 The Fast Controls

The various optical and electrical components of the interferometer are driven by local, standalone, controls. Several components can be correlated by a higher level process (like the Global control for locking & alignment) acting through local controls and using information from various photodiodes. During setting up, any local control can be operated using the supervisor. The figure 5000.5 is a sketch of this general control architecture.

Figure 5000.6 presents the chain of hardware components needed for the control implementation. It is a distributed digital servo loop running at a frequency equal to 10 kHz (this frequency is limited by the transfer time between the components, given their relative distances). The status of each component is controlled by the supervisor using the computer network, while the real time data are exchanged using dedicated hardware connections (DOL). The data exchanged in the links are :

- From signal detection : power seen by the various photodiodes in watts (DC and demodulated signals)
- From the local position measurement : three absolute positions and angles
- From the suspension control to the Global Control : the mirror absolute position from the local position, the force applied on the mirror and any relevant status information.
- From the Global Control to the suspension control : the position and angle error.

This scheme is basically the same for the longitudinal locking and for the alignment . Strong connections between them will be possible, though we will try to disconnect as much as possible all the functions.

50.3.2.2 The control and monitoring of the interferometer environment

These control are done using the Slow Monitoring Station. They are :

- - The Building control station
- - The Environment Monitoring Station
- - The Tube Control Station
- - The Tower Control Station
- - The calibrator control

50.3.3 Offline

The major offline activity is the data analysis aiming at the extraction of a gravity wave signal. This activity where imagination is very important should stay widely open within the collaboration. But one needs a set of tools and rules which should be managed in common to provide basic software environment and to allow for comparisons of different works.

There will be a simple analysis framework to provide the basic functionality of analysis jobs like read/write frames, simple monitoring, run the online selection. Such programs could already be tested with SIESTA.

During data analysis we will need some generic tools, usually in the area of histogramming, plotting and fitting. For this need, we will use as much as possible the tools developed at CERN. This is especially true for the histogramming with HBOOK and interactive plotting with PAW .

The offline reconstruction program which converts the raw data to an h value has also to be standard and identical to the online reconstruction run for the frame selection. Improvements in the knowledge of the transfer functions or of the calibration constants may justify an offline re-run of the h reconstruction.

50.3.4 System Commissioning

It is mandatory to allow for a progressive and independent commissioning of the various components of the experiment. To that purpose, the readout has been organized in autonomous subsystems capable of local standard data acquisition. To exercise locally and independently the various controls, one has to provide the necessary excitations and measurements devices. Once everything is set up, i.e. once the interferometer is running its beams, then a calibration device is foreseen to monitor permanently its sensitivity.

50.3.4.1 Controls commissioning

The suspension control is organized in independent system with local position measurement. This gives the capability to test all the actuators and the controls. For the global control, simulated data can be generated and sent in the data links. But we will have also the capability to illuminate the photodiodes with known signal and to test the effectiveness of the global controls.

50.3.5 Data acquisition commissioning

The DAQ of the experiment is performed by a central system which assembles the frames whose details are collected trough optical links fed by the local readouts. Once the local readouts have been set up, one certifies their frame building capability with appropriate test procedures which do not need any special hardware. As an example, the local readouts can be programmed to deliver a simulated output signal. This would allow for a test of the optical links and of all the procedures following the frame assembly.

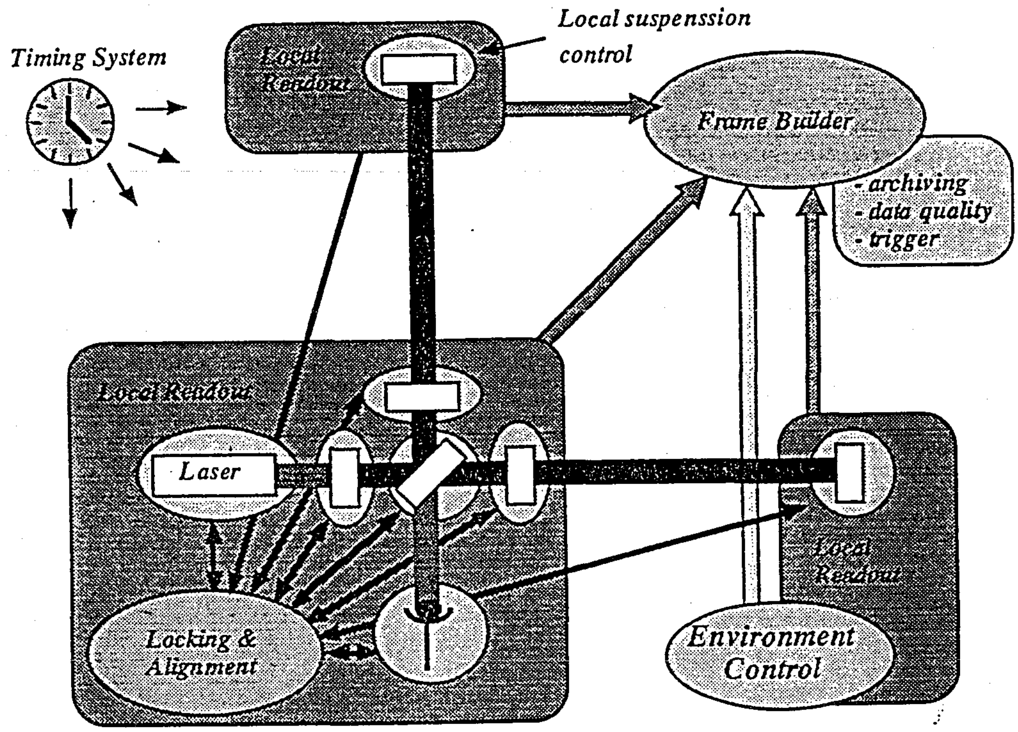

figure 5000.1 The online architecture

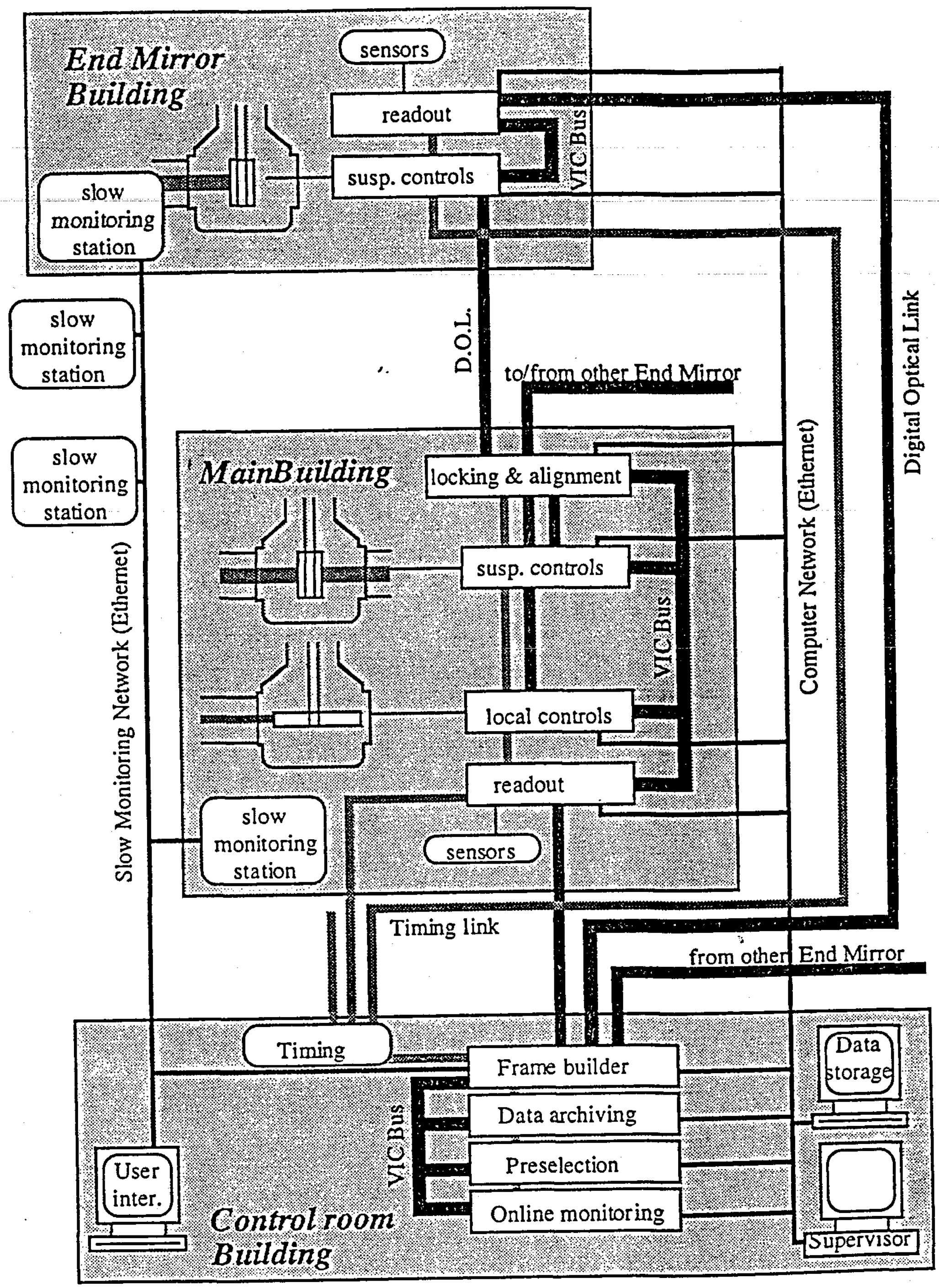

Figure 5000..2

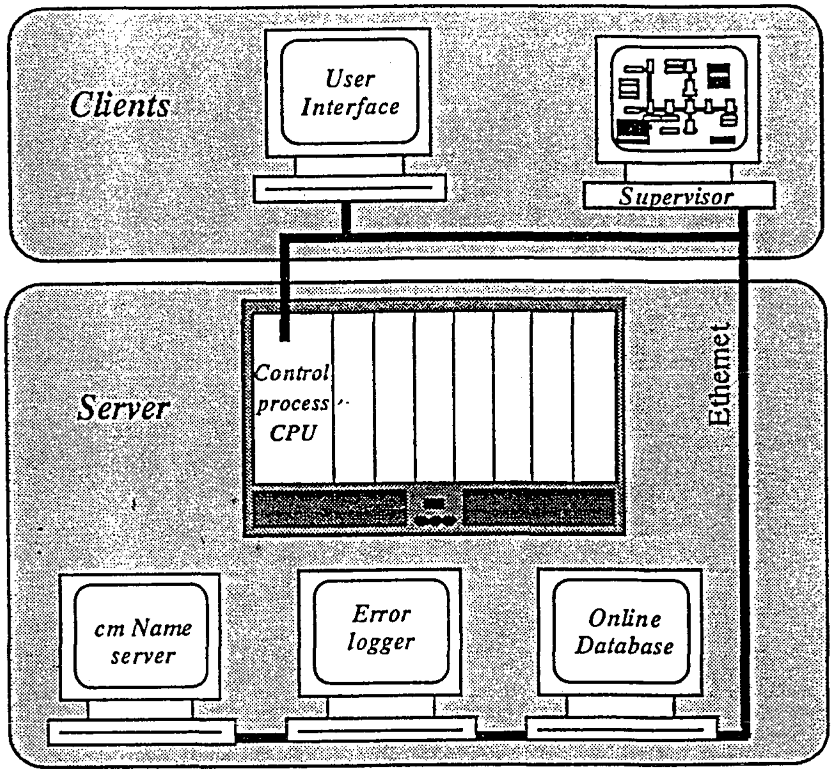

Figure 5000.3 client/server process organization

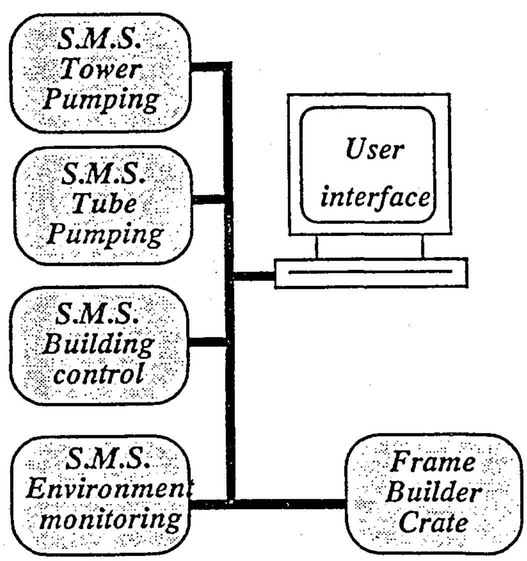

Figure 5000.4 Logical organization of the slow monitoring

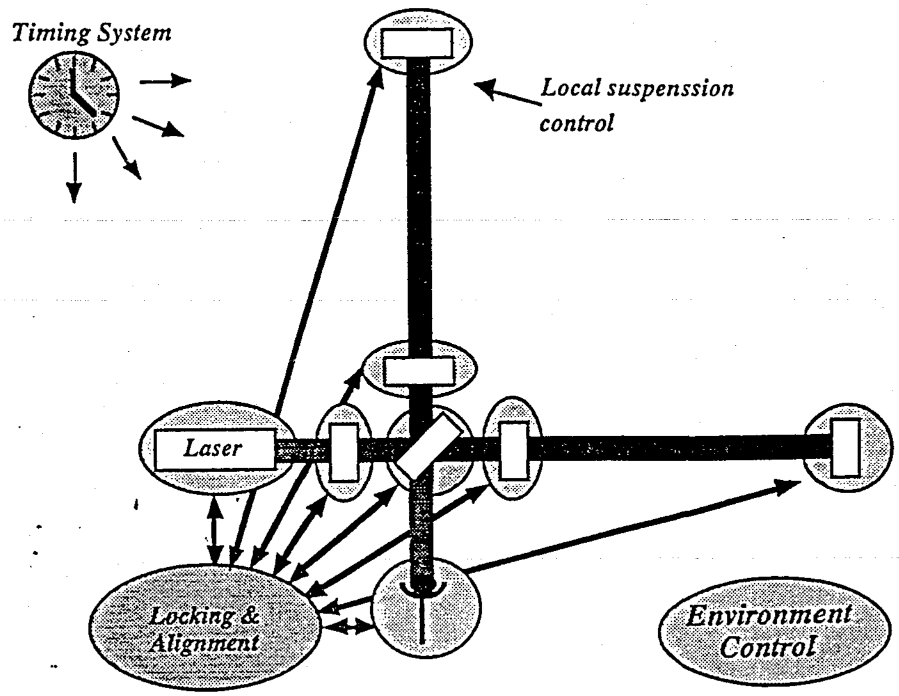

Figure 5000.5 Global view of the controls.

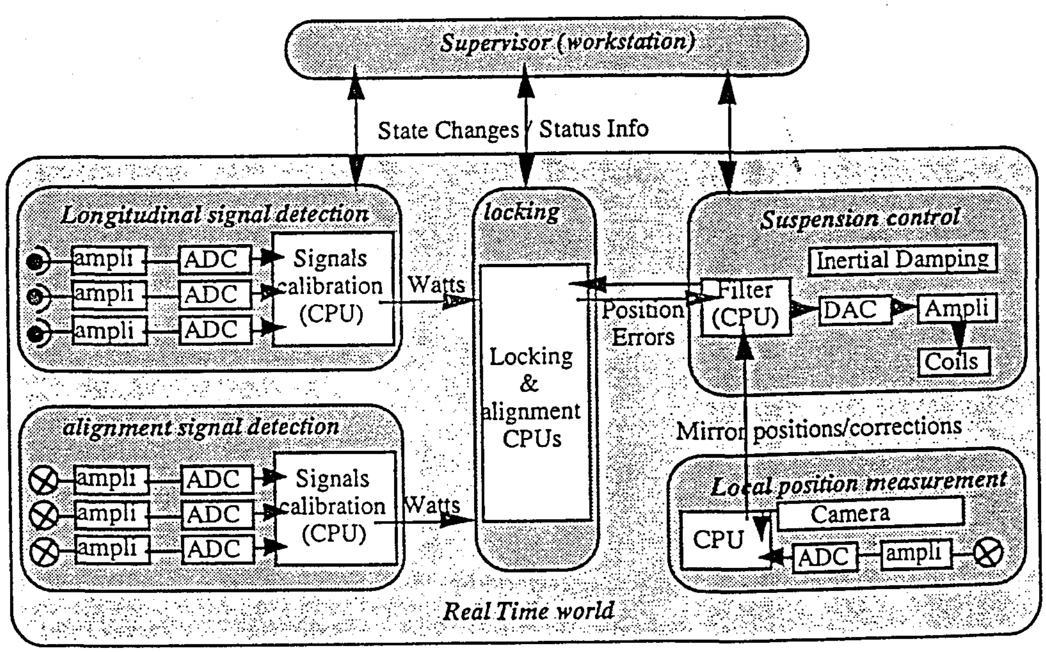

Figure 5000.6 Principle of the control implementation.

51. Global Control

51.1 Real Time Global Control (RIOT)

The first component of the Global Control is located in the RIOT (Real tIme glObal conTrol) crate, in the main building : it is completed by the Global Control Survey in the control room.

RIOT is activated by the Supervisor once all the needed sub-systems have reached their running mode. At setting up (non-linear regime), RIOT has to bring the different components of the interferometer close enough to the ideal positions in order to activate the ``running" algorithms. In running mode (linear regime), RIOT is in charge of the longitudinal locking and alignment of the interferometer.

The Global Control software is flexible enough to accommodate different kinds of locking schemes, to handle longitudinal as well as alignment drifts, and to be able to guarantee smooth operation of the interferometer both in its linear and non-linear regime.

A set of three processors is foreseen. This hierarchy is based on the time response needed for the various processes ; each one uses its own (more or less sophisticated and, hence, time consuming) model of the interferometer.

In the running mode, one is dedicated to the longitudinal locking, another one to the alignment. The third higher level processor does monitoring and checks the validity of the work done by the other two processors. If some troubles are detected, the models used at the lower levels can be updated. When necessary, it can take care directly of the locking and alignment.

In the starting mode, the higher processor is the only one at work. Through a dedicated user interface, it can perform manual operations using general ressources (beam-imaging system for example) and/or photodiodes signals and run predefined algorithms in order to bring the interferometer in the linear regime. When the conditions are fulfilled or the user wishes, it starts the lower processors and goes to survey mode.

RIOT uses the signals provided by the various signal detection systems to compute the time dependent parameters needed to describe the status of the interferometer. It is also kept informed of the relevant actions decided locally, for example, by the servo-loops in charge of the suspension chains or of the second stabilisation stage of the laser. Its main task is to compute the corrections to be applied on the main optical elements. These correction requests are sent to the corresponding local controls which are in charge of implementing them. The corrections, together with the error signals and the status of RIOT and local servo-loops are sent to the DAQ, for monitoring and for the Global Control Survey.

51.2 Global Control Survey

The second component of the Global Control is the Global Control Survey, complement of RIOT. Its main role is to detect unwanted trends in the various servo-loops and, more generally, to react on faulty behaviours thwarting the locking of the interferometer. It should be in position to perform all correlations deemed necessary to fulfil its task. Its decisions are reached on the basis of the overall response of the interferometer, taking into account as much as possible, all the information available at this level. Its other function is to permit the development online of Global Control softwares.

52. Standardized components

52.1 Standardization and Software rules

52.1.1 Language

- Lynx OS for real time VME CPU (or OS9 for G64 crates)
- UNIX system for workstation
- Motif and X window for graphic
- C with C++ style for language

The software running on various processors will be written in C language as much as possible in order to be able to use it in the simulation and analysis programs if needed. This is also true for monitoring tasks running on the front end workstations which are in charge of the control and monitoring of the real time processors.

52.1.2 Coding rules

Here is a short list of the main coding rules to be followed :

- Use `double` instead of `float` (for 'scientific' calculations),
- use `long` instead of `int` (to make sure we have 32 bits).
- use a naming convention:
    - all function names, structure types and variables which are not local should start with the two key letters of the library. Example : `frrawdata`
    - keep upper case for `define`.
    - start local variables with lower case.
    - start global variables with upper case.
    - to build composed words use upper case instead of underscore.
- write `simple' C code
- only one instruction per line (except for `for`, `while`)
- use indentation for loops, if... (at least 2 spaces)
- no C++ keyword to allow a futur migration to C++. As a reminder here is the list of C++ keywords : asm, catch, class, delete, friend, inline, new, operator, private, protected, public, template, try, this, throw, virtual.
- use comments, especially in the header file to describe each variable defined in a structure.

52.1.3 File organization

The file organization is presented in figure 5200.1. The reference version for the VIRGO software is stored in the machine virgoa1.in2p3.fr for the time being. It will be moved on the site when computers will be available. This directory and the software documentation could be accessed using WWW at the following address :

http://lapphp.in2p3.fr/virgo/sdoc/doc.html

All packages are stored in a separate directory. A readme file should give some basic information like the person in charge of this package and who to contact in case of problem. The list of the current packages and their key words and manager is included in the `/virgoApp` directory. Each package has a single person in charge of the updates. The standard version of the software is found by using the 'pro' directory which contains logical links on the various packages. When several people are working on the same package, CVS is used as code manager.

52.1.4 The list of Slow Monitoring Stations

Here is the list of the foreseen slow monitoring stations with their name :

Tube control station :	TW01,TW02,...TW11,TN01,...TN11 (for west & north arm)
Tower control :	TOIB (input bench), TOMC (mode cleaner),
	TOPR (power recycling), TOBS (beam splitter),
	TOIN (input mirror north), TOEN (end mirror north)
	TOIW (input mirror west), TOEW (end mirror west)
	TOSR (signal recycling), TODB (detection bench)
Building control :	BCCE (for central building), BCMC(for mode cleaner)
	BCEW (for end west), BCEN(for end north)
Environment monit :	EMCE (for central building), EMMC(for mode cleaner)
	EMEW (for end west), EMEN(for end north)
Laser control :	LASR
Benchs :	IBEN (input), DBEN (detection), NBEN (north arm bench),
	WBEN (west arm bench)
Calibrator :	CALI

52.1.5 Data format on tape :

Frame number and sampling number are limited to 65536 in order to store them in a single word in the timing board. Frames collected with the same experimental condition are grouped in 'Run' identified with a run number.

When frames are exchanged between client and server, we just send one binary file per frame with the same format as the one used to write on tape. More information about data format and examples could be found in the FrameLib (Fr) directory.

52.1.6 Information distribution

News can be broadcast to a list of VIRGO people by sending a mail to VIRGO-L@IN2P3.FR. WWW servers are available in most of the labs. More information about the news system and old news could be found at :

http://lapphp.in2p3.fr/virgo/news/news.html

52.2 The timing system

A central timing system is required to synchronize the interferometer controls, servo loops and readout systems. This is achieved with a master clock driving a bunch of timers which reduce the original frequency to the frequency specific to a given device (see figure 5200.4). Practically, the master clock is derived from a GPS system located in the control room building. Clocking signals are distributed by an optical fiber link to the different buildings where they are converted to TTL signals for local use.

Whereas the different sensors and controls are sampled and operated at rates adapted to their sensitivities, the basic acquisition cycle is set to the sampling frequency of the dark fringe. The timing system produces the necessary interrupts (at 20 kHz) to trigger the acquisitions with a 'sampling number' for their later identification. Depending on the required sensitivity, one may be led to group together several acquisition cycles, covering thus larger time intervals called frames. The timing system provides the frame number for their later identification. The frame starting time is given by the GPS system at reception of this interrupt. It is the time stamp of the data acquisition.

The different controls and feedbacks are operated on fractions or multiples (i.e 1MHz) of the basic acquisition cycle. Their action is thus precisely known with respect to the acquisition time. The implementation of this clocking sequence is a corner stone of the safe operation of the detector.

For simplification, the number of clocks will be minimized. We foresee three basic clocks :

• The fast servo loop clock (about 1 MHz). It will be used to oversample ADC's used for precise measurements (signal detection or suspension damping)

• The sampling frequency (10 to 20 kHz). It will be used for most of the digital servo loops (locking, suspension control) and for the main data acquisition

• The seismic frequency (100 Hz). It will be used to record monitoring accelerometers.

Each timing board is able to generate a frequency signal by its own in order to guarantee a clock signal to the ADC and DAC boards, even if the connection with the master source is lost. There is a timing server for each crate holding a timing board.

The full timing system could be tested and will be permanently monitored by measuring the sampling time in each local readout crate using independent GPS boards or by using a return signal for fast servo loops.

52.3 Workstations

Workstations are used to run the Graphical User Interfaces and control programs. Powerful workstations are needed to handle the large amount of data provided by the various detectors. Detail of the possible solutions can be found in the document VIR-TRE-LAPP-5200-102.

52.3.1 Control Room & Computer Room

The Control room will contain two clusters of identical workstations (Figure 5200.2). Even though they will be able to run any user interface, they will be dedicated to one or two specific types of control. Two clusters will be used instead of one in order to do system maintenance without stopping VIRGO.

Here is the list of the foreseen workstations :

- W1 : Tube control & Tower control (on slow mon. net.)
- W2 : Building control & Environment control (on slow mon. net.)
- W3 : Laser & input bench control
- W4 : Detection bench control & Signal detection
- W5 : Suspension control
- W6 : Locking & Linear alignement
- W7 : Name Server, Supervisor & Timing control
- W8 : Non Linear Alignement & Beam Imaging
- W9 : Local Readout & Frame Builder
- W10 : Data distribution control & Data archiving

- W11 : Trigger control & Data Monitoring
- W12 : Data distribution : This workstation is located inside the computer room. It is a more powerful workstation with lot of disk space and special hardware.
- W13 : Network analyser
- W14 : Software distribution

The rack content is the following :

- R1 Cabling arrival
- R2 Network Hardware
- R3 Master timing (1 c.) Frame Buidler(1.c) Reconstruction & Trigger (1c.) Data monitoring (1 c.)
- R4 Data archiving (1crate + space for tape drives and disks)
- R5 Free (could hold CPU monitors)

52.3.2 Main Building

A few workstations (or X terminals) will be available in the Data acquisition room to locally work on the control. They will be on the same cluster as those in the Control Room.

Here is the list :

- W21 : Tower control & Tube control (on slow mon. net.)
- W22 : (for W3,W6)
- W23 : (for W4)
- W24 : (for W6)
- W25 : (for W8)

The rack content is the following :

- R11 Cabling arrival
- R12 Network Hardware
- R13 Detection Bench control (1.c) Signal detection (2 c.)
- R14 Detection Bench Suspension control (2 crates)
- R15 local readout(1c.), Calibration (1 c.), Env. monit & Build control (1c.)
- R16 Input North and Input West Suspension control (2x2 crates) (These crates may need to be closer to these towers)
- R17 Recycling and Beam Split. Suspension control (2x2 crates)
- R18 Locking&alignment(1c.), alignement signals(1c.),
- R19 Detection Bench (2 crates)
- R20 Laser control (1 c.), Input bench control (1c.)

52.3.3 Mode Cleaner or End Mirror Building

One general purpose workstation (W31, 32, 33) and one X Terminal will be available next to the tower. There will be also one rack with 2 crates for the suspension control and one for the local readout.

52.4 The Video system

The requirement for the video system will evolve with time, from the survey of the mirror installation to the control of the smooth running of the interferometer. Therefore the video system should be easily reconfigurable. This means that we will have standardized cameras, monitors, cables and plugs.

We described here a reference solution where most of the monitors will be located in the control room. Since we have a large number of cameras, we will have choosers in the control room to decide which cameras are displayed. We will also use 'quadravision' to group four cameras in one monitor. It will be possible to forward the image of a few selected monitors to the data acquisition room or near the optical benches to help for their tuning. It will be also always possible to insert a local monitor near the corresponding camera. A tape recorder will be available in the control room to keep track of some installation procedures or of the interferometer start-up for instance.

52.4.1 List of cameras

Human activity control :

The purpose of these cameras is to monitor the various rooms, the benches and mirrors installation and to survey their operations. The corresponding monitors will be installed near the Building control workstations. Colour cameras will be used to survey the halls to improve the visual resolution (cameras V1 to V8). During the mirror installation inside the tower, we will use the alignment cameras to monitor the operations. We should foresee a different set of lenses to increase their field. The list of cameras is the following :

V1	Clean Room	(colour)
V2,3	Gallery 1 ang 2	(colour)
V4,5	Hall 1 and 2	(colour)
V6	Data Acquisition Room	(colour)
V7	Mode Cleaner Hall	(colour)
V8	Laser room	(colour)
V9	Laser Bench	(black & white)
V10	outside Input Bench	(black & white)
V11	outside Detection Bench	(black & white)
V12	North End Mirror Hall	(black & white)
V13	West End Mirror Hall	(black & white)
V14	North End Mirror Gallery	(black & white)
V15	West End Mirror Gallery	(black & white)
V16	North End Mirror Bench	(black & white)
V17	West End Mirror Bench	(black & white)
V18,19	Central building views	(black & white)

To reduce the cost of the 3.2km transmission, the camera signals from an end mirror building will be grouped together with a "quadravision", with a monitor in the end building and another one in the control room.

Mirrors and Benches position measurements :

The position of each suspended object is monitored with two cameras, one with lens and one without lens (see alignment section of the FD). These are high precision cameras read by a VME board. The purpose of the video monitors is to provide a fast check for the auxiliary laser beams and for the camera operation and also to survey the mirror using the cameras equipped with lens. During the running of the interferometer, we will mostly display in the control room the cameras imaging a mirror (6 cameras).

V21 Input Bench Positioning	V31	(camera with lens)
V22 Mode Cleaner Mirror Positioning	V32	(camera with lens)
V23 Recycling Mirror Positioning	V33	(camera with lens)
V24 Beam Splitter Positioning	V34	(camera with lens)
V25 Detection Bench Positioning	V35	(camera with lens)
V26 Signal Recycling Positioning	V36	(camera with lens)

V27 Input North Positioning	V37	(camera with lens)
V28 Input West Positioning	V38	(camera with lens)
V29 End North Positioning	V39	(camera with lens)
V30 End West Positioning	V40	(camera with lens)

Beam Imaging :

A set of high precision cameras read by a VME board is installed to image the beam at various positions in the interferometer. They are used to align the benches and the interferometer and also to monitor the running conditions. The purpose of the video monitors is to have a fast check in addition to the digital images.

V41,V42,V43,V44	Laser & Input Bench
V45	Recycling mirror screen
V46	Mode Cleaner
V47	End of north arm bench
V48	End of west arm bench
V50,51,52,53	Detection Bench

Tower separating roof position measurements :

The position of suspension wire inside the conductance will be monitored by a camera. A mirror located near the conductance will provide a side view of the wire position. Therefore we will use a set of black and white cameras. Their images will be displayed in the control room to survey separating roof displacement. Additional monitors could be installed near the tower .

V61	Recycling Mirror separating roof positioning
V62	Beam Splitter separating roof positioning
V63	Input North separating roof positioning
V64	Input West separating roof positioning
V65	End North separating roof positioning
V66	End West separating roof positioning

52.4.2 Digital processing of the signals

In order to get a fast treatment for the position measurements we will have one processor for each couple of cameras looking at one mirror or bench (10 CPU's). Then six more processors will be dedicated to the beam imaging. One for the cameras located in the laser and input bench, one at the end of the mode cleaner, one at the end of each arm, one for the recycling mirror screen and one for the cameras located on the detection bench. Of course we need one VME interface for each camera. A software (GalaXie, GX) is developped to process the images. This includes simple image presentation, local position measurement and tools for the non linear algnment. Most of the image processing is done by the local VME processor. But the image presentation and the non linear alignment analysis will be performed on various workstations and especially on the imaging workstation.

52.4.3 Monitor installation in the Control room

Two colour monitors will be reserved in the control room to view the various halls (cameras V1 to V8). A chooser will select 2 of the 8 inputs. These monitors will be installed near the building control workstation. One of this input will be forwarded to a colour screen located in the data acquisition room.

The bench monitors and the end mirror building survey will be sent to another chooser also located near the building control workstation. The separating roof positioning images will be sent to the same chooser. For the end mirror, the separating roof positioning will replace the gallery camera in the quadravision during the permanent operations.

The signals coming from the alignment cameras (V21 to 28 and V31 to 36) will be send to a chooser (16 inputs, 2 outputs) located near the alignment workstation.

Four monitors will display the most useful information for the interferometer running : the signals coming from the input and output benches (V41 to 44 and V50 to 53), the four images of the transmitted beam (V45 to 49) grouped in one image and the images of the four mirror cavities (V37 to 40) also grouped in one image.

The figure 5200.5 summarises all the components of the system. Few additional monitors will be availabletemporarilly during the installation of the interferometer.

52.4.4 Cabling :

4 cameras in the mode cleaner, 33 in the central building and 6 in each end mirror building are foreseen. Taking into account of a few cables to send images to the computer room (1 to the mode cleaner building and 6 to the central building) and adding some spare cables the following cables are needed.

- 3 optical fibers to each end mirror building (4 cameras are grouped by a quadravision)
- 8 coaxial cables (150m of KX6) to the mode cleaner building
- 40 coaxial cables (150m of KX6) to the central building

The optical fibers are from the standard cabling. Dedicated patch panels for the coaxial cables will be installed in the data acquisition room, computer room and mode cleaner room near the network patch panels

52.5 Standardization : Hardware

The hardware standard components are as follows :

- VME bus with A24D32 addressing mode for fast system or G64 for slow monitoring system like vacuum control
- VME crate 21 slots 9U (basic package reference : 70-204-45 from ELMA). Power supplies 500W (+5V/80A; +12V;10A; +12V/2A; -12V/10A), Automatic daisy chain, J1 and J2. Cooling with 3 fans.
- VME Crate 7 slots 4U (basic package reference : 70-204-25 from ELMA). Power supplies 250W (+5V/40A; +12V;6A; -12V/2.5A). Automatic daisy chain, J1 and J2. Cooling with 1 fan.
- CPU : CES (RIO2-8061FA) and 604 from CETIA (only for the Data Archiving and DIstribution)
- Timing : board from LAPP
- TTL/OPTO and OPTO/TTL : copper to fiber converter for timing signals
- GPS : BC637-VME from Bankcom
- The Digital Optical Link (DOL) for fast crate to crate connections. These links are seen has a FIFO on each crate. The data rate on the 3 km optical fiber is 14 Mbytes/s
- BNC connector for cables

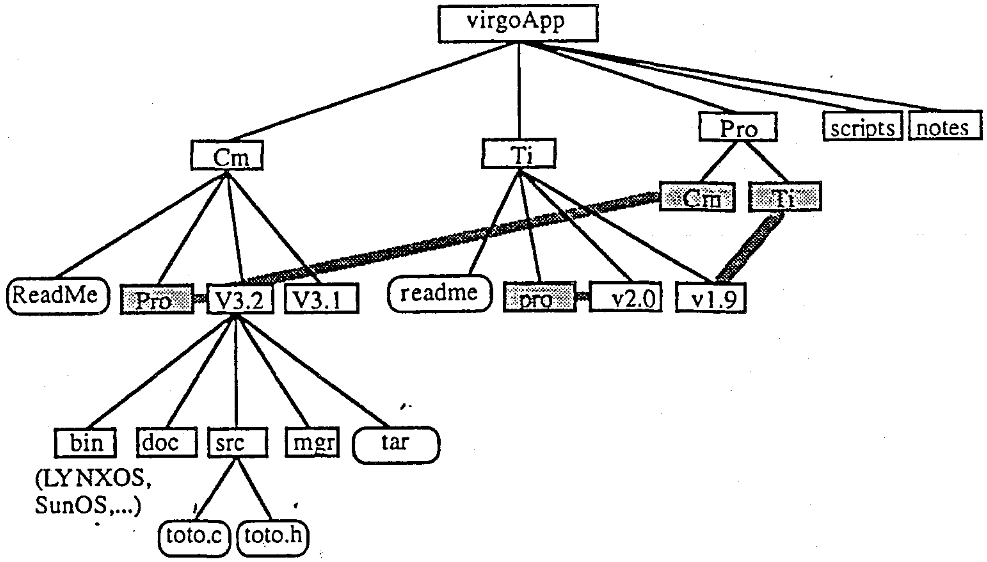

Figure 5200.1 The file organization

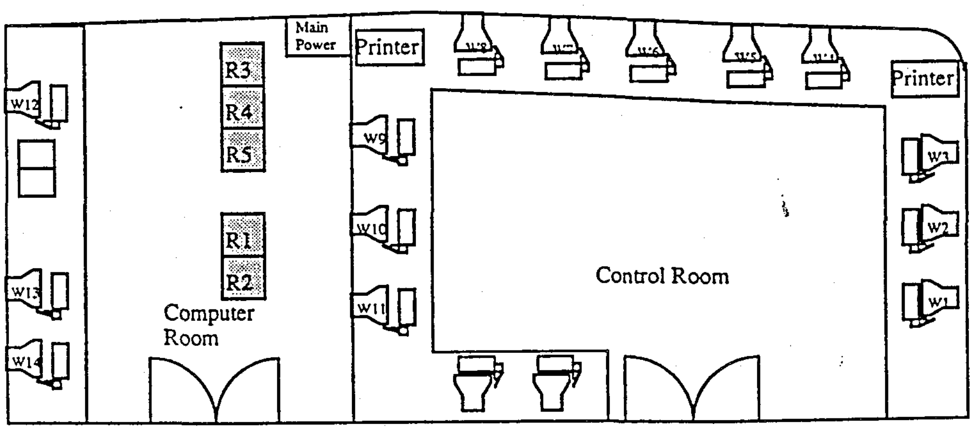

Figure 5200.2 Control Room and Computer room. Video monitor (for beam imaging or for room survey) will be installed above the workstation

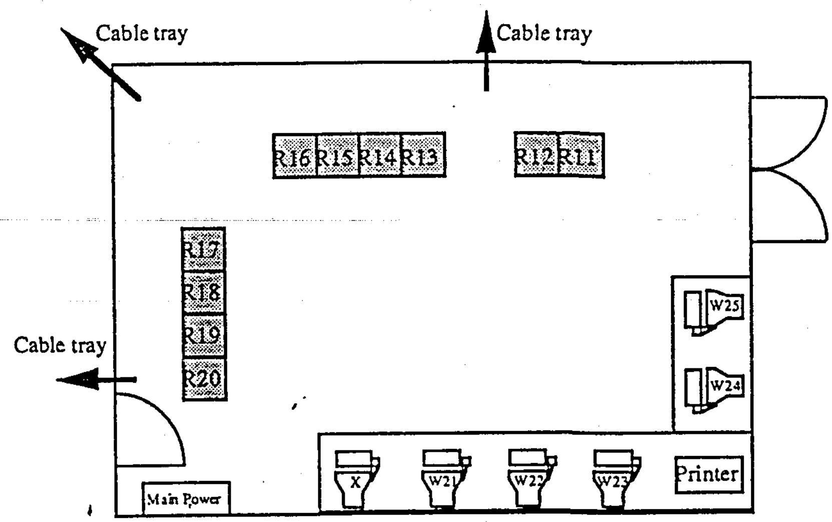

Figure 5200.3 Control Room and Computer room. Video monitor (for beam imaging or for room survey) will be installed above the workstation

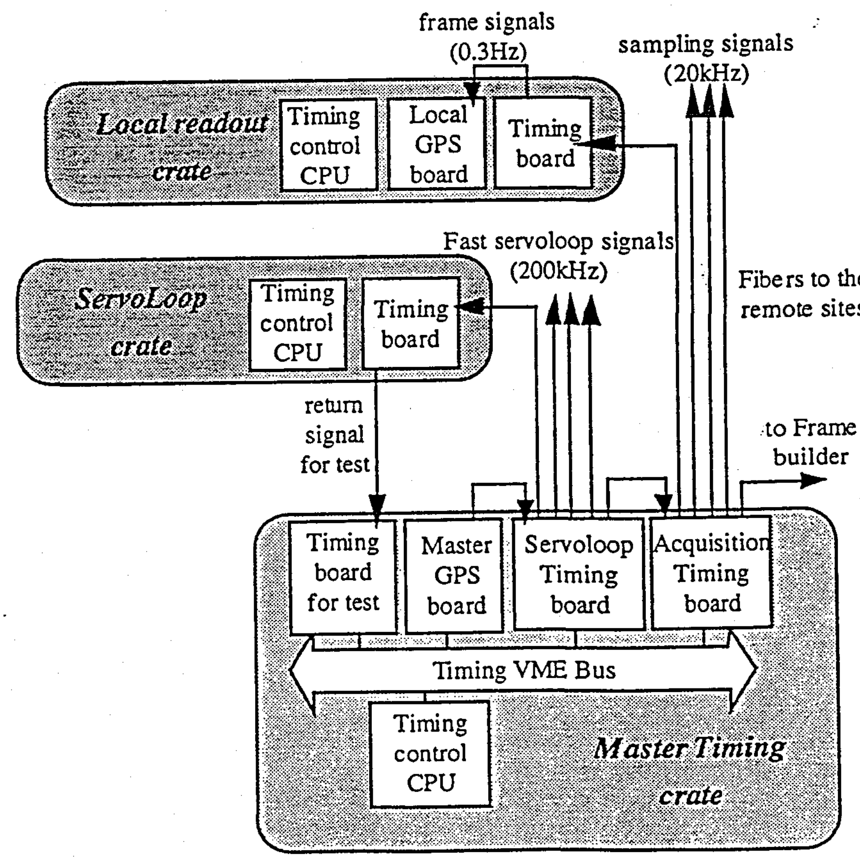

figure 5200.4 The timing system

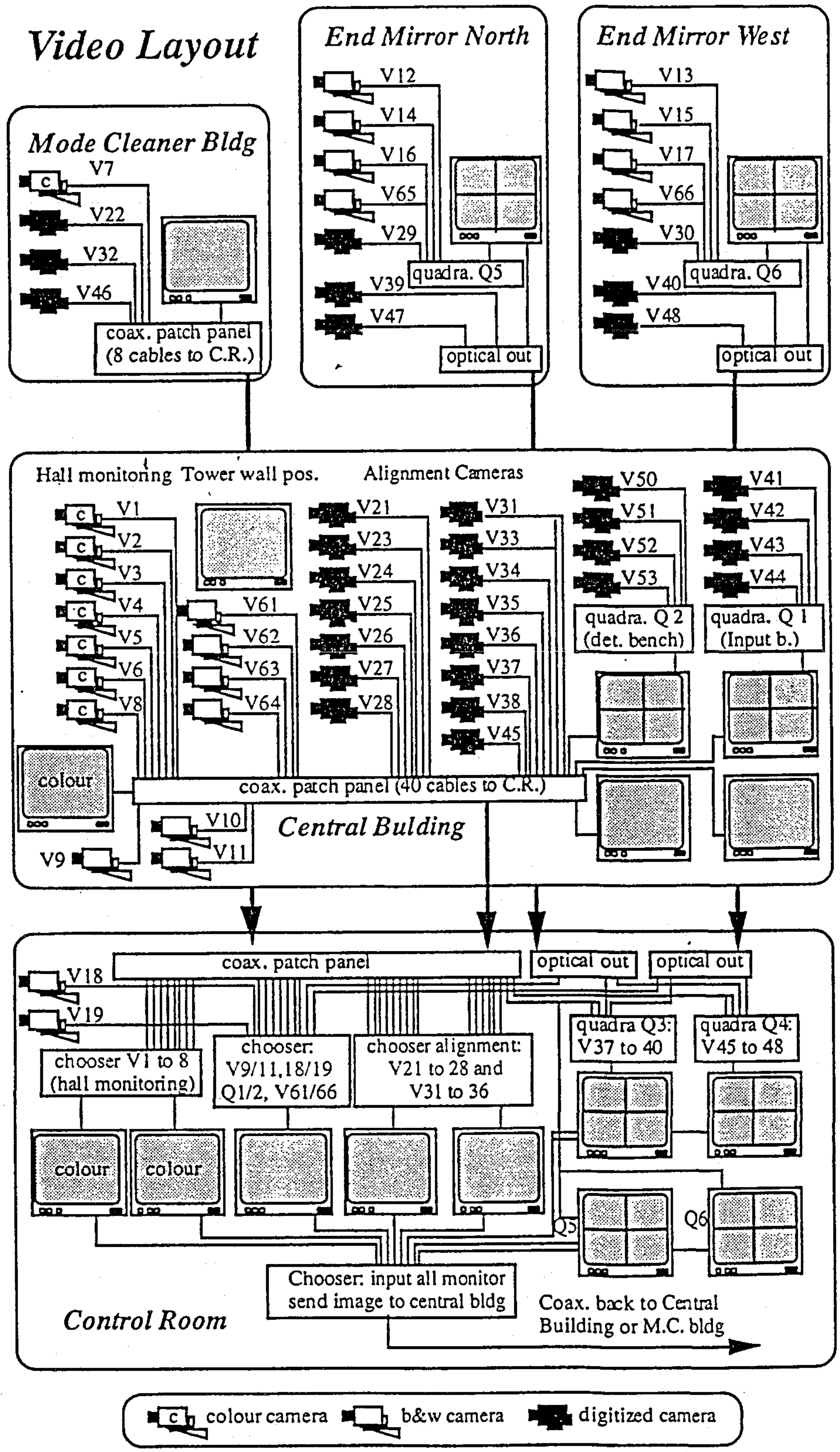

Figure 5200.5. Schematic view of the VIRGO Video system. The digital part of the system (VME interfaces, processors) is not presented.

53. Networks

The cabling necessary for the networks of VIRGO can be divided as follows :

- Optical Links for high speed transfers: this applies to the distribution of the time signal, to the servoloops control and to the acquisition.
- Slow Monitoring Network: this applies to the monitoring of all parameters collected from many crates in all buildings, towers, pumping stations, etc...
- Computer Network: this applies to the connection of all computers, workstations and some of the VME crates.
- Telephone : this applies to ordinary telephone lines in all rooms of all buildings.
- Video: this applies to video monitoring of remote places and of surroundings.

The VIRGO net, which includes the Slow Monitoring Network and the Computer Network is shown in Figure 5300.1.

The cabling we propose conforms to the standard EIA/TIA 568 for cabling, and is generally referred to as "structured cabling". This means a hierarchical organization from a central point to peripheral points, with radial configuration of cables departing from each system and with a maximum length of 100 meters for each cable, reaching a "telematic outlet" placed wherever necessary.

It is necessary to use fibers from one building to another, and twisted pairs within the buildings, as far as possible; these latter can be ScTP (Screened Twisted Pairs with shielded RJ45 connectors. This kind of cabling accomodates both audio communications (telephone) and video (remote monitoring), as well as ETHERNET (10 base T) Serial (RS432) and FDDI (over copper). Optical fibers will also be used to reach dedicated systems, e.g. for control of servoloops, timing and acquisition.

The central system will be placed in the Control room.

We can give the number of fibres needed between the buildings in figure 5300.2. Taking into account some reserve we have : 150m of cable with 36 fibers, 13 km of cable with 18 fibers, 6.6km of cable with 12 fibers and 22km of cable with 6 fibers.

In the 5 buildings of VIRGO, we find a Fiber Distribution Panel which receives all the fibers and distributes them to the Hub for networking, or to the other systems as necessary. All this is done via a Patch Panel for both fibers and copper.

In different buildings, each distribution system is in a rack (Secondary); the number of racks is dictated by the necessity to have only 100m cables from Sec to "outlets". Each rack accomodates a "patch panel" for configuring each outlet according to needs, and a "hub" with the intelligent part for computer network, or slow monitoring (repeaters, bridges, terminal servers...). The racks have to be powered via Uninterrupted Power Supplies, and use in total about 1kW.

The main system is also a rack, which contains a router for connections to INFNet, a module for connection to a telephone system (PBX) as well as a "hub" for communication via fibres with the secondary systems

Each "outlet" shall have 4 connectors of RJ45 type, all identical for phone, video, computers, and so on. The destination will be made on the patch panel in the SEC system, not in the outlets. The cable from the outlet to the equipment may change according to needs.

A line for Telecommunications to CNUCE in PISA (this latter is on the backbone of the 2 Mbit/s Italian Network) is needed.

Figure 5300.1 VirgoNet

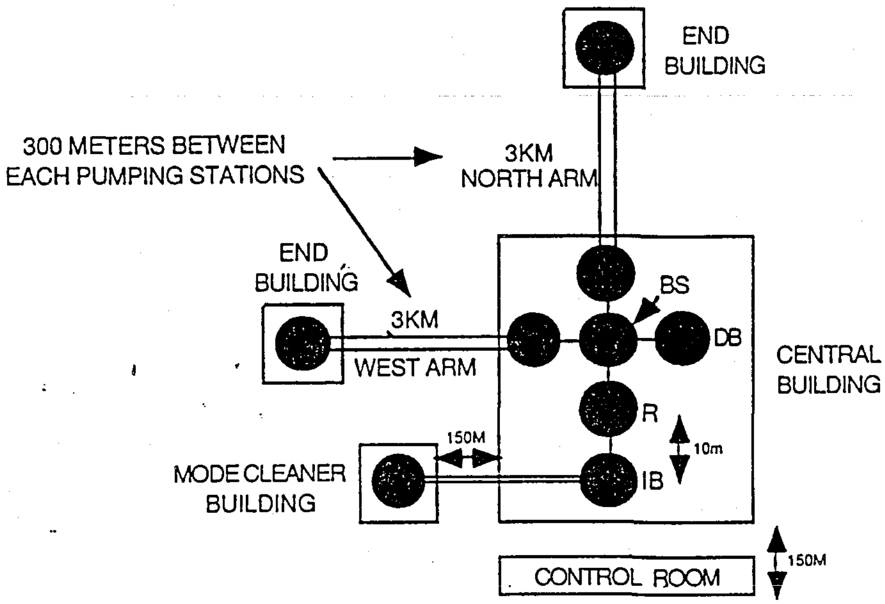

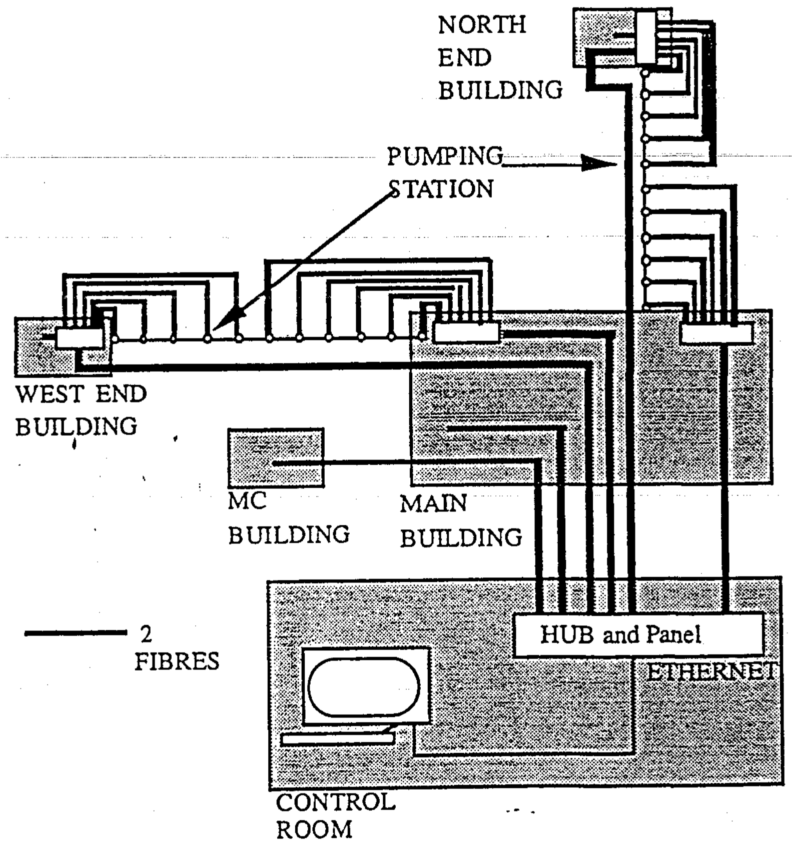

Figure 5300.3 The slow monitoring network.

54. Data Acquisition System

54.1 Requirements

The Data Acquisition system (DAQ) is part of the overall online system and will fulfill the following experimental requirements :

- handle 5 Mbytes of continuous data per second with burst at 10 Mbytes/s,
- operate at a sampling frequency of 20 kHz,
- synchronize on the GPS based signals generated by the Timing System,
- implement a distributed readout system,
- use the Frame format as a common data format.

Moreover, the DAQ functional requirements are the following :

- collect VIRGO Raw Data and perform Data Compression if needed,
- assume data transport between DAQ components,
- structure RAW Data into frames,
- distribute frames to the online processing tasks,
- perform Online Data Quality check,
- operate the Online Data Preselection before the Data storage.

54.2 Architecture and Components

The DAQ architecture is shown on figure 5400.1. The DAQ system is broken down into components according to its primary functions.

The Local Readout is the front end component of the DAQ system. Four of these are implemented on the experimental site. In each building, a Local Readout collects from the various sub-systems the available data which are not used in any controls or servoloops and sends them to a Local Frame builder via a Digital Optical Link (DOL).

Records from Slow Monitoring Stations (SMS) are passed to the DAQ system through the SMS Frame builder. Data samplings are structured into frames by two Local Frame builders.

The Main Frame builder combines the data samplings collected into frames with the associated status information and distributes them to the storage and online processing units.

The DAQ system receives timing data from the Timing system which synchronizes the readout operations and makes extensive use of the Digital Optical Links.

All the DAQ components follow the standard hardware and software options defined by the Electronics & Software system.

The DAQ system also requires the precise definition of data channels (amount and rate) to be read out. The table below recalls the amount of data to be recorded and gives the set up of each Local Readout according to VIRGO VME Crate list which is maintained in the Standardized Components "sub-system".

Local Readout	Crates	Slots used	ADCs	Channels	Rates
Main building	C39	12	4	≥ 49 8 acoustic noise 8 em. noise 5 line voltage 4 calibration 8x3 seismic noise ≥ 8 laser DAQ	 20 kHz 20 kHz 20 kHz 20 kHz 1 kHz
Mode Cleaner	C61	5	1	12 2 acoustic noise 2 em. noise 2 line voltage 2x3 seismic noise	 20 kHz 20 kHz 20 kHz 1 kHz
End buildings	C74 C84	5	1	15 2 acoustic noise 2 em. noise 2 line voltage 3x3 seismic noise	 20 kHz 20 kHz 20 kHz 1 kHz

54.3 Data Acquisition interfaces

As shown on figure 5400.1, the Data Acquisition system is interfaced at various levels with most of the others online sub-systems. Some interfaces are provided by dedicated hardware, others may be supplied by software package, format definition, dataflow specifications or even proper information exchange.

Interfaces which will be typically designed and provided by the DAQ sub-system in accordance with other sub-systems requirements will be shortly described.

54.3.1 Interface with Slow Monitoring

The readout of status information (SMS records) is assumed by Slow Monitoring sub-systems. However, the DAQ system provides a dedicated front end interface for the purpose of collecting SMS records (the so-called Slow Monitoring Frame builder). The Slow Monitoring Frame builder is a dedicated software DAQ component which is adapted to the Slow monitoring network organization as it has been already described.

54.3.2 Interface with the Fast Controls

Data Collection is supplied by so-called Local Readout or User Readout systems, depending whether the data concerned include controls and feedback values or not. User Readouts are part of the Contols system as data contribute to the various servo loops but the information is also passed to the DAQ system.

The DAQ system is then interfaced to all the Controls sub-systems such as the Detection bench. It provides a standardized User Readout interface to the Local Frame builder level which includes the definition of the format for the data transport mechanism between DAQ components over the

DOL links. The interface specifies the way the DOL boards capabilities are used in this specific case and the data format which needs to be used over such connections. The DAQ system recommends this as a standard for all data transports to the Local Frame Builder level.

54.3.3 Interface with Data Archiving and Global Control

The interface with those sub-system is assumed by the dataflow scheme used for the Frame distribution. It is based on a common agreement on hardware and software mechanisms.

54.3.4 Interface with Supervisor

The DAQ system will operate under the central DAQ Supervisor. DAQ software is developed in respect of the software specifications and tools defined by the Supervisor sub-system.

DAQ software components follow the Online client/server organization. Communications tools and protocol for the message exchange allow to interface the various DAQ control processes and the Supervisor.

54.3.5 Interface with off-line activity, simulation and Data Management

The DAQ system uses the same Frame format as any on-line or off-line sub-system involved in VIRGO Data Managment. The Frame format is the VIRGO standard data format. In this respect, it is one of the major guideline for interfacing sub-systems accessing VIRGO data.

The DAQ sub-system may also enhance the use of SIESTA. The integration of all the different components is one of the most important aspects and SIESTA can be also conceived as an on-line tool for the DAQ commissionning. For this, we may use SIESTA capabilities of generating signals for the data readout and simulating the signal processing.

54.4 System Description

54.4.1 Data Collection

The Data Acquisition system assumes the function of collecting data through :

- four Local Readouts (in End Mirrors, Mode Cleaner, and Central buildings),
- the User Readout interface for the Control and Locking information,
- and the Slow Monitoring Frame builder

54.4.1.1 Local Readout

54.4.1.1.1 Hardware Components and Connections

Figure 5400.3 provides a detailed view of the components which make up a Local Readout crate. Local Readout crate will be controlled by a Power PC based RISC I/O board (RIO2 8061) from CES running the LynxOS real time operating system.

The CPU board will perform the following functions :

- to run the Local Readout control process,

- to perform Interrupt handling functions and data readout operations,
- VME bus controller,
- to provide sockets based interface to Ethernet,
- to build DAQ packets and supervise DOL access.

The Timing board receives four TTL signals (run, frame, sampling, 1MHz) from the remote timing crate. It provides the following :

- sampling and frame counting,
- generation of VME interrupt to trigger the DAQ process,
- distribution of the external trigger to the ADC boards according to user needs,
- generation of all needed signals using the local oscillator (standalone mode),
- generation of secondary clock (as odd sampling signal).

Each sampling is tagged by Local Readout using the GPS system. The BANCOMM bc635VME board provides :

- global Time stamp on VME demand or on External event capture.

The DOL board enables the optical fiber connection with the Local Frame builder crate housed in the main building. It provides :,

- up to 3.2 km point to point connection,
- one emision channel per board associated with 16kwords (32 bits) of output buffer memory,
- 135 Mbits/s parallel throughout.
- A24 A32 D32 BLT32 slave VME access.

The ETEP-734 ADC board will be used to digitize signals acquired by Local Readouts. Up to 64 channels per crate is foreseen. Required specifications are :

- 16 individual, differential inputs,
- 16-bits ADC,
- User selectable input range : +/- 5V or +/- 10V,
- 8 to 100 kHz sampling rates,
- 2 x 128 Kwords (16 bits) onboard flip-flop memory,
- A32 D32 BLT32 slave VME data readout,
- external trigger inputs.

54.4.1.1.2 Operational overview

This section is intented to give an overview of the way the Local Readout operate in normal DAQ mode. This is defined as the DAQ system has been configured and armed to run and continuous data acquisition is taking place. According to Figure 5400.2, we consider a Local Readout in charge of collecting 20K data samples per second from 4 ADCs boards. Lower rate ADC channels are ignored here as they are not so critical regarding to the methods and timing.

Data flow through the Local Readout is shown on Figure 5400.3. During data acquisition, the sampling signal is received by the Timing board and wired to the ADC modules which perform continuous digitization at the supplied clock frequency of 20 kHz. Each ADC sample is stored in the onboard flip-flop memory which is controlled by the odd sampling signal. This buffer may handle several samples ready for readout. In coincidence with the odd sampling signal, the 10 kHz VME interrupt dedicated to the data acquisition process is generated by the Timing board.

The timing board capabilities allow to generate any useful secondary clock according to the user needs.

At this point, the VME interrupt is detected by an Interrupt Service Routine (ISR) in the CPU. The readout process reads data from ADC modules into one of the two memory plans while they continue to digitize and store new data into the second plan of their flip-flop memories. This is done in BLock Transfer (BLT). Data are then formatted and written into the FIFO memory standing on the DOL module which is ready to transfer data words. The transmission time over DOL is then hidden by the BLT VME transfer time.

The foreseen timing sequence is shown on figure 5400.4. The readout performances will firstly depend on the interrupt dispatch time which is measured by the maximum delay between the receipt of an interrupt and the execution of the corresponding interrupt routine. The « worst case » value was measured has 30 microseconds under LynxOS. Readout operations will be handled before the receipt of the next 10 kHz interrupt signal.Within 100 microseconds, lightweight processing such as data compression could be performed if required.

54.4.1.1.3 Configuration

Configuration of a Local Readout consists in the VME devices setting up. It should describe describe what data collect, where and how fast. The needed information is organized in C structures (as shown on figure 5400.5) including a header and a set of informations related to each device which will be accessed.

Local readout may be configured in a very flexible way according to the needs. It is able to take into account any device access described by such items as :

- the access function (selected from a predefined set : CTRL, READ, WRITE...),
- the cycle which specifies the rate of this access (1 corresponds to the data acquisition rate),
- its VME address,
- the size in bytes of the data exchanged,
- the data value if any ...

Configuration information is passed to the local readout control process as tables which are interpreted to fill in the C structures just described. All the needed parameters may be edited from the Local Readout User interface and stored in configuration files. An example of configuration file is given below. It describes a sequence including initialisation cycles performed once (cycle ratio is set to 0 in this case) and readout cycles at the data acquisition rate (for which the cycle ratio set to 1). The devices concerned here include a GPS board, both Timing and DOL units, and an ADC module from ETEP. The test sequence described here consists of reading 4 ADC channels in block transefer bytes and writing data and control information (sample, frame and time stamp) into the DOL.

Function	Cycle	VME address - hex	Register offset- hex	Access mode	Adress modifier -hex	Data width in bytes - dec	Comment	Value -hex
TAS	0	0xee2100	0x0	CPU	0x3d	1	DOL init.	
WRITE	0	0xee2100	0x4	CPU	0x3d	4	DOL init.	0x2010000
WRITE	0	0xee2100	0x4	CPU	0x3d	4	DOL init.	0x10200000
WRITE	0	0xe000	0x24	CPU	0x2d	2	GPS init.	0x9
WRITE	0	0x100000	0x2	CPU	0x39	2	ADC init.	0x7
WRITE	0	0x100000	0x2	CPU	0x39	2	ADC init	0x3
WRITE	0	0x100000	0x2	CPU	0x39	2	ADC init	0x7
WRITE	0	0x100000	0x2	CPU	0x39	2	ADC init	0x3
WRITE	0	0x100000	0x2	CPU	0x39	2	ADC init	0x7
CTRL	1	0xee2200	0x30	CPU	0x3d	4	Sampl&Frame	
CTRL	1	0xe000	0x1c	CPU	0x2d	2	Fix. Time	
READ	1	0x100000	0x0	BLT	0x39	2	read ADC chan	0x4
WRITE	1	0xee2100	0x20	BLT	0x3f	4	Write in DOL	

54.4.1.2 Data Transport and Format

This section describes data transport and format from readout crates to local frame builder crates. For moving data at this level, the use of Digital Optical Link has been chosen and DOL boards are now operational. The DAQ system will precise the way the capabilities of DOL boards are used in this specific case and recommend this as a standard for all data transports between readout units and the Local Frame Builder level. The data format used over those connections will also be specified. The underlying goal is the definition of an efficient interface for all readout components including fast readouts which are parts of the Control system.

54.4.1.3 Local Frame Builder

54.4.1.3.1 Hardware Components and Connections

Local Frame builder structures data samplings received from readout crates into frames. The SMS Frame builder (crate C2) provides a similar function with regard to SMS records. DAQ front end interface to other online systems, namely Slow Monitoring and Controls and Locking systems is achieved at this level. Two Local Frame builder A-B crates (C55-C56) are foreseen. Connections arrangement with all the readout crates is not yet fixed.

Figure 5400.6 gives a detailed view of the components which make up a Local Frame builder crate.

54.4.1.3.2 Operational Overview

The DAQ system will specify the way the Local Builder Crate operate.

54.4.1.4 Frame Format

VIRGO Data taking operates as a continuous process which acquires data from various channels sampled at different frequencies. In this context, data format has been designed as a « frame » structure with the following requirements :

- to afford a little overhead for data organization
- to handle different data and various informations
- to organize a data set of few seconds lenght
- to allow data content evolution
- to afford large data rate by efficient input/ouput mechanisms
- to enhance software reusability by an identical format everywhere (on-line, off-line, test).

A frame is a unit of information containing all the information necessary for the understanding of the interferometer behaviour over a finite time interval which integrates several samplings. It contains thus not only the sampling performed during the integrated time interval, but also those performed at a frequency smaller than the frame frequency.

To simplify its manipulation, a frame is organized as a set of C structures described by a header holding pointers to additional structures and values of parameters expected to be stable over the integrated time interval : the starting time of the frame, its duration, values produced by the slow monitoring. This header is followed by an arbitrary number of additional structures, each holding the values of a rapidly varying parameter like the main signal, the seismic noise. Each active element producing data at a rate higher than the frame rate is thus accumulated in a dedicated structure.

This frame structure (figure 5000.7) is a standard which is conserved over the various stages of the analysis. Frame history, detector geometry, trigger results, monitoring data, reconstructed data, simulation results lead thus just to additional structures. It is always possible to add new structures or to drop old ones.

The input and output routines used for their creation and the specifications of their format are unique and kept as stable as possible. Their format is saved on tape to allow for automatic processing.

54.4.1.5 Main Frame Builder and Frame Distribution

The Main Frame Builder combines information received, from Local Frame Builders A and B with the associated status information into final frames. It also performe the frames distribution to the Online Processing units over a Reflective Memory Network.

The Figure 5400.8 shows the Main Frame Builder crate (C3) as it is foreseen.

54.4.2 Data Quality

This online task will survey permanently the data quality produced by the interferometer. It uses the signal induced by the calibrators, the noise level, and runs data quality algorithms. It should provide a fast feedback in case of problems. It is a real time data quality check. The corresponding informations are stored in the data storage system to allow further data selection according to the data quality requirements of the offline analysis. It may be run as part of the Trigger system.

54.4.3 Data Preselection

Let us remember the typical data rate of 2 MBytes/sec in continuous mode. This means about 2 DAT tapes (4 GBytes) every hour and translates into about 16000 tapes/year. Such an amount of data is not a problem for the online writing or for the storage, but it may very quickly overflow any data analysis. Therefore it may be wise to reduce their amount for the detailed data analysis. A typical goal would be a reduction of more than one order of magnitude. The final reduction factor will in fact be driven by our data analysis capability and by the data production rate. Remember that this rate is also function of our operational efficiency.

Prior to any kind of physics analysis one has to convert raw data (i.e. ADC counts provided by the main feedback and the remaining dark fringe signal) to physical quantities and to compute the h values. This is the first task of the trigger. This computation requires the knowledge of the 'transfer functions' of the various controls and of the calibration constants. These quantities are available from a special database accessible from any VIRGO laboratory. This reconstruction should be the same as the offline reconstruction.

Then trigger algorithms looking for burst events are run. Triggered frames are defined within 'time windows' during which binary coalescence or burst candidates may occur. These candidates will be selected using simple and robust search algorithms to minimize a possible bias in the further offline analysis : selection efficiency has to supersede rejection efficiency. Random triggers are recorded to monitor the trigger algorithm efficiency. To cover a large type of astrophysical events, several trigger algorithms will be run in parallel.

The informations kept after trigger selection are written to Data Summary Tapes (DST). They are the following for each frame :

- reconstructed h value at 20 kHz and eventually reconstructed h resampled at lower frequency (2 kHz) : this represents less than 100 kBytes per second.
- slow monitoring records (less than 5 kBytes per second) to follow permanently the interferometers environment.

For 'triggered frames":

- all the raw data required to perform a full analysis of the signal candidates.

The triggered frames are sent to the data storage system using a standard network.

Of course, false signals will be selected. But this filtering is not the final data analysis and a lot of work is still needed to extract and prove the existence of a gravitational wave signal from the DST tapes. The achieved data reduction should provide the conditions for a fast analysis and a fast data dispatching over the collaboration. Most of the data analysis will thus be performed on this filtered sample. But remember that it will always be possible to start again from the original raw data sample.

The filtering algorithms will be designed and tuned using simulated and real data. They will certainly change and improve with some learning experience. This is why we are prepared to reprocess the original raw data. Dedicated computers will be installed on the site for this purpose.

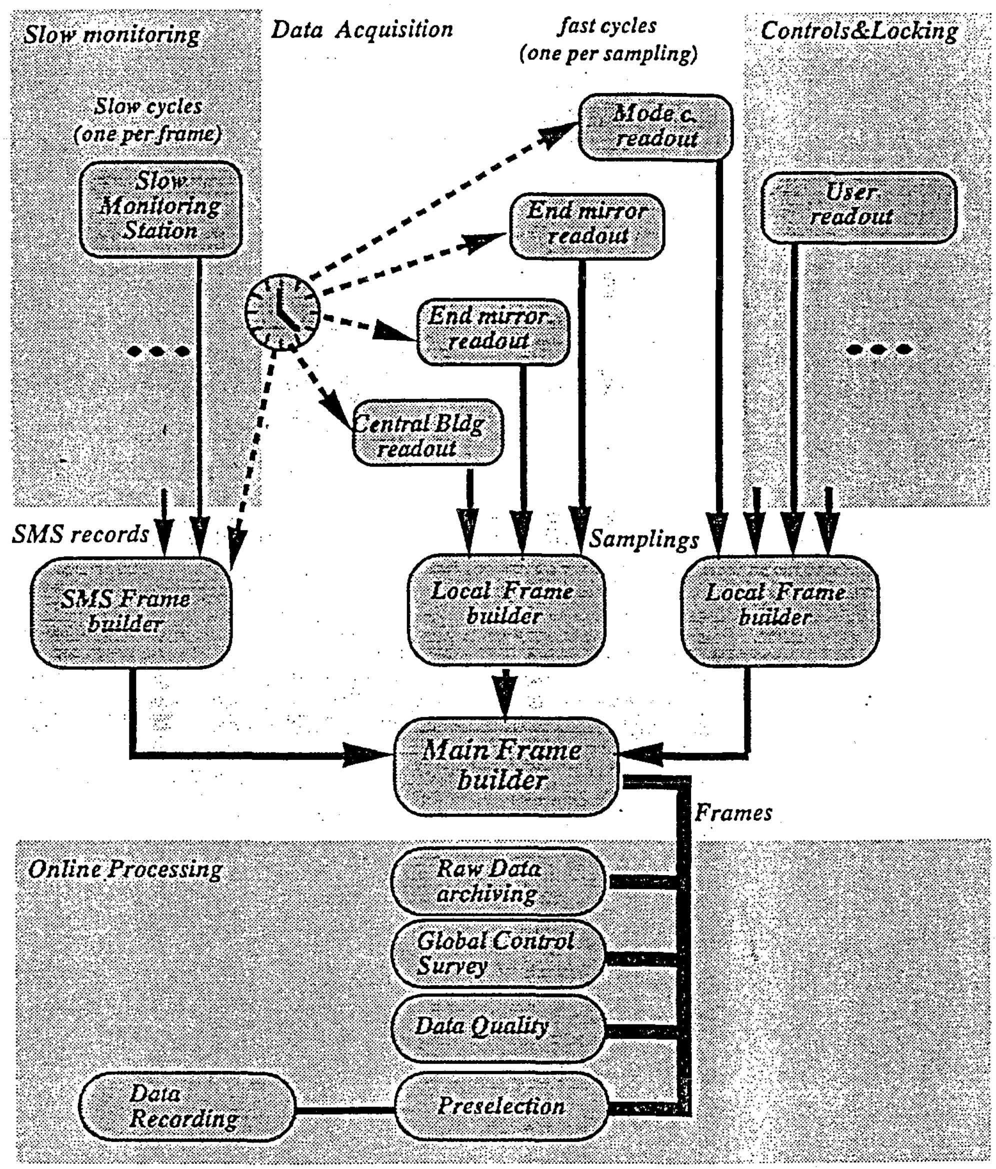

Figure 5400.1 : Virgo Data Acquisition System

From the remote Timing crate (run, frame, sampling and 1 MHz signals)

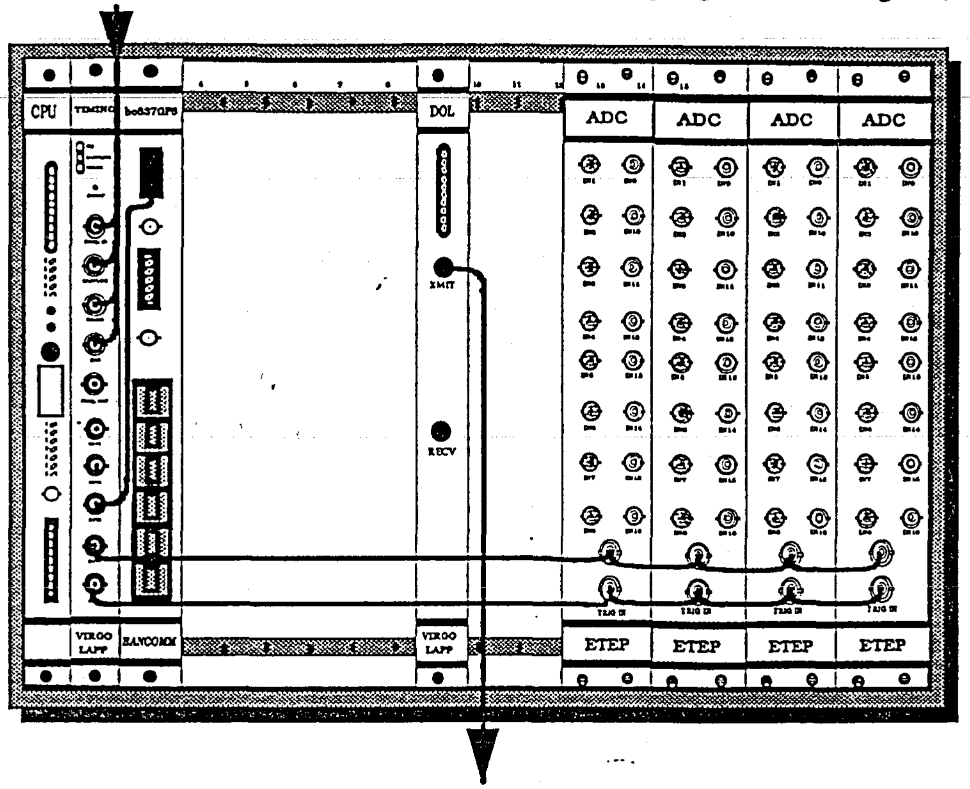

To Local Frame Builder

Figure 5400.2 : The Local Readout Crate (Components and Connections)

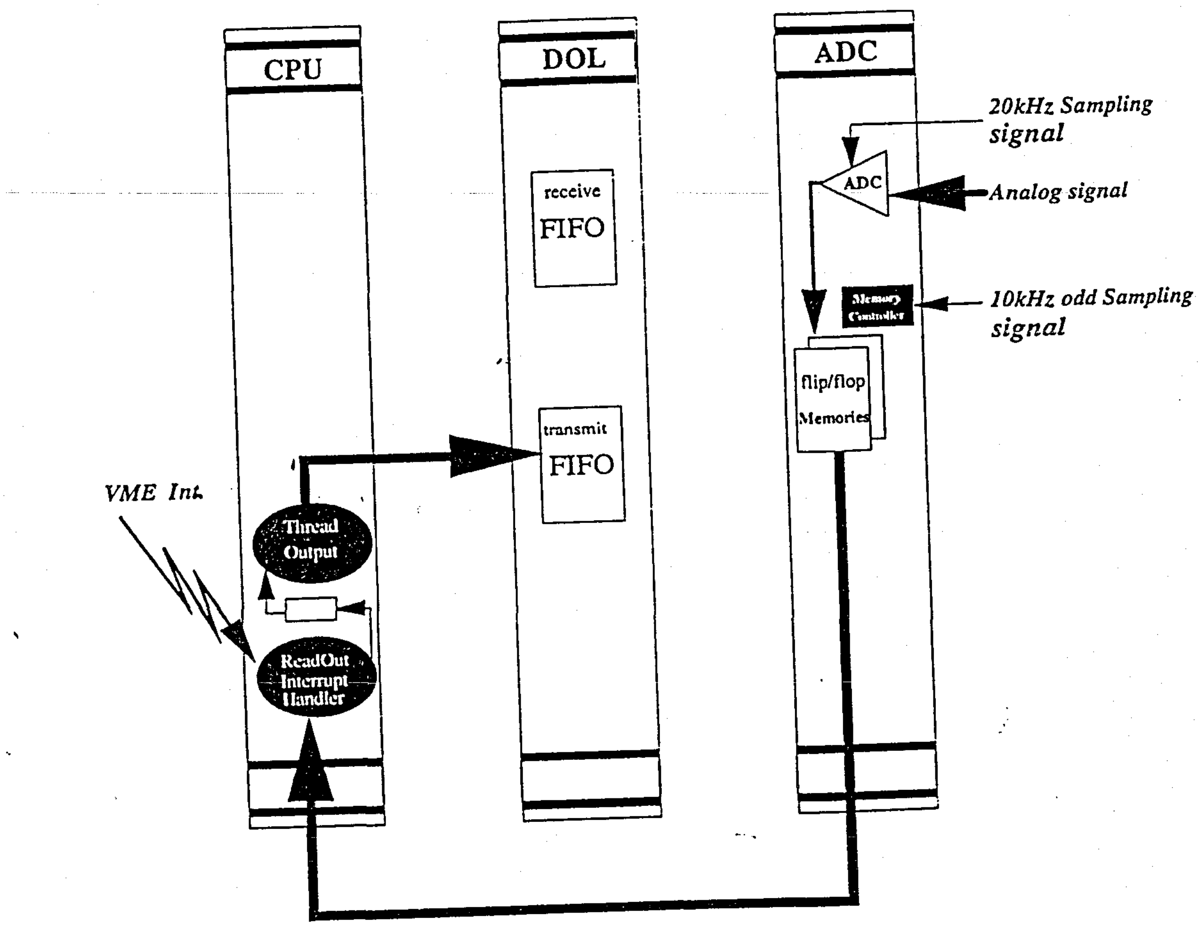

Figure 5400.3 : The Local Readout Data Flow

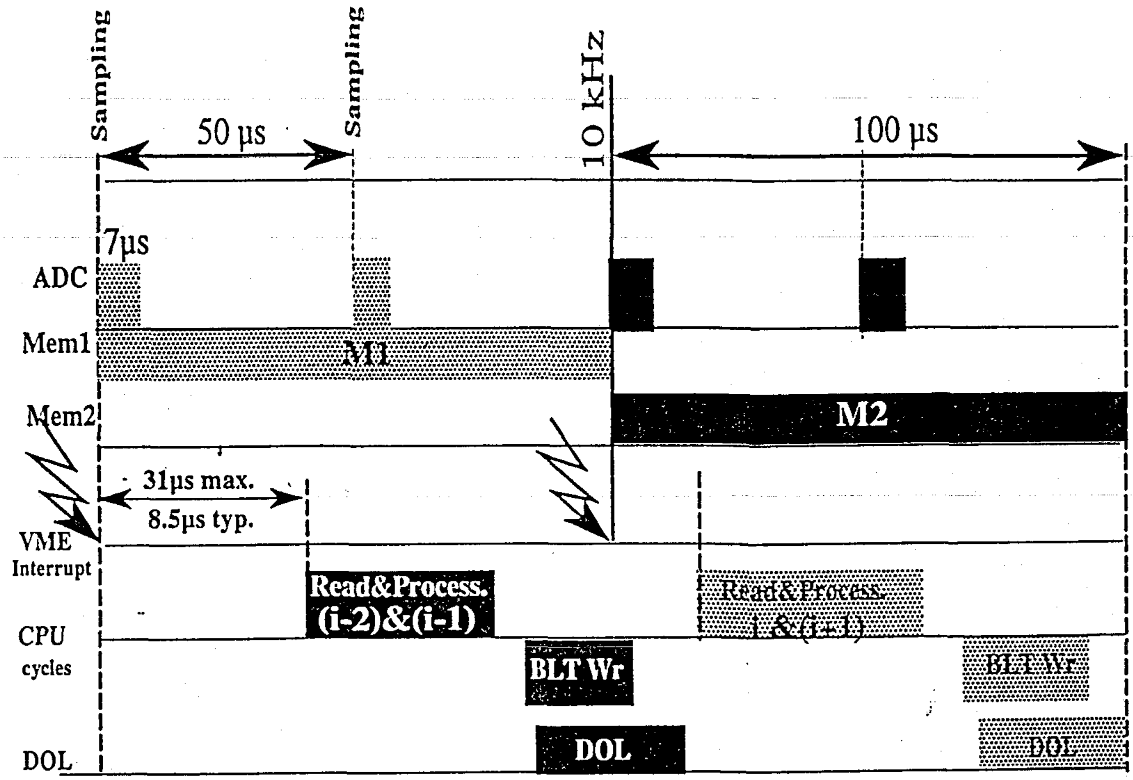

Figure 5400.4 : The Local Readout Timing Sequence

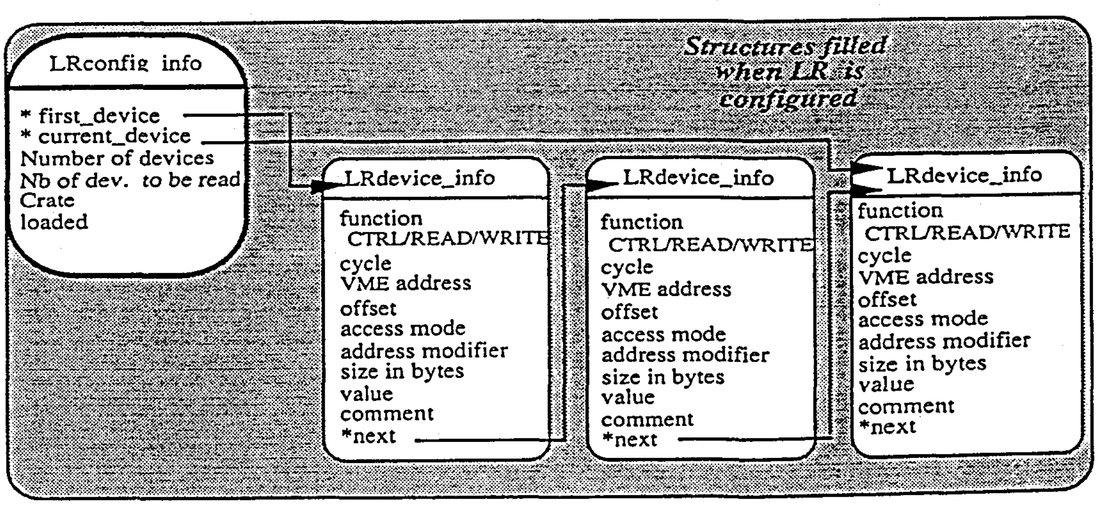

Figure 5400.5 : The Local Readout configuration Information

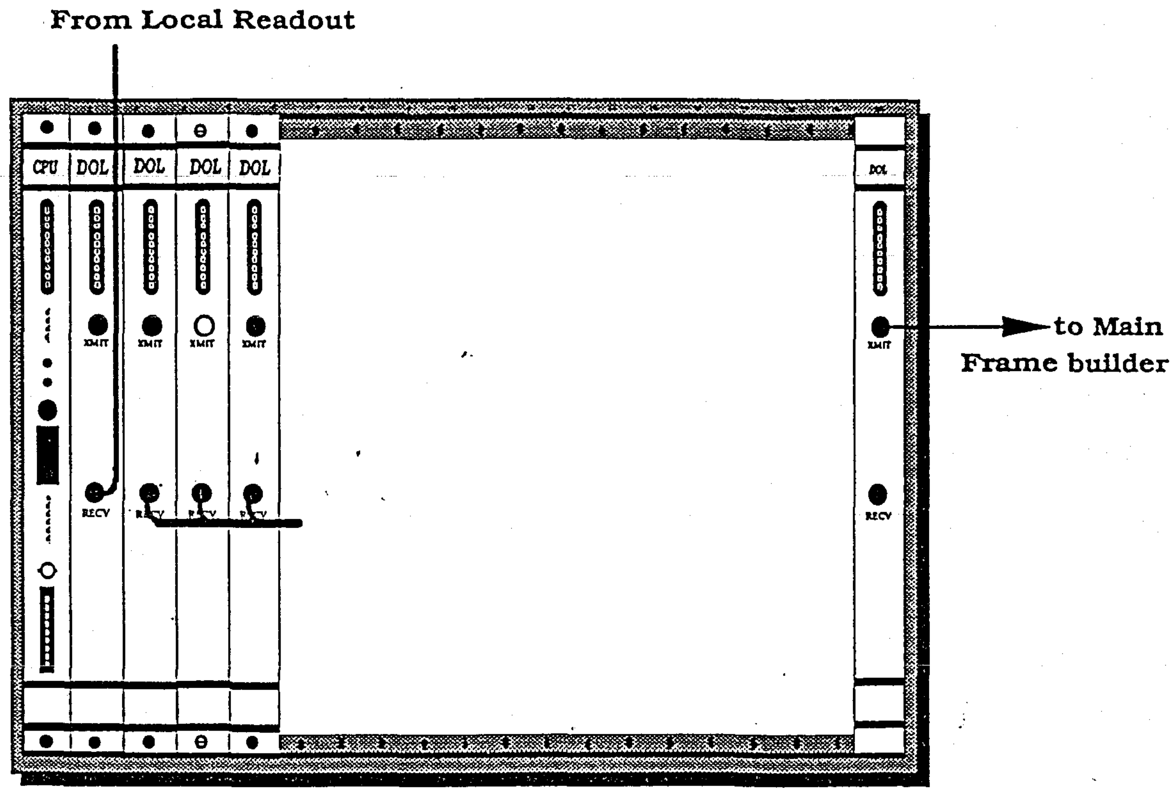

Figure 5400.6 : The Local Frame Builder Crate

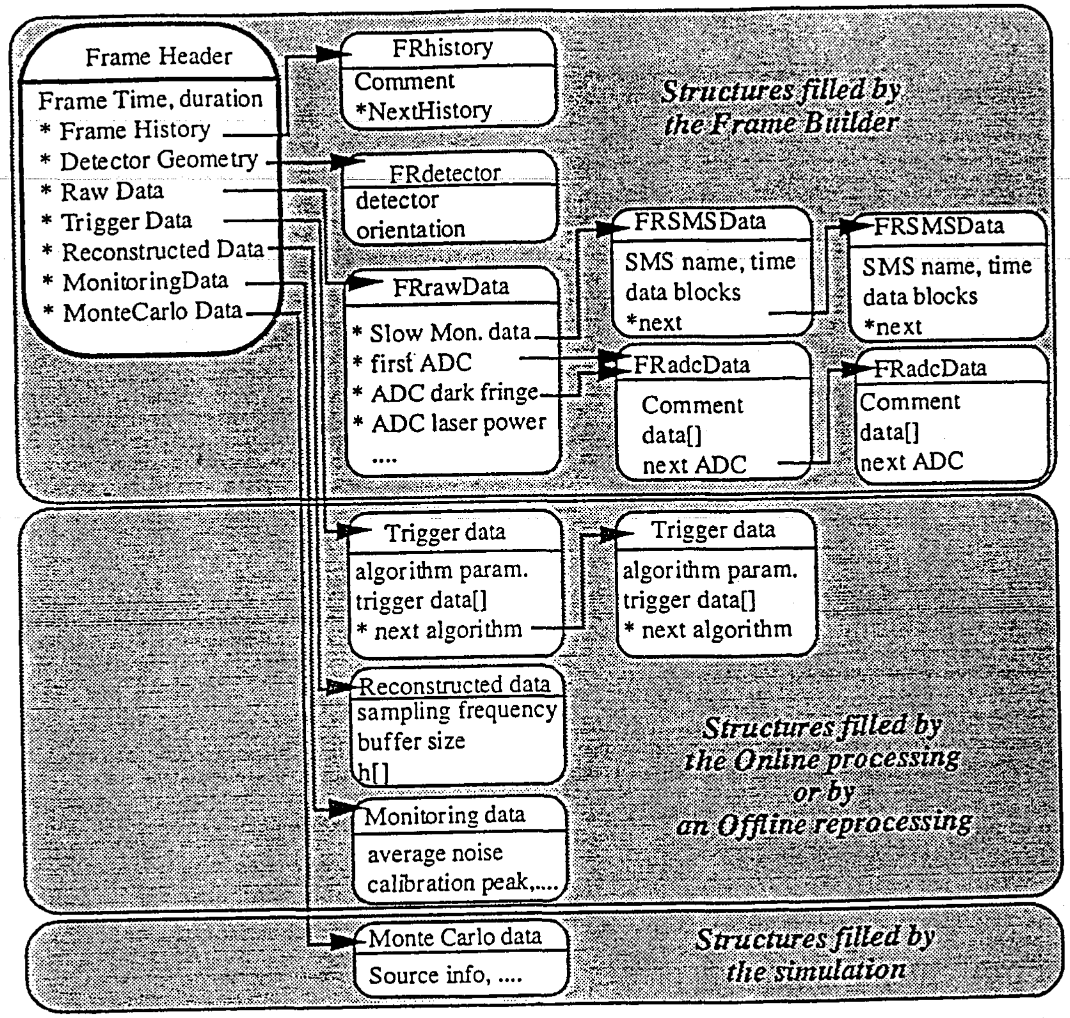

Figure 5400.7 The frame structure

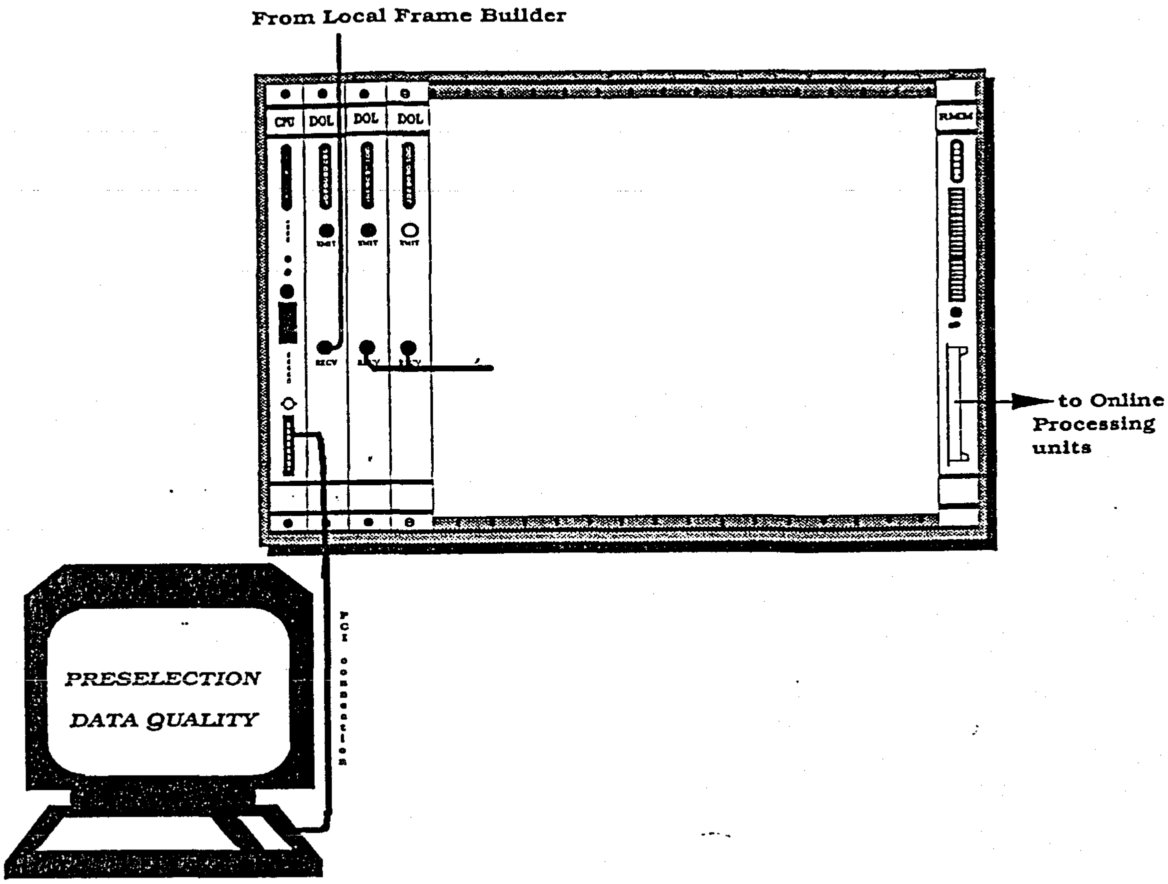

Figure 5400.8 The Main Frame Builder Crate

55. Data Distribution & Archiving

The Data Distribution & Archiving is the Virgo sub-system which takes care of the on-line and off-line archive and distribution of Virgo data. The large amount of expected data (from 1- 5 Mbyte/sec in continuous mode, but up to 10 Mbyte/sec in burst mode) and the different needs of accessing totally or partially these data have suggested the specialization of this system into two subsystems, strongly related but different for structure and use : the Raw Data Archiving System and the Data Distribution System.

55.1 Function and concept

In Figure 5500.1 the scheme of principle of the Data Distribution & Archiving and its connection with the Frame Builder and On-Line Processing are shown.

As described in section 5400, all Virgo data are organized in frames, that is the unitary information which records the Virgo behaviour over a finite time interval. Each frame, organized as a set of C structures described by a header, is basically made of three parts :

- structures filled by the Frame Builder, which contain all the raw data collected by detectors and probes;
- structures filled by the On-line Processing (or by the Off-line Reprocessing), which contain the reconstructed data ([t,h] pairs at the sampling frequency of 20 kHz) and the necessary auxiliary information;
- structures filled by the Simulation, which are necessary for comparison of the behaviour of the interferometer with the modelled one.

The Raw Data Archiving System collects and stores all the frames produced by the Frame Builder (raw data). These data are necessary for any reprocessing starting from the original data like the improvement of the reconstructed data if more refined off-line data analyses are implemented or the study and check of the Virgo performances along the time. According to the requirements on the continuous data flow rate, the amount of data to be archived spans from 86,4 Gbyte/day (1Mbyte/sec data flow rate) to 432 Gbyte/day (5 Mbyte/sec data flow rate). Such a large amount of data cannot be maintained on-line according to the status of the technology. For this reason the Raw Data Archiving System archives all the frames on RDT (Raw Data Tapes), while the Raw Data Retrieval and Off-line Data Reprocessing is a Data Distribution System task.

The Data Distribution System archives all the frames selected by the on-line Data Analysis Algorithms (i.e. the frames which include also the structures filled by the On-line Processing and by the Simulation). These frames should contain the gravitational wave events and, for this reason, they need a more refined analysis. Actually, this on-line frame selection well applies to impulsive sources, but may be inadequate for continuous or quasi-countinuous sources, which may need very refined off-line analyses. For this reason, the Data Distribution System also stores all the [t,h] pairs and the necessary auxiliary information of all the frames at the real sampling rate (20 kHz). Unfortunately, also in this case the large amount of data limits the quantity of data which can be maintained on-line because of the costs of the disks and of the CPU's. In fact, about ≈ 12 Gbyte/day for the storage of the selected frames (i.e. 150 Kbytes/sec as mean data flow assuming 10 days of events over a year of acquisition at 5 Mbyte/sec data flow) and ≈ 10 Gbyte/day for the [t,h] pairs at the sampling rate of 20 kHz (including quality factor coefficients and the auxiliary information necessary for an off-line data analysis) would have been the necessary disk space for an on-line storage. For this reason, we split the Data Distribution System into two parts : on-line data distribution and off-line data distribution. The on-line data distribution allows the Virgo user to get all the data produced by Virgo in the last month via computer network. This task requires to maintain at least 500 Gbyte on-line (assuming a mean data flow of only 2 Mbyte/sec). At the same time all the content of the on-line archive is written on DST (Data Summary Tapes) and distributed on request to the Virgo laboratories. In order to optimise the data distribution and analysis, special DST are also foreseen according to the data analysis needs.

These solutions put no restrictions to the off-line data analyses made by Virgo users. In fact, every time a raw data reprocessing is necessary (i.e. for making correlation with environmental data, with other antennas, etc.) the RDT can be loaded and reprocessed by the Data Distribution System (Off-line Reprocessing) using the same tools implemented for the On-line Processing. For this reason a list of the contents of the data stored in RDT and in DST is maintained on-line on a Data Distribution System Database. These database also includes an on-line archive of the environmental parameters necessary for a check of the Virgo environmental status.

55.2 Requirements

As shown before, the requirements necessary to overcome the problem of data storage and distribution concern mainly the data flow and the amount of data storage. The requirements for the Raw Data Archiving System and for the Data Distribution System are summarised in Table 5500.I and Table 5500.II, respectively.

Raw Data Archiving System Requirements

Data Flow Rate	1-5	Mbyte/sec	continuous mode
	<10	Mbyte/sec	burst mode
Data Transfer Rate	<10	Mbyte/sec	from the Frame Builder

Table 5500.I Requirements for the Raw Data Archiving System

Data Distribution System Requirements

Data Flow Rate	<1	Mbyte/sec	continuous mode
	<10	Mbyte/sec	burst mode
Data Transfer Rate	<10	Mbyte/sec	from the On-line Processing
	<1	Mbyte/sec	to users via FDDI line
Data On-line	>500	Gbyte	1 month data

Table 5500.II Requirements for the Data Distribution System

55.3 Interfaces

The two systems require a direct connection with the main sub-systems of the electronics.

55.3.1 List of Data Distribution & Archiving interfaces

5100 Global Control
5200 Standardized Components
5300 Networks
5400 Data Acquisition
5600 Supervisor
5700 S/W Tools - Simulation

5800 Environment Monitoring
5900 S/W Tools - Distribution

55.3.2 Interface with Global Control

The Data Distribution and Archiving System uses the Cm package for communication within the system and with other related Virgo subsystems. In particular, it sends every error message to the Error Logger, while its on-line configuration is stored in the On-line Database.

55.3.3 Interface with Standardized Components

The Data Distribution and Archiving System is projected with great part of standard Virgo hardware and software components : this makes it easier their replacement and smaller the number of spare components. In particular, the CPU's (PPC604), the crates (VME), the operating systems (LynxOS and OSF/1), the language (C), the network (Ethernet and FDDI) and the tapes (DLT and DAT) are standard Virgo components (5200).

55.3.4 Interface with Networks

The Data Distribution and Archiving System requires the standard Virgo Ethernet line for internal connections (i.e. User Interface, Error Logger, On-line Database, Supervisor, etc.). On the other hand, due to the expected large data transfer rates (of the order of Mbyte/sec), the access of the Virgo users to the Data Distribution Systems is made via an independent Ethernet (and/or FDDI) line in order not to perturb the internal Virgo operations.

55.3.5 Interface with Data Acquisition

The data transfers [Frame Builder - Raw Data Archive] and [On-line Processing - Data Distribution] is made via VIC interfaces (data transfer rate up to 10 Mbyte/sec) or reflective memories (data transfer rate up to 40 Mbyte/sec).

55.3.6 Interface with Supervisor

The Supervisor keeps track, requests, allows or inhibits the modifications of the status of this subsystem and can act as an User Interface.

55.3.7 Interface with S/W Tools - Simulation

The S/W Tools - Simulation are used by the Data Distribution System during the reprocessing of the RDT for rebuilding the full frames.

55.3.8 Environment Monitoring

A database of the environmental quantities is maintained in its On-line Database. Some of the environmental data acquired by the Environment Monitoring for specific studies on environmental variables can be acquired and directly sent to the Data Distribution System, which stores them in its On-line Database.

55.3.9 Interface with S/W Tools - Distribution

The S/W Tools - Distribution are used by Virgo users for off-line data analysis for getting the data archived by the Data Distribution System via Ethernet (and/or FDDI) network choosing among the frames stored on-line and the frames stored in RDT and DST, whose list is maintained on-line.

55.4 Selection of solutions

Although the Raw Data Archiving System and the Data Distribution Systems are structurally different, the technical solutions are designed according to the following general criteria :

- system easy to use and to upgrade;
- system completely open to Virgo people :
  1. software sources available, documented, easy to change and to upgrade according to future Virgo needs ;
  2. standard and commercial hardware, whenever possible;
- system completely expandable : every further upgrade necessary for the improvement of the performances of the system can be obtained by simply adding components or upgrading part of them without changing the hardware and software structure of the system;
- system made of as many standard Virgo components as possible, in order to reduce the number of spare components.

55.5 Detailed description

In the following, detailed descriptions of the Raw Data Archiving System and Data Distribution System are reported.

55.5.1 Raw Data Archiving System

55.5.1.1 Function and concept

All the data generated by the different detectors and controls (raw data), collected by distributed local readout processes and slow monitoring systems and structured by the Frame Builder are then archived on RDT's by the Raw Data Archiving System. These data are the real output of the interferometer and are necessary for any eventual data reprocessing starting from the original data.

55.5.1.2 Detailed description

The architecture of the Raw Data Archiving System, shown in Figure 5510.1, is the typical client/server Virgo architecture, in which the Raw Data Archive (server) is configured and controlled by its User Interface (client). The configuration of the system is stored in the On-line Database while the Error Logger records all the error messages generated the Raw Data Archive. The Supervisor may act as an User Interface.

As said above the major technical specification for the Raw Data Archive is given by the need of storing a maximum burst data flow equal to 10 Mbyte/sec, although a continuous data flow from 1 to 5 Mbyte/sec is expected. On the basis of the actual technology such a large amount of data has necessarily to be maintained off-line. Although an off-line archive can use both optical disks and magnetic tapes, actually the only economical affordable solution is that of using magnetic tapes. At the moment the best candidate as media is the DLT (Digital Linear Tape) which is becoming a de-facto standard. These tapes have a good data storage capacity (20 Gbyte - 40 Gbyte in compressed mode [81,600 bit/in]) and a maximum sustained transfer rate of 3 Mbyte/sec (writing mode) with a synchronous peak transfer rate of 10 Mbyte/sec and an average file access time of 68s. Therefore, assuming the maximum continuous data flow of 5 Mbyte/sec and the maximum storage capacity of DLT (40 Gbyte), then about 4000 DLT/year/copy are necessary to maintain a Raw data Archive.

The DLT solution is much more efficient and reliable than a solution which would make use of the more diffused DAT, which are also de-facto standard and have a good storage capacity (4 Gbyte - 8 Gbyte in compressed mode) with a maximum sustained transfer rate of the order of 1.0 Mbyte/sec (writing mode) and an average file access time of 30s. In this case, assuming again the maximum continuous data flow of 5 Mbyte/sec and their maximum data storage capacity of 8 Gbyte, then at least 20000 DAT/year/copy would have been necessary.

The matching of the sustained transfer rate (writing mode) of the DLT with the requirement on the maximum continuous data flow and with the restriction of a sequential writing on DLT, which would render it easy every data distribution and retrieval, is obtained with the implementation of a two stage storage procedure. A modular solution to this problem, which can be easily integrated in Virgo, consists in the parallel staging of the data on disks (which can sustain a transfer data flow higher than 6 MByte/sec in writing mode and can have a storage capacity up to 4 - 9 Gbyte) and then copying the data on DLT.

The scheme of principle of the Raw Data Archiving System Server structure which implements this solution is shown in Figure 5510.2. The system is made of a dedicated VME crate controlled by a master CPU, running the operating system LynxOS and linking the Raw Data Archiving System Server to its User Interface, to the On-line Database, to the Error Logger and to the Supervisor via the network (Ethernet) using Cm for communication. In the same VME crate, n slave CPU's are housed, each one provided with disks and with a DLT autoloader. The master CPU controls the frame acquisition from the Frame Builder via VIC bus enabling the first slave CPU which writes the frames on its disks. When these disks are full, then the master CPU enables the second slave CPU to write the frames on its disks, while the first one starts to download the content of the disks on the first DLT. When it finishes, it changes the tape and waits until the master CPU enables it to write again. The procedure requires the number of CPU's necessary to match the data flow to the sustained transfer rate of the DLT. This solution makes it easy also to reconfigure the system on the basis of the actual data flow and to have higher data flows for short times if the disks and/or the RAM memory on board are used as buffers.

The temporal course of the storage procedure with DLT is shown in the scheme of Fig.5510.3 for a data flow equal to 5 Mbyte/sec and a sustained transfer rate of 2.5 Mbyte/sec on DLT. Three slave CPU's are necessary, each provided with 40 Gbyte total disk memory and autoloader with 7 media. In this configuration a full cycle lasts 24 ksec (approx 6.7 hours), that is new data are written on the same disk after 24 ksec. And assuming that the autoloader houses up to 7 DLT, a total memory of 840 Gbyte is foreseen and it is necessary to change the Cartridge Magazine of each slave CPU approximately every 48 hours. In order to increase this time it is necessary to provide each CPU with larger autoloaders or with more DLT autoloaders. This configuration has also the advantage of leaving the autoloaders enough dead time to rewind a DLT and to load another one on the same unit. Finally, this configuration is completely open and expandable and can easily sustain higher data flow rates.

Moreover, the hardware can be easily upgraded without changing substantially the software architecture.

Due to the importance of these data, which represent the real output of the Virgo interferometer, the Raw Data Archiving System is provided with a shadow companion in order to render the system fault tolerant. In this way, the system writes two copies of the archive which are located in two different places for safety.

On the basis of the above defined structure the Raw data Archiving System Server is made of a dedicated VME crate (12 units) controlled by a master CPU (PowerPC604 - 64 Mbyte RAM

Memory), running the operating system LynxOS and linking the Raw Data Archiving System to the network (Ethernet). In this crate a VIC bus (but we have already tested VME Reflective Memory Boards which allow a data transfer rate up to 40 Mbyte/sec) and 3 slave CPU's (PowerPC604 with 32 Mbyte RAM Memory), each provided with 40 GByte fast disks and a DLT unit with autoloader (with 7 or more media), are housed. This configuration has also the advantage of leaving the autoloaders enough dead time to rewind a DLT and to load another one on the same unit.

A Raw Data Archiving System Prototype has been implemented and is operational in the Napoli Virgo Lab. This prototype is made of a 7-slot VME crate, in which a master CPU (PPC604 - 100 MHz - 32 Mbyte RAM), running the operational system LynxOS, and two slave CPU's (PPC604 - 100 MHz - 32 Mbyte RAM), each provided with a 4 Gbyte fast disk and a DAT autoloader with 6 media are housed. On this prototype the whole software and hardware architecture has been developed and tested. Moreover, specific tests, which are valid for the final Virgo system have been performed. In particular, the test on the sustained data transfer rate on disk (writing mode) has reached 6 Mbyte/sec in continuous mode, while a sustained data transfer rate on DAT (writing mode) has reached 0.7 Mbyte/sec. Independent tests of writing speed on DLT have shown that the system works well also with these media. Finally the data retrieval from RDT has been also developed and tested.

55.5.2 Data Distribution System

55.5.2.1 Function and concept

The Data Distribution System collects the data produced by the On Line Processing System and stores them on disks (on-line data distribution) and on DLTs (and on DATs) (off-line data distribution - DST). These data contain all the useful information for the off-line data analysis, that are :

- Reconstructed h values ([t,h] pairs with quality coefficients and all the necessary auxiliary information) (maximum continuos data flow ≈ 120 kByte/sec at 20 kHz sampling rate).
- Slow monitoring records for monitoring the interferometer environment. These data are organized in a On-line Database (Historical Monitoring) and can be accessed at any time for checking and analysis of the environmental variables (maximum continuous data flow ≈ 5 kByte/sec).
- Frames selected by the Virgo real-time data analysis algorithms running in parallel on the On-Line Processing. These frames contain all the raw data required to perform a full analysis of the signal candidates (maximum equivalent continuous data flow ≈ 150 kbyte/sec assuming 10 days of events at 5 Mbyte/sec data flow).
- Raw data, retrieved from the RDT's of the archive, to be reprocessed by the Data Distribution System in order to reconstruct the full frame, or data retrieved from DST's.

The organisation of the data in the Data Distribution System is hierarchical. The frame directory, the slow monitoring variables and all the derived data and auxiliary information are stored in classic database (a commercial database is used for a full compatibility with other scientific databases), while the frames selected by the On Line Processing System are stored according to a tree structure, as shown in Fig.5520.1.

Actually, such a large amount of data (≈ 300 kbyte/sec) cannot be archived on-line for a long time by the Data Distribution System, because it would make the archive too expensive. For this reason we limit the content of the on-line archive to the data produced by Virgo in the last month, which requires to maintain about 500 Gbyte on-line (at least 80 disks, assuming 9 Gbyte capacity and a global data flow of 2 Mbyte/sec). At the same time, all the content of the on-line archive is also written on DST's. Although the content of special DST's can be defined according to the data analysis needs, the standard DST's contains the following information :

- All the frames with reconstructed h data and slow monitoring records at the sampling rate (20 kHz) for performing a full data analysis for all the sources on the whole band of the interferometer. The storage of these data requires a maximum amount of 3600 Gbyte/year.
- All the frames with slow monitoring records and reconstructed [t,h] pairs data resampled at lower frequency (2 kHz) for performing a specific research on continuous sources (i.e. pulsar search). The storage of these data requires a maximum amount of 360 GByte/year.
- Frames selected by the parallel real-time data analysis algorithms running on the On Line Processing System for performing a specific research on bursts or coalescing binaries, which contain all the necessary raw data. Assuming 10 days of these data, then the storage of these data requires a maximum amount of 4400 GByte/year.

On the basis of the assumptions made, then the storage of data on DST's requires a maximum amount of $\approx$ 8400 Gbyte/year on tape, that corresponds to $\approx$ 210 DLT/year.

All the data archived by the Data Distribution System are available to the authorised Virgo users via standard network (Ethernet and/or FDDI) or directly on DST for the off-line analysis. They can get them using the Software Tools - Data Distribution (5900), choosing them within the list of contents of the data stored in RDT's and in DST's, which is maintained on-line on the Data Distribution System.

55.5.2.2 Detailed description

The architecture of the Data Distribution System is shown in Fig.5520.2. An User Interface (client) configures and controls the Data Distribution (server) according to the typical client/server Virgo Architecture, setting the configuration (stored in the On Line Database System), checking the errors (recorded by the Error Logger System), accessing the stored data for changing their structure, for deleting and moving files and for all the relevant operations of management of the system. Standard Virgo User Interfaces access the stored data in read only mode using the Software Tools - Data Distribution (5900). In particular, the history of each stored quantity can be displayed on these workstations using the Historical Monitoring software. Due to the large amount of data and to avoid any possible interference between the Virgo data collection and the data distribution, the Data Distribution System uses separate standard network lines. In synthesis, the Data Distribution System has two main tasks :

- Data Acquisition and Storage from the On-Line Processing.
- Data Distribution to Virgo users.

The Data Distribution System has been designed in order to perform these two tasks in a nearly completely independent way following two different philosophies, giving full priority to the Data Acquisition and Storage tasks if access conflicts exist. In particular the Data Acquisition and Storage section is designed according to the real-time VME acquisition techniques, while the Data Distribution section follows the standard computer networking techniques (Fig 5520.3).

The Data Acquisition and Storage section, whose main tasks are the data acquisition from the On-line Processing System, the data retrieval from raw data (RDT) and data output (DST) is a VME based system in which a master CPU (all the Data Acquisition CPU's are provided with up to 4 PCI bus interfaces on board) runs the operating systems LynxOS. On the same VME bus slave CPU's are housed, each one handling a number of disks connected to its native SCSI bus or to added PCI-SCSI interfaces. The master CPU acquires the data from the On-line Processing via a VIC bus (or reflective memories) and distributes them to the designated slave CPU (via VME bus or via reflective memory VME boards if the slave CPU's are not housed in the same crate of the master), which store them on disk. At the same time the master CPU send to the Data Distribution section the part of the frame relative to the environment monitoring parameters together with the information of the location and the content of the stored frames, necessary for any data retrieval and content list making.

The Data Distribution section, which manages the requests of the Virgo users, follows a standard networking procedure. For this task, a fully expandable server (Alpha server), which can accommodate multiple Alpha CPU's running the operating systems OSF/1, memory boards, PCI peripherals buses for the I/O which supports several SCSI buses to which it is possible to attach disks and tapes, is used. The link between with the master VME CPU is made via a VME-PCI bus-to-bus adapter interface. This channel is used by the server to receive all the working information (and part of the data) necessary for checking the correct working of the Data Acquisition and Storage section and to send commands (configuration, upgrading of directories, etc.). All this information is stored in an on-line database. The data retrieval is done using a FDDI internal network. For this reason, each slave VME CPU is provided with a FDDI-PCI interface which is used by the server for accessing the data stored in the disks.

A Data Distribution System Prototype has been implemented and is operational in the Napoli Virgo Lab. This prototype is made of a 3 VME crates, in which a master CPU (PPC601 - 100 MHz - 64 Mbyte RAM), running the operational system LynxOS, and three slave CPU's (PPC604 - 100 MHz - 32 Mbyte RAM with 2 PCI slots on board), each provided with a 2 4 Gbyte fast disks and a DAT are housed. The Alpha Server is a 2100 Alpha Server VME running the operating system OSF/1. On this prototype the whole software and hardware architecture has been developed and tested. Moreover, specific tests, which are valid for the final Virgo system ,have already been performed.

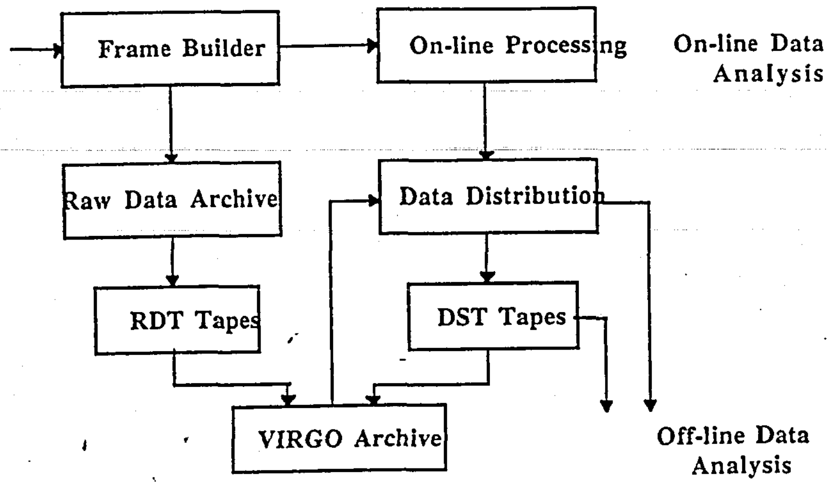

Figure 5500.1 Scheme of principle of the Data Distribution & Archiving

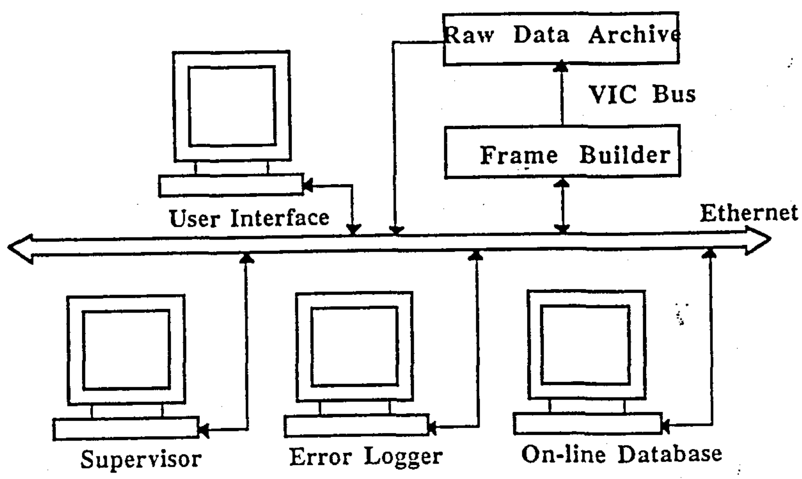

Figure 5510.1 Architecture of the Raw Data Archiving System

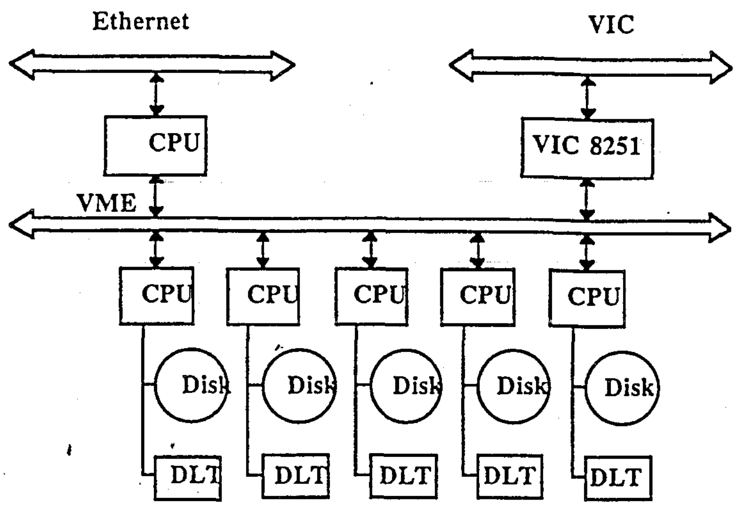

Figure 5510.2 Raw Data Archiving System Hardware Structure

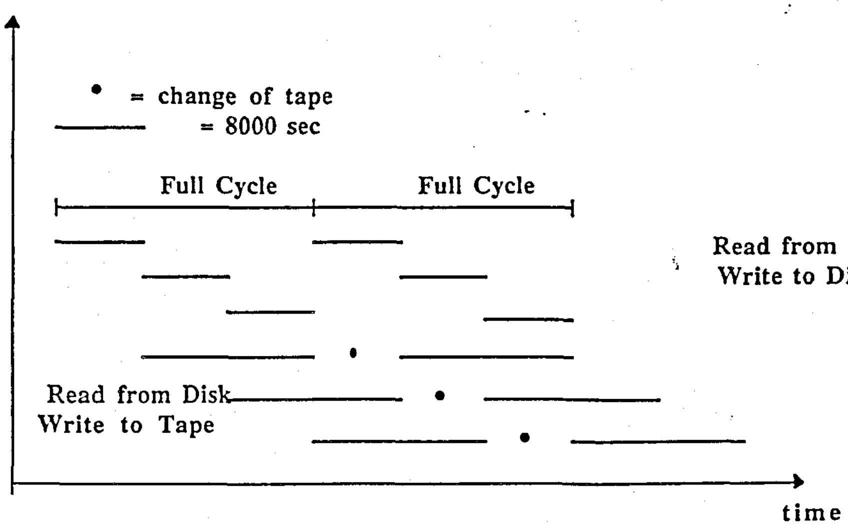

Figure 5510.3 Time Course of the Data Storage Procedure

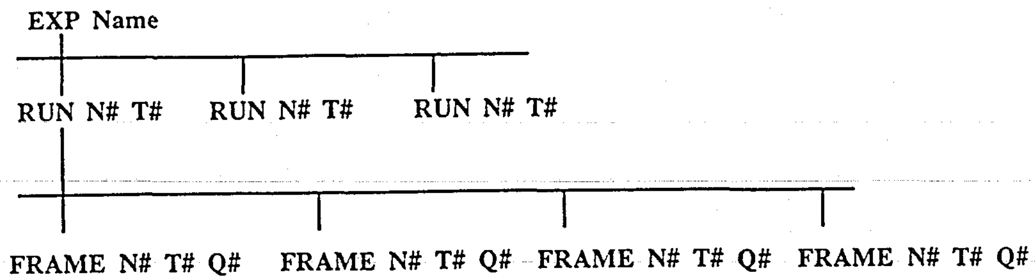

with N# = number, T# = time, Q# = quality factor

Figure 5520.1 Structure of the Stored Frames in Data Distribution System

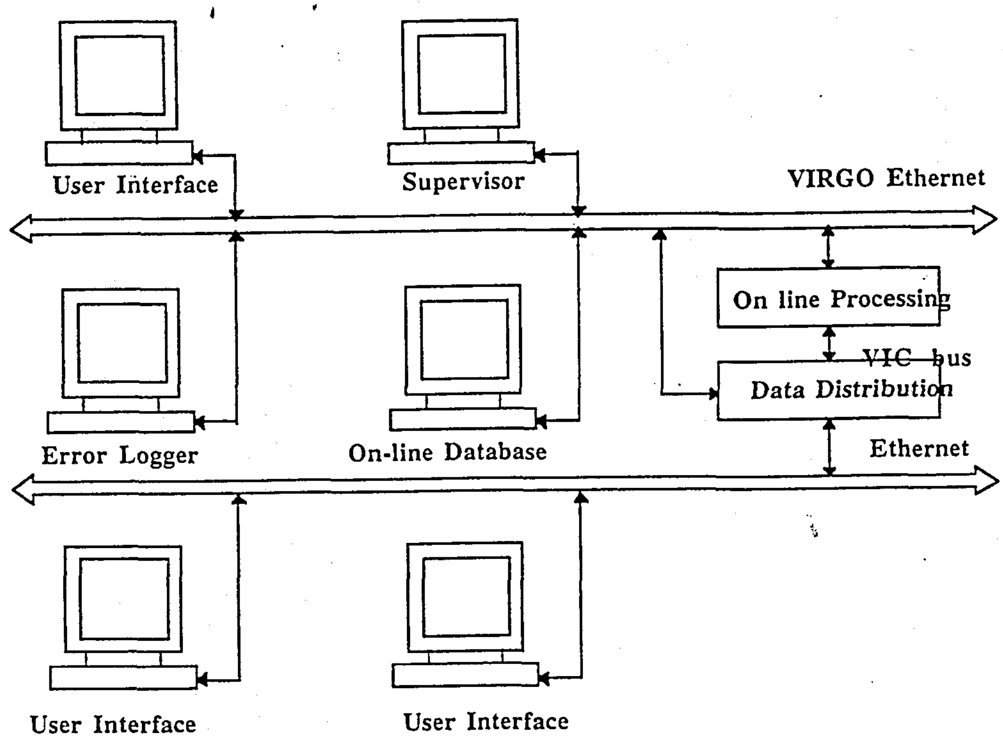

Figure 5520.2 Architecture of the Data Distribution System

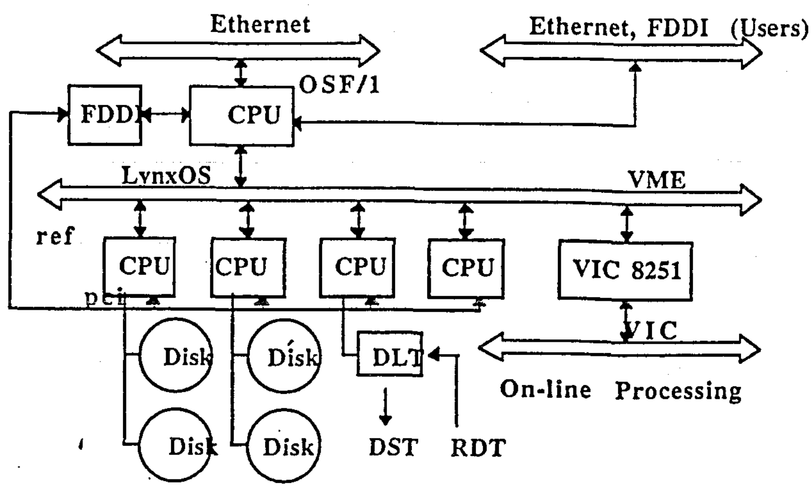

Figure 5520.3 Data Distribution System Hardware Structure

56. Supervisor & associated software

56.1 The Supervisor

The function of the Supervisor is to keep track of, to request, allow or inhibit modifications of the status of the various components of the interferometer. With respect to this functionality directed towards Organisation and Security, it is intended to provide the overall user interface (the master client) of VIRGO. The Supervisor, in particular, provides a graphic display of the status of all the VIRGO components. It will also use the output of the Data Monitoring programs and should later house the expert system in charge of the interferometer. A set of automatic sequences will be available for the interferometer start up for instance.

The Supervisor controls all the servers using the messages described in table 5000.1. It displays the status of all the available servers. When a special action is required for a given server it can start the corresponding client and delegate its privileges.

The list of servers controlled by the supervisor is called the partition. This partition which can be modified, is described in the supervisor configuration. The supervisor is in fact the 'front page' of VIRGO as it provides a very short description of the status of all available tasks using a color code. The possible status are :

- Not in partition	grey
- In partition but not connected	black
- Connected and no configuration file	red
- Connected and config available	orange
- Connected and config loaded	yellow
- Connected and running	blue
- Connected and stable	green

In addition, the type of client can be specified (master which is the default, or ordinary client) and a message displayed. A changing status is indicated by a flashing color. The figure 5100.1 shows a possible supervisor.

By clicking within the Supervisor panel on a server icon, one may perform the following actions on a server with the help of a pop up menu :

- add or remove from the partition
- configure (set parameters like server names,...)
- start server (task)
- ask for connection
- read status
- read and load server configuration file
- run and stop the action performed by the server
- start the corresponding user interface
- kill the server
- become master or slave user

Under smooth conditions there is only one Supervisor running in the control room with all the privileges for the hardware access. It collects the status information from the servers and checks the error logger for warning or error messages. It asks periodically for status. A non answering server could be considered as an error message. Additional supervisors without privileges for the hardware access could be run in different places to monitor the interferometer.

56.2 The communication tool

This package manages task to task communications by providing a wide range of mechanisms required to manipulate transparently the network layer (TCPIP) and unifornly across the various platforms. A complete description is available within the Cm distribution kit. However, one may summarize the basic features it implements as follows :

Cm is meant to manage the task to task communications (sending or receiving messages) running on heterogenous machines (with different architectures or operating systems) without limitations on the number of active connections apart from those induced by the operating systems.

The set of tasks or applications that may participate this network define a Cm domain managed by one special application - the NameServer - in charge of the physical addressing scheme, allowing several independant such domains to coexist.

An application with which a connection is requested is referenced by a name, that must be unique within one Cm domain and that does not need to mention anyhow the machine on which it runs, nor the transport charectiristics (such as TCPIP parameters).

The central manager application NameServer is in charge of every mechanism for name registration, port number allocation, and physical addressing operations transparently for the user application.

The Cm Message part handles the formatting issues, insuring that a structured information frame is transmitted across the network (reaching heterogenous architectures) without loosing its integrity.

Elements of security management are introduced by the internal protocole, by transmitting the host name and user name of the message senders.

56.3 The ErrorLogger

The error logger collects the information and error messages from all the processes. The messages are sent using the El library which uses Cm.

Each message contains a severity code and a text. The levels of severity are :

- info — just information message
- warning — their is some problem but the standard operation can continue
- severe — some non standard procedure has to be followed to fix the problem. The server goes one state down for severe error.
- fatal — the server is stopped or going to kill. It goes more than one state down.

The error display is the error logger client which provides the tools to select and display error messages collected by the error logger.

Query operations can be requested by aplications giving selection criteria based on the date, the severity, the source, the message. The diagnostics and monitoring applications will be the normal users of the error logger.

56.4 The Online DataBase

This package is meant to handle the online configuration database. It is based on one server (although several servers may coexist) responsible for the accesses to the stored objects (controling the protections, the selections and the manipulations) and of the effective storage medium for the objects. Access to the data base will be achieved from any application through the network. (DB is based on Cm)

Data items consist on named C objects and can be of most legal C type.

Management of items is centralized in a DB server (that also handles access control on objects)

Items (or objects) are accessed by their nam transparently over the network and selections of set-of-objects can be done with various criteria (name pattern, conditions on nvalue, ...)

An history of the contents evolution for every object is maintained by the system and recoveries of object values are possible on the basis of azbsolute or relative time and date specifications.

Objects are eventually stored into textual files (using a human readable format) that may even permit a non-network access to objects.

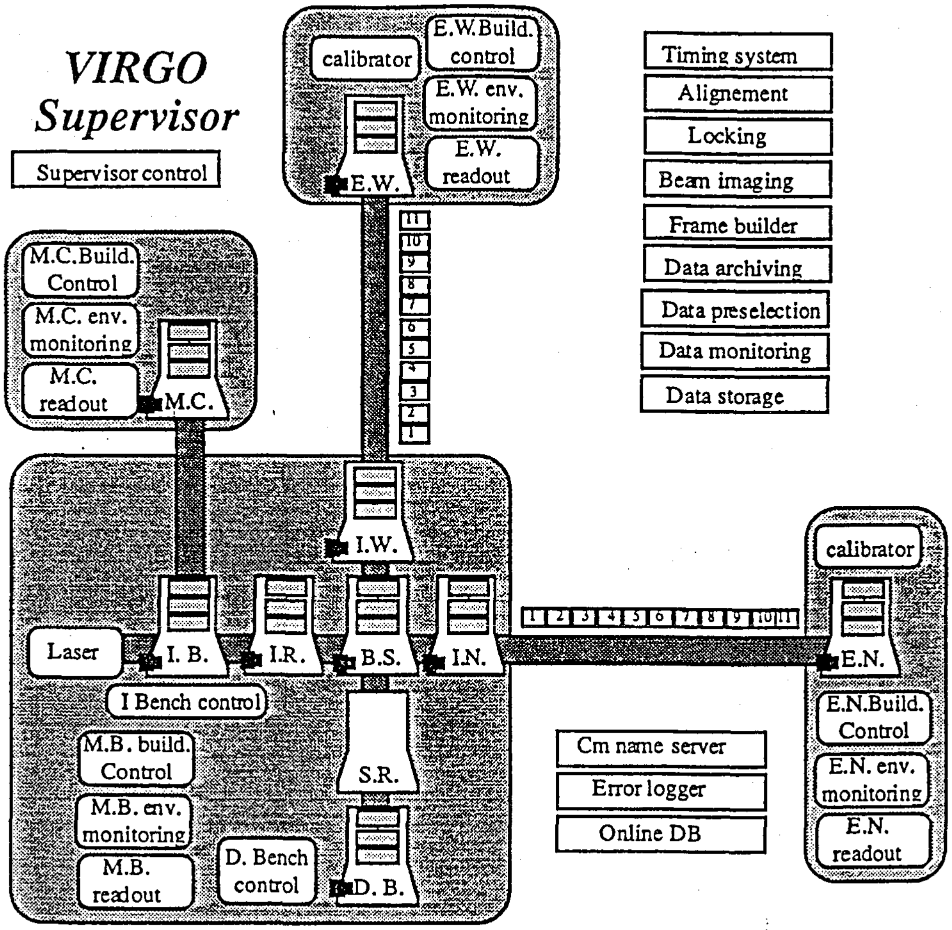

Figure 5600.1 The Supervisor

57. Software Tools - Simulation

57.1 General Description

The simulation software tool of VIRGO is SIESTA. It is an integrated, general purpose simulation program. One of its goals is to provide a tool for the detector design and commissioning, especially as far as the control of the interferometer is concerned. To reach this goal, a global simulation of the interferometer operation is needed , not only for the case when the interferometer is around its working point, but also for the lock acquisition phase. The other major goal of SIESTA is to provide simulated data for data analysis, in order to develop search and trigger algorithms. Moreover, an effort has been made to make the software modular enough so that some pieces may be used in connection with other VIRGO softwares.

57.2 Interfaces

SIESTA is interfaced to the FrameLib package that allows to write/read formatted data.

57.3 Selection of solutions

One of the choices has been to perform the simulation in the time domain. This is important for data analysis since it allows to produce the same type of simulated data as real data. It is also useful when non-linear effects have to be taken into account, such as non-lin earitiesin the interferometer optical response or in the electronics.

SIESTA is written in the C language, and is based on an object-oriented structure that is most suitable to build an integrated simulation involving many different aspects. The implemented framework allows to integrate the generation of gravitational wave events with the simulation of the most relevant aspects of the detector operation : behavior of suspended mirrors, interferometer optical response, control, DAQ (see figure 5700.1). Since the level of accuracy needed for some aspects of the simulation may vary according to the issue investigated, various models are made available as options whenever possible.

Not all the simulation developments are integrated into SIESTA : very specific issues have been addressed through dedicated simulation tools that need not be integrated in the general software.

57.4 Detailed description

For a detailed description we refer to the SIESTA user's guide that is available with the SIESTA package and can be found at the following http address :

http://lapphp.in2p3.fr/virgo/sDoc/dirvirgoApp.

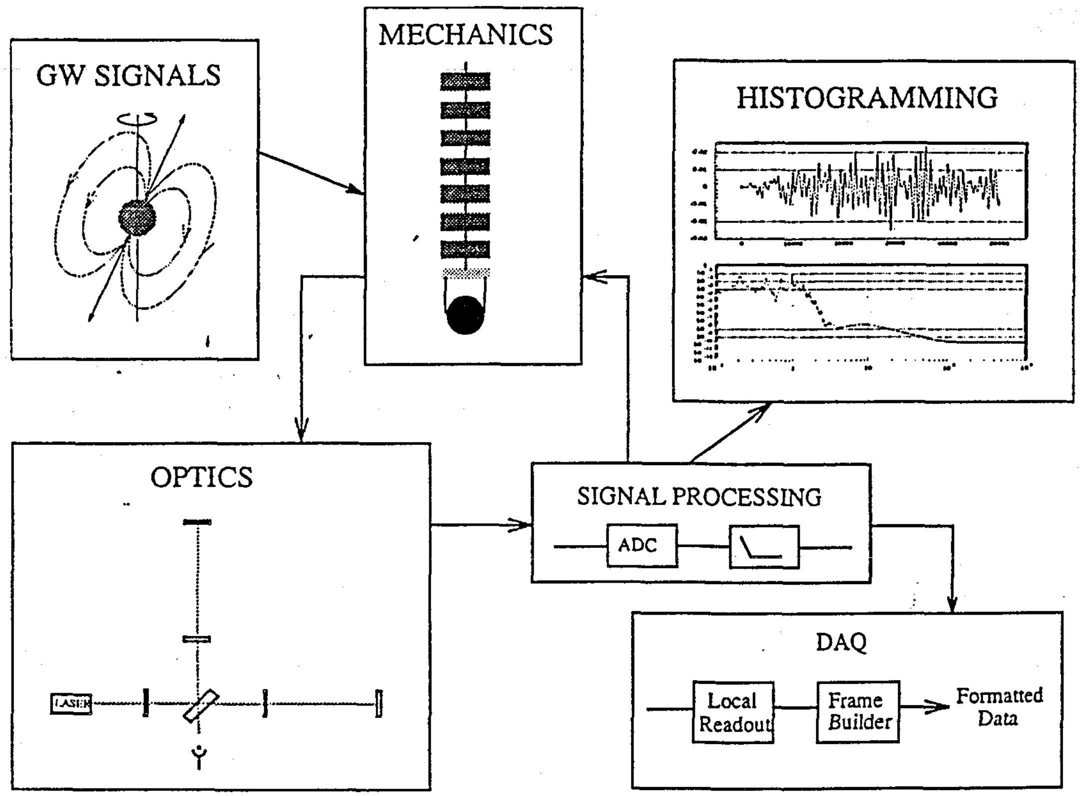

Figure 5700.1: Different modules integrated into SIESTA

58. Environment Monitoring

The Environment Monitoring System monitors all the environmental quantities which can have effects on the sensitivity of Virgo. This monitoring is necessary both for understanding any possible malfunctioning of the interferometer due to environmental causes and for providing the data analysis algorithms with the necessary environmental data for reducing the false alarm probability of gravitational wave events detection by means of correlation techniques.

58.1 Function and concept

The environmental sources of noise can be divided into two groups : the building noise (i.e. the noises due to the big appliances, like the power supply noises, the air conditioning noises, etc., of the Virgo buildings), which are monitored by the Building Monitoring System through a distributed acquisition network, and the environmental noise (i.e. acoustic noise, electromagnetic noise, etc.), which are monitored and analysed by the Environment Monitoring System.

The Environment Monitoring takes care of both continuos and impulsive noise sources. But while the continuous noise sources are theoretically predictable and can be experimentally checked once for all (together with their effects on the sensitive curve of Virgo), on the other hand, accidental causes, which can last also for a long time and can mime a gravitational wave event, must be experimentally measured, even if the corresponding continuous noise is some orders of magnitude below the Virgo sensitivity curve, and continuously monitored. For these reasons, the Environment Monitoring must be a an extremely flexible system, which must be adapted to the real needs of Virgo : without any substantial change of the hardware and software architecture of the system, it must allow an easy increase (or decrease) in the number and type of probes and changes of their positions for a improving their sensitivity. For this reason the Building Monitoring Servers and the Environment Monitoring Servers (one for each building) are characterised by an open architecture which makes it easy to add other probes, if necessary, or simply to change the type of probe used. Moreover, for making it easy to position the probes and to make all the necessary tests, also during the normal Virgo data acquisition phase, the Environment Monitoring is provided with the necessary computing power on board for performing all the necessary analysis on the environmental quantities and the capability of sending all these data directly to the On-line Database of the Data Distribution System, without perturbing in any way the Virgo acquisition procedures. In Figure 5800.1 the structure of principle of the Environment Monitoring in connection with the other Virgo systems is shown.

A preliminary study on the type and the number of environmental quantities which need to be monitored has led to the Table 5800.1.I. More precise indications on the actual number and final position of the probes is going to be obtained both from better theoretical approaches, by direct measurements on the existing Virgo prototypes and, later on, on site with the interferometer working.

Environment Monitoring Parameters

Parameter	CB	MCB	NB	WB	NT	WT	Frequency	Timing
Electromagnetic	8	2	2	2	-	-	20 kHz	yes
Acoustic	8	2	2	2	-	-	20 kHz	yes
Power Supply	5	2	2	2	-	-	20 Khz	yes
Seismic (3)	8	2	3	3	-	-	1 kHz	yes
Env. Temp.	8	2	3	3	-	-	1 Hz	no
Env. Press.	8	2	3	3	-	-	1 Hz	no
Env. Hum.	8	2	3	3	-	-	1 Hz	no
Wind Speed	1	-	1	1	-	-	1 Hz	no
Wind Direction	1	-	1	1	-	-	1 Hz	no
Rain	1	-	1	1	-	-	1 Hz	no

Table 5800.I Environment Monitoring Parameters

CB = Central Building	MCB = Mode Cleaner Building
NB = Nord End Building	WB = West End Building
NT = Nord Tunnel	WT = West Tunnel

In particular, as it is possible to see in this Table, the sampling frequency is not the same for all of the environmental quantities, because of the different bands of the noises and the different effects on the sensitivity curve of Virgo. In fact, the same sampling rate of the output signal of the interferometer (20 kHz) and a precise timing is necessary for some of them (i.e. electromagnetic noise, acoustic noise, etc.) while a lower frequency sampling rate with no precise timing definition is sufficient for other quantities (i.e. temperature, pressure, humidity, etc.). On the basis of the structure of the Virgo systems, then the best solution for the acquisition of the environmental parameters is the following :

- The acquisition of fast variables which need precise timing is integrated within a fast VME data acquisition system (local readout), which makes it easy to handle the data and to transfer them to the Frame Builder. For this reason the fast ADCs of the Environments Monitoring are housed within the Local readout System. At the same time these variables are acquired for checks and for spectral analysis by the Environment Monitoring System, which record and send their main characteristics to the Frame Builder and to the Data Distribution System via the Slow Monitoring Netowrk (Ethernet).
- The acquisition of slow variables is made by the Environment Monitoring Servers, which send them directly to the Frame Builder by means of the Slow Monitoring Network (Ethernet).
- The acquisition of quantities related to the noise of the Building is made by the Building Monitoring Servers, which send them directly to the Frame Builder by means of the Slow Monitoring Network (Ethernet).

The architecture of the Environment Monitoring is shown in Fig.5800.2. A user interface running on one of the control room workstations manages the whole Environment Monitoring Network, sets the configuration of each server (stored in the On-line Database System), of all the fast and slow acquisition boards and of the probes, checks the errors (recorded by the Error Logger System). Such user interface has a graphical page for each type of variable and can display the main characteristics and the history of each environment monitoring parameter, using the Historical Monitoring software in connection with the Data Distribution System.

58.2 Requirements

The main requirements relative to the Environment Monitoring concern the sampling frequency and the sampling accuracy. The requirements for the Building Monitoring System and Environment Monitoring System are shown in Table 5800.II and Table 5800.III, respectively.

Building Monitoring System Requirements

Data Acquisition			
Distributed	<=3	km	distributed
Sampling Frequency	<= 1	kHz	
ADC bit Number	12 - 16	bit	
Data Flow Rate	<=2	kbyte/sec	VME continuous mode
	<=200	kbyte/sec	ETN continuous mode
Data Transfer Rate	<=2	kbyte/sec	continuous mode
	<=200	kbyte/sec	burst mode - User Interface

Table 5800.1 Building Monitoring System Requirements

Environment Monitoring System Requirements

Data Acquisition			
Sampling Frequency	<= 20	kHz	
ADC bit Number	16	bit	
Data Flow Rate	<=2	Mbyte/sec	VME continuous mode
Data Transfer Rate	<=2	kbyte/sec	continuous mode
	<=200	kbyte/sec	burst mode - User Interface

Table 5800.2 Environment Monitoring System Requirements

58.3 Interface

The two systems require a direct connection with the main components of the electronics.

58.3.1 List of Environment Monitoring interfaces

2000 Infrastructure
5100 Global Control
5200 Standardized components
5300 Networks
5400 Data Acquisition
5500 Data Distribution & Archiving
5600 Supervisor

58.3.2 Interface with Infrastructure

The Environment monitoring (Building Monitoring System) is connected with the infrastructure, because it has to monitor the status of the buildings and the status of the appliances installed in the buildings.

58.4 Interface with Global Control

The Environment Monitoring uses the Cm package for communication within the system and with other related Virgo subsystems. In particular, it sends every error message to the Error Logger, while its on-line configuration is stored in the On-line Database.

58.4.1 Interface with Standardized Components

The Environment Monitoring uses, where possible, standard Virgo hardware and software components : this makes it easy their replacement and smaller the number of spare components. In particular, the CPU's (PPC604), the crates (VME), the operating systems (LynxOS), the language (C) and the network (Ethernet) are standard Virgo components (5200).

58.4.2 Interface with Networks

The Environment Monitoring requires the standard Virgo Ethernet line for internal connections (i.e. User Interface, Error Logger, On-line Database, Supervisor, Frame Builder, Data Distribution, etc.).

58.4.3 Interface with Data Acquisition

All the fast environmental quantities (20 kHz) which need the timing are acquired by the Local Readout using the ADCs of the Environment monitoring, while the slow quantities and the main parameters of the all the fast ones acquired and processed by the Environment Monitoring are transferred to the Frame Builder is made via the slow monitoring network (Ethernet).

58.4.4 Interface with Data Distribution & Archiving

Some environmental data acquired by the Environment Monitoring for specific studies on environmental variables can be directly sent to the Data Distribution System, which stores them in its On-line Database.

58.4.5 Interface with Supervisor

The Supervisor keep track, request allow od inhibits the modifications of the status of this subsystem and can act as an User Interface.

58.5 Selection of solutions

Although the Building Monitoring System and Environment Monitoring System are structurally different, the technical solutions are designed according to the following general criteria :

- system easy to use and to upgrade;
- system completely open to Virgo people :
    1. software sources available, documented and easy to change and to upgrade according to future Virgo needs;
    2. standard commercial hardware components when possible;
- system completely expandable, that is every further upgrade necessary for the improvement of the performances of the system can be obtained by simply adding components or upgrading part of them without changing the hardware and software structure of the whole system.
- system made of as many standard Virgo components as possible, in order to reduce the number of spare components..

58.6 Detailed description

In the following sections detailed descriptions of the Building Monitoring System and Environment Monitoring System are reported.

58.6.1 Building Monitoring System

58.6.1.1 Function and concept

The Building Monitoring System monitors the appliances installed in the buildings (i.e. power supply systems, air conditioning systems, etc.) and the main actuators in the buildings. At the same time, it acquires all the relevant quantities describing the status of the buildings (i.e. temperature, pressure, humidity, etc.).

58.6.1.2 Detailed description

The architecture of the Buildings Monitoring System, shown in Fig.5810.1, is a typical client/server Virgo architecture, in which the Building Monitoring (server) is configured and controlled by its User Interface (client). The configuration of the server is stored in the On- line Database, while the Error Logger records all the error messages generated by the Building Monitoring. The Supervisor may act as an User Interface.

As pointed above, the main characteristic of the Building Monitoring is that of monitoring appliances and noises over a distributed area and of displaying, if necessary, their history. Moreover, it must have the necessary characteristics of flexibility of being configured and modified also during the construction and test phases of Virgo.

These characteristics are obtained using a distributed I/O control protocol system (ETN system - Enhanced Tecnint Network) both for acquisition and control. This system is interfaced to a standard VME environment via a slave CPU controller. All the boards are serially connected using a RS485 serial connection. The standard characteristics of this distributed I/O is that for a 200 m length of the serial cable (but a maximum of 6 km is allowed with repeaters), it can sustain a maximum transmission speed of 1.5 Mbit/sec with an acquisition time for every 16 bit transaction equal to 100μs, that is a maximum of 10,000 transactions per second. Beyond the standard foreseen VME ADC boards, the system is integrated with standard RS232 interface VME boards for the data acquisition from all the probes which are interfaced with this standard. For this reason, the server supports a distributed RS232 network developed in Napoli Virgo Lab. This systems consists in distributed addressable micro-controllers systems provided with on-boards 8-bit ADCs, which locally acquire the quantities, make some eventual local on-line processing on them and send the results to the server via the RS232 interface.

A PC based version of the server permits the control of those appliances for which the control software is directly provided by the factories for MS-DOS operating system.

A Building Control Server is foreseen for each building. Each server consists of a dedicated VME crate, controlled by a local CPU, running the operating system LynxOS and linking each server to the Slow Monitoring Network (or a PC with both operating systems MS-DOS and LynxOS).

A Building Monitoring System Prototype has been implemented and is operational in the Napoli Virgo Lab. This prototype of the server is made of a 5-slot VME crate, in which a master CPU (68040- 25 Mhz - 16 Mbytre RAM), running the operational system LynxOS. In this server a TVM-221 CPU (68020) board from Tecnint with a TVM-922 piggyback as ETN controller and a TVM-580 memory board for data transfer in shared memory, interfaces the ETN with the VME. This controller has on board a driver of type master which automatically controls the serial communication process with the acquisition distributed boards. On this system a RS232 interface VME board (VCPH4A - 4 RS232 from Cetia) is also housed for data acquisition using the RS232 standard which provide the server with the link to the RS232 micro-controllers for data acquisition. A PC prototype of Building Monitoring with ETN is also operational in Napoli.

58.6.2 Environment Monitoring System

58.6.2.1 Function and concept

The Environment Monitoring System monitors all the environment variables, which are not directly related to the status of interferometer, but necessary for the correlation analysis with the interferometer output signals. At the same time is acquires and processes the data relative to the environment quantities which are necessary to analyse in more detail.

58.6.2.2 Detailed description

The architecture of the Environment Monitoring System, shown in Fig.5820.1, is a typical client/server Virgo architecture, in which the Environment Monitoring (server) is configured and controlled by its User Interface (client). The configuration of the server is stored in the On-line Database, while the Error Logger records all the error messages generated by the Building Monitoring. The Supervisor may act as an User Interface.

As pointed above, the main characteristic of the Environment Monitoring is that of monitoring all the environmental quantities which can have effects on Virgo, eventually processing them in order to study in detail each quantity and displaying, if necessary, their history. For these reasons, it must have the necessary characteristics of flexibility of being configured and modified also during the construction and test phases of Virgo.

These characteristics are obtained using a VME system on which DSP boards and ADC boards are housed which use the fast bus for data transfer, and standard CPU's which use the VSB bus for data acquisition from the ADC boards in order to maintain their sustained data flow rate if working in multiplexing mode. Moreover, the server supports VME boards with RS232 interface and the distributed RS232 network developed in Napoli Virgo Lab, as shown for the Building Monitoring System.

An Environment Monitoring System Prototype has been implemented and is operational in the Napoli Virgo Lab. This prototype of the server is made of a 12-slot VME crate, in which a master CPU (PPC601 - 100 Mhz - 16 Mbytre RAM), running the operational system LynxOS. In this server a DSP DV96 from Loughborough is housed which acquires data from ADC via its bus and processes them. Two ADC 16 bit 8 channels 50 kHz sampling rate (MPV912A from Pentland) are used by the PCC601 for data acquisition.

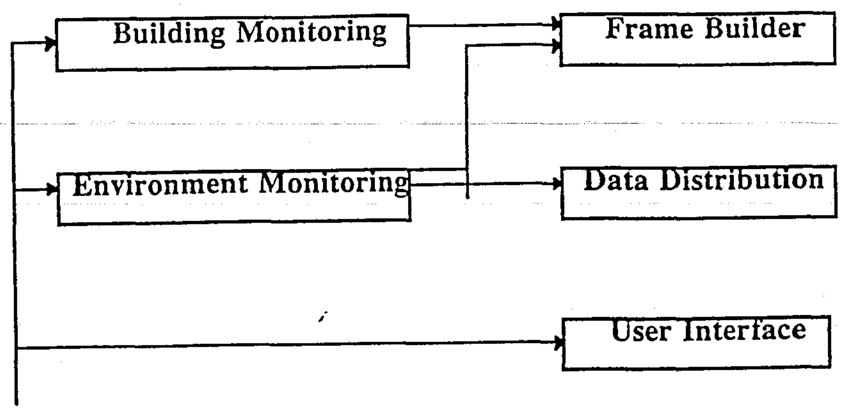

Figure 5800.1 Scheme of principle of the Environment Monitoring

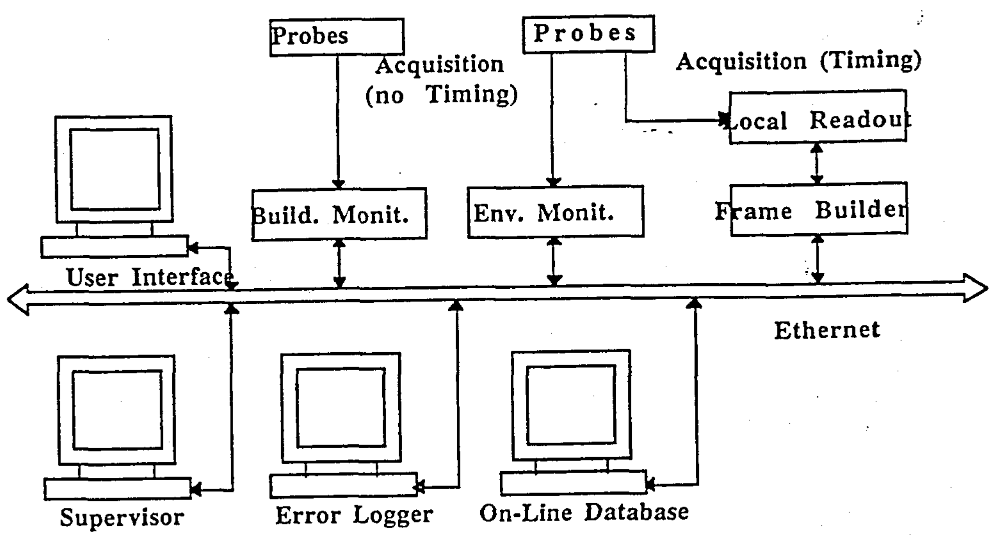

Figure 5800.2 Architecture of the Environment Monitoring

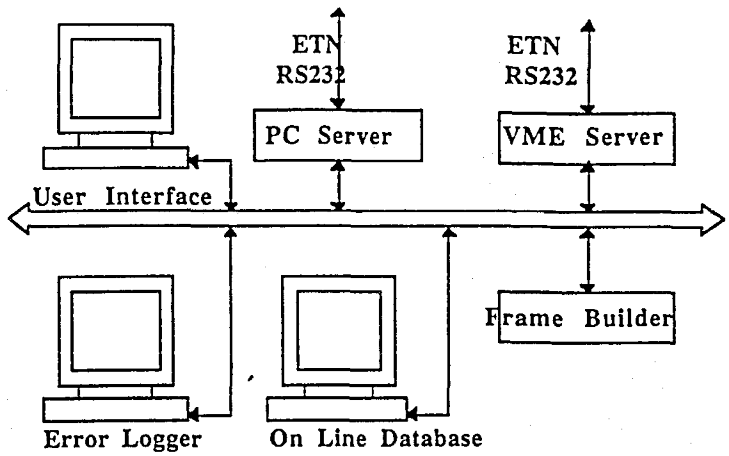

Figure 5810.1 Architecture of the Building Monitoring System

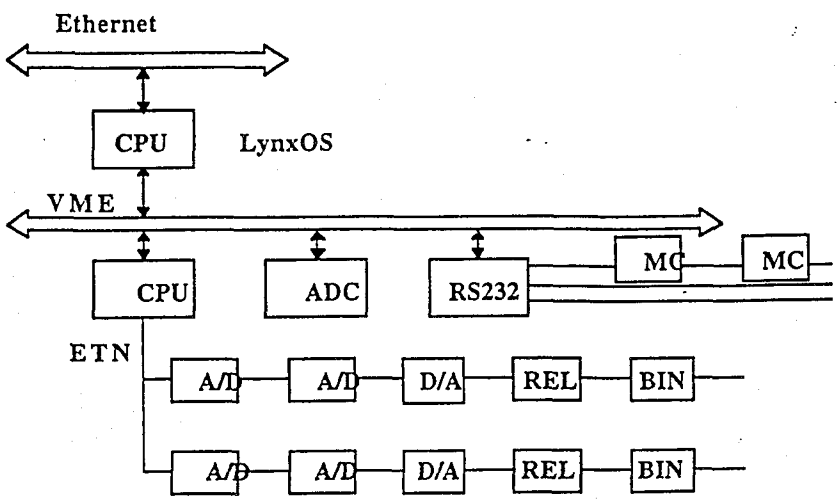

Figure 5810.2 Architecture of the Building Monitoring Server

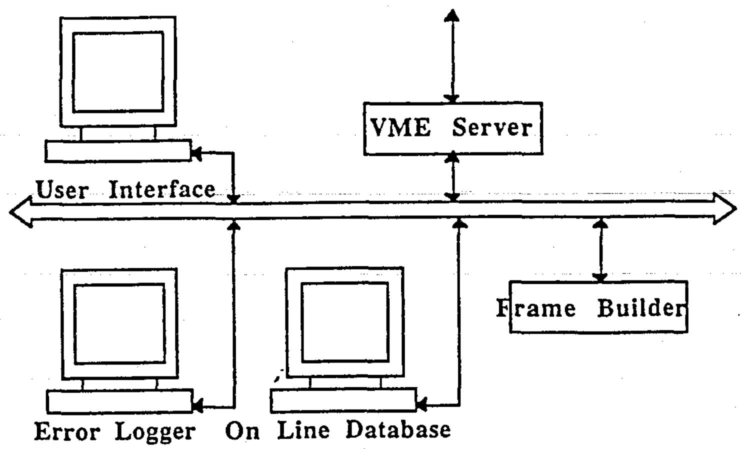

Figure 5820.1 Architecture of the Environment Monitoring System

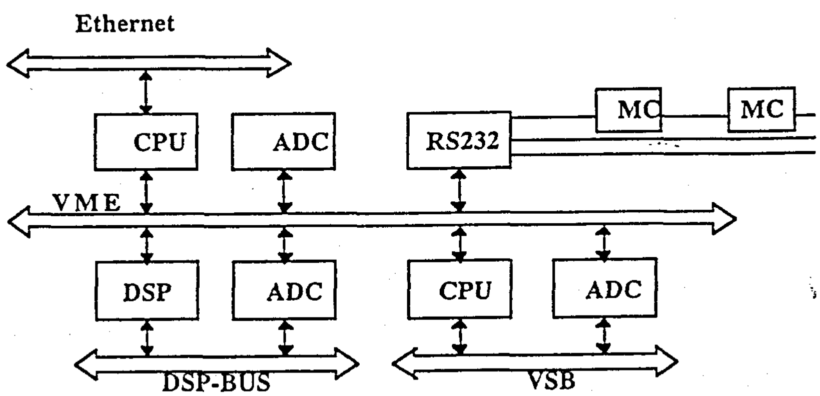

Figure 5820.2 Architecture of the Environment Monitoring Server

59. Software Tools - Distribution

The off-line Software Tools Distribution provides all the software for data retrival and distribuiton that the Virgo users will use for every access to the Virgo Data Archive (on-line and off-line). This software will allow the user to extract, to view, to process and to reconstruct all the stored information useful for data analysis and general checks on Virgo.

59.1 Function and concept

The off-line S/W Tools are organized in such a way that the Virgo users can extract, view, process, reconstruct and download all the data stored in RDT's, DST's and on the on-line databases of the Data Distribution System in the easiest way. It uses, where they exists, the S/W Tools designed and used also in other subsystems in such a way to define an unique Virgo standard, without any duplication of work.

59.2 Requirements

The only requirements are relative to use a standard procedure and languages for data retrieval and reprocessing according to the Virgo standards and to satisfy the maximum data transfer rate of 1 Mbyte/sec which is in the requirements of the Data Distribution & Archiving (5500).

59.3 Interfaces

This system requires a direct connection with the main software delevoped for other systmes of the electronics.

59.3.1 List of S/W Tools - Distribution interfaces

5400 Data Acquisition
5500 Data Distribution & Archiving
5700 S/W Tools - Simulation

59.3.2 Interface with Data Acquisition

The system uses some tools developed for the Data Acquisition, like the Data Display, On-line Processing, etc.

59.3.3 Interface with Data Distribution & Archiving

The S/W Tools -Distribution have access to the data on-line stored in the Data Distribution, to DST's and to the RDT's.

59.3.4 Interface with S/W Tools - Distribution

The S/W Tools - Simulation must be used by the S/W Tools - Distribution for the reprocessing of RDT's for rebuilding the frames after their retrieval.

59.4 Selection of solutions

The system is developed according to the following general criteria :

- to implement the system and easy to use and to upgrade.
- to implement a system completely open to Virgo people with software sources available, documented and easy to change and to upgrade according to the future Virgo needs.

59.5 Detailed description

The structure of the S/W tools - Distribution is organised in modules, written in C language for portability. These modules include many modules developed for other subsystems which are keep as they ,are in order to have standard Virgo software. Other software, including the software for the data distribution via network, is written ad hoc or standard software with large diffusion is used.

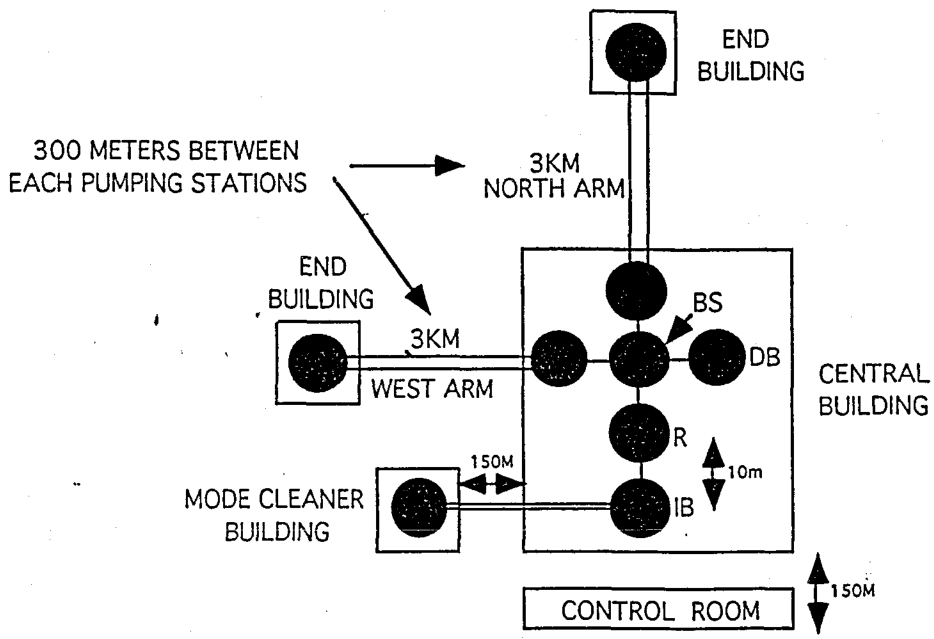

figure 5300.2 VIRGO Buildings

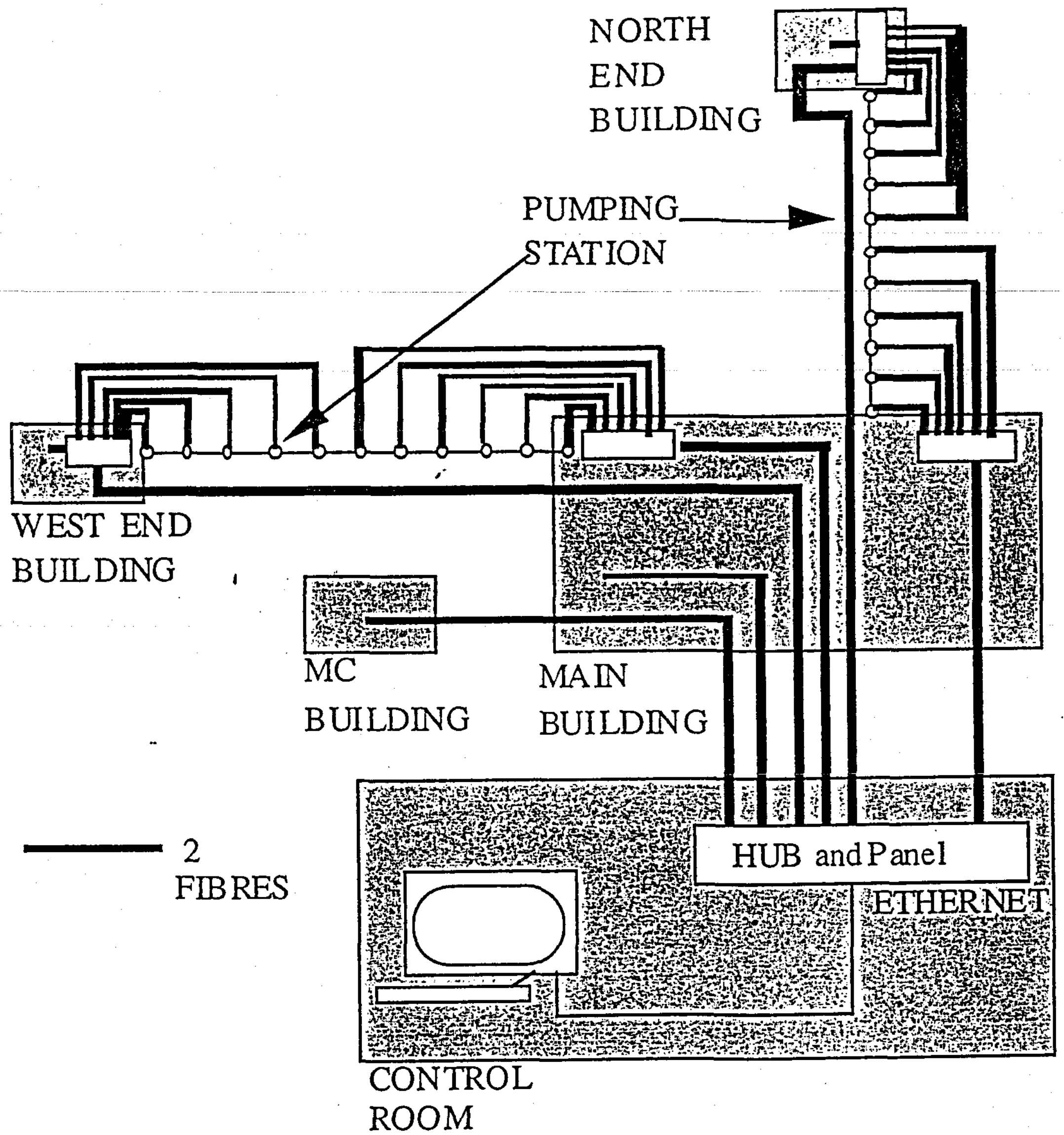

Figure 5300.3 The slow monitoring network.

The VIRGO Collaboration on January 1997

Direction and Project Office

Acker Y.
Benfatti P.
Brillet A.
Enard D.
Errico A.
Giazotto A.
Tofani C.

ITALIAN LABORATORIES

INFN-Firenze
Cecchini R.
Ciuffi F.
Mazzoni M.
Pelfer P.G.
Stanga R.

INFN-Frascati
Babusci D.
Cima E.
Fang H.
Giordano G.
Iannarelli M.
Matone G.
Turri E.

INFN-Napoli
Barone F.
Calloni E.
Di Fiore L.
Flagiello M.
Garufi F.
Grado A.
Longo M.
Lops M.
Marano S.
Milano L.
Solimeno S.

INFN-Perugia
Aragona A.
Babucci E.
Cagnoli F.
Gammaitoni L.
Kovalik J.
Marchesoni F.
Punturo M.

INFN - Pisa
Beccaria M.
Bernardini M.
Braccini S.
Bradaschia C.
Cella G.
Ciampa A.
Cosci R.
Cuoco E.
Curci G.
D'Ambrosio E.
Dàttilo V.
De Carolis G.
de Salvo R.
Di Virgilio A.
Ferrante I.
Fidecaro F.
Gaddi A.
Gennai A.
Giassi A.
La Penna P.
Losurdo G.
Maggiore M.
Mancini S.
Palla F.
Pan H. B.
Paoletti F.
Pasqualetti A.
Passuello D.
Poggiani R.
Popolizio P.
Raffaelli F.
Ragonesi A.
Ruberti R.
Vicere' A.
Zhang Z.

INFN - Roma
Astone P.
Bronzini F.
Capradossi G.
Ferrari V.
Frasca S.
Majorana E.
Mattei A.
Papa M. A.
Pellegrino F.
Perciballi M.
Puppo P.
Rapagnani P.
Ricci F.
Serrani E.

FRENCH LABORATORIES

ESPCI - Paris
Boccara C.
Deban J.B.
Germain O.
Gleyzes P.
Leliboux M.
Loriette V.
Nahum R.
Roger J.P.

IPN - LYON
Dognin L.
Ganau P.
Lagrange B.
Mackowski J.M.
Michel C.
Morgado N.
Morgue M.
Napolitano M.
Pinard L.

LAL - Orsay
Arnault C.
Barrand G.
Beney J. L.
Bilhaut R.
Brisson V.
Cavalier F.
Chiche R.
Combeau R.
Corona P.
Coulon J. P.
Cuzon S.
Davier M.
Dehamme M.
Dialinas M.
Ducorps A.
Eder C.
Garnier C.
Gaspard M.
Hello P.
Heusse P.
Jules E.
Lissilour G.
Marie M.
Marin P.
Marrucho J.C
Matone L.
Mencik M.
Reboux A.
Rivoirard P.
Roudier P.
Taurigna M.

LAPP - Annecy
Bellachia F.
Bermond M
Boget D.
Buskuluc D.
Caron B.
Carron T.
Castellazzi D
Chollet F.
Daguin G.
David P. Y.
Dedieu M. L.
Derome L.
Drezen C.
Dufournaud D.
Flaminio R.
Gaillard G.
Giacobone L.
Girard C.
Grave X.
Hermel R.
Lacotte J.C.
Le Marec J.C.
Lieunard B.
Marion F.
Massonet L.
Mehmel C.
Morand R.
Mours B.
Mugnier P.
Sannibale V.
Sottile R.
Verkindt D.
Yvert M

LAS - Orsay
Barillet R.
Barsuglia M.
Berthet J.P.
Bindzi Ph.
Cachenaut J.
Cleva F.
Gourgoulhon E.
Heitmann H.
Lucenay J. C.
Man Nary C.
Marck J-A.
Pelat D.
Pham-Tu M.
Redon T.
Reita V.
Taubman M.
Vinet J.Y.

50. ELECTRONICS AND SOFTWARE

Table of Contents